

UCLA

UCLA Electronic Theses and Dissertations

Title

Developing Prodrug Strategies for the Controlled Delivery and Release of Therapeutic Small Molecules and Proteins

Permalink

<https://escholarship.org/uc/item/1wv5f5d2>

Author

Rose, Douglas

Publication Date

2021

Peer reviewed|Thesis/dissertation

UNIVERSITY OF CALIFORNIA

Los Angeles

Developing Prodrug Strategies for the Controlled Delivery and
Release of Therapeutic Small Molecules and Proteins

A dissertation submitted in partial satisfaction of the
requirements for the degree Doctor of Philosophy
In Chemistry

by

Douglas Rose

2021

© Copyright by

Douglas Rose

2021

ABSTRACT OF THE DISSERTATION

Developing Prodrug Strategies for the Controlled Delivery and Release of Therapeutic Small
Molecules and Proteins

by

Douglas Rose

Doctor of Philosophy in Chemistry

University of California, Los Angeles, 2021

Professor Heather Maynard, Chair

Therapeutic agents including small molecules, peptides, and proteins comprise most of the pharmaceuticals currently on the market and are an invaluable piece of modern medicine. Many of these therapeutics have some level of instability and/or off-target effects when administered in vivo that ultimately limits their effectiveness. Covalent modification of such therapeutics into an inactive prodrug prior to administration is a common modality used within the field of drug delivery to increase the circulation time or limit off-target effects, thus enhancing the therapeutic efficacy compared to administration of the unaltered drug. Due to the large diversity in chemical reactivities across various therapeutics, a wide array of strategies has been developed to covalently modify functional groups of interest. This thesis outlines the development of two such prodrug modalities; the first for the targeted delivery of oxycodone to the small intestine to prevent

nonprescribed forms of administration and the second being a platform for the tunable release of peptides and proteins for enhanced circulation time.

Biologics including peptides, proteins, and oligonucleotides are an important class of macromolecules that have received an increasing amount of attention over the past few decades for their therapeutic potential. Their widespread adoption has lacked, in part, due to issues with chemical instability and immunogenicity *in vivo*. One particular avenue towards mitigating these effects is through PEGylation of the biologics, which can lead to enhanced stability and circulation times *in vivo*. However, PEGylation typically results in decreased binding or activity and in some cases can turn these off altogether. To mitigate these effects, researchers developed small molecule linkages that can be placed in between the protein and polymer, which cleave slowly over time to release native protein with restored binding/activity. Chapter 1 outlines the current strategies used within the field of traceless peptide/protein conjugation, including lonapegsomatropin-tcgp and NKTR-214 the only two traceless protein-polymer conjugates currently approved by the FDA, along with insights into potential future directions for this field.

Prescription opioids, although necessary for pain management, are highly addictive and have led to the dramatic increase of opioid involved overdoses over the past 20 years. Abuse-deterrent (AD) opioid formulations are an important avenue towards addressing this national health crisis by increasing the difficulty for abusers to easily obtain large amounts of active opioid. However, there are currently only ten AD formulations on the market, a majority of which are easily circumvented by motivated users. Chapter 2 outlines the design and preparation of a slow-release elastomeric opioid formulation, which requires the presence of two proteases found within the small intestine in order to release the drug. This strategy limits the common abusive routes of administration, including, nasal insufflation and intravenous injection through the protease

mediated activation step. In order to do this, the opioid was modified with a dual-enzyme responsive peptide sequence, whereupon proteolytic cleavage by chymotrypsin followed by trypsin triggers a self-immolative based release of the active opioid. The resulting elastomeric formulation was shown to be stable towards mechanical deformation testing following periods of heating and cooling, as well as hydrolytic degradation across a pH range of 2-10.

It was later identified that the elastomeric opioid carrier was not entirely necessary for the abuse deterrent properties of the formulation, but rather the same properties could be demonstrated in a small molecule peptide-opioid prodrug. Therein, Chapter 3 highlights the development of a second-generation abuse-deterrent peptide prodrug without the elastomeric carrier. The peptide-opioid prodrug sequence was optimized to mitigate any nonspecific protease cleavage, while also enhancing the rate of trypsin and chymotrypsin cleavage, the two enzymes responsible for activation in the small intestine. Notably, the composition of the amino acid sequence was highly crucial in determining the protease promiscuity which was identified as an issue with the first-generation prodrug. In addition, a third level of protection from abuse was incorporated into the prodrug through an acid mediated activation step to unmask a tyrosine residue. This activation rapidly occurs in simulated gastric fluid producing *t*-butanol and allows for chymotrypsin to bind and subsequently cleave the tyrosine residue.

The development of traceless linkers, outlined in Chapter 1, demonstrates the interest in creating prodrug like protein-polymer conjugates, allowing for the systemic administration of therapeutic peptides and proteins that were previously cleared too rapidly to be clinically useful. To this end, Chapter 4 outlines the development of a new amine reactive benzylamine traceless linker as an alternative to the commonly used carbamate linkages. A small molecule model system was initially used to probe the release kinetics of a primary amine, simulating lysine release from

a protein-polymer conjugate. Varying the electronics within the aromatic core of the linker played a vital role in modulating the rate of release, resulting in half-lives ranging from 144 to 20 hours. The most promising linker was then incorporated into as a PEG-end group and used to conjugate to prepare traceless lysozyme-PEG conjugates. These conjugates released more than 95% native lysozyme over the course of 48 hours at a pH of 7.4 with a restoration of lysozyme activity upon release, whereas less than 25% native lysozyme was released within 96 hours at a pH of 4.0.

Building upon the results from Chapter 4 and mechanistic insights from density functional theory (DFT) calculations carried out in collaboration with members from the Houk Lab, Chapter 5 discusses the synthetic pursuits, kinetics studies, and protein conjugation studies toward developing a second-generation linker. These linkers incorporate an intramolecular trap to decrease the lifetime of the quinone methide intermediate, which in turn enhanced the rate of release to a 4.5 hour half-life using a small molecule model system. Additionally, these second-generation benzylamine linkers were used to prepare two traceless lysozyme-PEG conjugates with varying electronics and rates of release. The lysozyme-PEG conjugate containing the more electron rich linker demonstrated 98% release of native lysozyme within 12 days while restoring lysozyme activity, whereas the less electron rich linker showed only 50% release within the same time frame. This new class of linkers with tunable release rates expands the traceless linkers toolbox for a variety of bioconjugation applications.

The dissertation of Douglas Rose is approved.

Richard B. Kaner

Kendall N. Houk

Christopher J. Evans

Heather D. Maynard, Committee Chair

University of California, Los Angeles

2021

*This dissertation is dedicated to my family,
especially my parents, Jack and Beth Rose for
their unwavering love and support.*

Table of Contents

ABSTRACT OF THE DISSERTATION	ii
Table of Contents	viii
List of Figures.....	xii
List of Tables	xxv
List of Schemes.....	xxvi
List of Abbreviations	xxviii
Acknowledgements	xxxii
Vitae	xxxiv
Chapter 1 Traceless Linkers Used for Reversible Protein Modifications	1
1.1 Introduction.....	2
1.2 Lysine Modifications	3
1.2.1 Anhydride Linkers	3
1.2.2 Bicin Linkers.....	4
1.2.3 β -Mercaptocarbamate Linkers	5
1.2.4 Trimethyl Lock Linkers	6
1.2.5 1,6-Benzyl Carbamate Linkers	7
1.2.6 E1cB Linkers	9
1.2.7 Retro-Michael Addition Linkers.....	10
1.2.8 β -Elimination Linkers	11
1.2.9 Photocleavable Linkers.....	13
1.3 Cysteine Modifications	14

1.3.1	Retro-Michael Addition Linkers.....	14
1.3.2	Disulfide Stapling Linkers	20
1.4	Noncovalent Traceless Linkages	24
1.4.1	Host-Guest Complexes	25
1.4.2	Hydrophobic Interactions.....	27
1.4.3	Metal Coordination Complexes	29
1.4.4	Ionic Interactions	30
1.5	Future Outlook.....	31
1.6	References.....	33

Chapter 2 Development of a Dual-Enzyme Responsive Elastomeric Abuse-Deterrent

Opioi	Formulation	53
2.1	Introduction.....	54
2.2	Results and Discussion	60
2.2.1	Evaluation of Common Opioids for Reversible Modification.....	60
2.2.2	Preparation of a Peptide-Opioid Prodrug.....	62
2.2.3	Development of a Polysiloxane Based Prodrug Formulation.....	65
2.2.4	Development of a Crosslinked PEG Prodrug Formulation.....	69
2.3	Conclusions.....	72
2.4	Experimental.....	72
2.4.1	Materials	72
2.4.2	Analytical Techniques	73
2.4.3	Methods.....	74
2.5	References.....	87
2.6	Appendix B.....	89

Chapter 3 Development of a Dual-Enzyme Responsive Abuse-Deterrent Opioid

Prodrug 98

3.1	Introduction.....	99
3.2	Results and Discussion	100
3.2.1	Determining the Cause of Chymotrypsin Promiscuity	100
3.2.2	Optimization of Peptide Sequence to Enhance the Efficiency of Release.....	103
3.2.3	Preparation of Oxycodone Electrophile.....	109
3.2.4	Preparation and Characterization of Ac-Lys[Tyr-Ala-Ala-Ala]-Oxycodone Prodrug as an Abuse-Deterrent Formulation	111
3.3	Conclusions.....	113
3.4	Experimental.....	113
3.4.1	Materials	113
3.4.2	Analytical Techniques	114
3.4.3	Methods.....	115
3.5	References.....	148
3.6	Appendix B.....	150

Chapter 4 Self-Immolative Benzylamine Linkers for Traceless Protein Conjugation. 158

4.1	Introduction.....	159
4.2	Results and Discussion	162
4.2.1	Preparation of a Benzylamine Model System for Release Kinetics	162
4.2.2	Preparation of mPEG-(2,6-dimethoxybenzaldehyde) for protein conjugation.....	164
4.2.3	Preparation of mPEG- β -thioester-(2,6-dimethoxybenzaldehyde)-Lysozyme Conjugate and Traceless Release of Lysozyme.....	165

4.2.4	Preparation of mPEG-glutarate-(2,6-dimethoxybenzaldehyde)-Lysozyme Conjugate and Traceless Release of Lysozyme	171
4.3	Conclusions.....	177
4.4	Experimental.....	178
4.4.1	Materials	178
4.4.2	Analytical Techniques	178
4.5	Methods	179
4.6	References.....	193
4.7	Appendix C	200
Chapter 5 Development of Second Generation Benzylamine Linkers for Traceless Protein Conjugation..... 223		
5.1	Introduction.....	224
5.2	Results and Discussion	227
5.2.1	Preparation of Second Generation Benzylamine Linkers with Release Kinetics ...	227
5.2.2	Synthesis of Benzaldehyde Precursors for Traceless Conjugation.....	229
5.2.3	Preparation of Traceless mPEG-Lysozyme Conjugates	232
5.2.4	Traceless Release of Lysozyme and Activity Recovery Studies.....	234
5.3	Conclusions.....	236
5.4	Experimental.....	237
5.4.1	Materials	237
5.4.2	Analytical Techniques	237
5.4.3	Methods.....	238
5.5	References.....	283
5.6	Appendix C	285

List of Figures

Figure 1.1. Traceless hydrolytic release of native protein from a PEGylated conjugate through use of a bicin linker.	5
Figure 1.2. Thioester or disulfide (top and bottom respectively) triggered mechanism of protein release for the β -mercaptocarbamate traceless linkers.....	6
Figure 1.3. Design of the NQO1-Catalyzed Chemical Modification of a Protein and Its Intracellular Delivery for Potent Protein Activation in Living Cells for a Potential Targeted Cancer Therapy.	7
Figure 1.4. Acendis Pharmaceutical's Lonapegsomatropin-tcgp long acting traceless hGH-PEG conjugate.....	9
Figure 1.5. Meldrums acid derived traceless linker relying on a retro-Michael addition to facilitate protein release (R represents either cysteine or glutathione).....	10
Figure 1.6. NKTR-214 is a CD122-biased cytokine agonist conjugated with multiple releasable chains of PEG located at the interface of IL2 and IL2R $\alpha\beta\gamma$. The PEG chains slowly release at physiological pH, creating conjugated-IL2 species with fewer PEG chains and increased bioactivity. Sustained signaling through the heterodimeric IL2 receptor pathway (IL2R $\beta\gamma$) preferentially activates and expands effector CD8 T and NK cells over Tregs.....	12
Figure 1.7. Functionalization and release of the Grb2 SH2 Domain (L111C) with dibromomaleimide.	16
Figure 1.8. Synthesis of trifunctional pyridazinedione-protein derivatives.....	18
Figure 1.9. Chemical switch for bonding and debonding using Triggerable Michael Acceptors (TMAc). (A) Schematic illustration of the trigger-to-release process as a universal strategy	

for uncaging of functional groups (left) and the trigger-to-reverse process, the reversibility of which can be structurally customized (right). (B) Proposed thiol-based trigger-to-release. (C) Proposed amine-based trigger-to-release.....	19
Figure 1.10. sCT disulfide bridging with ATRP generated PEGMA via dibromomaleimide linker	21
Figure 1.11. Strategy for supramolecular PEGylation. (A) A copper-free “click” reaction between a cucurbit[7]uril (CB[7]) supramolecular host molecule bearing a single azide moiety (CB[7]–N ₃) and a dibenzocyclooctyne-functional poly(ethylene glycol) polymer (PEG–DBCO) (M _n = 5, 10, or 30 kDa) yields CB[7]–PEG upon triazole formation. (B) Cartoon depicting supramolecular PEGylation of the insulin protein through strong noncovalent binding of the CB[7] moiety to the N-terminal phenylalanine residue.	27
Figure 1.12. Design concept of the cholesterol end-modified poly(ethyleneglycol) (Chol-U-Pr-mPEG) for by-product-free intact modification of insulin.	29
Figure 2.1. Number of deaths per year in the United States attributed to drug overdose. Chart plotted from data made available from the National Institute on Drug Abuse. ⁵	55
Figure 2.2. Abuse-deterrent elastomeric extended-release opioid prodrug formulation comprised of a dual enzyme-responsive peptide prodrug covalently bound within a PEG matrix.....	59
Figure 2.3. Commonly prescribed opioids and their conserved reactive handles highlighted.	60
Figure 2.4. Stability of peptide prodrug (6) to (a) common household solvents and (b) 50 mM citrate-phosphate (McIlvaine) buffer within a pH range of 2 to 10.....	63
Figure 2.5. Protease responsive release of naltrexone from naltrexone-peptide prodrug (6) in the presence of either trypsin or chymotrypsin or both monitored by HPLC and confirmed by LCMS (n = 3 samples, error bars are smaller than markers).....	64

Figure 2.6. Abuse-deterrent elastomeric extended-release opioid prodrug formulation comprised of a dual enzyme-responsive peptide prodrug in a polysiloxane-PEG matrix.....	65
Figure 2.7. SEM characterization of elastomer lyophilized from (a) water or (b) benzene followed by incubation in water for 12 h.	67
Figure 2.8. Protease responsive release of naltrexone from naltrexone-peptide-PMVS elastomer (9) in the presence of either trypsin or chymotrypsin or both monitored by HPLC and confirmed by LCMS.	68
Figure 2.9. Protease responsive release of naltrexone from naltrexone-peptide-PEG hydrogel (9) in the presence of either trypsin or chymotrypsin or both monitored by HPLC and confirmed by LCMS (n = 3, error bars are smaller than markers).	71
Figure 2.10. Elastomeric prodrug stability to Coca-Cola measured via HPLC over 12 hours. No appearance of Naltrexone was confirmed by LCMS.	75
Figure 2.11. Elastomeric prodrug stability to lemon juice measured via HPLC over 12 hours. No appearance of Naltrexone was confirmed by LCMS.	75
Figure 2.12. Elastomeric prodrug stability to vinegar measured via HPLC over 12 hours. No appearance of Naltrexone was confirmed by LCMS.	76
Figure 2.13. Standard curve of Naltrexone via HPLC with integrated absorbance values (254nm) across multiple concentrations.	77
Figure 2.14. ¹ H NMR Spectrum of OMe-Naltrexone in CDCl ₃	90
Figure 2.15. ¹³ C NMR Spectrum of OMe-Naltrexone in CDCl ₃	91
Figure 2.16. ¹ H NMR Spectrum of O-Me Naltrexone-enol-thionocarbonate-pentafluorophenol in CD ₃ CN.	92

Figure 2.17. ¹³ C NMR Spectrum of O-Me Naltrexone-enol-thionocarbonate-pentafluorophenol in CD ₃ CN.	93
Figure 2.18. ¹ H NMR Spectrum of 2,2,2-trifluoro-N-(2-(methylamino)ethyl)acetamide in CD ₃ CN.	94
Figure 2.19. ¹³ C NMR Spectrum of 2,2,2-trifluoro-N-(2-(methylamino)ethyl)acetamide in CD ₃ CN.	95
Figure 2.20. ¹ H NMR Spectrum of 2,2,2-trichloroethyl (2-aminoethyl)(methyl)carbamate in CD ₃ CN.	96
Figure 2.21. ¹³ C NMR Spectrum of 2,2,2-trichloroethyl (2-aminoethyl)(methyl)carbamate in CD ₃ CN.	97
Figure 3.1. Sequence dependent <i>p</i> NP release from peptide substrates in the presence of only chymotrypsin monitored via the absorbance at 405 nm (n=3).	102
Figure 3.2. Peptide sequence optimization (a) peptide-prodrug mimic for monitoring rate of <i>p</i> NP release via absorbance at 405 nm (b) Michaelis-Menten kinetics parameters comparison between peptide sequences (ND: not determined).....	105
Figure 3.3. Abuse-deterrent opioid formulation comprised of a pH and dual enzyme-responsive peptide prodrug.	108
Figure 3.4. Protease responsive release of <i>p</i> NP from peptide- <i>p</i> NP prodrug (a) 18 in the presence of either trypsin or chymotrypsin or both monitored by absorbance at 405nm (n=3) in 35 mM HEPES pH 7.4 (b) 18 with or without the t-butyl ether protecting group masking the phenol in the presence of both trypsin and chymotrypsin (n=3).	108

Figure 3.5. Michaelis Menten enzyme kinetics monitoring competitive inhibition of (a) Ac-K[YAA]-pNP using YAA as an inhibitor and (b) Ac-K[YAAA]-pNP using YAAA as an inhibitor.....	109
Figure 3.6. (a) Stability of Ac-K[YAAA]-oxycodone prodrug to household chemicals and solvents as well as (b) in 50 mM citrate-phosphate (McIlvaine) buffer across a pH range of 2 to 10.	112
Figure 3.7. Standard curve of p-nitrophenol via UV absorbance (405 nm) on a plate reader across multiple concentrations.....	116
Figure 3.8. ¹ H NMR Spectrum of Compound 1 in CDCl ₃	150
Figure 3.9. ¹³ C NMR Spectrum of Compound 1 in CDCl ₃	151
Figure 3.10. ¹ H NMR Spectrum of Compound 2 in CD ₃ CN.....	152
Figure 3.11. ¹³ C NMR Spectrum of Compound 2 in CD ₃ CN.....	153
Figure 3.12. ¹ H NMR Spectrum of Compound 3 in CD ₃ CN.....	154
Figure 3.13. ¹³ C NMR Spectrum of Compound 3 in CD ₃ CN.....	155
Figure 3.14. ¹ H NMR Spectrum of Compound 11 in CD ₃ CN.....	156
Figure 3.15. ¹³ C NMR Spectrum of Compound 11 in CD ₃ CN.....	157
Figure 4.1. Strategies to prepare traceless bioconjugates: (a) fluorenyloxycarbamate (Fmoc) linker and (b) benzyl carbamate linker compared to (c) benzylamine linker.....	160
Figure 4.2. (a) Library of traceless linkers prepared for model release study with experimentally determined rate constants. (b) Pseudo-first order plot of phenethylamine release kinetics from the benzylamine linker model compounds (n = 3 for each sample) carried out at 5 mM of linker in a 1:1 mixture of methanol and buffer.	162

Figure 4.3. (a) SDS-PAGE of lysozyme and mPEG- β -thioester-lysozyme conjugate (lanes 2 and 3 respectively) (b) MALDI-TOF spectrum of mPEG- β -thioester-DMOB-lysozyme conjugate.	170
Figure 4.4. Traceless release of mPEG- β -thioester-Lysozyme (a) Release kinetics as measured by released 2,6-dimethoxybenzyl alcohol (n = 3, error bars are smaller than markers). (b) MALDI-TOF of lysozyme conjugate 72 hours after incubation at pH 7.1.	171
Figure 4.5. Characterization of mPEG-glutarate-lysozyme by (a) SDS-PAGE and (b) MALDI-TOF mass spectrum.	174
Figure 4.6. Traceless release of lysozyme. (a) Release kinetics as measured by released 2,6-dimethoxybenzyl alcohol (n = 3, error bars are smaller than markers) via HPLC. (b) SDS-PAGE of the mPEG-glutarate-DMOB-lysozyme conjugate before and after the traceless release at both pH 4.0 and 7.4.	175
Figure 4.7. MALDI-TOF mass spectrum of the mPEG-glutarate-(2,6-dimethoxybenzaldehyde)-Lysozyme conjugate incubated for 3 days at (a) pH 7.4 and (b) pH 4.0.	176
Figure 4.8. Lysozyme activity of the mPEG-glutarate-(2,6-dimethoxybenzaldehyde)-lysozyme conjugate before and after traceless release (n = 3, error bars represent standard deviation, *** $p < 0.005$).	177
Figure 4.9. Phenethylamine standard curve from HPLC integration values at 254nm.	191
Figure 4.10. 4-Hydroxy-2,6-dimethoxybenzyl alcohol standard curve from HPLC integration values at 280nm.	192
Figure 4.11. Lysozyme standard curve from ENZChek fluorescence assay (excitation 485 nm, emission 530 nm).	193
Figure 4.12. ^1H NMR Spectrum of Compound 1 in CD_3CN	200

Figure 4.13. ^{13}C NMR Spectrum of Compound 1 in CD_3CN	201
Figure 4.14. ^1H NMR Spectrum of Compound 2 in CD_3CN	202
Figure 4.15. ^{13}C NMR Spectrum of Compound 2 in CD_3CN	203
Figure 4.16. ^1H NMR Spectrum of Compound 3a in CD_3CN	204
Figure 4.17. ^{13}C NMR Spectrum of Compound 3a in CD_3CN	205
Figure 4.18. ^1H NMR Spectrum of Compound 4a in CD_3CN	206
Figure 4.19. ^{13}C NMR Spectrum of Compound 4a in CD_3CN	207
Figure 4.20. ^1H NMR Spectrum of Compound 3b in CD_3CN	208
Figure 4.21. ^{13}C NMR Spectrum of Compound 3b in CD_3CN	209
Figure 4.22. ^1H NMR Spectrum of Compound 9 in CDCl_3	210
Figure 4.23. ^{13}C NMR Spectrum of Compound 9 in CDCl_3	211
Figure 4.24. ^1H NMR Spectrum of Compound 4b in CD_3CN	212
Figure 4.25. ^{13}C NMR Spectrum of Compound 4b in CD_3CN	213
Figure 4.26. ^1H NMR Spectrum of 2 kDa mPEG-COOH in DMSO-d_6	214
Figure 4.27. ^1H NMR Spectrum of 2 kDa mPEG-(2,6-dimethoxybenzaldehyde) in CD_3CN	215
Figure 4.28. ^1H NMR Spectrum of 2 kDa mPEG-phthalimide in CD_3CN	216
Figure 4.29. ^1H NMR Spectrum of 2 kDa mPEG-NH ₂ in CD_2Cl_2	217
Figure 4.30. ^1H NMR Spectrum of 2 kDa mPEG-glutaric acid in CD_3CN	218
Figure 4.31. ^1H NMR Spectrum of 2 kDa mPEG-glutaric-(2,6-dimethoxybenzaldehyde) in CDCl_3	219
Figure 4.32. ^1H NMR Spectrum of 2 kDa mPEG-vinyl in CD_3CN	220
Figure 4.33. ^1H NMR Spectrum of 2 kDa mPEG- β -thioacid in CDCl_3	221

Figure 4.34. ¹ H NMR Spectrum of 2 kDa mPEG-β-thioester-(2,6-dimethoxybenzaldehyde) in CDCl ₃	222
Figure 5.1. (a) Observed cyclic dimeric, trimeric, and tetrameric products from the phenethylamine kinetics release assay (b) structures calculated at the B3LYP-D3/6-31G(d) level of theory.	225
Figure 5.2. Pseudo-first order plot of phenethylamine release kinetics from the benzylamine linker model compounds (n = 3, error bars are smaller than markers) carried out at 5 mM of linker in a 1:1 mixture of methanol and buffer. Release kinetics of 4a and 4b were taken from Figure 4.2. as a comparison.....	229
Figure 5.3. Traceless linkers prepared for protein conjugation.	230
Figure 5.4. Traceless release of lysozyme from Lyz-mPEG conjugates in phosphate buffer (pH 7.4) monitored via HR-LCMS.	235
Figure 5.5. Lysozyme activity assay comparison between each mPEG-Lyz conjugate before (blue) and after (red) traceless release.....	236
Figure 5.6. LCMS-QTOF of deconvoluted lysozyme-linker-6 mass 72 hours into the reaction	241
Figure 5.7. LCMS-QTOF of deconvoluted lysozyme-linker-7 mass 72 hours into the reaction	242
Figure 5.8. LCMS-QTOF of deconvoluted lysozyme-linker-8 mass 72 hours into the reaction	243
Figure 5.9. FPLC Trace of crude mPEG-6-Lysozyme (GE-Superdex 75 10/300 column, 0.5 mL/min, 100 mM PBS)	244
Figure 5.10. (a) SDS-PAGE analysis of conjugation (b) FPLC Trace of crude mPEG-7-Lysozyme (GE-Superdex 75 10/300 column, 0.5 mL/min, 100 mM PBS)	245
Figure 5.11. (a) SDS-PAGE analysis of conjugation (b) FPLC Trace of crude mPEG-8-Lysozyme (GE-Superdex 75 10/300 column, 0.5 mL/min, 100 mM PBS)	246

Figure 5.12. FPLC Trace Comparison of the three mPEG-Lysozyme conjugations (GE-Superdex 75 10/300 column, 0.5 mL/min, 100 mM PBS)	247
Figure 5.13. Traceless release of lysozyme from mPEG-7-lysozyme conjugate in phosphate buffer (pH 7.4) monitored via HR-LCMS.....	248
Figure 5.14. Traceless release of lysozyme from mPEG-8-lysozyme conjugate in phosphate buffer (pH 7.4) monitored via HR-LCMS.....	249
Figure 5.15. Representative deconvoluted LCMS-QTOF mass spectrum of lysozyme after traceless release.....	249
Figure 5.16. Standard curve of lysozyme activity via the ENZChek fluorescence assay (excitation 485 nm, emission 530 nm).....	250
Figure 5.17. ¹ H NMR Spectrum of Compound 1 in CD ₃ CN.....	285
Figure 5.18. ¹³ C NMR Spectrum of Compound 1 in CD ₃ CN.....	286
Figure 5.19. ¹ H NMR Spectrum of Compound 2 in CD ₃ CN.....	287
Figure 5.20. ¹³ C NMR Spectrum of Compound 2 in CD ₃ CN.....	288
Figure 5.21. ¹ H NMR Spectrum of Compound 3a in CD ₃ CN.....	289
Figure 5.22. ¹³ C NMR Spectrum of Compound 3a in CD ₃ CN.....	290
Figure 5.23. ¹ H NMR Spectrum of Compound 4a in CD ₃ CN.....	291
Figure 5.24. ¹³ C NMR Spectrum of Compound 4a in CD ₃ CN.....	292
Figure 5.25. ¹ H NMR Spectrum of Compound 3b in CD ₃ CN.....	293
Figure 5.26. ¹³ C NMR Spectrum of Compound 3b in CD ₃ CN.....	294
Figure 5.27. ¹ H NMR Spectrum of Compound 9 in CDCl ₃	295
Figure 5.28. ¹³ C NMR Spectrum of Compound 9 in CDCl ₃	296
Figure 5.29. ¹ H NMR Spectrum of Compound 4b in CD ₃ CN.....	297

Figure 5.30. ^{13}C NMR Spectrum of Compound 4b in CD_3CN	298
Figure 5.31. ^1H NMR Spectrum of Compound 10 in CD_3CN	299
Figure 5.32. ^{13}C NMR Spectrum of Compound 10 in CD_3CN	300
Figure 5.33. ^1H NMR Spectrum of Compound 11 in CDCl_3	301
Figure 5.34. ^{13}C NMR Spectrum of Compound 11 in CDCl_3	302
Figure 5.35. ^1H NMR Spectrum of Compound 12a in CD_3CN	303
Figure 5.36. ^{13}C NMR Spectrum of Compound 12a in CDCl_3	304
Figure 5.37. ^1H NMR Spectrum of Compound 13a in CD_3CN	305
Figure 5.38. ^{13}C NMR Spectrum of Compound 13a in CD_3CN	306
Figure 5.39. ^1H NMR Spectrum of Compound 14a in CDCl_3	307
Figure 5.40. ^{13}C NMR Spectrum of Compound 14a in CDCl_3	308
Figure 5.41. ^1H NMR Spectrum of Compound 15a in CD_3CN	309
Figure 5.42. ^{13}C NMR Spectrum of Compound 15a in CD_3CN	310
Figure 5.43. ^1H NMR Spectrum of Compound 16a in CD_3CN	311
Figure 5.44. ^{13}C NMR Spectrum of Compound 16a in CD_3CN	312
Figure 5.45. ^1H NMR Spectrum of Compound 17a in CD_3CN	313
Figure 5.46. ^{13}C NMR Spectrum of Compound 17a in CD_3CN	314
Figure 5.47. ^1H NMR Spectrum of Compound 5a in CD_3CN	315
Figure 5.48. ^{13}C NMR Spectrum of Compound 5a in CD_3CN	316
Figure 5.49. ^1H NMR Spectrum of Compound 18 in CDCl_3	317
Figure 5.50. ^{13}C NMR Spectrum of Compound 18 in CDCl_3	318
Figure 5.51. ^1H NMR Spectrum of Compound 12b in CD_3CN	319
Figure 5.52. ^{13}C NMR Spectrum of Compound 12b in CD_3CN	320

Figure 5.53. ^1H NMR Spectrum of Compound 13b in CD_3CN	321
Figure 5.54. ^{13}C NMR Spectrum of Compound 13b in CD_3CN	322
Figure 5.55. ^1H NMR Spectrum of Compound 14b in CD_3CN	323
Figure 5.56. ^{13}C NMR Spectrum of Compound 14b in CD_2Cl_2	324
Figure 5.57. ^1H NMR Spectrum of Compound 15b in CD_3CN	325
Figure 5.58. ^{13}C NMR Spectrum of Compound 15b in CD_3CN	326
Figure 5.59. ^1H NMR Spectrum of Compound 16b in CD_3CN	327
Figure 5.60. ^{13}C NMR Spectrum of Compound 16b in CD_3CN	328
Figure 5.61. ^1H NMR Spectrum of Compound 17b in CD_3CN	329
Figure 5.62. ^{13}C NMR Spectrum of Compound 17b in CD_3CN	330
Figure 5.63. ^1H NMR Spectrum of Compound 5b in CD_3CN	331
Figure 5.64. ^{13}C NMR Spectrum of Compound 5b in CD_3CN	332
Figure 5.65. ^1H NMR Spectrum of Compound 33 in CDCl_3	333
Figure 5.66. ^{13}C NMR Spectrum of Compound 33 in CDCl_3	334
Figure 5.67. ^1H NMR Spectrum of Compound 5c in CD_3CN	335
Figure 5.68. ^{13}C NMR Spectrum of Compound 5c in CD_3CN	336
Figure 5.69. ^1H NMR Spectrum of Compound 19 in CDCl_3	337
Figure 5.70. ^{13}C NMR Spectrum of Compound 19 in CDCl_3	338
Figure 5.71. ^1H NMR Spectrum of Compound 20 in CDCl_3	339
Figure 5.72. ^{13}C NMR Spectrum of Compound 20 in CDCl_3	340
Figure 5.73. ^1H NMR Spectrum of Compound 8 in CD_2Cl_2	341
Figure 5.74. ^{13}C NMR Spectrum of Compound 8 in CD_2Cl_2	342
Figure 5.75. ^1H NMR Spectrum of Compound 21 in CDCl_3	343

Figure 5.76. ^{13}C NMR Spectrum of Compound 21 in CDCl_3	344
Figure 5.77. ^1H NMR Spectrum of Compound 22 in CD_3CN	345
Figure 5.78. ^{13}C NMR Spectrum of Compound 22 in CD_3CN	346
Figure 5.79. ^1H NMR Spectrum of Compound 23 in CD_3CN	347
Figure 5.80. ^{13}C NMR Spectrum of Compound 23 in CD_3CN	348
Figure 5.81. ^1H NMR Spectrum of Compound 24 in CD_3CN	349
Figure 5.82. ^{13}C NMR Spectrum of Compound 24 in CD_3CN	350
Figure 5.83. ^1H NMR Spectrum of Compound 25 in CD_3OD	351
Figure 5.84. ^{13}C NMR Spectrum of Compound 25 in CD_3OD	352
Figure 5.85. ^1H NMR Spectrum of Compound 26 in CD_3CN	353
Figure 5.86. ^{13}C NMR Spectrum of Compound 26 in CD_3OD	354
Figure 5.87. ^1H NMR Spectrum of Compound 27 in CD_3CN	355
Figure 5.88. ^{13}C NMR Spectrum of Compound 27 in CD_3CN	356
Figure 5.89. ^1H NMR Spectrum of Compound 28 in CD_3CN	357
Figure 5.90. ^{13}C NMR Spectrum of Compound 28 in CD_3CN	358
Figure 5.91. ^1H NMR Spectrum of Compound 7 in CD_2Cl_2	359
Figure 5.92. ^{13}C NMR Spectrum of Compound 7 in CD_2Cl_2	360
Figure 5.93. ^1H NMR Spectrum of Compound 29 in CD_3CN	361
Figure 5.94. ^{13}C NMR Spectrum of Compound 29 in CD_3CN	362
Figure 5.95. ^1H NMR Spectrum of Compound 30 in CD_3CN	363
Figure 5.96. ^{13}C NMR Spectrum of Compound 30 in CD_3CN	364
Figure 5.97. ^1H NMR Spectrum of Compound 31 in CDCl_3	365
Figure 5.98. ^{13}C NMR Spectrum of Compound 31 in CDCl_3	366

Figure 5.99. ^1H NMR Spectrum of Compound 32 in CDCl_3	367
Figure 5.100. ^{13}C NMR Spectrum of Compound 32 in CDCl_3	368
Figure 5.101. ^1H NMR Spectrum of Compound 6 in CDCl_3	369
Figure 5.102. ^{13}C NMR Spectrum of Compound 6 in CDCl_3	370

List of Tables

Table 1.1. Binding affinities of select noncovalent linkages applied for bioconjugates of proteins and peptides.	25
Table 2.1. List of FDA approved abuse-deterrent opioid formulations. ⁷	57
Table 2.3. Stability of polysiloxane based elastomer to physical manipulation under thermal stress. Pass refers to the elastomer maintaining structural integrity to crushing and cutting.	69
Table 4.1. Stability of mPEG- β -thioester-DMOB monitoring the loss of starting material over five hours after incubation in 50 mM citrate/phosphate buffer ranging from pH 4-8.	168
Table 4.2. Stability of mPEG-glutarate-(DMOB) monitoring the loss of starting material over five hours after incubation in 50 mM citrate/phosphate buffer at either pH 4.0 or 7.5.	172
Table 5.1. Reductive amination screen using the benzaldehyde linker 7 and lysozyme in either buffer A (25 mM citric acid), B (100 mM HEPES), or C (100 mM borate). The % modification was monitored using LCMS to determine the number of linkers conjugated to each lysozyme.	239

List of Schemes

Scheme 2.1. Synthesis of peptide-naltrexone prodrug (6) prepared from Ac-C(Trt)AAK(Boc).	62
Scheme 2.2. Preparation of elastomeric prodrug (9) via a thiol-ene conjugation of the cysteine containing peptide to the vinyl-containing backbone followed by a thiol-ene crosslinking with 4-arm PEG-SH.	66
Scheme 2.3. Preparation of prodrug hydrogel (11) via a thiol-maleimide conjugation of the cysteine containing peptide to a bismaleimido-diethyleneglycol crosslinker followed by crosslinking with 4-arm PEG-SH.	70
Scheme 3.1. Synthesis of peptide-naltrexone prodrug (6) prepared from Ac-C(trt)AAK(boc).	101
Scheme 3.2. Synthesis of Ac-Lys[Phe-R]- <i>p</i> NP substrates for enzyme kinetics experiments.	104
Scheme 3.3. Synthesis of Ac-Lys[Tyr-Ala-Ala-R]- <i>p</i> NP substrates 17 and 18 for enzyme kinetics experiments.	106
Scheme 3.4. Synthesis of Ac-Ala-Lys[Tyr-Ala-Ala]- <i>p</i> NP substrate for enzyme kinetics experiments.	107
Scheme 3.5. Preparation of the O-enol linked <i>p</i> NP-oxycodone electrophile (11) via an enolate formation and subsequent trapping with <i>p</i> NP-thionochloroformate (1).	110
Scheme 3.6. Synthesis of Ac-Lys[Tyr-Ala-Ala-Ala]-oxycodone prodrug 14L. The negative control 14D was also prepared using a D-tyrosine residue in replace of the L-tryosine.	112
Scheme 4.1. Synthesis of mPEG-(2,6-dimethoxybenzaldehyde) with a phenolic ester trigger for protein conjugation.	165
Scheme 4.2. Acid mediated hydrolysis of β -thioesters.	166
Scheme 4.3. Synthesis of PEG- β -thioester-(2,6-dimethoxybenzaldehyde) with a β -thioester trigger for protein conjugation.	167

Scheme 4.4. Conjugation of Lysozyme to mPEG- β -thioester-(2,6-dimethoxybenzaldehyde) by reductive amination.....	169
Scheme 4.5. Synthesis of mPEG-glutarate-(DMOB) with a phenolic ester trigger for protein conjugation.....	172
Scheme 4.6. Conjugation of lysozyme to mPEG-glutarate-DMOB by reductive amination.	173
Scheme 5.1. Mechanism of release for benzylamine linkers with quenching of the quinone methide by a phenoxide.	224
Scheme 5.2. Mechanism of release for benzylamine linkers containing a pendant arm for intramolecularly quenching the quinone methide intermediate.....	226
Scheme 5.3. Synthesis of benzylamine traceless linker with the incorporated intramolecular trapping arm.	228
Scheme 5.4. Synthesis of traceless benzaldehyde precursor 8.	230
Scheme 5.5. Synthesis of traceless benzaldehyde precursors 6 and 7 from 4-fluorobenzonitrile.	231
Scheme 5.6. Representative stepwise protein conjugation scheme for the preparation of traceless mPEG-7-Lyz conjugate.	233

List of Abbreviations

5MP	5-Methylene Pyrrolones
AD	Abuse Deterrent
ATRP	Atom Transfer Radical Polymerization
BCN	Bicyclo[6.1.0]nonyne
boc	tert-Butyloxycarbonyl
CB[7]	cucurbit[7]uril
Cbz	Carboxybenzyl
CD	Cyclodextrin
CDC	Centers for Disease Control and Prevention
CuAAC	Copper Mediated Azide Alkyne Cycloaddition
Cyt C	Cytochrome C
DBCO	Dibenzocyclooctyl
DCM	Dichloromethane
DE	Distortion Energy
DFT	Density Functional Theory
DIBAL	Diisobutylaluminum Hydride
DIPEA	Diisopropylethylamine
DME	Dimethoxyethane
DMF	Dimethylformamide
DMOB	2,6-Dimethoxybenzaldehyde
DMSO	Dimethylsulfoxide
EDT	Ethane-1,2-Dithiol

ESI	Electrospray Ionization
EtOAc	Ethyl Acetate
FDA	Food and Drug Administration
FITC	Fluorescein Isothiocyanate
Fmoc	Fluorenylmethyloxycarbonyl
FRET	Förster Resonance Energy Transfer
G-CSF	Granulocyte Colony-Stimulating Factor
GC	Gas Chromatography
GFP	Green Fluorescent Protein
GI	Gastrointestinal
GSH	Glutathione
HATU	1-[Bis(dimethylamino)methylene]-1H-1,2,3-triazolo[4,5-b]pyridinium 3-oxide hexafluoro-phosphate
HEPES	(4-(2-hydroxyethyl)-1-piperazineethanesulfonic acid
HFIP	Hexafluoroisopropanol
hGH	Human Growth Hormone
HPLC	High Performance Liquid Chromatography
HSA	Human Serum Albumin
IGF-1	Insulin like Growth Factor 1
IL2	Interleukin 2
IPA	Isopropanol
IR	Infrared
KHMDS	Potassium Bis(trimethylsilyl)amide

LCMS	Liquid Chromatography-Mass Spectrometry
Lyz	Lysozyme
MALDI-TOF	Matrix-Assisted Laser Desorption/Ionization-Time of Flight
MeCN	Acetonitrile
MeOH	Methanol
mPEG	Monomethyl Ether Poly(Ethylene Glycol)
Myo	Myoglobin
NMP	N-Methylpyrrolidinone
NMR	Nuclear Magnetic Resonance
NQO1	NADPH Dehydrogenase [Quinone] 1
NTA	Nitrilotriacetic Acid
PBS	Phosphate Buffered Saline
PEG	Poly(Ethylene Glycol)
PEGMA	Poly(Ethylene Glycol) Methacrylate
PFP	Pentafluorophenol
PFPTC	Pentafluorophenyl Thionochloroformate
pI	Isoelectric Point
PMVS	Poly(Methylvinylsiloxane)
pNP	<i>para</i> -Nitrophenol
pNP-TCI	<i>para</i> -Nitrophenyl Thionochloroformate
QPN	Quinone Propionic Acid
RAFT	Reversible Addition Fragmentation Chain Transfer
RNase A	Ribonuclease A

sCT	Salmon Calcitonin
SDS-PAGE	Sodium Dodecylsulfate-Polyacrylamide Gel Electrophoresis
SEM	Scanning Electron Microscopy
SET-LRP	Single-Electron Transfer Living Radical Polymerization
tBu	tert-Butyl Ether
TCEP	Tris(2-carboxyethyl)phosphine
TEMPO	(2,2,6,6-Tetramethylpiperidin-1-yl)oxyl or (2,2,6,6-tetramethylpiperidin-1-yl)oxidanyl
TFA	Trifluoroacetic Acid
THF	Tetrahydrofuran
TIPS	Triisopropylsilane
TMAc	Triggerable Michael Acceptor
TMEDA	Tetramethylethylenediamine
trityl	Triphenylmethyl
Troc	2,2,2-Trichloroethoxycarbonyl
US	United States
βLGb	β-Lactoglobulin B

Acknowledgements

I am incredibly grateful for all the professional and personal support I have received over the years from a vast collection of people. Without them, I would not have become the scientist or man I am today. First, I would like to thank all my scientific mentors, starting with my advisor Heather Maynard, for all the guidance and opportunities she provided for me over the past five years. To my mentors in the Maynard lab Dr. Natalie Boehnke, Dr. Jacquelin Kammeyer, and Dr. Liang Sun, thank you for building my skills and confidence in the laboratory, without which I may not have made it through graduate school. I would also like to thank my past scientific mentors, Professor Eric McCloud, Professor Julian Davis, Professor Brandon Field, and especially Professor Edmir Wade for sparking my curiosity in research and more specifically organic chemistry and starting me on this incredible journey.

A huge thank you to all the Maynard Lab members, both past and present, that have been there to discuss research ideas and provide an overall great work environment. Neil Forsythe, you have become a great friend of mine and I certainly can't imagine having made it to this point without you. Kyle Tamshen, it's difficult to explain how much our friendship and proximity in the office helped with my development as a scientist. Our impromptu discussions on everything from experimental results to management styles helped to refine my scientific and personal abilities to an incredible extent. Prier Panescu, I truly appreciate our friendship and all the times you helped to keep me sane over the past five years. Additionally, I would like to thank Billy Treacy for his help, both intellectually and experimentally, across many chapters throughout this thesis. It has been great working alongside you, and I am looking forward to seeing the great accomplishments you achieve throughout your career. Furthermore, I have received large amounts of help and encouragement from many other Maynard lab members for which I am eternally grateful including

Dr. Samantha Raftery, Dr. Jeong-Hoon Ko, Dr. Emma Pelegri-O'Day, Dr. Marco Messina, Arvind Bhattacharya, Kathleen Chen, Dr. Kathryn Messina, Nikolas Theopold, Dr. Madeline Gelb, Dr. Daniele Vinciguerra, Jane Yang, Hayden Montgomery, Mikayla Tan, Grace Kunkel, Hallie Lower, and Ellie Puente. I would be remiss if I did not throw in a specific thank you for all the members of the UCLA facilities, without whom my research would have ground to a screeching halt, most especially Ricky Ruiz.

My collaborations outside of the Maynard Lab have also played a vital role in my graduate studies beginning with my doctoral committee, Professor Richard Kaner, Professor Kerriann Backus, and Professor Christopher Evans for their helpful guidance and encouragement over the years. Additionally, I thank Professor Catherine Cahill and her students who have made most of the work in chapters 2 and 3 possible through intellectual and experimental support over the past 4 years. I also need to express my sincerest appreciation to both Dr. Robert Taylor and Dr. Ta-Chung Ong as well as Dr. Ignacio Martini for allowing me to work in the NMR facility as a teaching assistant. This experience greatly broadened my scientific knowledge base and placed me in direct contact with researchers from a diverse background of specialties both of which greatly influenced the scientist I have become.

In addition to my scientific peers and colleagues I would like to thank my family for their unwavering support throughout the past five years. This experience would not have been possible without you all and I cannot express how truly grateful I am to have you in my life.

Vitae

Education:

University of California, Los Angeles, Department of Chemistry, Los Angeles, CA

Ph. D. in Chemistry, Expected Fall 2021

University of Southern Indiana, Evansville, IN

Bachelor of Science in Biochemistry, May 2015

Publications:

1. Panescu, P.; **Rose, D.**; Chen, K.; Kashanchi, G.; Maynard, H. “Mesotrione Conjugation Strategies to Create Proherbicides with Reduced Soil Mobility” *ACS Sustain. Chem. Eng.* 2021, Accepted with Minor Revisions
2. **Rose, D.**; Treacy, J.; Yang, Z.; Ko, J.; Houk, K.; Maynard, H. “Electronically Modulated Self-Immolative Benzylamine Linkers for Traceless Protein-Polymer Conjugation” Manuscript in Preparation
3. **Rose, D.**; Treacy, J.; Tamshen, K.; Boehnke, N.; Sun, L.; Ko, J.; Maynard, H. “Development of a Stimuli-Responsive Elastomeric Abuse-Deterrent Opioid Formulation” Manuscript in Preparation
4. **Rose, D.**; Tamshen, K.; Treacy, J.; Boehnke, N.; Cahill, C.; Maynard, H. “A Multi-Stimuli-Responsive Prodrug for Use as an Abuse-Deterrent Opioid Formulation” Manuscript in Preparation
5. **Rose, D.**; Vinciguerra, D.; Panescu, P.; Chao, E.; Maynard, H. “The Use of Traceless Linkers in the Preparation of Protein-Polymer Conjugates” *Manuscript in Preparation*

Presentations:

1. “Dual Enzyme Responsive Peptides for Drug Delivery” Johnson Symposium, Stanford University. 2017. Poster Presentation.

Selected Awards and Honors:**University of California, Los Angeles**

Dr. Yuh Guo Pan Dissertation Award in Organic Chemistry

University of Southern Indiana

Dean’s List (2011-2014)

Chapter 1

Traceless Linkers Used for Reversible Protein Modifications

1.1 Introduction

Protein conjugation is a versatile tool that allows for the alteration of a protein's stability, activity, and functionality.¹ Protein-polymer conjugates are one useful application of this tool for therapeutically relevant proteins, often resulting in an increased stability and circulation time *in vivo*.² Currently, there are several protein-PEG conjugates used in the clinic; however, the addition of polyethylene glycol (PEG) typically leads to a significant loss of activity compared to that of their unmodified counterpart and in some cases, activity is abrogated completely.³⁻⁵ To minimize such undesired effects, site-specific conjugation techniques can be employed to ensure that placement of the polymer is distant from the active site.⁶ This is not broadly applicable to all proteins of interest and requires a tailor-made strategy for each protein, resulting in a significant investment of time and resources. In addition to the preparation of protein-polymer conjugates, proteins and peptides are commonly modified with other modalities including fluorophores or binding substrates. The former is commonly employed to track the presence *in vivo*, while the latter (for example, biotin tag) is commonly used as a handle for protein purification purposes. Even in the case of small molecule modifications, protein activity can be significantly hampered and the potential for protein aggregation can increase.

As a means to circumvent this loss of activity, researchers place unstable linkages between the protein and the polymer/fluorophore/binding substrate in order to create a reversible linkage. This in turn allows for a stimulus-dependent release of the native protein and recovered protein activity. These reversible linkages that release native protein are referred to as traceless linkers. The reversibility of these traceless linkers is an important aspect when designing protein conjugates, especially when protein activity is of a high importance. To that end, this review will overview various types of traceless conjugation chemistries. It is meant to be a guide to help

bioconjugation chemists decide which linker to use for any given application, rather than a comprehensive review.

1.2 Lysine Modifications

The lysine residue is the most commonly used handle for traceless conjugation due to the high prevalence and reactivity of protein lysines.⁷ Modifications of these peripheral lysines, especially residues near the protein binding site can significantly hamper binding/activity. This observation is particularly drastic when conjugating a polymer which typically form a polymeric coating around the protein, in turn sterically inhibiting the protein's binding ability. Even with the dramatic decrease in protein activity, the increased circulation time *in vivo* is often worth the downsides. Traceless linkers have made a significant impact on the field of protein-polymer conjugates over the past decade, wherein one conjugate was recently approved by the FDA for clinical use and another is currently undergoing phase 3 clinical trials. The high prevalence and reactivity of lysine residues across a wide array of proteins, has led to the largest diversity in traceless linker conjugation strategies, which will be summarized below.

1.2.1 Anhydride Linkers

The first recorded demonstration of reversible protein modifications arises from the use of maleic anhydride to reversibly modify the lysine residues of proteins prior to a tryptic digest or purification methods.⁸⁻¹⁰ The linkers are subsequently reversed by hydrolysis under acidic conditions (pH 2-4), however, these early works showed little data on the rate of release, which was not the primary focus of the work. Once identified as a potential reversible strategy it was quickly demonstrated that a substituted maleic anhydride could initially mask the lysine residues of lysozyme followed by the attachment of a variety of functionalities including sulfonates, sugars,

fluorophores, and polymers to modify the proteins solubility, stability, or functionality.¹¹⁻¹³ Herein, it was demonstrated that at pH 2.5, $\geq 90\%$ of the protein activity was restored within a period of 30 hours, indicating that the process is truly reversible and does not lead to any protein degradation. More recently there have been deeper examinations into the anhydride linkers demonstrating the release kinetics for a variety of different payloads across multiple proteins. It was shown that the rate of release at pH 5 is sufficient to achieve $>80\%$ release within 12 hours for both human serum albumin and green fluorescent protein.¹⁴ These release experiments were designed to mimic the endosomal conditions of cells, thus demonstrating the pH sensitive delivery of ribonuclease A (RNase A). Additionally, RNase A was conjugated to histidine rich cationic oligomer for enhanced protein transduction, whereupon entering the acidic environment of the endosome the linker was cleaved and the oligomer was free to mediate endosomal escape releasing native RNase A into the cytosol.¹⁵

1.2.2 Bicin Linkers

Another cyclization-based linker, the bicin linker, was initially demonstrated by Greenwald *et al.*, which allows for the hydrolysis of an amide linkage to the protein through the anchimeric assistance of two ethyl alcohol-based appendages (Figure 1.1). These ester-containing appendages once hydrolyzed then backbite on the amide, thus favoring release of the amine and the resulting 4-(2-hydroxyethyl)morpholin-2-one byproduct. This was originally demonstrated through the conjugation of either a branched or linear PEG to lysozyme to form the monopegylated conjugate. Whereupon incubation of the conjugate in rat plasma at 37 °C native lysozyme was slowly released with half-lives of the conjugates ranging from 5 to 20 hours, depending on the linker structure.^{16,17} This strategy was then adapted by Filpula *et al.* for the delivery of SS1P, a recombinant anti-mesothelin immunotoxin. The SS1P was PEGylated with either a linear or branched PEG-bicin

derivative, attaching an average of 3 to 4 PEG groups per immunotoxin. These conjugates showed an increased half-life of 5 hours compared to native SS1P *in vivo*, where the linear and branched conjugates reduced tumor size by 68 and 92% respectively using a xenografted tumor in a mouse model.¹⁸

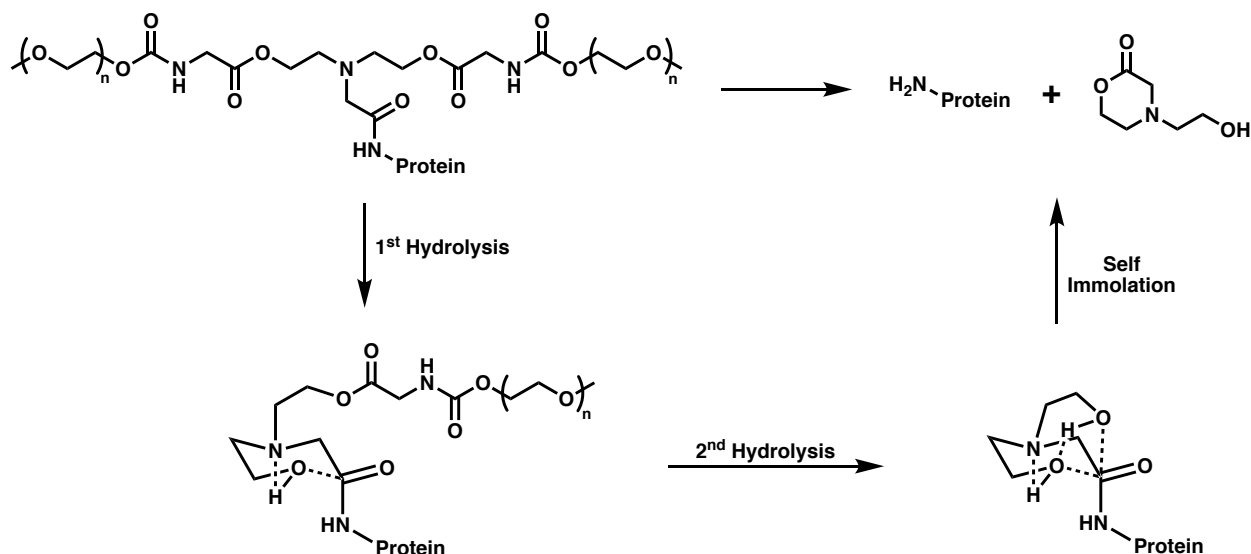


Figure 1.1. Traceless hydrolytic release of native protein from a PEGylated conjugate through use of a bicin linker.

1.2.3 β -Mercaptocarbamate Linkers

The β -mercaptocarbamate linkage was initially developed as an alternative stimuli-responsive traceless protein linker by Chen *et al.* to include a thiol specific triggering mechanism.¹⁹ In the presence of 5 mM glutathione (GSH), the β -mercaptocarbamate would undergo a thiol-thioester exchange, which unmasked the sulfhydryl, resulting in an intramolecular cyclization to release the native protein along with carbon dioxide and ethylene sulfide byproducts (Figure 1.2). This strategy was demonstrated through the mono-PEGylation of lysozyme; the conjugate had a half-life of 0.73 hours in PBS at 37 °C in the presence of 5 mM GSH, simulating cytosolic conditions. Following the lysosome release, protein activity was recovered showing no significant

difference when compared to fresh lysozyme. However, no release or recovery of activity was observed following incubation in the absence of GSH, signifying its importance in the release mechanism.

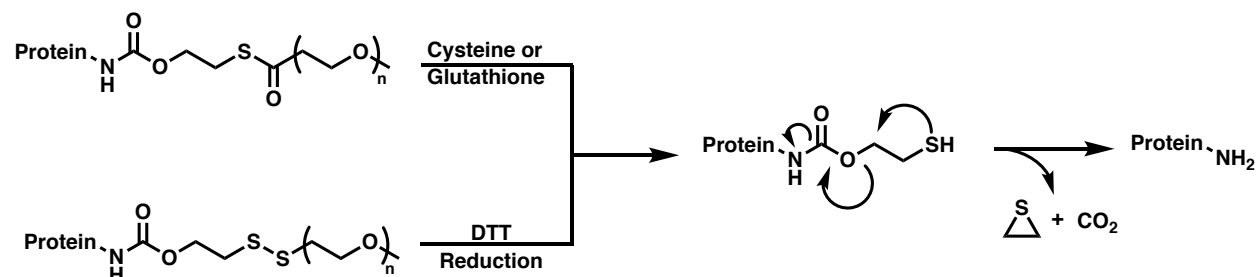


Figure 1.2. Thioester or disulfide (top and bottom respectively) triggered mechanism of protein release for the β -mercaptocarbamate traceless linkers.

Following this report, researchers began using disulfides as an alternative thiol sensitive trigger to the thioesters (Figure 1.2). Dutta *et al.* demonstrate this switch by using cytochrome C (CytC) to crosslink poly(methyl methacrylate) functionalized with the a β -mercaptocarbonate side chain.²⁰ The resulting nanogels were shown to release fully active CytC after incubation under reducing conditions for 4 hours at 37 °C. Recently, Scherger *et al.* demonstrated the ability to carry out a post-polymerization modification of a reversible addition-fragmentation chain transfer (RAFT)-polymerization-based thiocarbonylthio end-group to an activated β -mercaptocarbonate.²¹ This polymer was then conjugated to either lysozyme or a nanobody, followed by the traceless cleavage of the polymer under reducing conditions. This highlighted the first demonstration of a non-crosslinked traceless protein-polymer conjugate using the β -mercaptocarbamate linkage.

1.2.4 Trimethyl Lock Linkers

A newly demonstrated traceless linker referred to as the ‘trimethyl lock’ was initially developed by Amsberry *et al.* using a small molecule prodrug approach.^{22,23} This linker was comprised of a masked phenol, which upon cleavage undergoes an intramolecular cyclization with

a pendant amide bond to form the resultant substituted coumarin derivative. This linker was recently adapted to protein conjugation by Chang *et al.* wherein a small molecule quinone propionic acid (QPN) was conjugated to a protein of interest, shutting off all activity.²⁴ When the conjugate came in contact with a tumor cell specific NADPH dehydrogenase [quinone] 1 (NQO1), the quinone was reduced to a phenol. The resulting phenol then cyclized to form a substituted coumarin byproduct along with the native protein. This was demonstrated using both CytC and RNase A, both of which regained activity upon incubation with NQO1 and the RNase A conjugate showed enhanced cytotoxicity towards NQO1 producing HeLa cells and tumor xenograft. Although there are no current publications demonstrating the use of the trimethyl lock linker in regards to protein-polymer conjugates we believe the chemistry is an interesting new alternative traceless linker for lysine conjugations that could prove valuable in the field of traceless protein-polymer conjugation.

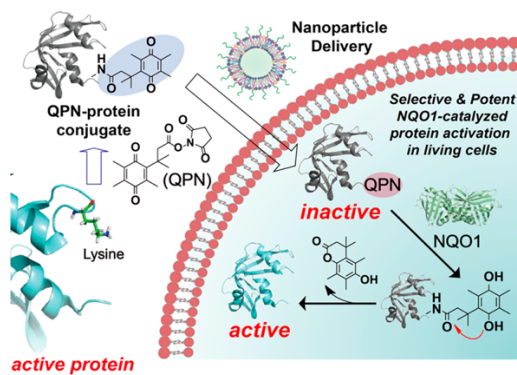


Figure 1.3. Design of the NQO1-Catalyzed Chemical Modification of a Protein and Its Intracellular Delivery for Potent Protein Activation in Living Cells for a Potential Targeted Cancer Therapy.

1.2.5 1,6-Benzyl Carbamate Linkers

The 1,6-benzyl carbamate class of linkers is the most prevalent and diverse set of traceless linkers for the lysine modifications. The masking of a phenol or aniline head group with a protecting group specific for a biologically relevant stimulus is what leads to the large diversity in

this class of linkers. The first demonstration of this technology was performed using a small molecule model system wherein an aniline-based linker was masked with a lysine residue.²⁵ Upon cleavage of the lysine residue using trypsin, the aniline underwent a 1,6-elimination to release p-nitroaniline as a colorimetric reporter molecule. Following the seminal publication, the applicability of this linker was quickly identified and diversified using a variety of strategies to unmask the protecting groups including disulfide reduction,²⁶⁻²⁹ ester hydrolysis,^{30,31} carbamate hydrolysis,³² and boronate reduction.^{33,34} All of these examples result in the unmasking of either a phenol, thiophenol, or aniline head group that subsequently undergoes the 1,6-benzyl elimination reaction to release the protein and CO₂ as a byproduct.³⁵

Recently the FDA approved Ascendis Pharmaceutical's lonapegsomatropin-tcgp for use as a human growth hormone (hGH) replacement in pediatric patients.^{32,36} hGH is a perfect example of a protein that is ideal for the use of a traceless linker due to its short half-life of 20 minutes and PEGylated hGH has less than 10% activity when compared to the native hGH. This drug is in fact a monoPEGylated version of hGH containing a 4-arm PEG group attached to the hGH through a carbamate masked 1,6-benzyl carbamate linkage (Figure 1.4). The release of native hGH was monitored *in vitro* and shown to have a half-life of 75 hours in PBS at 37 °C. Further studies in cynomolgus monkeys showed that a single administration of the PEGylated hGH prodrug resulted in higher levels of insulin-like growth factor 1 (IGF-1), a pharmacodynamic marker for hGH, when compared to daily hGH administration. This was later confirmed in a study comparing a once weekly subcutaneous administration of the lonapegsomatropin prodrug at 0.24 mg/kg which outperformed daily hGH injections in pediatric patients with human growth hormone deficiency. This particular example demonstrates the usefulness of these traceless linkers, specifically as

protein-polymer prodrug therapeutics, in reducing the number of therapeutic injections on a weekly basis and thereby increasing the patient's experience.

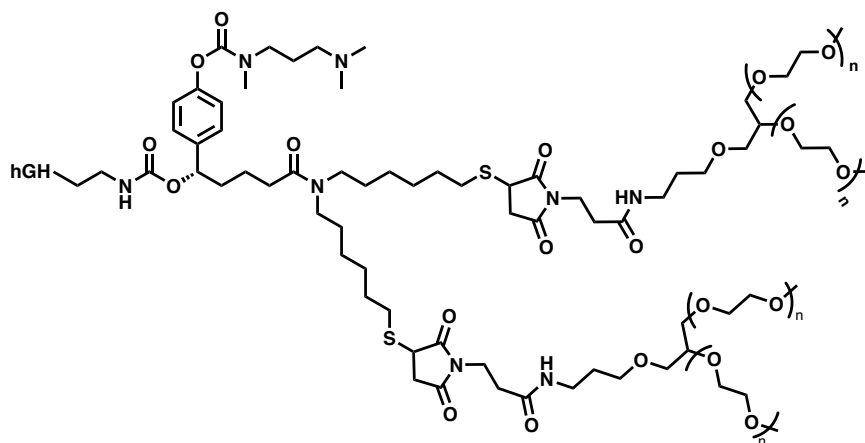


Figure 1.4. Acendis Pharmaceutical's Lonapegsomatropin-tcgp long acting traceless hGH-PEG conjugate.

1.2.6 E1cB Linkers

The E1cB linker is comprised of an aryl carbamate linkage directly to the protein through the lysine residues. In neutral to basic aqueous conditions the linkage undergoes an elimination to form an isocyanate intermediate, which is rapidly hydrolyzed to release the primary amine and CO₂ byproduct. This strategy was initially demonstrated by Brandl *et al.* who modified the end-group of a 4-arm PEG species to contain an activated aryl carbonate.³⁷ Lysozyme was then used to crosslink the multi-arm PEG species to form a hydrogel. Degradation of the resulting hydrogel was monitored over 96 hours at pH 9.0 and 50 °C, where there was an initial 24-hour onset prior to any native lysozyme release. A similar strategy was carried out by Hammer *et al.*, who used a linear PEG derivative rather than the multi-arm PEG species to modify lysozyme.³⁸ They also diversified the structure of the E1cB linker by varying the electronics of the aromatic core, which in turn displayed different rates of lysozyme release varying from 63% lysozyme released in 24 hours to 44% released over 28 days. This linker demonstrated a maximum release threshold of 63%, which the authors hypothesized was due a side reaction between the amines on the protein

reacting with the isocyanate intermediate produced, resulting in protein dimerization, which was observed via sodium dodecyl sulphate-polyacrylamide gel electrophoresis (SDS-PAGE).

1.2.7 Retro-Michael Addition Linkers

The retro-Michael addition has recently been investigated as a mechanism of release for lysine-based traceless linkers. This concept was initially demonstrated by Diehl *et al.* who showed that the Michael addition of a primary amine onto a derivative of Meldrums acid could be reversed in the presence of a thiol containing “decoupling agent” like dithiothreitol, cysteine, or ethanedithiol (Figure 1.5).³⁹ To demonstrate the ability of this linker to function as a traceless linker, the researchers functionalized the lysine residues on myoglobin followed by a secondary addition of PEG-thiol. This PEGylated protein was then incubated with the decoupling agent for 36 hours, which showed the release of the native myoglobin by LCMS.

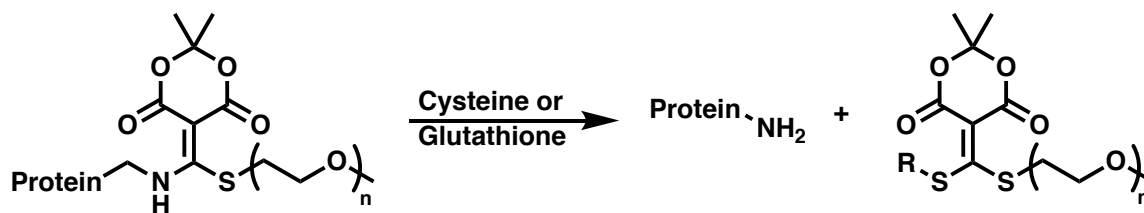


Figure 1.5. Meldrums acid derived traceless linker relying on a retro-Michael addition to facilitate protein release (R represents either cysteine or glutathione).

Zhuang *et al.* more recently demonstrated an alternative approach through the use of a functionalized α,β -unsaturated carbonyl compound.⁴⁰ These linkers were demonstrated as traceless through their initial modification of β -lactoglobulin B and subsequent displacement by 2-(2-methoxyethoxy)ethanethiol over the course of two hours. However, this reaction is not specific for the lysine residue and does simultaneously modify cysteine residues, both of which are reversible. Ultimately, further work was carried out to selectively modify cysteine residues which will be discussed further in a latter section.

1.2.8 β -Elimination Linkers

The β -elimination linkers are the second most prevalent traceless linker used in the preparation of protein conjugates. These linkers were initially implemented via the small molecule Fmoc groups reversibly modifying any surface accessible lysines present on the protein of interest to toggle activity on and off.⁴¹⁻⁴³ This was later advanced to using a sulfonated Fmoc containing PEG species to modify the lysine residues of various therapeutically relevant proteins including interferon α ,⁴⁴ human growth hormone,⁴⁵ insulin,⁴⁶ and enkephalin⁴⁷. These traceless protein conjugates all demonstrated an increased circulation time *in vivo* with a steady release of native protein over the course of that time frame. The steady rate of release and versatility of this linker has led Nektar therapeutics to develop a long acting interleukin-2 (IL-2) protein polymer conjugate relying on an fluorenylmethyloxycarbonyl (Fmoc) derived β -elimination linker, which is currently in clinical trials.⁴⁸⁻⁵⁰ This traceless protein-polymer conjugate consists of 6 PEG chains conjugated to each IL2 resulting in a 4-fold increase of the half-life *in vivo* compared to the non-PEGylated control.

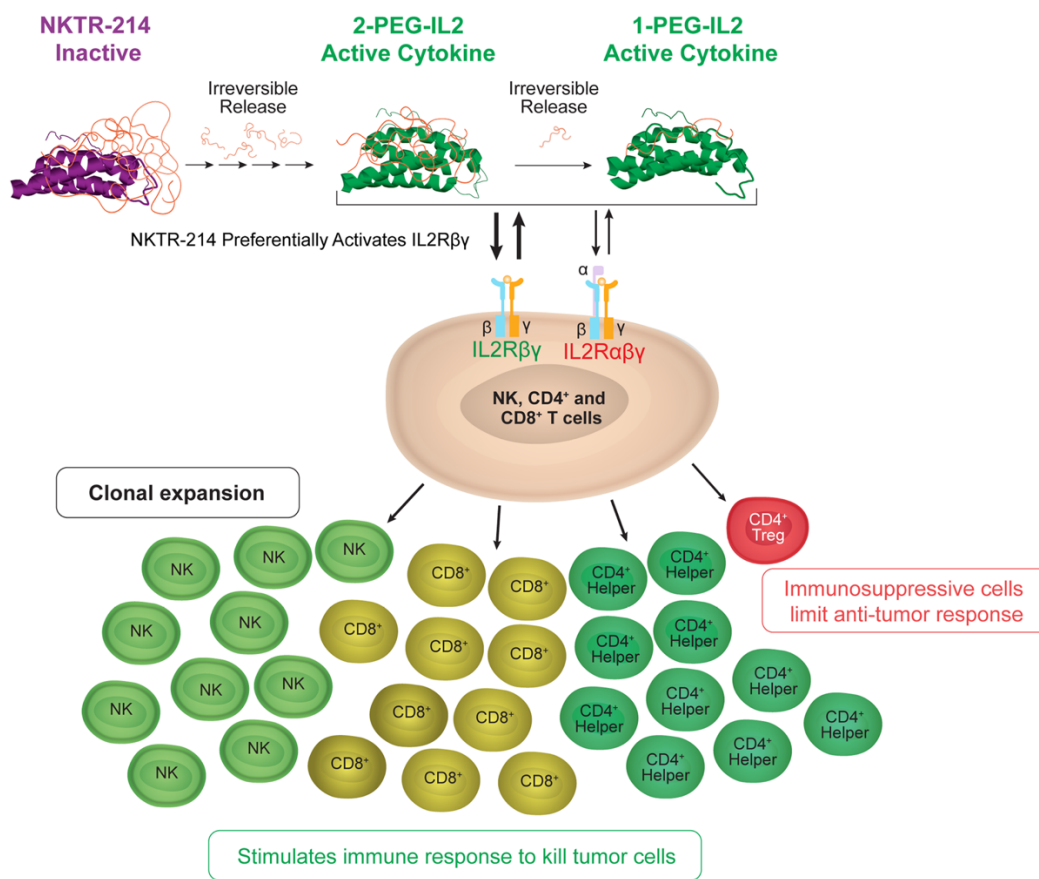


Figure 1.6. NKTR-214 is a CD122-biased cytokine agonist conjugated with multiple releasable chains of PEG located at the interface of IL2 and IL2R $\alpha\beta\gamma$. The PEG chains slowly release at physiological pH, creating conjugated-IL2 species with fewer PEG chains and increased bioactivity. Sustained signaling through the heterodimeric IL2 receptor pathway (IL2R $\beta\gamma$) preferentially activates and expands effector CD8 T and NK cells over Tregs.

An alternative β -elimination traceless linker was recently developed by Santi *et al.* who created a tunable set of traceless linkers by modulating the pK_a of the proton β to the carbamate linkage.⁵¹ This was controlled using an electronic modulator, which in turn created a set of linkers with half-lives ranging from 14 to 10,500 hours at a pH of 7.4 and 37 °C. This technology was applied to the prolonged release of exenatide, a glucagon-like peptide-1 agonist through the conjugation of the peptide to a traceless PEG or the incorporation into a degradable hydrogel

material.^{52–54} In both instances, the peptide was linked to the polymeric material through the aforementioned β -elimination linkers. The resulting release of the peptide was monitored *in vivo* and demonstrated a 56-fold increase to the half live compared to that of the unmodified peptide.

1.2.9 Photocleavable Linkers

Photocleavable linkers have long been used as an orthogonal protecting group strategy towards the protection of amines typically through the use of an *o*-nitrobenzyl group. This concept was initially brought into the field of protein polymer conjugates as a traceless linker by Georgianna *et al.* by modifying a PEG end-group with an *o*-nitrobenzyl group.⁵⁵ This was then used to modify the lysine side chains of lysozyme producing an average of 4 PEG chains per protein. Irradiation of the conjugate with 365nm light for 30 minutes results in the release of native lysozyme with full activity. This concept was replicated by Takamori *et al.* using a biotinylated *o*-nitrobenzyl linker as opposed to the PEGylation reagent to allow for a biotin pull-down purification of lysozyme followed by the linker removal under irradiation at 365nm.⁵⁶ A similar strategy was used by Karas *et al.* towards the synthesis of an amyloid- β peptide fragment.⁵⁷ The peptide was highly prone to aggregation, making solid-phase peptide synthesis and the subsequent high-performance liquid chromatography (HPLC) purification challenging. The incorporation of a triethylene glycol tag through a *o*-nitrobenzyl group to a lysine residue on the peptide reduced aggregation prior to cleavage from the resin and during HPLC purification. The triethylene glycol tag was subsequently removed via irradiation at 365nm, allowing for the study of the aggregated fibril formation.

1.3 Cysteine Modifications

Second only to lysine as a convenient covalent conjugation handle, cysteine offers numerous advantages over other residues. For instance, due to its natural low abundance in proteins, cysteine residues are often targeted when site-selective conjugation is desired. Additionally, the unique nucleophilicity of the thiol containing cysteine residue allows for relatively quick and efficient conjugation reactions.^{58,59} Nonetheless, some proteins do not contain any cysteine residues, or the few present are hidden in hydrophobic pockets or involved in disulfide linkages. In these cases, cysteine can be introduced using protein engineering techniques such as mutagenesis, however these protocols can be quite laborious.^{60,61}

Importantly, due to their peculiar reactivity, cysteine residues are often structural components of the protein active site and their modification can greatly diminish protein activity.^{62,63} Therefore, developing conjugation strategies able to reversibly bind to cysteine and subsequently release the native protein in a traceless fashion is of particular significance for this amino acid. In this section, we will explore reversible conjugation reactions that target specifically cysteines or disulfide bridges.

1.3.1 Retro-Michael Addition Linkers

Although for years the gold standard in cysteine conjugation has been the use of pyridyl disulfide to form a disulfide bond,⁶⁴⁻⁶⁶ this strategy will not be discussed in detail in this review, which will focus instead on approaches involving small molecule linkers. The most commonly used are maleimides, which are known for their reactivity towards thiols as Michael acceptors. Generally, these are regarded as stable and non-reversible linkages, however, it has been demonstrated that in specific cases they can undergo retro and exchange reactions in the presence

of other thiols. An important factor when designing these linkers is that this reversibility can be shut off upon a hydrolytic ring-opening reaction.^{67–69}

Due to the difficulties in controlling the fate of this thioether bond, maleimide analogues carrying leaving groups, such as bromine atoms have been designed. The resulting vinyl sulfide adduct has a higher propensity to undergo thiol-exchange reactions, which in turn regenerates the native peptide.^{70–75} For instance, the Grb2 adaptor protein containing a single cysteine mutation (L111C) was reacted with 1 equivalent of N-methylbromomaleimide, resulting in complete conversion within one hour. The reaction was selective for the cysteine residue over the 8 surface accessible lysine residues present on the protein. When the conjugate was treated with an excess of tris(2-carboxyethyl)phosphine (TCEP), 85% of the native protein was promptly released. Using a dibromo-substituted maleimide, a second functionalization can be performed, as was demonstrated with glutathione or thioglucose. In each case, an excess of 2-mercaptoethanol or glutathione was required in order to release the native protein (Figure 1.7).⁷¹ It was observed that native protein was released within 4 hours under conditions mimicking the cell cytoplasm. Interestingly, the incorporation of an electron withdrawing N-substituent, e.g. N-phenylmaleimides, increases the propensity for the undesirable ring-opening side-reaction, thus creating an irreversible conjugate unable to release the protein.⁷² In a comparative study, bromo or dibromomaleimides were employed to synthesize green fluorescent protein (GFP)–rhodamine conjugates as Förster resonance energy transfer (FRET) pairs. These conjugates were transfected into live HeLa cells and GFP release was followed by time-lapse fluorescence microscopy, revealing that dibromomaleimides are cleaved at a faster rate.⁷³

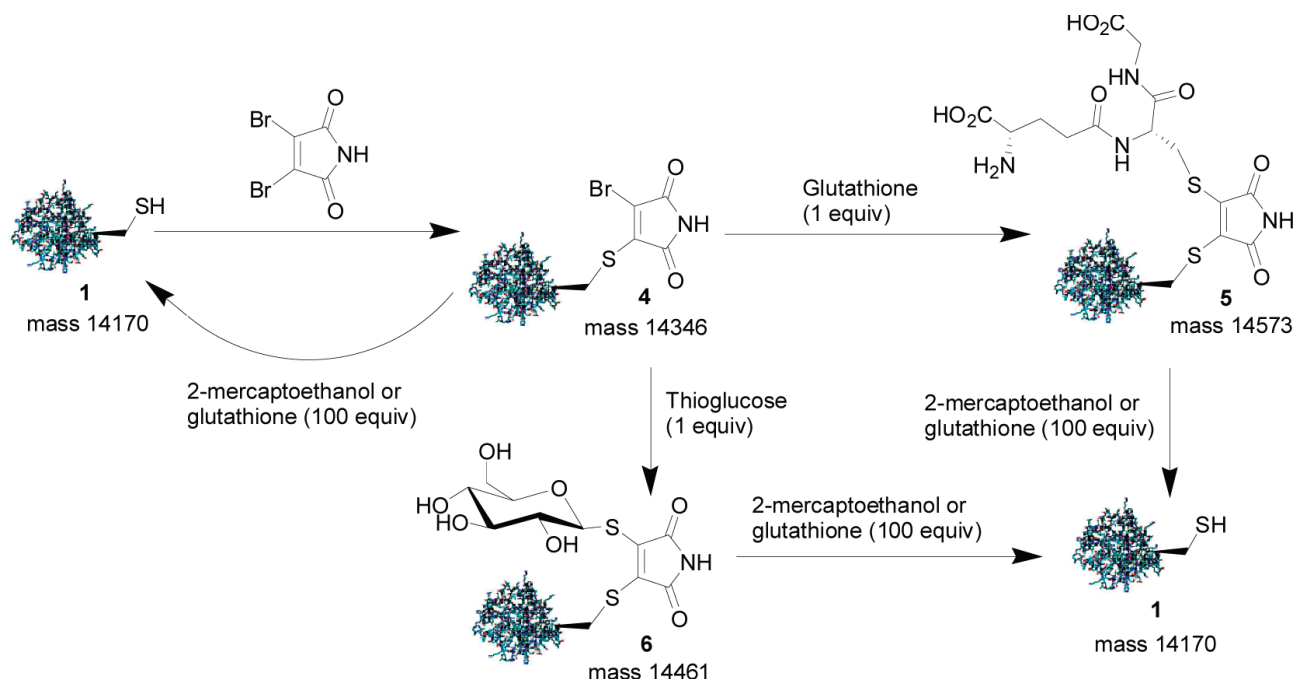


Figure 1.7. Functionalization and release of the Grb2 SH2 Domain (L111C) with dibromomaleimide.

A direct application of these linkers was the development of affinity tags for use as a pull-down purification tag. A N-modified biotin bromomaleimide was reacted with the Grb2 SH2 Domain (L111C) and the conjugate was applied to neutravidin-coated agarose beads. The native protein was released over the course of two hours after suspension in phosphate buffered saline (PBS) buffer with 25 mM 2-mercaptoethanol, resulting in 77% protein recovery.⁷² The approach was later improved with the discovery that hydrophobic N-substituents, such as butyl or cyclohexylmethyl, increased the hydrolytic stability of the maleimide at 37 °C and pH 8. Moreover, a more efficient release protocol requiring only equimolar 1,2-ethanedithiol to facilitate release of the protein was presented.⁷⁴ Another application was the employment of chemical vapor deposition polymerization of 4-(3,4-dibromomaleimide)[2.2]paracyclophane to form a polymer coating able to react with and release thiolated peptides. This strategy could be applied for the functionalization of biomedical sensing and diagnostic materials.⁷⁵

Other classes of Michael acceptors exist and are utilized as reversible and traceless linkers, often with improved properties over maleimides. For instance, 5-methylene pyrrolones (5MPs) exhibit high thiol specificity, improved stability under physiological conditions and traceless release at basic pH or by thiol exchange. 5MPs were synthesized bearing different moieties as N-substituents including biotin, fluorescein or doxorubicin. These were subsequently conjugated to a histone H4 mutant (H4-R45C) containing a single cysteine. The conjugation was selective for cysteine and proceeded to greater than 95% conversion within two hours at a pH of 7.5. The protein was subsequently incubated in either a pH 9.5 solution or in the presence of glutathione at pH 7.5, both of which led to traceless release of the native protein.⁷⁶ Bromo and dibromopyridazinedione were also designed to reversibly bind cysteine, while also demonstrating lower rates of hydrolysis compared to maleimides, with four possible points of chemical attachment. The conjugation reaction necessitated a large excess of linker (100 equiv.) to achieve quantitative conversion within one hour. The chemical reversibility was demonstrated upon incubation in the presence of a large excess of 2-mercaptoethanol or cytosolic glutathione concentrations, which released native protein within one hour.⁷⁷ The high versatility of this scaffold was later demonstrated when three different functionalities were incorporated within a single pyridazinedione-protein conjugate. A dual clickable dibromo pyridazinedione bearing an azide and a tetrazine was designed, synthesized and reacted initially with the protein, and subsequently with bicyclo[6.1.0]nonyne (BCN)-fluorescein and dibenzocyclooctyl-(DBCO)-biotin, to attach the tetrazine and the azide, respectively. The remaining bromo group was subsequently displaced by either a cysteine-containing peptide or an azide functionalized aniline, which was later used to incorporate PEG (Figure 1.8). Neither of the conjugates released the protein at healthy blood concentrations of glutathione over 24 hours and were stable in serum for 7 days. Only the conjugates incorporating the cysteine-containing peptides

released native protein in the presence of high glutathione concentrations, while the aniline conjugates showed no cleavage of the pyridazinedione. The increased stability of the aniline conjugate was attributed to decreased electrophilicity of the resulting linker, preventing the thiol displacement necessary to release native protein.⁷⁸ Alternatively, incorporation of a cysteine containing protein within a saturated pyridazinedione scaffold via a Michael addition allows for the release of native protein via a retro-Michael pathway without encountering any ring hydrolysis and avoiding any reactivity towards blood thiols.⁷⁹

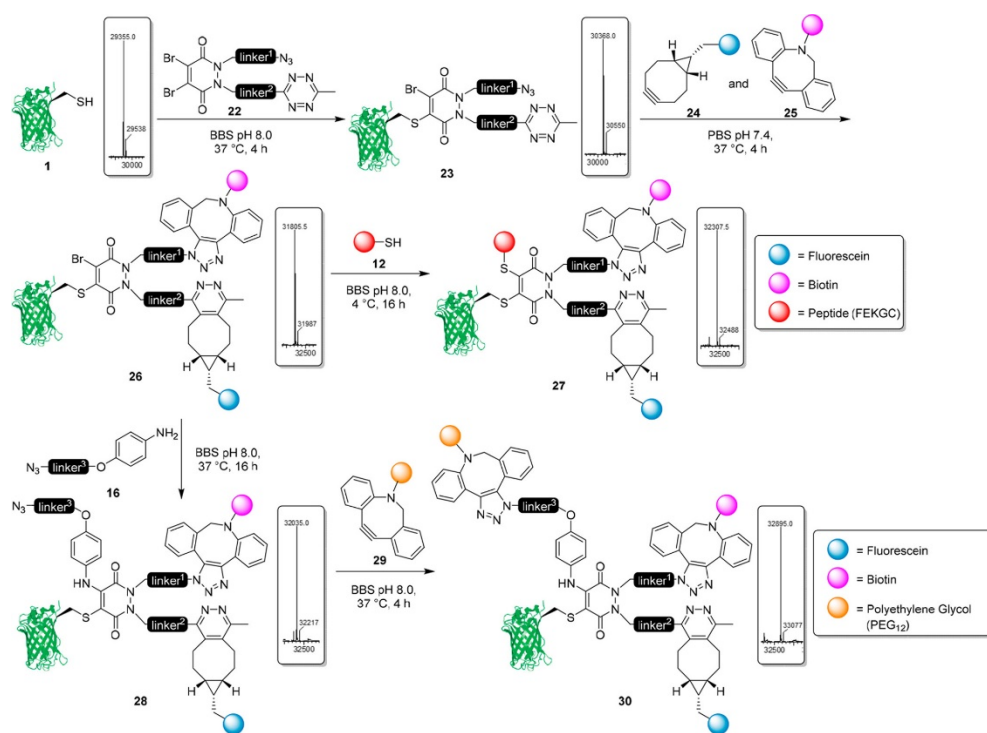


Figure 1.8. Synthesis of trifunctional pyridazinedione-protein derivatives.

Recently, Zhuang *et al.* developed a chemical switch based on a Triggerable Michael Acceptor (TMAc) bearing a good leaving group at the β position. The acceptor is initially coupled to a nucleophile, resulting in the formation of an α,β -unsaturated carbonyl. The presence of a second stronger nucleophile results in a Michael addition and subsequent release of the initial nucleophile. The unique structure of the TMAc allows for a modular electronic design of the linker

to fine tune the kinetics of the system. The concept was applied to selectively modify β -lactoglobulin B (β LGb) on its free cysteine using the appropriate TMAc. After, myoglobin (Myo) was modified with another TMAc and subsequently released with an excess of thiol within 2 hours.⁴⁰ A similar concept was employed using a 4-substituted cyclopentenone with fast kinetics. In the presence of a Michael donor, the conjugated protein underwent a traceless release with no observable impact on protein structure or functionality. UBXD protein was used as a model protein and reacted with the cyclopentenone. The reaction occurred within one hour with a high specificity for cysteine residues while showing no impact on the protein structure. The linker could be removed in 3 hours with an excess of mercaptoethanol.⁸⁰

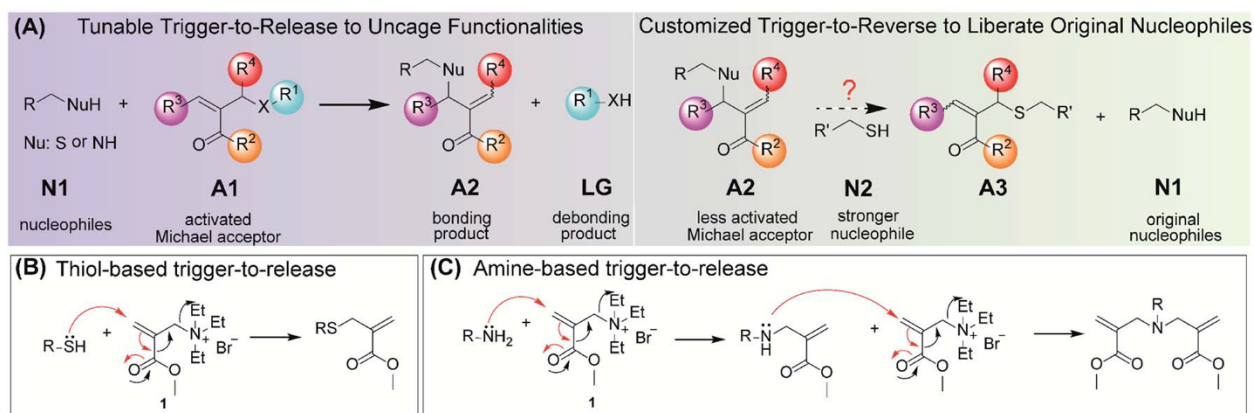


Figure 1.9. Chemical switch for bonding and debonding using Triggerable Michael Acceptors (TMAc). (A) Schematic illustration of the trigger-to-release process as a universal strategy for uncaging of functional groups (left) and the trigger-to-reverse process, the reversibility of which can be structurally customized (right). (B) Proposed thiol-based trigger-to-release. (C) Proposed amine-based trigger-to-release.

Unfortunately, not many examples report conjugation with polymers, largely because model studies are easier to carry out with small molecules. Nevertheless, we believe most of the presented strategies could be applied to the polymer-protein conjugate field. Moreover, not many papers investigate how the chemical modifications effect protein activity before and after traceless release. Assessment of protein activity before and after conjugation and after release should

become more widespread in order to verify that the reversible release is indeed traceless and the chemistry does not negatively impact the protein functionality.

1.3.2 Disulfide Stapling Linkers

Disulfide bridges are found naturally in proteins and are often accessible on the surface. Their primary function is to impart stability to the protein tertiary structure and therefore need to be preserved to maintain protein functionality.⁸¹ Brocchini *et al.* pioneered site-specific modification of various protein's disulfide bridges using bis-thiol alkylating PEG reagent.^{82,83} This chemistry resulted in irreversible conjugation, which can be detrimental for the retention of protein activity. For instance, in the case of human interferon α -2b it led to a 92 % loss of activity *in vitro*.⁸³

More recently, new linkers have been developed in an effort to achieve reversible conjugates, the most prevalent being the maleimide derivatives. The first example was provided by Smith *et al.* who developed dibromomaleimide as a new class of reversible maleimide linker. TCEP was used to reduce the disulfide present in somatostatin, a 15 amino acid cyclic peptide, analogues of which are used in the treatment of acromegaly and gastroenteropancreatic tumors, followed by treatment with dibromomaleimide, which resulted in complete conversion to the bridged peptide. Choosing a functional maleimide, this strategy was utilized to rapidly conjugate fluorescein to somatostatin. Exposure of the conjugate to another nucleophilic thiol, such as 2-mercaptoethanol, regenerated the reduced somatostatin.⁷¹ Once identified as a viable approach, this strategy was quickly extended to other peptides and explored for polymer conjugation. For instance, dibromomaleimide was functionalized with PEG via a modified Mitsunobu reaction and conjugated to salmon calcitonin (sCT), a 32 amino acid peptide used in clinic for the treatment of various bone condition. The authors then proceeded to demonstrate their method using atom transfer radical polymerization (ATRP) generated poly(ethylene glycol) methacrylate (PEGMA).

The initial attempt of employing a dibromomaleimide functionalized initiator proved unsuccessful due to retardation of the polymerization by the maleimide moiety. To circumvent this issue, a strategy involving a postpolymerization modification of the initiator via a copper mediated azide alkyne cycloaddition (CuAAC) click reaction or condensation reaction with dibromomaleic anhydride, was used to introduce the maleimide functionality. The conjugation reactions with sCT proceeded smoothly in less than 30 minutes (Figure 1.10).⁸⁴ The same strategy was used also for antibody functionalization with PEG, fluorescein, biotin or a spin label moiety.⁸⁵ The elegant methodology presented shows obvious advantages such as short reaction time and no purification required due to the use of stoichiometric amount of reagents; however the release and retention of activity of the native peptide was not investigated. Moreover, an initial reduction step is required, which could lead to protein unfolding, aggregation⁸⁶ or disulfide scrambling⁸⁷ due to the presence of free thiols before the conjugation can be performed.

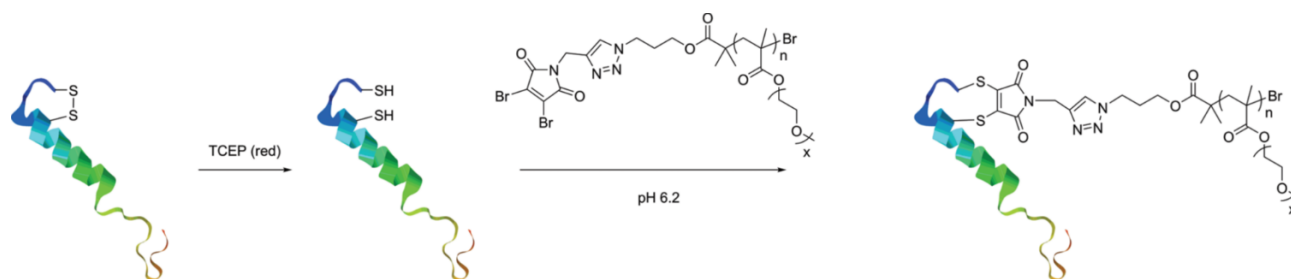


Figure 1.10. sCT disulfide bridging with ATRP generated PEGMA via dibromomaleimide linker

To solve this issue, dithiophenolmaleimides, another class of maleimide derivatives, was developed for use in one-pot reactions with a reducing agent to limit any disulfide formation that occurs prior to addition of the linker.⁸⁸⁻⁹⁰ The approach was demonstrated first by conjugating PEG to somatostatin. Initially, the two-step reaction, (reduction with TCEP followed by conjugation) led to complete bridging in 10 minutes with an equimolar amount of linker, which was a considerable improvement compared to aliphatic dithiomaleimide, requiring 10 equivalents

and 1 hour to achieve complete functionalization. Later, a one-step reaction proved to be possible and quantitatively completed in 20 minutes, whereas use of dibromomaleimide resulted in only 60% functionalization due to side reactions.⁸⁸ The conjugate showed retention of activity, but the possibility to release the native peptide was not demonstrated at this stage. Due to the higher tolerance of dithiophenolmaleimide to TCEP, the authors explored the possibility to use the linker as initiator for ATRP without any protecting groups. The PEGMA polymerization proceeded with acceptable linear first order kinetics, but similarly no release was shown.⁸⁹ Some years later, Collins *et al.* studied the reversibility of this strategy by conjugating a dithiophenolmaleimide bearing PEGMA to oxytocin, a cyclic peptide used to prevent postpartum hemorrhaging which has very limited stability in solution due to the high reactivity of its disulfide bond. The peptide disulfide was first reduced with TCEP, followed by reaction with the functional polymer overnight at 10 °C. After purification, the resulting conjugate was tested for stability which was greatly improved compared to the native peptide (passing from 97.5% to 10% degradation after 28 days in accelerated conditions). Finally, when the conjugate was exposed to an excess of GSH in the biorelevant range the native peptide was quantitatively released over 4 days.⁹⁰ Aryloxymaleimides are another class of maleimide derivatives with attenuated reactivity, which have a preferential selectivity for the disulfide bridging over the bis-adduct formation, a common byproduct formed when using dibromomaleimide. They are also resistant to TCEP, allowing for a one step *in situ* conjugation. Depending upon the peptide chosen, the conjugation reaction was shown to be reversible. Additionally, due to the intrinsic equilibrium of the reaction, the bridged peptide could be treated with another functionalized bromomaleimide leading to reversible dual-functionalization.⁹¹ Other than maleimide derivatives, bis-sulfone reagents can be used to bridge disulfides. The resulting bis-sulfide bond was reversible *in vitro* in MCF-7 breast cancer cells,

where GSH concentration is higher (10 mM), but not at the lower GSH concentrations present in plasma (20 μ M), making this system ideal for cancer targeting delivery systems.⁹² Moreover, dibromopyridazinedione was utilized to bridge the somatostatin disulfide, followed by the release of reduced somatostatin over 72 hours when exposed to an excess of 2-mercaptoethanol.⁷⁷

Interestingly, the high affinity between metals and disulfides can also be exploited as a bridging system. Arylarsenous acid was conjugated to sCT in less than 2 minutes *via* either an *in situ* or a two-step reduction-conjugation approach. The bond was cleavable by exposure to an excess of ethane-1,2-dithiol (EDT). Notably, the specificity for disulfide bonds compared to free thiols present in the same protein was higher than dibromomaleimide. The arsenic containing initiator could also be used to prepare PEGMA via single-electron transfer living radical polymerization (SET-LRP). The resulting polymer was found to be an order of magnitude less toxic across multiple cell lines when compared to the arsenical small molecules. Quantitative conjugation of the polymer to sCT was achieved by treating first the polymer with GSH to stabilize the arsenous acid As(III) and by increasing the amount of polymer used. The native peptide could be released following treatment with an excess of EDT or reduced lipoic acid in 107 or 30 minutes, respectively.⁹³

Unfortunately, very few of these papers explore the possible loss of activity of the peptide or protein after release. Moreover, most of these approaches provide the reduced peptide, which would require a further oxidation step to reform their disulfide linkages, necessary to maintain the natural conformation and avoid loss of activity. Therefore, the development of a method affording the disulfide without the need for a subsequent oxidation reaction, which could be harmful for other protein residues, would be of great importance.

Despite being outside the scope of this review, a similar approach was employed in the area of reversible peptide stapling, which are constrained peptides for various applications, and avoid or inhibit protein-protein interactions, increase stability, enhance cell-uptake or improve target binding affinity. The already thoroughly discussed dibromomaleimides found application also in this field,^{94,95} whereas examples of new approaches include the use of dithioaryl(TCEP)pyridazinedione, as a 2 in 1 reagent with both reducing and rebridging function,⁹⁶ a photocleavable *s*-tetrazine linker,⁹⁷ or 1,3,5-tris((pyridin-2-yl)disulfanyl)methyl)benzene (TPSMB) as a planar, trivalent, sulfhydryl-specific linker.⁹⁸

1.4 Noncovalent Traceless Linkages

While covalent traceless strategies effectively mitigate loss of a biomolecules' activities, they still present synthetic challenges. Covalent linkers require chemical reactions between the polymer and protein (or peptide) followed by purification, where these additional processes could be harmful and might reduce scalability. Noncovalent conjugation strategies that rely on physical polymer-protein interactions can circumvent these issues.⁹⁹ Through selective and thermodynamically stable noncovalent complexes, polymers can strongly interact with proteins and peptides without chemically modifying their structures; these high-affinity complexes are what distinguish noncovalent conjugates from typical protein excipients. For example, lectin-specific complexation of a fucose-capped PEG with fucose-binding lectin has yielded noncovalent, multivalent protein-polymer complexes with micromolar binding dissociation.¹⁰⁰ For bioconjugates of other proteins, molecular recognition usually occurs via host-guest, hydrophobic, metal coordination, or ionic interactions (Table 1.1). Noncovalent linkages through these interactions are considered traceless if they demonstrate reversibility in relevant physiological conditions.

Table 1.1. Binding affinities of select noncovalent linkages applied for bioconjugates of proteins and peptides.

Interaction Type	Noncovalent linkage	Affinity (K_a) (M^{-1})	Ref.
Host-Guest	Biotin + Streptavidin	10^{15}	101
	CB[7] + N-terminal aromatic amino acids (e.g. tryptophan and phenylalanine)	10^6	102
	CB[7] + midchain aromatic or cationic ammonium residues	10^3 to 10^4	102
Hydrophobic interactions	Insulin + cholesterol-PEG	1.14×10^5	103
	Insulin + cholane-PEG	3.98×10^4	103
Metal Coordination Complexes	G-CSF + 8-arm PEG-(NTA) ₈	4.7×10^9	104
Ionic interactions	Keratinocyte growth factor-2 + pentosane polysulfate-PEG20	1.1×10^7	105
	Bovine serum albumin + hyaluronic acid	4×10^2	106

1.4.1 Host-Guest Complexes

Bontempo *et al.* demonstrated an example of using host-guest chemistry to create a protein-polymer conjugate.¹⁰⁷ Leveraging the high affinity of streptavidin and biotin, *N*-isopropylacrylamide was polymerized by “grafting from” a novel streptavidin-biotin ATRP macro initiator. The resulting conjugate was stable, demonstrated thermoresponsive behavior by precipitating when heated, and was reversible in a dimethylformamide (DMF)/water mixture at 90

°C for 1 hour. This work was expanded to form heterotelechelic polymers that could form dimers of bovine serum albumin with streptavidin.¹⁰⁸ While these host-guest bioconjugates demonstrate promising proof-of-concept, the *in vivo* reversibility and activity was not demonstrated, making it difficult to define these examples as truly “traceless” conjugations.

In contrast to the last example, most other host-guest bioconjugations apply the protein as the guest and polymer as the host molecule. Insulin has been coordinated and stabilized with cyclodextrin (CD)- or cucurbit[7]uril (CB[7])-functionalized polymeric host molecules.^{109–112} Webber and Appel *et al.* modified PEG with CB[7] and demonstrated binding with the N-terminal aromatic phenylalanine residue of insulin as well as weaker interactions with midchain residues of glucagon and an antibody for human CD20 (Figure 1.11).¹¹⁰ The resulting conjugates improved the *in vitro* stability and function of the proteins. For insulin, the polymeric bioconjugate preserved stability and activity for 100 days in physiological conditions (pH 7.4, 37 °C) with agitation. This was greatly improved compared to free insulin and insulin + CB[7] (non-polymeric), which both aggregated and lost significant activity within ~14 hours. Insulin with CB[7]-PEG was further evaluated and demonstrated extended *in vivo* activity (with PEG ≥ 10 kDa)¹¹⁰ as well as enhanced occurrence of fast-acting, monomeric insulin.¹¹¹ Moreover, CB[7]-PEG binding did not affect insulin’s diffusivity or its association state. While host-guest chemistry relies on hydrophilic and hydrophobic interactions, noncovalent conjugates can also be assembled via other non-polar interactions.

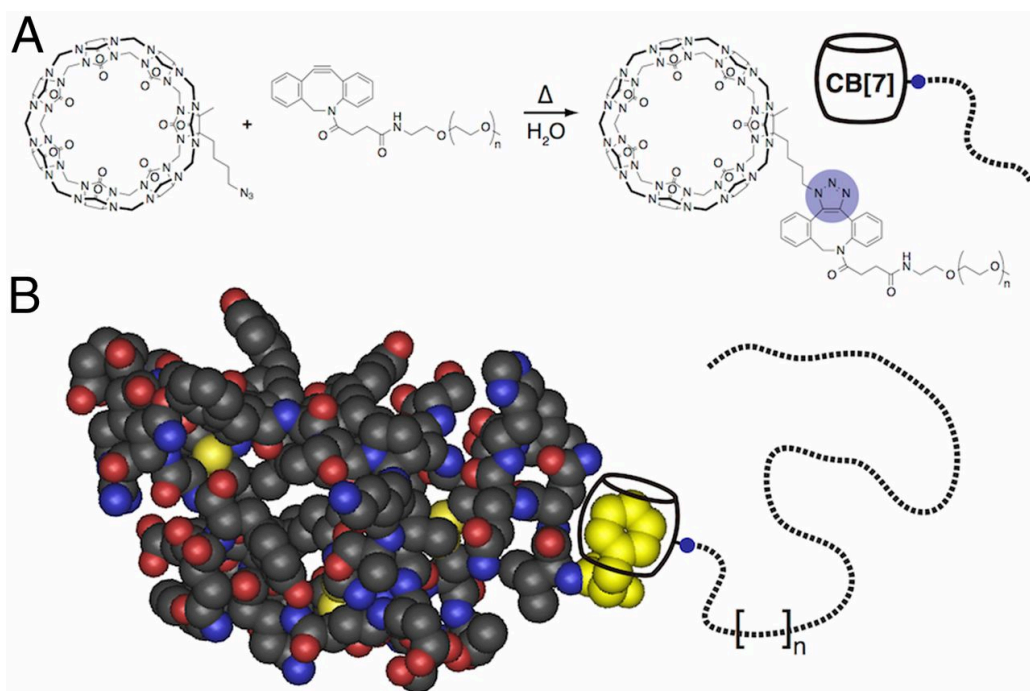


Figure 1.11. Strategy for supramolecular PEGylation. (A) A copper-free “click” reaction between a cucurbit[7]uril (CB[7]) supramolecular host molecule bearing a single azide moiety (CB[7]–N₃) and a dibenzocyclooctyne-functional poly(ethylene glycol) polymer (PEG–DBCO) (M_n = 5, 10, or 30 kDa) yields CB[7]–PEG upon triazole formation. (B) Cartoon depicting supramolecular PEGylation of the insulin protein through strong noncovalent binding of the CB[7] moiety to the N-terminal phenylalanine residue.

1.4.2 Hydrophobic Interactions

Proteins are amphiphilic and will oftentimes unfold to present non-polar patches in solution. These hydrophobic areas are then available to interact with other non-polar moieties through hydrophobic interactions. Hydrophobic interactions are hypothesized to block surface absorption-induced protein aggregation and denaturation. As a result, studies which create PEG modifications with hydrophobic dansyl-,¹¹³ tryptophan-,¹¹⁴ phenylbutylamine-,¹¹⁵ benzyl-,¹¹⁵ cholesteryl-,^{103,115,116} and cholane-¹⁰³ groups have examined the efficacy of stabilizing proteins and peptides. Asayama *et al.* synthesized a cholesteryl-PEG polymer attached through a urethane linkage.¹¹⁶ The polymer associated with insulin through cholesterol interaction with non-polar

amino acids in insulin, such as alanine, valine, leucine, isoleucine, and phenylalanine (Figure 1.12). The urethane linkage promoted additional noncovalent interactions via hydrogen bonding with hydrogen-bond-forming amino acids, such as serine, threonine, tyrosine, glutamine, and asparagine. The authors demonstrated that the cholesteryl-PEG bioconjugation to insulin improved the protein's stability to protease digestion and enhanced insulin's *in vivo* activity as demonstrated through suppressed levels of glucose in mice, although this bioconjugate performed similarly to a covalently PEGylated insulin bioconjugate. The authors hypothesized that the cholesteryl-PEG bioconjugates would degrade in serum at 37 °C, however further studies are required to validate this claim. Aside from complexes based on polarity, traceless bioconjugates have been conducted with other types of noncovalent interactions, such as the coordination of metals with chelators.

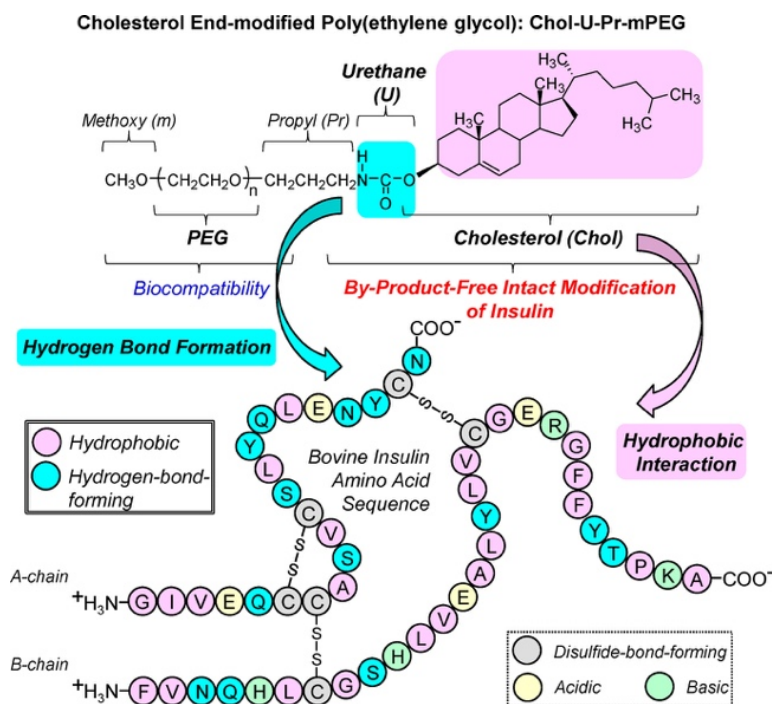


Figure 1.12. Design concept of the cholesterol end-modified poly(ethyleneglycol) (Chol-U-Pr-mPEG) for by-product-free intact modification of insulin.

1.4.3 Metal Coordination Complexes

Metal coordination complexes applied for protein stabilization typically leverage the strong interactions of metal ions (such as Ni^{2+} or Cu^{2+}), nitrilotriacetic acid (NTA), and histidine. For example, there are examples of synthetically-created hexahistidine (His_6)-tagged proteins that have been complexed with Ni^{2+} and NTA-polystyrene,¹¹⁷ NTA-PEG,¹¹⁸ or NTA-poly(*N*-acryloylmorpholine-*stat*-*N*-acryloxysuccinimide).¹¹⁹ While effective for site-specific labelling and protein stabilization, these examples require native protein modification, and are therefore not considered “traceless”. However, there is an example of a naturally histidine-rich protein, granulocyte colony-stimulating factor (G-CSF), which was able to bind to Cu^{2+} and flexible, multi-arm 8-arm PEG-(NTA)₈ polymer.¹⁰⁴ These G-CSF bioconjugates were demonstrated as stable in the presence of human serum albumin (HAS) at 22 °C, although unfortunately, the *in vivo* half-

life of G-CSF was unaffected by the addition of polymer indicating that the rate of traceless release is too fast to produce a steady release of native G-CSF. The authors hypothesized that this was due to dissociation through dilution and/or competition with plasma proteins, which reduced the *in vivo* half-life of the complex. Another study demonstrated metal coordination of native transferrin protein via Werner complexation.¹²⁰ Here, a PEG-amine and transferrin, specifically the protein's amines, were coordinated with Co^{2+} . *In vitro* studies demonstrated rapid ligand exchange with competitive binder ethanolamine, but the *in vivo* functionality and reversibility of bioconjugates created through metal coordination complexes must be further investigated.

1.4.4 Ionic Interactions

Ionic interactions are an additional alternative noncovalent traceless conjugation strategy, wherein recently a mono-ion complexation of a diethylaminoethyl end-modified PEG to catalase was studied.¹²¹ This noncovalent bioconjugate preserved protein activity, including in the presence of protease, trypsin or 10% fetal bovine serum, with similar efficacy compared to a covalent PEG-catalase conjugate, while keeping the native protein conformation intact. However, no data was presented demonstrating its traceless release which will need to be evaluated further. Most other examples of ionic interactions used for protein stabilization are via polyelectrolytes.^{105,122–127} These are important multivalent, reversible complexes, but will not be discussed further here as polyelectrolyte-protein interactions have been recently reviewed in detail elsewhere¹²⁸ and their specificity decreases with increased ionic strength of the experimental media,¹²⁹ making these interactions less practical for *in vivo* studies. In fact, hydrophobic groups, specifically, ethyl, 1-hydroxyethyl, and benzyl, have been utilized to overcome these competing ionic interactions; they were quarternized to poly(*N,N*-dimethylaminoethyl methacrylate)-block-PEG to form cationic polyelectrolytes with enhanced affinity toward α -amylase in saline conditions.¹³⁰ As seen in Table

1.1, ionic interaction binding affinities vary widely, probably due to the many possible variations in experimental and materials (for example, discrepancies in polymer hydrodynamic radius and charge).

There is a lack of studies that demonstrate the efficacy of noncovalent complexes *in vivo*. Noncovalent traceless strategies require physical interactions that are specific and thermodynamically- and kinetically- favored, even in dilute solutions with competitive interactions. It follows that *in vivo* application is challenging due to the many additional proteins and small molecules that can disrupt molecular recognition events, thus lowering the complex binding affinity. Alternatively, if the noncovalent interaction is too robust, it may be difficult for the biomolecule to release within a therapeutically relevant timeframe. More experiments need to be conducted to confirm the ideal binding affinity for efficacious noncovalent, traceless bioconjugates.

1.5 Future Outlook

This review highlights the diversity and breadth of traceless linkers currently in the field of reversible peptide and protein modifications. The purpose of this review is to outline the different strategies for each conjugation handle, in order to allow readers to decide which linker design would fit best for their application design. No one traceless linker design is a perfect fit across all applications, but rather the specific constraints around each application can inform the bioconjugation chemist which linker is most appropriate. As traceless linkers are adapted towards more and more specific applications, the specificity of the linker designs is likely to increase. This includes the design of traceless linkers that are primarily cleaved under tissue specific conditions which would require more precise triggering conditions, as compared to the more commonly used hydrolysis and reductive triggering functionalities. Additionally, as the field of protein

conjugation grows, the number of residue specific chemistries has begun to broaden which in turn may lead to alternative traceless linkers for entirely new conjugation handles.

1.6 References

- (1) Gunnoo, S. B.; Madder, A. Bioconjugation – Using Selective Chemistry to Enhance the Properties of Proteins and Peptides as Therapeutics and Carriers. *Org. Biomol. Chem.* **2016**, *14* (34), 8002–8013. <https://doi.org/10.1039/C6OB00808A>.
- (2) Pelegri-O’Day, E. M.; Lin, E.-W.; Maynard, H. D. Therapeutic Protein–Polymer Conjugates: Advancing Beyond PEGylation. *J. Am. Chem. Soc.* **2014**, *136* (41), 14323–14332. <https://doi.org/10.1021/ja504390x>.
- (3) Morgenstern, J.; Gil Alvaradejo, G.; Bluthardt, N.; Beloqui, A.; Delaittre, G.; Hubbuch, J. Impact of Polymer Bioconjugation on Protein Stability and Activity Investigated with Discrete Conjugates: Alternatives to PEGylation. *Biomacromolecules* **2018**, *19* (11), 4250–4262. <https://doi.org/10.1021/acs.biomac.8b01020>.
- (4) Lucius, M.; Falatach, R.; McGlone, C.; Makaroff, K.; Danielson, A.; Williams, C.; Nix, J. C.; Konkolewicz, D.; Page, R. C.; Berberich, J. A. Investigating the Impact of Polymer Functional Groups on the Stability and Activity of Lysozyme–Polymer Conjugates. *Biomacromolecules* **2016**, *17* (3), 1123–1134. <https://doi.org/10.1021/acs.biomac.5b01743>.
- (5) Tucker, B. S.; Stewart, J. D.; Aguirre, J. I.; Holliday, L. S.; Figg, C. A.; Messer, J. G.; Sumerlin, B. S. Role of Polymer Architecture on the Activity of Polymer–Protein Conjugates for the Treatment of Accelerated Bone Loss Disorders. *Biomacromolecules* **2015**, *16* (8), 2374–2381. <https://doi.org/10.1021/acs.biomac.5b00623>.
- (6) Wang, Y.; Wu, C. Site-Specific Conjugation of Polymers to Proteins. *Biomacromolecules* **2018**, *19* (6), 1804–1825. <https://doi.org/10.1021/acs.biomac.8b00248>.

- (7) Hacker, S. M.; Backus, K. M.; Lazear, M. R.; Forli, S.; Correia, B. E.; Cravatt, B. F. Global Profiling of Lysine Reactivity and Ligandability in the Human Proteome. *Nat. Chem.* **2017**, *9* (12), 1181–1190. <https://doi.org/10.1038/nchem.2826>.
- (8) Butler, P. J.; Harris, J. I.; Hartley, B. S.; Leberman, R. Reversible Blocking of Peptide Amino Groups by Maleic Anhydride. *Biochem. J.* **1967**, *103* (3), 78-79P.
- (9) Hanai, R.; Wang, J. C. Protein Footprinting by the Combined Use of Reversible and Irreversible Lysine Modifications. *Proc. Natl. Acad. Sci.* **1994**, *91* (25), 11904–11908. <https://doi.org/10.1073/pnas.91.25.11904>.
- (10) Palacián, E.; López-Rivas, A.; Pintor-Toro, J. A.; Hernández, F. Dissociation of the Protein Components from Chromatin by Reversible Modification with Dimethylmaleic Anhydride. *Mol. Cell. Biochem.* **1981**, *36* (3), 163–167. <https://doi.org/10.1007/BF02357033>.
- (11) Schäfer, R. Synthesis and Application of Chemically Reactive Proteins by the Reversible Modification of Protein Amino Groups with Exo-Cis-3,6-Endo-Epoxy-4,5-Cis-Epoxyhexahydrophthalic Anhydride. *Biochem. J.* **1982**, *203* (2), 345–350. <https://doi.org/10.1042/bj2030345>.
- (12) Garman, A. J.; Barret Kalindjian, S. The Preparation and Properties of Novel Reversible Polymer-Protein Conjugates 2- ω -Methoxypolyethylene (5000) Glycoxymethylene-3-Methylmaleyl Conjugates of Plasminogen Activators. *FEBS Lett.* **1987**, *223* (2), 361–365. [https://doi.org/10.1016/0014-5793\(87\)80319-8](https://doi.org/10.1016/0014-5793(87)80319-8).
- (13) Sakata, K.; Hamase, K.; Zaitso, K. Reversible Fluorescence Labeling of Amino Groups of Protein Using Dansylaminomethylmaleic Anhydride. *J. Chromatogr. B* **2002**, *769* (1), 47–54. [https://doi.org/10.1016/S1570-0232\(01\)00629-8](https://doi.org/10.1016/S1570-0232(01)00629-8).

- (14) Maier, K.; Wagner, E. Acid-Labile Traceless Click Linker for Protein Transduction. *J. Am. Chem. Soc.* **2012**, *134* (24), 10169–10173. <https://doi.org/10.1021/ja302705v>.
- (15) Liu, X.; Zhang, P.; He, D.; Rödl, W.; Preiß, T.; Rädler, J. O.; Wagner, E.; Lächelt, U. PH-Reversible Cationic RNase A Conjugates for Enhanced Cellular Delivery and Tumor Cell Killing. *Biomacromolecules* **2016**, *17* (1), 173–182. <https://doi.org/10.1021/acs.biomac.5b01289>.
- (16) Greenwald, R. B.; Zhao, H.; Yang, K.; Reddy, P.; Martinez, A. A New Aliphatic Amino Prodrug System for the Delivery of Small Molecules and Proteins Utilizing Novel PEG Derivatives. *J. Med. Chem.* **2004**, *47* (3), 726–734. <https://doi.org/10.1021/jm030369+>.
- (17) Zhao, H.; Yang, K.; Martinez, A.; Basu, A.; Chintala, R.; Liu, H.-C.; Janjua, A.; Wang, M.; Filpula, D. Linear and Branched Bicin Linkers for Releasable PEGylation of Macromolecules: Controlled Release in Vivo and in Vitro from Mono- and Multi-PEGylated Proteins. *Bioconjug. Chem.* **2006**, *17* (2), 341–351. <https://doi.org/10.1021/bc050270c>.
- (18) Filpula, D.; Yang, K.; Basu, A.; Hassan, R.; Xiang, L.; Zhang, Z.; Wang, M.; Wang, Q.; Ho, M.; Beers, R.; Zhao, H.; Peng, P.; Zhou, J.; Li, X.; Petti, G.; Janjua, A.; Liu, J.; Wu, D.; Yu, D.; Zhang, Z.; Longley, C.; FitzGerald, D.; Kreitman, R. J.; Pastan, I. Releasable PEGylation of Mesothelin Targeted Immunotoxin SS1P Achieves Single Dosage Complete Regression of a Human Carcinoma in Mice. *Bioconjug. Chem.* **2007**, *18* (3), 773–784. <https://doi.org/10.1021/bc060314x>.
- (19) Chen, J.; Zhao, M.; Feng, F.; Sizovs, A.; Wang, J. Tunable Thioesters as “Reduction” Responsive Functionality for Traceless Reversible Protein PEGylation. *J. Am. Chem. Soc.* **2013**, *135* (30), 10938–10941. <https://doi.org/10.1021/ja405261u>.

- (20) Dutta, K.; Hu, D.; Zhao, B.; Ribbe, A. E.; Zhuang, J.; Thayumanavan, S. Templated Self-Assembly of a Covalent Polymer Network for Intracellular Protein Delivery and Traceless Release. *J. Am. Chem. Soc.* **2017**, *139* (16), 5676–5679. <https://doi.org/10.1021/jacs.7b01214>.
- (21) Scherger, M.; Räder, H. J.; Nuhn, L. Self-Immolative RAFT-Polymer End Group Modification. *Macromol. Rapid Commun.* **2021**, *42* (8), 2000752. <https://doi.org/10.1002/marc.202000752>.
- (22) Amsberry, K. L.; Gerstenberger, A. E.; Borchardt, R. T. Amine Prodrugs Which Utilize Hydroxy Amide Lactonization. II. A Potential Esterase-Sensitive Amide Prodrug. *Pharm. Res.* **1991**, *8* (4), 455–461. <https://doi.org/10.1023/A:1015890809507>.
- (23) Milstien, S.; Cohen, L. A. Rate Acceleration by Stereopopulation Control: Models for Enzyme Action. *Proc. Natl. Acad. Sci.* **1970**, *67* (3), 1143–1147. <https://doi.org/10.1073/pnas.67.3.1143>.
- (24) Chang, J.; Cai, W.; Liang, C.; Tang, Q.; Chen, X.; Jiang, Y.; Mao, L.; Wang, M. Enzyme-Instructed Activation of Pro-Protein Therapeutics In Vivo. *J. Am. Chem. Soc.* **2019**, *141* (45), 18136–18141. <https://doi.org/10.1021/jacs.9b08669>.
- (25) Carl, P. L.; Chakravarty, P. K.; Katzenellenbogen, J. A. A Novel Connector Linkage Applicable in Prodrug Design. *J. Med. Chem.* **1981**, *24* (5), 479–480. <https://doi.org/10.1021/jm00137a001>.
- (26) Zalipsky, S.; Mullah, N.; Engbers, C.; Hutchins, M. U.; Kiwan, R. Thiolytically Cleavable Dithiobenzyl Urethane-Linked Polymer–Protein Conjugates as Macromolecular Prodrugs: Reversible PEGylation of Proteins. *Bioconjug. Chem.* **2007**, *18* (6), 1869–1878. <https://doi.org/10.1021/bc7001902>.

- (27) Suma, T.; Cui, J.; Müllner, M.; Fu, S.; Tran, J.; Noi, K. F.; Ju, Y.; Caruso, F. Modulated Fragmentation of Proapoptotic Peptide Nanoparticles Regulates Cytotoxicity. *J. Am. Chem. Soc.* **2017**, *139* (11), 4009–4018. <https://doi.org/10.1021/jacs.6b11302>.
- (28) Qian, L.; Fu, J.; Yuan, P.; Du, S.; Huang, W.; Li, L.; Yao, S. Q. Intracellular Delivery of Native Proteins Facilitated by Cell-Penetrating Poly(Disulfide)s. *Angew. Chem. Int. Ed.* **2018**, *57* (6), 1532–1536. <https://doi.org/10.1002/anie.201711651>.
- (29) He, M.; Li, J.; Han, H.; Borges, C. A.; Neiman, G.; Røise, J. J.; Hadaczek, P.; Mendonsa, R.; Holm, V. R.; Wilson, R. C.; Bankiewicz, K.; Zhang, Y.; Sadlowski, C. M.; Healy, K.; Riley, L. W.; Murthy, N. A Traceless Linker for Aliphatic Amines That Rapidly and Quantitatively Fragments after Reduction. *Chem. Sci.* **2020**, *11* (33), 8973–8980. <https://doi.org/10.1039/D0SC00929F>.
- (30) Lee, S.; Greenwald, R. B.; McGuire, J.; Yang, K.; Shi, C. Drug Delivery Systems Employing 1,6-Elimination: Releasable Poly(Ethylene Glycol) Conjugates of Proteins. *Bioconjug. Chem.* **2001**, *12* (2), 163–169. <https://doi.org/10.1021/bc000064z>.
- (31) Greenwald, R. B.; Yang, K.; Zhao, H.; Conover, C. D.; Lee, S.; Filpula, D. Controlled Release of Proteins from Their Poly(Ethylene Glycol) Conjugates: Drug Delivery Systems Employing 1,6-Elimination. *Bioconjug. Chem.* **2003**, *14* (2), 395–403. <https://doi.org/10.1021/bc025652m>.
- (32) Rau, H.; Kindermann, S.; Lessmann, T.; RASMUSSEN, G. N.; Hersel, U.; Wegge, T.; Sprogøe, K. Pegylated Recombinant Human Growth Hormone Compounds. WO2009133137A2, November 5, 2009.
- (33) Wang, M.; Sun, S.; Neufeld, C. I.; Perez-Ramirez, B.; Xu, Q. Reactive Oxygen Species-Responsive Protein Modification and Its Intracellular Delivery for Targeted Cancer

- Therapy. *Angew. Chem. Int. Ed.* **2014**, *53* (49), 13444–13448. <https://doi.org/10.1002/anie.201407234>.
- (34) Liu, B.; Ianosi-Irimie, M.; Thayumanavan, S. Reversible Click Chemistry for Ultrafast and Quantitative Formation of Protein–Polymer Nanoassembly and Intracellular Protein Delivery. *ACS Nano* **2019**, *13* (8), 9408–9420. <https://doi.org/10.1021/acsnano.9b04198>.
- (35) Alouane, A.; Labruère, R.; Le Saux, T.; Schmidt, F.; Jullien, L. Self-Immolative Spacers: Kinetic Aspects, Structure–Property Relationships, and Applications. *Angew. Chem. Int. Ed.* **2015**, *54* (26), 7492–7509. <https://doi.org/10.1002/anie.201500088>.
- (36) Sprogøe, K.; Egesborg, H.; Jennsen, S.; Kurpiers, T. Long-Acting Growth Hormone Dosage Forms. US20170312342A1, November 2, 2017.
- (37) Brandl, F.; Hammer, N.; Blunk, T.; Tessmar, J.; Goepferich, A. Biodegradable Hydrogels for Time-Controlled Release of Tethered Peptides or Proteins. *Biomacromolecules* **2010**, *11* (2), 496–504. <https://doi.org/10.1021/bm901235g>.
- (38) Hammer, N.; Brandl, F. P.; Kirchhof, S.; Goepferich, A. M. Cleavable Carbamate Linkers for Controlled Protein Delivery from Hydrogels. *J. Controlled Release* **2014**, *183*, 67–76. <https://doi.org/10.1016/j.jconrel.2014.03.031>.
- (39) Diehl, K. L.; Kolesnichenko, I. V.; Robotham, S. A.; Bachman, J. L.; Zhong, Y.; Brodbelt, J. S.; Anslyn, E. V. Click and Chemically Triggered Declick Reactions through Reversible Amine and Thiol Coupling via a Conjugate Acceptor. *Nat. Chem.* **2016**, *8* (10), 968–973. <https://doi.org/10.1038/nchem.2601>.
- (40) Zhuang, J.; Zhao, B.; Meng, X.; Schiffman, J. D.; Perry, S. L.; Vachet, R. W.; Thayumanavan, S. A Programmable Chemical Switch Based on Triggerable Michael Acceptors. *Chem. Sci.* **2020**, *11* (8), 2103–2111. <https://doi.org/10.1039/C9SC05841A>.

- (41) Gershonov, E.; Shechter, Y.; Fridkin, M. New Concept for Long-Acting Insulin: Spontaneous Conversion of an Inactive Modified Insulin to the Active Hormone in Circulation: 9-Fluorenylmethoxycarbonyl Derivative of Insulin. *Diabetes* **1999**, *48* (7), 1437–1442. <https://doi.org/10.2337/diabetes.48.7.1437>.
- (42) Gershonov, E.; Goldwaser, I.; Fridkin, M.; Shechter, Y. A Novel Approach for a Water-Soluble Long-Acting Insulin Prodrug: Design, Preparation, and Analysis of [(2-Sulfo)-9-Fluorenylmethoxycarbonyl]3-Insulin. *J. Med. Chem.* **2000**, *43* (13), 2530–2537. <https://doi.org/10.1021/jm990533m>.
- (43) Shechter, Y.; Goldwaser, I.; Lavon, I.; Gershonov, E.; Mester, B.; Mironchik, M.; Pratt, L. P.; Fridkin, M. A New Approach for Prolonging the Half-Life of Peptides, Proteins and Low-Molecular-Weight Drugs in Vivo. *Drugs Future* **2001**, *26* (7), 669. <https://doi.org/10.1358/dof.2001.026.07.858711>.
- (44) Peleg-Shulman, T.; Tsubery, H.; Mironchik, M.; Fridkin, M.; Schreiber, G.; Shechter, Y. Reversible PEGylation: A Novel Technology To Release Native Interferon A2 over a Prolonged Time Period. *J. Med. Chem.* **2004**, *47* (20), 4897–4904. <https://doi.org/10.1021/jm0497693>.
- (45) Tsubery, H.; Mironchik, M.; Fridkin, M.; Shechter, Y. Prolonging the Action of Protein and Peptide Drugs by a Novel Approach of Reversible Polyethylene Glycol Modification*. *J. Biol. Chem.* **2004**, *279* (37), 38118–38124. <https://doi.org/10.1074/jbc.M405155200>.
- (46) Shechter, Y.; Mironchik, M.; Rubinraut, S.; Tsubery, H.; Sasson, K.; Marcus, Y.; Fridkin, M. Reversible Pegylation of Insulin Facilitates Its Prolonged Action in Vivo. *Eur. J. Pharm. Biopharm.* **2008**, *70* (1), 19–28. <https://doi.org/10.1016/j.ejpb.2008.03.018>.

- (47) Shechter, Y.; Heldman, E.; Sasson, K.; Bachar, T.; Popov, M.; Fridkin, M. Delivery of Neuropeptides from the Periphery to the Brain: Studies with Enkephalin. *ACS Chem. Neurosci.* **2010**, *1* (5), 399–406. <https://doi.org/10.1021/cn100001j>.
- (48) Bossard, M. J.; Ali, C. F.; Liu, X.; Charych, D. H.; Zappe, H.; Wang, Y.; Huang, J. Conjugates of an Il-2 Moiety and a Polymer. WO2012065086A1, May 18, 2012.
- (49) Addepalli, M. K.; Charych, D. H.; Kantak, S.; Lee, S. R. Il-2rbeta-Selective Agonists in Combination with an Anti-Ctla-4 Antibody or an an Anti-Pd-1 Antibody. WO2015125159A1, August 27, 2015.
- (50) Charych, D.; Khalili, S.; Dixit, V.; Kirk, P.; Chang, T.; Langowski, J.; Rubas, W.; Doberstein, S. K.; Eldon, M.; Hoch, U.; Zalevsky, J. Modeling the Receptor Pharmacology, Pharmacokinetics, and Pharmacodynamics of NKTR-214, a Kinetically-Controlled Interleukin-2 (IL2) Receptor Agonist for Cancer Immunotherapy. *PLOS ONE* **2017**, *12* (7), e0179431. <https://doi.org/10.1371/journal.pone.0179431>.
- (51) Santi, D. V.; Schneider, E. L.; Reid, R.; Robinson, L.; Ashley, G. W. Predictable and Tunable Half-Life Extension of Therapeutic Agents by Controlled Chemical Release from Macromolecular Conjugates. *Proc. Natl. Acad. Sci.* **2012**, *109* (16), 6211–6216. <https://doi.org/10.1073/pnas.1117147109>.
- (52) Schneider, E. L.; Henise, J.; Reid, R.; Ashley, G. W.; Santi, D. V. Hydrogel Drug Delivery System Using Self-Cleaving Covalent Linkers for Once-a-Week Administration of Exenatide. *Bioconjug. Chem.* **2016**, *27* (5), 1210–1215. <https://doi.org/10.1021/acs.bioconjchem.5b00690>.
- (53) Schneider, E. L.; Hearn, B. R.; Pfaff, S. J.; Reid, R.; Parkes, D. G.; Vrang, N.; Ashley, G. W.; Santi, D. V. A Hydrogel-Microsphere Drug Delivery System That Supports Once-

- Monthly Administration of a GLP-1 Receptor Agonist. *ACS Chem. Biol.* **2017**, *12* (8), 2107–2116. <https://doi.org/10.1021/acscchembio.7b00218>.
- (54) Schneider, E. L.; Reid, R.; Parkes, D. G.; Lutz, T. A.; Ashley, G. W.; Santi, D. V. A Once-Monthly GLP-1 Receptor Agonist for Treatment of Diabetic Cats. *Domest. Anim. Endocrinol.* **2020**, *70*, 106373. <https://doi.org/10.1016/j.domaniend.2019.07.001>.
- (55) Georgianna, W. E.; Lusic, H.; McIver, A. L.; Deiters, A. Photocleavable Polyethylene Glycol for the Light-Regulation of Protein Function. *Bioconjug. Chem.* **2010**, *21* (8), 1404–1407. <https://doi.org/10.1021/bc100084n>.
- (56) Takamori, S.; Yamaguchi, S.; Ohashi, N.; Nagamune, T. Sterically Bulky Caging for Light-Inducible Protein Activation. *Chem. Commun.* **2013**, *49* (29), 3013–3015. <https://doi.org/10.1039/C3CC38026B>.
- (57) Karas, J. A.; Noor, A.; Schieber, C.; Connell, T. U.; Separovic, F.; Donnelly, P. S. The Efficient Synthesis and Purification of Amyloid- β (1–42) Using an Oligoethylene Glycol-Containing Photocleavable Lysine Tag. *Chem. Commun.* **2017**, *53* (51), 6903–6905. <https://doi.org/10.1039/C7CC03147E>.
- (58) Chalker, J. M.; Bernardes, G. J.; Lin, Y. A.; Davis, B. G. Chemical Modification of Proteins at Cysteine: Opportunities in Chemistry and Biology. *Chem. Asian J.* **2009**, *4* (5), 630–640.
- (59) Gunnoo, S. B.; Madder, A. Chemical Protein Modification through Cysteine. *ChemBioChem* **2016**, *17* (7), 529–553.
- (60) Paluck, S. J.; Nguyen, T. H.; Maynard, H. D. Heparin-Mimicking Polymers: Synthesis and Biological Applications. *Biomacromolecules* **2016**, *17* (11), 3417–3440.

- (61) Li, Q.; White, J. B.; Peterson, N. C.; Rickert, K. W.; Lloyd, C. O.; Allen, K. L.; Rosenthal, K.; Gao, X.; Wu, H.; Dall'Acqua, W. F. Tumor Uptake of Pegylated Diabodies: Balancing Systemic Clearance and Vascular Transport. *J. Controlled Release* **2018**, *279*, 126–135.
- (62) Maurais, A. J.; Weerapana, E. Reactive-Cysteine Profiling for Drug Discovery. *Curr. Opin. Chem. Biol.* **2019**, *50*, 29–36.
- (63) Weerapana, E.; Wang, C.; Simon, G. M.; Richter, F.; Khare, S.; Dillon, M. B.; Bachovchin, D. A.; Mowen, K.; Baker, D.; Cravatt, B. F. Quantitative Reactivity Profiling Predicts Functional Cysteines in Proteomes. *Nature* **2010**, *468* (7325), 790–795.
- (64) Bontempo, D.; Heredia, K. L.; Fish, B. A.; Maynard, H. D. Cysteine-Reactive Polymers Synthesized by Atom Transfer Radical Polymerization for Conjugation to Proteins. *J. Am. Chem. Soc.* **2004**, *126* (47), 15372–15373.
- (65) Nauka, P. C.; Lee, J.; Maynard, H. D. Enhancing the Conjugation Yield of Brush Polymer–Protein Conjugates by Increasing the Linker Length at the Polymer End-Group. *Polym. Chem.* **2016**, *7* (13), 2352–2357.
- (66) Gok, O.; Erturk, P.; Sumer Bolu, B.; Gevrek, T. N.; Sanyal, R.; Sanyal, A. Dendrons and Multiarm Polymers with Thiol-Exchangeable Cores: A Reversible Conjugation Platform for Delivery. *Biomacromolecules* **2017**, *18* (8), 2463–2477.
- (67) Baldwin, A. D.; Kiick, K. L. Tunable Degradation of Maleimide–Thiol Adducts in Reducing Environments. *Bioconjug. Chem.* **2011**, *22* (10), 1946–1953.
- (68) Fontaine, S. D.; Reid, R.; Robinson, L.; Ashley, G. W.; Santi, D. V. Long-Term Stabilization of Maleimide–Thiol Conjugates. *Bioconjug. Chem.* **2015**, *26* (1), 145–152. <https://doi.org/10.1021/bc5005262>.

- (69) Wu, H.; LeValley, P. J.; Luo, T.; Kloxin, A. M.; Kiick, K. L. Manipulation of Glutathione-Mediated Degradation of Thiol–Maleimide Conjugates. *Bioconjug. Chem.* **2018**, *29* (11), 3595–3605.
- (70) Mark, E. B. Bromomaleimides: New Reagents for the Selective and Reversible Modification of Cysteine. *Chem. Commun.* **2009**, No. 43, 6583–6585.
- (71) Smith, M. E.; Schumacher, F. F.; Ryan, C. P.; Tedaldi, L. M.; Papaioannou, D.; Waksman, G.; Caddick, S.; Baker, J. R. Protein Modification, Bioconjugation, and Disulfide Bridging Using Bromomaleimides. *J. Am. Chem. Soc.* **2010**, *132* (6), 1960–1965.
- (72) Ryan, C. P.; Smith, M. E. B.; Schumacher, F. F.; Grohmann, D.; Papaioannou, D.; Waksman, G.; Werner, F.; Baker, J. R.; Caddick, S. Tunable Reagents for Multi-Functional Bioconjugation: Reversible or Permanent Chemical Modification of Proteins and Peptides by Control of Maleimide Hydrolysis. *Chem Commun* **2011**, *47* (19), 5452–5454. <https://doi.org/10.1039/C1CC11114K>.
- (73) Moody, P.; Smith, M. E.; Ryan, C. P.; Chudasama, V.; Baker, J. R.; Molloy, J.; Caddick, S. Bromomaleimide-Linked Bioconjugates Are Cleavable in Mammalian Cells. *ChemBioChem* **2012**, *13* (1), 39.
- (74) Nathani, R. I.; Chudasama, V.; Ryan, C. P.; Moody, P. R.; Morgan, R. E.; Fitzmaurice, R. J.; Smith, M. E.; Baker, J. R.; Caddick, S. Reversible Protein Affinity-Labeling Using Bromomaleimide-Based Reagents. *Org. Biomol. Chem.* **2013**, *11* (15), 2408–2411.
- (75) Ross, A.; Durmaz, H.; Cheng, K.; Deng, X.; Liu, Y.; Oh, J.; Chen, Z.; Lahann, J. Selective and Reversible Binding of Thiol-Functionalized Biomolecules on Polymers Prepared via Chemical Vapor Deposition Polymerization. *Langmuir* **2015**, *31* (18), 5123–5129.

- (76) Zhang, Y.; Zhou, X.; Xie, Y.; Greenberg, M. M.; Xi, Z.; Zhou, C. Thiol Specific and Tracelessly Removable Bioconjugation via Michael Addition to 5-Methylene Pyrrolones. *J. Am. Chem. Soc.* **2017**, *139* (17), 6146–6151.
- (77) Chudasama, V.; Smith, M. E. B.; Schumacher, F. F.; Papaioannou, D.; Waksman, G.; Baker, J. R.; Caddick, S. Bromopyridazinedione-Mediated Protein and Peptide Bioconjugation. *Chem Commun* **2011**, *47* (31), 8781–8783. <https://doi.org/10.1039/C1CC12807H>.
- (78) Bahou, C.; Szijj, P. A.; Spears, R. J.; Wall, A.; Javaid, F.; Sattikar, A.; Love, E. A.; Baker, J. R.; Chudasama, V. A Plug-and-Play Platform for the Formation of Trifunctional Cysteine Bioconjugates That Also Offers Control over Thiol Cleavability. *Bioconjug. Chem.* **2021**, *32* (4), 672–679.
- (79) Bahou, C.; Spears, R. J.; Aliev, A. E.; Maruani, A.; Fernandez, M.; Javaid, F.; Szijj, P. A.; Baker, J. R.; Chudasama, V. Use of Pyridazinediones as Extracellular Cleavable Linkers through Reversible Cysteine Conjugation. *Chem. Commun.* **2019**, *55* (98), 14829–14832.
- (80) Yu, J.; Yang, X.; Sun, Y.; Yin, Z. Highly Reactive and Tracelessly Cleavable Cysteine-Specific Modification of Proteins via 4-Substituted Cyclopentenone. *Angew. Chem.* **2018**, *130* (36), 11772–11776.
- (81) Hogg, P. J. Disulfide Bonds as Switches for Protein Function. *Trends Biochem. Sci.* **2003**, *28* (4), 210–214.
- (82) Brocchini, S.; Balan, S.; Godwin, A.; Choi, J.-W.; Zloh, M.; Shaunak, S. PEGylation of Native Disulfide Bonds in Proteins. *Nat. Protoc.* **2006**, *1* (5), 2241–2252.

- (83) Shaunak, S.; Godwin, A.; Choi, J.-W.; Balan, S.; Pedone, E.; Vijayarangam, D.; Heidelberger, S.; Teo, I.; Zloh, M.; Brocchini, S. Site-Specific PEGylation of Native Disulfide Bonds in Therapeutic Proteins. *Nat. Chem. Biol.* **2006**, *2* (6), 312–313.
- (84) Jones, M. W.; Strickland, R. A.; Schumacher, F. F.; Caddick, S.; Baker, J. R.; Gibson, M. I.; Haddleton, D. M. Polymeric Dibromomaleimides as Extremely Efficient Disulfide Bridging Bioconjugation and Pegylation Agents. *J. Am. Chem. Soc.* **2012**, *134* (3), 1847–1852.
- (85) Schumacher, F. F.; Sanchania, V. A.; Tolner, B.; Wright, Z. V.; Ryan, C. P.; Smith, M. E.; Ward, J. M.; Caddick, S.; Kay, C. W.; Aeppli, G. Homogeneous Antibody Fragment Conjugation by Disulfide Bridging Introduces ‘Spinostics.’ *Sci. Rep.* **2013**, *3* (1), 1–8.
- (86) Petersen, M. T. N.; Jonson, P. H.; Petersen, S. B. Amino Acid Neighbours and Detailed Conformational Analysis of Cysteines in Proteins. *Protein Eng.* **1999**, *12* (7), 535–548.
- (87) Eldjarn, L.; Pihl, A. The Equilibrium Constants and Oxidation-Reduction Potentials of Some Thiol-Disulfide Systems¹. *J. Am. Chem. Soc.* **1957**, *79* (17), 4589–4593.
- (88) Schumacher, F. F.; Nobles, M.; Ryan, C. P.; Smith, M. E.; Tinker, A.; Caddick, S.; Baker, J. R. In Situ Maleimide Bridging of Disulfides and a New Approach to Protein PEGylation. *Bioconjug. Chem.* **2011**, *22* (2), 132–136.
- (89) Jones, M. W.; Strickland, R. A.; Schumacher, F. F.; Caddick, S.; Baker, J. R.; Gibson, M. I.; Haddleton, D. M. Highly Efficient Disulfide Bridging Polymers for Bioconjugates from Radical-Compatible Dithiophenol Maleimides. *Chem. Commun.* **2012**, *48* (34), 4064–4066.
- (90) Collins, J.; Tanaka, J.; Wilson, P.; Kempe, K.; Davis, T. P.; McIntosh, M. P.; Whittaker, M. R.; Haddleton, D. M. In Situ Conjugation of Dithiophenol Maleimide Polymers and

- Oxytocin for Stable and Reversible Polymer–Peptide Conjugates. *Bioconjug. Chem.* **2015**, *26* (4), 633–638.
- (91) Marculescu, C.; Kossen, H.; Morgan, R. E.; Mayer, P.; Fletcher, S. A.; Tolner, B.; Chester, K. A.; Jones, L. H.; Baker, J. R. Aryloxymaleimides for Cysteine Modification, Disulfide Bridging and the Dual Functionalization of Disulfide Bonds. *Chem. Commun.* **2014**, *50* (54), 7139–7142.
- (92) Wang, T.; Ng, D. Y.; Wu, Y.; Thomas, J.; TamTran, T.; Weil, T. Bis-Sulfide Bioconjugates for Glutathione Triggered Tumor Responsive Drug Release. *Chem. Commun.* **2014**, *50* (9), 1116–1118.
- (93) Wilson, P.; Anastasaki, A.; Owen, M. R.; Kempe, K.; Haddleton, D. M.; Mann, S. K.; Johnston, A. P. R.; Quinn, J. F.; Whittaker, M. R.; Hogg, P. J.; Davis, T. P. Organic Arsenicals As Efficient and Highly Specific Linkers for Protein/Peptide–Polymer Conjugation. *J. Am. Chem. Soc.* **2015**, *137* (12), 4215–4222. <https://doi.org/10.1021/jacs.5b01140>.
- (94) Grison, C. M.; Burslem, G. M.; Miles, J. A.; Pilsl, L. K.; Yeo, D. J.; Imani, Z.; Warriner, S. L.; Webb, M. E.; Wilson, A. J. Double Quick, Double Click Reversible Peptide “Stapling.” *Chem. Sci.* **2017**, *8* (7), 5166–5171.
- (95) Lindsey-Crosthwait, A.; Rodriguez-Lema, D.; Walko, M.; Pask, C. M.; Wilson, A. J. Structural Optimization of Reversible Dibromomaleimide Peptide Stapling. *Pept. Sci.* **2020**, e24157.
- (96) Lee, M. T.; Maruani, A.; Baker, J. R.; Caddick, S.; Chudasama, V. Next-Generation Disulfide Stapling: Reduction and Functional Re-Bridging All in One. *Chem. Sci.* **2016**, *7* (1), 799–802.

- (97) Brown, S. P.; Smith III, A. B. Peptide/Protein Stapling and Unstapling: Introduction of s-Tetrazine, Photochemical Release, and Regeneration of the Peptide/Protein. *J. Am. Chem. Soc.* **2015**, *137* (12), 4034–4037.
- (98) Ernst, C.; Heidrich, J.; Sessler, C.; Sindlinger, J.; Schwarzer, D.; Koch, P.; Boeckler, F. M. Switching Between Bicyclic and Linear Peptides—The Sulfhydryl-Specific Linker TPSMB Enables Reversible Cyclization of Peptides. *Front. Chem.* **2018**, *6*, 484.
- (99) Reichert, C.; Borchard, G. Noncovalent PEGylation, An Innovative Subchapter in the Field of Protein Modification. *J. Pharm. Sci.* **2016**, *105* (2), 386–390. <https://doi.org/10.1002/jps.24692>.
- (100) Antonik, P. M.; Eissa, A. M.; Round, A. R.; Cameron, N. R.; Crowley, P. B. Noncovalent PEGylation via Lectin-Glycopolymer Interactions. *Biomacromolecules* **2016**, *17* (8), 2719–2725. <https://doi.org/10.1021/acs.biomac.6b00766>.
- (101) Weber, P. C.; Ohlendof, D. H.; Wendoloskii, J. J.; Salemme, F. R. Structural Origins of High-Affinity Biotin Binding. *Science* **1989**, *243*, 85–88.
- (102) Urbach, A. R.; Ramalingam, V. Molecular Recognition of Amino Acids, Peptides, and Proteins by Cucurbit[n]uril Receptors. *Isr. J. Chem.* **2011**, *51* (5–6), 664–678. <https://doi.org/10.1002/ijch.201100035>.
- (103) Mastrotto, F.; Bellato, F.; Andretto, V.; Malfanti, A.; Garofalo, M.; Salmaso, S.; Caliceti, P. Physical PEGylation to Prevent Insulin Fibrillation. *J. Pharm. Sci.* **2020**, *109* (1), 900–910. <https://doi.org/10.1016/j.xphs.2019.10.020>.
- (104) Mero, A.; Ishino, T.; Chaiken, I.; Veronese, F. M.; Pasut, G. Multivalent and Flexible PEG-Nitrilotriacetic Acid Derivatives for Non-Covalent Protein Pegylation. *Pharm. Res.* **2011**, *28* (10), 2412–2421. <https://doi.org/10.1007/s11095-011-0468-8>.

- (105) Khondee, S.; Olsen, C. M.; Zeng, Y.; Middaugh, C. R.; Berkland, C. Noncovalent PEGylation by Polyanion Complexation as a Means to Stabilize Keratinocyte Growth Factor-2 (KGF-2). *Biomacromolecules* **2011**, *12* (11), 3880–3894. <https://doi.org/10.1021/bm2007967>.
- (106) Du, X.; Dubin, P. L.; Hoagland, D. A.; Sun, L. Protein-Selective Coacervation with Hyaluronic Acid. *Biomacromolecules* **2014**, *15* (3), 726–734. <https://doi.org/10.1021/bm500041a>.
- (107) Bontempo, D.; Maynard, H. D. Streptavidin as a Macroinitiator for Polymerization: In Situ Protein-Polymer Conjugate Formation. *J. Am. Chem. Soc.* **2005**, *127* (18), 6508–6509. <https://doi.org/10.1021/ja042230+>.
- (108) Heredia, K. L.; Grover, G. N.; Tao, L.; Maynard, H. D. Synthesis of Heterotelechelic Polymers for Conjugation of Two Different Proteins. *Macromolecules* **2009**, *42* (7), 2360–2367. <https://doi.org/10.1021/ma8022712>.
- (109) Wang, L.; Yang, Y. W.; Zhu, M.; Qiu, G.; Wu, G.; Gao, H. β -Cyclodextrin-Conjugated Amino Poly(Glycerol Methacrylate)s for Efficient Insulin Delivery. *RSC Adv.* **2014**, *4* (13), 6478–6485. <https://doi.org/10.1039/c3ra47150k>.
- (110) Webber, M. J.; Appel, E. A.; Vinciguerra, B.; Cortinas, A. B.; Thapa, L. S. Supramolecular PEGylation of Biopharmaceuticals. **2016**, No. 19, 3–8. <https://doi.org/10.1073/pnas.1616639113>.
- (111) Maikawa, C. L.; Smith, A. A. A.; Zou, L.; Meis, C. M.; Mann, J. L.; Webber, M. J.; Appel, E. A. Stable Monomeric Insulin Formulations Enabled by Supramolecular PEGylation of Insulin Analogues. *Adv. Ther.* **2020**, *3* (1), 1900094. <https://doi.org/10.1002/adtp.201900094>.

- (112) Maikawa, C. L.; Smith, A. A. A.; Zou, L.; Roth, G. A.; Gale, E. C.; Stapleton, L. M.; Baker, S. W.; Mann, J. L.; Yu, A. C.; Correa, S.; Grosskopf, A. K.; Liong, C. S.; Meis, C. M.; Chan, D.; Troxell, M.; Maahs, D. M.; Buckingham, B. A.; Webber, M. J.; Appel, E. A. A Co-Formulation of Supramolecularly Stabilized Insulin and Pramlintide Enhances Mealtime Glucagon Suppression in Diabetic Pigs. *Nat. Biomed. Eng.* **2020**, *4* (May). <https://doi.org/10.1038/s41551-020-0555-4>.
- (113) Mueller, C.; Capelle, M. A. H.; Arvinte, T.; Seyrek, E.; Borchard, G. Noncovalent Pegylation by Dansyl-Poly(Ethylene Glycol)s as a New Means against Aggregation of Salmon Calcitonin. *J. Pharm. Sci.* **2011**, *100* (5), 1648–1662. <https://doi.org/10.1002/jps.22401>.
- (114) Mueller, C.; Capelle, M. A. H.; Arvinte, T.; Seyrek, E.; Borchard, G. Tryptophan-MPEGs: Novel Excipients That Stabilize Salmon Calcitonin against Aggregation by Non-Covalent PEGylation. *Eur. J. Pharm. Biopharm.* **2011**, *79* (3), 646–657. <https://doi.org/10.1016/j.ejpb.2011.06.003>.
- (115) Mueller, C.; Capelle, M. A. H.; Seyrek, E.; Martel, S.; Carrupt, P. A.; Arvinte, T.; Borchard, G. Noncovalent PEGylation: Different Effects of Dansyl-, l-Tryptophan-, Phenylbutylamino-, Benzyl- and Cholesteryl-PEGs on the Aggregation of Salmon Calcitonin and Lysozyme. *J. Pharm. Sci.* **2012**, *101* (6), 1995–2008. <https://doi.org/10.1002/jps.23110>.
- (116) Asayama, S.; Nagashima, K.; Negishi, Y.; Kawakami, H. Byproduct-Free Intact Modification of Insulin by Cholesterol End-Modified Poly(Ethylene Glycol) for in Vivo Protein Delivery. *Bioconjug. Chem.* **2018**, *29* (1), 67–73. <https://doi.org/10.1021/acs.bioconjchem.7b00593>.

- (117) Cho, H. Y.; Kadir, M. A.; Kim, B. S.; Han, H. S.; Nagasundarapandian, S.; Kim, Y. R.; Ko, S. B.; Lee, S. G.; Paik, H. J. Synthesis of Well-Defined (Nitrilotriacetic Acid)-End-Functionalized Polystyrenes and Their Bioconjugation with Histidine-Tagged Green Fluorescent Proteins. *Macromolecules* **2011**, *44* (12), 4672–4680. <https://doi.org/10.1021/ma200480f>.
- (118) Kim, T. H.; Swierczewska, M.; Oh, Y.; Kim, A.; Jo, D. G.; Park, J. H.; Byun, Y.; Sadegh-Nasseri, S.; Pomper, M. G.; Lee, K. C.; Lee, S. Mix to Validate: A Facile, Reversible Pegylation for Fast Screening of Potential Therapeutic Proteins in Vivo. *Angew. Chem. - Int. Ed.* **2013**, *52* (27), 6880–6884. <https://doi.org/10.1002/anie.201302181>.
- (119) Duret, D.; Haftek-Terreau, Z.; Carretier, M.; Ladavière, C.; Charreyre, M. T.; Favier, A. Fluorescent RAFT Polymers Bearing a Nitrilotriacetic Acid (NTA) Ligand at the α -Chain-End for the Site-Specific Labeling of Histidine-Tagged Proteins. *Polym. Chem.* **2017**, *8* (10), 1611–1615. <https://doi.org/10.1039/c6py02222g>.
- (120) Nguyen, D. T.; Cavazos, R. J.; Harris, A. N.; Petros, R. A. Werner Complexes Viewed Anew: Utilizing Cobalt Coordination Chemistry for ‘Traceless’ Stimuli-Responsive Bioconjugation Involving Therapeutic Nanoparticles, Protein PEGylation, and Drug-(Bio)Polymer Conjugates. *Comments Inorg. Chem.* **2014**, *34* (3–4), 59–77. <https://doi.org/10.1080/02603594.2014.940103>.
- (121) Asayama, S.; Nagashima, K.; Kawakami, H. Facile Method of Protein PEGylation by a Mono-Ion Complex. *ACS Omega* **2017**, *2* (5), 2382–2386. <https://doi.org/10.1021/acsomega.7b00462>.
- (122) Kurinomaru, T.; Shiraki, K. Noncovalent PEGylation of L-Asparaginase Using PEGylated Polyelectrolyte. *J. Pharm. Sci.* **2015**, *104* (2), 587–592. <https://doi.org/10.1002/jps.24217>.

- (123) Kurinomaru, T.; Kuwada, K.; Tomita, S.; Kameda, T.; Shiraki, K. Noncovalent PEGylation through Protein-Polyelectrolyte Interaction: Kinetic Experiment and Molecular Dynamics Simulation. *J. Phys. Chem. B* **2017**, *121* (28), 6785–6791. <https://doi.org/10.1021/acs.jpcc.7b02741>.
- (124) Kurinomaru, T.; Tomita, S.; Kudo, S.; Ganguli, S.; Nagasaki, Y.; Shiraki, K. Improved Complementary Polymer Pair System: Switching for Enzyme Activity by PEGylated Polymers. *Langmuir* **2012**, *28* (9), 4334–4338. <https://doi.org/10.1021/la2043312>.
- (125) Nieto-Orellana, A.; Di Antonio, M.; Conte, C.; Falcone, F. H.; Bosquillon, C.; Childerhouse, N.; Mantovani, G.; Stolnik, S. Effect of Polymer Topology on Non-Covalent Polymer-Protein Complexation: Miktoarm versus Linear MPEG-Poly(Glutamic Acid) Copolymers. *Polym. Chem.* **2017**, *8* (14), 2210–2220. <https://doi.org/10.1039/c7py00169j>.
- (126) Nieto-Orellana, A.; Coghlan, D.; Rothery, M.; Falcone, F. H.; Bosquillon, C.; Childerhouse, N.; Mantovani, G.; Stolnik, S. Dry-Powder Formulations of Non-Covalent Protein Complexes with Linear or Miktoarm Copolymers for Pulmonary Delivery. *Int. J. Pharm.* **2018**, *540* (1–2), 78–88. <https://doi.org/10.1016/j.ijpharm.2018.02.008>.
- (127) Tsiourvas, D.; Sideratou, Z.; Sterioti, N.; Papadopoulos, A.; Nounesis, G.; Paleos, C. M. Insulin Complexes with PEGylated Basic Oligopeptides. *J. Colloid Interface Sci.* **2012**, *384* (1), 61–72. <https://doi.org/10.1016/j.jcis.2012.06.068>.
- (128) Gao, S.; Holkar, A.; Srivastava, S. Protein – Polyelectrolyte Complexes and Micellar Assemblies. *Polymers* **2019**, *11*, 1097.
- (129) Seyrek, E.; Dubin, P. L.; Tribet, C.; Gamble, E. A. Ionic Strength Dependence of Protein-Polyelectrolyte Interactions. *Biomacromolecules* **2003**, *4* (2), 273–282. <https://doi.org/10.1021/bm025664a>.

- (130) Kuwada, K.; Kurinomaru, T.; Tomita, S.; Shiraki, K. Noncovalent PEGylation-Based Enzyme Switch in Physiological Saline Conditions Using Quaternized Polyamines. *Colloid Polym. Sci.* **2016**, *294* (10), 1551–1556. <https://doi.org/10.1007/s00396-016-3916-5>.

Chapter 2

Development of a Dual-Enzyme Responsive

Elastomeric Abuse-Deterrent Opioid

Formulation

2.1 Introduction

The United States has a tumultuous past with opioids dating back to late 19th century. The rise in prescription opioid use throughout the United States over the past few decades has been traced back to multiple factors including an unsubstantiated letter to the editor published in the New England Journal of Medicine,¹ aggressive promotional tactics employed by pharmaceutical companies, as well as a lack of oversight and education for regulators and physicians alike.² The overreliance on opioids has been exacerbated over the past 20 years, resulting in a 6-fold increase in opioid associated deaths. The centers for disease control and prevention (CDC) reported that in 2018 around 10 million people within the United States (US) have reported misusing prescription opioids which led to 17 thousand opioid-associated deaths.³ Economists have calculated that the opioid crisis has cost the US an estimated \$1.02 trillion for 2017 alone, emphasizing the magnitude of this epidemic.⁴ It is now widely recognized that despite their effectiveness for reducing both acute and chronic pain, these highly addictive opioids have been heavily overprescribed, and some form of intervention is required to mitigate the costs to our society and prevent further loss of life.

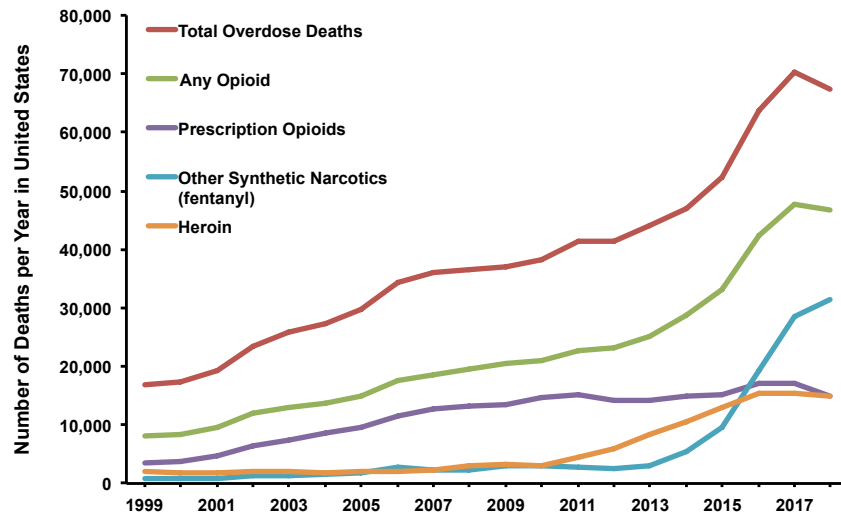


Figure 2.1. Number of deaths per year in the United States attributed to drug overdose. Chart plotted from data made available from the National Institute on Drug Abuse.⁵

In 2017 the US Department of Health and Human Services formally recognized the opioid epidemic as a national health crisis and a plan of action was implemented to reverse the damage done by this class of pharmaceuticals.⁶ The scale and complexity of this issue require a multifaceted approach with many measures working in conjunction to effectively combat the crisis. One of the proposed countermeasures included the development of opioid formulations that contain abuse-deterrent (AD) engineering controls, which are designed to mitigate the typical forms of abuse.⁷ Prescription opioids are most commonly abused by ingesting a dose that is larger than prescribed, which results in a euphoric sensation.⁸ Most prescription opioids are designed for relatively slow, sustained release over time, so while orally ingesting more than a prescribed dose will provide a rewarding euphoric sensation, alternative routes of administration such as nasal insufflation or intravenous injection elicit a faster onset of effects along with higher potency.⁸ Opioid formulations without engineered safeguards against these routes of administration are therefore associated with greater abuse potential, highlighting the FDA’s call for AD opioid formulations.^{9,10}

The FDA has described 5 general strategies for developing AD formulations including: physical or chemical barriers to mechanical alteration, agonist/antagonist combinations, coformulation with aversive substances released upon tampering, unconventional delivery systems (subcutaneous implants), and prodrugs which are only activated after oral administration.¹¹ These AD formulations increase the difficulty for patients to extract out large amounts of the active ingredient (i.e. hydrocodone or oxycodone) for instant release in pursuit of the euphoric effects. This is commonly done via ethanol extraction or crushing of the pills for intravenous/intranasal administration.⁸ The AD formulations currently approved by the FDA all rely on a noncovalent encapsulation strategy, wherein the opioid is sequestered within a porous polymeric network that slowly releases the opioid.⁷ The polymeric networks typically employed possess a high mechanical strength and rigidity, thus ensuring they cannot be crushed into a fine powder. In addition to this, many AD formulations currently utilize hydrophilic polymers that swell in the presence of water or ethanol (common solvents used in the extraction process), which prevents extracted material from being pulled through the needle of a syringe prior to intravenous injection. Lastly, some formulations contain a core of sequestered antagonist, which only release upon tampering with the formulation thus counteracting any instant-release effects of the opioid. The ten FDA approved AD formulations employ one or more of these strategies to deliver hydrocodone, oxycodone, or morphine safely to the patient (Table 2.1).

Brand Name	Active Ingredients	Sequestered Antagonist	Year of FDA Approval
OxyContin	Oxycodone	–	2010
Xtampza ER	Oxycodone	–	2016
Troxyca ER	Oxycodone	Naltrexone	2016
Targiniq ER	Oxycodone	Naloxone	2014

Roxybond	Oxycodone	–	2017
Hysingla ER	Hydrocodone	–	2014
Vantrella ER	Hydrocodone	–	2017
Embeda	Morphine	Naltrexone	2014
Morphabond ER	Morphine	–	2015
Arymo ER	Morphine	–	2017

Table 2.1. List of FDA approved abuse-deterrent opioid formulations.⁷

Even with these engineering controls in place, many of the AD formulations currently on the market can be circumvented by knowledgeable addicts using household supplies, reducing their effectiveness.^{12,13} Typical routes to circumvent these AD formulations include depressing the temperature of the polymeric network below its T_g thus decreasing its mechanical strength and allowing it to be ground into a fine powder. To circumvent any swelling of the formulation during the extraction process, a simple filtration prior to intravenous administration prevents any clogging of the needle.

A promising alternative to these noncovalent abuse-deterrent strategies is to employ covalent modifications that control the release parameters of the opioid. This strategy relies on a prodrug designed to sequester opioid release within the gastrointestinal tract, safeguarding against the intravenous and intranasal routes of abuse.¹⁴ An abuse-deterrent prodrug should also be resistant against physical and chemical manipulations, thus ensuring that abusers cannot release the opioid to its full potency prior to ingestion. Ideally, the rate of opioid release from the prodrug would contain a rate limiting step independent of concentration, so that even oral administration of elevated dosages will not necessarily translate into elevated levels of the opioid in circulation. This prodrug strategy is currently being pursued by three separate companies all of which are in

phase three clinical trials.¹⁴ Two of these prodrugs take advantage of the acidic conditions in the stomach to cleave either an ester or phosphoester modification to the opioid. The third relies on trypsin, a protease found in the small intestine, which enzymatically cleaves the prodrug and releases oxycodone. Unfortunately, these prodrug strategies can still be easily circumvented by fairly simple chemical manipulations using household supplies, allowing users to quickly bypass the engineering controls.

In this chapter, we report the design and synthesis of a dual-enzyme responsive opioid prodrug that addresses the shortcomings of currently available abuse-deterrent formulations (Figure 2.2). This prodrug was developed based on our group's previously reported dual-enzyme responsive peptide that effectively released a small molecule reporter upon incubation with digestive enzymes trypsin and chymotrypsin.¹⁵ First, chymotrypsin is required to cleave the isopeptide bond between a phenylalanine residue and the ϵ -amine of a lysine residue. Once cleaved, the lysine residue is unmasked and can further be processed by trypsin, which further cleaves the lysine C-terminally and releases a primary amine. This primary amine can then rapidly cyclize and release an attached, active opioid, forming 1-methylimidazolidine-2-thione as a nontoxic byproduct.¹⁶ As an additional layer of protection, the prodrug was covalently attached within a polymeric matrix to resist any physical manipulations or extractions.

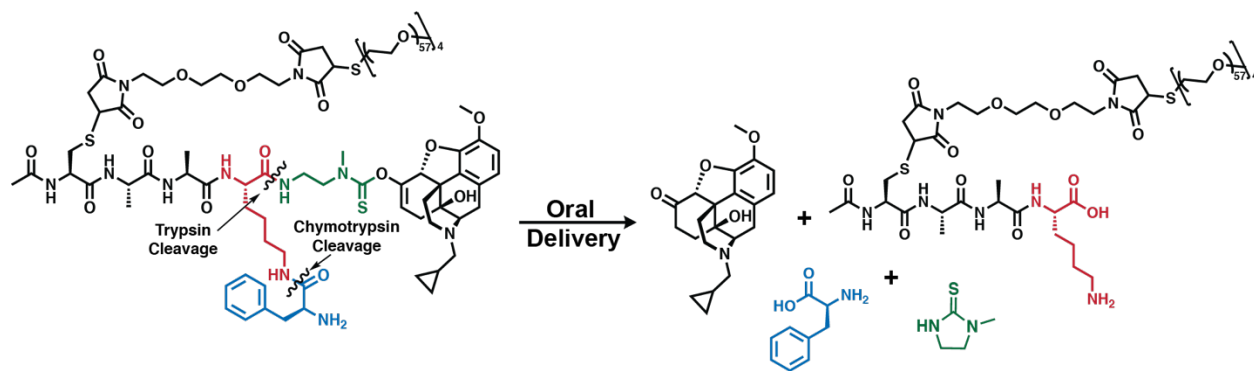


Figure 2.2. Abuse-deterrent elastomeric extended-release opioid prodrug formulation comprised of a dual enzyme-responsive peptide prodrug covalently bound within a PEG matrix.

Our AD-formulation design possesses several layers of protection against unintentional release (Figure 2.2). First, the polymeric backbone comprising the structural integrity of the formulation imparts a high mechanical strength, which inhibits any physical manipulation under household accessible temperatures. Second, two separate digestive enzymes are required to release the active opioid, making it significantly more difficult for individuals to chemically or biochemically manipulate the formulation and achieve burst release. Additionally, since these enzymes are only present in the gastrointestinal tract, administration by other routes will be ineffectual to release active opioid. Third, our prodrug is composed of stable, but reversible linkages that are resistant to unintended release that is most commonly facilitated by hydrolysis. Lastly, because enzymes control release of the opioid from the prodrug scaffold, the release rate may be sufficiently slow so that even if the prodrug is orally overdosed, only a limited amount of the prodrug may be enzymatically processed, thereby mitigating burst release. We expect that this platform will therefore offer significant improvements to the currently available abuse-deterrent formulations.

In the following sections, we report the development of chemistry to activate functional groups common across most opioids for conjugation to our dual-enzyme responsive peptide

platform in order to synthesize an abuse-deterrent opioid prodrug. We then demonstrate the application of this chemistry into a crosslinked polymeric network for increased mechanical strength and evaluate the stability of the formulation to a broad pH range. Finally, we describe optimization of this chemistry, elucidation of possible downstream bottlenecks, and redesign our system in order to mitigate them.

2.2 Results and Discussion

2.2.1 Evaluation of Common Opioids for Reversible Modification

Oxycodone and hydrocodone are the two most commonly prescribed opioids for acute pain with 9 of the 10 FDA approved AD formulations containing one of these active ingredients.⁷ Conserved across these two opioids is the ketone, which we identified as a potential linkage point for the peptide (Figure 2.3). We postulated that if we could selectively prepare the O-enolate by trapping it with either a chloroformate or thionochloroformate, this could be used as an electrophile to subsequently attach to the peptide. Due to the highly controlled nature of these opioids, we chose to use O-methylated naltrexone as a surrogate for oxycodone and hydrocodone due to the conserved structural features of interest.

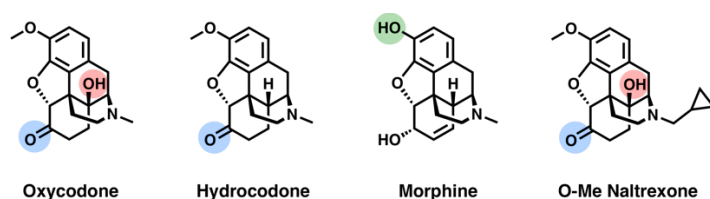


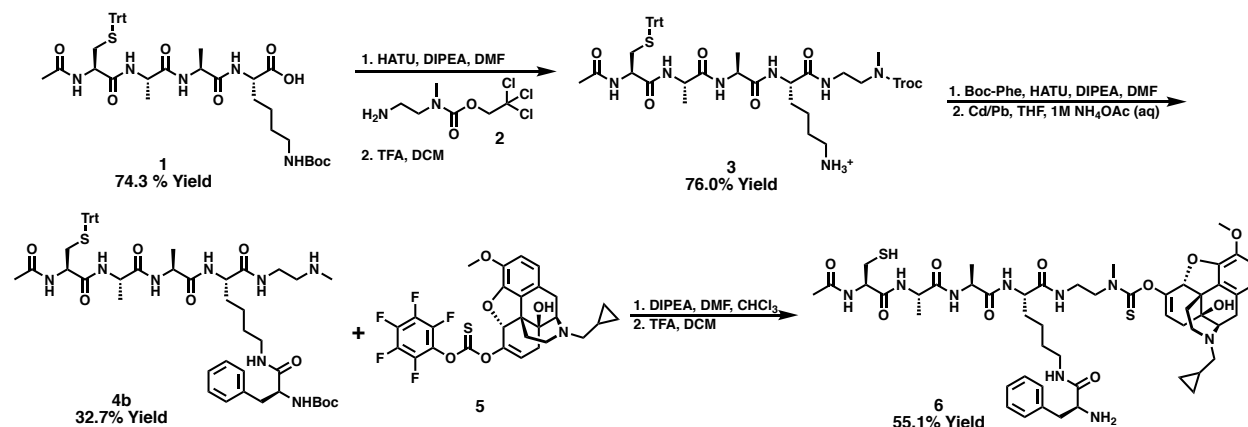
Figure 2.3. Commonly prescribed opioids and their conserved reactive handles highlighted.

Initially, we were worried that the tertiary alcohol on naltrexone and oxycodone was accessible as a secondary point of conjugation therefore minimizing the selectivity of this strategy. In order to circumvent this issue, we attempted to protect this alcohol, however all such attempts

resulted in no modification. Looking at the modeled structure it is clear that the steric congestion around that alcohol makes it inaccessible for any modifications. This observation enhanced our optimism for an enolate linkage strategy with minimal cross reactivity for both oxycodone and hydrocodone substrates.

With the thionocarbamate linkage strategy in mind, the next step was to selectively O-acylate the enolate. To this end, conditions were screened to selectively favor the O-acylation of the enolate over the corresponding C-acylation products. It has been previously shown that the use of a coordinating solvent and a hard electrophile favors O-acylation. We found that the use of potassium bis(trimethylsilyl)amide (KHMDs) as a base, dimethoxyethane (DME) as a solvent, and pentafluorophenyl thionochloroformate (PFPTC) as an electrophile minimized C-acylation products and progressed to full conversion. The resulting thionocarbonate electrophile was stable to HPLC purification and prolonged storage increasing its usefulness compared to the carbonate electrophile which rapidly hydrolyzed under similar conditions. Additionally, studies were carried out to compare the carbamate and thionocarbamate linkages with the peptide, which showed that the thionocarbamate linkage was significantly more stable across a range of pH's. This was likely due to the diminished electrophilicity at the carbon atom of the thionocarbamate as a result of the significantly less electronegative sulfur atom. Thus, the thionocarbamate linkage was chosen for all future modifications.

2.2.2 Preparation of a Peptide-Opioid Prodrug



Scheme 2.1. Synthesis of peptide-naltrexone prodrug (**6**) prepared from Ac-C(Trt)AAK(Boc).

The peptide portion of the prodrug was designed based on our previous work using dual enzyme responsive linkers to include both a trypsin and chymotrypsin recognition sequence masking one another (Figure 2.1). In addition, we included a cysteine residue to provide a thiol for thiol-ene conjugation to a vinyl containing polymeric matrix. Due to the unique branching structure of the prodrug, it was not feasible to prepare it entirely on resin. Instead, we chose to prepare the cysteine-alanine-alanine-lysine peptide backbone on resin to use as a scaffolding. With this protected peptide in hand, we then coupled **2** to the C-terminus of the peptide. The 2,2,2-trichloroethoxycarbonyl (Troc) protecting group was chosen as an orthogonal protecting group to the acid labile tert-butyloxycarbonyl (Boc) and triphenylmethyl (trityl) protecting groups where the deprotection conditions are not sensitive to the presence of thiols. Following the addition of the protected diamine, the Boc protecting group on the lysine's ϵ -amine was selectively deprotected over the trityl using a mixture of trifluoroacetic acid (TFA) and dichloromethane (DCM) which did not contain any scavenger. At this point, the Boc-phenylalanine was coupled to the lysine side chain, after which, the Troc was selectively removed using a zinc-lead couple. This

peptide was then coupled to the naltrexone electrophile **5** under basic conditions followed by the simultaneous deprotection of the trityl and Boc groups to afford the final prodrug.

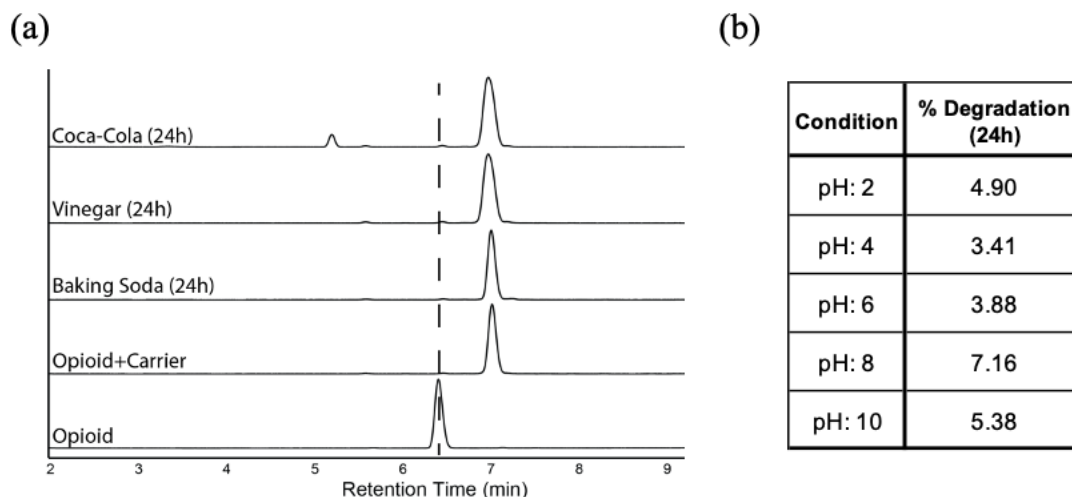


Figure 2.4. Stability of peptide prodrug (**6**) to (a) common household solvents and (b) 50 mM citrate-phosphate (McIlvaine) buffer within a pH range of 2 to 10.

The water solubility of the prodrug was also considered when designing the peptide-prodrug structure. It was found that while more hydrophobic peptides would increase participation in the polysiloxane modifications, the decreased water solubility reduced the enzymatic rate of release. To that end, there needed to be at least one free amine present on the prodrug (other than the one on the opioid) to ensure the right hydrophilicity and enzymatic rate of release. The final structure shown above proved to be the optimal candidate based on enzymatic release profiles, water solubility, and synthetic feasibility. In addition, the stability of the prodrug (**6**) was monitored over 24 hours across a range of pH's. It was found that the stability of the carbamate linkage was resilient to a wide range of conditions with minimal release of opioid. The absence of naltrexone was confirmed by liquid chromatography-mass spectrometry (LCMS) analysis.

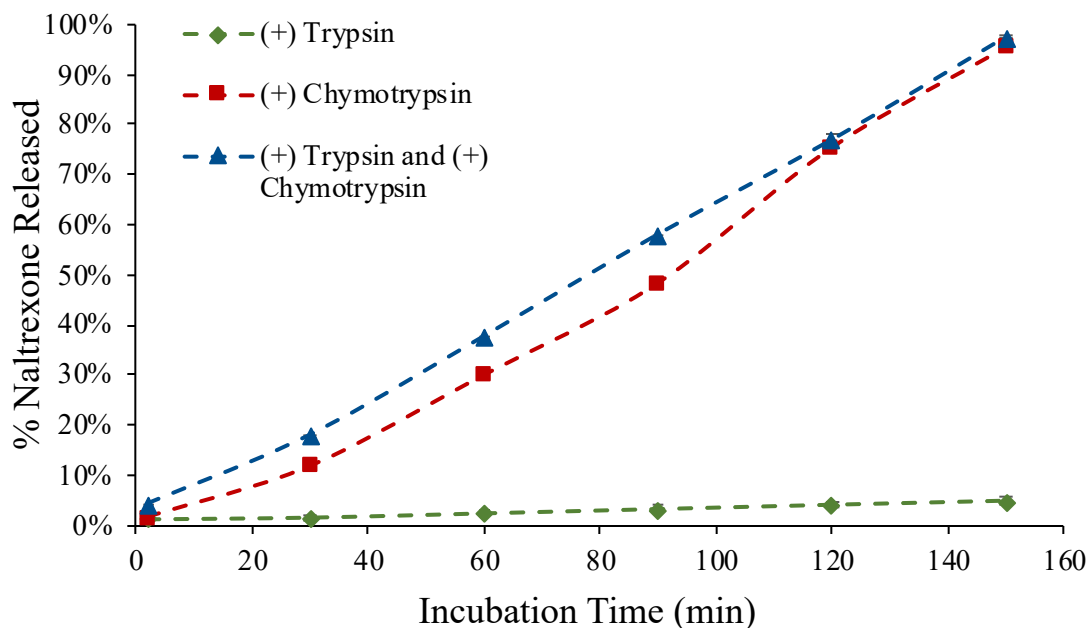


Figure 2.5. Protease responsive release of naltrexone from naltrexone-peptide prodrug (6) in the presence of either trypsin or chymotrypsin or both monitored by HPLC and confirmed by LCMS (n = 3 samples, error bars are smaller than markers).

In vitro simulated digestion assays were carried out in the presence of either trypsin, chymotrypsin, or both using 2 mM prodrug substrate at a 25:1 ratio to each protease in 35 mM (4-(2-hydroxyethyl)-1-piperazineethanesulfonic acid (HEPES) buffer (pH 7.4). Naltrexone release was monitored via HPLC, which showed 100% release within 2.5 hours in the presence of both enzymes. It was observed, however, that when the prodrug was incubated in the presence of only chymotrypsin there was significant background cleavage leading to unintended release of the opioid. The peptide was carried forward as is for use in preparing the elastomeric formulations, and optimization of the peptide sequence in order to mitigate this phenomenon is detailed in Chapter 3.

2.2.3 Development of a Polysiloxane Based Prodrug Formulation

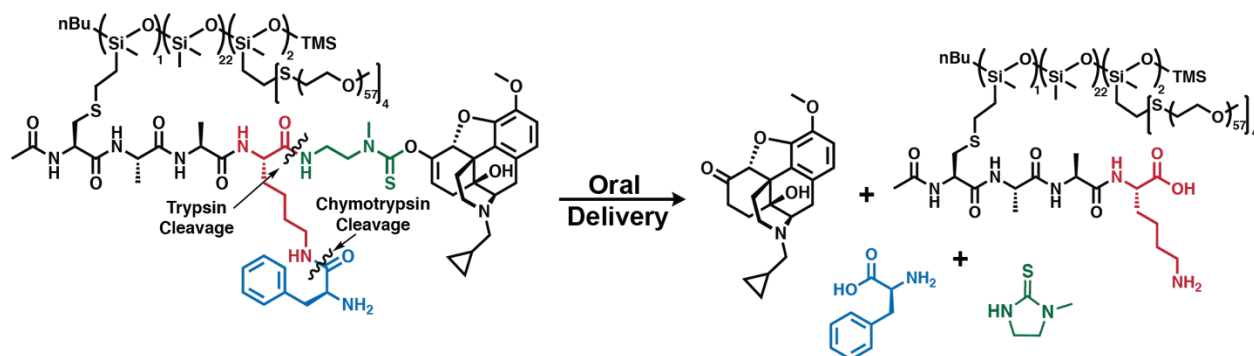
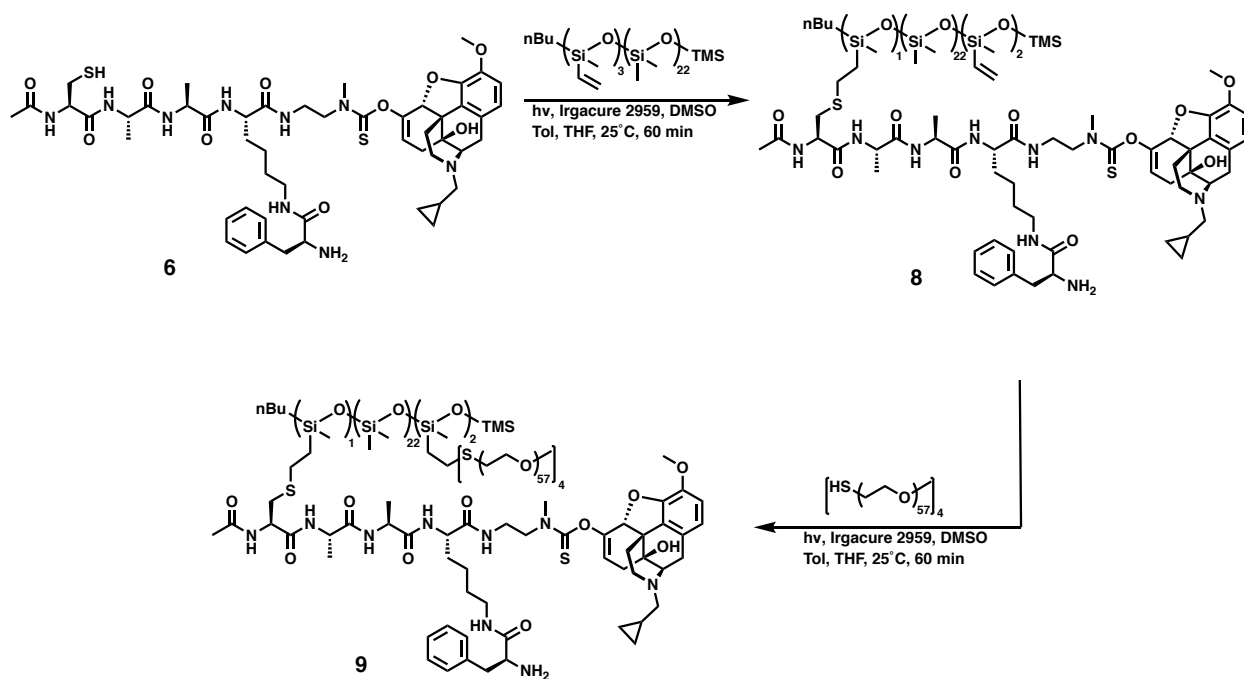


Figure 2.6. Abuse-deterrent elastomeric extended-release opioid prodrug formulation comprised of a dual enzyme-responsive peptide prodrug in a polysiloxane-PEG matrix.

Our initial design of the elastomeric prodrug relied on the use of a vinyl containing polysiloxane backbone that could be crosslinked through a radical thiol-ene reaction (Scheme 2.2). Polysiloxane was chosen as the polymeric matrix due to its low T_g and high mechanical strength once crosslinked, making it resistant towards crushing and shaving.¹⁷ Poly(vinylmethylsiloxane) (PMVS) has a T_g of $-130\text{ }^\circ\text{C}$ which is lower than a typical abuser would feasibly be able to achieve using household appliances. In addition, we found that the crosslinked elastomer (without the prodrug) was able to resist significant mechanical deformation using a hammer or razor blade even when cooled to $-190\text{ }^\circ\text{C}$. Our initial attempts to incorporate the peptide onto the vinyl containing polysiloxane backbone showed significant backbone crosslinking preferential to peptide incorporation when using either (30%-vinylmethylsiloxane)-dimethylsiloxane copolymer or PMVS. We hypothesized that the high prevalence of vinyl groups in close proximity to each other lead to backbone crosslinking rather than the intended peptide incorporation. When the vinyl incorporation was reduced below 0.25 vinyl groups per repeat unit the backbone crosslinking was minimized and prodrug incorporation efficiency increased. Therefore, we settled with a (12%-

vinylmethylsiloxane)-dimethylsiloxane copolymer which showed minimal crosslinking and effective thiol-ene reactivity (Scheme 2.2).



Scheme 2.2. Preparation of elastomeric prodrug (9) via a thiol-ene conjugation of the cysteine containing peptide to the vinyl-containing backbone followed by a thiol-ene crosslinking with 4-arm PEG-SH.

The polysiloxane elastomers proved to be very hydrophobic and fully collapsed in an aqueous environment which minimized the likelihood of proteolytic prodrug cleavage within the elastomer. To circumvent this issue, it was decided to incorporate a hydrophilic crosslinking agent that would not detract from the mechanical properties of the final elastomer. Although linear PEG dithiols did form hydrophilic elastomers, they were easily crushed after cooling to 0 °C. Further increasing the crosslinking density by using a 4-arm PEG thiol (10 kDa) afforded elastomers that maintained a high level of mechanical strength with an enhanced hydrophilicity (Scheme 2.2). With rigid elastomers in hand, scanning electron microscopy (SEM) was run to ensure that the pore size was large enough for the enzymes to permeate into the elastomeric network. It was observed that the elastomer had a significantly higher porosity, averaging 13 nm in diameter when

freeze dried from benzene, when compared to the nonporous surface after freeze drying from water (Figure 2.7). This phenomenon can be explained by the hydrophobic polysiloxane backbone collapsing in an aqueous environment. However, if the elastomer was incubated in an aqueous solution following its freeze drying from benzene, the porosity remained unaltered signifying that the morphology was locked into place. The locked conformation ensures that the porosity will be maintained during passage through the gastrointestinal tract, allowing the proteases to interact with the peptide sequence.

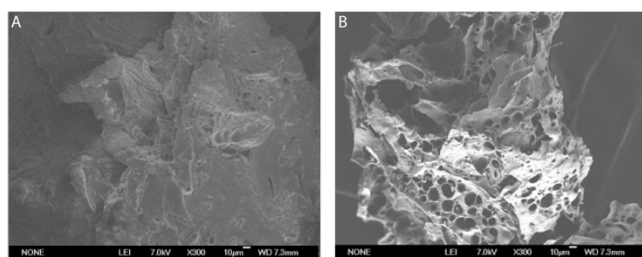


Figure 2.7. SEM characterization of elastomer lyophilized from (a) water or (b) benzene followed by incubation in water for 12 h.

With the hydrophilicity, mechanical strength, and porosity of the elastomer optimized, we began running naltrexone release studies. *In vitro* simulated digestion assays were once again carried out in the presence of either trypsin, chymotrypsin, or both using elastomer containing 2 mM of the prodrug at a 25:1 ratio to each protease in 35 mM HEPES buffer (pH 7.4). Naltrexone release reached 32% within 90 minutes, showing a slight reduction in the rate of release compared to the peptide-prodrug prior to attachment to the elastomer (Figure 2.8). This is likely caused by the reduced permeability of the proteases within the elastomer resulting in the rate reduction of 55%. In addition, the release of naltrexone in the presence of only chymotrypsin was observed similarly to that of the peptide-prodrug.

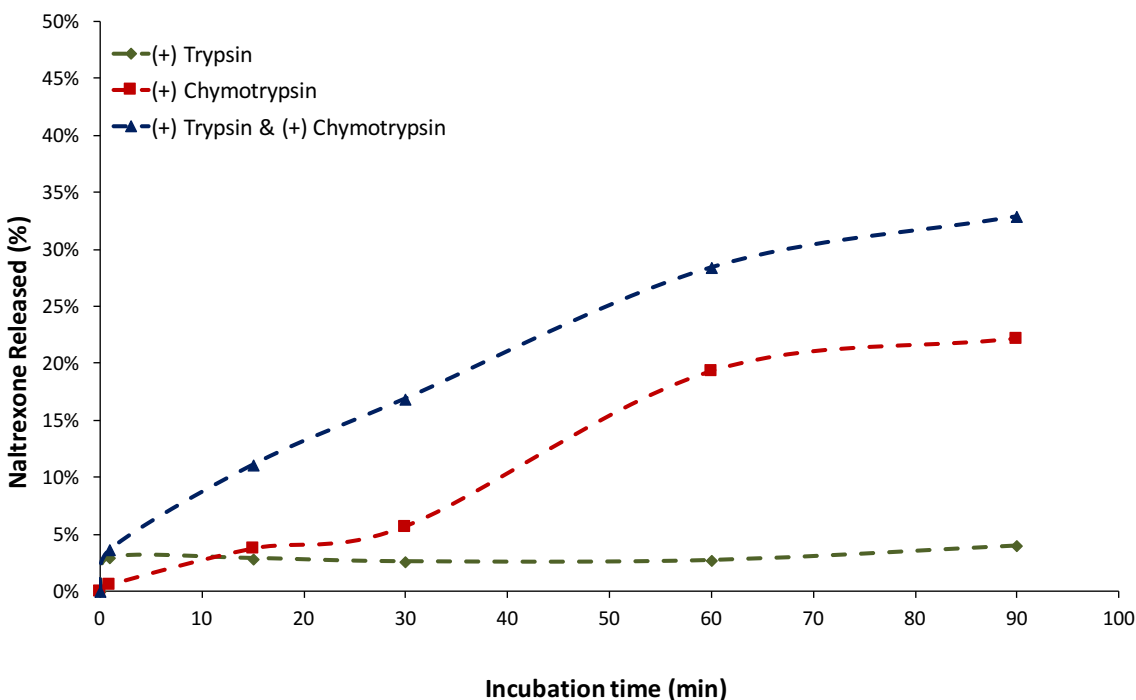


Figure 2.8. Protease responsive release of naltrexone from naltrexone-peptide-PMVS elastomer (9) in the presence of either trypsin or chymotrypsin or both monitored by HPLC and confirmed by LCMS.

Following confirmation of naltrexone release, the stability of the elastomeric prodrug to mechanical and chemical degradation was tested. The stability to mechanical deformation was carried out by attempting to crush and or shave the elastomer into fine particles after subjection to thermal stresses. The elastomer was unphased by subjection to microwave radiation (5 minutes or less), heating to 260 °C, and cooling to -20 °C (Table 2.3), three household accessible means commonly used to circumvent the AD formulations currently on the market. Exposure to microwave radiation for longer than 5 minutes resulted in a charred surface, and extractions with aqueous and polar protic solvents following this period showed no presence of opioid via HPLC analysis. In addition, the elastomer was stable to a suite of household chemicals including; lemon

juice, Coca-Cola, and aqueous saturated sodium bicarbonate, all resulting in a negligible amount of released naltrexone (see section 2.4.3).

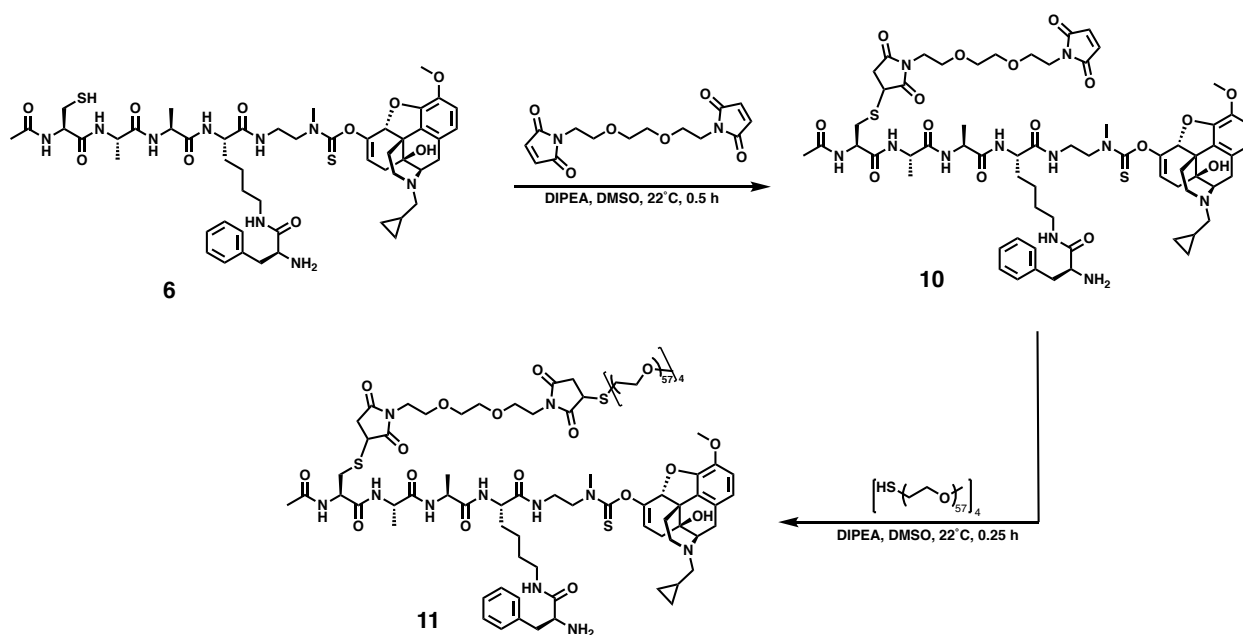
Condition	Time Subjected (h)	Pass/Fail
Microwave	0.02	Pass
Microwave	0.08	Pass
Microwave	0.17	Burnt
Heat to 260 °C	0.25	Pass
Heat to 260 °C	0.50	Pass
Heat to 260 °C	1	Pass
Cooling to -20 °C	12	Pass
Cooling to -20 °C	24	Pass

Table 2.2. Stability of polysiloxane based elastomer to physical manipulation under thermal stress. Pass refers to the elastomer maintaining structural integrity to crushing and cutting.

2.2.4 Development of a Crosslinked PEG Prodrug Formulation

Although enough elastomer was prepared for the naltrexone release assay and stability studies, the scale of the peptide conjugation step was limited. Attempting the conjugation on a scale larger than 100 mg of polysiloxane resulted in insufficient peptide incorporation and/or significant backbone crosslinking. It was decided that an alternative strategy should be pursued since any progression forward with the project would require a substantial increase in the synthetic output. The leading cause of the inefficient conjugation was the incompatible solubilities of the polysiloxane and peptide substrates. This led to an immiscibility of both substrates in any one solvent and only a very precise solution of multiple solvents allowed the thiol-ene reaction to

proceed efficiently. Rather than continuing to optimize this system we elected to remove the polysiloxane backbone which was at the heart of the synthetic issues within this project. Along with the removal of the polysiloxane, the system was modified to the more efficient and robust thiol-maleimide conjugation using a multi-arm PEG framework (Scheme 2.3). This reduced the elastomer's stability towards low temperature physical manipulations; however, the enzymatic release would limit any significant “dose dumping” effects and protect against non-oral routes of administration.



Scheme 2.3. Preparation of prodrug hydrogel (11) via a thiol-maleimide conjugation of the cysteine containing peptide to a bismaleimido-diethyleneglycol crosslinker followed by crosslinking with 4-arm PEG-SH.

The updated PEG delivery system was prepared by initially conjugating bismaleimido-diethyleneglycol onto the peptide-prodrug (6) under basic conditions (Scheme 2.3). Without any purification the four-arm PEG-thiol was then added to the maleimide-peptide-prodrug to form the crosslinked hydrogel network. Initial attempts at the preparation of 11 using a higher crosslinking density formed rigid hydrogels, however no naltrexone release was observed from these hydrogels.

It was surmised that the crosslinking density must be kept low in order to ensure that the mesh size was larger than the hydrodynamic radius of the enzymes.

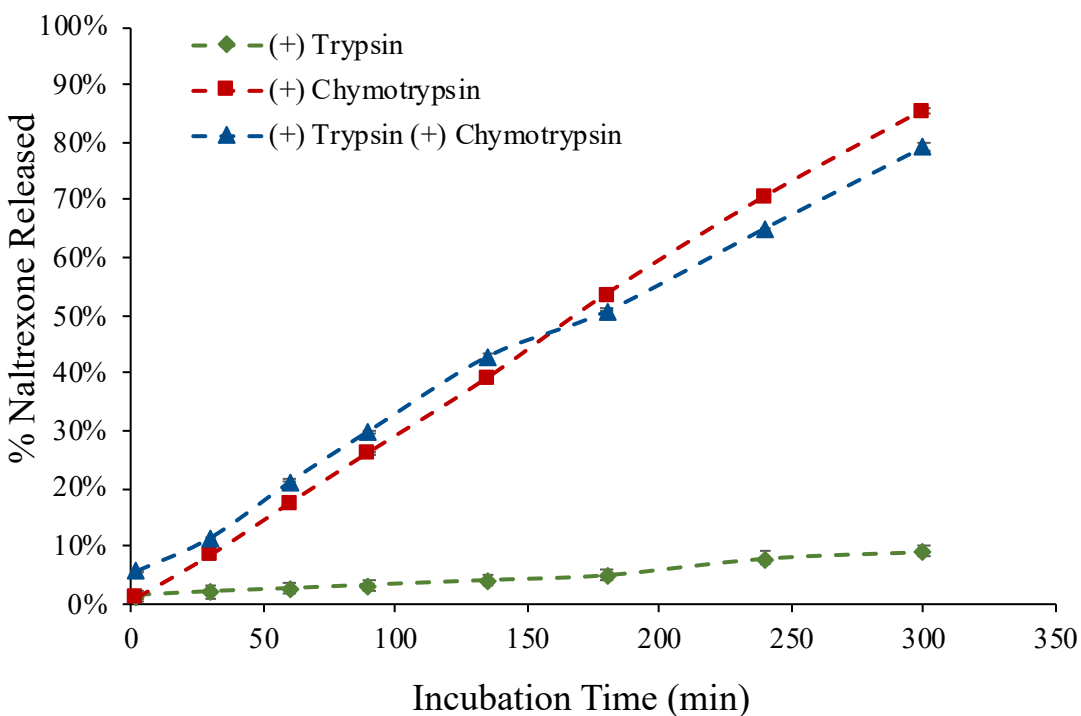


Figure 2.9. Protease responsive release of naltrexone from naltrexone-peptide-PEG hydrogel (9) in the presence of either trypsin or chymotrypsin or both monitored by HPLC and confirmed by LCMS ($n = 3$, error bars are smaller than markers).

In vitro simulated digestion assays were once again carried out in the presence of either trypsin, chymotrypsin, or both using hydrogel containing 2 mM of the prodrug at a 25:1 ratio to each protease in 35 mM HEPES buffer (pH 7.4). Naltrexone release reached 30% within 90 minutes, showing a comparable rate of release with the polysiloxane elastomer. The naltrexone continued to release over the course of 5 hours where it reached 86%. The stability of the elastomer to aqueous solutions ranging from pH 2.5 to 10 showed no release of naltrexone, which was confirmed by LCMS analysis.

This system appears to be ideal for a slow sustained opioid delivery via an oral administration pathway. The incorporation of the opioid into an enzymatically responsive prodrug protects against any routes of administration other than oral, while the hydrogel helps to control the rate of release. The combination of these two engineering controls surpasses the level of security employed by any of the AD formulations currently on the market or in clinical trials and presents a valuable step forward in the design of AD opioid formulations.

2.3 Conclusions

With the ongoing opioid epidemic claiming thousands of lives in the United States each year, development of technologies to deter the abuse of these necessary, but highly addictive analgesic agents have become a high priority. In this chapter, we report the development of a dual-enzyme responsive peptide-oxycodone prodrug and incorporation of this prodrug into a polymeric network for oral administration. Our initial design of the elastomeric system proved effective on small scales, however, preparing larger quantities of material proved difficult. The system was redesigned to avoid these pitfalls and resulted in a formulation that demonstrated excellent stability to a broad pH range and could be prepared on a reasonable scale. We anticipate that the design of our abuse deterrent formulation and the chemistry used for its preparation will contribute towards combatting the opioid epidemic.

2.4 Experimental

2.4.1 Materials

Naltrexone was purchased from MedChem Express, polysiloxane's were purchased from Gelest Inc., and all other chemicals were used as purchased unless otherwise noted from Acros, Alfa Aesar, Sigma Aldrich, Chem-Impex, or Fisher Scientific. All reactions were performed using

dry solvents under an inert Argon atmosphere unless otherwise noted. Dichloromethane (DCM) was distilled over CaH_2 and stored under argon. Tetrahydrofuran (THF) was distilled over sodium/benzophenone and stored under argon. 1,2-dimethoxyethane, methanol (MeOH), acetonitrile (MeCN) and other dry solvents were dried by purging with nitrogen and passage through activated alumina columns prior to use. Tetramethylethylenediamine (TMEDA) was freshly distilled and stored over 3Å molecular sieves prior to use. KHMDS were stored in a Vacuum Atmospheres Genesis stainless steel glove box under nitrogen atmosphere. Representative procedures are provided for each reaction.

2.4.2 Analytical Techniques

Nuclear magnetic resonance (NMR) spectra were obtained using either Bruker AV400, AV500, DRX500, or AV600 spectrometers. Electrospray ionization (ESI) mass spectra were obtained using either a Waters Acquity LCT Premier XE equipped with an autosampler and direct injection port or an Agilent 6530 QTOF-ESI with a 1260 Infinity LC with autosampler. Infrared (IR) absorption spectra were obtained using a PerkinElmer FT-IR equipped with an ATR accessory. Normal phase flash column chromatography was carried out using a Biotage Isolera One Flash Purification Chromatography system. Analytical reverse phase HPLC was carried out on a Agilent 1260 Infinity II HPLC system equipped with an autosampler and a UV detector using a Poroshell 120 2.7 μm C18 120 Å column (analytical: 2.7 μm , 4.6 \times 100 mm) with monitoring at $\lambda = 220$ and 280 nm and with a flow rate of 0.8 ml/min. Peptide-drug conjugates were analyzed using a mobile phase consisting of 10-100% MeCN + 0.1% TFA in water beginning with a 1 min isocratic at 10%, then up to 100% over 10 min in a linear gradient, followed by an isocratic hold at 100% MeCN + 0.1% TFA for 4 min (total time was 15 min). Purification was carried out on the same system using a Zorbax SB-C18 5.0 μm C18 120 Å column (semi-preparative: 5.0 μm , 9.4 \times

250 mm) with monitoring at $\lambda = 220$ and 280 nm and with a flow rate of 3.0 ml/min. Peptide-drug conjugates were purified using a mobile phase consisting of 10-100% MeCN + 0.1% TFA in water beginning with a 3 min isocratic at 10%, then up to 100% over 15 min in a linear gradient, followed by an isocratic hold at 100% MeCN + 0.1% TFA for 4 min (total time was 22 min). Preparatory reverse phase HPLC was carried out on a Shimadzu high performance liquid chromatography system equipped with a UV detector using a Luna 5 μm C18 100 Å column (preparatory: 5 μm , 250 \times 21.2 mm) with monitoring at $\lambda = 215$ and 254 nm and with a flow rate of 20 ml/min. Enolate trapped drug products were purified using a mobile phase consisting of 40-95% MeCN + 0.1% trifluoroacetic acid (TFA) in water beginning with 1 min isocratic at 10%, then up to 95% over 15 min in a linear gradient, followed by an isocratic hold at 95% MeCN + 0.1% TFA for 4 min (total time was 20 min). Scanning electron microscopy images were taken of the elastomer samples freeze-dried from either water or benzene. The resulting dried elastomers were then Au-coated using a sputter coater (Anatech Hummer 6.2) before being visualized via SEM (JEOL JSM-6700F).

2.4.3 Methods

Stability of Elastomeric Prodrug to Household Solvents

Elastomeric prodrug samples were combined with either lemon juice, Coca-Cola, or vinegar. Aliquots were removed periodically and analyzed via analytical HPLC to determine the amount of free naltrexone in solution corresponding to the instability of the elastomeric prodrug.

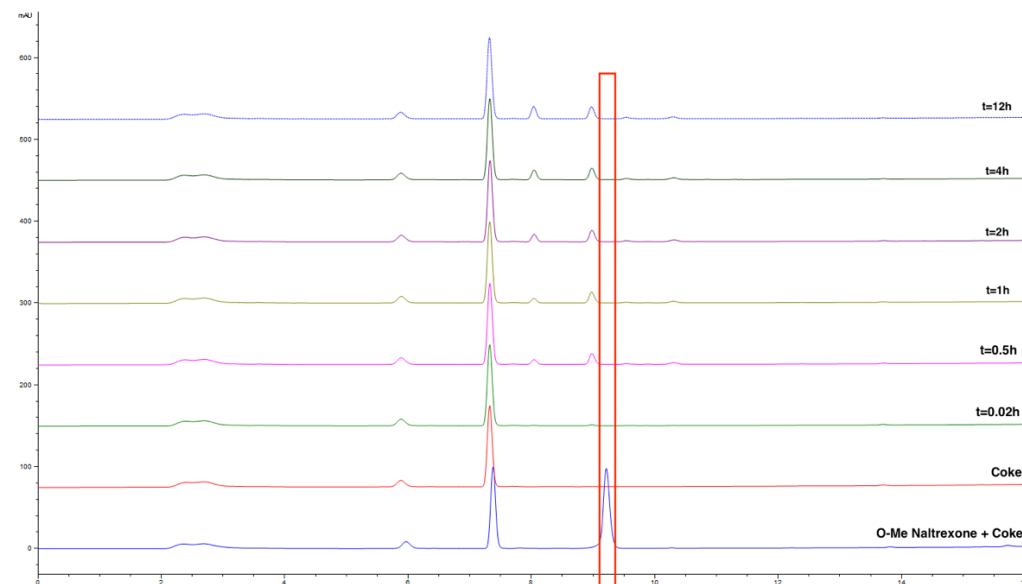


Figure 2.10. Elastomeric prodrug stability to Coca-Cola measured via HPLC over 12 hours. No appearance of Naltrexone was confirmed by LCMS.

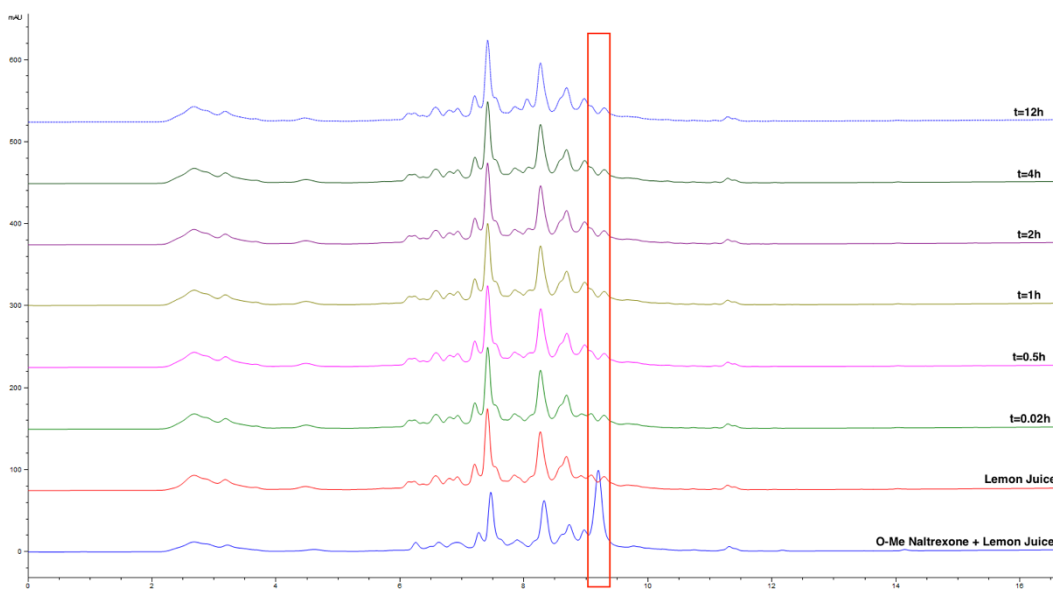


Figure 2.11. Elastomeric prodrug stability to lemon juice measured via HPLC over 12 hours. No appearance of Naltrexone was confirmed by LCMS.

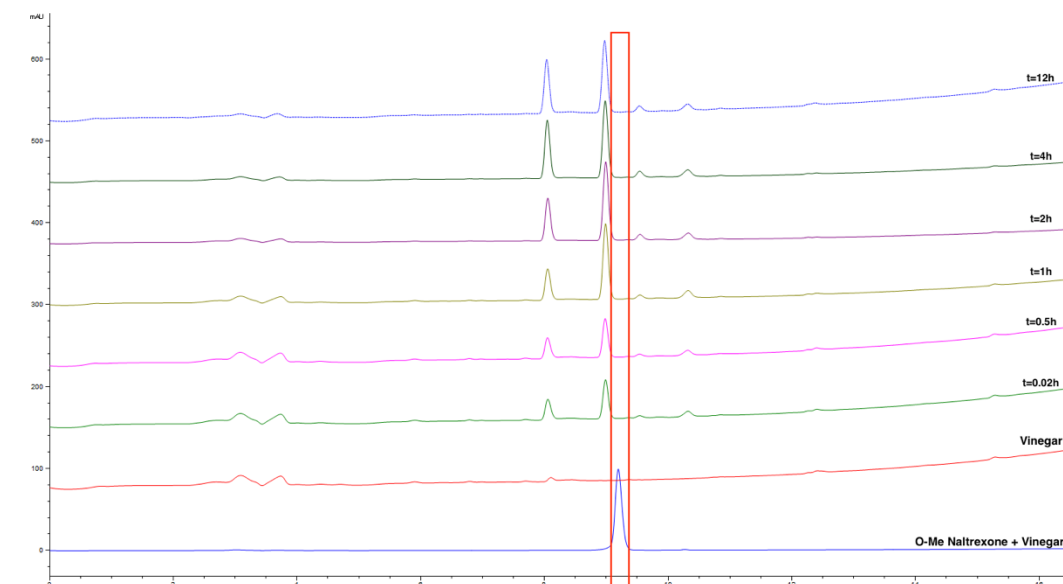


Figure 2.12. Elastomeric prodrug stability to vinegar measured via HPLC over 12 hours. No appearance of Naltrexone was confirmed by LCMS.

General Naltrexone Release Studies

Peptide or elastomer was dissolved in dimethylsulfoxide (DMSO) and diluted using 35 mM HEPES buffer (pH 7.4). Four solutions were prepared by adding either no protease, trypsin only, chymotrypsin only, or both proteases (15 to 1 ratio of peptide to protease). The solutions were placed in an incubator at 37 °C for the remainder of the experiment. Aliquots were removed from the samples over the course of the experiment. These solutions were then filtered and run on an analytical HPLC using a 95/5% to 50/50% H₂O/MeCN gradient with 0.1% TFA over 11 minutes followed by a 4-minute isocratic hold at 100% MeCN. The cleavage was monitored by integrating the appearance of the O-Me Naltrexone peak at 9 min. Naltrexone appearance was confirmed using LCMS.

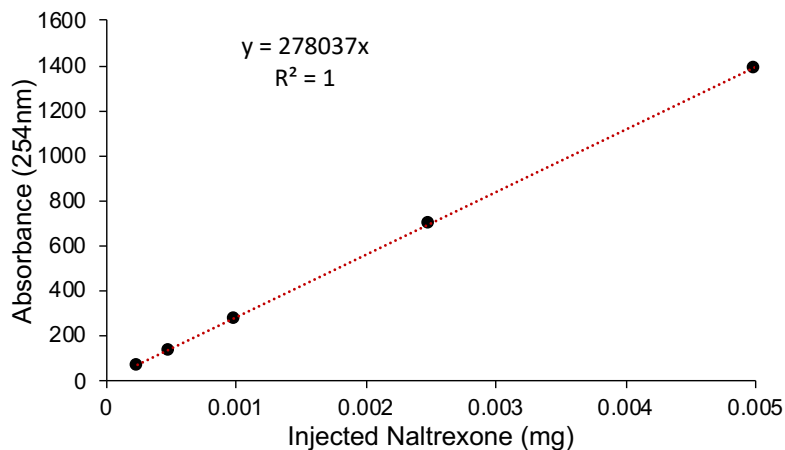
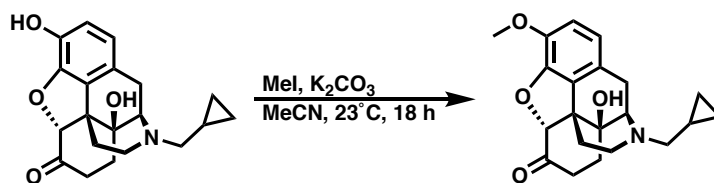


Figure 2.13. Standard curve of Naltrexone via HPLC with integrated absorbance values (254nm) across multiple concentrations.

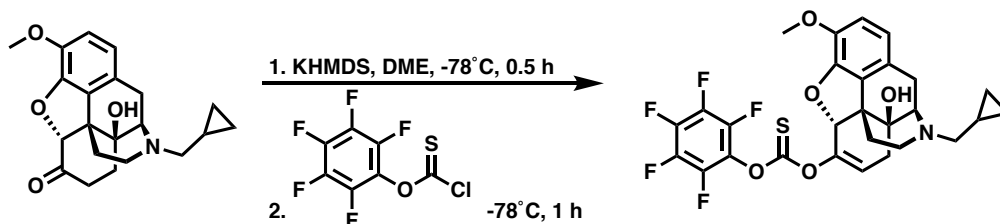
Synthesis of O-Me Naltrexone



To a solution of naltrexone (0.50 g, 1 Eq, 1.46 mmol) in DCM (10 mL) was added potassium carbonate (1.01 g, 5 Eq, 7.32 mmol) and iodomethane (1.82 mL, 20 Eq, 29.3 mmol). The reaction was stirred for 18 hours at 23 °C. Following full conversion of naltrexone, the reaction contents were diluted with DCM (200 mL). This was washed with sat. aq. NaHCO₃ sodium bicarbonate (3 x 75 mL), sat. aq. NaCl (75 mL), dried over MgSO₄, and concentrated under reduced pressure to afford **7** as a beige solid (0.515 g, 99.0% yield). ¹H NMR (600 MHz, CDCl₃) δ 6.69 (d, J = 8.2 Hz, 1H), 6.61 (d, J = 8.2 Hz, 1H), 5.22 (s, 1H), 4.67 (s, 1H), 3.89 (s, 3H), 3.19 (d, J = 4.4 Hz, 1H), 3.03 (m, 2H), 2.70 (dd, J = 11.7, 4.4 Hz, 1H), 2.58 (dd, J = 6.0, 18.5 Hz, 1H), 2.42 (m, 3H), 2.30 (td, J = 3.1, 14.3 Hz, 1H), 2.13 (td, J = 12.2, 3.8 Hz, 1H), 1.88 (m, 1H), 1.63 (dt, J = 3.4, 14.0 Hz, 1H), 1.57 (dd, J = 2.5, 12.8 Hz, 1H), 0.87 (t, J = 6.4 Hz, 1H), 0.55 (q, J = 3.1

Hz, 2H), 0.14 (d, $J = 4.6$ Hz, 2H). ^{13}C NMR (101 MHz, CDCl_3) δ 208.56, 145.04, 142.97, 129.57, 124.95, 119.39, 114.93, 90.44, 70.18, 62.11, 59.24, 56.86, 50.85, 43.63, 36.21, 31.54, 30.73, 22.64, 9.43, 3.99, 3.84. HRMS (ESI): $[\text{M}+\text{H}]^+$ calcd for $\text{C}_{21}\text{H}_{26}\text{NO}_4^+$, 356.1856; found 356.1705.

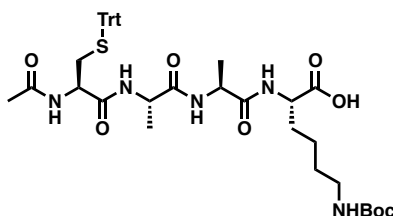
Synthesis of O-Me Naltrexone-enol-thionocarbonate-pentafluorophenol (5)



A solution potassium bis(trimethylsilyl)amide (KHMDS, 84.0 mg, 3 Eq, 0.42 mmol) in anhydrous dimethoxyethylene glycol (DME, 5 mL) in an oven dried flask under argon was cooled to -78°C . A solution of **7** (50.0 mg, 1 Eq, 0.14 mmol) in anhydrous DME (2 mL) was added dropwise and stirred at -78°C for 30 minutes. Following the enolate preparation, a solution of the pentafluorophenyl chlorothionoformate (PFPTC, 136 μL , 3 Eq, 0.84 mmol) in anhydrous DME (3 mL) was prepared in a separate oven dried flask. The solution was then cooled to -78°C in a dry ice/acetone bath. The solution containing **7** was cannulated into the flask containing the electrophile. Upon full addition, the reaction contents were stirred at -78°C for 30 minutes, warmed to 23°C and stirred for an additional 60 minutes. The reaction was then concentrated under reduced pressure, redissolved in a minimal amount of DCM, and precipitated in hexanes. Lastly, the crude product was purified by preparative HPLC (60-100% MeCN gradient against H_2O with 0.1% TFA, 15-minute gradient followed by a 5-minute isocratic hold at 100% MeCN) to afford **5** as a yellow solid (40.3 mg, 49.1% yield). ^1H NMR (600 MHz, CDCl_3) δ 7.46 (s, 1H), 6.89 (d, $J = 8.3$ Hz, 1H), 6.79 (d, $J = 8.3$ Hz, 1H), 5.85 (dd, $J = 2.2, 6.2$ Hz, 1H), 5.25 (d, $J = 1.4$ Hz, 1H), 4.07 (d, $J = 6.7$ Hz, 1H), 3.79 (s, 3H), 3.33 (d, $J = 20.0$ Hz, 1H), 3.28 (m, 1H), 3.20 (m, 1H), 2.91 (m, 1H),

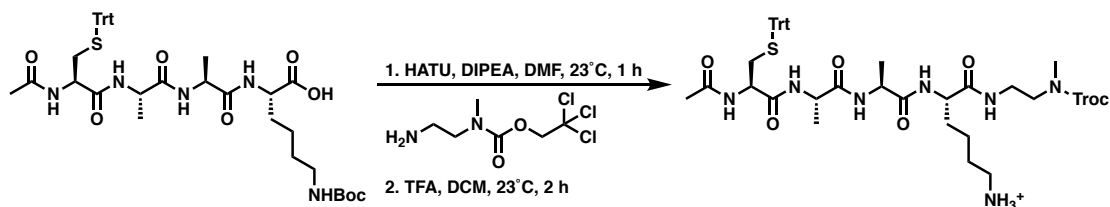
2.77 (m, 1H), 2.59 (dt, J = 5.1, 13.5 Hz, 1H), 2.44 (dd, J = 6.2, 18.5 Hz, 1H), 2.26 (td, J = 2.2, 18.5 Hz, 1H), 1.81 (dd, J = 13.8, 3.1 Hz, 1H), 1.07 (m, 1H), 0.79 (m, 1H), 0.71 (m, 1H), 0.45 (m, 2H). ^{13}C NMR (126 MHz, CD₃CN) δ 190.22, 146.67, 144.29, 144.24, 142.16, 140.16, 139.25, 137.22, 128.56, 122.27, 120.35, 119.66, 115.42, 83.80, 70.46, 61.76, 57.92, 56.17, 46.30, 45.83, 31.63, 27.64, 23.54, 5.61, 4.83, 2.77. HRMS (ESI): [M+H]⁺ calcd for C₂₈H₂₅F₅NO₅S⁺, 582.1368; found 582.0905.

Synthesis of Ac-Cys(trt)-Ala-Ala-Lys(boc)-OH (1)



The peptide was synthesized using standard Fmoc solid-phase chemistry with a 2-chlorotrityl chloride resin (1.0 g, 0.9 mmol/g substitution). N-termini were acetylated prior to cleavage from the resin using 50 eq. acetic anhydride and diisopropylethylamine (DIPEA) in dimethylformamide (DMF) for 30 min. Peptides were cleaved from the resin using a 20% hexafluoroisopropanol (HFIP) solution in dichloromethane (DCM). The cleavage solution was concentrated under reduced pressure and precipitated into cold diethyl ether affording **1** as a white solid (518.8 mg, 74.3% yield). HRMS (ESI/QTOF): [M+Na]⁺ calcd for C₄₁H₅₃N₅O₈SNa⁺, 798.3507; found 798.3524.

Synthesis of Ac-Cys(trt)-Ala-Ala-Lys-ethyl-2-amino-N-methyl-N-((2,2,2-trichloroethoxy) carbonyl) (3)



To a solution of **1** (200 mg, 1 Eq, 0.26 mmol) in DMF (5 mL) was added HATU (108 mg, 1.1 Eq, 0.28 mmol), followed by DIPEA (135 μ L, 3 Eq, 0.77 mmol). This solution was stirred at room temperature for 10 minutes to ensure complete activation. Following this, a solution of **2** (89 mg, 1.25 Eq, 0.32 mmol) in DMF (2 mL) and DIPEA (90 μ L, 2 Eq, 0.52 mmol) was added to the electrophile solution dropwise over 5 minutes. This solution was stirred at 23 °C for 40 minutes, following which, the reaction mixture was precipitated into water and concentrated under reduced pressure to afford an off-white solid. The presence of the intermediate peptide was confirmed via LCMS and carried forward without any further purification. HRMS (ESI/QTOF): $[M+H]^+$ calcd for $C_{47}H_{63}N_7O_9SCl_3^+$, 1006.3468; found 1006.3661.

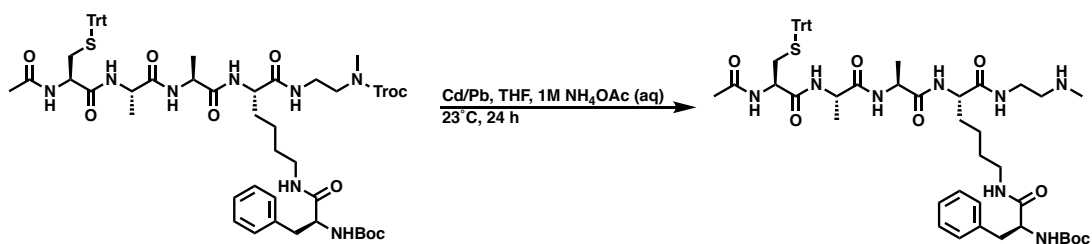
The dried product was dissolved in a 17:3 mixture of DCM and TFA (10 mL) and stirred for 2 hours at 23 °C. Following full conversion of the starting material, the solution was concentrated under reduced pressure and precipitated into cold diethyl ether to afford **3** as a white powder (183 mg, 76.0% yield). HRMS (ESI/QTOF): $[M+H]^+$ calcd for $C_{42}H_{55}N_7O_7SCl_3^+$, 906.2944; found 906.3005.

Synthesis of Ac-Cys(trt)-Ala-Ala-Lys[N-boc-Phe]-ethyl-2-amino-N-methyl-N-((2,2,2-trichloroethoxy)carbonyl) (4a)



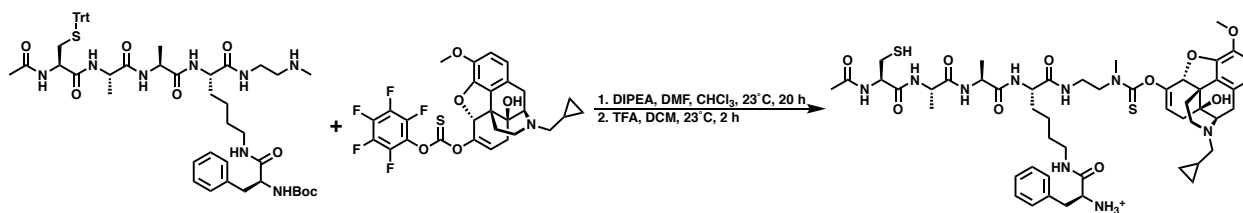
To a solution of N-(tert-butoxycarbonyl)-L-phenylalanine (73 mg, 1.5 Eq, 0.27 mmol) and 1-[Bis(dimethylamino)methylene]-1H-1,2,3-triazolo[4,5-b]pyridinium 3-oxide hexafluorophosphate (HATU, 104 mg, 1.5 Eq, 0.27 mmol) in DMF (2 mL) was added DIPEA (159 μ L, 5 Eq, 0.91 mmol), which formed a yellow solution. This solution was stirred for 10 minutes to ensure complete activation. Following the activation, a solution of **3** (170 mg, 1 Eq, 0.18 mmol) in DMF (2 mL) and DIPEA (95 μ L, 3 Eq, 0.55 mmol) was combined with the electrophile solution. The reaction contents were stirred at 23 °C for 40 min and conversion was monitored via analytical HPLC. Following full conversion, the crude reaction contents were purified on preparative HPLC (30-100% MeCN gradient against H₂O with 0.1% TFA, 15-minute gradient followed by a 5-minute isocratic hold at 100% MeCN) to afford **4a** as a beige solid (108 mg, 50.2% yield). HRMS (ESI/QTOF): [M+H]⁺ calcd for C₅₆H₇₂N₈O₁₀SCl₃⁺, 1153.4152; found 1153.4201.

Synthesis of Ac-Cys(trt)-Ala-Ala-Lys[N-boc-Phe]-ethyl-2-amino-N-methyl (4b)



To a vigorously stirred solution of **4a** (108 mg, 1 Eq, 0.035 mmol) in THF (4 mL) and 1M aq. ammonium acetate (2 mL) was added Pb/Zn couple (473 mg, 5 Eq, 1.74mmol) in 4 portions over 4 hours. Following this, the solution was vigorously stirred for an additional 20 hours. The crude product was then purified by preparative HPLC (10-100% MeCN gradient against H₂O with 0.1% TFA, 15-minute gradient followed by a 5-minute isocratic hold at 100% MeCN) to afford **4b** as a white solid (22.2 mg, 65.1% yield). HRMS (ESI/QTOF): [M+H]⁺ calcd for C₅₃H₇₁N₈O₈S⁺, 979.5110; found 979.5140.

Synthesis of Ac-Cys-Ala-Ala-Lys[Phe]-ethylamino-N-methyl-N-Naltrexone (**6**)

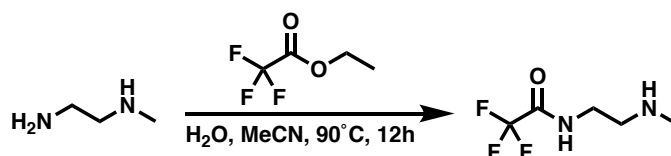


To a solution of **4b** (125 mg, 1 Eq, 0.113 mmol) in chloroform (5 mL) and DMF (0.5 mL), was added DIPEA (98.7 μL, 5 Eq, 0.567 mmol). This solution was added dropwise to a solution of **5** (86.7 mg, 1.1 Eq, 0.125) in chloroform (2 mL) over two minutes. This reaction was then stirred at 23 °C for 20 hours, after which, the chloroform was removed under reduced pressure and remaining DMF solution was precipitated into a solution of 1:1 diethyl ether: hexane. The white precipitate was reclaimed, characterized via LCMS (to confirm the identity), and carried forward without any further purification. HRMS (ESI/QTOF): [M+H]⁺ calcd for C₇₅H₉₄N₉O₁₂S₂⁺, 1376.6458; found 1376.6544.

The dried product was dissolved in an 8:2 mixture of DCM and TFA solution (10 mL) with an additional 0.25 mL of triisopropylsilane (TIPS) as a quenching agent, all of which was stirred for 2 hours at 23 °C. Following full conversion of the starting material, the solution was concentrated

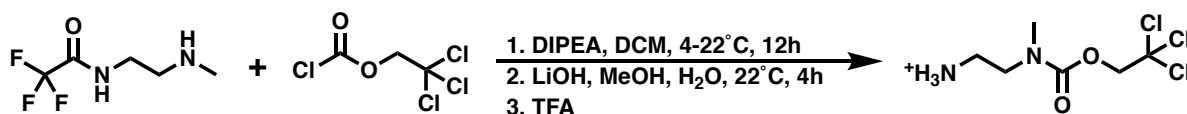
under reduced pressure. This crude product was then purified via preparative HPLC (10-100% MeCN gradient against H₂O with 0.1% TFA, 15-minute gradient followed by a 5-minute isocratic hold at 100% MeCN) to afford **6** as a white solid (79 mg, 55.1% yield). HRMS (ESI/QTOF): [M+H] calcd for C₅₁H₇₂N₉O₁₀S₂⁺, 1034.4838; found 1034.4872.

Synthesis of 2,2,2-trifluoro-N-(2-(methylamino)ethyl)acetamide (**12**)



To a solution of N-methylethylene diamine (1.5 mL, 1 Eq, 17 mmol) in water (1.0 mL) and MeCN (9 mL) was slowly added ethyl trifluoroacetate (4.7mL, 2.3 Eq, 40 mmol) at 23 °C under an inert atmosphere. This solution was then warmed to 90 °C under a reflux condenser for 12 hours. Following this, the solution was cooled back down to room temperature and all solvent was removed under reduced pressure. The resulting brown oil was combined with isopropanol (3 mL) and again all solvent was removed under reduced pressure. This last step was repeated 2 additional times eventually resulting in a brown solid. This crude product was recrystallized using DCM to afford **9** (4.7 g, 97.2% yield). ¹H NMR (500 MHz, CD₃CN) δ 9.08 (s, 2H), 3.59 (q, J = 5.4 Hz, 2H), 3.16 (t, J = 5.4 Hz, 2H), 2.63 (s, 3H). ¹³C NMR (126 MHz, CD₃CN) δ 159.59, 116.53, 47.96, 36.16, 32.84. HRMS (ESI/QTOF) [M+H]⁺ calcd for C₅H₁₀F₃N₂O⁺, 171.0740; found 171.0763.

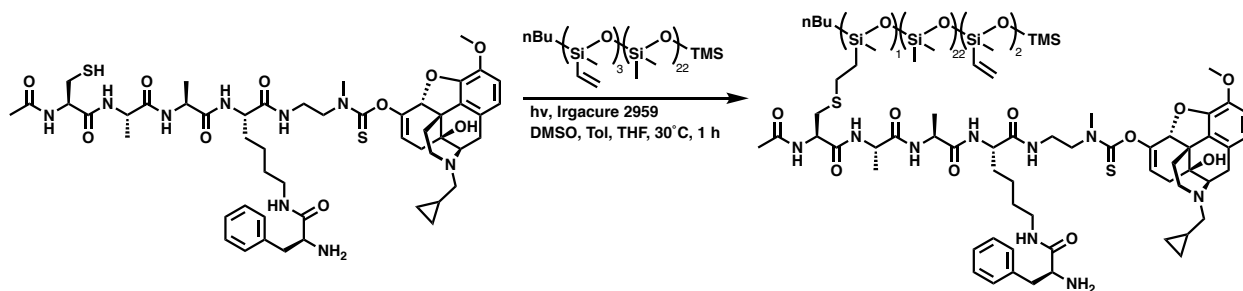
Synthesis of 2,2,2-trichloroethyl (2-aminoethyl)(methyl)carbamate (**2**)



To a solution of **9** (500mg, 1 Eq, 1.76 mmol) in anhydrous DCM (5 mL) was added DIPEA (337 μ L, 1.1 Eq, 1.94 mmol) and the solution was cooled to 4 °C. Separately a solution of 2,2,2-trichloroethyl chloroformate (266 μ L, 1.1 Eq, 1.94 mmol) in anhydrous DCM (5 mL) was prepared and added to the cooled solution dropwise over 15 minutes. This solution was slowly warmed up to room temperature and stirred for an additional 3 hours. The reaction contents were then diluted with ethyl acetate (EtOAc) (300 mL) and washed with sat. aq. NaHCO₃ (2 x 75 mL), 0.1M aq. HCl (3 x 75 mL), and sat. aq. NaCl (75 mL). The organic layer was dried over MgSO₄, concentrated under reduced pressure, and the crude product was further purified by running a silica plug (15% MeOH in DCM). The product was carried forward with no further purification.

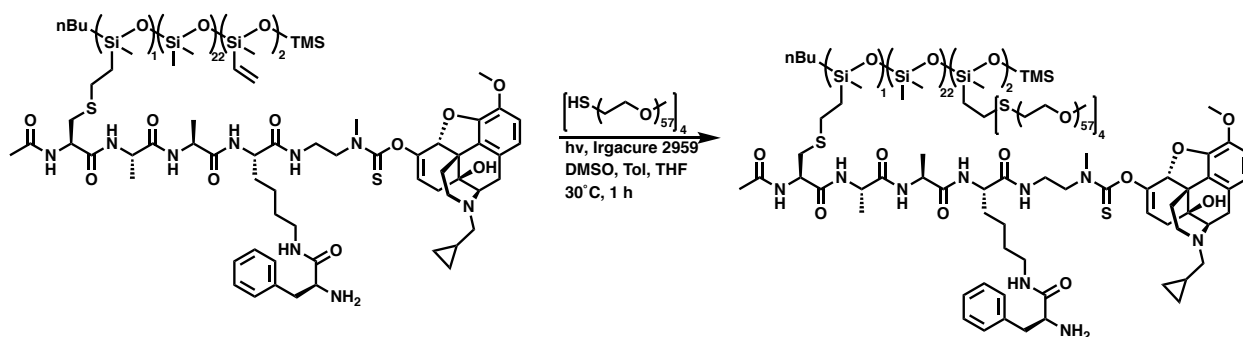
The intermediate was then combined with MeOH (10 mL), H₂O (3 mL), and K₂CO₃ (1.46 g, 6 Eq, 10.6 mmol) where it was stirred at 22 °C for 16 hours. The reaction contents were then concentrated under reduced pressure and extracted using a 3:1 solution of CHCl₃ and IPA (2 x 75 mL). The combined organic layers were washed with sat. aq. NaHCO₃ (2 x 75 mL), sat. aq. NaCl (75 mL), dried over MgSO₄, and concentrated under reduced pressure. The residual liquid was dissolved in ether (5 mL) and added dropwise into a solution of ether (45 mL) and TFA (1 mL) to afford **2** as a white precipitate (381 mg, 59.6% yield). ¹H NMR (500 MHz, CD₃CN) δ 7.75 (s, 3H), 4.77 (s, 2H), 3.61 (m, 2H), 3.17 (m, 2H), 2.97 (d, J = 21.3 Hz, 3H). ¹³C NMR (126 MHz, CD₃CN) δ 155.53, 95.54, 74.98, 46.89, 38.00, 34.21. HRMS (ESI/QTOF) [M+H]⁺ calcd for C₆H₁₂Cl₃N₂O₂⁺, 248.9959; found 248.9985.

Conjugation of peptide-prodrug onto (12%-vinylmethylsiloxane)-dimethylsiloxane copolymer (8)



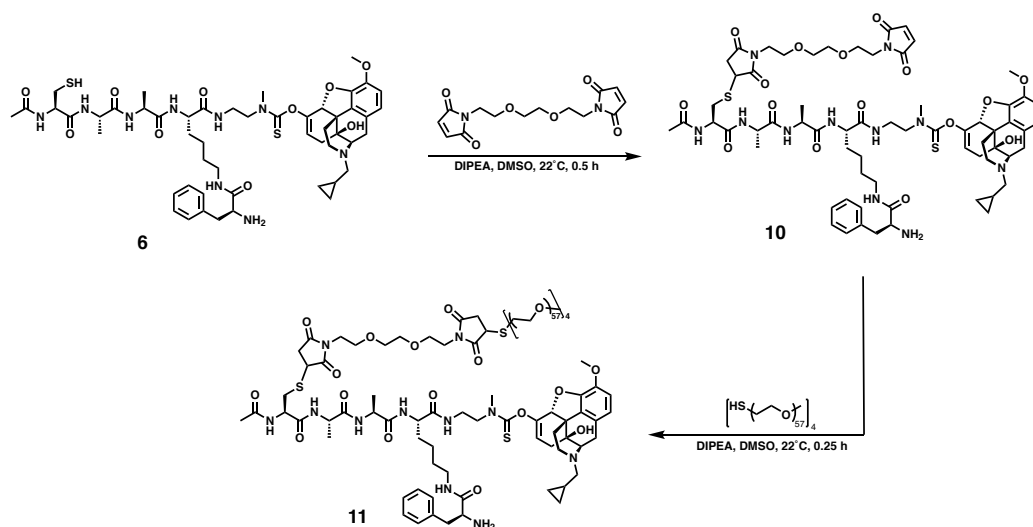
A solution of **6** (19.7 mg, 1 Eq, 15.6 μmol) was prepared in DMSO (50 μL) and THF (150 μL), a solution of Irgacure 2959 (1.4 mg, 0.398 Eq, 6.2 μmol) was prepared in THF (100 μL), and a solution of (12%-vinylmethylsiloxane)-dimethylsiloxane copolymer (226 kDa, 10 mg, 0.003 Eq, 44 nmol, 15.6 μmol of vinyl) was prepared in toluene (30 μL) and THF (200 μL). These solutions were then combined in a vial and degassed via 3 cycles of freeze-pump-thaw. The resulting vial was then capped under argon and irradiated under UV light for 60 minutes with vigorous stirring. The % modification was monitored via ^1H NMR where the reduction in vinyl protons corresponds to the peptide incorporation and was deemed complete with a 50% reduction of the vinyl peaks. This resulting polymer was purified by precipitating into a 25% MeOH in H_2O solution resulting in pure **8** (20 mg).

Crosslinking polymer-prodrug conjugate with 4-arm PEG-thiol (9)



A solution of **8** (20 mg, 1 Eq, 44 nmol, 7.8 μmol of vinyl) in DMSO (30 μL) and THF (300 μL) was combined with 4-arm PEG-thiol (10 kDa, 46.4 mg, 0.10 Eq, 3.09 μmol , 12.4 μmol of thiol) and Irgacure 2959 (1.39 mg, 0.2 Eq, 6.18 μmol). This solution was degassed via 3 cycles of freeze-pump-thaw, sealed under argon, and irradiated under UV light for 60 minutes. This resulting elastomer was washed with MeOH (4 x 1 mL) and freeze-dried from benzene to afford the spongy elastomeric prodrug **9**.

Preparation of peptide-prodrug PEG hydrogel (**11**)



To a solution of the **6** (30.0 mg, 0.5 Eq, 23.7 μmol) in DMSO (200 μL) was added a solution of 1,8-bismaleimido-diethyleneglycol (8.78 mg, 0.6 Eq, 28.5 μmol) in DMSO (200 μL) followed by DIPEA (16.5 μL , 2 Eq, 95.0 μmol). This solution was stirred for 30 minutes, after which the modification was confirmed via LCMS. HRMS (ESI/QTOF) $[\text{M}+\text{H}]^+$ calcd for $\text{C}_{65}\text{H}_{88}\text{N}_{11}\text{O}_{16}\text{S}_2^+$, 1342.5846; 1342.5094. At this point, a solution of the 4-arm PEG-SH (190 mg, 0.4 Eq, 19.0 μmol) in DMSO (500 μL) was added and a gel formed almost immediately upon addition. The gel was then washed with DMSO, MeOH, DCM, and benzene. The resulting gel was then freeze-dried from benzene to ensure a porous architecture.

2.5 References

- (1) Leung, P. T. M.; Macdonald, E. M.; Stanbrook, M. B.; Dhalla, I. A.; Juurlink, D. N. A 1980 Letter on the Risk of Opioid Addiction. *N. Engl. J. Med.* **2017**, *376* (22), 2194–2195. <https://doi.org/10.1056/NEJMc1700150>.
- (2) Doctor, J. N.; Nguyen, A.; Lev, R.; Lucas, J.; Knight, T.; Zhao, H.; Menchine, M. Opioid Prescribing Decreases after Learning of a Patient’s Fatal Overdose. *Science* **2018**, *361* (6402), 588–590. <https://doi.org/10.1126/science.aat4595>.
- (3) Hoots, B. E.; Xu, L.; Kariisa, M.; Wilson, N. O.; Rudd, R. A.; Scholl, L.; Schieber, L.; Seth, P. 2018 Annual Surveillance Report of Drug-Related Risks and Outcomes -- United States. **2018**.
- (4) Florence, C.; Luo, F.; Rice, K. The Economic Burden of Opioid Use Disorder and Fatal Opioid Overdose in the United States, 2017. *Drug Alcohol Depend.* **2021**, *218*, 108350. <https://doi.org/10.1016/j.drugalcdep.2020.108350>.
- (5) *Multiple Cause of Death 1999 - 2018 on CDC WONDER Online Database, Released January, 2020*; National Center for Health Statistics, 2020.
- (6) *The President’s Commission on Combating Drug Addiction and the Opioid Crisis*; The White House, 2017; p 138.
- (7) Litman, R. S.; Pagán, O. H.; Cicero, T. J. Abuse-Deterrent Opioid Formulations. *Anesthesiol. J. Am. Soc. Anesthesiol.* **2018**, *128* (5), 1015–1026. <https://doi.org/10.1097/ALN.0000000000002031>.
- (8) Gasior, M.; Bond, M.; Malamut, R. Routes of Abuse of Prescription Opioid Analgesics: A Review and Assessment of the Potential Impact of Abuse-Deterrent Formulations. *Postgrad. Med.* **2016**, *128* (1), 85–96. <https://doi.org/10.1080/00325481.2016.1120642>.

- (9) Lankenau, S. E.; Teti, M.; Silva, K.; Bloom, J. J.; Harocopos, A.; Treese, M. Initiation into Prescription Opioid Misuse amongst Young Injection Drug Users. *Int. J. Drug Policy* **2012**, *23* (1), 37–44. <https://doi.org/10.1016/j.drugpo.2011.05.014>.
- (10) Budman, S. H.; Grimes Serrano, J. M.; Butler, S. F. Can Abuse Deterrent Formulations Make a Difference? Expectation and Speculation. *Harm. Reduct. J.* **2009**, *6* (1), 8. <https://doi.org/10.1186/1477-7517-6-8>.
- (11) *Abuse-Deterrent Opioids — Evaluation and Labeling*; U.S. Department of Health and Human Services, Food and Drug Administration, Center for Drug Evaluation and Research, 2015; p 29.
- (12) Vosburg, S. K.; Haynes, C.; Besharat, A.; Green, J. L. Changes in Drug Use Patterns Reported on the Web after the Introduction of ADF OxyContin: Findings from the Researched Abuse, Diversion, and Addiction-Related Surveillance (RADARS) System Web Monitoring Program. *Pharmacoepidemiol. Drug Saf.* **2017**, *26* (9), 1044–1052. <https://doi.org/10.1002/pds.4248>.
- (13) McNaughton, E. C.; Coplan, P. M.; Black, R. A.; Weber, S. E.; Chilcoat, H. D.; Butler, S. F. Monitoring of Internet Forums to Evaluate Reactions to the Introduction of Reformulated OxyContin to Deter Abuse. *J. Med. Internet Res.* **2014**, *16* (5), e3397. <https://doi.org/10.2196/jmir.3397>.
- (14) Gudin, J. A.; Nalamachu, S. R. An Overview of Prodrug Technology and Its Application for Developing Abuse-Deterrent Opioids. *Postgrad. Med.* **2016**, *128* (1), 97–105. <https://doi.org/10.1080/00325481.2016.1126186>.
- (15) Boehnke, N.; Maynard, H. D. Design of Modular Dual Enzyme-Responsive Peptides. *Biopolymers* **2017**, *108* (5), 1–6. <https://doi.org/10.1002/bip.23035>.

- (16) Ruddick, J. A.; Newsome, W. H.; Nash, L. Correlation of Teratogenicity and Molecular Structure: Ethylenethiourea and Related Compounds. *Teratology* **1976**, *13* (3), 263–266.
<https://doi.org/10.1002/tera.1420130304>.
- (17) Mark, J. E.; Allcock, H. R.; West, R. *Inorganic Polymers*, 2nd edition.; Oxford University Press: New York, 2005.

2.6 Appendix B

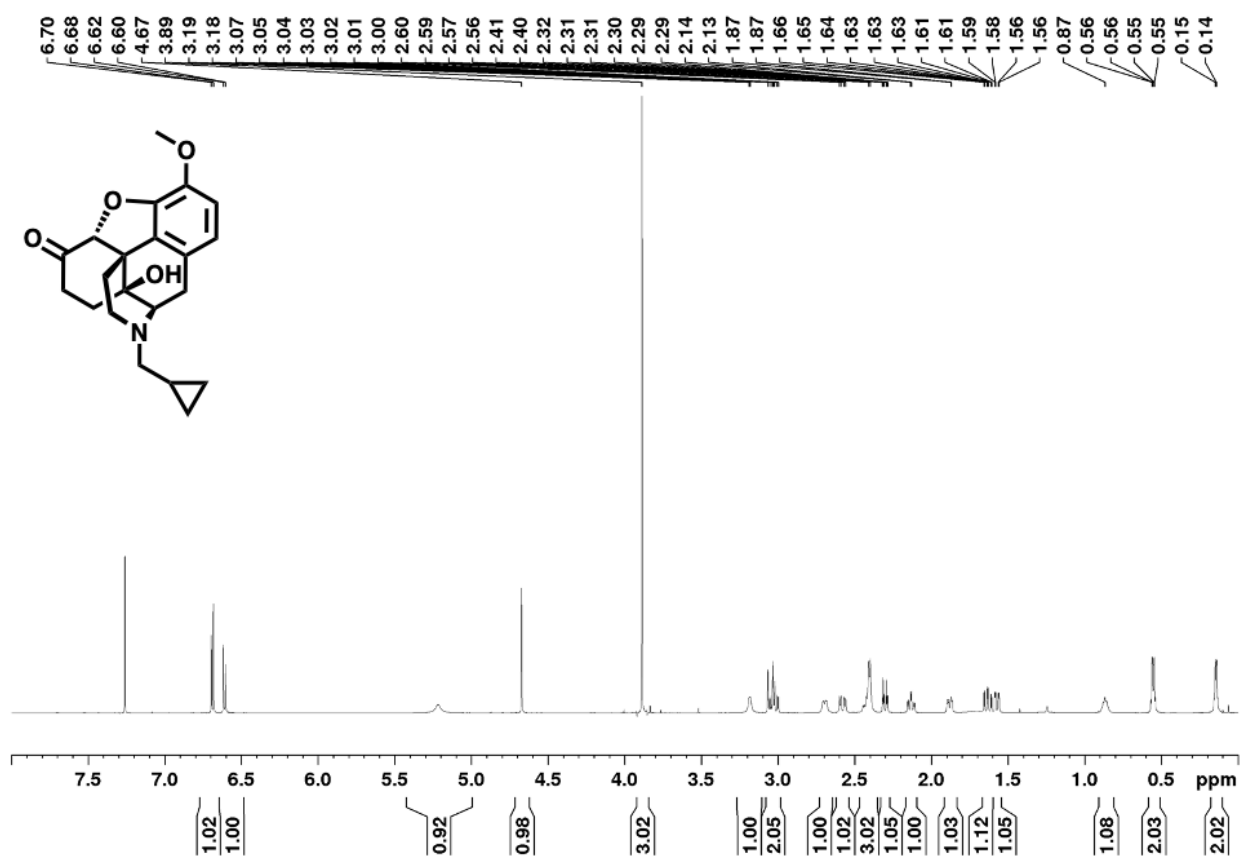


Figure 2.14. ¹H NMR Spectrum of OMe-Naltrexone in CDCl₃.

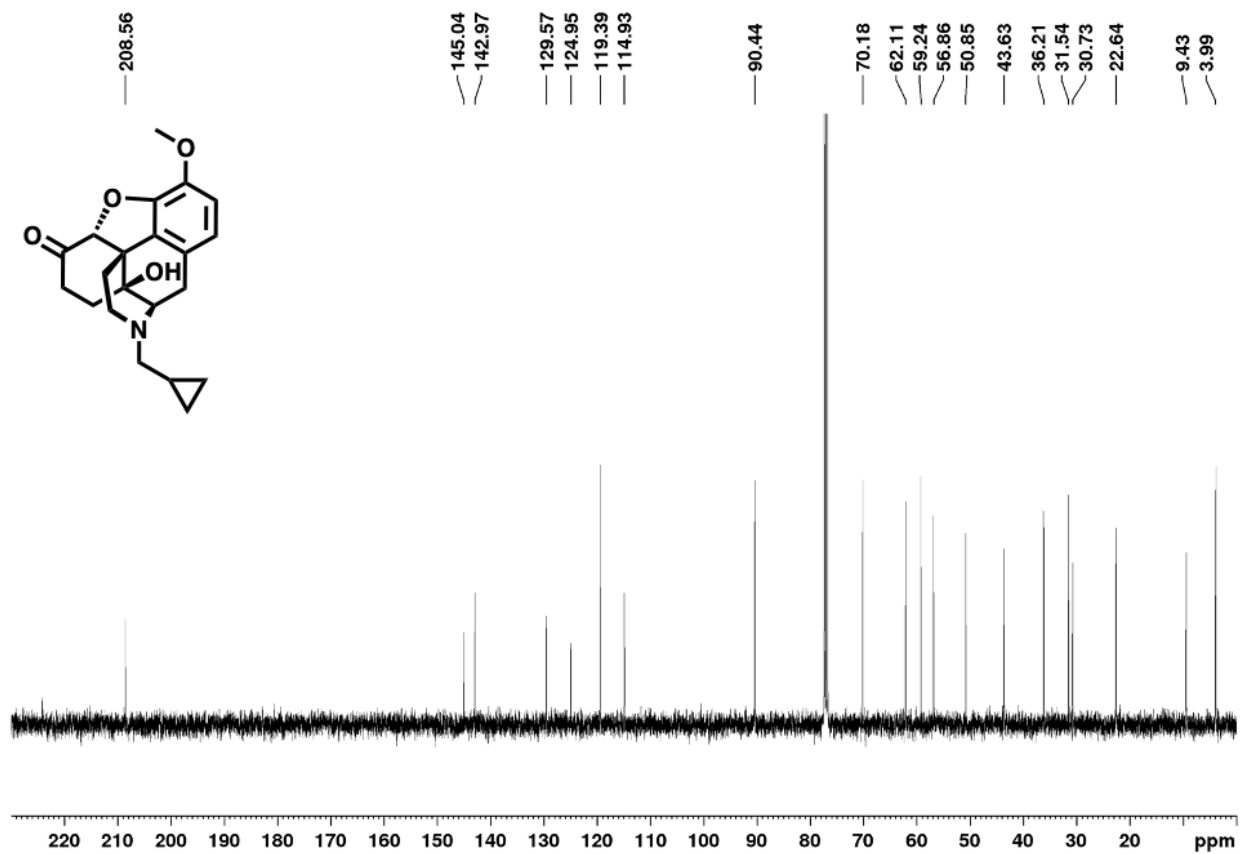


Figure 2.15. ^{13}C NMR Spectrum of OMe-Naltrexone in CDCl_3 .

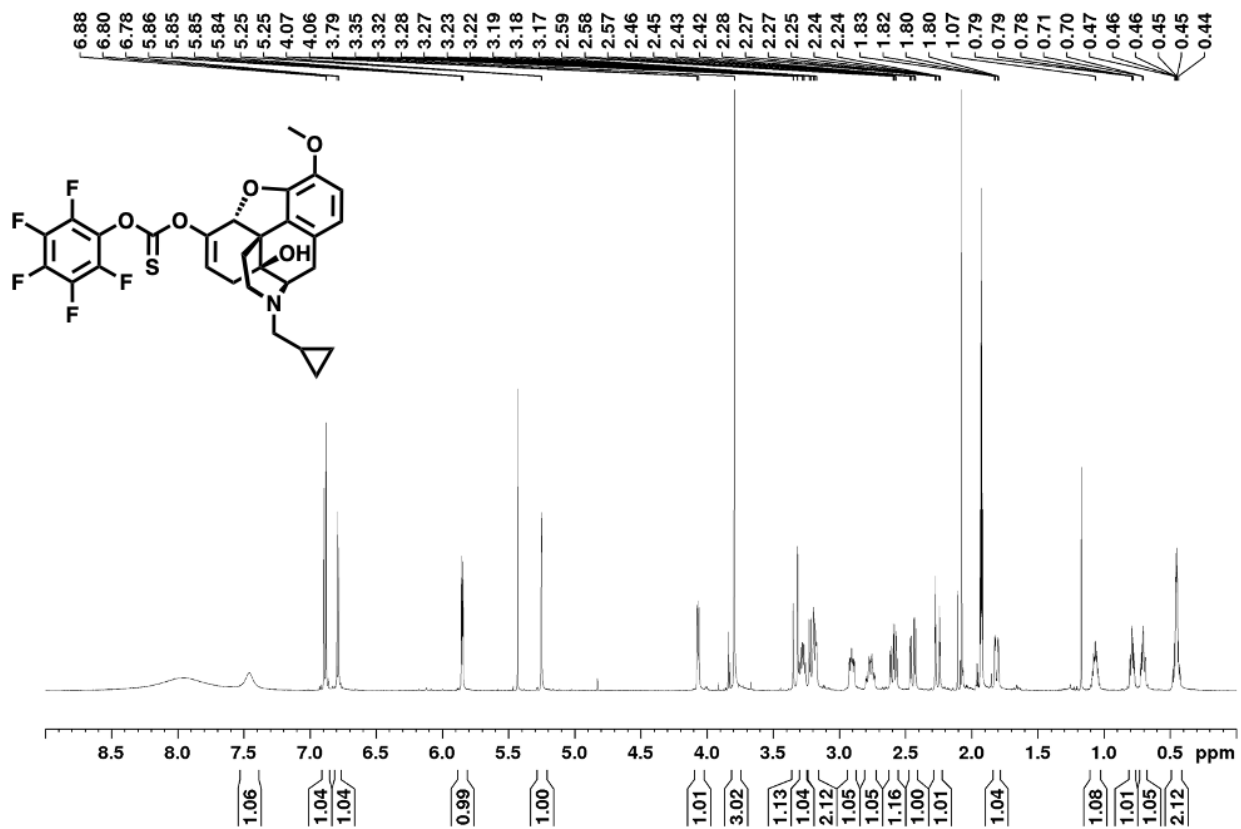


Figure 2.16. ¹H NMR Spectrum of O-Me Naltrexone-enol-thionocarbonate-pentafluorophenol in CD₃CN.

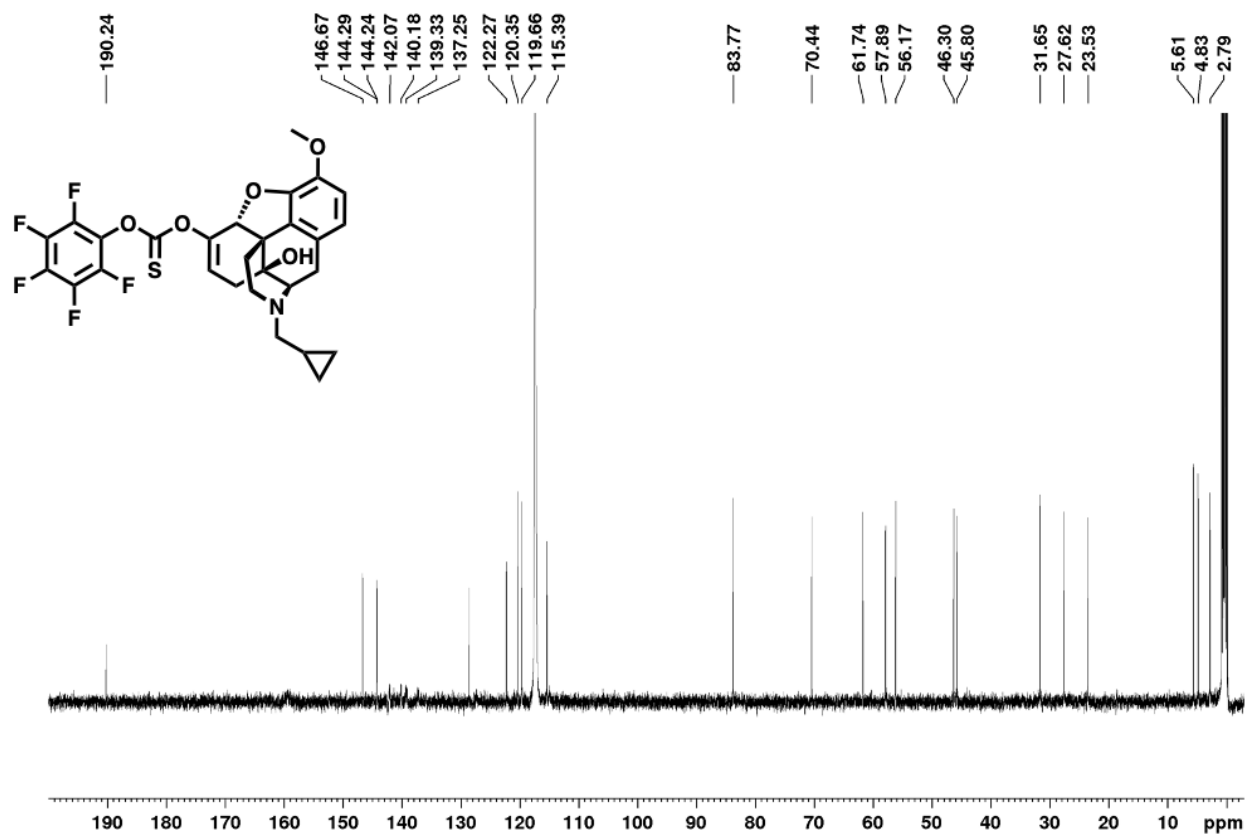


Figure 2.17. ^{13}C NMR Spectrum of O-Me Naltrexone-enol-thionocarbonate-pentafluorophenol in CD_3CN .

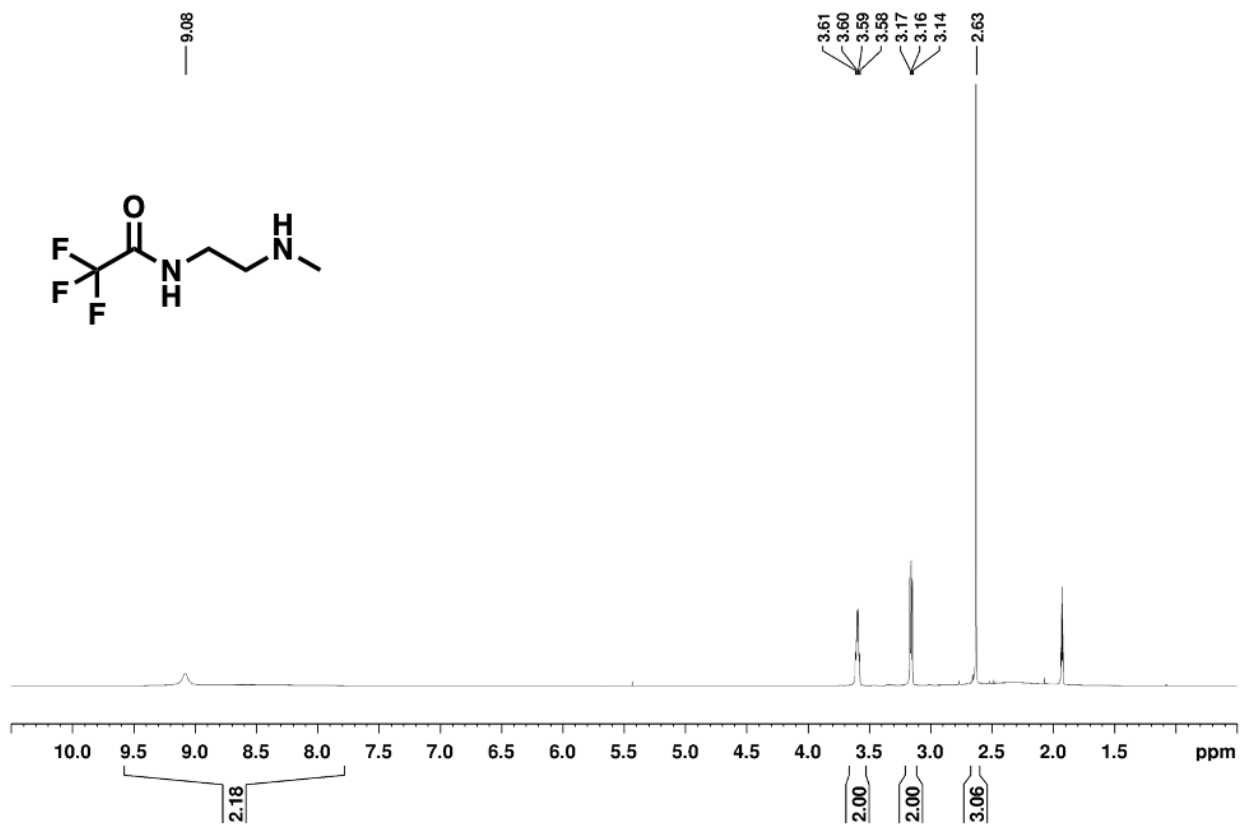


Figure 2.18. ¹H NMR Spectrum of 2,2,2-trifluoro-N-(2-(methylamino)ethyl)acetamide in CD₃CN.

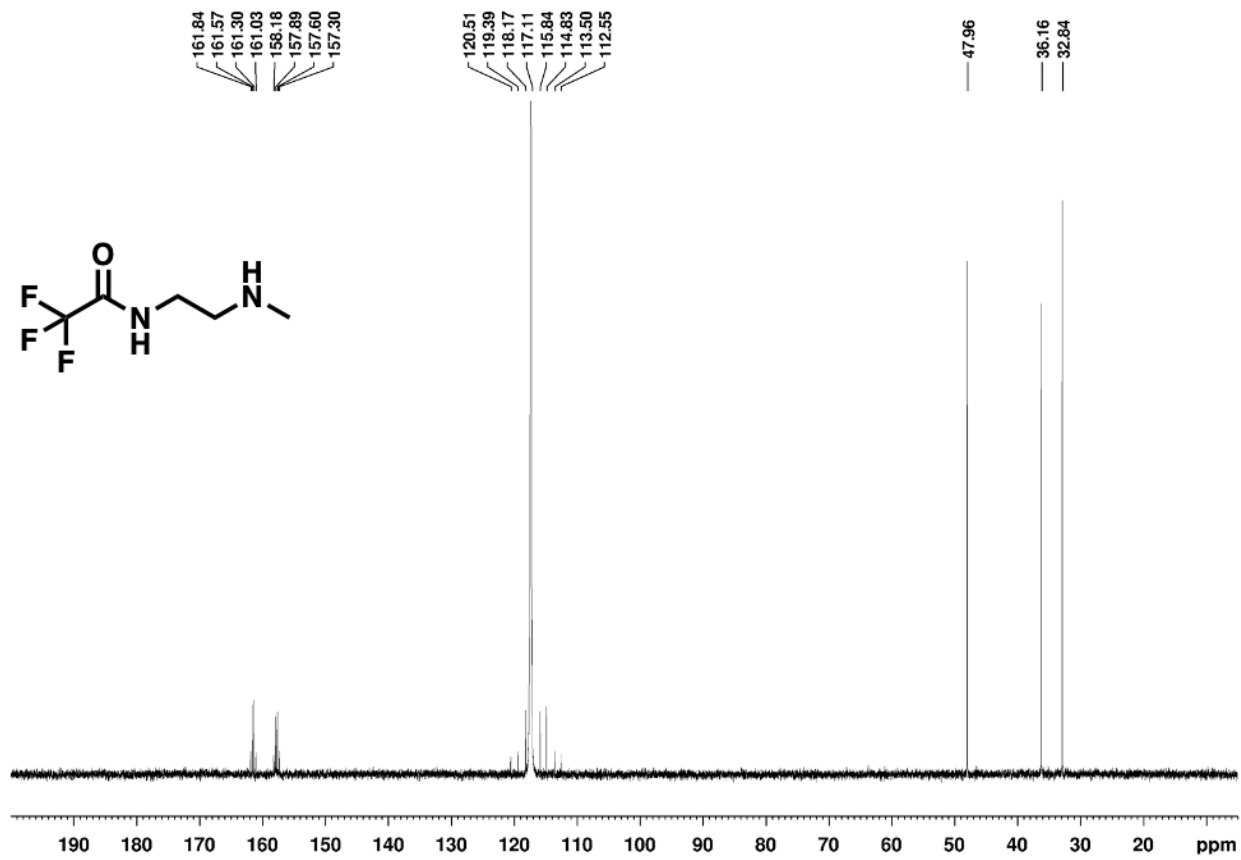


Figure 2.19. ¹³C NMR Spectrum of 2,2,2-trifluoro-N-(2-(methylamino)ethyl)acetamide in CD₃CN.

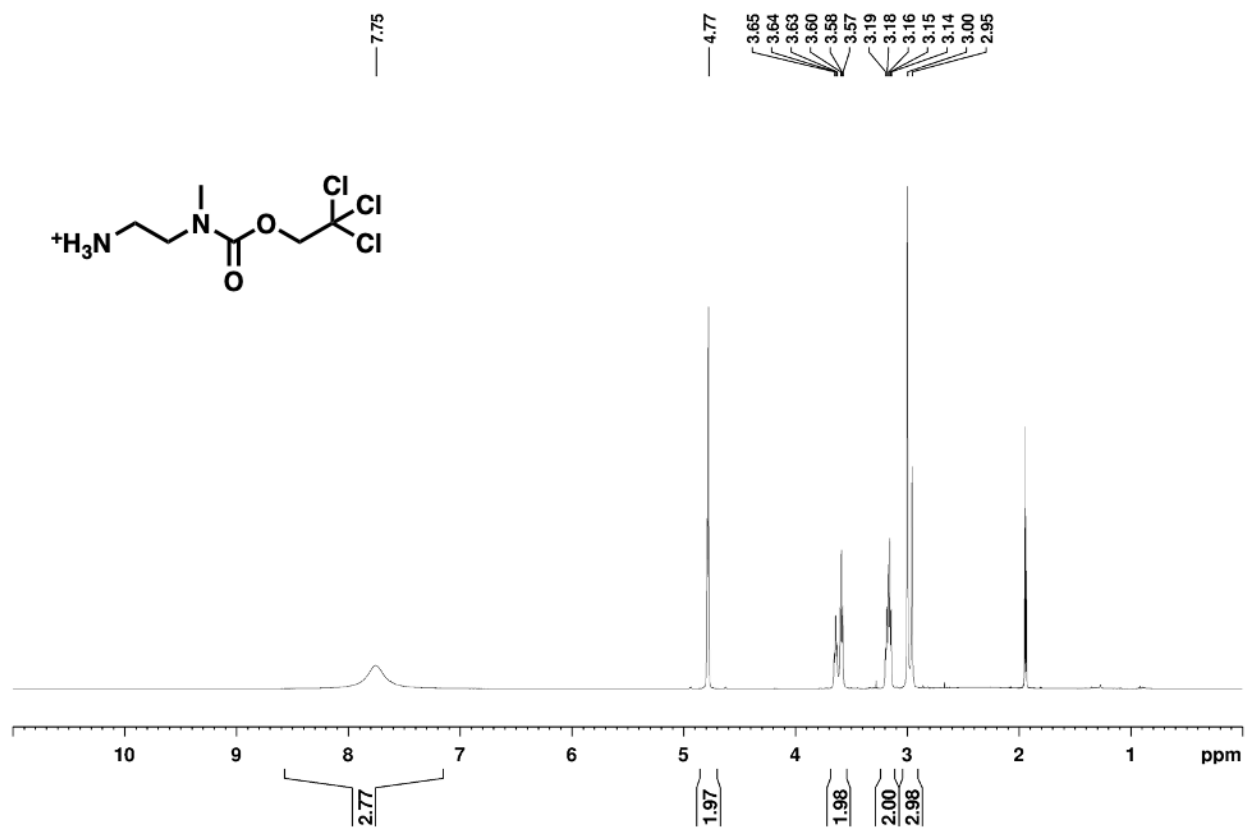


Figure 2.20. ¹H NMR Spectrum of 2,2,2-trichloroethyl (2-aminoethyl)(methyl)carbamate in CD₃CN.

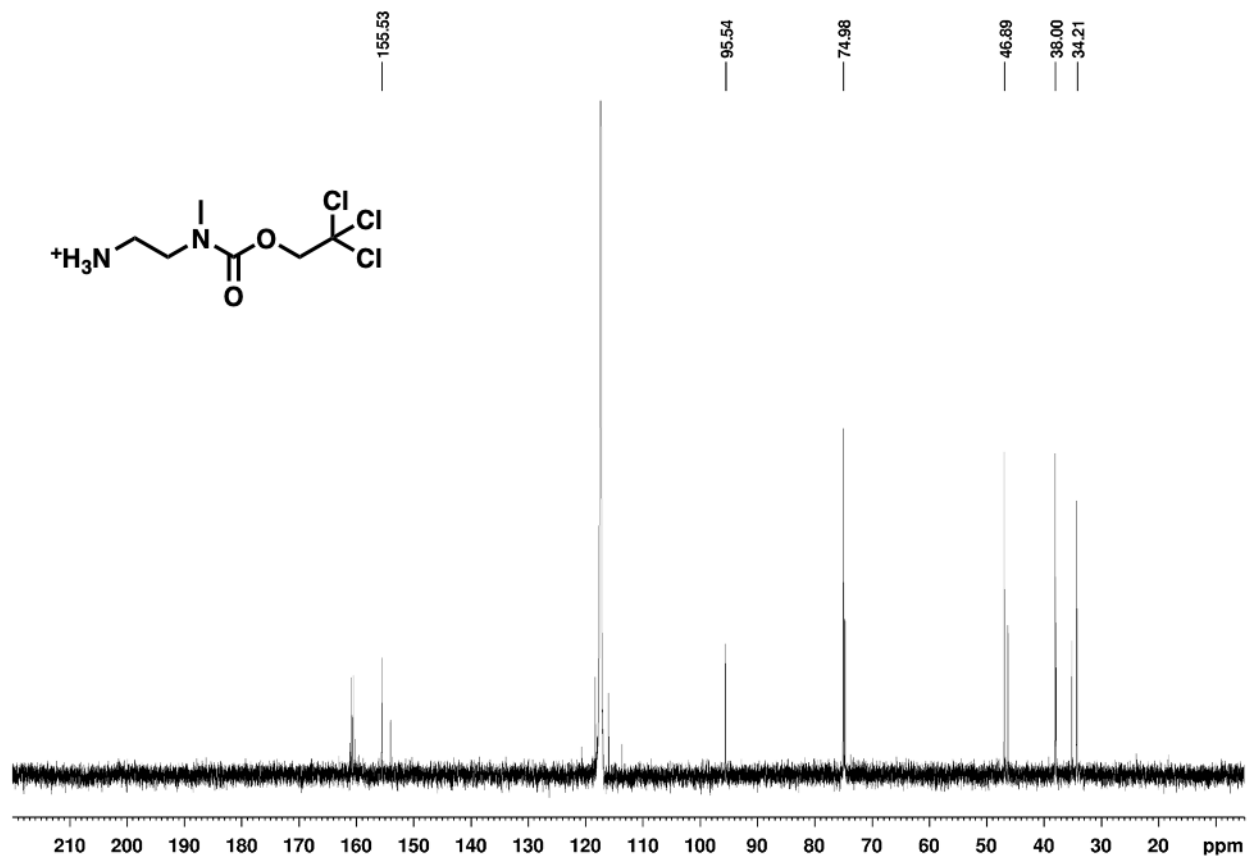


Figure 2.21. ¹³C NMR Spectrum of 2,2,2-trichloroethyl (2-aminoethyl)(methyl)carbamate in CD₃CN.

Chapter 3

Development of a Dual-Enzyme Responsive

Abuse-Deterrent Opioid Prodrug

3.1 Introduction

Chapter 2 outlined the design and preparation of an abuse-deterrent elastomeric opioid prodrug formulation. During the course of the project, a few drawbacks which would limit the general applicability of the formulation were identified in the project design. First, the distribution of the opioid within the elastomeric network was unknown and it would prove significantly challenging to quantify any homogeneity or inhomogeneity. Any amount of uneven distribution within the formulation would lead to inconsistent dosages and varied rates of release, which would certainly not pass FDA inspection. Second, increasing the scale of the elastomer synthesis resulted in significant complications. The polysiloxane modifications were readily synthesized when using less than 100 mg; however, larger quantities led to insufficient functionalization and/or significant backbone crosslinking. Third, the inability to physically alter the formulation made carrying out animal studies difficult. Although the intent behind the formulation was to minimize physical manipulation, the formulations gel like nature would not pass through an oral gavage during attempts to administer to mice for toxicity and analgesia studies. Fourth, the prodrug before and after covalent attachment to the polysiloxane backbone would release naltrexone in the presence of only chymotrypsin. This limits the security of the formulation since chymotrypsin can be easily obtained over the internet or as a digestive aid at convenience stores. Finally, the polysiloxane backbone was used to prevent crushing or extraction of the formulation prior to administration, but neither of these methods of abuse are concerning when using a prodrug, if it was indeed dual enzyme responsive, which would be more difficult to tamper with. A dual-enzyme responsive prodrug ensures that the opioid must be ingested orally and controls the rate of release independently of the elastomer.

In this chapter, we report the design and synthesis of a dual-enzyme responsive opioid prodrug that addresses the shortcomings of currently available abuse-deterrent formulations. This prodrug was developed based on our group's previously reported dual-enzyme responsive peptide that effectively released a small molecule reporter upon incubation with digestive enzymes trypsin and chymotrypsin.¹ First, chymotrypsin is required to cleave the isopeptide bond between a phenylalanine residue and the ϵ -amine of a lysine residue. Once cleaved, the lysine residue is unmasked and can further be processed by trypsin, which further cleaves the lysine C-terminally and releases a primary amine. This primary amine can then rapidly cyclize and release an attached, active opioid, forming 1-methylimidazolidine-2-thione as a nontoxic byproduct.²

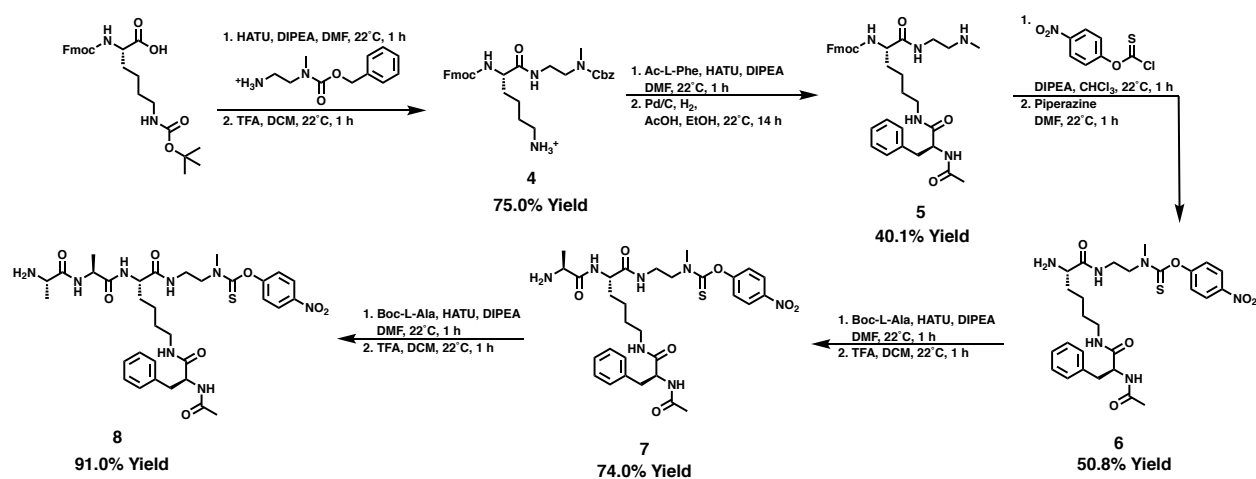
In the following sections, we report the optimization of our dual-enzyme responsive peptide platform towards a more efficient abuse-deterrent opioid prodrug. We then describe the application of the resulting target peptides towards developing oxycodone prodrugs while simultaneously enhancing the security of the formulation through a required pH-based activation step. Finally, we describe optimization of this chemistry, in vitro release assays, and monitoring the stability of the formulation towards a variety of chemical manipulations.

3.2 Results and Discussion

3.2.1 Determining the Cause of Chymotrypsin Promiscuity

During the preparation of the abuse-deterrent opioid formulation in Chapter 2, we observed a significant amount of release in the presence of only chymotrypsin. Based on the mechanism of release, the chymotrypsin should only cleave after the phenylalanine residue and therefore require the presence of trypsin in order to finish the release of naltrexone. Our initial explanations centered around contamination, yet repurchasing chymotrypsin from high quality vendors at a high purity

($\geq 99\%$ purity) showed no effect on the release. We next hypothesized that the branching nature of the peptide placed the peptide backbone in a twisted conformation within the binding pocket of chymotrypsin that led to the cleavage after the lysine residue.³ In this case, the peptide sequence itself was the cause for the unintentional release and modifications to the sequence would potentially reverse the unintended release phenomenon. In order to probe which part of the peptide sequence, if any, was the cause of the unintended chymotrypsin cleavage, we designed a model system to monitor enzymatic cleavage in a more streamlined manner. Initially, studying enzymatic release by HPLC created a major time barrier, limiting the amount of time points obtained during the release and requiring a relatively large amount of prodrug. The updated design now relied on the attachment of *p*-nitrophenol thionochloroformate (*p*NP-TCl) to the peptide in place of the opioid. Upon enzymatic cleavage of the prodrug and the subsequent diamine self-immolative cyclization, *p*-nitrophenol (*p*NP) would be released into solution, which was monitored at 405 nm on a plate reader, thus increasing the sampling frequency and throughput of the assay.



Scheme 3.1. Synthesis of peptide-naltrexone prodrug (**6**) prepared from Ac-C(trt)AAK(boc).

We initially prepared the prodrugs **6**, **7**, and **8** to elucidate whether the peptide backbone length had any effect on the chymotrypsin release phenomenon. These prodrugs did not have the

cysteine (**6**), and either 1 Ala (**7**) or no Ala (**8**). They were prepared from Fmoc-lysine(Boc) by initially installing a carboxybenzyl-protected diamine followed by removal of the Boc group. The free ϵ -amine was then coupled to acetyl-phenylalanine and the carboxybenzyl (Cbz) group was subsequently removed through a palladium mediated hydrogenolysis. The resulting secondary amine was coupled to *p*NP-TC followed by the removal of the Fmoc protecting group on the α -amine of lysine to furnish **6**. The length of the peptide backbone was then elongated through the iterative coupling of two additional alanine residues to afford **7** and **8**, respectively.

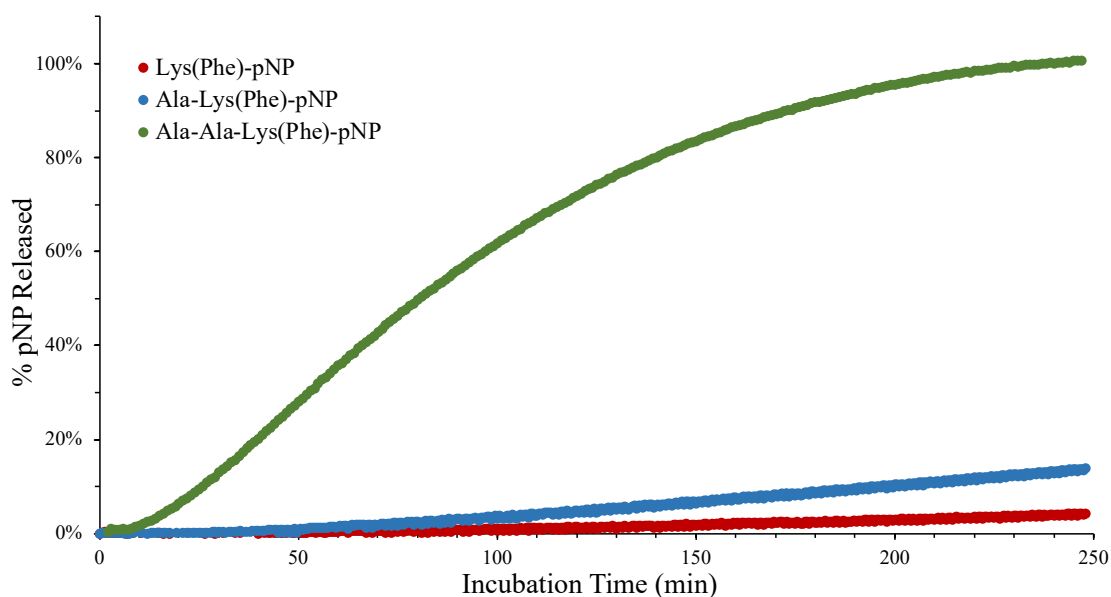


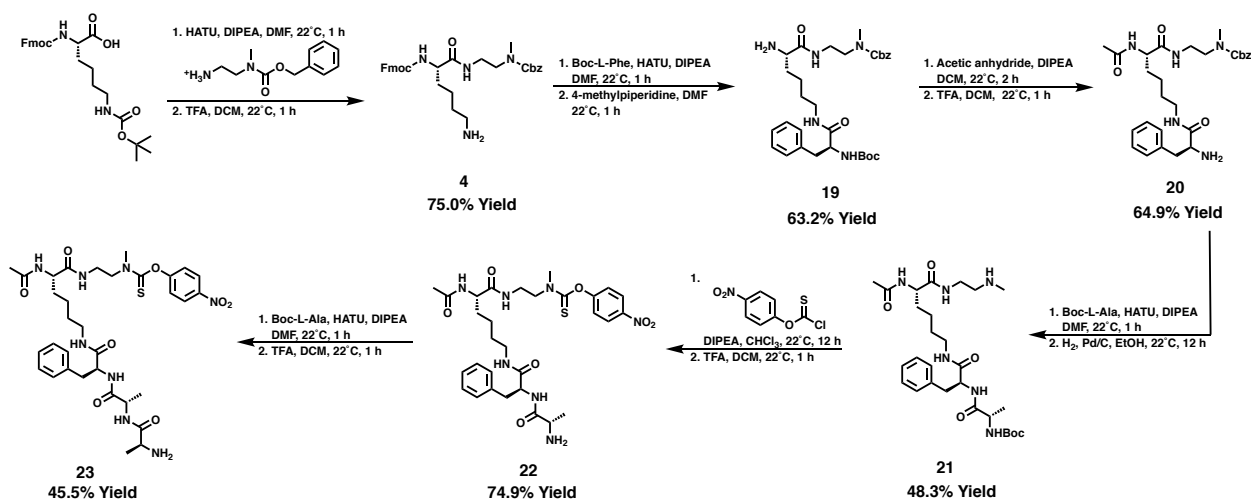
Figure 3.1. Sequence dependent *p*NP release from peptide substrates in the presence of only chymotrypsin monitored via the absorbance at 405 nm (n=3).

With the three prodrugs synthesized, we next monitored the *p*NP release from each of them in the presence of chymotrypsin. Substrates **6** and **7** both showed less than 10% release over the course of four hours. However, substrate **8** reached greater than 90% *p*NP release within three hours. This effectively illustrated that the increasing length of the peptide backbone by at least two amino acids directly facilitated the onset of the chymotrypsin cleavage. Whether the loss of these two alanine residues affected the conformation of the peptide sequence in the chymotrypsin

binding pocket was not investigated; however, identifying a prodrug with minimal release in the presence of only chymotrypsin was successful, so we proceeded towards further optimization of the prodrug sequence.

3.2.2 Optimization of Peptide Sequence to Enhance the Efficiency of Release

In order to ensure the prodrug was effectively cleaved in the small intestine, we decided to optimize the peptide sequence to enhance the substrate efficiency. This enhanced substrate would ensure that all of the opioid is released in the gastrointestinal (GI) tract and minimize the amount of secreted waste. Our observation that peptides with more than one Ala attached to the α -amine of lysine activated the chymotrypsin promiscuity, limited the peptide sequence diversity on this part of the prodrug. However, previous studies have shown through the crystal structure of chymotrypsin co-crystallized with substrates, that substrate binding is selective towards phenylalanine and tyrosine and this binding can be enhanced through additional non-bulky amino acid groups following the phenylalanine or tyrosine.⁴⁻⁷ These additional amino acids increase the number of hydrogen bonds between the substrate and the enzyme which enhances the alignment of the substrate in the binding pocket, and therefore enhances the catalytic turnover. With this knowledge, we decided to further probe the length of the peptide sequence by adding alanine residues to the α -amine of phenylalanine.



Scheme 3.2. Synthesis of Ac-Lys[Phe-R]-pNP substrates for enzyme kinetics experiments.

These prodrugs were prepared from Fmoc-lysine(Boc) by initially installing a carboxybenzyl-protected diamine followed by the removal of the Boc group (Scheme 3.2). The free ϵ -amine was then coupled to Boc-Phe followed by removal of the Fmoc group through a base mediated deprotection. The resulting amine was acetylated and thereupon the Boc group was removed via an acidic deprotection. The resulting α -amine was then coupled to Boc-alanine followed by cleavage of the Cbz group via a palladium mediated hydrogenolysis. The resulting secondary amine was then coupled to pNP-TC followed by a Boc deprotection to afford **22**. Lastly, the peptide was once again coupled to another Boc-alanine and the Boc group was subsequently removed to afford **23**. Once prepared, we ran Michaelis-Menten enzyme kinetics experiments to compare the enzymatic efficiency between each substrate (Figure 3.2). Substrate **6** was chosen as a starting point, however, there was a negligible amount of release over the course of 4 hours. Substrates **22** and **7** both showed comparable substrate specificity (K_{cat}/K_M) and the additional alanine on **23** resulted in a significant enhancement to that specificity.

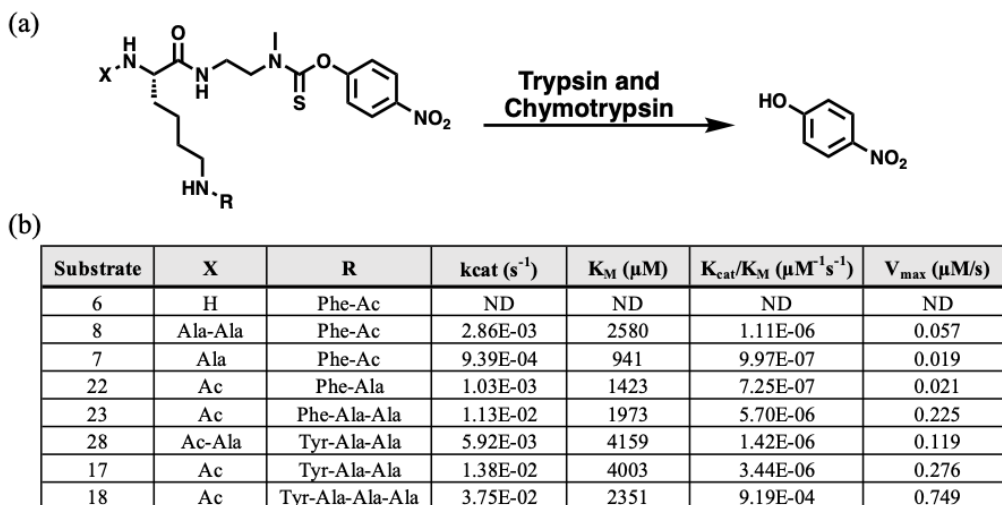
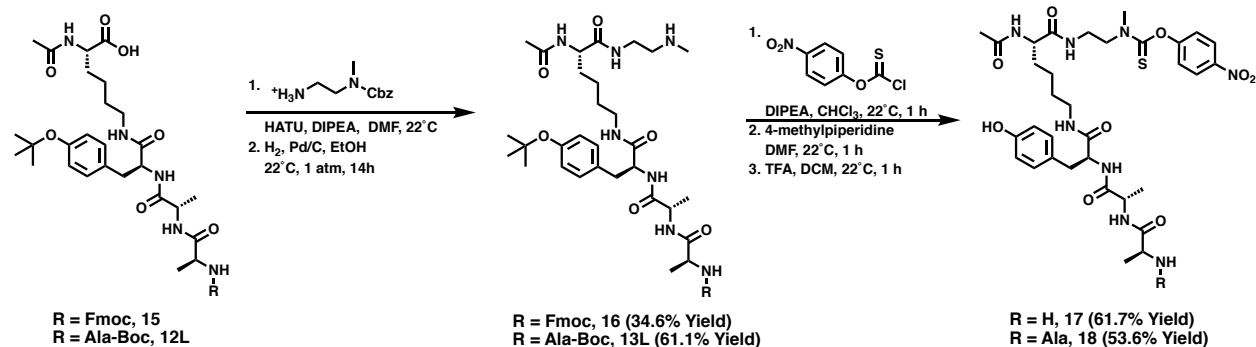


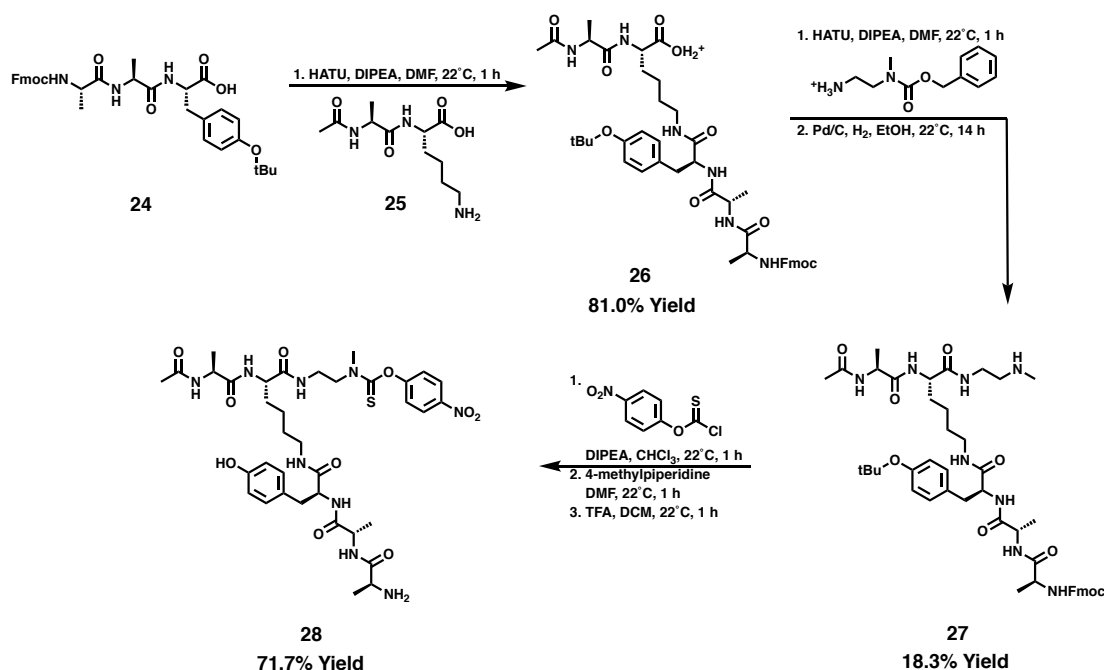
Figure 3.2. Peptide sequence optimization (a) peptide-prodrug mimic for monitoring rate of *p*NP release via absorbance at 405 nm (b) Michaelis-Menten kinetics parameters comparison between peptide sequences (ND: not determined).

Further analysis of the literature showed that a tyrosine residue was preferred in the chymotrypsin binding pocket over a phenylalanine residue, which could further enhance the substrate specificity of our peptide sequence.^{5,6} To determine what extent the tyrosine substitution would have on the substrate specificity, **17** and **18** were prepared (Scheme 3.4). The peptide backbones were prepared entirely on resin followed by the installation of a carboxybenzyl-protected diamine and subsequent removal of the Cbz group. The resulting secondary amine was then coupled to *p*NP-TC followed by the removal of all protecting groups to afford **17** and **18**. Comparing the substrate specificity between **17** and **23** showed a minor enhancement in favor of the phenylalanine residue, however the addition of another alanine in substrate **18** showed a 265-fold enhancement compared to **17** (Figure 3.2).



Scheme 3.3. Synthesis of Ac-Lys[Tyr-Ala-Ala-R]-*p*NP substrates 17 and 18 for enzyme kinetics experiments.

The previous comparison between substrates **6** and **7** showed that the addition of one alanine residue to α -amine of lysine does enhance the substrate specificity without turning on the chymotrypsin promiscuity. To determine whether this trend remained applicable for the newer generation of substrates, **28** was prepared. This was done by separately synthesizing **24** and **25** on resin and then coupling them together to deliver **26**. Thereupon the installation of a carboxybenzyl-protected diamine and subsequent removal of the Cbz group furnished **27**. The resulting secondary amine was coupled to *p*NP-TC followed by the removal of all protecting groups to afford **28**. This addition to the α -amine of lysine minimally affected the substrate affinity (K_M) of **28**; however, the V_{\max} was reduced by half leading to a decrease in the substrate specificity.



Scheme 3.4. Synthesis of Ac-Ala-Lys[Tyr-Ala-Ala]-pNP substrate for enzyme kinetics experiments.

When comparing all the prodrugs it was found that substrate **18** had the highest K_{cat}/K_M and fastest rate of release (V_{max}). While the addition of another alanine residue to **23** may result in a comparable K_{cat}/K_M , the use of tyrosine incorporated a phenol onto the peptide backbone. The presence of a phenol gives an additional handle to functionalize, which could be modified to add another layer of security within the prodrug. We hypothesized that by protecting the phenol via a t-butyl ether (tBu) we could shut off any chymotrypsin recognition prior to passage through the acidic conditions in the stomach where the t-butyl ether would be removed.⁸ This additional security measure removes a user's ability to pretreat the prodrug with store bought digestive enzymes, many of which contain both trypsin and chymotrypsin.

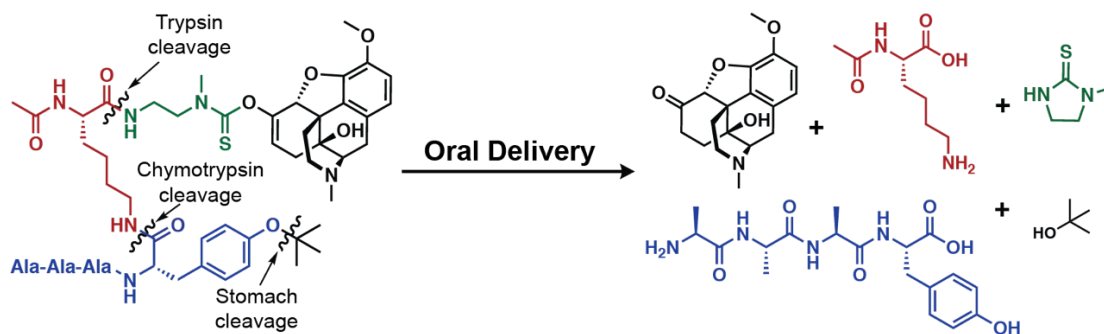


Figure 3.3. Abuse-deterrent opioid formulation comprised of a pH and dual enzyme-responsive peptide prodrug.

To probe our hypothesis, *in vitro* simulated digestion assays were carried out in the presence of either trypsin, chymotrypsin, or both. All *in vitro* assays were carried out using 0.5 mM prodrug substrate at a 25:1 ratio to the respective protease in 35 mM HEPES buffer at pH 7.4. *p*-Nitrophenol release from **18** was only observed in the presence of both proteolytic enzymes and the presence of a *t*-butyl ether masking the phenol completely abrogates any release, confirming that the additional acidic pretreatment was required for this prodrug system.

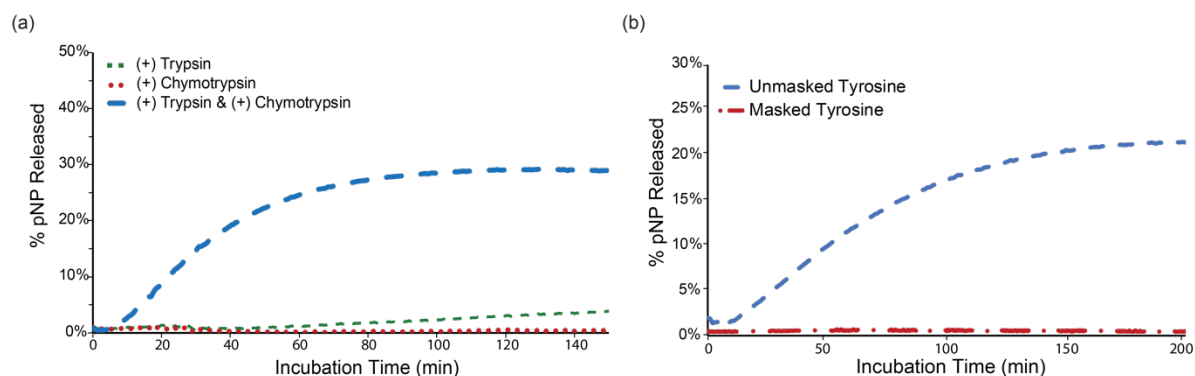


Figure 3.4. Protease responsive release of *p*NP from peptide-*p*NP prodrug (a) **18** in the presence of either trypsin or chymotrypsin or both monitored by absorbance at 405nm (n=3) in 35 mM HEPES pH 7.4 (b) **18** with or without the *t*-butyl ether protecting group masking the phenol in the presence of both trypsin and chymotrypsin (n=3).

Prior to moving forward towards analgesia studies in mice, we wanted to ensure that the YAAA byproduct (**29**) from the cleavage was not competitively inhibiting the *p*NP release. This

would be an issue once *in vivo* as the PEPT1 transepithelial transporter for peptides in the digestive tract has a very low binding affinity for tetrapeptides.⁹ A lack of transport for the byproduct could lead to the accumulation of YAAA and if this competitively inhibits chymotrypsin the opioid release could be shut off before reaching high levels of release. To test whether this would prove to be an issue, we ran Michaelis-Menten competitive inhibition enzyme kinetics experiments on the two best performing peptide sequences (**17** and **18**). The stepwise reduction in enzyme velocity shown in the Michaelis-Menten plot clearly demonstrates that increasing amounts of the YAA byproduct (**30**) inhibited the rate of release for **17** (Figure 3.5a). However, the inhibition of **18** proved to be negligibly affected by the presence of the YAAA inhibitor with no statistical difference between conditions (Figure 3.5b). This observation meaningfully enhanced our confidence in using substrate **18** for analgesia studies.

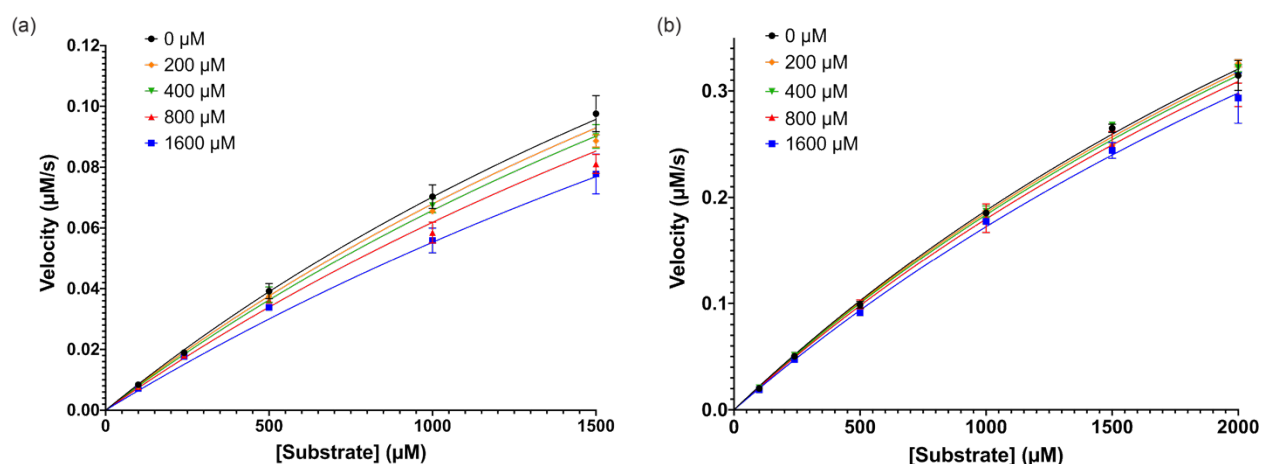
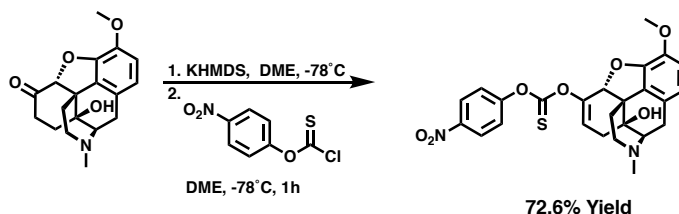


Figure 3.5. Michaelis Menten enzyme kinetics monitoring competitive inhibition of (a) Ac-K[YAA]-*p*NP using YAA as an inhibitor and (b) Ac-K[YAAA]-*p*NP using YAAA as an inhibitor.

3.2.3 Preparation of Oxycodone Electrophile

Initial attempts to prepare the oxycodone electrophile were carried out using the same preparation as the naltrexone-PFP electrophile from Chapter 4. Briefly, the oxycodone enolate was prepared in DME using KHMDS at -78 °C and this was cannulated into a separate solution of

pentafluorophenyl thionochloroformate. This procedure was optimized with Naltrexone to regularly return yields above 50%, however, upon switching to oxycodone, the yield dropped precipitously to ~10%. Considering that oxycodone is highly regulated and difficult to obtain, it was not feasible to continue forward with this procedure. During these initial attempts, we observed that the drop in yield was not due to low conversion but rather a lack of stability to the purification conditions. Our conjecture is that the increased hydrophilicity of oxycodone decreased the stability of the thionocarbonate and therefore reduced the lifetime during reverse phase purification. Attempts to purify the reaction mixture via normal phase column chromatography proved impractical due to the inability to separate the intended thionocarbonate from various PFP byproducts. In an effort to avoid chromatography, a precipitation-based purification strategy was attempted by precipitating out the PFP-oxycodone product into hexanes. Unfortunately, the product was soluble in hexanes, and therefore the strategy proved futile.



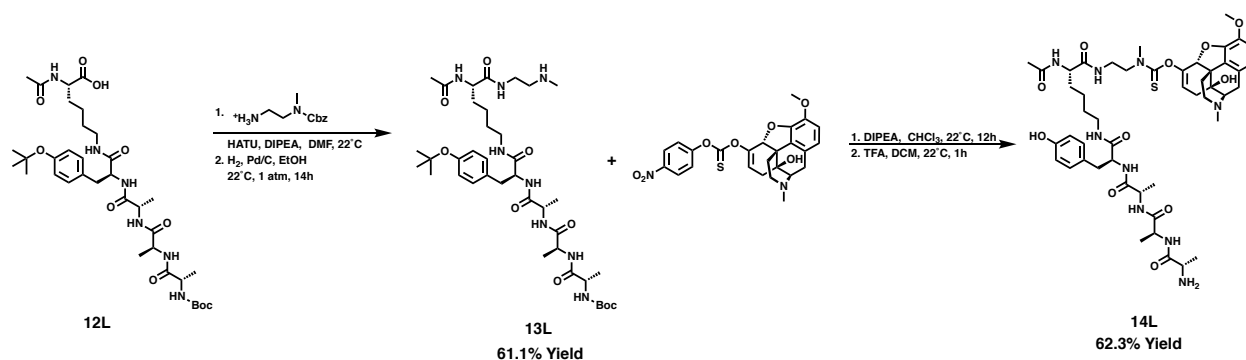
Scheme 3.5. Preparation of the O-enol linked *p*NP-oxycodone electrophile (**11**) via an enolate formation and subsequent trapping with *p*NP-thionochloroformate (**1**).

Rather than continuing to optimize purification conditions, we decided to modify the electrophile in order to alter the solubility. To this end, the oxycodone-*p*NP allyl enol thionocarbonate electrophile (**11**) was prepared as a hydrophilic alternative to the PFP derivative, allowing for a precipitation-based purification. Conditions for the preparation of this electrophile were optimized and found that 2 equivalences of potassium bis(trimethylsilyl)amide (KHMDS) and 1.6 equivalence of **1** resulted in 100% conversion of the oxycodone to the allyl enol

thionocarbonate with minimal byproduct formation. The crude reaction mixture was then immediately washed, and concentrated under vacuum. All attempts to concentrate the reaction prior to the washes, led to the formation of unidentified oxycodone byproducts that were difficult to separate by chromatography and this approach was therefore avoided. The resulting semi-pure solid was iteratively precipitated into hexanes resulting in oxycodone-*p*NP allyl enol thionocarbonate electrophile of $\geq 95\%$ purity. In the end, this reaction was scaled up to 150 mg of oxycodone resulting in yields on average of 73%, surpassing the higher yields obtained from the naltrexone modifications.

3.2.4 Preparation and Characterization of Ac-Lys[Tyr-Ala-Ala-Ala]-Oxycodone Prodrug as an Abuse-Deterrent Formulation

When designing the analgesia studies, we decided that the use of an inactive substrate would prove to be an effective control. This was carried out by using the D-tyrosine residue for the L-tyrosine, which would no longer be recognized by chymotrypsin. This would aid us in understanding if the release pathway proceeds through an enzymatic release mechanism. The synthesis of these prodrugs was carried out in tandem, through the initial preparation of **12** entirely on resin. Thereupon the C-terminus was coupled to the Cbz-protected diamine followed by a hydrogenolysis to furnish **13**. The resulting amine was then coupled to the oxycodone-*p*NP allyl enol thionocarbonate electrophile (**11**) followed by a global deprotection to afford **14**.



Scheme 3.6. Synthesis of Ac-Lys[Tyr-Ala-Ala-Ala]-oxycodone prodrug 14L. The negative control 14D was also prepared using a D-tyrosine residue in replace of the L-tyrosine.

The resulting prodrug was then tested for its stability to aqueous buffers ranging in pH from 2 to 12. Additionally, the prodrug's stability to household chemicals as well as store bought digestive enzymes was monitored. Across all attempts to degrade the prodrug, none of the conditions resulted in a significant amount of opioid released.

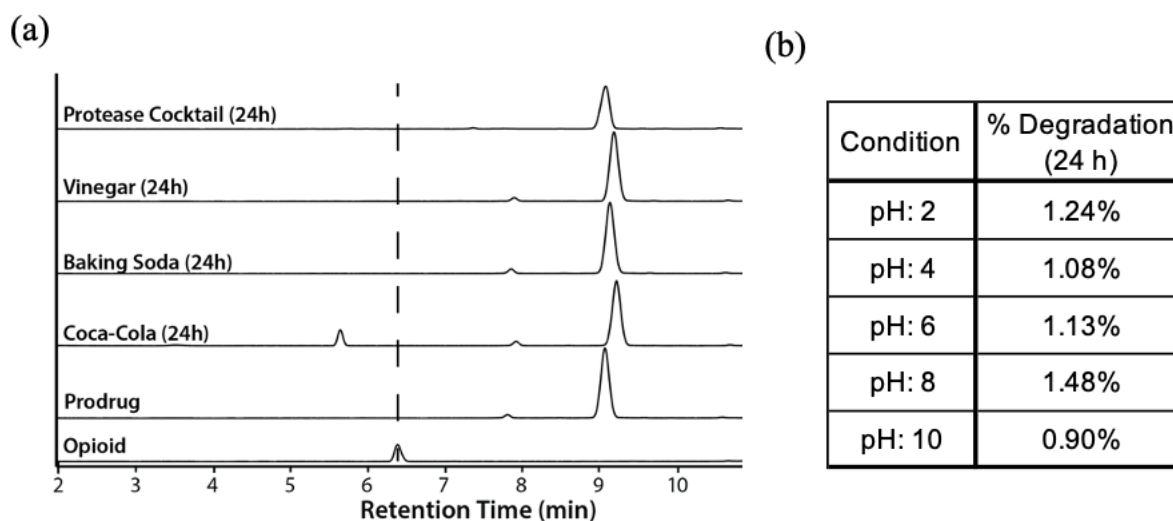


Figure 3.6. (a) Stability of Ac-K[YAAA]-oxycodone prodrug to household chemicals and solvents as well as (b) in 50 mM citrate-phosphate (McIlvaine) buffer across a pH range of 2 to 10.

The final peptide-oxycodone prodrug was delivered to Professor Catherine Cahill in the UCLA Department of Neuroscience who, at the time of writing, is studying the analgesic effects

of the prodrug in mice. A comparison between the prodrugs containing either an L or D tyrosine in the peptide backbone will further ensure that the release is progressing through a protease mediated cleavage process *in vivo*.

3.3 Conclusions

With the ongoing opioid epidemic claiming thousands of lives in the United States each year, development of technologies to mitigate the abuse of these necessary, but highly addictive analgesic agents have become of paramount importance. In this chapter, we report the synthetic development of a dual-enzyme responsive peptide-oxycodone prodrug for oral administration, improving upon our previous abuse-deterrent formulation. The design of this prodrug relies on an initial passage through the stomach to activate the peptide sequence, followed by the enzymatically triggered release of active oxycodone. The improvement in the prodrug design was carried out through peptide sequence optimization to ensure the requirement of trypsin and chymotrypsin while simultaneously enhancing the release kinetics. Preparation of the oxycodone allyl enol thionocarbonate electrophile was not easily translated from previous naltrexone modifications and therefore synthetic conditions were optimized to achieve consistent and high yielding results. We expect that the chemistry and abuse-deterrent opioid prodrug that we have developed in this chapter will contribute to efforts to combat the opioid epidemic.

3.4 Experimental

3.4.1 Materials

Oxycodone was supplied by our collaborators Chris Evans and Catherine Cahill in the UCLA Department of Neurosciences who are licensed through the DEA. All other chemicals were used as purchased unless otherwise noted from Acros, Alfa Aesar, Sigma Aldrich, Chem-Impex,

or Fisher Scientific. All reactions were performed using dry solvents under an inert Argon atmosphere unless otherwise noted. Dichloromethane (DCM) was distilled over CaH₂ and stored under argon. Tetrahydrofuran (THF) was distilled over sodium/benzophenone and stored under argon. 1,2-dimethoxyethane, methanol, acetonitrile (MeCN) and other dry solvents were dried by purging with nitrogen and passage through activated alumina columns prior to use. TMEDA was freshly distilled and stored over 3Å molecular sieves prior to use. KHMDS was stored in a Vacuum Atmospheres Genesis stainless steel glove box under nitrogen atmosphere. Representative procedures are provided for each reaction.

3.4.2 Analytical Techniques

NMR spectra were obtained using either Bruker AV400, AV500, DRX500, or AV600 spectrometers. ESI mass spectra were obtained using either a Waters Acquity LCT Premier XE equipped with an autosampler and direct injection port or an Agilent 6530 QTOF-ESI with a 1260 Infinity LC with autosampler. Infrared absorption spectra were obtained using a PerkinElmer FT-IR equipped with an ATR accessory. Normal phase flash column chromatography was carried out using a Biotage Isolera One Flash Purification Chromatography system. Analytical reverse phase HPLC was carried out on a Agilent 1260 Infinity II HPLC system equipped with an autosampler and a UV detector using a Poroshell 120 2.7 µm C18 120 Å column (analytical: 2.7 µm, 4.6 × 100 mm) with monitoring at λ = 220 and 280 nm and with a flow rate of 0.8 ml/min. Peptide-drug conjugates were analyzed using a mobile phase consisting of 10-100% MeCN + 0.1% TFA in water beginning with a 1 min isocratic at 10%, then up to 100% over 10 min in a linear gradient, followed by an isocratic hold at 100% MeCN + 0.1% TFA for 4 min (total time was 15 min). Purification was carried out on the same system using a Zorbax SB-C18 5.0 µm C18 120 Å column (semi-preparative: 5.0 µm, 9.4 × 250 mm) with monitoring at λ = 220 and 280 nm and with a flow

rate of 3.0 ml/min. Peptide-drug conjugates were purified using a mobile phase consisting of 10-100% MeCN + 0.1% TFA in water beginning with a 3 min isocratic at 10%, then up to 100% over 15 min in a linear gradient, followed by an isocratic hold at 100% MeCN + 0.1% TFA for 4 min (total time was 22 min). Preparatory reverse phase HPLC was carried out on a Shimadzu high performance liquid chromatography system equipped with a UV detector using a Luna 5 μ m C18 100 Å column (preparatory: 5 μ m, 250 \times 21.2 mm) with monitoring at λ = 215 and 254 nm and with a flow rate of 20 ml/min. Enolate trapped drug products were purified using a mobile phase consisting of 40-95% MeCN + 0.1% TFA in water beginning with 1 min isocratic at 10%, then up to 95% over 15 min in a linear gradient, followed by an isocratic hold at 95% MeCN + 0.1% TFA for 4 min (total time was 20 min).

3.4.3 Methods

Stability of Elastomeric Prodrug to Household Solvents

Prodrug samples (1 mg/mL) were combined with either lemon juice, Coca-Cola, vinegar, or a predissolved solution of a digestive enzymes kit containing both trypsin and chymotrypsin. Aliquots were removed periodically to determine the amount of free oxycodone in solution corresponding to the instability of the prodrug.

General *p*-Nitrophenol Release Kinetics Studies

The peptide was dissolved in DMSO and diluted using 35 mM HEPES buffer (pH 7.5) to a final substrate concentration of 2.0, 1.5, 1.0, 0.5, 0.24, and 0.1 mM maintain a constant concentration of DMSO across all conditions. These solutions were then combined with trypsin and chymotrypsin to afford a final concentration of 0.02 mM for each enzyme. Immediately upon addition of the proteases, the 96-well plate was inserted into the plate reader and the absorbance

at 405 nm was monitored over the course of 4 hours. All conditions were carried out in triplicate and reported as the average between the three replicates. Michaelis-Menten enzyme kinetic analysis was carried out using GraphPad Prism 8.4.3.

For the inhibition studies, the above procedure was carried out with an additional presence of the inhibitor. The inhibitor was added to yield a final concentration of either 1.6, 0.8, 0.4, or 0.2 mM. Michaelis-Menten enzyme inhibition kinetic analysis was carried out using GraphPad Prism 8.4.3.

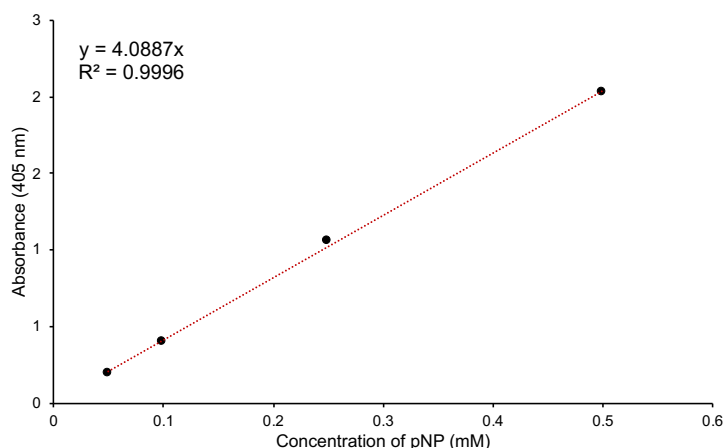
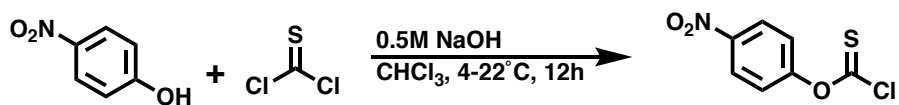


Figure 3.7. Standard curve of p-nitrophenol via UV absorbance (405 nm) on a plate reader across multiple concentrations.

Synthesis of pNP-thionochloroformate (1)

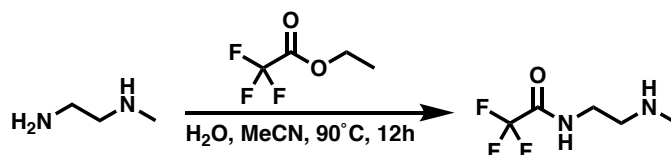


A solution of 4-nitrophenol (2.0 g, 1 Eq, 14.4 mmol) in aq. sodium hydroxide (575 mg, 28.8 mL, 0.500 molar, 1 Eq, 14.4 mmol) was cooled down to 4 °C using an ice bath. Separately, a solution of thiophosgene (1.1 mL, 1 Eq, 14.4 mmol) in CHCl₃ (20 mL) was prepared and then

added dropwise to the cooled solution over the course of 10 minutes. This solution was then stirred at 4 °C for 1 hour, slowly warmed up to 22 °C, and stirred for an additional 12 hours at 22 °C.

At this point the chloroform was removed under reduced pressure and the resulting suspension was transferred to a separatory funnel along with EtOAc (300 mL). The organic layer was then washed with sat. aq. NaHCO₃ (3 x 75 mL), sat. aq. NaCl (50 mL), dried over MgSO₄, and concentrated under reduced pressure directly onto silica (2 g). The crude product was purified by flash column chromatography (50 g silica gel, 5-50% EtOAc gradient against hexanes 10 column volumes) to afford the product (1.84 g, 58.8 % yield) as a yellow solid. TLC: R_f 0.73 (9:1 hexanes:EtOAc). ¹H NMR (400 MHz, CD₃CN): δ 8.35 (d, *J* = 9.2 Hz, 2H), 7.35 (d, *J* = 9.2 Hz, 2H). ¹³C NMR (101 MHz, CD₃CN): δ 184.66, 158.16, 146.49, 125.80, 122.72. m.p.: T_{on} 62.3 °C: T_{peak} 63.7 °C.

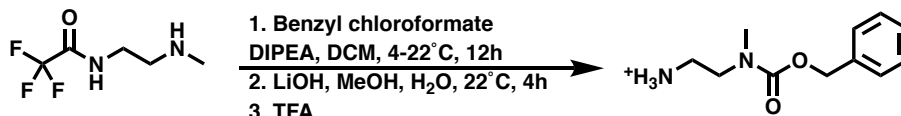
Synthesis of 2,2,2-trifluoro-N-(2-(methylamino)ethyl)acetamide (2)



To a solution of N-methylethylene diamine (1.5 mL, 1 Eq, 17 mmol) in water (1.0 mL) and MeCN (9 mL) was slowly added ethyl trifluoroacetate (4.7mL, 2.3 Eq, 40 mmol) at 23 °C under an inert atmosphere. This solution was then warmed to 90 °C under a reflux condenser for 12 hours. Following this, the solution was cooled back down to room temperature and all solvent was removed under reduced pressure. The resulting brown oil was combined with isopropanol (3 mL) and again all solvent was removed under reduced pressure. This last step was repeated two additional times eventually resulting in a brown solid. This crude product was recrystallized using DCM to afford the product (4.7 g, 97.2% yield) as a beige solid. ¹H NMR (500 MHz, CD₃CN): δ

9.08 (s, 2H), 3.59 (q, $J = 5.4$ Hz, 2H), 3.16 (t, $J = 5.4$ Hz, 2H), 2.63 (s, 3H). ^{13}C NMR (126 MHz, CD_3CN): δ 159.59, 116.53, 47.96, 36.16, 32.84. HRMS (ESI/Q-TOF): $[\text{M}+\text{H}]^+$ calcd for $\text{C}_5\text{H}_{10}\text{F}_3\text{N}_2\text{O}^+$, 171.0740; found 171.0763. m.p.: T_{on} 209.9 °C: T_{peak} 239.8 °C

Synthesis of benzyl (2-aminoethyl)(methyl)carbamate (3)

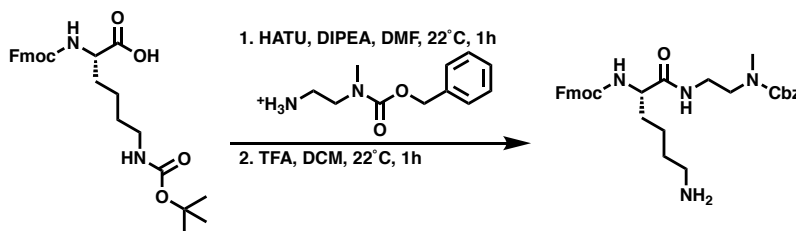


To a solution of **2** (1.5 g, 1 Eq, 5.28 mmol) in anhydrous DCM (15 mL) was added anhydrous DIPEA (1.0 mL, 1.1 Eq, 6.25 mmol) and the reaction contents were brought down to 4°C. A separately prepared solution of benzyl chloroformate (0.79 mL, 1.05 Eq, 5.54 mmol) in anhydrous DCM (5 mL) was then added to the cooled solution dropwise over the course of 15 minutes. The reaction contents were then slowly brought up to 22 °C and stirred for 12 hours under an inert atmosphere. At this point the reaction contents were transferred to a separatory funnel along with EtOAc (300 mL). The organic layer was washed with sat. aq. NaHCO_3 (75 mL), 0.1M aq. HCl (75 mL), sat. aq. NaCl (75 mL), dried over MgSO_4 , and concentrated under reduced pressure to afford the bis-protected diamine as a yellow oil (1.48 g, 92.0% yield). This was carried forward as-is with no further purification. HRMS (ESI/Q-TOF): $[\text{M}+\text{H}]^+$ calcd for $\text{C}_{13}\text{H}_{16}\text{F}_3\text{N}_2\text{O}_3^+$, 305.1108; found 305.0673.

This intermediate was then dissolved in methanol and combined with a solution of LiOH (0.70 g, 6 Eq, 29.2 mmol) in H_2O (5 mL). This was stirred at 22 °C for 3 hours where it reached full conversion. The solvent was then removed under reduced pressure and the resulting oil was transferred to a separatory funnel along with CHCl_3 (225 mL) and isopropanol (75 mL). The organic layer was washed with sat. aq. NaHCO_3 (75 mL), sat. aq. NaCl (75 mL), dried over

MgSO₄, and concentrated under reduced pressure to produce a tan oil. This oil was then precipitated into a mixture of diethyl ether (45 mL) and TFA (1 mL) to afford the product (1.05 g, 66.8% yield) as a white solid. ¹H NMR (500 MHz, CD₃CN): δ 7.36 (m, J = 5.2 Hz, 8H), 5.10 (s, 2H), 3.54 (s, 2H), 3.14 (s, 2H), 2.92 (s, 3H). ¹³C NMR (126 MHz, CD₃CN): δ 157.62, 136.86, 128.50, 128.00, 127.73, 67.24, 46.67, 38.76, 34.20. HRMS (ESI/Q-TOF): [M+H]⁺ calcd for C₁₁H₁₇N₂O₂⁺, 209.1285; found 209.1239. m.p.: T_{on} 103.3 °C: T_{peak} 107.6 °C.

Synthesis of Fmoc-Lys-(2-(Cbz)methyl)ethylamino (4)

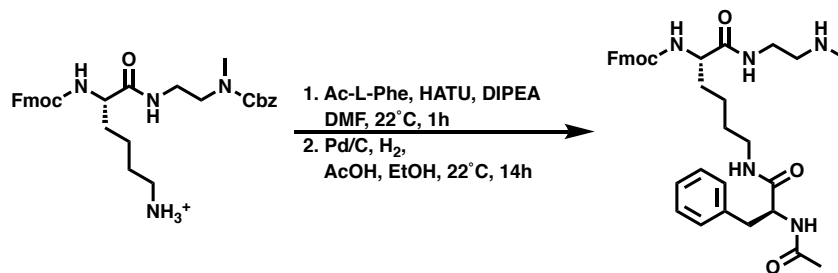


To a solution of Fmoc-lysine(boc) (400.0 mg, 1 Eq, 854 μmol) in DMF (5 mL) was added (1-[Bis(dimethylamino)methylene]-1H-1,2,3-triazolo[4,5-b]pyridinium-3-oxide hexafluorophosphate (HATU) (357 mg, 1.1 Eq, 939 μmol) and DIPEA (410 μL, 3 Eq, 2.56 mmol) forming a bright yellow solution. This solution was stirred for 10 minutes to ensure complete activation. Separately, a solution of **3** (303.0 mg, 1.1 Eq, 939 μmol) was prepared in DMF (2 mL) and then added dropwise to the activated peptide. This solution was stirred for 30 minutes at 22 °C before HPLC analysis showed full conversion. The reaction contents were then concentrated under reduced pressure and precipitated into H₂O (45 mL) to afford the intermediate as a white solid. This was carried forward without any further purification. HRMS (ESI/Q-TOF): [M+H]⁺ calcd for C₄₈H₆₈N₉O₁₁S⁺, 659.3439; found 659.2946.

This resulting peptide was dissolved in a 25% TFA solution in DCM (10 mL) with 1% TIPS and H₂O. This was stirred at 22 °C for 30 minutes and then concentrated under reduced

pressure. The resulting crude product was then purified via preparative HPLC (C18, 10-50% MeCN gradient against H₂O with a 0.1% TFA additive over 12 minutes) to afford **4** (1.53 g, 75.0% yield). HRMS (ESI/Q-TOF): [M+H]⁺ calcd for C₄₈H₆₈N₉O₁₁S⁺, 559.2915; found 559.3320.

Synthesis of Fmoc-Lys[(Ac)Phe]-2-methylethylamino (**5**)



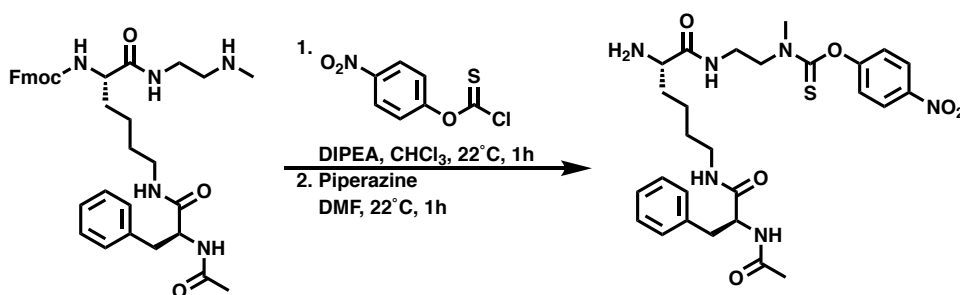
To a solution of Ac-L-phenylalanine (72.5 mg, 1.1 Eq, 350 μmol) in DMF (5 mL) was added HATU (133 mg, 1.1 Eq, 350 μmol) and DIPEA (166 μL, 3 Eq, 0.95 mmol) forming a bright yellow solution. This solution was stirred for 10 minutes to ensure complete activation. Separately, a solution of **4** (214 mg, 1 Eq, 318 μmol) was prepared in DMF (2 mL) and then added dropwise to the activated peptide. This solution was stirred for 30 minutes at 22 °C before HPLC analysis showed full conversion. The reaction contents were then concentrated under reduced pressure and precipitated into H₂O (45 mL) to afford the intermediate as a white solid. This was carried forward without any further purification. HRMS (ESI/Q-TOF): [M+H]⁺ calcd for C₄₃H₅₀N₅O₇⁺, 748.3705; found 748.4602.

The product was then dissolved in ethanol (20 mL) and acetic acid (324 μL, 20 Eq, 5.67 mmol) and combined with Pd/C (30 mg, 0.1 Eq). This solution was then sparged with argon, sealed under an atmosphere of hydrogen, and stirred at 22 °C for 14 hours (note 1). The reaction contents were then filtered over celite and concentrated under reduced pressure. The crude product was then purified via preparative HPLC (C18, 10-100% MeCN gradient against H₂O with a 0.1%

TFA additive over 12 minutes) to afford **5** (92 mg, 40.1% yield). HRMS (ESI/Q-TOF): $[M+H]^+$ calcd for $C_{38}H_{65}N_8O_9^+$, 614.3337; found 614.3444.

Note 1. The reaction was carried out in a 50 mL 1-neck RB flask and capped with a rubber septum. A double-layered balloon connected to a 3 mL syringe with a 3 cm needle was filled and hydrogen and placed on the round-bottom (RB) flask. The solution was sparged for 5 minutes with hydrogen before allowing it to stir for 14 hours.

Synthesis of Lys[(Ac)Phe]-(2-(*p*NP-thionocarbamate)methyl)ethylamino (**6**)



To a solution of **5** (92.0 mg, 1 Eq, 84.2 μ mol) in $CHCl_3$ (2.5 mL) and DMF (0.5 mL) was added DIPEA (66.1 μ L, 3 Eq, 379 μ mol). This solution was stirred for 5 minutes before a solution of **1** (52.2 mg, 1.25 Eq, 105 μ mol) in $CHCl_3$ (1.0 mL) was added. This solution was then vigorously stirred at $22^\circ C$ for 12 hours. At this point, the reaction contents were concentrated under vacuum and then precipitated into H_2O . The resulting precipitate was identified as the product via LCMS and shown to be greater than 95% pure. HRMS (ESI/Q-TOF): $[M+H]^+$ calcd for $C_{42}H_{47}N_6O_8S^+$, 795.3171; found 795.3326.

This resulting peptide was dissolved in DMF (2 mL) with piperazine (67.0 mg, 10 Eq, 780 μ mol). This was stirred at $22^\circ C$ for 30 minutes and then concentrated under reduced pressure. The resulting crude product was then purified via preparative HPLC (C18, 10-50% MeCN gradient

against H₂O with a 0.1% TFA additive over 12 minutes) to afford **6** (44 mg, 50.8% yield). HRMS (ESI/Q-TOF): [M+H]⁺ calcd for C₂₇H₃₇N₆O₆S⁺, 573.2490; found 573.2581.

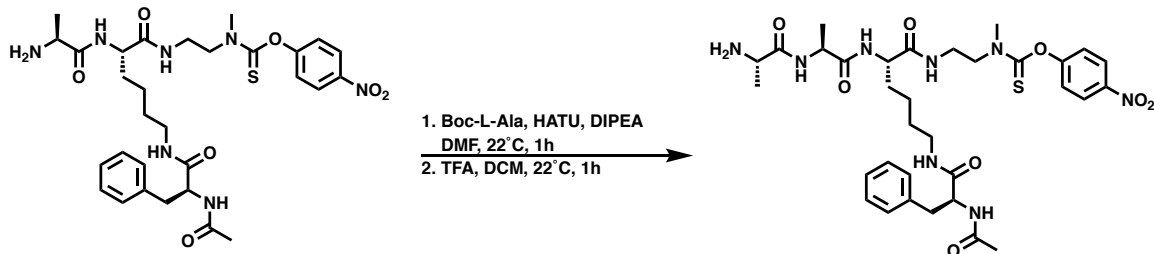
Synthesis of Ala-Lys[(Ac)Phe]-(2-(*p*NP-thionocarbamate)methyl)ethylamino (**7**)



To a solution of Boc-L-alanine (31 mg, 1.5 Eq, 170 μ mol) in DMF (5 mL) was added HATU (63 mg, 1.5 Eq, 170 μ mol) and DIPEA (96 μ L, 5 Eq, 0.55 mmol) forming a bright yellow solution. This solution was stirred for 10 minutes to ensure complete activation. Separately, a solution of **6** (76 mg, 1 Eq, 110 μ mol) was prepared in DMF (2 mL) and then added dropwise to the activated peptide. This solution was stirred for 30 minutes at 22 °C before HPLC analysis showed full conversion. The reaction contents were then concentrated under reduced pressure and precipitated into H₂O (45 mL) to afford the intermediate as a white solid. This was carried forward without any further purification. HRMS (ESI/Q-TOF): [M+H]⁺ calcd for C₃₅H₅₀N₇O₉S⁺, 744.3385; found 744.3480.

This resulting peptide was dissolved in a 25% TFA solution in DCM (10 mL) with 1% TIPS and H₂O. This was stirred at 22 °C for 30 minutes and then concentrated under reduced pressure. The resulting crude product was then purified via preparative HPLC (C18, 10-80% MeCN gradient against H₂O with a 0.1% TFA additive over 12 minutes) to afford **7** (62 mg, 74.0% yield). HRMS (ESI/Q-TOF): [M+H]⁺ calcd for C₃₀H₄₂N₇O₇S⁺, 644.2861; found 644.2968.

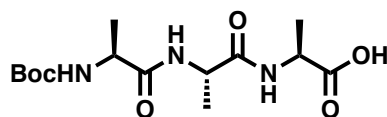
Synthesis of Ala-Ala-Lys[(Ac)Phe]-(2-(*p*NP-thionocarbamate)methyl)ethylamino (**8**)



To a solution of Boc-L-alanine (16 mg, 1.5 Eq, 85 μ mol) in DMF (5 mL) was added HATU (32 mg, 1.5 Eq, 85 μ mol) and DIPEA (49 μ L, 5 Eq, 0.28 mmol) forming a bright yellow solution. This solution was stirred for 10 minutes to ensure complete activation. Separately, a solution of **7** (43 mg, 1 Eq, 57 μ mol) was prepared in DMF (2 mL) and then added dropwise to the activated peptide. This solution was stirred for 30 minutes at 22 °C before HPLC analysis showed full conversion. The reaction contents were then concentrated under reduced pressure and precipitated into H₂O (45 mL) to afford the intermediate as a white solid. This was carried forward without any further purification. HRMS (ESI/Q-TOF): [M+H]⁺ calcd for C₃₈H₅₅N₈O₁₀S⁺, 815.3863; found 815.3863.

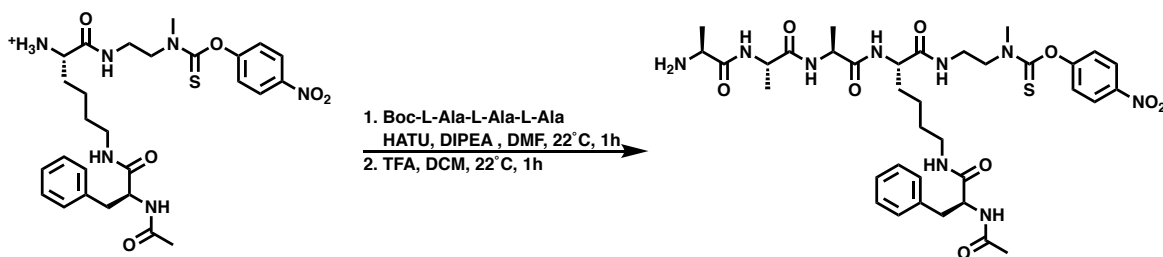
This resulting peptide was dissolved in a 25% TFA solution in DCM (10 mL) with 1% TIPS and H₂O. This was stirred at 22 °C for 30 minutes and then concentrated under reduced pressure. The resulting crude product was then purified via preparative HPLC (C18, 10-80% MeCN gradient against H₂O with a 0.1% TFA additive over 12 minutes) to afford **8** (43 mg, 91.0% yield). HRMS (ESI/Q-TOF): [M+H]⁺ calcd for C₃₃H₄₇N₈O₈S⁺, 715.3232; found 715.3345.

Synthesis of Boc-Ala-Ala-Ala (**9**)



The peptide was synthesized via standard Fmoc Solid Phase Peptide Synthesis conditions. The peptide was prepared starting from a 2-Chlorotrityl chloride resin (0.89 meq/g ChemImpex). The resin was initially swelled in DCM for 60 minutes prior to any modifications. The initial Alanine coupling was carried out using two equivalence of Fmoc-alanine and 6 equivalence of DIPEA. This was done in a 50/50 DCM & NMP mixture and shaken for 90 minutes. Each amino acid residue thereafter was loaded using a 3:3:6 ratio of amino acid: HATU: DIPEA in NMP for 30 minutes. The couplings were followed by deprotection in 20% 4 methyl-piperidine (in DMF) for 20 minutes. After coupling the third alanine residue, the Boc protecting group was NOT cleaved. The resin was dried under vacuum for 120 minutes and then swelled in DCM for 40 minutes. The peptide was cleaved from the resin while maintaining the Boc protecting group by using a 20% HFIP in DCM cleavage cocktail. Approximately 10mL of the cleavage cocktail was added to the resin/peptide and mixed for 2 minutes. The solution was filtered and the solvent removed under vacuum. This process was repeated 4 additional times. After each removal of HFIP and DCM under vacuum the concentrate was precipitated into chilled diethyl ether (-20.0°C) to afford **9** (148 mg, 49.6% yield). HRMS (ESI/Q-TOF): $[M+Na]^+$ calcd for $C_{14}H_{25}N_3O_6Na^+$, 354.1636; found 354.1689.

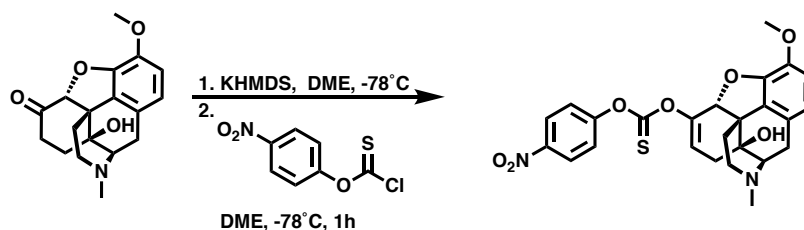
Synthesis of Ala-Ala-Ala-Lys[(Ac)Phe]-(2-(*p*NP-thionocarbamate)methyl)ethylamino (**10**)



To a solution of **9** (18 mg, 1.5 Eq, 55 μmol) in DMF (3 mL) was added HATU (21 mg, 1.5 Eq, 55 μmol) and DIPEA (32 μL , 5 Eq, 0.18 mmol) forming a bright yellow solution. This solution was stirred for 10 minutes to ensure complete activation. Separately, a solution of **6** (25 mg, 1 Eq, 36 μmol) was prepared in DMF (2 mL) and then added dropwise to the activated peptide. This solution was stirred for 30 minutes at 22 $^{\circ}\text{C}$ before HPLC analysis showed full conversion. The reaction contents were then concentrated under reduced pressure and precipitated into H_2O (45 mL) to afford the intermediate as a white solid. This was carried forward without any further purification. HRMS (ESI/Q-TOF): $[\text{M}+\text{H}]^+$ calcd for $\text{C}_{41}\text{H}_{60}\text{N}_9\text{O}_{11}\text{S}^+$, 886.4128; found 886.4228.

This resulting peptide was dissolved in a 25% TFA solution in DCM (10 mL) with 1% TIPS and H_2O . This was stirred at 22 $^{\circ}\text{C}$ for 30 minutes and then concentrated under reduced pressure. The resulting crude product was then purified via preparative HPLC (C18, 10-80% MeCN gradient against H_2O with a 0.1% TFA additive over 12 minutes) to afford **10** (29 mg, 89.0% yield). HRMS (ESI/Q-TOF): $[\text{M}+\text{H}]^+$ calcd for $\text{C}_{36}\text{H}_{52}\text{N}_9\text{O}_9\text{S}^+$, 786.3603; found 786.3682.

Synthesis of pNP-oxycodone thionocarbonate (11)



To a solution of Oxycodone (150.5 mg, 1 Eq, 477.2 μmol) (free base) in anhydrous DME (5 mL) at -78 $^{\circ}\text{C}$ was slowly added a solution of KHMDS (190.4 mg, 2 Eq, 954.4 μmol) in anhydrous DME (2 mL) (note 1). This solution was then vigorously stirred at -78 $^{\circ}\text{C}$ for about 20 minutes under an inert atmosphere. Separately, a solution of **1** (166.2 mg, 1.6 Eq, 763.5 μmol) in anhydrous DME (30 mL) was cooled to -78 $^{\circ}\text{C}$. Once cooled, the oxycodone solution was slowly

cannulated into the solution of 1 over the course of 10 minutes. Upon complete transfer, an additional amount of anhydrous DME (~3 mL) was used to rinse the oxycodone flask and was also transferred into the reaction mixture. The reaction contents were then stirred at -78 °C for 20 minutes, at which point HPLC indicated full conversion had been achieved.

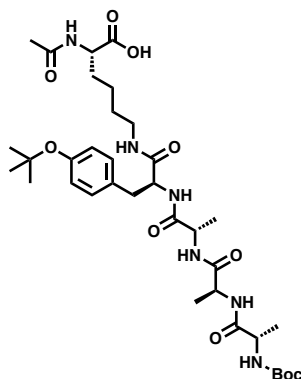
The reaction contents were immediately transferred to a separatory funnel along with H₂O (200 mL) (note 2). The aq. solution was then extracted with EtOAc (2 x 100 mL) and the combined organic layers were washed with H₂O (3 x 50 mL), sat. aq. NaCl (50 mL), dried over MgSO₄, and concentrated under reduced pressure to afford a yellow solid. This solid is then reconstituted in a minimal amount of DCM and precipitated into hexanes chilled to 0 °C. The precipitate is collected and the precipitation is repeated an additional three times to afford the oxycodone electrophile (172 mg, 72.6% yield) (note 3) as a beige solid. ¹H NMR (500 MHz, CD₃CN): δ 8.31 (d, J = 9.1 Hz, 2H), 7.36 (d, J = 9.1 Hz, 2H), 6.74 (d, J = 8.3 Hz, 1H), 6.67 (d, J = 8.2 Hz, 1H), 5.74 (dd, J = 1.9, 6.0 Hz, 1H), 5.23 (s, 1H), 3.84 (s, 3H), 3.20 (d, J = 18.9 Hz, 1H), 3.16 (s, 1H), 2.75 (dd, J = 18.7, 5.5 Hz, 1H), 2.65 (s, 1H), 2.52 (s, 3H), 2.39 (m, 3H), 2.21 (d, J = 17.6 Hz, 1H), 1.68 (dd, J = 2.5, 12.9 Hz, 1H), 1.25 (s, 1H). ¹³C NMR (126 MHz, CD₃CN): δ 191.87, 157.53, 146.52, 145.95, 144.52, 143.80, 130.30, 125.37, 124.68, 123.27, 120.35, 119.24, 114.18, 85.27, 70.47, 64.18, 56.54, 46.91, 45.44, 42.86, 31.78, 30.28, 22.60. HRMS (ESI/Q-TOF): [M+H]⁺ calcd for C₂₂H₂₅N₂O₇S⁺, 497.1377; found 497.1447.

Note 1. Oxycodone was azeotropically dried from anhydrous toluene prior to use in this experiment.

Note 2. It is important to quickly transfer the cold reaction contents to the separatory funnel with H₂O. Leaving the reaction contents at elevated temperatures (> -78 °C) for prolonged periods of time leads to side product formation.

Note 3. To maximize the % recovery the supernatant can be concentrated back down and put through the precipitation process again to reclaim more product. This method of purification was chosen due to the electrophile's instability to chromatographic forms of purification.

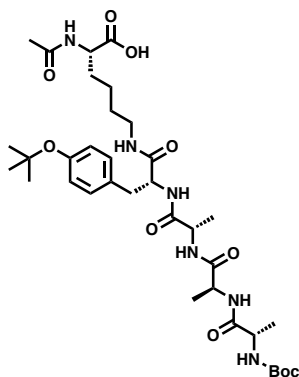
Synthesis of Ac-Lys[Tyr(tBu)-Ala-Ala-Ala-boc] (12L)



The peptide was synthesized via standard Fmoc Solid Phase Peptide Synthesis conditions. The peptide was prepared starting from a 2-Chlorotrityl chloride resin (0.89 meq/g ChemImpex). The resin was initially swelled in DCM for 60 minutes prior to any modifications. The initial lysine coupling was carried out using two equivalence of acetylated-lysine(Fmoc) and 6 equivalence of DIPEA. This was done in a 50/50 DCM & NMP mixture and shaken for 90 minutes. Each amino acid residue thereafter was loaded using a 3:3:6 ratio of amino acid: HATU: DIPEA in NMP for 30 minutes (note 1). The couplings were followed by deprotection in 20% 4 methyl-piperidine (in DMF) for 20 minutes (note 2). After coupling the third alanine residue, the Boc protecting group was NOT cleaved. The resin was dried under vacuum for 120 minutes and then swelled in DCM for 40 minutes. The peptide was cleaved from the resin while maintaining the Boc and t-butyl

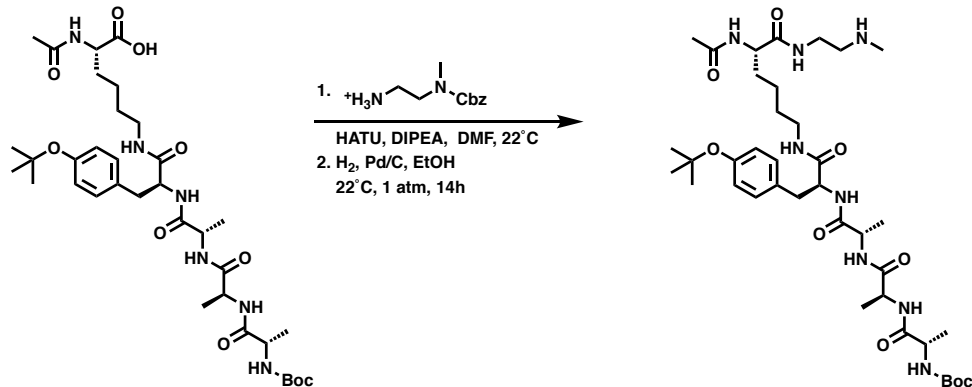
protecting groups by using a 20% HFIP in DCM cleavage cocktail. Approximately 10mL of the cleavage cocktail was added to the resin/peptide and mixed for 2 minutes. The solution was filtered and the solvent removed under vacuum. This process was repeated 4 additional times. After each removal of HFIP and DCM under vacuum the concentrate was precipitated into chilled diethyl ether (-20.0°C) to afford **12L** (540 mg, 56.2% yield). HRMS (ESI/Q-TOF): $[M+H]^+$ calcd for $C_{35}H_{57}N_6O_{10}^+$, 721.4131; found 721.3825.

Synthesis of Ac-Lys[Tyr(tBu)-Ala-Ala-Ala-boc] (12D)



Prepared following the procedure for **5L**, however, N-Fmoc-D-tyrosine(tBu) was used rather than the L-amino acid to afford **12D** (565.2 mg, 58.8% yield). HRMS (ESI/Q-TOF): $[M+H]^+$ calcd for $C_{35}H_{57}N_6O_{10}^+$, 721.4131; found 721.3799.

Synthesis of Ac-Lys[Tyr(*t*Bu)-Ala-Ala-Ala-boc]-2-methylethylamino (13L**)**

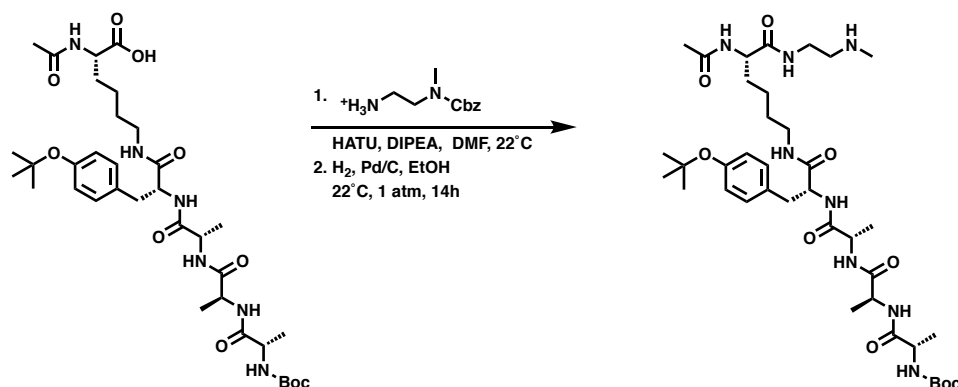


To a solution of **12L** (540.3 mg, 1 Eq, 749.5 μmol) in DMF (10 mL) was added HATU (313.5 mg, 1.1 Eq, 824.5 μmol) and DIPEA (392 μL , 3 Eq, 2.249 mmol) forming a bright yellow solution. This solution was stirred for 15 minutes to ensure complete activation. Separately, a solution of **3** (265.7 mg, 1.1 Eq, 824.5 μmol) was prepared in DMF (2 mL) and then added dropwise to the activated peptide. This solution was stirred for 30 minutes at 22 °C before HPLC analysis showed full conversion. The reaction contents were then concentrated under reduced pressure and precipitated into H_2O (45 mL) to afford the intermediate as a white solid. This was carried forward without any further purification.

The product was then dissolved in ethanol (30 mL) and combined with Pd/C (80 mg, 0.1 Eq). This solution was then sparged with argon, sealed under an atmosphere of hydrogen, and stirred at 22 °C for 14 hours (note 1). The reaction contents were then filtered over celite and concentrated under reduced pressure. The crude product was then purified via preparative HPLC (C18, 10-75% MeCN gradient against H_2O with a 0.1% TFA additive over 12 minutes) to afford **13L** (355.3 mg, 61.1% yield). HRMS (ESI/Q-TOF): $[\text{M}+\text{H}]^+$ calcd for $\text{C}_{38}\text{H}_{65}\text{N}_8\text{O}_9^+$, 777.4869; found 777.4898.

Note 1. The reaction was carried out in a 50 mL 1-neck RB flask and capped with a rubber septum. A double-layered balloon connected to a 3 mL syringe with a 3 cm needle was filled and hydrogen and placed on the RB flask. The solution was sparged for 5 minutes with hydrogen before allowing it to stir for 14 hours.

Synthesis of *Ac-Lys[Tyr(*t*Bu)-Ala-Ala-Ala-boc]-2-methylethylamino (13D)*



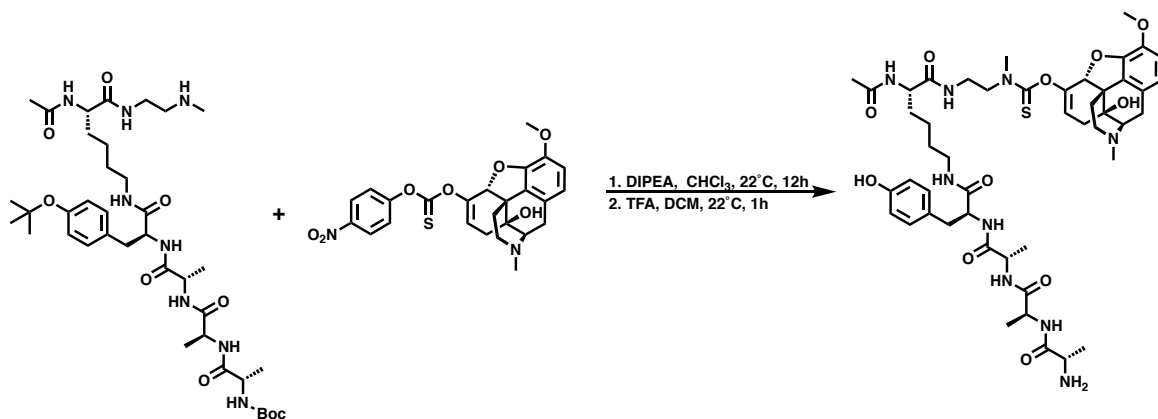
To a solution of **12D** (565.2 mg, 1 Eq, 784.1 μmol) in DMF (10 mL) was added HATU (327.9 mg, 1.1 Eq, 862.5 μmol) and DIPEA (410 μL , 3 Eq, 2.35 mmol) forming a bright yellow solution. This solution was stirred for 15 minutes to ensure complete activation. Separately, a solution of **3** (278.0 mg, 1.1 Eq, 862.5 μmol) was prepared in DMF (2 mL) and then added dropwise to the activated peptide. This solution was stirred for 30 minutes at 22 °C before HPLC analysis showed full conversion. The reaction contents were then concentrated under reduced pressure and precipitated into H_2O (45 mL) to afford the intermediate as a white solid. This was carried forward without any further purification.

The product was then dissolved in ethanol (30 mL) and combined with Pd/C (84 mg, 0.1 Eq). This solution was then sparged with argon, sealed under an atmosphere of hydrogen, and stirred at 22 °C for 14 hours (note 1). The reaction contents were then filtered over celite and concentrated under reduced pressure. The crude product was then purified via preparative HPLC

(C18, 10-75% MeCN gradient against H₂O with a 0.1% TFA additive over 12 minutes) to afford **13D** (355.3 mg, 61.1% yield). HRMS (ESI/Q-TOF): [M+H]⁺ calcd for C₃₈H₆₅N₈O₉⁺, 777.4869; found 777.4964.

Note 1. The reaction was carried out in a 50 mL 1-neck RB flask and capped with a rubber septum. A double-layered balloon connected to a 3 mL syringe with a 3 cm needle was filled and hydrogen and placed on the RB flask. The solution was sparged for 5 minutes with hydrogen before allowing it to stir for 14 hours.

Synthesis of Ac-Lys[Tyr-Ala-Ala-Ala]-(2-(Oxycodone-thionocarbamate)methyl)ethylamino (14L)

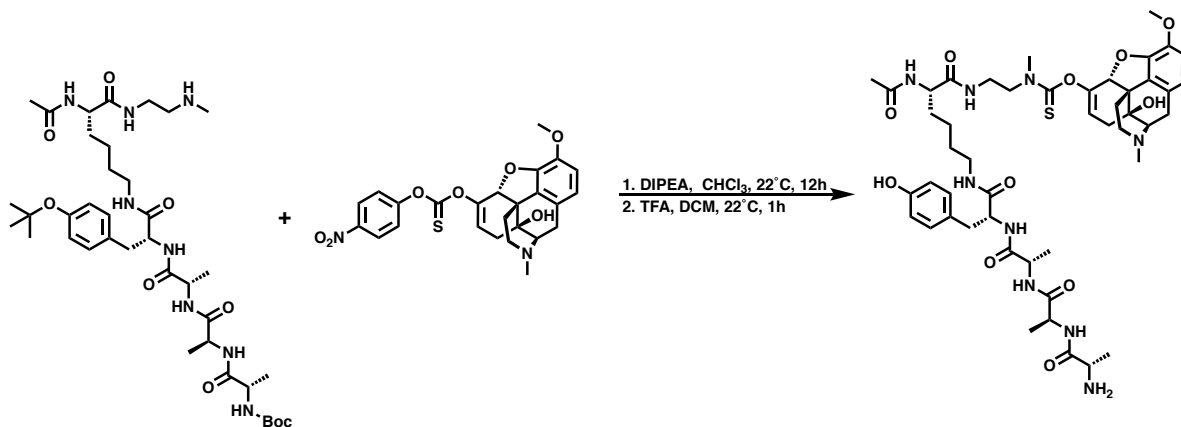


To a solution of **6L** (76.0 mg, 1 Eq, 85.3 μmol) in CHCl₃ (2.5 mL) and DMF (0.5 mL) was added DIPEA (0.15 mL, 10 Eq, 853 μmol). This solution was stirred for 5 minutes before a solution of **4** (52.9 mg, 1.25 Eq, 107 μmol) in CHCl₃ (1.0 mL) was added. This solution was then vigorously stirred at 22 °C for 12 hours. At this point, the reaction contents were concentrated under vacuum and then precipitated into H₂O. The resulting precipitate was identified as the

product via LCMS and shown to be greater than 90% pure. HRMS (ESI/Q-TOF): $[M+H]^+$ calcd for $C_{57}H_{84}N_9O_{13}S^+$, 1134.5904; found 1134.5998.

This resulting peptide was dissolved in a 25% TFA solution in DCM (10 mL) with 1% TIPS and H_2O . This was stirred at 22 °C for 30 minutes and then concentrated under reduced pressure. The resulting crude product was then purified via preparative HPLC (C18, 10-50% MeCN gradient against H_2O with a 0.1% TFA additive over 12 minutes) to afford **14L** (58.1 mg, 62.3% yield). HRMS (ESI/Q-TOF): $[M+H]^+$ calcd for $C_{48}H_{68}N_9O_{11}S^+$, 978.4754; found 978.4779.

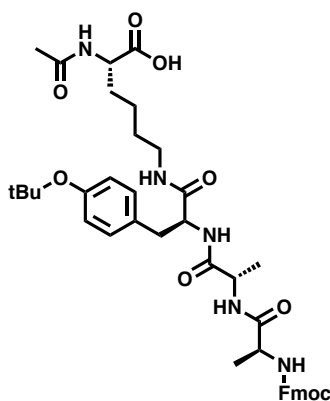
Synthesis of Ac-Lys[Tyr-Ala-Ala-Ala]-(2-(Oxycodone-thionocarbamate)methyl)ethylamino (14D)



To a solution of **6D** (75.0 mg, 1 Eq, 84.2 μ mol) in $CHCl_3$ (2.5 mL) and DMF (0.5 mL) was added DIPEA (0.15 mL, 10 Eq, 842 μ mol). This solution was stirred for 5 minutes before a solution of **4** (52.2 mg, 1.25 Eq, 105 μ mol) in $CHCl_3$ (1.0 mL) was added. This solution was then vigorously stirred at 22 °C for 12 hours. At this point, the reaction contents were concentrated under vacuum and then precipitated into H_2O . The resulting precipitate was identified as the product via LCMS and shown to be greater than 90% pure. HRMS (ESI/Q-TOF): $[M+H]^+$ calcd for $C_{57}H_{84}N_9O_{13}S^+$, 1134.5904; found 1134.5998.

This resulting peptide was dissolved in a 25% TFA solution in DCM (10 mL) with 1% TIPS and H₂O. This was stirred at 22 °C for 30 minutes and then concentrated under reduced pressure. The resulting crude product was then purified via preparative HPLC (C18, 10-50% MeCN gradient against H₂O with a 0.1% TFA additive over 12 minutes) to afford **14D** (22.4 mg, 24.0% yield). HRMS (ESI/Q-TOF): [M+H]⁺ calcd for C₄₈H₆₈N₉O₁₁S⁺, 978.4754; found 978.4317.

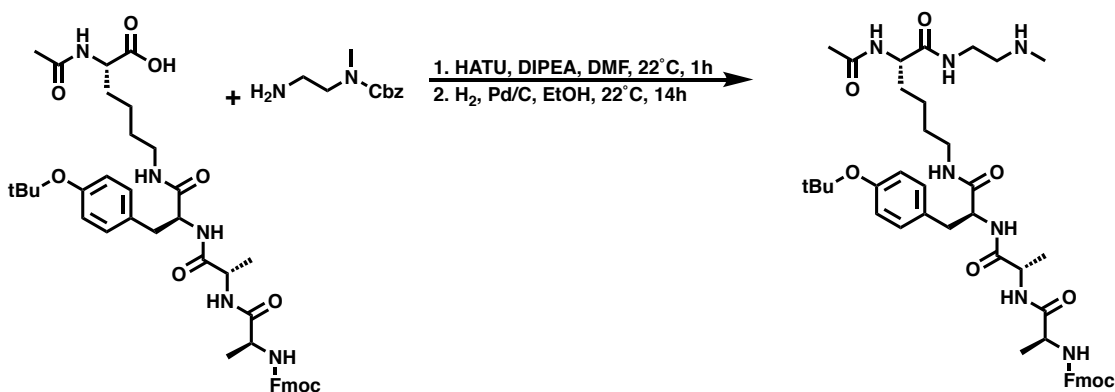
Synthesis of Ac-Lys[Tyr(tBu)-Ala-Ala-Fmoc] (15)



The peptide was synthesized via standard Fmoc Solid Phase Peptide Synthesis conditions. The peptide was prepared starting from a 2-Chlorotrityl chloride resin (0.89 meq/g ChemImpex). The resin was initially swelled in DCM for 60 minutes prior to any modifications. The initial lysine coupling was carried out using two equivalence of Ac-lys(Fmoc)-OH and 6 equivalence of DIPEA. This was done in a 50/50 DCM & NMP mixture and shaken for 90 minutes. Each amino acid residue thereafter was loaded using a 3:3:6 ratio of Amino Acid: HATU: DIPEA in NMP for 30 minutes. The couplings were followed by deprotection in 20% 4 methyl-piperidine (in DMF) for 20 minutes. After coupling the second alanine residue, the Fmoc protecting group was not cleaved. The resin was dried under vacuum for 120 minutes and then swelled in DCM for 40 minutes. The peptide was cleaved from the resin while maintaining the tBu protecting group by using a 20% HFIP in DCM cleavage cocktail. Approximately 10mL of the cleavage cocktail was added to the

resin/peptide and mixed for 2 minutes. The solution was filtered and the solvent removed under vacuum. This process was repeated 4 additional times. After each removal of HFIP and DCM under vacuum, the concentrate was precipitated into chilled diethyl ether (-20.0°C) to afford **15** (386.5 mg, 63.1% yield). HRMS (ESI/Q-TOF): $[M+H]^+$ calcd for $C_{42}H_{54}N_5O_9^+$, 772.3916; found 772.3973.

Synthesis of Ac-Lys[Tyr(tBu)-Ala-Ala-Fmoc]-2-methylethylamino (**16**)



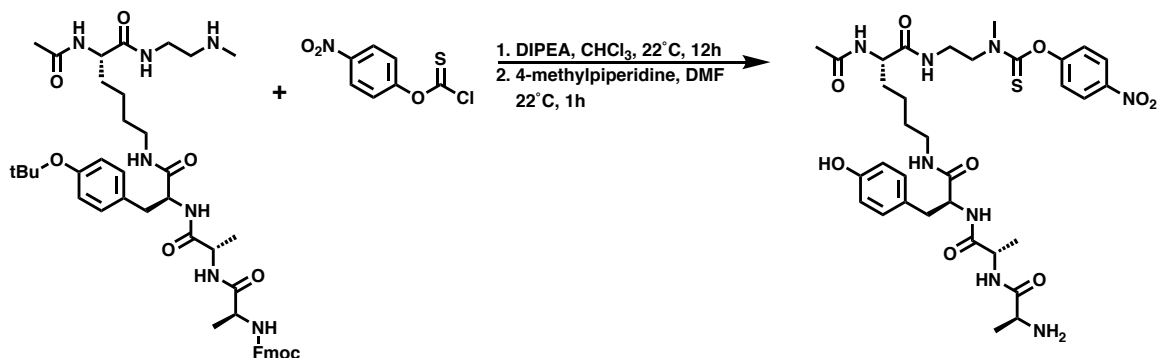
To a solution of **15** (378.9 mg, 1 Eq, 491 μ mol) in DMF (10 mL) was added HATU (224 mg, 1.2 Eq, 589 μ mol) and DIPEA (428 μ L, 5 Eq, 2.45 mmol) forming a bright yellow solution. This solution was stirred for 15 minutes to ensure complete activation. Separately, a solution of **3** (153.3 mg, 1.5 Eq, 737 μ mol) was prepared in DMF (2 mL) and then added dropwise to the activated peptide. This solution was stirred for 30 minutes at 22 °C before HPLC analysis showed full conversion. The reaction contents were then concentrated under reduced pressure and precipitated into H₂O (45 mL) to afford the intermediate as a white solid. This was carried forward without any further purification.

The product was then dissolved in ethanol (30 mL) and combined with Pd/C (84 mg, 0.1 Eq). This solution was then sparged with argon, sealed under an atmosphere of hydrogen, and stirred at 22 °C for 14 hours (note 1). The reaction contents were then filtered over celite and

concentrated under reduced pressure. The crude product was then purified via preparative HPLC (C18, 10-75% MeCN gradient against H₂O with a 0.1% TFA additive over 12 minutes) to afford **16** (140.7 mg, 34.6% yield). HRMS (ESI/Q-TOF): [M+H]⁺ calcd for C₄₅H₆₂N₇O₈⁺, 828.4654; found 828.4782.

Note 1. The reaction was carried out in a 50 mL 1-neck RB flask and capped with a rubber septum. A double-layered balloon connected to a 3 mL syringe with a 3 cm needle was filled and hydrogen and placed on the RB flask. The solution was sparged for 5 minutes with hydrogen before allowing it to stir 14 hours.

Synthesis of Ac-Lys[Tyr-Ala-Ala]-(2-(*p*NP-thionocarbamate)methyl)ethylamino (**17**)

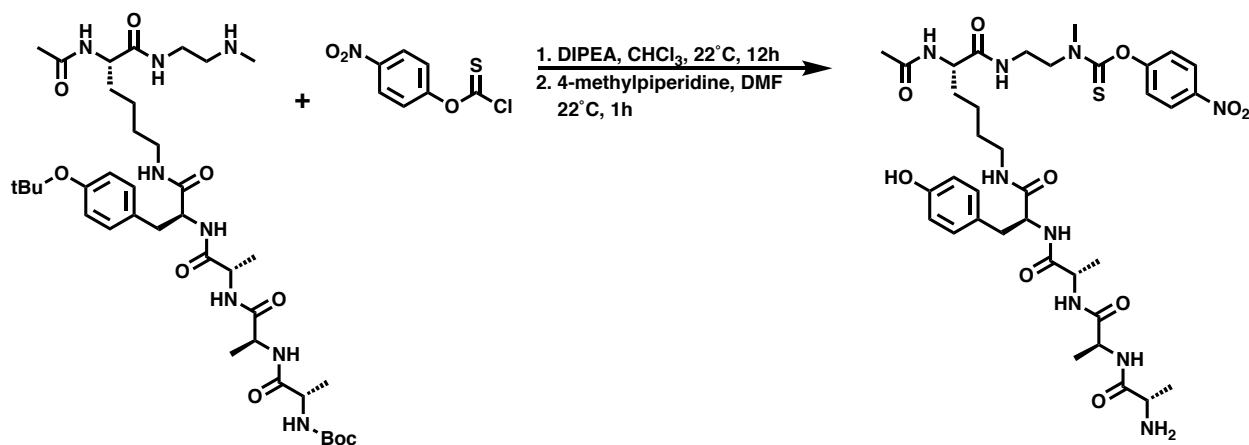


To a solution of **16** (25.0 mg, 1 Eq, 32.4 μ mol) in CHCl₃ (2.5 mL) and DMF (0.5 mL) was added DIPEA (17.0 μ L, 3 Eq, 97 μ mol). This solution was stirred for 5 minutes before a solution of **1** (10.6 mg, 1.5 Eq, 48.6 μ mol) in CHCl₃ (1.0 mL) was added. This solution was then vigorously stirred at 22 °C for 12 hours. At this point, the reaction contents were concentrated under vacuum and then precipitated into H₂O. The resulting precipitate was identified as the product via HPLC and shown to be greater than 90% pure (calculated from peak integrations at 254 nm).

This resulting peptide was dissolved in DMF (2 mL) with piperazine (67.0 mg, 10 Eq, 780 μ mol). This was stirred at 22 °C for 30 minutes and then concentrated under reduced pressure.

The resulting crude product was then acidified using 1 M aq. HCl and stirred for an additional 60 minutes, after which it was purified via preparative HPLC (C18, 10-100% MeCN gradient against H₂O with a 0.1% TFA additive over 12 minutes) to afford **17** (14.6 mg, 61.7% yield). HRMS (ESI/Q-TOF): [M+H]⁺ calcd for C₃₃H₄₇N₈O₉S⁺, 731.3181; found 731.3244.

Synthesis of Ac-Lys[Tyr-Ala-Ala-Ala]-(2-(*p*NP-thionocarbamate)methyl)ethylamino (**18**)

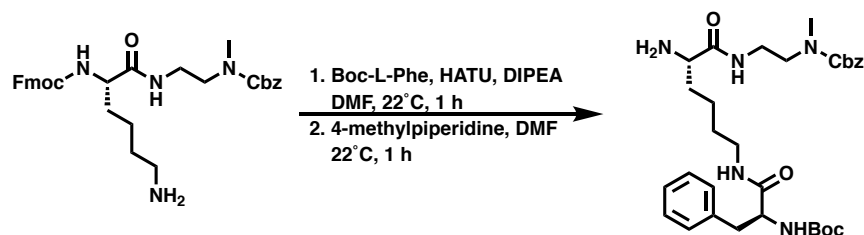


To a solution of **13L** (25.0 mg, 1 Eq, 27.8 μ mol) in CHCl₃ (2.5 mL) and DMF (0.5 mL) was added DIPEA (17.0 μ L, 3 Eq, 83 μ mol). This solution was stirred for 5 minutes before a solution of **1** (8.5 mg, 1.4 Eq, 39.0 μ mol) in CHCl₃ (1.0 mL) was added. This solution was then vigorously stirred at 22 °C for 12 hours. At this point, the reaction contents were concentrated under vacuum and then precipitated into H₂O. The resulting precipitate was identified as the product via LCMS and shown to be greater than 90% pure (calculated from peak integrations at 254 nm).

This resulting peptide was dissolved in DCM (4 mL) with TFA (1 mL). This was stirred at 22 °C for 30 minutes and then concentrated under reduced pressure. The resulting crude product was then purified via preparative HPLC (C18, 10-100% MeCN gradient against H₂O with a 0.1%

TFA additive over 12 minutes) to afford **18** (12.8 mg, 53.6% yield). HRMS (ESI/Q-TOF): $[M+H]^+$ calcd for $C_{36}H_{52}N_9O_{10}S^+$, 802.3552; found 802.3570.

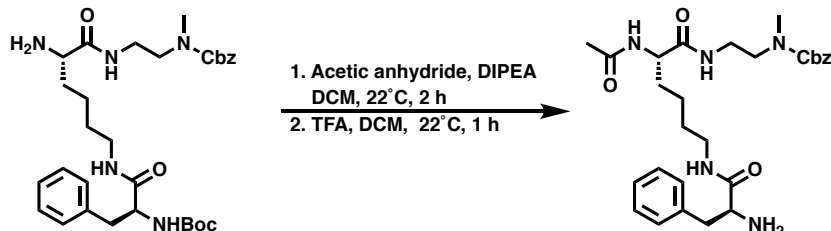
Synthesis of Lys[(Boc)Phe]-(2-(Cbz)methyl)ethylamino (**19**)



To a solution of Boc-phenylalanine (475 mg, 2 Eq, 1.79 mmol) in DMF (5 mL) was added HATU (681 mg, 2 Eq, 1.79 mmol) and DIPEA (780 μ L, 5 Eq, 4.48 mmol) forming a bright yellow solution. This solution was stirred for 10 minutes to ensure complete activation. Separately, a solution of **4** (500 mg, 1 Eq, 0.90 mmol) was prepared in DMF (2 mL) and then added dropwise to the activated peptide. This solution was stirred for 30 minutes at 22 °C before HPLC analysis showed full conversion. The reaction contents were then concentrated under reduced pressure and precipitated into H₂O (45 mL) to afford the intermediate as a white solid. This was carried forward without any further purification.

This resulting intermediate was dissolved in a 5% 4-methylpiperidine solution in DMF (5 mL). This was stirred at 22 °C for 30 minutes and then concentrated under reduced pressure. The resulting crude product was then purified via preparative HPLC (C18, 10-100% MeCN gradient against H₂O with a 0.1% TFA additive over 12 minutes) to afford **19** (380 mg, 63.2% yield). HRMS (ESI/Q-TOF): $[M+H]^+$ calcd for $C_{31}H_{46}N_5O_6^+$, 584.3443; found 584.3550.

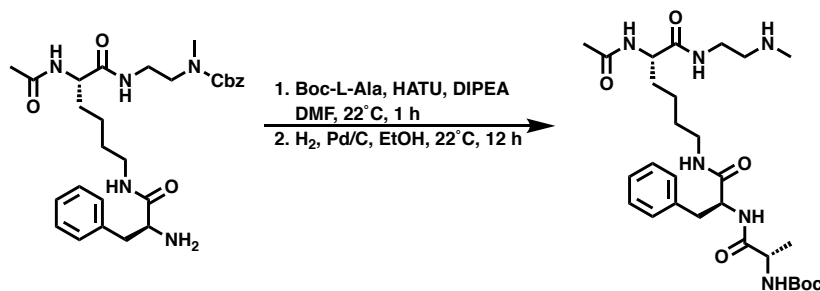
Synthesis of Ac-Lys[Phe]-(2-(Cbz)methyl)ethylamino (20)



To a solution of **19** (380 mg, 1 Eq, 0.68 mmol) in DCM (15 mL) was added DIPEA (593 μ L, 5 Eq, 3.40 mmol) and acetic anhydride (193 μ L, 3 Eq, 2.04 mmol). This solution was stirred for 2 hours at 22 °C before HPLC analysis showed full conversion. The reaction contents were then concentrated under reduced pressure and precipitated into 50/50 solution of diethyl ether and DCM (45 mL) to afford the intermediate as a white solid. This was carried forward without any further purification.

This resulting intermediate was dissolved in a 15% TFA solution in DCM (10 mL), which was stirred at 22 °C for 30 minutes and then concentrated under reduced pressure. The resulting crude product was then purified via preparative HPLC (C18, 10-80% MeCN gradient against H₂O with a 0.1% TFA additive over 12 minutes) to afford **20** (232 mg, 64.9% yield). HRMS (ESI/Q-TOF): [M+H]⁺ calcd for C₂₈H₄₀N₅O₅⁺, 526.3024; found 526.3006.

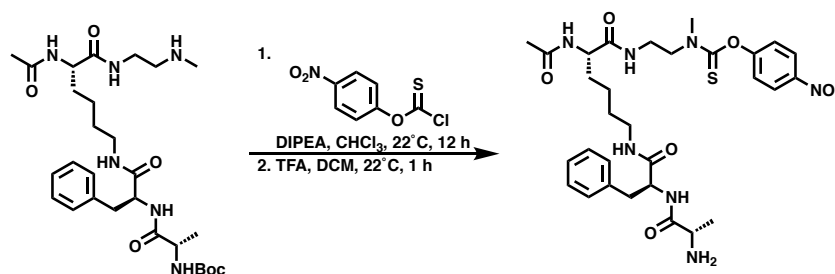
Synthesis of Ac-Lys[Phe-Ala(boc)]-2-methylethylamino (21)



To a solution of Boc-alanine (100 mg, 1.2 Eq, 530 μmol) in DMF (5 mL) was added HATU (202 mg, 1.2 Eq, 530 μmol) and DIPEA (385 μL , 5 Eq, 2.21 mmol) forming a bright yellow solution. This solution was stirred for 10 minutes to ensure complete activation. Separately, a solution of **20** (232 mg, 1 Eq, 442 μmol) was prepared in DMF (2 mL) and then added dropwise to the activated peptide. This solution was stirred for 30 minutes at 22 $^{\circ}\text{C}$ before HPLC analysis showed full conversion. The reaction contents were then concentrated under reduced pressure and precipitated into H₂O (45 mL) to afford the intermediate as a white solid. This was carried forward without any further purification.

The product was then dissolved in ethanol (30 mL) and combined with Pd/C (40 mg, 0.1 Eq). This solution was then sparged with argon, sealed under an atmosphere of hydrogen, and stirred at 22 $^{\circ}\text{C}$ for 12 hours. The reaction contents were then filtered over celite and concentrated under reduced pressure. The crude product was then purified via preparative HPLC (C18, 10-85% MeCN gradient against H₂O with a 0.1% TFA additive over 12 minutes) to afford **21** (120 mg, 48.3% yield). HRMS (ESI/Q-TOF): $[\text{M}+\text{H}]^{+}$ calcd for C₂₈H₄₇N₆O₆⁺, 563.3552; found 563.3320.

Synthesis of Ac-Lys[Phe-Ala(boc)]-(2-(*p*NP-thionocarbamate)methyl)ethylamino (**22**)

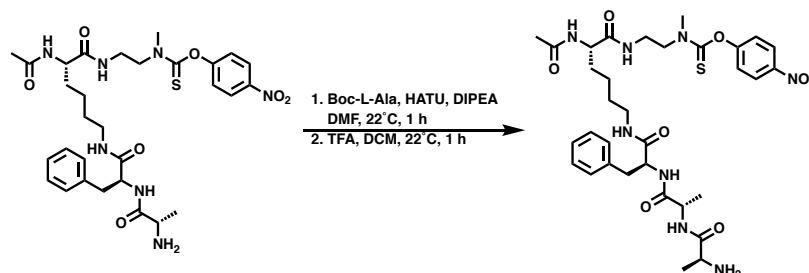


To a solution of **21** (35.0 mg, 1 Eq, 62.2 μmol) in CHCl₃ (2.5 mL) and DMF (0.5 mL) was added DIPEA (43.4 μL , 4 Eq, 249 μmol). This solution was stirred for 5 minutes before a solution of **1** (20.3 mg, 1.5 Eq, 93.4 μmol) in CHCl₃ (1.0 mL) was added. This solution was then vigorously

stirred at 22 °C for 12 hours. At this point, the reaction contents were concentrated under vacuum and then precipitated into H₂O. The resulting precipitate was identified as the product via LCMS and shown to be greater than 90% pure (calculated from peak integrations at 254 nm).

This resulting intermediate was dissolved in a 15% TFA solution in DCM (10 mL), which was stirred at 22 °C for 30 minutes and then concentrated under reduced pressure. The resulting crude product was then purified via preparative HPLC (C18, 10-100% MeCN gradient against H₂O with a 0.1% TFA additive over 12 minutes) to afford **22** (30.0 mg, 74.9% yield). HRMS (ESI/Q-TOF): [M+H]⁺ calcd for C₃₀H₄₂N₇O₇S⁺, 644.2861; found 644.2857.

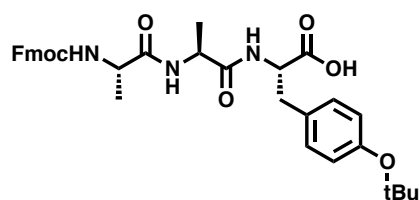
Synthesis of Ac-Lys[Phe-Ala-Ala]-(2-(*p*NP-thionocarbamate)methyl)ethylamino (**23**)



To a solution of Boc-alanine (9.5 mg, 1.2 Eq, 50.4 μmol) in DMF (2 mL) was added HATU (19.2 mg, 1.2 Eq, 50.4 μmol) and DIPEA (37 μL, 5 Eq, 210 μmol) forming a bright yellow solution. This solution was stirred for 10 minutes to ensure complete activation. Separately, a solution of **22** (27.0 mg, 1 Eq, 42.0 μmol) was prepared in DMF (1 mL) and then added dropwise to the activated peptide. This solution was stirred for 30 minutes at 22 °C before HPLC analysis showed full conversion. The reaction contents were then concentrated under reduced pressure and precipitated into H₂O (45 mL) to afford the intermediate as a white solid. This was carried forward without any further purification.

This resulting intermediate was dissolved in a 15% TFA solution in DCM (10 mL), which was stirred at 22 °C for 30 minutes and then concentrated under reduced pressure. The resulting crude product was then purified via preparative HPLC (C18, 10-90% MeCN gradient against H₂O with a 0.1% TFA additive over 12 minutes) to afford **23** (13.6 mg, 45.5% yield). HRMS (ESI/Q-TOF): [M+H]⁺ calcd for C₃₃H₄₇N₈O₈S⁺, 715.3232; found 715.3348.

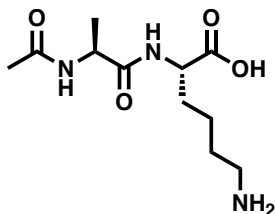
Synthesis of Tyr(tBu)-Ala-Ala-Fmoc (24)



The peptide was synthesized via standard Fmoc Solid Phase Peptide Synthesis conditions. The peptide was prepared starting from a 2-Chlorotrityl chloride resin (0.89 meq/g ChemImpex). The resin was initially swelled in DCM for 60 minutes prior to any modifications. The initial Lysine coupling was carried out using two equivalence of Fmoc-tyrosine(tBu)-OH and 6 equivalence of DIPEA. This was done in a 50/50 DCM/NMP mixture and shaken for 90 minutes. Each amino acid residue thereafter was loaded using a 3:3:6 ratio of amino acid: HATU: DIPEA in NMP for 30 minutes. The couplings were followed by deprotection in 20% 4 methyl-piperidine (in DMF) for 20 minutes. After coupling the second alanine residue, the Fmoc protecting group was not cleaved. The resin was dried under vacuum for 120 minutes and then swelled in DCM for 40 minutes. The peptide was cleaved from the resin while maintaining the Boc and t-butyl protecting groups by using a 20% HFIP in DCM cleavage cocktail. Approximately 10mL of the cleavage cocktail was added to the resin/peptide and mixed for 2 minutes. The solution was filtered and the solvent removed under vacuum. This process was repeated 4 additional times. After each

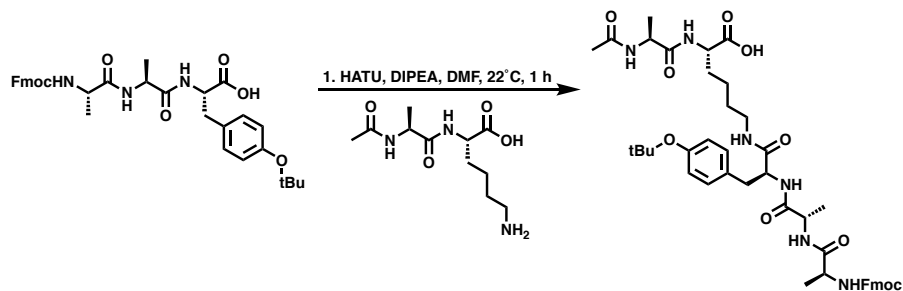
removal of HFIP and DCM under vacuum the concentrate was precipitated into chilled diethyl ether (-20.0°C) to afford **24** (455 mg, 69.2% yield). **HRMS (ESI/Q-TOF):** [M+H]⁺ calcd for C₃₄H₄₀N₃O₇⁺, 602.2861; found 602.2903.

Synthesis of Ac-Ala-Lys (**25**)



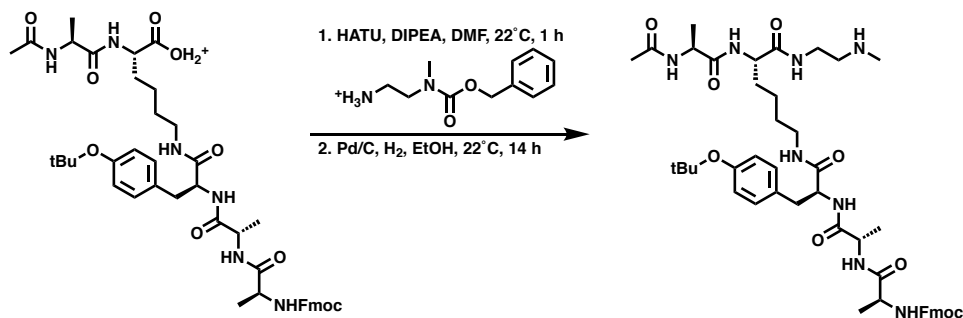
The peptide was synthesized via standard Fmoc Solid Phase Peptide Synthesis conditions. The peptide was prepared starting from a 2-Chlorotrityl chloride resin (0.89 meq/g ChemImpex). The resin was initially swelled in DCM for 60 minutes prior to any modifications. The initial lysine coupling was carried out using two equivalence of Fmoc-lysine(Boc)-OH and 6 equivalence of DIPEA. This was done in a 50/50 DCM/NMP mixture and shaken for 90 minutes. The following acetyl-alanine was loaded using a 3:3:6 ratio of amino acid: HATU: DIPEA in NMP for 30 minutes. The initial coupling was followed by deprotection in 20% 4 methyl-piperidine (in DMF) for 20 minutes. The resin was dried under vacuum for 120 minutes and then swelled in DCM for 40 minutes. The peptide was cleaved from the resin while simultaneously removing the Boc protecting group by using a 20% TFA in DCM cleavage cocktail containing 0.5% TIPS. Approximately 10mL of the cleavage cocktail was added to the resin/peptide and mixed for 2 minutes. The solution was filtered and the solvent removed under vacuum. This process was repeated 4 additional times. After each removal of TFA and DCM under vacuum the concentrate was precipitated into chilled diethyl ether (-20.0°C) to afford **25** (268 mg, 94.5% yield). **HRMS (ESI/Q-TOF):** [M+H]⁺ calcd for C₁₁H₂₂N₃O₄⁺, 260.1605; found 260.1669.

Synthesis of Ac-Ala-Lys[Tyr(tBu)-Ala-Ala-Fmoc] (26)



To a solution of **24** (443 mg, 1.1 Eq, 737 μmol) in DMF (5 mL) was added HATU (280 mg, 1.1 Eq, 737 μmol) and DIPEA (467 μL , 4 Eq, 2.68 mmol) forming a bright yellow solution. This solution was stirred for 10 minutes to ensure complete activation. Separately, a solution of **25** (250 mg, 1 Eq, 670 μmol) was prepared in DMF (1 mL) and then added dropwise to the activated peptide. This solution was stirred for 30 minutes at 22 °C before HPLC analysis showed full conversion. The reaction contents were then concentrated under reduced pressure and precipitated into H₂O (45 mL) to afford **26** as a white solid (458.6 mg, 81.0% yield). This was carried forward without any further purification. HRMS (ESI/Q-TOF): $[\text{M}+\text{H}]^+$ calcd for C₄₅H₅₉N₆O₁₀⁺, 843.4287; found 843.4309.

Synthesis of Ac-Ala-Lys[Tyr(tBu)-Ala-Ala-Fmoc]-2-methylethylamino (27)

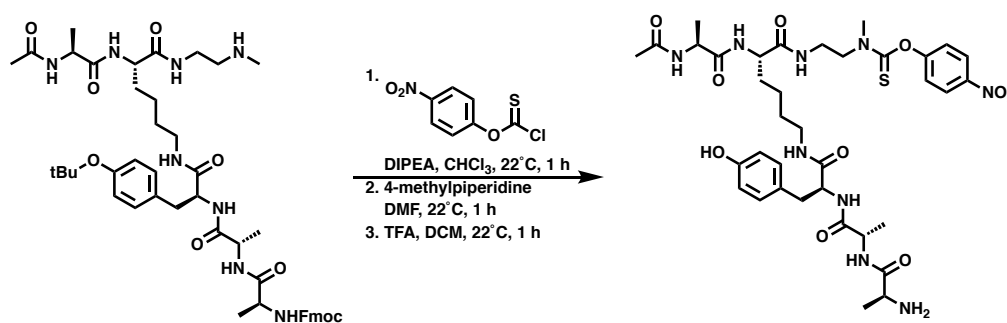


To a solution of **26** (456 mg, 1 Eq, 540 μmol) in DMF (7 mL) was added HATU (226 mg, 1.1 Eq, 595 μmol) and DIPEA (471 μL , 5 Eq, 2.70 mmol) forming a bright yellow solution. This

solution was stirred for 10 minutes to ensure complete activation. Separately, a solution of **3** (158 mg, 1.2 Eq, 649 μmol) was prepared in DMF (2 mL) and then added dropwise to the activated peptide. This solution was stirred for 30 minutes at 22 °C before HPLC analysis showed full conversion. The reaction contents were then concentrated under reduced pressure and precipitated into H₂O (45 mL) to afford the intermediate as a white solid. This was carried forward without any further purification. HRMS (ESI/Q-TOF): $[\text{M}+\text{H}]^+$ calcd for C₅₆H₇₃N₈O₁₁⁺, 1033.5393; found 1033.5392.

The product was then dissolved in ethanol (30 mL) and combined with Pd/C (95 mg, 0.1 Eq). This solution was then sparged with argon, sealed under an atmosphere of hydrogen, and stirred at 22 °C for 14 hours. The reaction contents were then filtered over celite and concentrated under reduced pressure. The crude product was then purified via preparative HPLC (C18, 10-75% MeCN gradient against H₂O with a 0.1% TFA additive over 12 minutes) to afford **27** (89.0 mg, 18.3% yield). HRMS (ESI/Q-TOF): $[\text{M}+\text{H}]^+$ calcd for C₄₅H₆₂N₇O₈⁺, 899.5026; found 899.5102.

Synthesis of Ac-Ala-Lys[Tyr-Ala-Ala]-(2-(*p*NP-thionocarbamate)methyl)ethylamino (**28**)



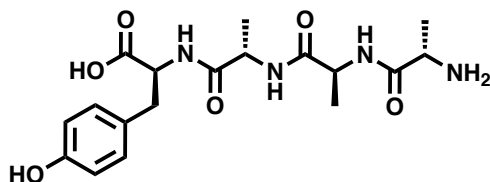
To a solution of **27** (25.0 mg, 1 Eq, 27.8 μmol) in CHCl₃ (2.5 mL) and DMF (0.5 mL) was added DIPEA (43.4 μL , 3 Eq, 83.5 μmol). This solution was stirred for 5 minutes before a solution of **1** (8.5 mg, 1.4 Eq, 39.0 μmol) in CHCl₃ (1.0 mL) was added. This solution was then vigorously stirred at 22 °C for 1 hour. At this point, the reaction contents were concentrated under vacuum

and then precipitated into H₂O. The resulting precipitate was identified as the product via LCMS and shown to be greater than 90% pure (calculated from peak integrations at 254 nm).

This resulting intermediate was dissolved in a 5% 4-methylpiperidine solution in DMF (5 mL), which was stirred at 22 °C for 60 minutes and then concentrated under reduced pressure. The resulting crude product was then purified via preparative HPLC (C18, 10-100% MeCN gradient against H₂O with a 0.1% TFA additive over 12 minutes) to afford the *t*Bu protected peptide. HRMS (ESI/Q-TOF): [M+H]⁺ calcd for C₄₀H₆₀N₉O₁₀S⁺, 858.4178; found 858.4241.

The resulting peptide was dissolved in a 15% TFA solution in DCM (10 mL), which was stirred at 22 °C for 30 minutes and then concentrated under reduced pressure. The resulting crude product was then precipitated into cold diethyl ether (-20 °C) to afford the **28** (17.1 mg, 71.7% yield). HRMS (ESI/Q-TOF): [M+H]⁺ calcd for C₃₆H₅₂N₉O₁₀S⁺, 802.3552; found 802.3548.

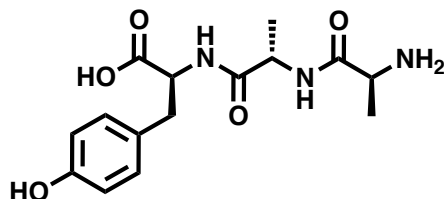
Synthesis of Tyr-Ala-Ala-Ala (**29**)



The peptide was synthesized via standard Fmoc Solid Phase Peptide Synthesis conditions. The peptide was prepared starting from a 2-Chlorotrityl chloride resin (0.73 meq/g ChemImpex). The resin was initially swelled in DCM for 60 minutes prior to any modifications. The initial tyrosine coupling was carried out using two equivalence of Fmoc-tyrosine(*t*Bu)-OH and 6 equivalence of DIPEA. This was done in a 50/50 DCM/NMP mixture and shaken for 90 minutes. Each amino acid residue thereafter was loaded using a 3:3:6 ratio of amino acid: HATU: DIPEA in NMP for 30 minutes. The couplings were followed by deprotection in 20% 4 methyl-piperidine

(in DMF) for 20 minutes. The third alanine residue was coupled as a Boc-alanine and left intact following the coupling. The resin was dried under vacuum for 120 minutes and then swelled in DCM for 40 minutes. The peptide was cleaved from the resin while simultaneously removing the Boc and t-butyl protecting groups by using a 20% TFA in DCM cleavage cocktail (with 0.25% TIPS). Approximately 10mL of the cleavage cocktail was added to the resin/peptide and mixed for 2 minutes. The solution was filtered and the solvent removed under vacuum. This process was repeated 4 additional times. After each removal of TFA and DCM under vacuum the concentrate was precipitated into chilled diethyl ether (-20.0°C) to afford **29** (286 mg, 99.5% yield). HRMS (ESI/Q-TOF): $[M+H]^+$ calcd for $C_{18}H_{27}N_4O_6^+$, 395.1925; found 395.2605.

Synthesis of Tyr-Ala-Ala (**30**)



The peptide was synthesized via standard Fmoc Solid Phase Peptide Synthesis conditions. The peptide was prepared starting from a 2-Chlorotrityl chloride resin (0.73 meq/g ChemImpex). The resin was initially swelled in DCM for 60 minutes prior to any modifications. The initial tyrosine coupling was carried out using two equivalence of Fmoc-tyrosine(tBu)-OH and 6 equivalence of DIPEA. This was done in a 50/50 DCM/NMP mixture and shaken for 90 minutes. Each amino acid residue thereafter was loaded using a 3:3:6 ratio of amino acid: HATU: DIPEA in NMP for 30 minutes. The couplings were followed by deprotection in 20% 4 methyl-piperidine (in DMF) for 20 minutes. The second alanine residue was coupled as a Boc-alanine and left intact following the coupling. The resin was dried under vacuum for 120 minutes and then swelled in

DCM for 40 minutes. The peptide was cleaved from the resin while simultaneously removing the Boc and t-butyl protecting groups by using a 20% TFA in DCM cleavage cocktail (with 0.25% TIPS). Approximately 10mL of the cleavage cocktail was added to the resin/peptide and mixed for 2 minutes. The solution was filtered and the solvent removed under vacuum. This process was repeated 4 additional times. After each removal of TFA and DCM under vacuum the concentrate was precipitated into chilled diethyl ether (-20.0°C) to afford **29** (163 mg, 67.3% yield). **HRMS (ESI/Q-TOF):** [M+H]⁺ calcd for C₁₅H₂₂N₃O₅⁺, 324.1554; found 324.1578.

3.5 References

- (1) Boehnke, N.; Maynard, H. D. Design of Modular Dual Enzyme-Responsive Peptides. *Pept. Sci.* **2017**, *108* (5), n/a-n/a. <https://doi.org/10.1002/bip.23035>.
- (2) Ruddick, J. A.; Newsome, W. H.; Nash, L. Correlation of Teratogenicity and Molecular Structure: Ethylenethiourea and Related Compounds. *Teratology* **1976**, *13* (3), 263–266. <https://doi.org/10.1002/tera.1420130304>.
- (3) Cohen, S. G.; Vaidya, V. M.; Schultz, R. M. Active Site of α -Chymotrypsin Activation by Association-Desolvation. *Proc. Natl. Acad. Sci.* **1970**, *66* (2), 249–256. <https://doi.org/10.1073/pnas.66.2.249>.
- (4) Appel, W. Chymotrypsin: Molecular and Catalytic Properties. *Clin. Biochem.* **1986**, *19* (6), 317–322. [https://doi.org/10.1016/S0009-9120\(86\)80002-9](https://doi.org/10.1016/S0009-9120(86)80002-9).
- (5) Bizzozero, S. A.; Baumann, W. K.; Dutler, H. Kinetic Investigation of the α -Chymotrypsin-Catalyzed Hydrolysis of Peptide Substrates. *Eur. J. Biochem.* **1982**, *122* (2), 251–258. <https://doi.org/10.1111/j.1432-1033.1982.tb05874.x>.
- (6) Baumann, W. K.; Bizzozero, S. A.; Dutler, H. Specificity of α -Chymotrypsin. Dipeptide Substrates. *FEBS Lett.* **1970**, *8* (5), 257–260. [https://doi.org/10.1016/0014-5793\(70\)80280-0](https://doi.org/10.1016/0014-5793(70)80280-0).
- (7) Kezdy, F. J.; Bender, M. L. The Kinetics of the α -Chymotrypsin-Catalyzed Hydrolysis of p-Nitrophenyl Acetate. **1962**, *1* (6), 10.
- (8) Kahns, A. H.; Bundgaard, H. Prodrugs of Peptides. 14. Bioreversible Derivatization of the Tyrosine Phenol Group to Effect Protection of Tyrosyl Peptides against α -Chymotrypsin. *Int. J. Pharm.* **1991**, *76* (1), 99–112. [https://doi.org/10.1016/0378-5173\(91\)90348-R](https://doi.org/10.1016/0378-5173(91)90348-R).

- (9) Vig, B. S.; Stouch, T. R.; Timoszyk, J. K.; Quan, Y.; Wall, D. A.; Smith, R. L.; Faria, T. N. Human PEPT1 Pharmacophore Distinguishes between Dipeptide Transport and Binding. *J. Med. Chem.* **2006**, *49* (12), 3636–3644. <https://doi.org/10.1021/jm0511029>.

3.6 Appendix B

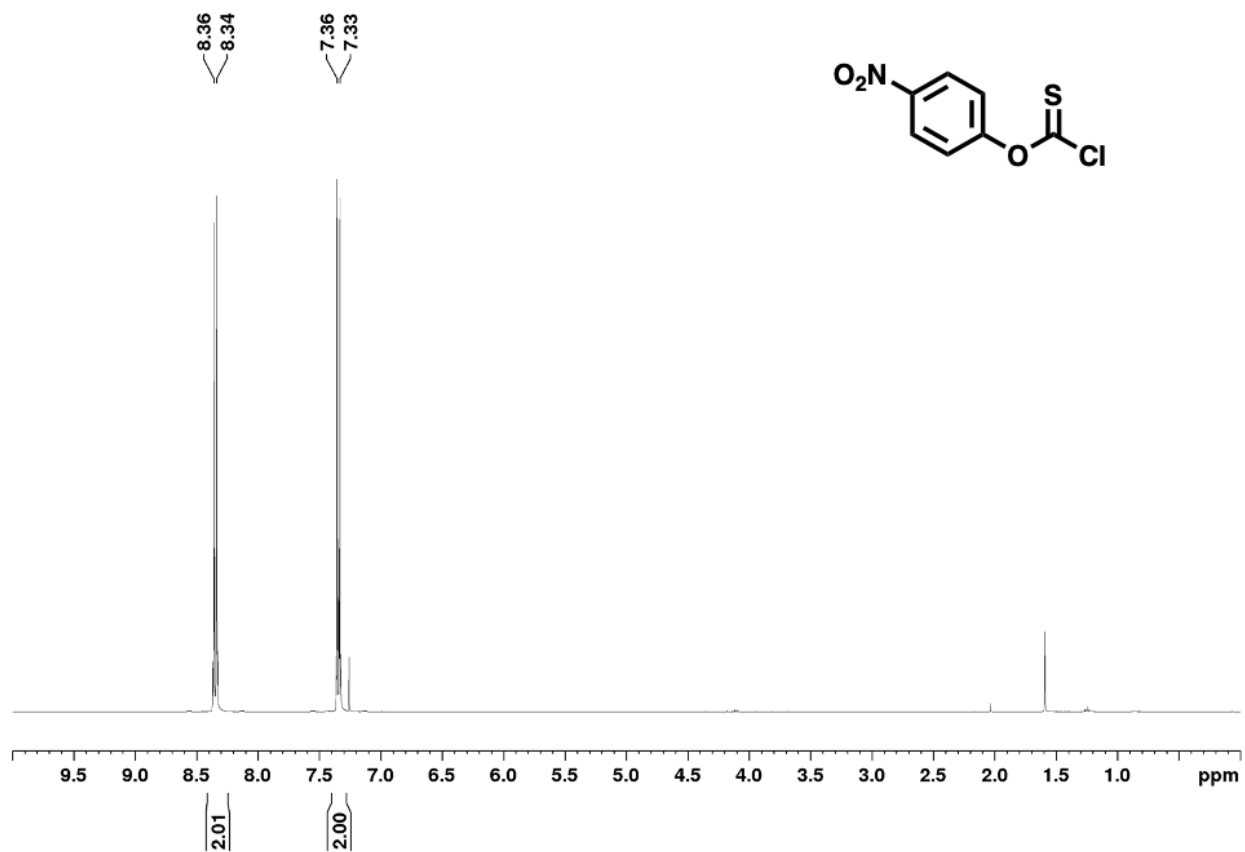


Figure 3.8. ¹H NMR Spectrum of Compound 1 in CDCl₃

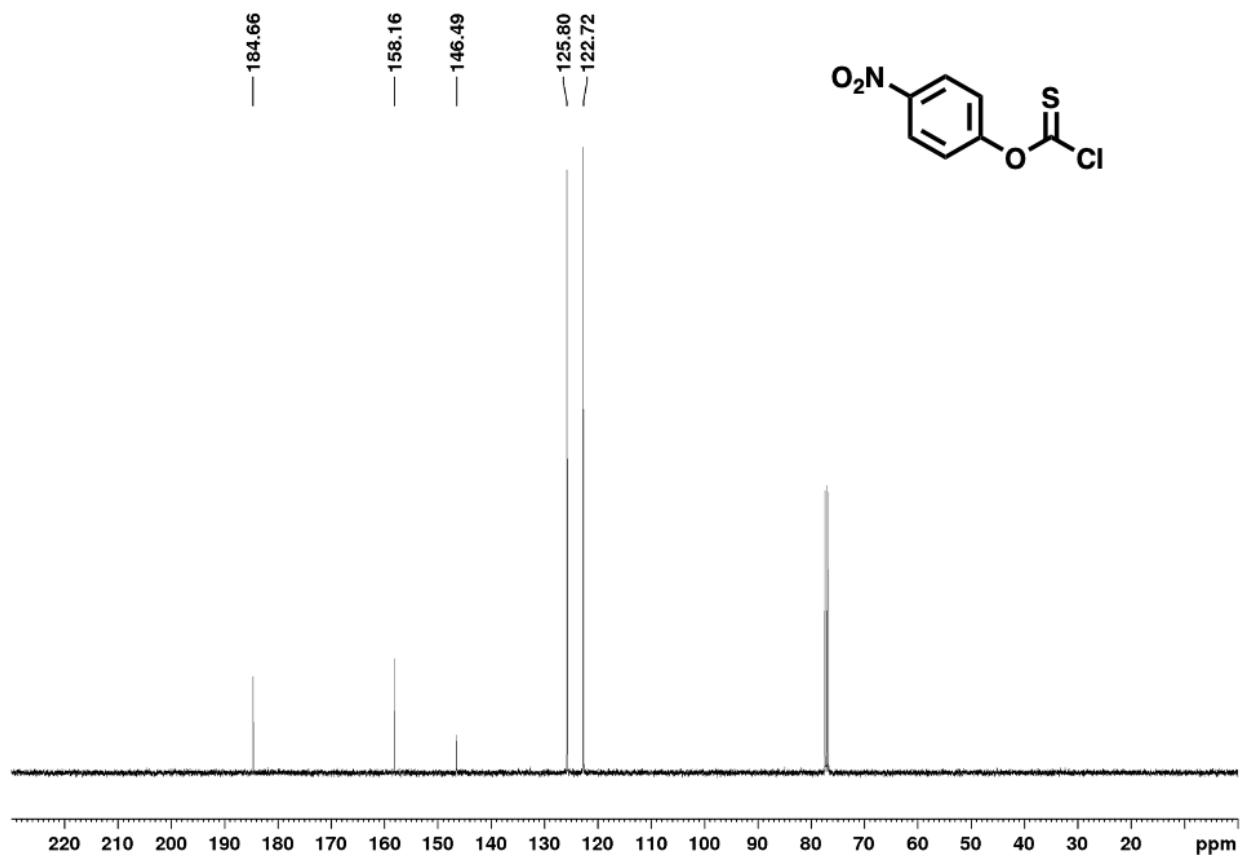


Figure 3.9. ^{13}C NMR Spectrum of Compound 1 in CDCl_3

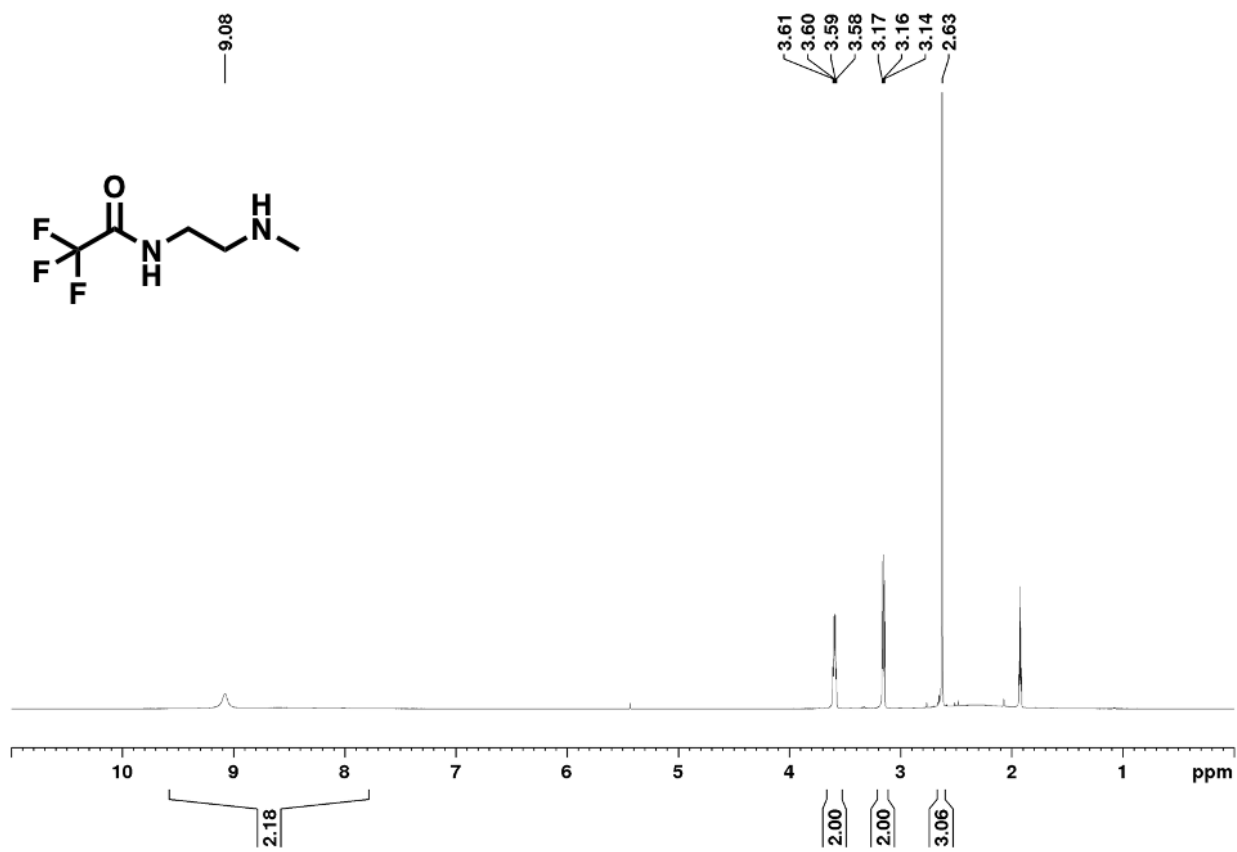


Figure 3.10. ¹H NMR Spectrum of Compound 2 in CD₃CN

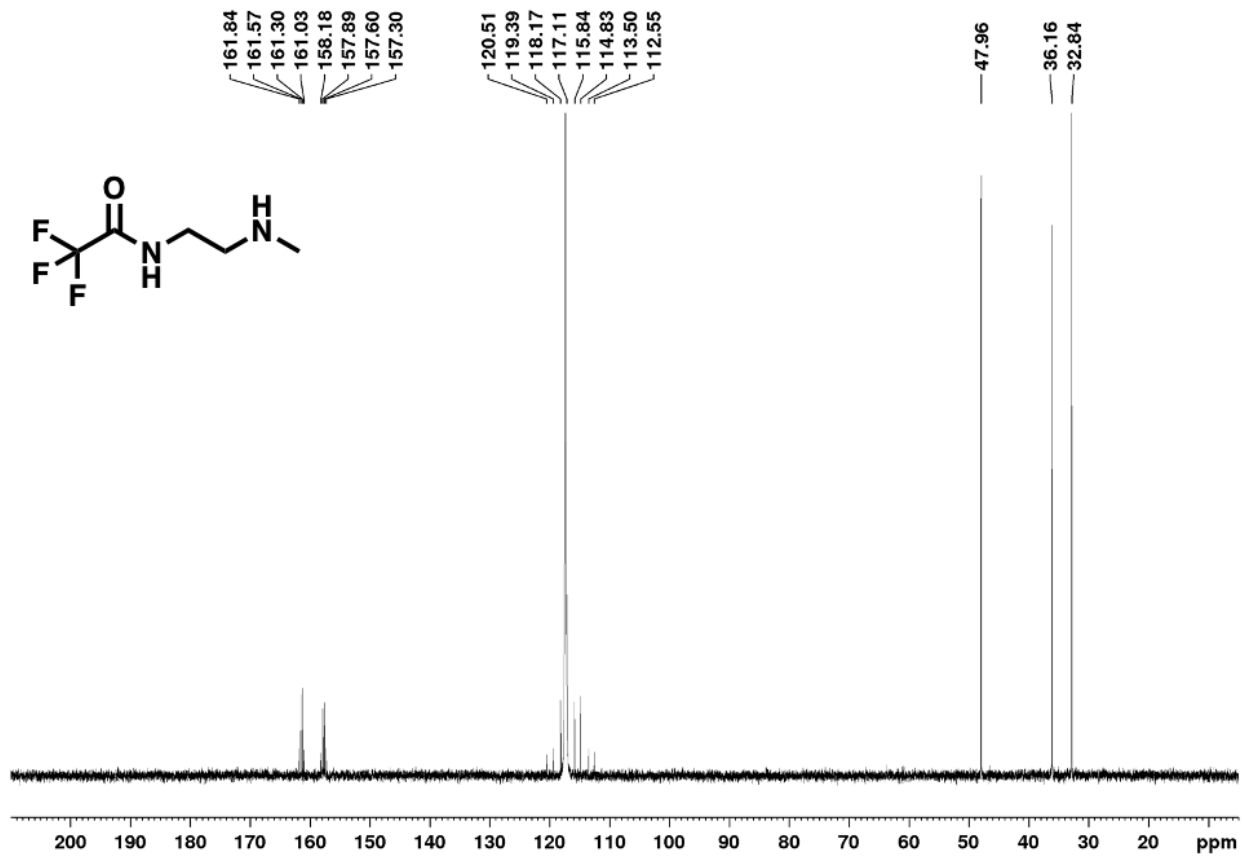


Figure 3.11. ¹³C NMR Spectrum of Compound 2 in CD₃CN



Figure 3.12. ^1H NMR Spectrum of Compound 3 in CD_3CN

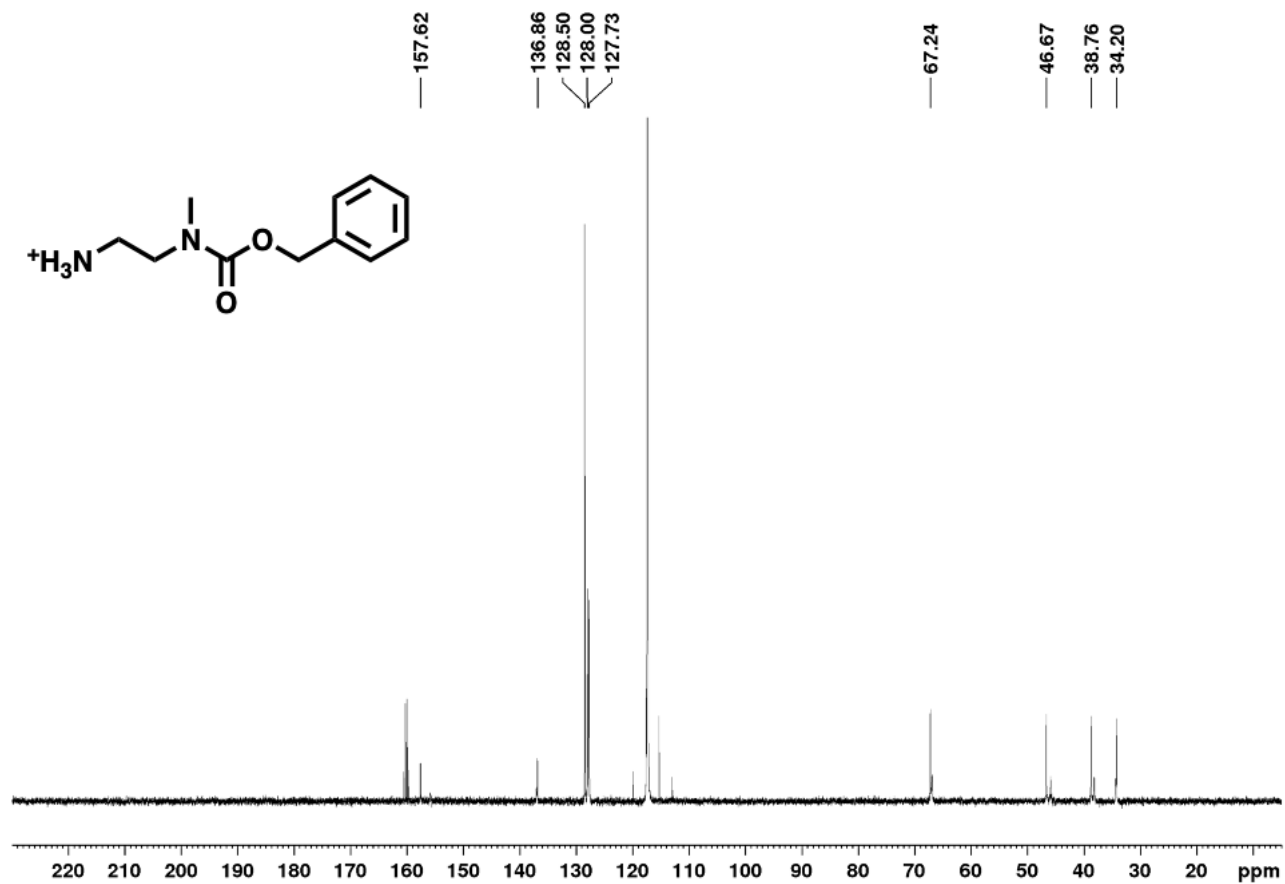


Figure 3.13. ¹³C NMR Spectrum of Compound 3 in CD₃CN

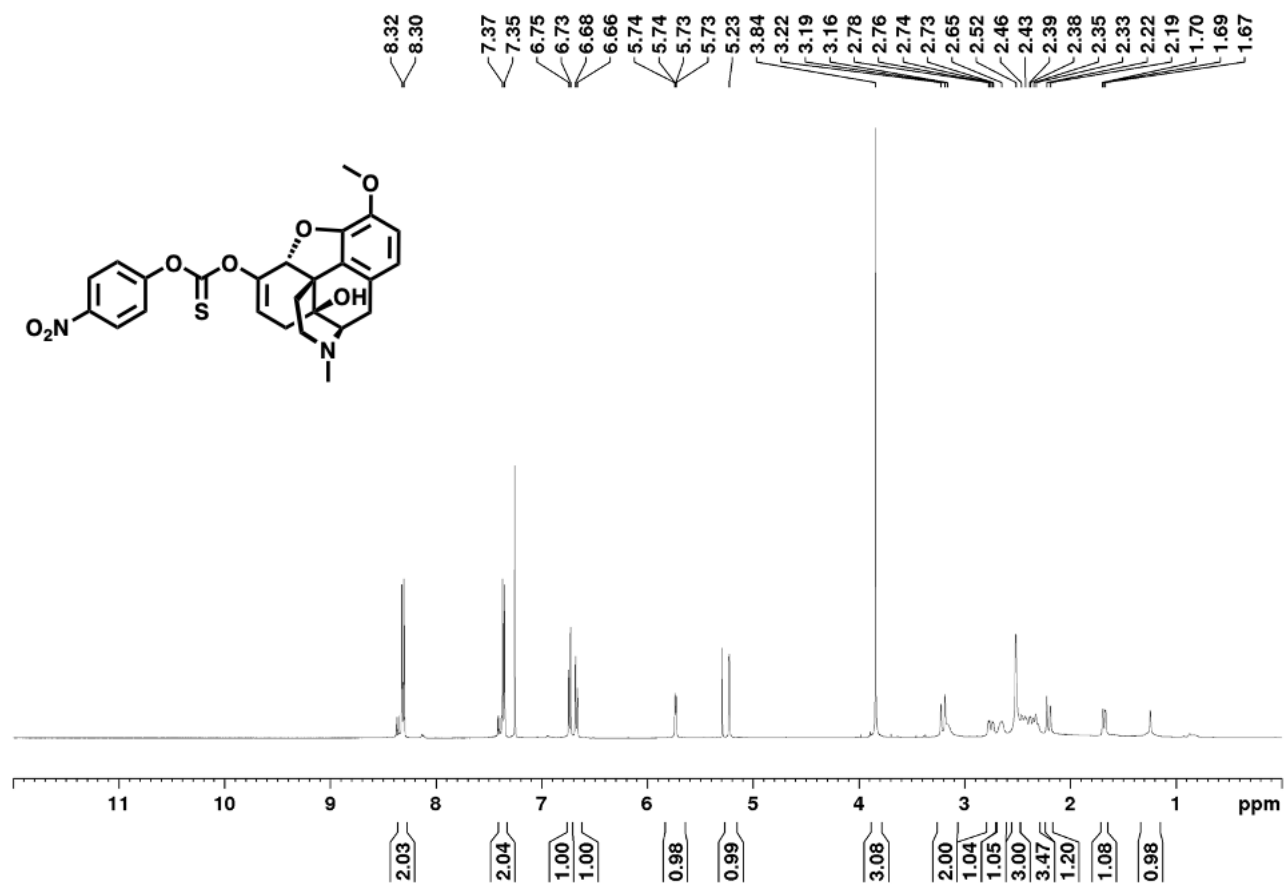


Figure 3.14. ¹H NMR Spectrum of Compound 11 in CD₃CN

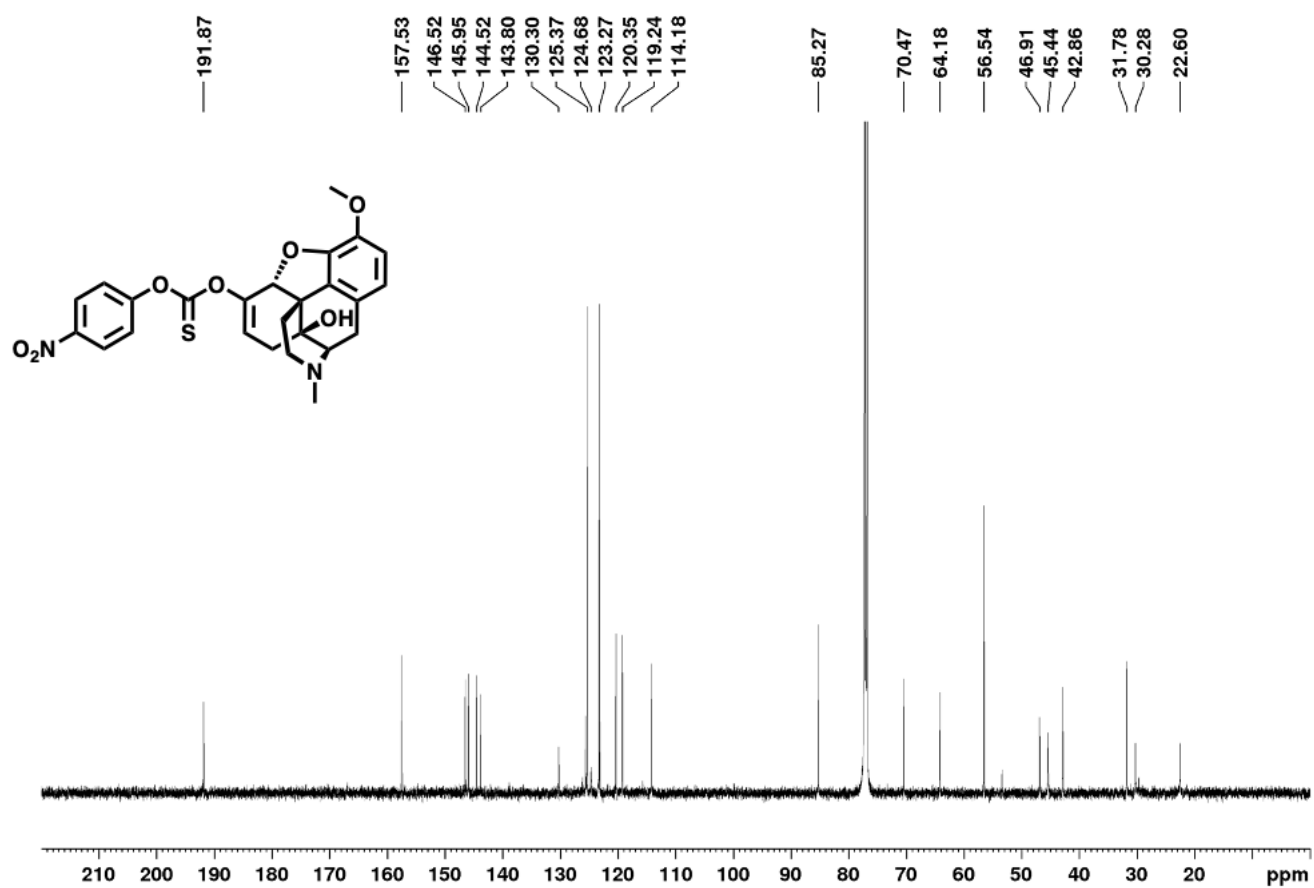


Figure 3.15. ¹³C NMR Spectrum of Compound 11 in CD₃CN

Chapter 4

Self-Immolative Benzylamine Linkers for Traceless Protein Conjugation

4.1 Introduction

Protein conjugation is a versatile tool that allows for the alteration of a protein's stability, activity, and functionality.¹ Protein-polymer conjugates are a useful application of this tool for therapeutically relevant proteins, often resulting in an increased stability and circulation time *in vivo*.² Currently, there are several protein-polyethylene glycol (PEG) conjugates used in the clinic; however, the addition of PEG typically leads to a significant loss of activity compared to that of their unmodified counterpart and in some cases, activity is shut off completely.³⁻⁵ To minimize such undesired effects, site-specific conjugation techniques can be employed to ensure that placement of the polymer is distant from the active site.⁶ This is not broadly applicable to all proteins of interest and requires a tailor-made strategy for each protein, resulting in a significant investment of time and resources.

As an alternative strategy to circumvent activity loss, researchers place unstable linkages between the protein and the polymer.⁷ These linkages slowly reverse to return lost activity incurred by the presence of the attached polymer. These reversible linkages that release native protein leave no indication that the protein was covalently modified and are deemed traceless linkers. This conjugation strategy primarily targets either lysine or cysteine residues and a variety of strategies have been developed for each.⁸⁻¹³ Although traceless cysteine conjugation is very effective, the necessary free and accessible cysteine is not available across all proteins of interest. Comparatively, lysines are highly prevalent across a wide range of proteins, many of which are accessible for covalent modification.¹⁴

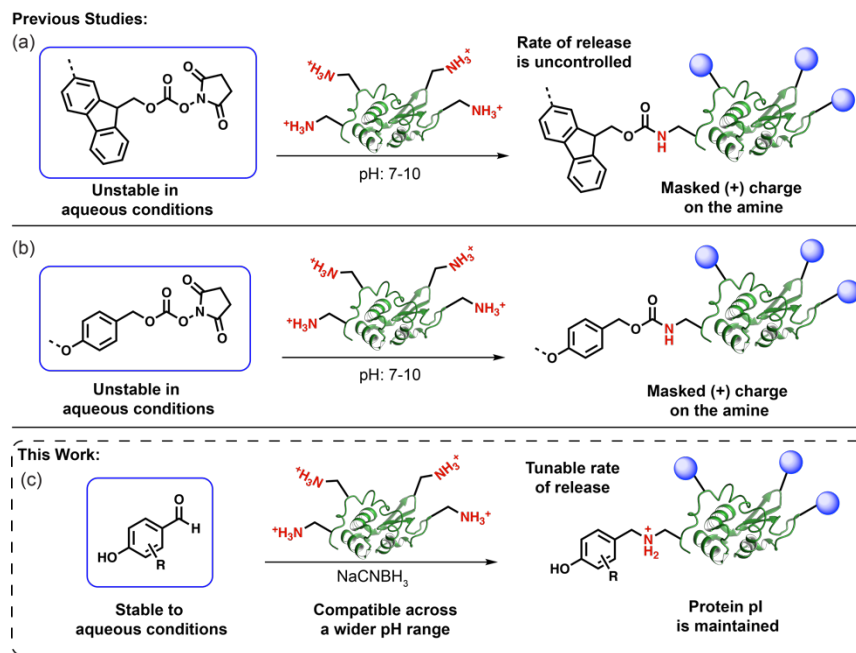


Figure 4.1. Strategies to prepare traceless bioconjugates: (a) fluorenyloxycarbamate (Fmoc) linker and (b) benzyl carbamate linker compared to (c) benzylamine linker.

One common traceless lysine conjugation strategy is the fluorenyloxycarbamate (Fmoc) linkage (Figure 1a).¹¹ Cleavage proceeds through a β -elimination pathway that is entirely mediated by the pH. This strategy works well for applications requiring a slow passive release *in vivo*, perfectly exemplified by Bempegaldesleukin, a slow release interleukin-2 PEG conjugate that is currently in phase 3 clinical trials.¹⁵ This passive release does, however, limit the amount of control over both the rate and site of release. Conversely, the benzyl carbamate linkage (Figure 1b) is stable across a wide pH range and requires an initial unmasking of the aniline or phenol in order to proceed through the release mechanism.⁹ Taking advantage of this reactivity, one can mask the phenol/aniline position with a diverse array of stimuli-responsive functionalities, adding a trigger dependent release to the system.¹⁶ This ensures the release is confined to locations where the stimulus is present, imparting a level of spatial and temporal control to the system. While these linkers are used for stimuli-responsive release across a variety of bioconjugation applications, they

are also used as passive traceless linkers within protein-polymer conjugation as demonstrated by Lonapegsomatropin, a long-acting human growth hormone PEG conjugate that is currently undergoing phase 3 clinical trials.¹⁷ Even with widespread adoption, these strategies contain a few limitations creating room for further development: (1) loss of the positive charge on the lysine residues that can destabilize the protein; (2) hydrolytic instability of carbonate precursors; and (3) high pH conditions for conjugations.

In order to address these limitations, we developed a class of benzylamine-based traceless linkers with tunable rates of release (Figure 1c). Taking inspiration from recent work showing the release of drugs containing tertiary amines and work showing the electronic effects on the strength of benzylic bonds, we hypothesized that electronically stabilizing the quinone methide intermediate would favor release of a primary amine.^{18,19} The use of a benzylamine linkage introduces the possibility of using reductive amination as a conjugation strategy with benzaldehyde precursors (Figure 1c). Reductive amination with benzaldehydes is commonly used in the preparation of irreversible protein conjugates due to its straightforward and versatile nature.^{20,21} These conjugations are carried out in an acidic to mildly basic pH solution, which complements the basic conditions used in the preparation of the benzyl carbamate linkers. This opens up the use of traceless linkers to proteins with isoelectric points (pI) between 7-9 that are incompatible with the carbamate conjugation conditions. Additionally, the resulting benzylamine conjugate retains the positive charge on the amines, which has been shown to minimize denaturation and aggregation incurred by a shift in the isoelectric point.^{22,23}

4.2 Results and Discussion

4.2.1 Preparation of a Benzylamine Model System for Release Kinetics

For the carbamate linkers, loss of CO₂ serves as the principle driving force for the amine release. Currently, conjugations using benzaldehyde derivatives lack such a driving force and are only utilized for permanent conjugations.^{20,21,24} Yet, we hypothesized that installing electron rich substituents on the aromatic core would facilitate dearomatization and stabilize the transient positive charge on the benzylic carbon to favor 1,6-elimination of a primary amine.^{19,25–27}

To test this hypothesis, we initially prepared a small library of model compounds using commercially available benzaldehydes, and measured the release of an amine payload (**1**, **2**, **3a**, **4a**, Figure 4.2a). The four benzaldehydes were chosen due to their varying levels of electron-donating abilities: benzaldehyde (**1**, $\sigma_p = 0.00$ for -H), dimethylbenzaldehyde (**2**, $\sigma_p = -0.17$ for each -Me), dimethoxybenzaldehyde (**3a**, $\sigma_p = -0.27$ for each -OMe), and dimethylaminobenzaldehyde (**4a**, $\sigma_p = -0.83$ for -NMe₂).²⁸ In the case of **1**, **2**, and **3a** σ_p Hammett

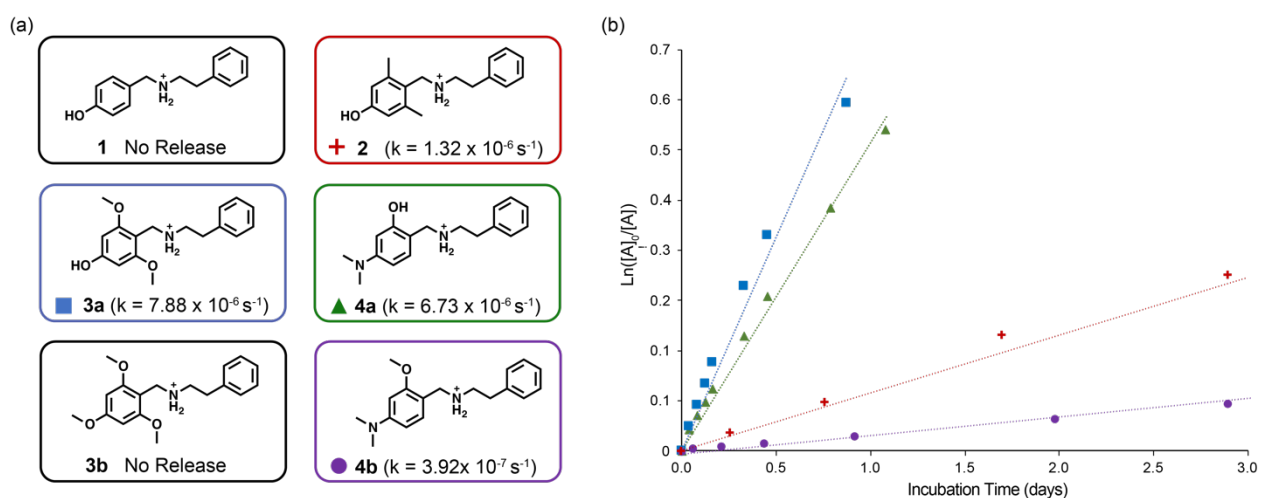


Figure 4.2. (a) Library of traceless linkers prepared for model release study with experimentally determined rate constants. (b) Pseudo-first order plot of phenethylamine release kinetics from the benzylamine linker model compounds ($n = 3$ for each sample) carried out at 5 mM of linker in a 1:1 mixture of methanol and buffer.

parameters were used, which have been found to be a good estimate for the *ortho*-substituents donating ability excluding sterically bulky groups. These four model compounds were prepared via reductive amination with phenethylamine, which was chosen as a surrogate to lysine due to its lower limit of detection when monitored by high-performance liquid chromatography (HPLC) for kinetic analysis.

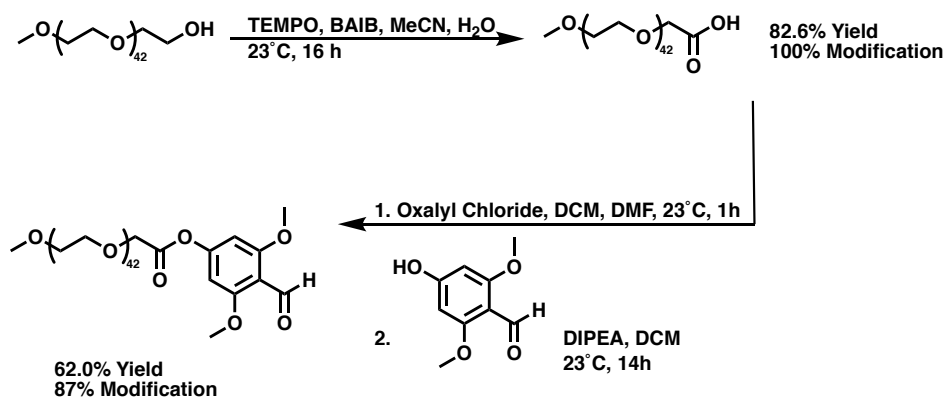
The release studies were carried out using a 5 mM solution of the linker in a 1:1 mixture of methanol and Tris buffer (pH 7.4, 100 mM), where the appearance of phenethylamine was monitored via HPLC. As expected, the unsubstituted linker **1** showed no release over 25 days whereas linker **2** had fully released within the same time period ($t_{1/2}$: 144 hours). Increasing the electron donation of the substituents to the more electron-rich methoxy groups in linker **3a** resulted in faster release ($t_{1/2}$: 20 hours), however, further increasing the electron density with linker **4a** led to a slower release ($t_{1/2}$: 29 hours). Pseudo-first order rate constants calculated from this plot (Figure 4.2b) showed that the rate increased 6-fold between linkers **2** and **3a** ($1.32 \times 10^{-6} \text{ s}^{-1}$ vs. $7.88 \times 10^{-6} \text{ s}^{-1}$ respectively, see Figure 4.2a). To better understand the mechanism of release, we prepared two additional linkers to act as negative controls by methylating the phenols. As expected, this completely shut off the release for **3b**. However, linker **4b**, did still release phenethylamine, albeit with a 17-fold reduction in the rate ($t_{1/2}$: 495 hours). This observation, along with a decreased rate of release under more acidic conditions, indicates the release pathway proceeds through an initial deprotonation of the phenol. Presumably, linker **4b** subverts the requisite deprotonation through a 1,6-elimination pathway, proceeding through an azaquinone methide intermediate to release the phenethylamine.

Excluding **4a**, linkers **1**, **2**, and **3a** clearly demonstrate that increasing the electron donation of the aryl substituents leads to a faster rate of release. The structural difference between **4a** and

the other linkers was initially identified as a potential culprit for this discrepancy, however, previous studies have shown the 1,4-elimination rate to be similar to that of the 1,6-elimination.²⁹ Yet, these studies were carried out with carbamate linkages and one could envision that the *ortho*-structure of this benzylamine linker might facilitate hydrogen bonding between the benzylic amine and the phenol. This hydrogen bonding may affect the phenol's participation in the release mechanism, leading to the observed discrepancy. Additionally, the use of the σ_p values for linkers **2** and **3a** in place of σ_o , may not be perfectly translatable for the *ortho*-substituents, which would modify our expected trend.

4.2.2 Preparation of mPEG-(2,6-dimethoxybenzaldehyde) for protein conjugation

As a proof-of-concept demonstration, we decided to modify the end-group of monomethyl ether poly(ethylene glycol) (mPEG) to use for protein conjugation. We chose linker **3a** for the mPEG end-group due to its superior performance in the model studies. For the stimuli responsive trigger, we chose a phenolic ester that has been shown to selectively hydrolyze in neutral to basic conditions.³⁰ The selectivity of this trigger is perfectly compatible with the reductive amination conditions and can subsequently be tested for release by exposure of the conjugate to neutral pH. The mPEG-2,6-dimethoxybenzaldehyde (mPEG-DMOB) polymer was prepared through an initial oxidation of mPEG using a hypervalent iodine species (diacetoxyiodobenzene) as the stoichiometric oxidant and catalytic TEMPO to afford mPEG-COOH. This species was then coupled to the 2,6-dimethoxy benzaldehyde (DMOB) via an acyl chloride intermediate using oxalyl chloride and catalytic DMF to afford mPEG-DMOB. This strategy was selected for its high efficiency across each step, thus ensuring a high conversion to the benzaldehyde end-group for protein conjugation.

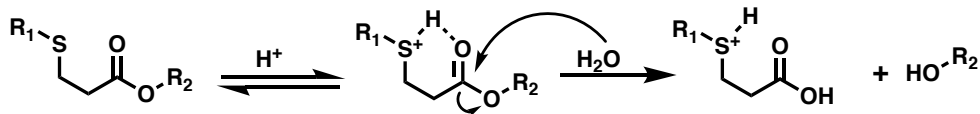


Scheme 4.1. Synthesis of mPEG-(2,6-dimethoxybenzaldehyde) with a phenolic ester trigger for protein conjugation.

Prior to any protein modification, the mPEG-DMOB was tested for its aqueous stability to ensure the competing ester hydrolysis remained minimal under the acidic reductive amination conditions. It was found that 50 % of the mPEG-DMOB hydrolyzed in a pH 5 solution, within one hour. Considering that the protein conjugation is typically carried out for at least two hours this strategy proved to be incompatible and a new triggering mechanism was developed.

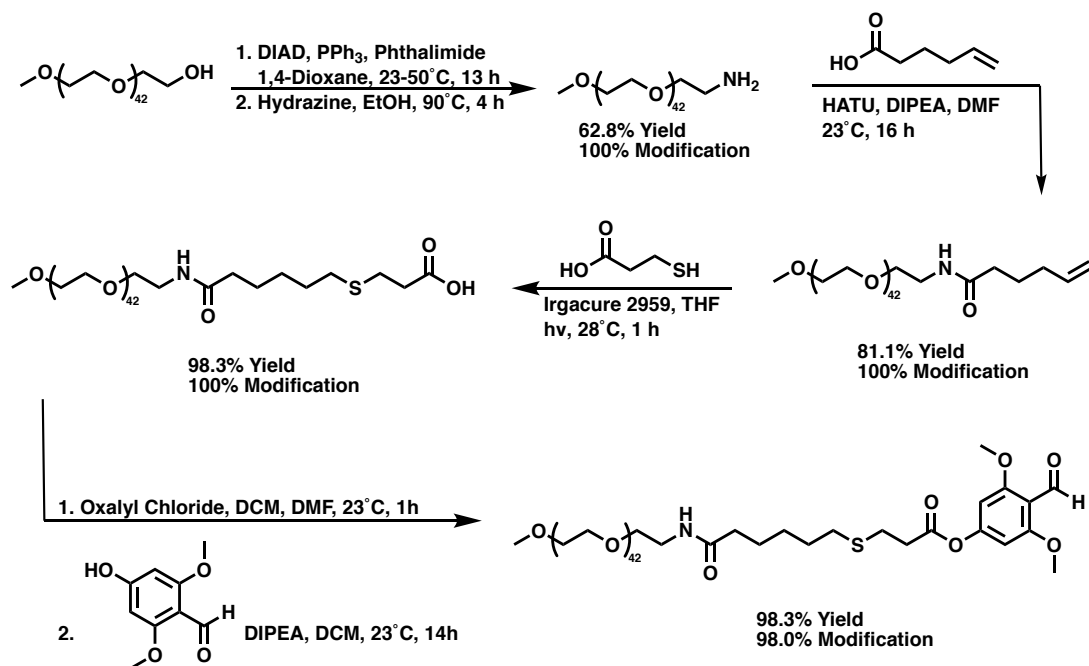
4.2.3 Preparation of mPEG- β -thioester-(2,6-dimethoxybenzaldehyde)-Lysozyme Conjugate and Traceless Release of Lysozyme

In order to circumvent the hydrolytic instability of mPEG-DMOB, it was decided to pursue the use of a β -thioester trigger, which selectively hydrolyzes under acidic conditions (Scheme 4.2).³¹ Although this triggering mechanism would cleave the ester under the acidic conditions typically used for reductive amination, it was pursued knowing that the conjugation can also be carried out at a slightly basic pH, where the ester hydrolysis should prove minimal.



Scheme 4.2. Acid mediated hydrolysis of β-thioesters.

To prepare the β-thioester containing PEG species, mPEG was converted to mPEG-phthalimide via a Mitsunobu reaction followed by deprotection with hydrazine to give mPEG-NH₂ (Scheme 4.3). This was succeeded by an amide coupling between the amine end-group and 5-hexenoic acid facilitated by O-(7-Azabenzotriazol-1-yl)-N,N,N',N'-tetramethyluronium hexafluorophosphate (HATU) to afford mPEG-vinyl. Subjection of the mPEG-vinyl to a radical mediated thiol-ene click reaction with 3-mercaptopropionic acid delivered the mPEG-β-thioacid. Mirroring the mPEG-DMOB synthesis, this carboxylic acid was converted to the acyl chloride and thereupon coupled to 2,6-dimethoxybenzaldehyde furnishing the mPEG-β-thioester-DMOB.



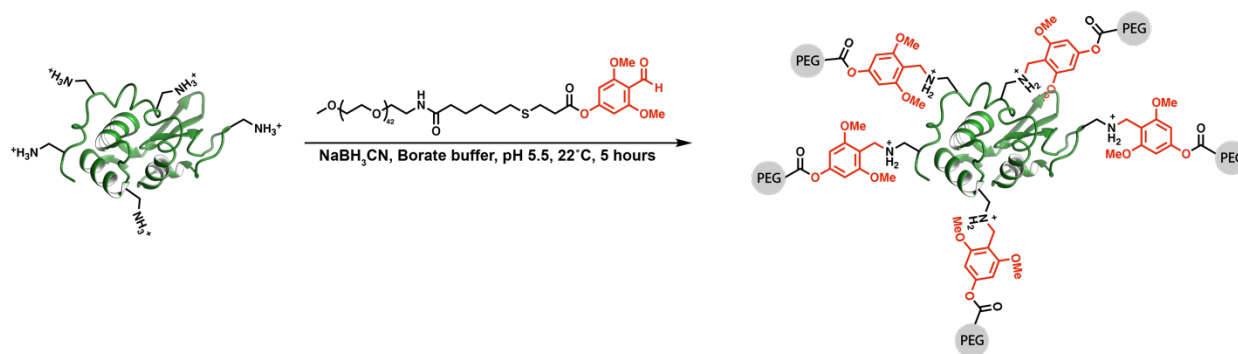
Scheme 4.3. Synthesis of PEG- β -thioester-(2,6-dimethoxybenzaldehyde) with a β -thioester trigger for protein conjugation.

With the mPEG- β -thioester-(2,6-dimethoxybenzaldehyde) in hand we then probed the hydrolytic stability of the phenolic β -thioester across a pH range of 4 to 8. HPLC analysis comparing initial time points to those after five hours indicated the percent degradation, further confirmed by the appearance of DMOB. Contrary to the previously demonstrated release of β -thioesters in the literature, this linkage appears to be undergoing a base mediated release more consistent within the phenolic ester literature. Yet, there is minimal background hydrolysis of the β -thioester under acidic conditions, which is ideal for the reductive amination conditions.

pH	% Released over 5 h
4	7.1%
5	14.3%
6	21.4%
7	44.6%
8	75.0%

Table 4.1. Stability of mPEG- β -thioester-DMOB monitoring the loss of starting material over five hours after incubation in 50 mM citrate/phosphate buffer ranging from pH 4-8.

Lysozyme (Lyz) was chosen as a model protein for conjugation, due to its 6 solvent accessible lysines including the N-terminal lysine,³² and that the activity assay is well-established. Reductive amination conditions were initially optimized to find that a pH of 5.5 and 65 equivalence of the mPEG- β -thioester-DMOB would functionalize an average of 2.5 lysine residues on lysozyme in five hours. Longer reaction times or elevated temperatures, as an attempt to raise the percent modification, only increased the competing ester hydrolysis and consequently decreased the overall conjugation efficiency. The percent modification, by sodium dodecyl sulphate-polyacrylamide gel electrophoresis (SDS-PAGE) and matrix-assisted laser desorption/ionization-time of flight mass spectrometry (MALDI-TOF), showed a distribution of 1-5 PEG species attached to each lysozyme.



Scheme 4.4. Conjugation of Lysozyme to mPEG- β -thioester-(2,6-dimethoxybenzaldehyde) by reductive amination.

The traceless release of lysozyme from the mPEG- β -thioester-DMOB-Lysozyme conjugates was monitored at a pH of 7.1 and 4.0. The amount of released 4-hydroxy-2,6-dimethoxybenzyl alcohol byproduct was used to calculate the percent released from each conjugate, with an average of 2.5 mPEG groups per protein. The conjugate fully released ($\geq 94\%$) within 42 hours at pH 7.1, however, the conjugate at pH 4.0 only showed 32% release at that time. The resulting lysozyme was characterized via MALDI-TOF following the release assay, which showed the primary product to be native lysozyme after 72 hours at a pH of 7.1, confirming that this was in fact a traceless release.

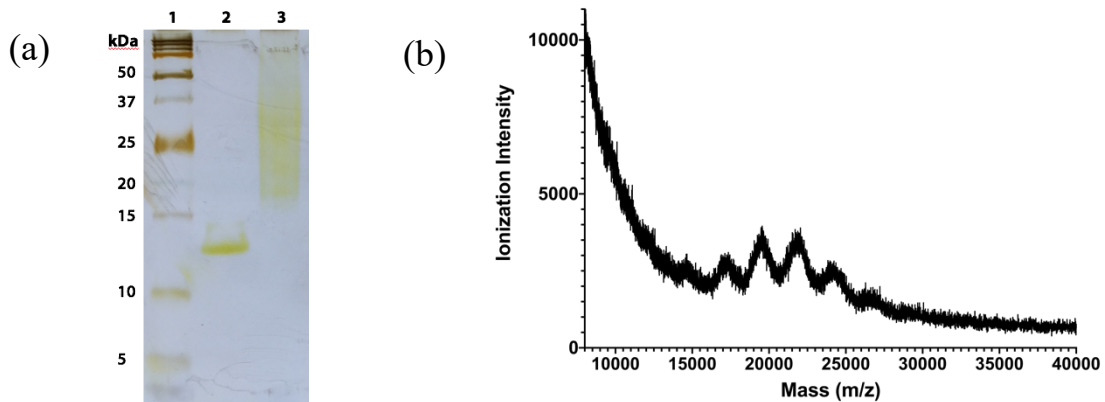


Figure 4.3. (a) SDS-PAGE of lysozyme and mPEG- β -thioester-lysozyme conjugate (lanes 2 and 3 respectively) (b) MALDI-TOF spectrum of mPEG- β -thioester-DMOB-lysozyme conjugate.

Although the enhanced stability of the phenolic β -thioester reduced the rate of release under acidic conditions, the conjugate still surpassed 50% release within 72 hours. This level of release under stable conditions does not constitute a high sense of control over release.

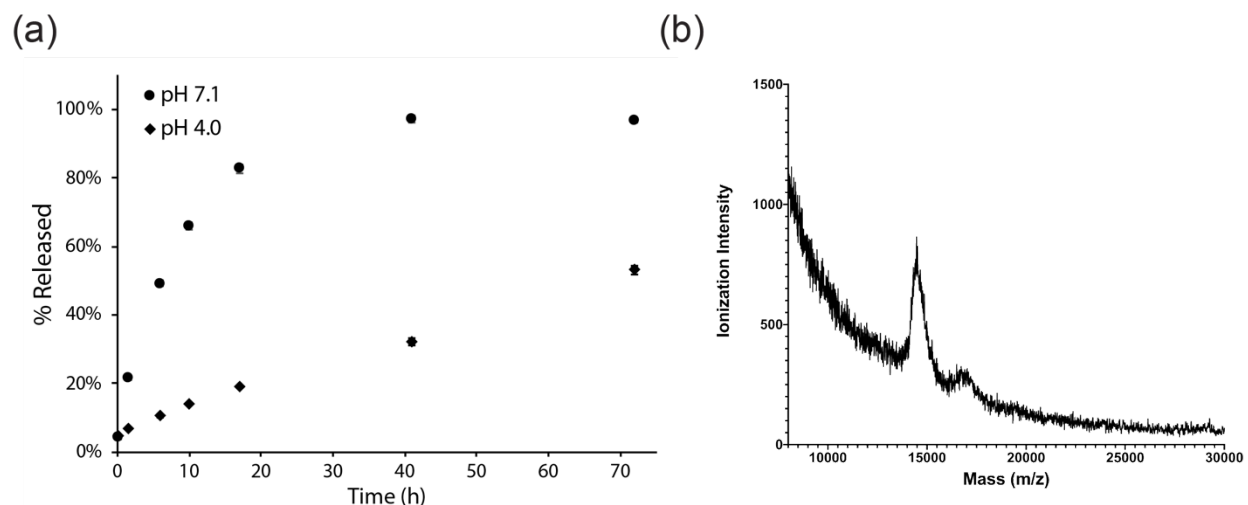
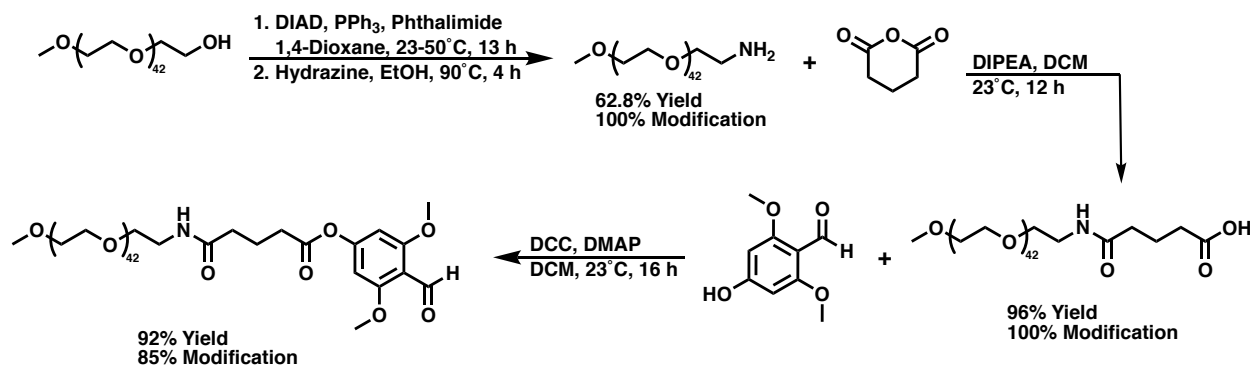


Figure 4.4. Traceless release of mPEG- β -thioester-Lysozyme (a) Release kinetics as measured by released 2,6-dimethoxybenzyl alcohol ($n = 3$, error bars are smaller than markers). (b) MALDI-TOF of lysozyme conjugate 72 hours after incubation at pH 7.1.

4.2.4 Preparation of mPEG-glutarate-(2,6-dimethoxybenzaldehyde)-Lysozyme Conjugate and Traceless Release of Lysozyme

The base mediated release pathway of the mPEG β -thioester indicated that the phenolic ester was the primary driving force of the release mechanism.³⁰ This suggested that the β -thioester is not required for the release and in fact it may be the primary driver behind the instability of the phenolic ester under acidic conditions. We hypothesized that the enhanced stability of the β -thioester compared to that of the initial phenolic ester likely was a result of the increased hydrophobicity in the spacer placed between that of the mPEG and benzaldehyde groups.³³



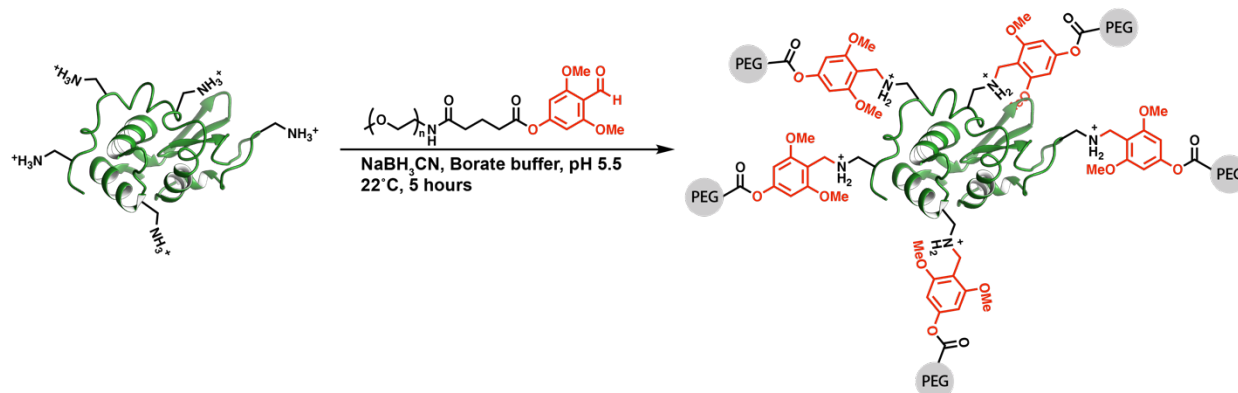
Scheme 4.5. Synthesis of mPEG-glutarate-(DMOB) with a phenolic ester trigger for protein conjugation.

To determine if the β -thioester was necessary for release and how much of an impact it had on the hydrolytic stability and pH selectivity of release, we prepared mPEG-glutarate-DMOB (Scheme 4.5). To prepare this mPEG species with a hydrophobic spacer, mPEG-NH₂ was converted to mPEG-glutaric acid through a ring opening of glutaric anhydride. The resulting carboxylic acid was then coupled to DMOB through a Steglich esterification to afford the mPEG-glutarate-DMOB.

pH	% Released over 5 h
4.0	0.9%
7.5	42.2%

Table 4.2. Stability of mPEG-glutarate-(DMOB) monitoring the loss of starting material over five hours after incubation in 50 mM citrate/phosphate buffer at either pH 4.0 or 7.5.

The hydrolytic stability of mPEG-glutarate-DMOB was then accessed showing minimal release at pH 4.0 while releasing 42.2% at pH 7.5 within 5 hours. The increased disparity between the hydrolysis at pH 4.0 and 7.5 suggests that any conjugate prepared with this mPEG species would selectively release under neutral to basic conditions with little to no background release under acidic conditions.



Scheme 4.6. Conjugation of lysozyme to mPEG-glutarate-DMOB by reductive amination.

Optimized reductive amination conditions were carried forward from the β -thioester bioconjugations at pH 5.5 using 65 equiv. of benzaldehyde per amine (Scheme 4.6). This time the conjugation efficiency was increased to afford the perfunctionalized lysozyme as characterized by MALDI-TOF and SDS-PAGE (Figure 4.5), with no unmodified lysozyme remaining in solution. This was further confirmed by measuring the % amine modification by both *o*-phthalaldehyde (90% modified) and fluorescamine assays (95% modified). We believe the increased conjugation efficiency was a result of the enhanced ester stability to the acidic reductive amination conditions.

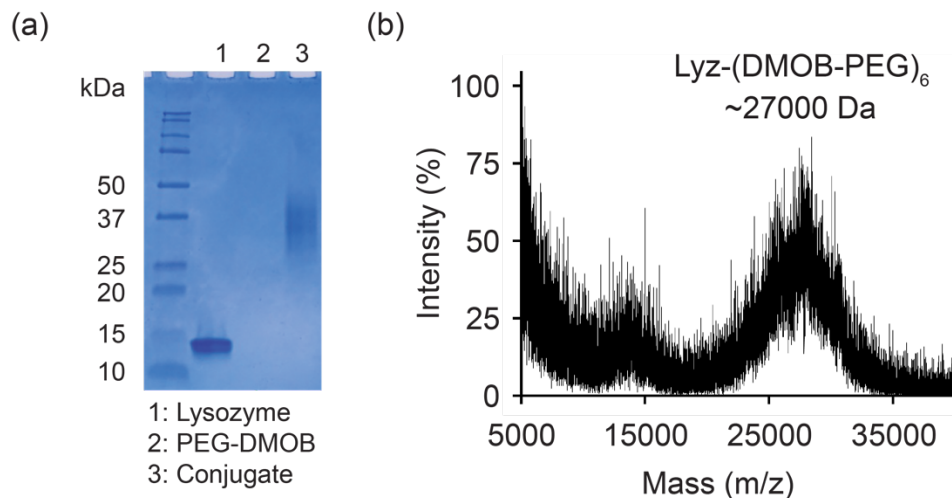


Figure 4.5. Characterization of mPEG-glutarate-lysozyme by (a) SDS-PAGE and (b) MALDI-TOF mass spectrum.

The traceless release of lysozyme was then tested (Figure 4.6a). Kinetics were obtained by measuring the amount of released 4-hydroxy-2,6-benzyl alcohol byproduct in solution over time. The phenolic ester hydrolysis was suppressed at pH 4 resulting in less than 20% released over 4 days, while at pH 7.4 the ester hydrolysis triggered the traceless release ($t_{1/2} = 10$ h) of lysozyme at a rate comparable to the small molecule model study (Figure 4.2).

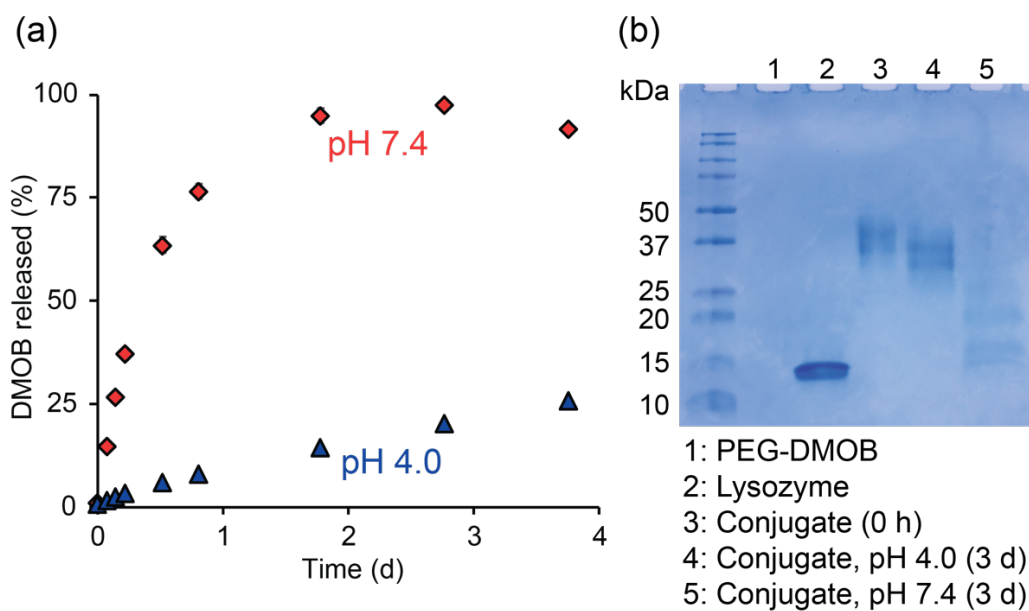


Figure 4.6. Traceless release of lysozyme. (a) Release kinetics as measured by released 2,6-dimethoxybenzyl alcohol ($n = 3$, error bars are smaller than markers) via HPLC. (b) SDS-PAGE of the mPEG-glutarate-DMOB-lysozyme conjugate before and after the traceless release at both pH 4.0 and 7.4.

To ensure that the release was truly traceless, MALDI-TOF was taken of the conjugates after incubation at either pH 4.0 or 7.4 for 4 days. It was observed that the primary mass seen via MALDI-TOF after release at pH 7.4 belonged to native lysozyme with minor amounts of the mono- and di-pegylated conjugates as well (Figure 4.7). Contrastingly, the primary product from the pH 4.0 release study was PEGylated lysozyme conjugate with an average of 4.5 PEG chains per lysozyme, which was further corroborated by SDS-PAGE (Figure 4.6b). It should be noted that due to the multiple modifications, unmodified lysozyme was observed only at a high DMOB release; theoretically, even when the release has reached 90% the corresponding amount of unmodified lysozyme will account for only 53% of the population.

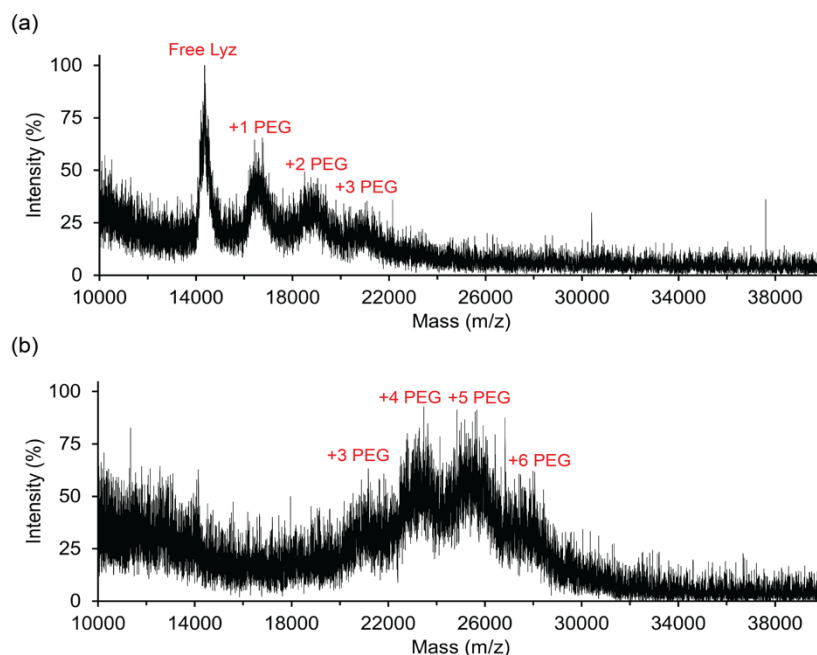


Figure 4.7. MALDI-TOF mass spectrum of the mPEG-glutarate-(2,6-dimethoxybenzaldehyde)-Lysozyme conjugate incubated for 3 days at (a) pH 7.4 and (b) pH 4.0.

Lysozyme activity before and after traceless release was monitored through the cell lysis of fluorescein isothiocyanate (FITC) labeled Gram-positive *Micrococcus lueus* in the EnzChek lysozyme activity assay (Figure 4.7) and after conjugation was 37% of unmodified. As anticipated, the activity was significantly decreased for the mPEG-glutarate-DMOB-lysozyme conjugate. Lysozyme breaks down bacterial cell walls and thus, the substrate for the enzyme is large and the binding is largely disrupted by steric hindrance from multiple attached polymers. This loss of activity was largely recovered, from 37% to 77%, upon traceless release at a pH of 7.4, whereas incubation at pH 4.0 for 4 days showed a slight increase to 43% activity. This suggests that lysozyme's tertiary structure was not compromised throughout the conjugation or release studies and that the steric blockage of the enzyme was the reason for the low activity of the conjugate. We believe that the minor amount of mPEG-lysozyme conjugate still present in solution explains why the lysozyme activity did not fully recover to 100%.

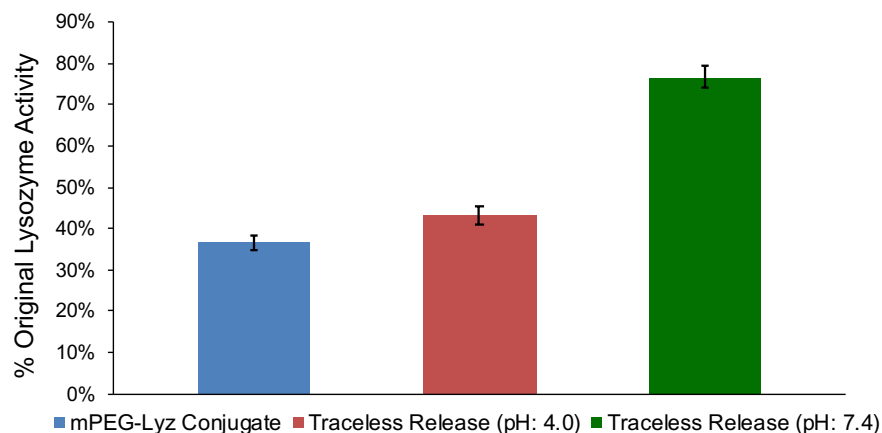


Figure 4.8. Lysozyme activity of the mPEG-glutarate-(2,6-dimethoxybenzaldehyde)-lysozyme conjugate before and after traceless release (n = 3, error bars represent standard deviation, *** $p < 0.005$).

Stimuli-triggered switching of protein activity has long been of interest in biotechnology,³⁴ and this strategy has potential for applications such as oral protein delivery and targeted drug delivery, reducing off-target effects.³⁵ This triggering of protein activity further demonstrates the utility of the benzaldehyde linkers in the context of traceless release. Theoretical insights into the factors that govern release kinetics gained from this study may help guide future design of these linkers to further slow or accelerate the release as desired.

4.3 Conclusions

In summary, we developed benzaldehyde-based traceless linkers that are readily accessible, have complementary conjugation conditions to previous linkers, and can reversibly change the level of protein activity. Near-complete modification of available lysines allowed the size and activity of the protein to be reversibly modulated. We chose phenolic ester as a trigger example, but other stimuli-responsive triggers³⁶ could easily be combined with this linker strategy. Given the desirable traits, these benzaldehyde handles are expected to be useful additions to the growing

library of traceless bioconjugate linkers that have found widespread use in chemical biology and biotechnology.

4.4 Experimental

4.4.1 Materials

All chemicals were used as purchased unless otherwise noted from Acros, Alfa Aesar, Sigma Aldrich, Combi-Blocks, Oakwood, or Fisher Scientific. Reagents were purchased at the highest commercial quality and used without further purification, unless otherwise stated. Dichloromethane (DCM) was distilled over CaH_2 and stored under argon. Tetrahydrofuran (THF) was distilled over sodium/benzophenone and stored under argon. 1,2-Dimethoxyethane, methanol, acetonitrile (MeCN) and other anhydrous solvents were dried by purging with nitrogen and passage through activated alumina columns prior to use. DIPEA was freshly distilled and stored over 3Å molecular sieves prior to use. All reactions were performed under an inert Argon atmosphere unless otherwise noted. Unless specifically mentioned, all solvents were purchased as ACS solvents and used without any further purification. Anhydrous solvents used were either freshly distilled or passed through activated alumina columns. Yields refer to isolated material, unless otherwise stated.

4.4.2 Analytical Techniques

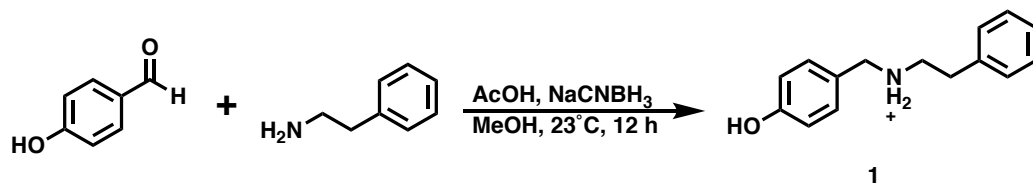
Reactions were monitored by GC/MS, LC/MS, and thin layer chromatography (TLC). TLC was performed using Millipore Sigma silica plates (60F-254), using short-wave UV light as the visualizing agent, acidic ethanolic anisaldehyde, or KMnO_4 and heat as developing agents. NMR spectra were recorded on Bruker AV-400, AV-500, and AV-600 instruments and are calibrated using residual undeuterated solvent (CHCl_3 at 7.26 ppm ^1H NMR, 77.16 ppm ^{13}C NMR). The

following abbreviations were used to explain multiplicities: s = singlet, d = doublet, t = triplet, q = quartet, m = multiplet. Column chromatography was performed using Silicycle silica (P60, particle size 40–63 μm) on a Biotage Isolera One 3.0 autocolumn instrument. All silica chromatography unless specifically stated otherwise was carried out on the Biotage using KP-Sil high-performance columns repacked using the Silicycle silica described above (column sizes described in experimental). ESI mass spectra were obtained using an Agilent 6530 QTOF-ESI in tandem with a 1260 Infinity LC. Analytical reverse phase high performance liquid chromatography (HPLC) was carried out on a Agilent 1260 Infinity II HPLC system equipped with an autosampler and a UV detector using a Poroshell 120 2.7- μm C18 120 \AA column (analytical: 2.7 μm , 4.6×100 mm) with monitoring at $\lambda = 220$ and 280 nm and with a flow rate of 0.8 mL/min. Preparatory reverse phase HPLC was carried out on an Agilent 1290 Infinity II high performance liquid chromatography system equipped with a UV detector using a Luna 5 μm C18 100 \AA column (preparatory: 5 μm , 250×21.2 mm) with monitoring at $\lambda = 220$ and 254 nm and with a flow rate of 25 mL/min. Melting points were recorded using a Mettler Toledo 3+ DSC wherein the melting points are listed as the onset temperature T_{on} and the peak temperature T_{peak} running under a nitrogen atmosphere at 5 $^{\circ}\text{C}/\text{min}$.

4.4.3 Methods

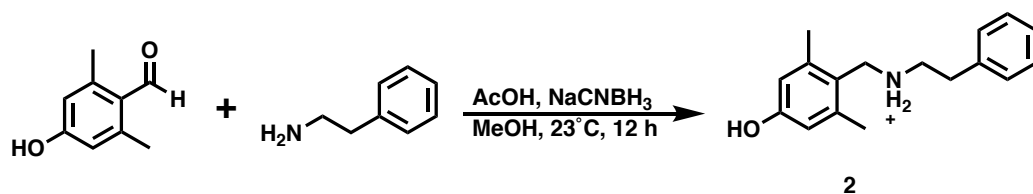
Synthesis of Compound 1

General Procedure A (reductive amination of benzaldehyde with phenethylamine).



To a solution of 4-hydroxybenzaldehyde (100.0 mg, 1 Eq, 818.9 μmol) in methanol (2 mL) was added acetic acid (245.9 mg, 234 μL , 5 Eq, 4.094 mmol), 2-phenylethan-1-amine (148.8 mg, 154 μL , 1.5 Eq, 1.228 mmol), and sodium cyanoborohydride (154.4 mg, 3 Eq, 2.457 mmol) sequentially. The reaction contents were then stirred for 12 hours at 23 $^{\circ}\text{C}$, where the conversion was monitored via analytical HPLC. The crude product was then purified on preparative HPLC (C18, 5-40% MeCN gradient against H_2O with a 0.1% TFA additive over 10 minutes) to afford **1** (138.1 mg, 49.4% yield) as a white solid. ^1H NMR (500 MHz, CD_3CN) δ 8.66 (s, 2H), 7.26 (m, $J = 8.9$ Hz, 7H), 6.81 (d, $J = 8.6$ Hz, 2H), 4.04 (s, 2H), 3.15 (t, $J = 8.1$ Hz, 2H), 2.97 (t, $J = 8.1$ Hz, 2H). ^{13}C NMR (126 MHz, CD_3CN) δ 158.17, 136.98, 131.67, 128.79, 128.76, 126.99, 122.00, 115.61, 50.60, 48.00, 31.74. IR (film): 3265, 3068, 3042, 2824, 1679, 1615, 1594, 1519, 1431, 1195, 1123 cm^{-1} . HRMS (ESI/Q-TOF) $[\text{M}+\text{H}]^+$ calcd for $\text{C}_{15}\text{H}_{18}\text{NO}^+$, 228.1383; found 228.1391. m.p.: T_{on} 115.1 $^{\circ}\text{C}$: T_{peak} 112.1 $^{\circ}\text{C}$

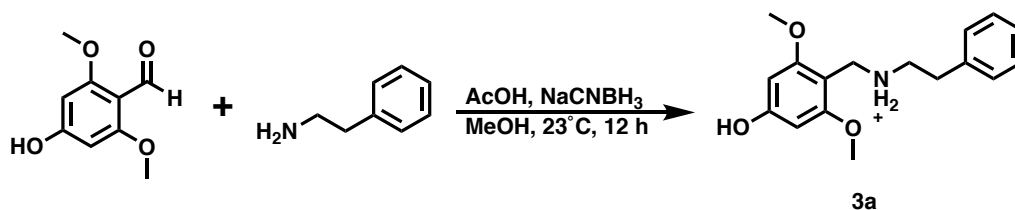
Synthesis of Compound 2



Following General Procedure A using 4-hydroxy-2,6-dimethylbenzaldehyde (100.0 mg, 665.9 μmol) afforded **2** (98.2 mg, 39.9% yield) as a white solid. ^1H NMR (500 MHz, CD_3CN) δ 7.83 (s, 2H), 7.35 (t, $J = 7.5$ Hz, 2H), 7.27 (d, $J = 7.7$ Hz, 3H), 6.55 (s, 2H), 4.16 (s, 2H), 3.32 (d, $J = 3.3$ Hz, 2H), 3.04 (t, $J = 8.2$ Hz, 2H), 2.30 (s, 6H). ^{13}C NMR (126 MHz, CD_3CN) δ 157.69, 140.37, 136.76, 128.86, 128.80, 127.11, 119.43, 115.34, 49.13, 45.55, 31.53, 19.17. IR (film):

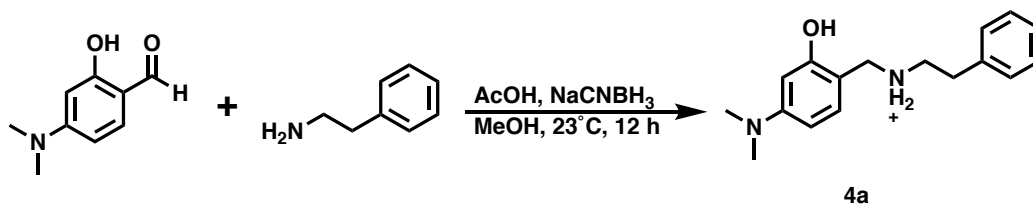
3034, 3012, 2825, 1664, 1613, 1593, 1465, 1307, 1191, 1122 cm^{-1} . HRMS (ESI/Q-TOF) $[\text{M}+\text{H}]^+$ calcd for $\text{C}_{17}\text{H}_{22}\text{NO}^+$, 256.1696; found 256.1599. m.p.: T_{on} 174.2 $^{\circ}\text{C}$: T_{peak} 178.9 $^{\circ}\text{C}$

Synthesis of Compound 3a



Following General Procedure A using 4-hydroxy-2,6-dimethoxybenzaldehyde (100.0 mg, 548.9 μmol) afforded **3a** (175.8 mg, 79.8% yield) as a white solid. ^1H NMR (500 MHz, CD_3CN) δ 7.86 (s, 2H), 7.33 (t, $J = 7.3$ Hz, 2H), 7.26 (t, $J = 7.4$ Hz, 1H), 7.21 (d, $J = 6.9$ Hz, 2H), 6.17 (s, 2H), 4.12 (s, 2H), 3.71 (s, 6H), 3.11 (s, 2H), 2.98 (t, $J = 7.8$ Hz, 2H). ^{13}C NMR (126 MHz, CD_3CN) δ 160.84, 159.80, 136.83, 128.84, 128.78, 127.06, 97.49, 91.87, 55.42, 47.40, 40.08, 31.40. IR (film): 3024, 3011, 2796, 1669, 1598, 1469, 1452, 1168, 1119 cm^{-1} . HRMS (ESI/Q-TOF) $[\text{M}+\text{H}]^+$ calcd for $\text{C}_{17}\text{H}_{22}\text{NO}_3^+$, 288.1594; found 288.1629. m.p.: T_{on} 134.7 $^{\circ}\text{C}$: T_{peak} 138.0 $^{\circ}\text{C}$

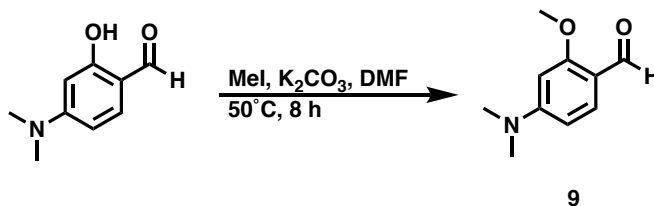
Synthesis of Compound 4a



Following General Procedure A using 4-(dimethylamino)-2-hydroxybenzaldehyde (100.0 mg, 605.4 μmol) afforded **4a** (179.7 mg, 59.6% yield) as a white solid. ^1H NMR (500 MHz, CD_3CN): δ 7.26 (m, $J = 4.8$ Hz, 6H), 6.99 (d, $J = 2.2$ Hz, 1H), 6.75 (dd, $J = 2.2, 8.4$ Hz, 1H), 4.15 (s, 2H), 3.20 (t, $J = 7.7$ Hz, 2H), 2.99 (s, 8H). ^{13}C NMR (126 MHz, CD_3CN): δ 157.33, 148.69,

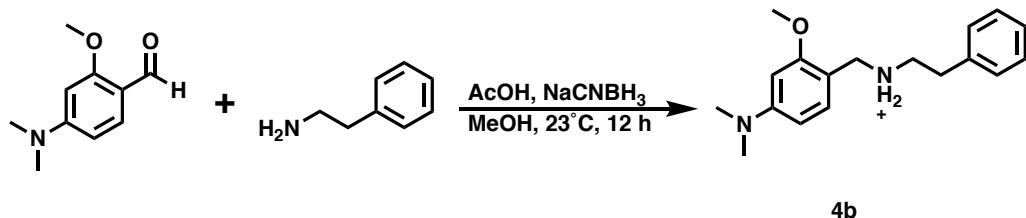
136.69, 132.74, 128.84, 128.74, 127.10, 113.03, 108.26, 104.34, 48.13, 46.77, 42.99, 31.61. IR (film): 3030, 2886, 1671, 1618, 1531, 1435, 1245, 1195, 1180, 1112 cm^{-1} . HRMS (ESI/Q-TOF): $[\text{M}+\text{H}]^+$ calcd for $\text{C}_{17}\text{H}_{23}\text{N}_2\text{O}^+$, 271.1805; found 271.1858. m.p.: T_{on} 74.6 $^{\circ}\text{C}$: T_{peak} 85.8 $^{\circ}\text{C}$.

Synthesis of Compound 9



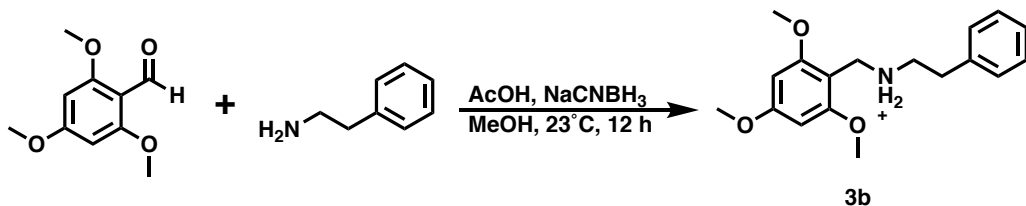
To a solution of 4-(dimethylamino)-2-hydroxybenzaldehyde (200 mg, 1 Eq, 1.21 mmol) in DMF (10 mL) was added potassium carbonate (837 mg, 5 Eq, 6.05 mmol) followed by iodomethane (1.72 g, 757 μL , 10 Eq, 12.1 mmol). The reaction contents were then sealed under argon and heated to 50 $^{\circ}\text{C}$ for 8 hours. The reaction was then combined with diethyl ether (150 mL), washed with sat. aq. NaHCO_3 (2 x 50 mL), water (50 mL), and sat. aq. NaCl (50 mL). The organic layer was then dried over MgSO_4 and concentrated under reduced pressure directly onto silica gel (2g). The crude product was then purified by flash column chromatography (25 g silica gel, 10-80% EtOAc gradient against hexanes over 10 column volumes) to afford benzaldehyde **9** (134.4 mg, 61.9% yield) as a pink solid. TLC: R_f 0.42 (1:1 hexanes:EtOAc). ^1H NMR (400 MHz, CD_3CN): δ 10.12 (d, $J = 0.5$ Hz, 1H), 7.67 (d, $J = 8.9$ Hz, 1H), 6.25 (dd, $J = 2.2, 8.9$ Hz, 1H), 5.99 (d, $J = 2.2$ Hz, 1H), 3.86 (s, 3H), 3.04 (s, 6H). ^{13}C NMR (101 MHz, CD_3CN): δ 187.41, 163.83, 155.98, 130.41, 114.56, 104.48, 92.89, 55.23, 40.17. IR (film): 2922, 2840, 1658, 1595, 1555, 1527, 1371, 1287, 1246, 1116 cm^{-1} . HRMS (ESI/Q-TOF): $[\text{M}+\text{H}]^+$ calcd for $\text{C}_{10}\text{H}_{14}\text{NO}_2^+$, 180.1019; found 180.1097. m.p.: T_{on} 60.1 $^{\circ}\text{C}$: T_{peak} 61.2 $^{\circ}\text{C}$.

Synthesis of Compound 4b



Following General Procedure A using 4-(dimethylamino)-2-methoxybenzaldehyde (30.0 mg, 167 μmol) afforded **4b** (55.26 mg, 82.9% yield) as an off white solid. ^1H NMR (500 MHz, CD_3CN): δ 7.99 (s, 2H), 7.34 (t, $J = 7.3$ Hz, 2H), 7.27 (q, $J = 5.3$ Hz, 1H), 7.21 (q, $J = 7.7$ Hz, 2H), 6.56 (d, $J = 2.3$ Hz, 1H), 6.52 (dd, $J = 2.3, 8.3$ Hz, 1H), 4.08 (s, 2H), 3.79 (s, 3H), 3.17 (s, 2H), 2.99 (s, 8H). ^{13}C NMR (126 MHz, CD_3CN): δ 158.96, 151.29, 136.74, 132.39, 128.87, 128.77, 127.12, 109.74, 106.39, 97.60, 55.17, 47.92, 47.03, 41.27, 31.53. IR (film): 2993, 1680, 1612, 1465, 1409, 1194, 1155, 1115 cm^{-1} . HRMS (ESI/Q-TOF): $[\text{M}+\text{H}]^+$ calcd for $\text{C}_{18}\text{H}_{25}\text{N}_2\text{O}^+$, 285.1961; found 284.9186. m.p.: T_{on} 59.6 $^\circ\text{C}$: T_{peak} 68.5 $^\circ\text{C}$

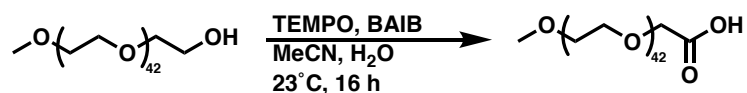
Synthesis of Compound 3b



Following General Procedure A using 2,4,6-trimethoxybenzaldehyde (100.0 mg, 509.7 μmol) afforded **3b** (145.2 mg, 68.6% yield) as a white solid. ^1H NMR (500 MHz, CD_3CN): δ 8.47 (s, 2H), 7.32 (t, $J = 7.3$ Hz, 2H), 7.26 (t, $J = 7.4$ Hz, 1H), 7.20 (d, $J = 6.9$ Hz, 2H), 6.20 (s, 2H), 4.13 (s, 2H), 3.79 (s, 3H), 3.76 (s, 6H), 3.11 (s, 2H), 2.99 (t, $J = 7.9$ Hz, 2H). ^{13}C NMR (126 MHz, CD_3CN): δ 162.83, 159.80, 137.08, 128.81, 128.76, 126.98, 99.12, 90.49, 55.59, 55.22, 47.43, 39.76, 31.46. IR (film): 3032, 2950, 2839, 1689, 1597, 1455, 1420, 1333, 1200, 1167, 1153, 1118

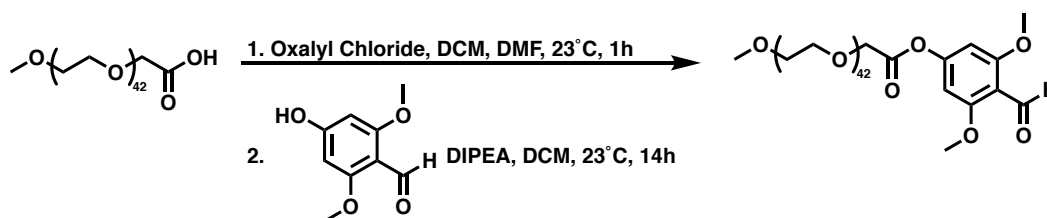
cm⁻¹. HRMS (ESI/Q-TOF): [M+H]⁺ calcd for C₁₈H₂₄NO₃⁺, 302.1751; found 302.1773. m.p.: T_{on} 127.8 °C: T_{peak} 132.1 °C.

Synthesis of 2 kDa mPEG-COOH



To a solution of mPEG-OH (2 kDa, 2.0 g, 1 Eq, 1 mmol) in a 50/50 mixture of water and MeCN (10 mL), was added (2,2,6,6-Tetramethylpiperidin-1-yl)oxyl (31 mg, 0.2 Eq, 0.2 mmol) and (bisacetoxyiodo)benzene (966 mg, 3 Eq, 3 mmol) and the resulting solution was stirred for 6 hours at 22 °C. The reaction contents were then concentrated under vacuum and precipitated into diethyl ether to afford the mPEG-COOH (1.7 g, 82.6% yield) as a white powder. ¹H NMR (500 MHz, DMSO-d₆) δ 3.97 (s, 2H), 3.47 (s, 185H), 3.20 (s, 3H). IR (film): 3480, 2884, 1737, 1467, 1341, 1280, 1239, 1104, 946, 841 cm⁻¹.

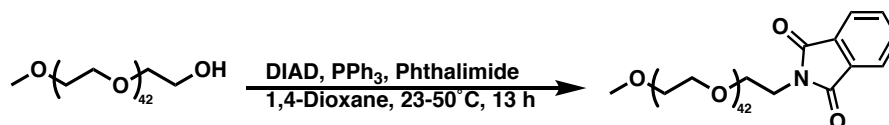
Synthesis of 2 kDa mPEG-(2,6-dimethoxybenzaldehyde)



A solution of DMF (940 μL, 0.1 Eq, 12 μmol) in anhydrous DCM (10 mL) was cooled to 4 °C and oxalyl chloride (52 μL, 5 Eq, 607 μmol) was subsequently added. This solution was warmed to room temperature where it was stirred for an additional 15 minutes. Separately, a solution of 2 kDa mPEG-COOH (250 mg, 1 Eq, 122 μmol) in anhydrous DCM (1 mL) was prepared and added to the reaction solution dropwise over 5 minutes. This solution was stirred at

40 °C for 1 hour forming a light-yellow solution. The reaction was concentrated under vacuum to remove all solvent and residual oxalyl chloride. The reaction contents were redissolved in anhydrous DCM (2 mL), after which a separate solution of 4-hydroxy-2,6-dimethoxybenzaldehyde (88 mg, 4 Eq, 486 μmol) and anhydrous DIPEA (529 μL , 25 Eq, 3.0 mmol) in anhydrous DCM (2 mL) was added dropwise to the acyl chloride solution. The resulting solution was stirred at 23 °C for 12 hours. The resulting reaction solution was dialyzed in methanol using a regenerated cellulose membrane (Spectra/Por, MWCO 1 kDa), and the solvent was removed under vacuum to afford the 2 kDa mPEG-(2,6-dimethoxybenzaldehyde) (155 mg, 62% yield) as a white solid. ^1H NMR (500 MHz, CD_3CN) δ 10.34 (s, 1H), 6.51 (s, 2H), 4.39 (s, 2H), 3.81 (s, 6H), 3.53 (s, 21H), 3.42 (m, 6H), 3.27 (s, 3H).

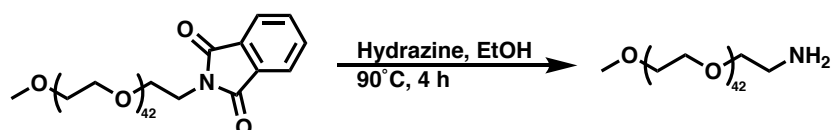
Synthesis of 2 kDa mPEG-phthalimide



To a solution of triphenylphosphine (2.6 g, 4 Eq, 10 mmol) in anhydrous 1,4-dioxane (5 mL) was added a solution of diisopropyl azodicarboxylate (2.6 g, 4 Eq, 10 mmol) in dioxane (1 mL). This solution was stirred for 30 minutes at 23 °C and then cannulated into a solution of mPEG (2 kDa, 5.0 g, 1 Eq, 2.5 mmol) in anhydrous 1,4-dioxane (10 mL). This solution was slowly warmed to 23 °C and stirred for an additional 30 minutes, after which phthalimide (1.5 g, 4 Eq, 10 mmol) was added. The resulting solution was stirred at 23 °C for 1 hour and then 50 °C for 13 hours. The resulting solution was concentrated under vacuum and the resulting viscous oil (~2 mL) was precipitated into diethyl ether. This precipitation was repeated 4 additional times, reconstituting in a minimal amount of DCM each time. The final precipitation noted zero yellow

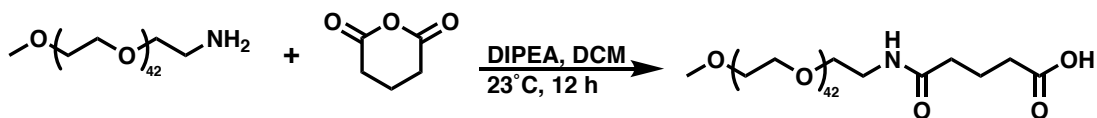
color present in the supernatant resulting in a white powder (4.61 g, 88.0% yield). ¹H NMR (500 MHz, CD₂Cl₂) δ 7.82 (q, *J* = 2.8 Hz, 2H), 7.72 (q, *J* = 2.8 Hz, 2H), 3.84 (t, *J* = 5.8 Hz, 2H), 3.59 (s, 200H), 3.32 (s, 3H). IR (film): 3458, 2870, 2896, 1711, 1638, 1454, 1408, 1348, 1340, 1297, 1250, 1091, 946, 841 cm⁻¹.

Synthesis of 2 kDa mPEG-NH₂



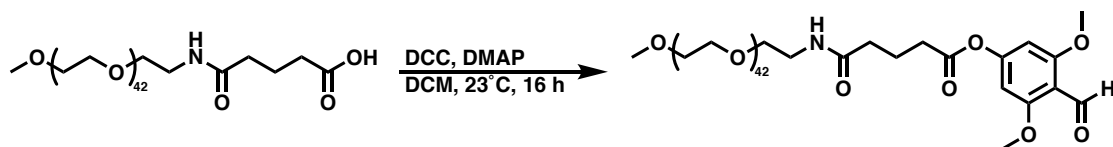
To a solution of mPEG-phthalimide (4.1 g, 1 Eq, 2.05 mmol) in ethanol (45 mL) was added a 78% hydrazine hydrate aqueous solution (1.3 mL, 10 Eq, 20.5 mmol). This solution was brought to 90 °C, where it was refluxed for 4 hours. The resulting solution was filtered and concentrated under vacuum to produce an off white solid. This solid was suspended in DCM (50 mL), filtered, and extracted with 1M aq. NaOH (10 mL). The aqueous layer was back extracted with DCM (25 mL), the organic layers were combined, dried over MgSO₄, and concentrated under vacuum to 5 mL. The resulting viscous solution was precipitated into cold diethyl ether to afford mPEG-NH₂ (2.79 g, 71.4% yield) as a white solid. ¹H NMR (500 MHz, CD₂Cl₂) δ 3.59 (s, 190H), 3.49 (q, *J* = 3.1 Hz, 2H), 3.44 (t, *J* = 5.3 Hz, 2H), 3.33 (s, 3H), 2.79 (t, *J* = 5.3 Hz, 2H). IR (film): 3458, 2870, 2896, 1647, 1454, 1348, 1340, 1290, 1246, 1088, 946, 841 cm⁻¹.

Synthesis of 2 kDa mPEG-glutaric acid



To a solution of mPEG-NH₂ (750 mg, 1 Eq, 0.375 mmol) in anhydrous DCM (10 mL) was added anhydrous DIPEA (327 μ L, 5 Eq, 1.88 mmol) followed by a solution of glutaric anhydride (214 mg, 5 Eq, 1.88 mmol) in DCM (2 mL). This solution was stirred at 23 $^{\circ}$ C for 14 hours, after which it was concentrated under vacuum. The resulting solution was dialyzed in a mixture of water and methanol (50/50) using a regenerated cellulose membrane (Spectra/Por, MWCO 1 kDa), and the solvent was removed under vacuum to afford the mPEG-glutaric acid (68 mg, 62% yield) as a white solid. ¹H NMR (500 MHz, CDCl₃) δ 6.58 (s, 1H), 3.53 (s, 194H), 3.45 (m, *J* = 3.2 Hz, 4H), 3.39 (q, *J* = 3.1 Hz, 1H), 3.28 (s, 5H), 2.16 (t, *J* = 7.1 Hz, 4H), 1.78 (t, *J* = 7.1 Hz, 2H). IR (film): 3458, 2870, 2896, 1748, 1711, 1647, 1454, 1348, 1340, 1290, 1246, 1088, 946, 841 cm⁻¹.

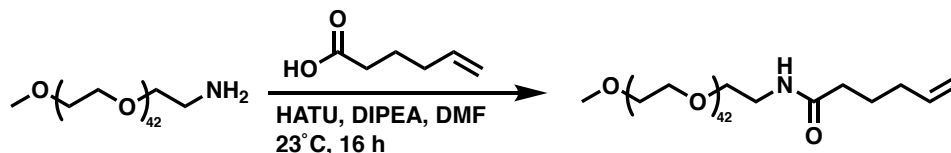
Synthesis of 2 kDa mPEG-glutaric-(2,6-dimethoxybenzaldehyde)



mPEG-glutaric acid (2.1 kDa, 100 mg, 0.048 mmol, 1 equiv) was dissolved in 1 mL dry toluene and dried in vacuo to remove water. Next, 4-(dimethylamino)pyridine (DMAP, 6 mg, 0.05 mmol, 1 equiv), 2,6-dimethoxy-4-hydroxybenzaldehyde (DMOB, 87 mg, 0.48 mmol, 10 equiv), and 4 mL dry DCM were added. The solution was cooled to 4 $^{\circ}$ C and stirred for 5 min. N,N'-Dicyclohexylcarbodiimide (DCC, 49 mg, 0.24 mmol, 5 equiv) in 1 mL dry DCM was added and the reaction mixture was allowed to warm to room temperature and stirred for 16 h. The reaction was concentrated in vacuo, and precipitated into cold diethyl ether. The polymer was dialyzed in methanol using a regenerated cellulose membrane (Spectra/Por, MWCO 1 kDa), and the solvent was removed under vacuum to yield the product with 82% conversion of the end group as determined by ¹H NMR (68 mg, 62% yield). ¹H NMR (500 MHz in CDCl₃) δ : 10.45–10.35 (1H),

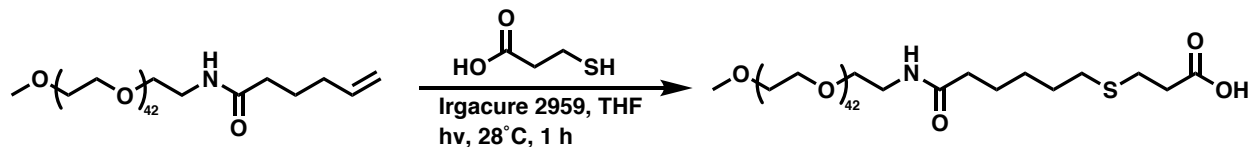
6.45–6.27 (2H), 3.91–3.84 (6H), 3.78–3.42 (180H), 3.39–3.35 (3H), 2.72–2.61 (2H), 2.40–2.29 (2H), 2.12–2.05 (2H). IR (film): 2882, 2741, 2695, 1766, 1676, 1600, 1466, 1408, 1359, 1340, 1279, 1240, 1146, 1103, 1059, 947, 841 cm^{-1} .

Synthesis of 2 kDa mPEG-vinyl



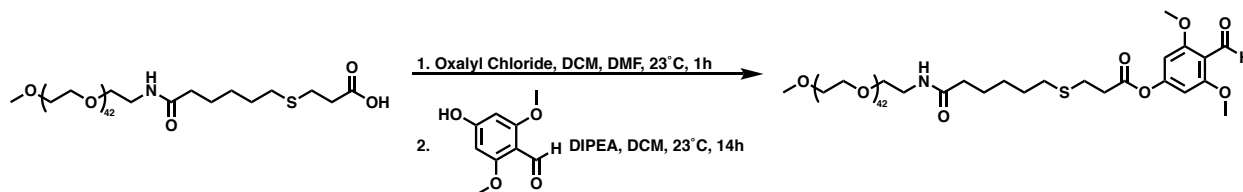
To a solution of 5-hexenoic acid (59 μL , 2 Eq, 500 μmol) in anhydrous DMF (3 mL) was added HATU (180 mg, 1.9 Eq, 475 μmol) and DIPEA (218 μL , 5 Eq, 1.25 mmol) forming a yellow solution that was stirred for 5 minutes. Separately, a solution of mPEG-NH₂ (500 mg, 1 Eq, 250 μmol) in anhydrous DMF (4 mL) was prepared and subsequently added to the activated hexanoic acid solution, which was stirred at 23 °C for 3 hours. The resulting solution was dialyzed in a mixture of water and methanol (80/20) using a regenerated cellulose membrane (Spectra/Por, MWCO 1 kDa), and the solvent was removed under vacuum to yield the product with 100% conversion of the end group as determined by ¹H NMR (426 mg, 81.1% yield). ¹H NMR (500 MHz, CD₃CN) δ 6.42 (s, 1H), 5.81 (m, 1H), 5.01 (qd, J = 1.8, 17.1 Hz, 1H), 4.94 (m, 1H), 3.67 (t, J = 4.7 Hz, 2H), 3.53 (s, 200H), 3.44 (m, 4H), 3.40 (t, J = 2.4 Hz, 1H), 3.26 (m, 5H), 2.09 (t, J = 7.5 Hz, 2H), 2.03 (q, J = 7.6 Hz, 2H), 1.62 (m, 2H). IR (film): 2883, 2740, 1646, 1541, 1466, 1455, 1413, 1352, 1340, 1279, 1240, 1146, 1103, 1060, 957, 841 cm^{-1} .

Synthesis of 2kDa mPEG- β -thioacid



To a solution of 2 kDa mPEG-vinyl (100 mg, 1 Eq, 50 μ mol) in THF (250 μ L) was added 3-mercaptopropionic acid (13 μ L, 3 Eq, 150 μ mol) and irgacure 2959 (1.1 mg, 0.1 Eq, 5 μ mol). This solution was sparged for 5 minutes with argon, sealed, and irradiated under UV for 1 hour. The resulting solution was dialyzed in a mixture of water and methanol (80/20) using a regenerated cellulose membrane (Spectra/Por, MWCO 1 kDa), and the solvent was removed under vacuum to yield the product with 100% conversion of the end group as determined by ^1H NMR (98.3 mg, 98.3% yield). ^1H NMR (500 MHz, CDCl_3) δ 6.37 (s, 1H), 3.76 (t, J = 4.8 Hz, 2H), 3.62 (s, 204H), 3.54 (m, 6H), 3.46 (dd, J = 4.7, 24.2 Hz, 4H), 3.36 (s, 3H), 2.77 (t, J = 6.9 Hz, 2H), 2.60 (s, 2H), 2.53 (t, J = 7.2 Hz, 2H), 2.19 (t, J = 7.4 Hz, 2H), 1.62 (m, 4H), 1.41 (m, 2H). IR (film): 3454, 2884, 2739, 1714, 1646, 1551, 1466, 1455, 1352, 1341, 1279, 1240, 1145, 1103, 1060, 958, 841 cm^{-1} .

Synthesis of 2 kDa mPEG- β -thioester-(2,6-dimethoxybenzaldehyde)



A solution of DMF (323 μ L, 0.1 Eq, 4 μ mol) in anhydrous DCM (10 mL) was cooled to 4 $^{\circ}\text{C}$ and oxalyl chloride (18 μ L, 5 Eq, 210 μ mol) was subsequently added. This solution was warmed to room temperature where it was stirred for an additional 15 minutes. Separately, a solution of 2 kDa mPEG- β -thioacid (93 mg, 1 Eq, 42 μ mol) in anhydrous DCM (1 mL) was

prepared and added to the reaction solution dropwise over 5 minutes. This solution was stirred at 40 °C for 1 hour forming a light-yellow solution. The reaction was concentrated under vacuum to remove all solvent and residual oxalyl chloride. The reaction contents were redissolved in anhydrous DCM (2 mL), after which a separate solution of 4-hydroxy-2,6-dimethoxybenzaldehyde (19 mg, 2.5 Eq, 105 μmol) and anhydrous DIPEA (37 μL , 5 Eq, 210 μmol) in anhydrous DCM (2 mL) was added dropwise to the acyl chloride solution. The resulting solution was stirred at 23 °C for 12 hours. The resulting reaction solution was dialyzed in methanol using a regenerated cellulose membrane (Spectra/Por, MWCO 1 kDa), and the solvent was removed under vacuum to afford the 2 kDa mPEG- β -thioester-(2,6-dimethoxybenzaldehyde) (98.3 mg, 98% yield) as a white solid. ^1H NMR (500 MHz, CDCl_3) δ 10.42 (s, 2H), 6.38 (s, 2H), 3.87 (s, 6H), 3.77 (t, $J = 4.9$ Hz, 2H), 3.63 (s, 240H), 3.56 (m, $J = 12$ H), 3.37 (s, 3H), 2.87 (t, $J = 3.2$ Hz, 4H), 2.60 (t, $J = 6.4$ Hz, 2H), 2.32 (t, $J = 6.9$ Hz, 2H), 1.65 (t, $J = 3.5$ Hz, 4H), 1.24 (s, 2H). IR (film): 2883, 2739, 1762, 1647, 1552, 1465, 1455, 1352, 1340, 1279, 1240, 1145, 1104, 1060, 956, 841 cm^{-1} .

pH Stability Study Procedure

The modified PEG species was prepared as a 1 mg/mL solution in 50 mM citrate-phosphate (McIlvaine) buffer within a pH range of 4.0 to 8.0. These samples were immediately analyzed on the analytical HPLC and the integration values were compared to a control prepared in MeCN. Each sample was prepared immediately prior to the first injection to ensure a consistent starting point across the three separate repeats. The reduction in the PEG peak compared to an initial time point was monitored over 5 hours and used to calculate the % hydrolysis.

Phenethylamine Release Study Procedure

The linker was prepared as a 10mM solution in MeOH in triplicate. Each aliquot was diluted to a final concentration of 5mM with 0.1M Tris buffer (pH: 7.4). This was immediately analyzed on the analytical HPLC to determine the amount of phenethylamine release using a phenethylamine standard curve. Each sample was prepared immediately prior to the first injection to ensure a consistent starting point across the three separate repeats. Time points were taken over a time frame of at least 10 days and longer if necessary.

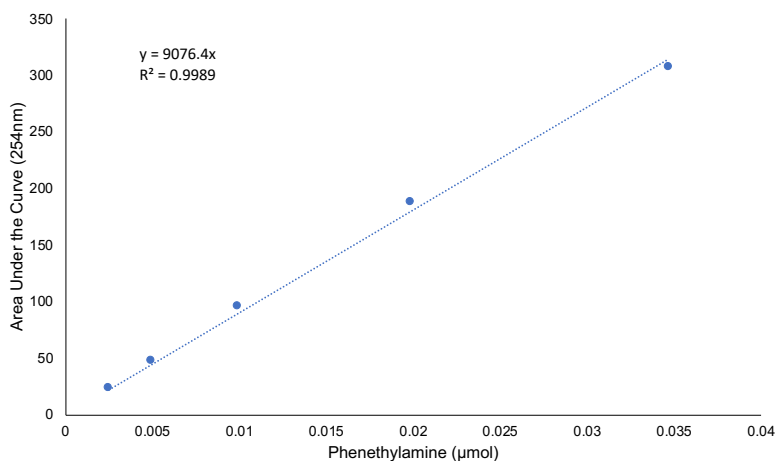


Figure 4.9. Phenethylamine standard curve from HPLC integration values at 254nm.

General Lysozyme PEG Conjugation

A solution of lysozyme (1.5 mg, 1 Eq, 0.105 mmol) in 0.2 M borate buffer (300 µL, pH 5.5) was added mPEG-benzaldehyde (450 µL, 15.1 M, 6.8 mmol, 65 equiv to lysozyme and 10.8 equiv to lysines) and NaBH₃CN (150 µL, 173 M, 26 mmol, 250 equiv) both in borate buffer. The mixture was incubated at 23 °C on a rocker for 5 h. The conjugate was purified by centrifugal filtration using the Centriprep™ tube (10 kDa molecular weight cut-off) and washed with 10% MeCN 12 times before resuspension into buffer.

Lysozyme release experiment

Lysozyme PEG conjugates were prepared at 0.5 mg/mL in 50 mM citrate-phosphate (McIlvaine) buffer at pH 4.0 or 7.4. This was immediately analyzed on the analytical HPLC to determine the amount of 4-hydroxy-2,6-dimethoxybenzyl alcohol released using a standard curve. Each sample was prepared immediately prior to the first injection to ensure a consistent starting point across the three separate repeats. Time points were taken over a time frame of 72 hours. The released lysozyme was characterized by sodium dodecyl sulfate-polyacrylamide gel electrophoresis (SDS-PAGE) and MALDI-MS.

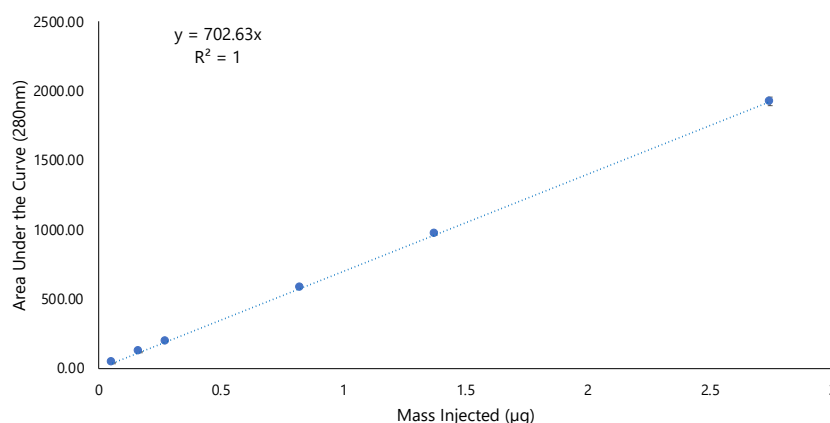


Figure 4.10. 4-Hydroxy-2,6-dimethoxybenzyl alcohol standard curve from HPLC integration values at 280nm.

Lysozyme Activity Assays

The lysozyme activity assay was conducted using the Invitrogen™ ENZChek™ assay kit, according to the manufacturer instructions. Briefly, 50 µL of sample (protein concentration was quantified by the bicinchoninic acid (BCA) assay) was mixed with 50 µL of fluorescein-labeled *Micrococcus luteus* in a 96-well plate and incubated at 37 °C. Recovered fluorescein fluorescence from cell lysis was measured (excitation 485 nm, emission 530 nm) and quantified using a standard curve.

Lysozyme Activity Standard Curve

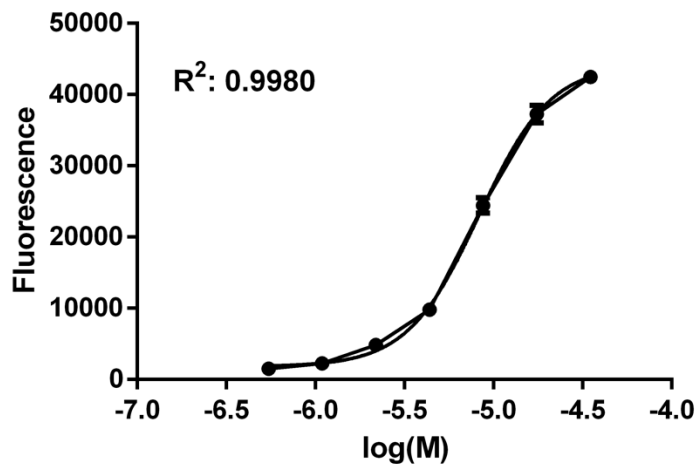


Figure 4.11. Lysozyme standard curve from ENZChek fluorescence assay (excitation 485 nm, emission 530 nm).

4.5 References

- (1) Gunnoo, S. B.; Madder, A. Bioconjugation – Using Selective Chemistry to Enhance the Properties of Proteins and Peptides as Therapeutics and Carriers. *Org. Biomol. Chem.* **2016**, *14* (34), 8002–8013. <https://doi.org/10.1039/C6OB00808A>.

- (2) Pelegri-O'Day, E. M.; Lin, E.-W.; Maynard, H. D. Therapeutic Protein–Polymer Conjugates: Advancing Beyond PEGylation. *J. Am. Chem. Soc.* **2014**, *136* (41), 14323–14332. <https://doi.org/10.1021/ja504390x>.
- (3) Morgenstern, J.; Gil Alvaradejo, G.; Bluthardt, N.; Beloqui, A.; Delaittre, G.; Hubbuch, J. Impact of Polymer Bioconjugation on Protein Stability and Activity Investigated with Discrete Conjugates: Alternatives to PEGylation. *Biomacromolecules* **2018**, *19* (11), 4250–4262. <https://doi.org/10.1021/acs.biomac.8b01020>.
- (4) Lucius, M.; Falatach, R.; McGlone, C.; Makaroff, K.; Danielson, A.; Williams, C.; Nix, J. C.; Konkolewicz, D.; Page, R. C.; Berberich, J. A. Investigating the Impact of Polymer Functional Groups on the Stability and Activity of Lysozyme–Polymer Conjugates. *Biomacromolecules* **2016**, *17* (3), 1123–1134. <https://doi.org/10.1021/acs.biomac.5b01743>.
- (5) Tucker, B. S.; Stewart, J. D.; Aguirre, J. I.; Holliday, L. S.; Figg, C. A.; Messer, J. G.; Sumerlin, B. S. Role of Polymer Architecture on the Activity of Polymer–Protein Conjugates for the Treatment of Accelerated Bone Loss Disorders. *Biomacromolecules* **2015**, *16* (8), 2374–2381. <https://doi.org/10.1021/acs.biomac.5b00623>.
- (6) Wang, Y.; Wu, C. Site-Specific Conjugation of Polymers to Proteins. *Biomacromolecules* **2018**, *19* (6), 1804–1825. <https://doi.org/10.1021/acs.biomac.8b00248>.
- (7) Gong, Y.; Leroux, J.-C.; Gauthier, M. A. Releasable Conjugation of Polymers to Proteins. *Bioconjug. Chem.* **2015**, *26* (7), 1172–1181. <https://doi.org/10.1021/bc500611k>.
- (8) Diehl, K. L.; Kolesnichenko, I. V.; Robotham, S. A.; Bachman, J. L.; Zhong, Y.; Brodbelt, J. S.; Anslyn, E. V. Click and Chemically Triggered Declick Reactions through Reversible

- Amine and Thiol Coupling via a Conjugate Acceptor. *Nat. Chem.* **2016**, *8* (10), 968–973.
<https://doi.org/10.1038/nchem.2601>.
- (9) Lee, S.; Greenwald, R. B.; McGuire, J.; Yang, K.; Shi, C. Drug Delivery Systems Employing 1,6-Elimination: Releasable Poly(Ethylene Glycol) Conjugates of Proteins. *Bioconjug. Chem.* **2001**, *12* (2), 163–169. <https://doi.org/10.1021/bc000064z>.
- (10) Zhao, H.; Yang, K.; Martinez, A.; Basu, A.; Chintala, R.; Liu, H.-C.; Janjua, A.; Wang, M.; Filpula, D. Linear and Branched Bicin Linkers for Releasable PEGylation of Macromolecules: Controlled Release in Vivo and in Vitro from Mono- and Multi-PEGylated Proteins. *Bioconjug. Chem.* **2006**, *17* (2), 341–351.
<https://doi.org/10.1021/bc050270c>.
- (11) Peleg-Shulman, T.; Tsubery, H.; Mironchik, M.; Fridkin, M.; Schreiber, G.; Shechter, Y. Reversible PEGylation: A Novel Technology To Release Native Interferon A2 over a Prolonged Time Period. *J. Med. Chem.* **2004**, *47* (20), 4897–4904.
<https://doi.org/10.1021/jm0497693>.
- (12) Garman, A. J.; Barret Kalindjian, S. The Preparation and Properties of Novel Reversible Polymer-Protein Conjugates 2- ω -Methoxypolyethylene (5000) Glycoxymethylene-3-Methylmaleyl Conjugates of Plasminogen Activators. *FEBS Lett.* **1987**, *223* (2), 361–365.
[https://doi.org/10.1016/0014-5793\(87\)80319-8](https://doi.org/10.1016/0014-5793(87)80319-8).
- (13) Brocchini, S.; Godwin, A.; Balan, S.; Choi, J.; Zloh, M.; Shaunak, S. Disulfide Bridge Based PEGylation of Proteins. *Adv. Drug Deliv. Rev.* **2008**, *60* (1), 3–12.
<https://doi.org/10.1016/j.addr.2007.06.014>.

- (14) Hacker, S. M.; Backus, K. M.; Lazear, M. R.; Forli, S.; Correia, B. E.; Cravatt, B. F. Global Profiling of Lysine Reactivity and Ligandability in the Human Proteome. *Nat. Chem.* **2017**, *9* (12), 1181–1190. <https://doi.org/10.1038/nchem.2826>.
- (15) Bossard, M. J.; Ali, C. F.; Liu, X.; Charych, D. H.; Zappe, H.; Wang, Y.; Huang, J. Conjugates of an Il-2 Moiety and a Polymer. WO2012065086A1, May 18, 2012.
- (16) Peterson, G. I.; Larsen, M. B.; Boydston, A. J. Controlled Depolymerization: Stimuli-Responsive Self-Immolative Polymers. *Macromolecules* **2012**, *45* (18), 7317–7328. <https://doi.org/10.1021/ma300817v>.
- (17) Rau, H.; Kindermann, S.; Lessmann, T.; RASMUSSEN, G. N.; Hersel, U.; Wegge, T.; Sprogøe, K. Pegylated Recombinant Human Growth Hormone Compounds. WO2009133137A2, November 5, 2009.
- (18) Staben, L. R.; Koenig, S. G.; Lehar, S. M.; Vandlen, R.; Zhang, D.; Chuh, J.; Yu, S.-F.; Ng, C.; Guo, J.; Liu, Y.; Fourie-O'Donohue, A.; Go, M.; Linghu, X.; Segraves, N. L.; Wang, T.; Chen, J.; Wei, B.; Phillips, G. D. L.; Xu, K.; Kozak, K. R.; Mariathasan, S.; Flygare, J. A.; Pillow, T. H. Targeted Drug Delivery through the Traceless Release of Tertiary and Heteroaryl Amines from Antibody–Drug Conjugates. *Nat. Chem.* **2016**, *8* (12), 1112–1119. <https://doi.org/10.1038/nchem.2635>.
- (19) Schmid, K. M.; Jensen, L.; Phillips, S. T. A Self-Immolative Spacer That Enables Tunable Controlled Release of Phenols under Neutral Conditions. *J. Org. Chem.* **2012**, *77* (9), 4363–4374. <https://doi.org/10.1021/jo300400q>.
- (20) Sun, G.; Fang, H.; Cheng, C.; Lu, P.; Zhang, K.; Walker, A. V.; Taylor, J.-S. A.; Wooley, K. L. Benzaldehyde-Functionalized Polymer Vesicles. *ACS Nano* **2009**, *3* (3), 673–681. <https://doi.org/10.1021/nn8007977>.

- (21) Liu, Y.; Lee, J.; Mansfield, K. M.; Ko, J. H.; Sallam, S.; Wesdemiotis, C.; Maynard, H. D. Trehalose Glycopolymer Enhances Both Solution Stability and Pharmacokinetics of a Therapeutic Protein. *Bioconjug. Chem.* **2017**, *28* (3), 836–845. <https://doi.org/10.1021/acs.bioconjchem.6b00659>.
- (22) Kinstler, O. B.; Brems, D. N.; Lauren, S. L.; Paige, A. G.; Hamburger, J. B.; Treuheit, M. J. Characterization and Stability of N-Terminally PEGylated RhG-CSF. *Pharm. Res.* **1996**, *13* (7), 996–1002. <https://doi.org/10.1023/A:1016042220817>.
- (23) Baker, S. L.; Murata, H.; Kaupbayeva, B.; Tasbolat, A.; Matyjaszewski, K.; Russell, A. J. Charge-Preserving Atom Transfer Radical Polymerization Initiator Rescues the Lost Function of Negatively Charged Protein–Polymer Conjugates. *Biomacromolecules* **2019**, *20* (6), 2392–2405. <https://doi.org/10.1021/acs.biomac.9b00379>.
- (24) Samanta, D.; McRae, S.; Cooper, B.; Hu, Y.; Emrick, T.; Pratt, J.; Charles, S. A. End-Functionalized Phosphorylcholine Methacrylates and Their Use in Protein Conjugation. *Biomacromolecules* **2008**, *9* (10), 2891–2897. <https://doi.org/10.1021/bm8006715>.
- (25) Alouane, A.; Labruère, R.; Le Saux, T.; Schmidt, F.; Jullien, L. Self-Immolative Spacers: Kinetic Aspects, Structure–Property Relationships, and Applications. *Angew. Chem. Int. Ed.* **2015**, *54* (26), 7492–7509. <https://doi.org/10.1002/anie.201500088>.
- (26) Muranaka, K.; Ichikawa, S.; Matsuda, A. Development of the Carboxamide Protecting Group, 4-(Tert-Butyldimethylsiloxy)-2-Methoxybenzyl. *J. Org. Chem.* **2011**, *76* (22), 9278–9293. <https://doi.org/10.1021/jo201495w>.
- (27) Weinert, E. E.; Dondi, R.; Colloredo-Melz, S.; Frankenfield, K. N.; Mitchell, C. H.; Freccero, M.; Rokita, S. E. Substituents on Quinone Methides Strongly Modulate

- Formation and Stability of Their Nucleophilic Adducts. *J. Am. Chem. Soc.* **2006**, *128* (36), 11940–11947. <https://doi.org/10.1021/ja062948k>.
- (28) Hansch, Corwin.; Leo, A.; Taft, R. W. A Survey of Hammett Substituent Constants and Resonance and Field Parameters. *Chem. Rev.* **1991**, *91* (2), 165–195. <https://doi.org/10.1021/cr00002a004>.
- (29) Erez, R.; Shabat, D. The Azaquinone-Methide Elimination: Comparison Study of 1,6- and 1,4-Eliminations under Physiological Conditions. *Org. Biomol. Chem.* **2008**, *6* (15), 2669–2672. <https://doi.org/10.1039/B808198K>.
- (30) Baddar, F. G.; Wahhab, S. A.; Awad, B. M.; Guindy, N. M.; Wahba, M. Phenolic Esters. Part 1. Rate of Hydrolysis of Phenyl, p-Tolyli, and p-Chlorophenyl Hydrogen Succinate. 7.
- (31) Zou, J.; Zhang, F.; Zhang, S.; Pollack, S. F.; Elsabahy, M.; Fan, J.; Wooley, K. L. Poly(Ethylene Oxide)-Block-Polyphosphoester-Graft-Paclitaxel Conjugates with Acid-Labile Linkages as a PH-Sensitive and Functional Nanoscopic Platform for Paclitaxel Delivery. *Adv. Healthc. Mater.* **2014**, *3* (3), 441–448. <https://doi.org/10.1002/adhm.201300235>.
- (32) Masuda, T.; Ide, N.; Kitabatake, N. Structure–Sweetness Relationship in Egg White Lysozyme: Role of Lysine and Arginine Residues on the Elicitation of Lysozyme Sweetness. *Chem. Senses* **2005**, *30* (8), 667–681. <https://doi.org/10.1093/chemse/bji060>.
- (33) Gregoritza, M.; Messmann, V.; M. Goepferich, A.; P. Brandl, F. Design of Hydrogels for Delayed Antibody Release Utilizing Hydrophobic Association and Diels–Alder Chemistry in Tandem. *J. Mater. Chem. B* **2016**, *4* (19), 3398–3408. <https://doi.org/10.1039/C6TB00223D>.

- (34) Stayton, P. S.; Shimoboji, T.; Long, C.; Chilkoti, A.; Ghen, G.; Harris, J. M.; Hoffman, A. S. Control of Protein–Ligand Recognition Using a Stimuli-Responsive Polymer. *Nature* **1995**, *378* (6556), 472–474. <https://doi.org/10.1038/378472a0>.
- (35) Fuhrmann, G.; Grotzky, A.; Lukić, R.; Matoori, S.; Luciani, P.; Yu, H.; Zhang, B.; Walde, P.; Schlüter, A. D.; Gauthier, M. A.; Leroux, J.-C. Sustained Gastrointestinal Activity of Dendronized Polymer–Enzyme Conjugates. *Nat. Chem.* **2013**, *5* (7), 582–589. <https://doi.org/10.1038/nchem.1675>.
- (36) Seidi, F.; Jenjob, R.; Crespy, D. Designing Smart Polymer Conjugates for Controlled Release of Payloads. *Chem. Rev.* **2018**, *118* (7), 3965–4036. <https://doi.org/10.1021/acs.chemrev.8b00006>.

4.6 Appendix C

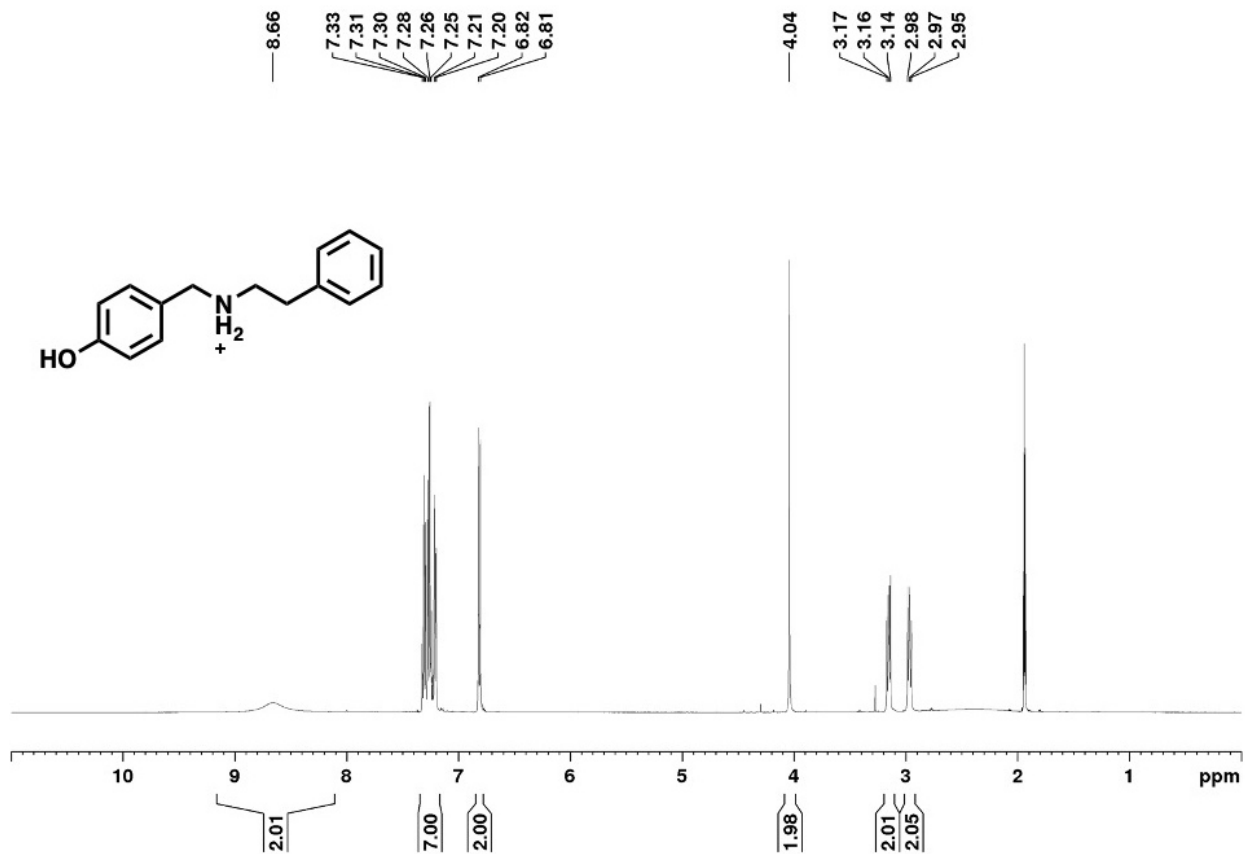


Figure 4.12. ^1H NMR Spectrum of Compound 1 in CD_3CN .

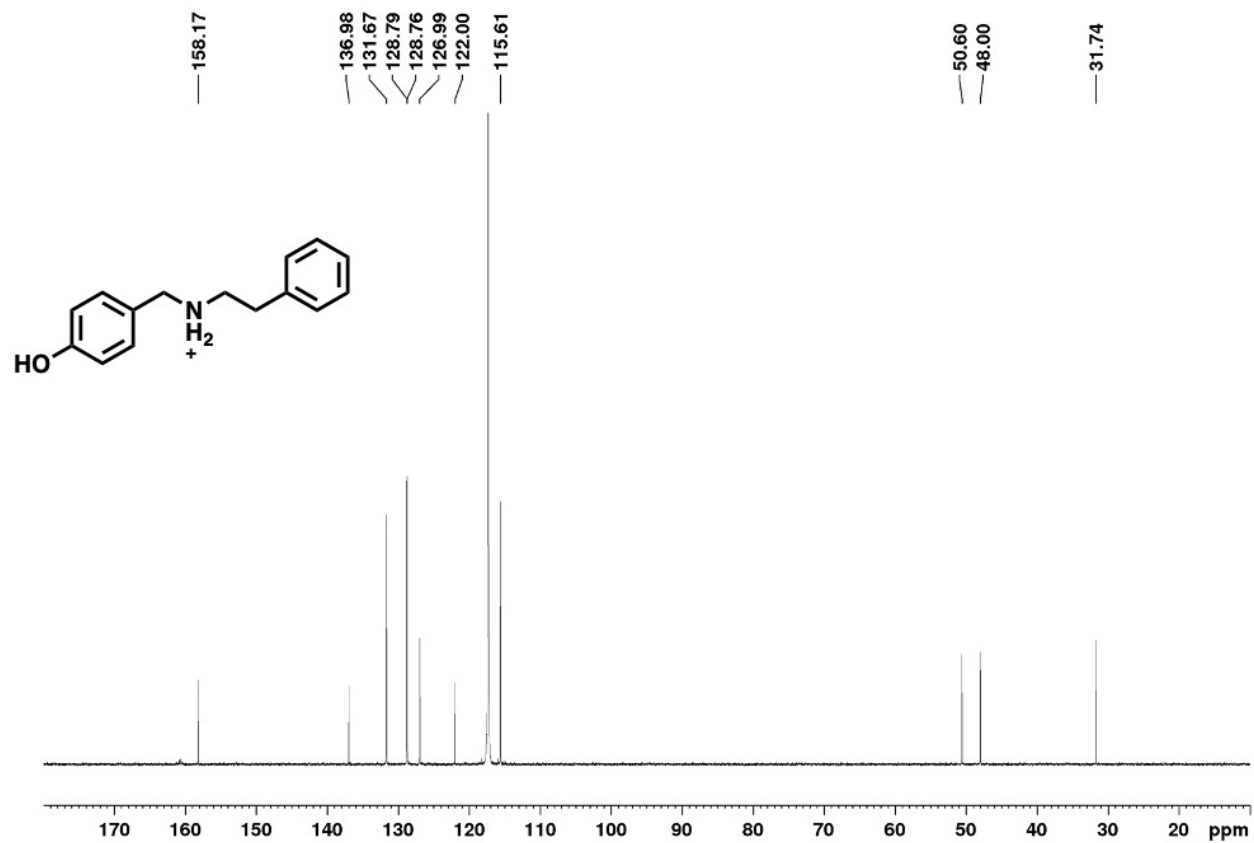


Figure 4.13. ^{13}C NMR Spectrum of Compound 1 in CD_3CN .

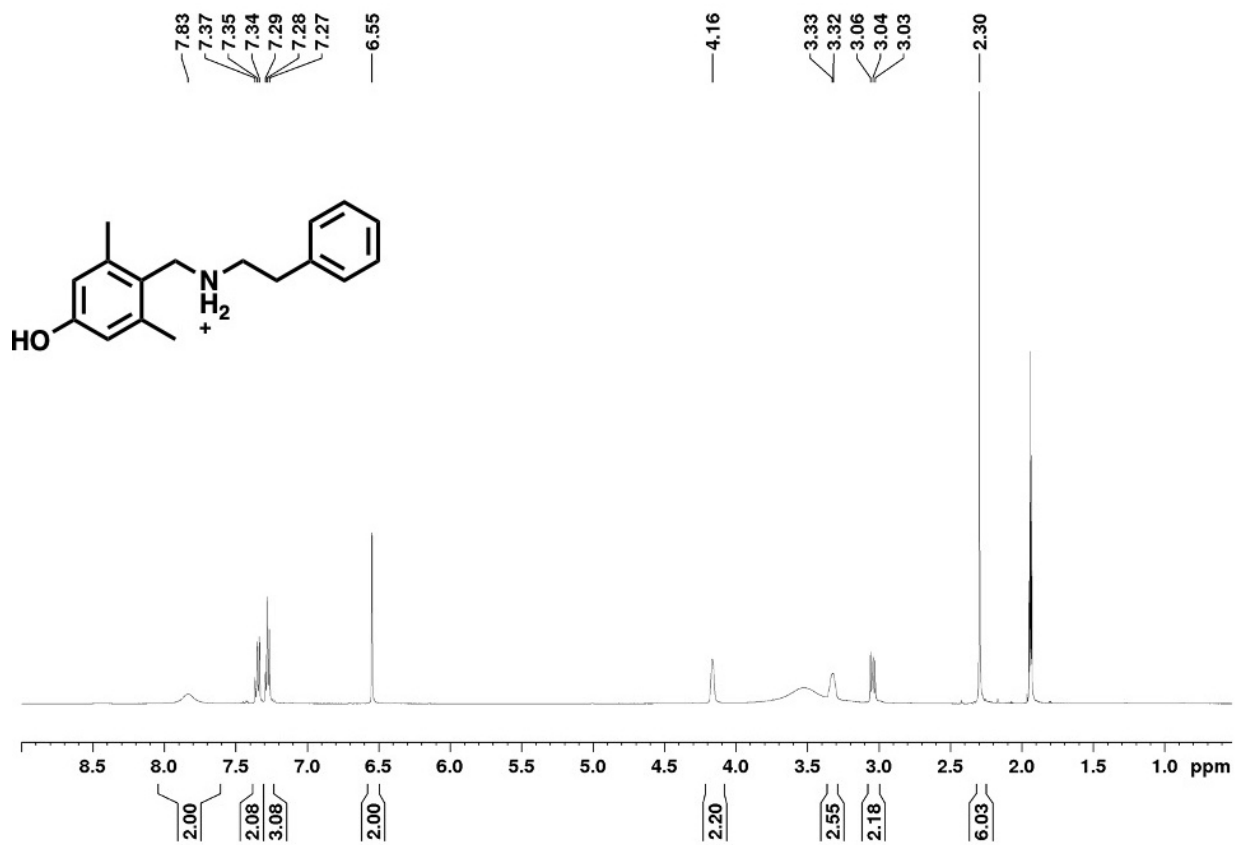


Figure 4.14. ¹H NMR Spectrum of Compound 2 in CD₃CN.

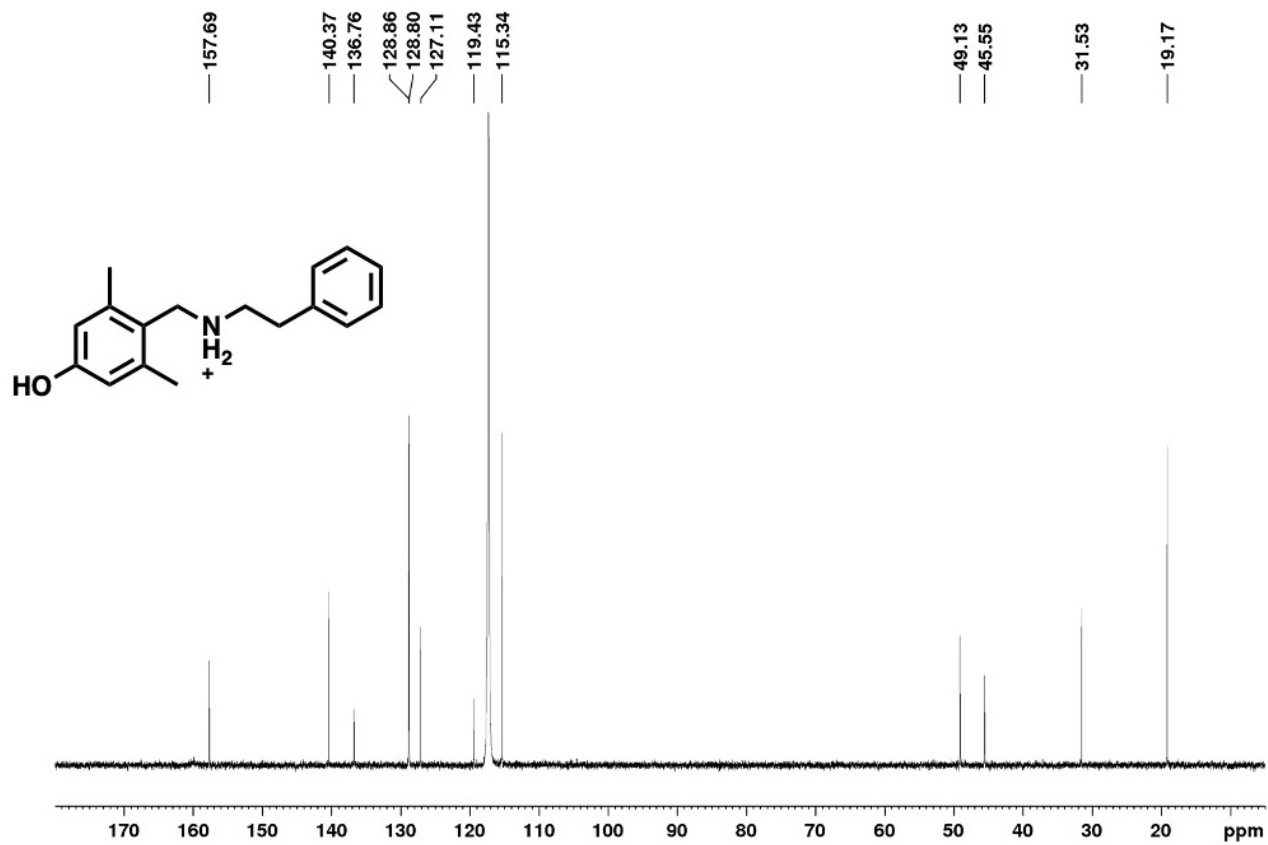


Figure 4.15. ^{13}C NMR Spectrum of Compound 2 in CD_3CN .

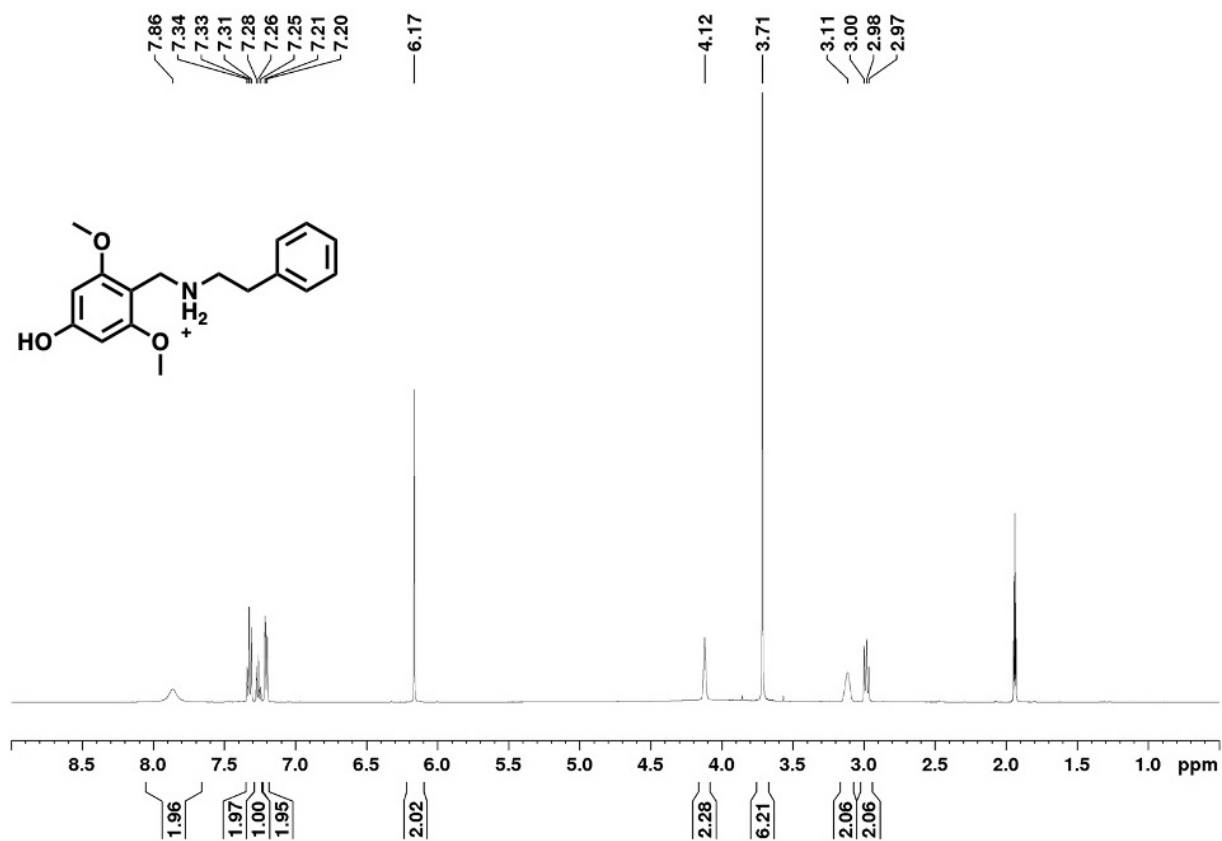


Figure 4.16. ¹H NMR Spectrum of Compound 3a in CD₃CN.

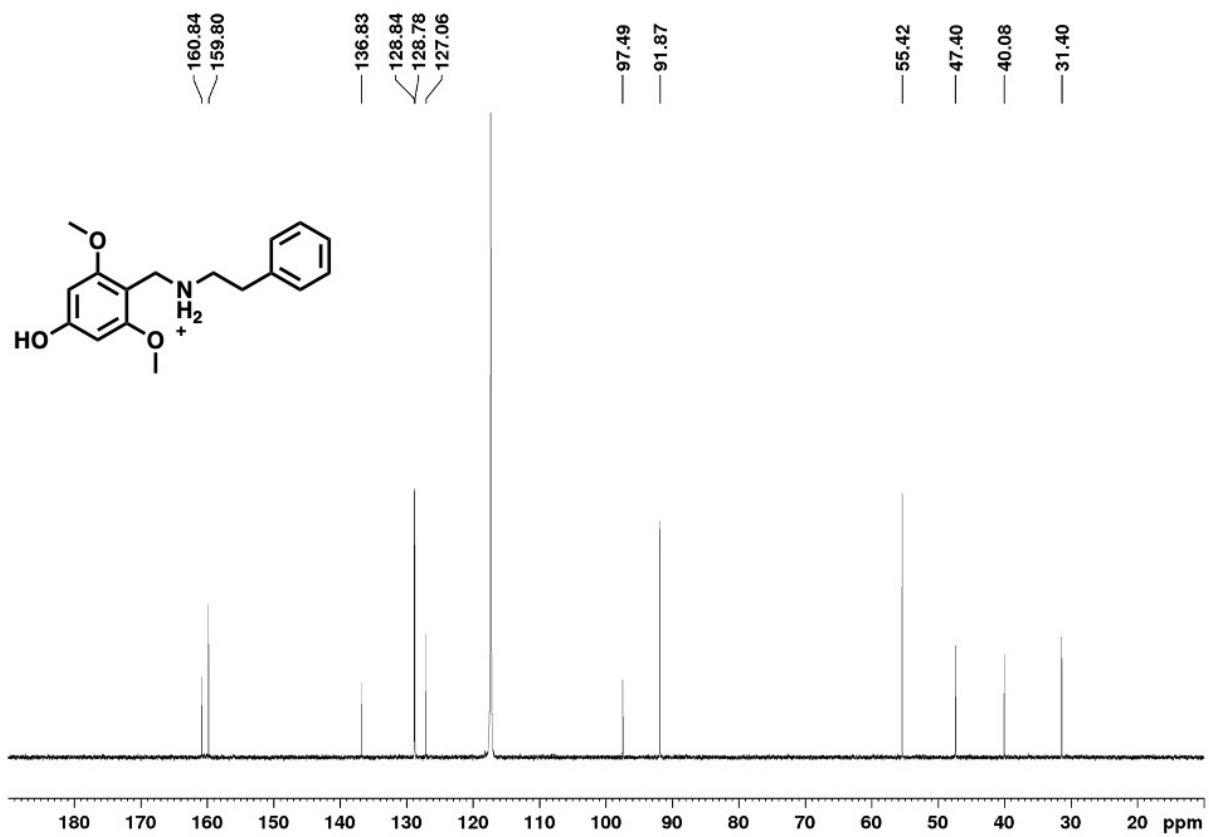


Figure 4.17. ¹³C NMR Spectrum of Compound 3a in CD₃CN.

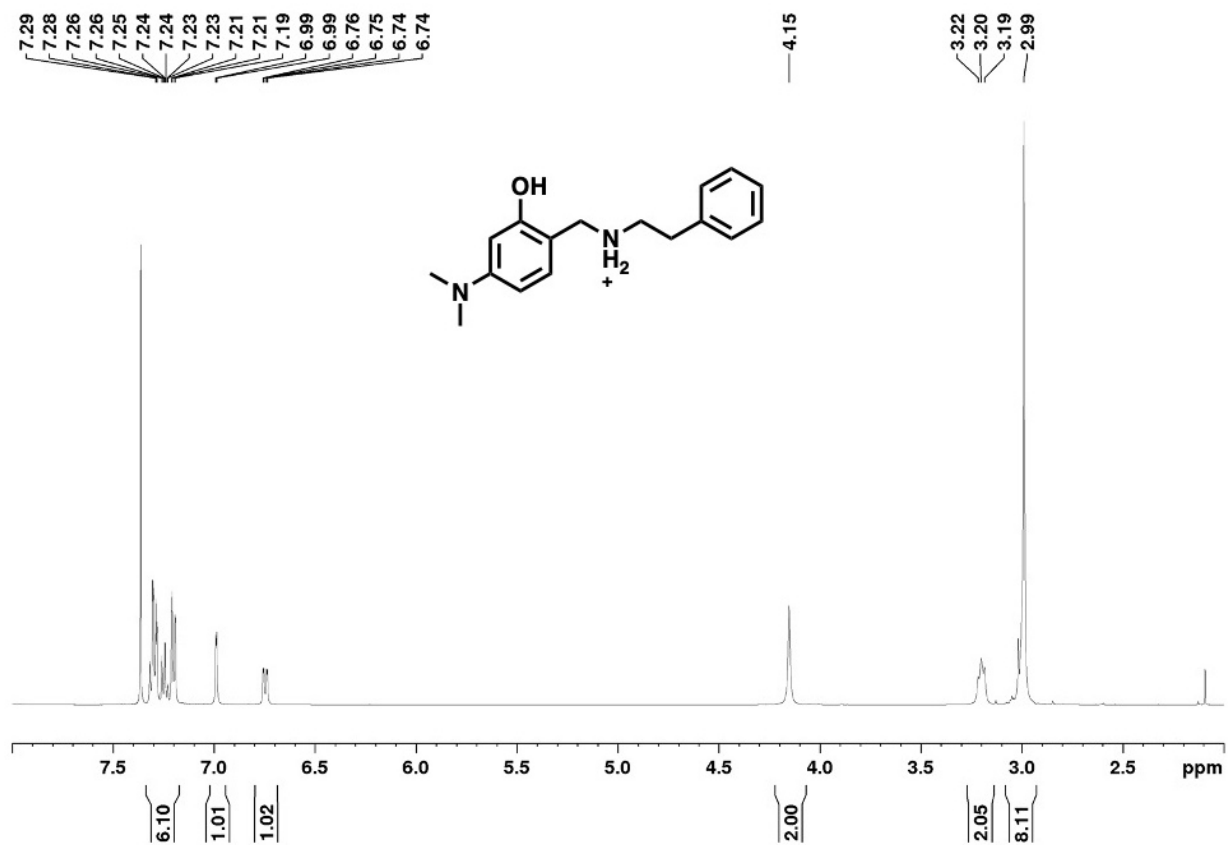


Figure 4.18. ^1H NMR Spectrum of Compound 4a in CD_3CN .

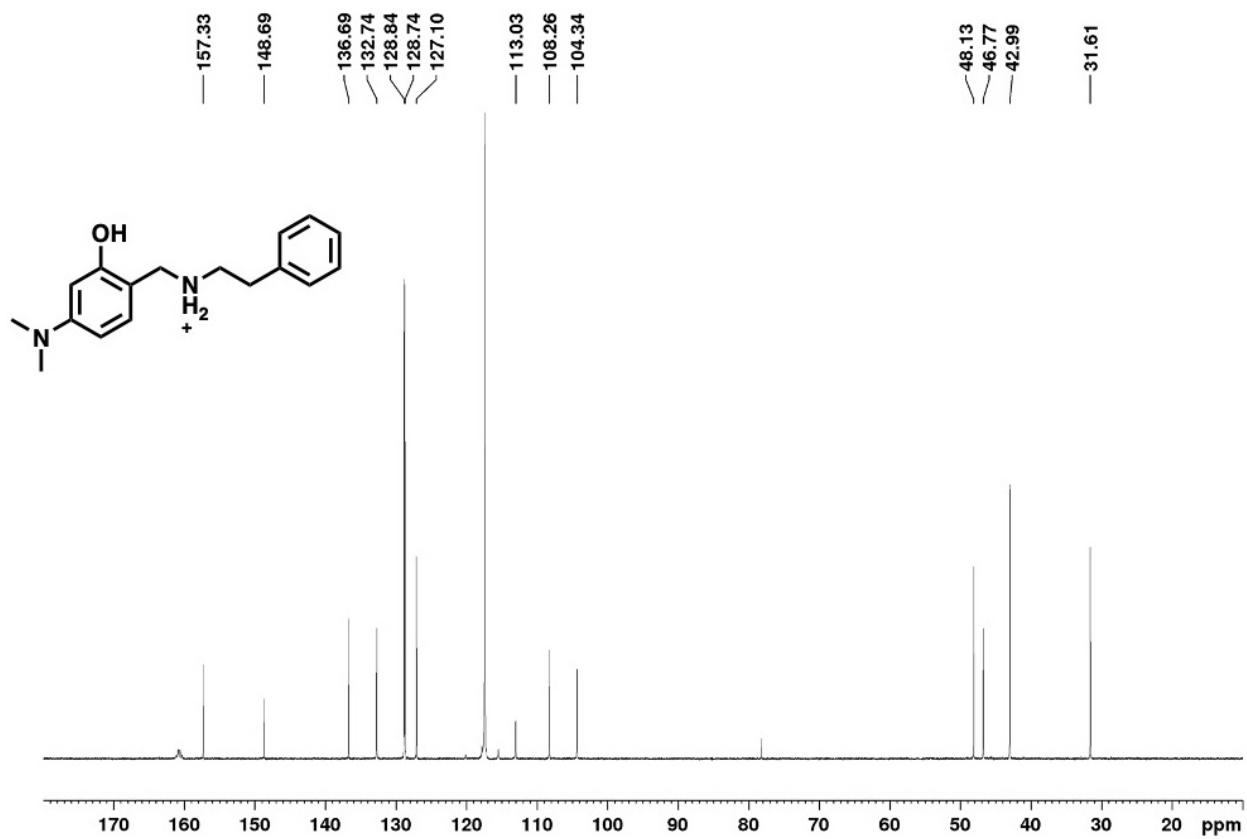


Figure 4.19. ^{13}C NMR Spectrum of Compound 4a in CD_3CN .

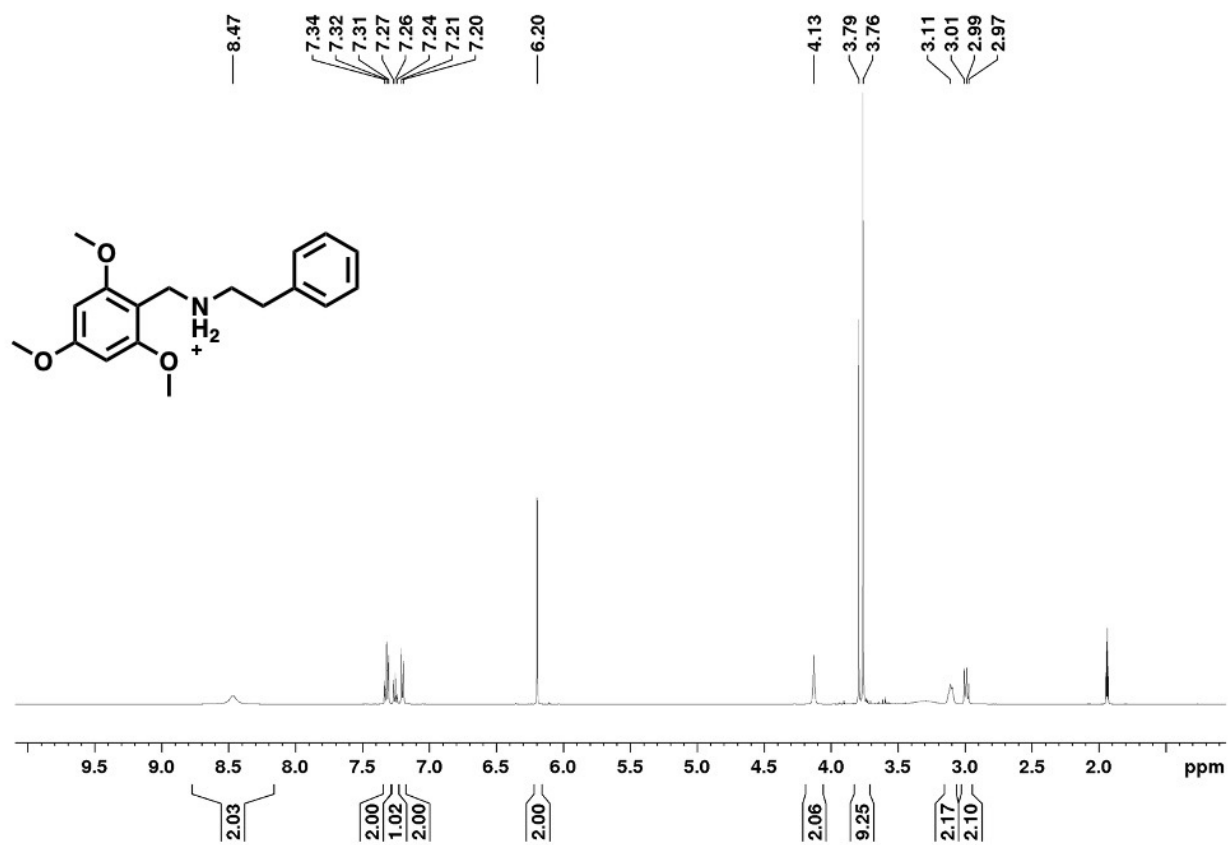


Figure 4.20. ¹H NMR Spectrum of Compound 3b in CD₃CN.

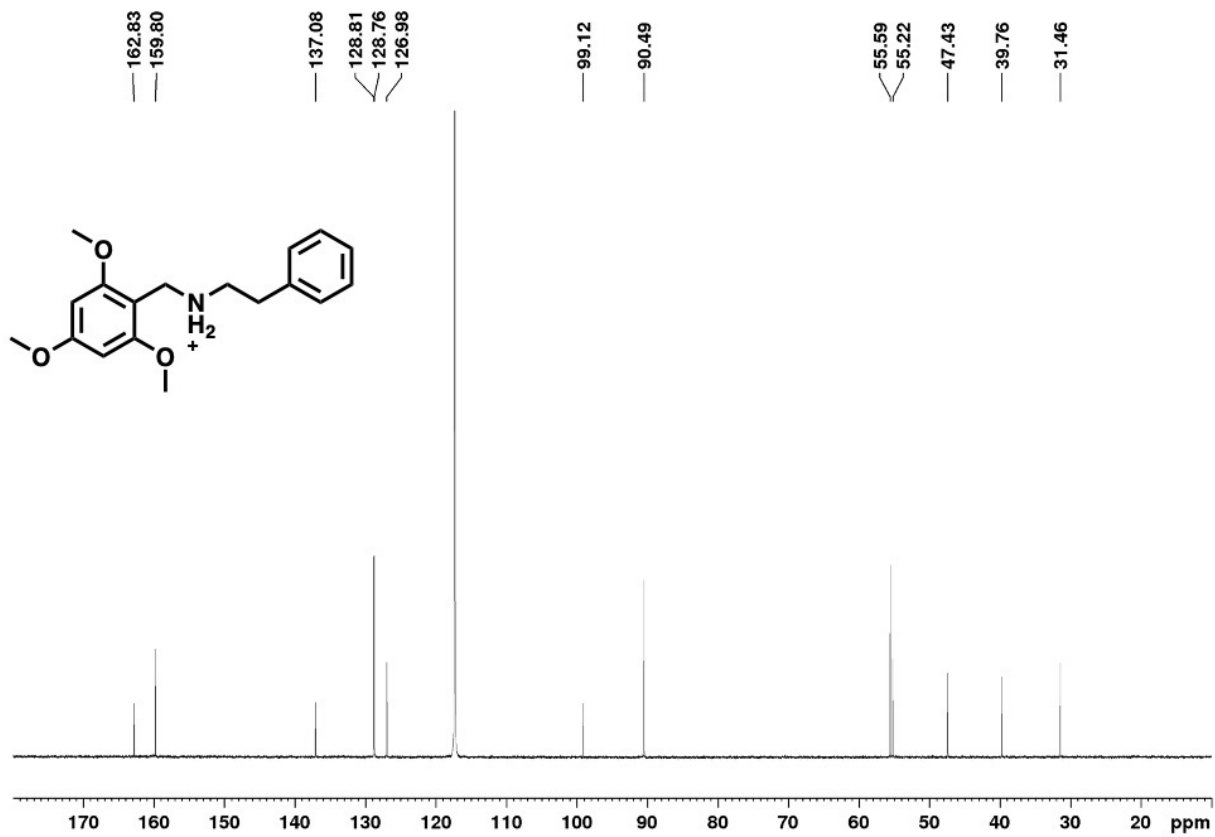


Figure 4.21. ¹³C NMR Spectrum of Compound 3b in CD₃CN.

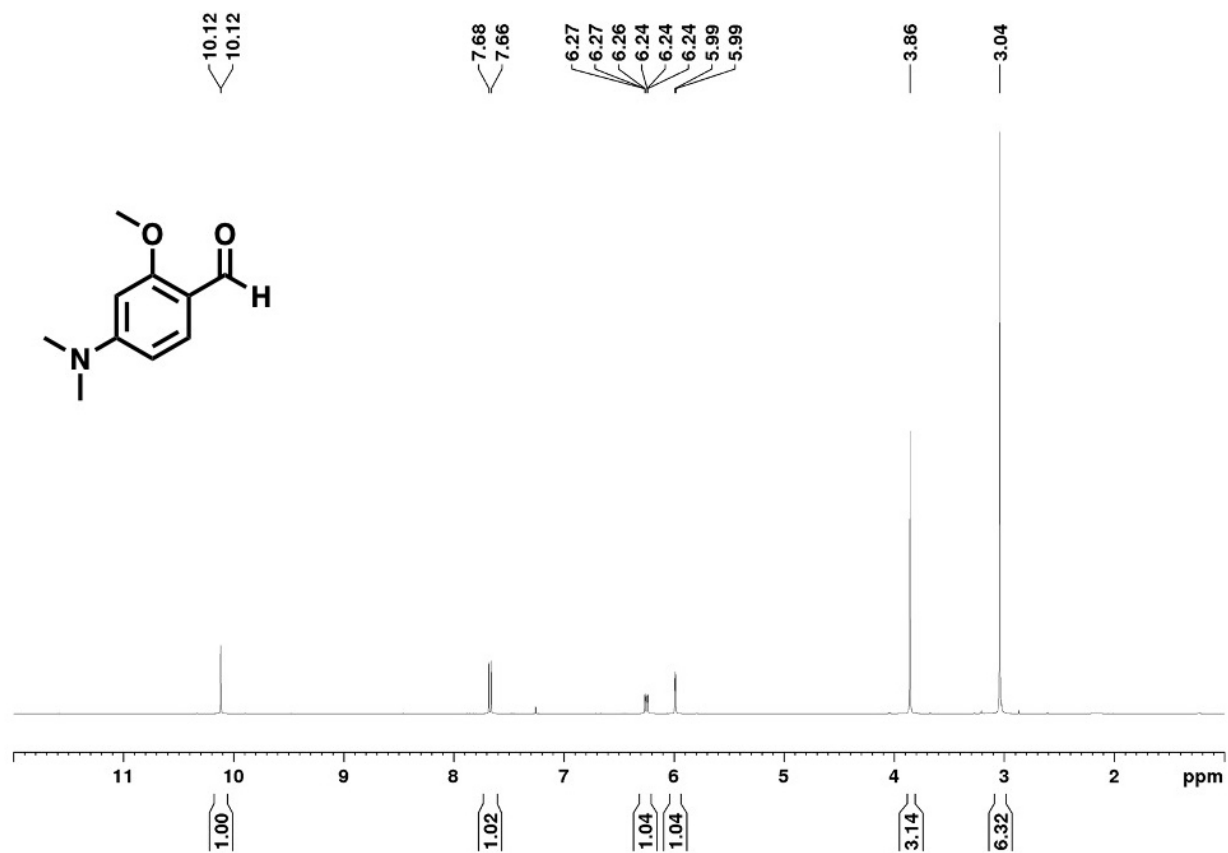


Figure 4.22. ^1H NMR Spectrum of Compound 9 in CDCl_3 .

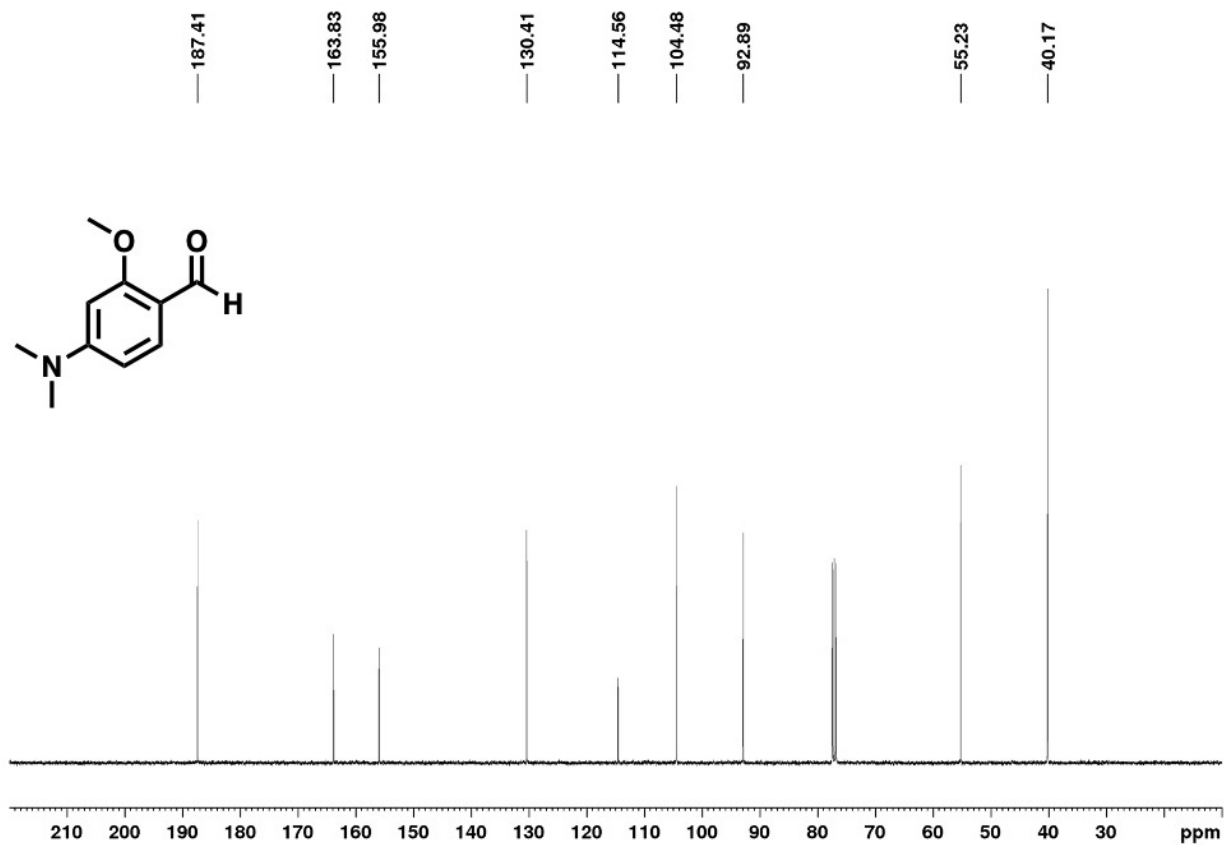


Figure 4.23. ^{13}C NMR Spectrum of Compound 9 in CDCl_3 .

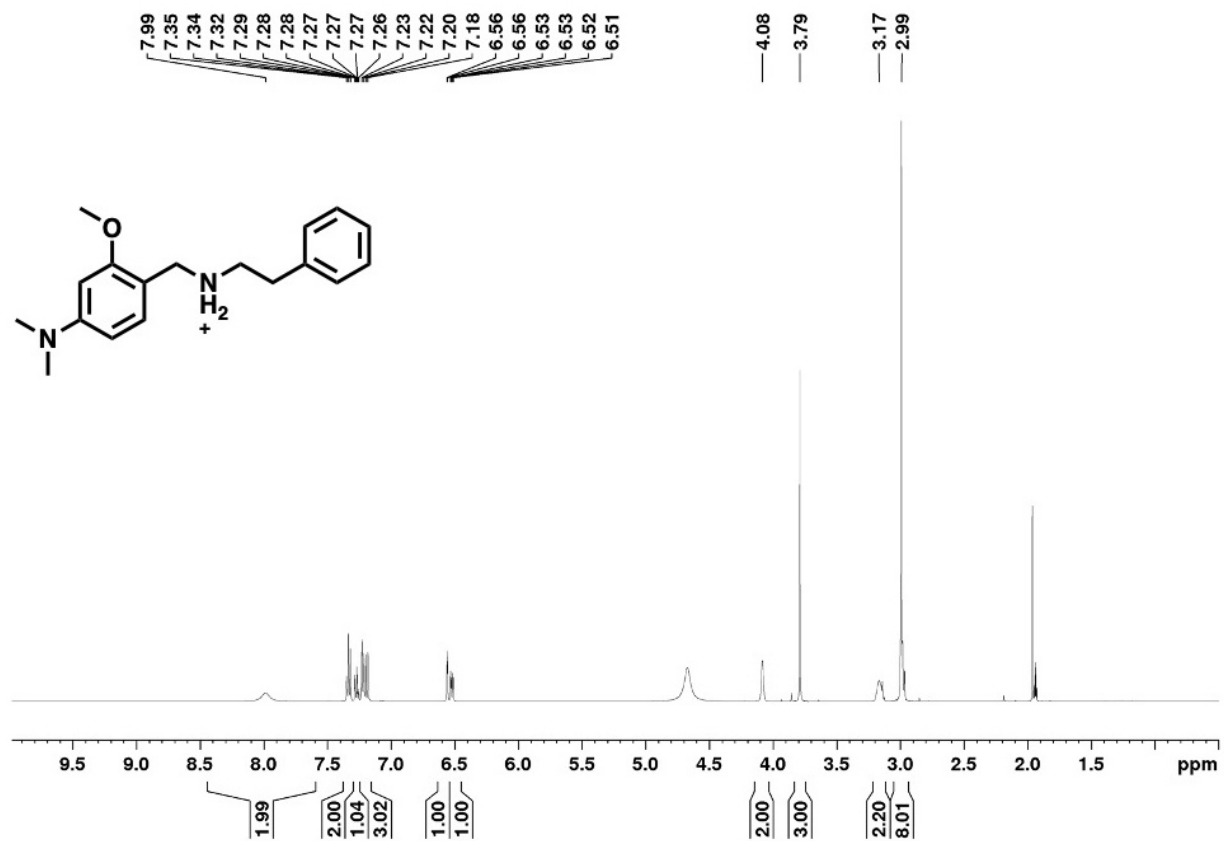


Figure 4.24. ¹H NMR Spectrum of Compound 4b in CD₃CN.

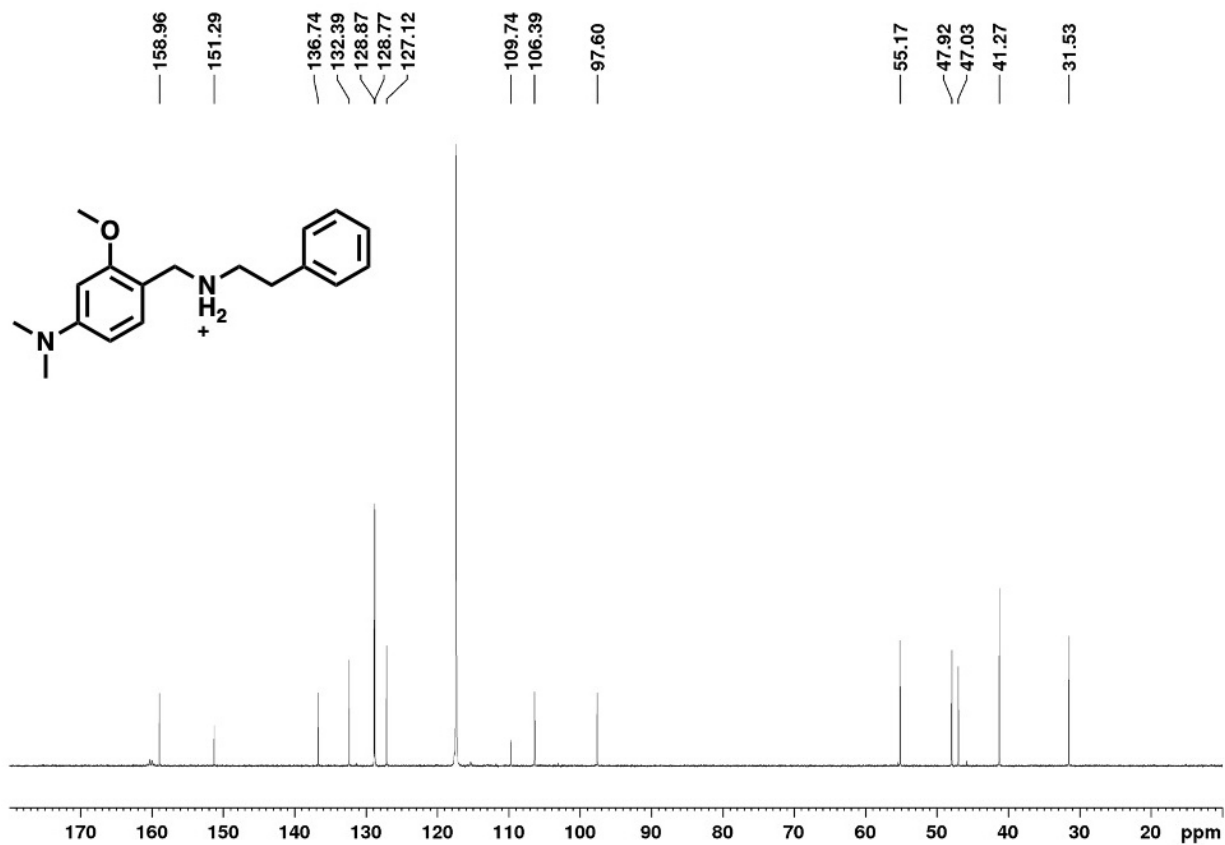


Figure 4.25. ^{13}C NMR Spectrum of Compound 4b in CD_3CN .

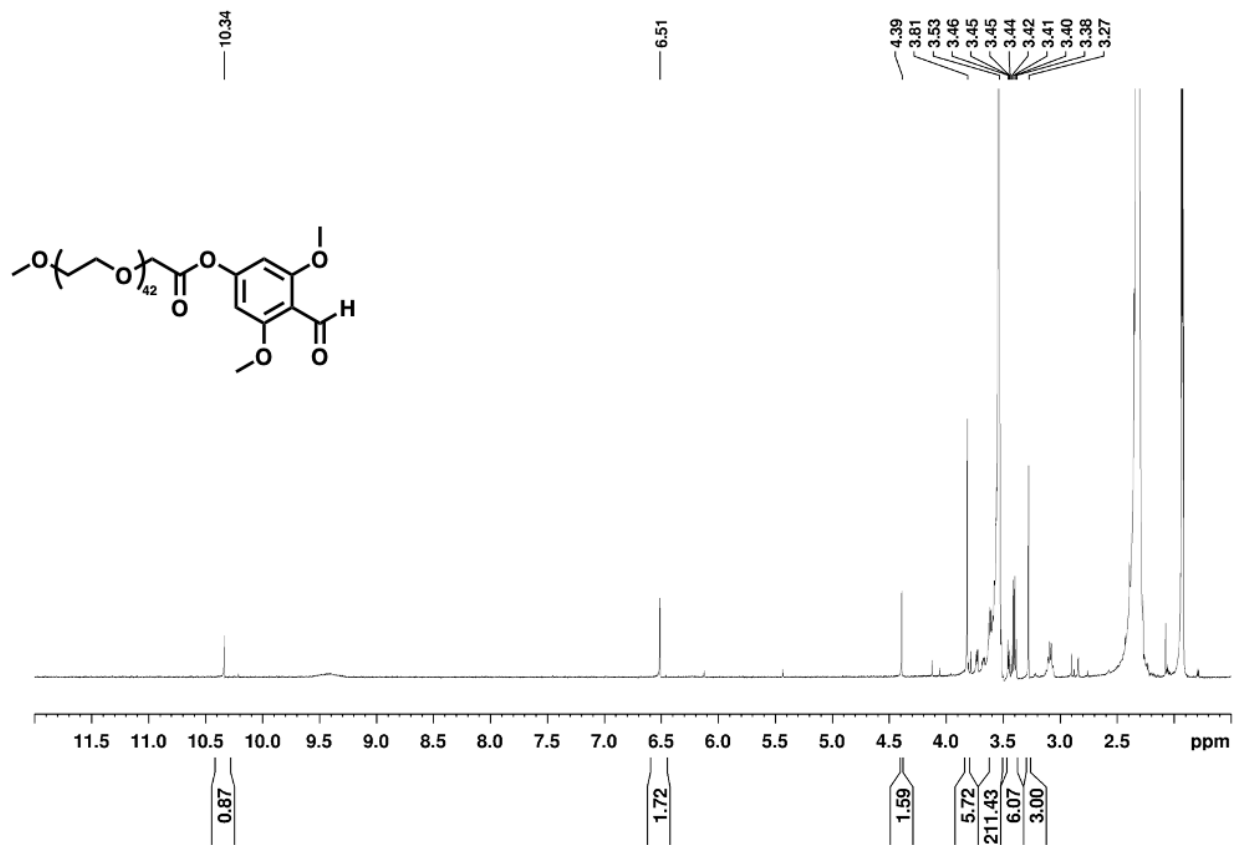


Figure 4.27. ¹H NMR Spectrum of 2 kDa mPEG-(2,6-dimethoxybenzaldehyde) in CD₃CN.

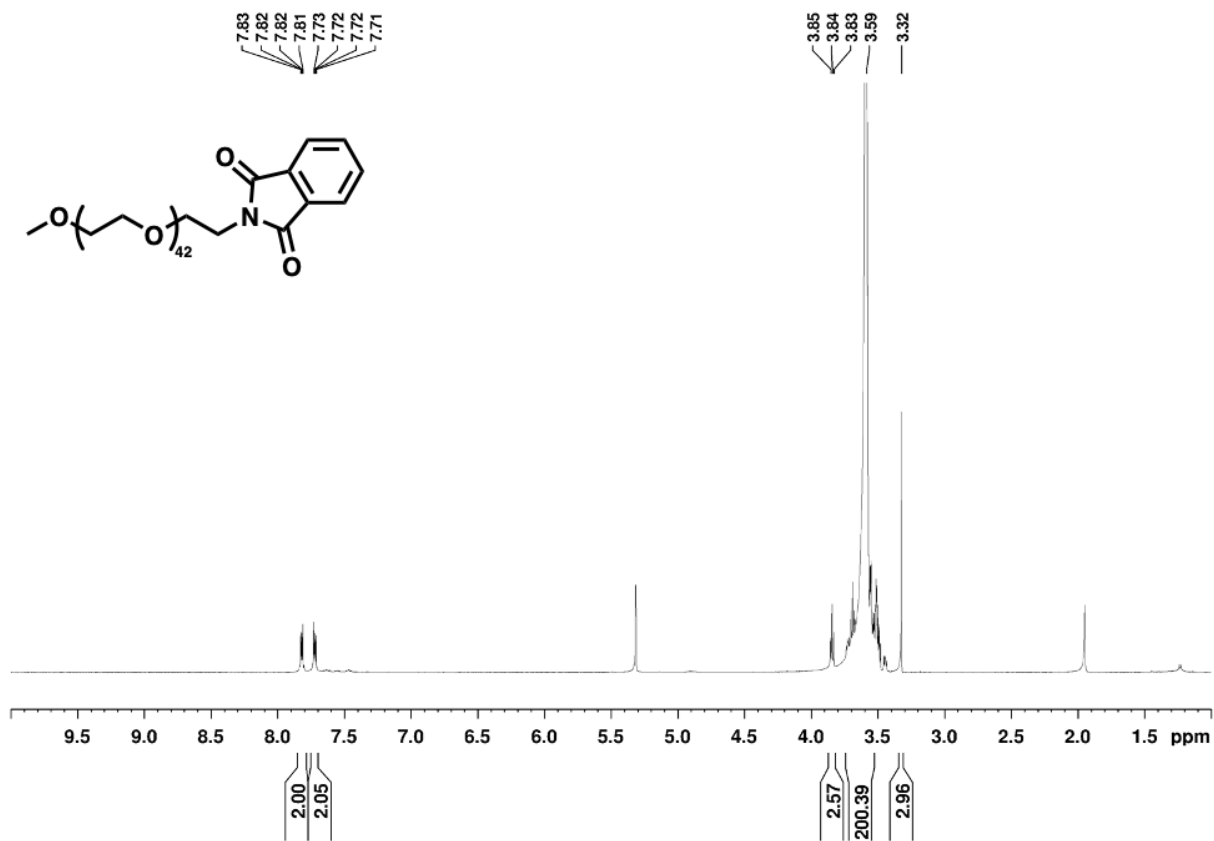


Figure 4.28. ¹H NMR Spectrum of 2 kDa mPEG-phthalimide in CD₃CN.

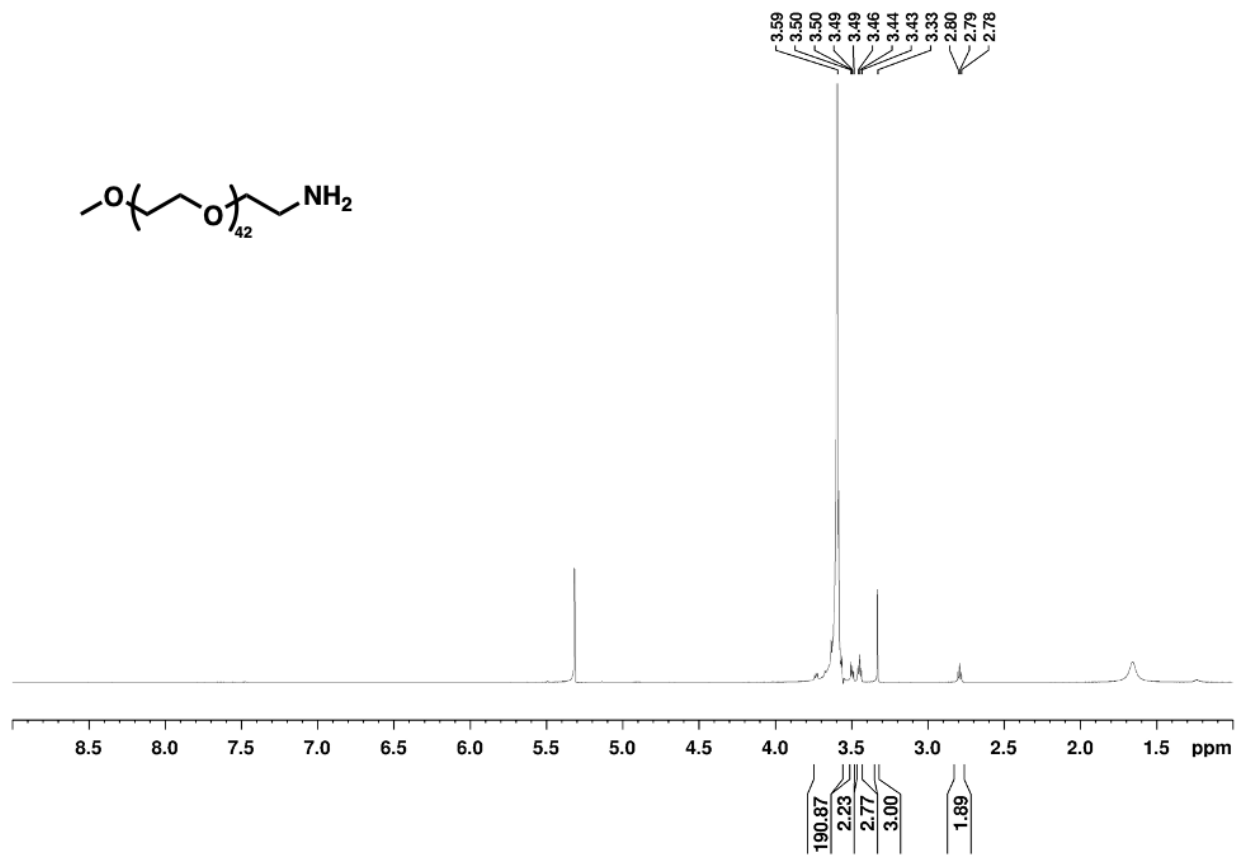


Figure 4.29. ¹H NMR Spectrum of 2 kDa mPEG-NH₂ in CD₂Cl₂.

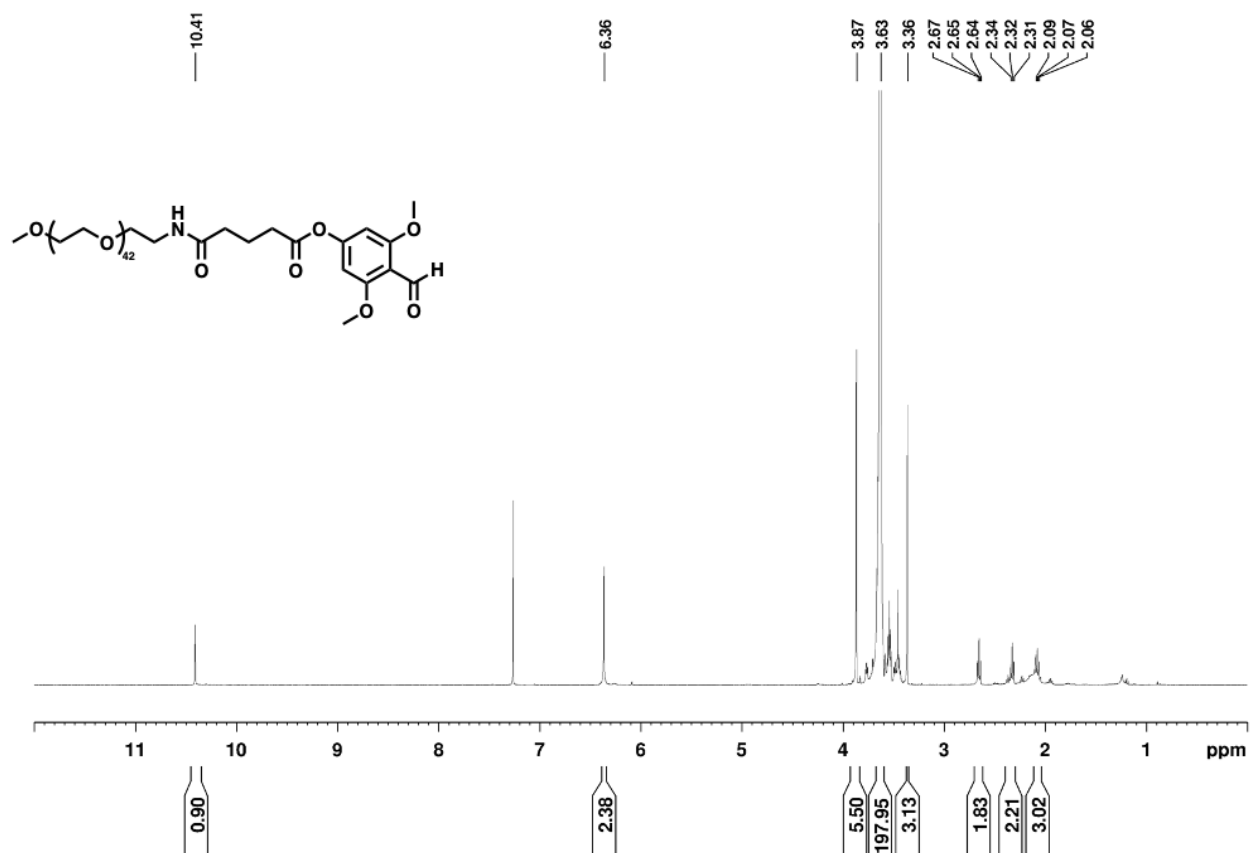


Figure 4.31. ¹H NMR Spectrum of 2 kDa mPEG-glutaric-(2,6-dimethoxybenzaldehyde) in CDCl₃.

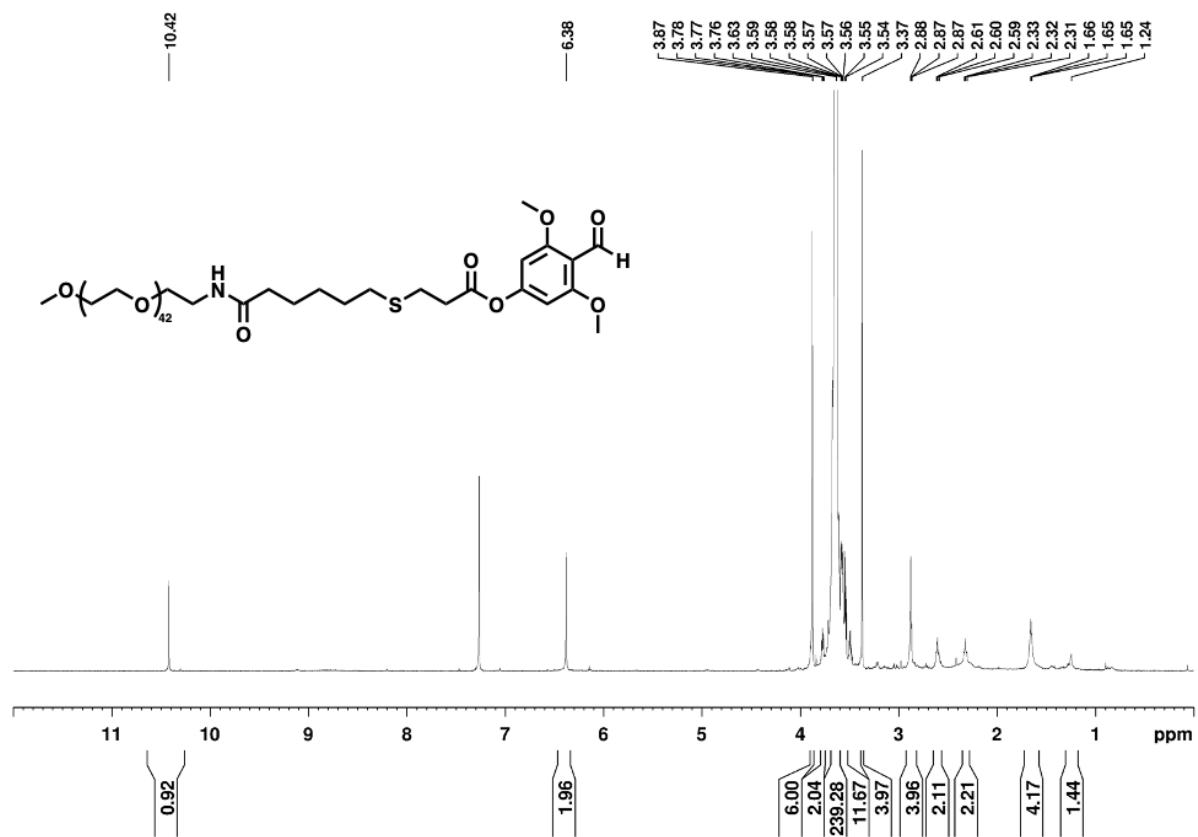


Figure 4.34. ¹H NMR Spectrum of 2 kDa mPEG- β -thioester-(2,6-dimethoxybenzaldehyde) in CDCl₃.

Chapter 5

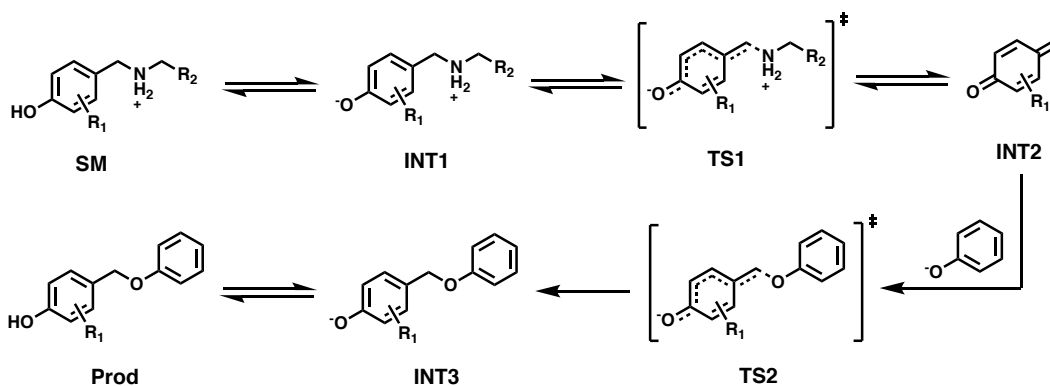
Development of Second Generation

Benzylamine Linkers for Traceless Protein

Conjugation

5.1 Introduction

The benzylamine linkers discussed in Chapter 4 proved to be highly effective for the traceless release of proteins from protein-polymer conjugates; however, there were two observations during that study which caused us to further exam the release. The first of which, was illuminated through density functional theory (DFT) calculations (performed by Joseph Treacy) on the release mechanism, which identified that the nucleophilic attack of the quinone methide intermediate (TS2) was the primary activation barrier rather than the loss of the amine (TS1) as initially hypothesized. Additionally, the initial phenol deprotonation and subsequent amine release to form INT2 appeared to be reversible (Scheme 5.1).



Scheme 5.1. Mechanism of release for benzylamine linkers with quenching of the quinone methide by a phenoxide.

The second observation was that the major products observed after the phenethylamine release studies were cyclic dimers and trimers, indicating that the quinone methide is not preferentially quenched with water but rather with the phenoxide. These two observations suggest drawbacks for the traceless benzylamine linkers if used in a complex biological setting. The reversibility of INT2 and the thermodynamically favored quenching of INT2 with a phenol, both ensure the formation of inadvertent byproducts which are nonideal for a controlled release system.

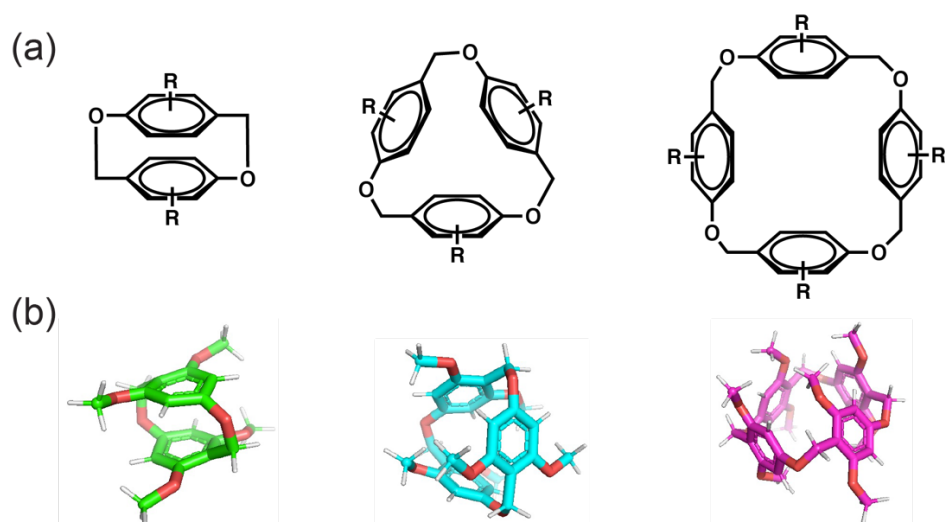
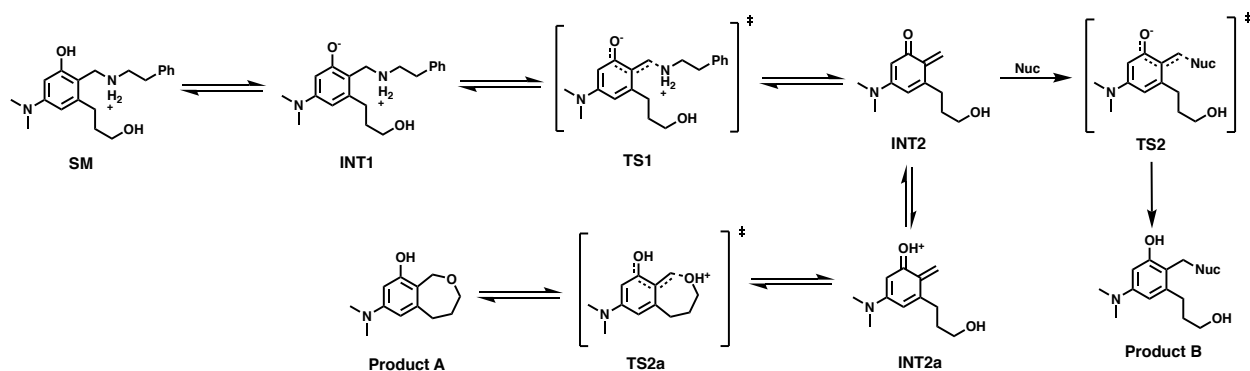


Figure 5.1. (a) Observed cyclic dimeric, trimeric, and tetrameric products from the phenethylamine kinetics release assay (b) structures calculated at the B3LYP-D3/6-31G(d) level of theory.

In order to prevent the reversibility of TS1 observed across the benzylamine linkers, we proposed that the addition of an intramolecular trapping agent would minimize the lifetime of INT2 and therefore limit any potential cross-reactivity *in vivo*. This intramolecular trapping arm could be augmented to increase the nucleophilicity of the pendant group to ensure quenching of the quinone methide and therefore limit any reversibility concerns. We hypothesized that the placement of an ethyl alcohol *ortho* to the benzylamine would quench the quinone methide intermediate through an intramolecular hydration to produce a 2-benzoxepine bicycle (Scheme 5.2 Product A).



Scheme 5.2. Mechanism of release for benzylamine linkers containing a pendant arm for intramolecularly quenching the quinone methide intermediate.

Prior to preparing this linker, DFT calculations were carried out (by Joseph Treacy) on the updated linker design to identify potential leads for synthesis. This exploration began with a pendant ethanol unit attacking the protonated quinone methide (TS2a), which was used as a model system for the quinone methide hydrogen bonding with water. The ΔG^\ddagger of the transition state was calculated to be 15.2 kcal/mol, but examination of the transition state geometry showed that this six-membered transition state was highly strained due to the coplanarity among four of the six atoms involved in the transition state.

To quantify this strain, intramolecular distortion energy calculations were developed, which showed a distortion energy of 12.0 kcal/mol for the ethanol arm. To relieve strain in the transition state, an additional methylene unit was added to form the propanol pendant arm, which showed a decrease in ΔG^\ddagger by 3.0 kcal/mol. This difference in ΔG^\ddagger between the propanol and ethanol arms can be attributed to the difference in distortion energy (DE) of the two linkers, 6.3 kcal/mol and 12.0 kcal/mol, respectively. With the distortion partially overcome, we sought to enhance the nucleophilicity by screening the propanethiol arm as well as the ethyl methyl ether and propyl methyl ether arms. The addition of the pendant methyl ether groups lowered the ΔG^\ddagger relative to the alcohol counterparts, with a negligible impact on the distortion energies. Interestingly, the

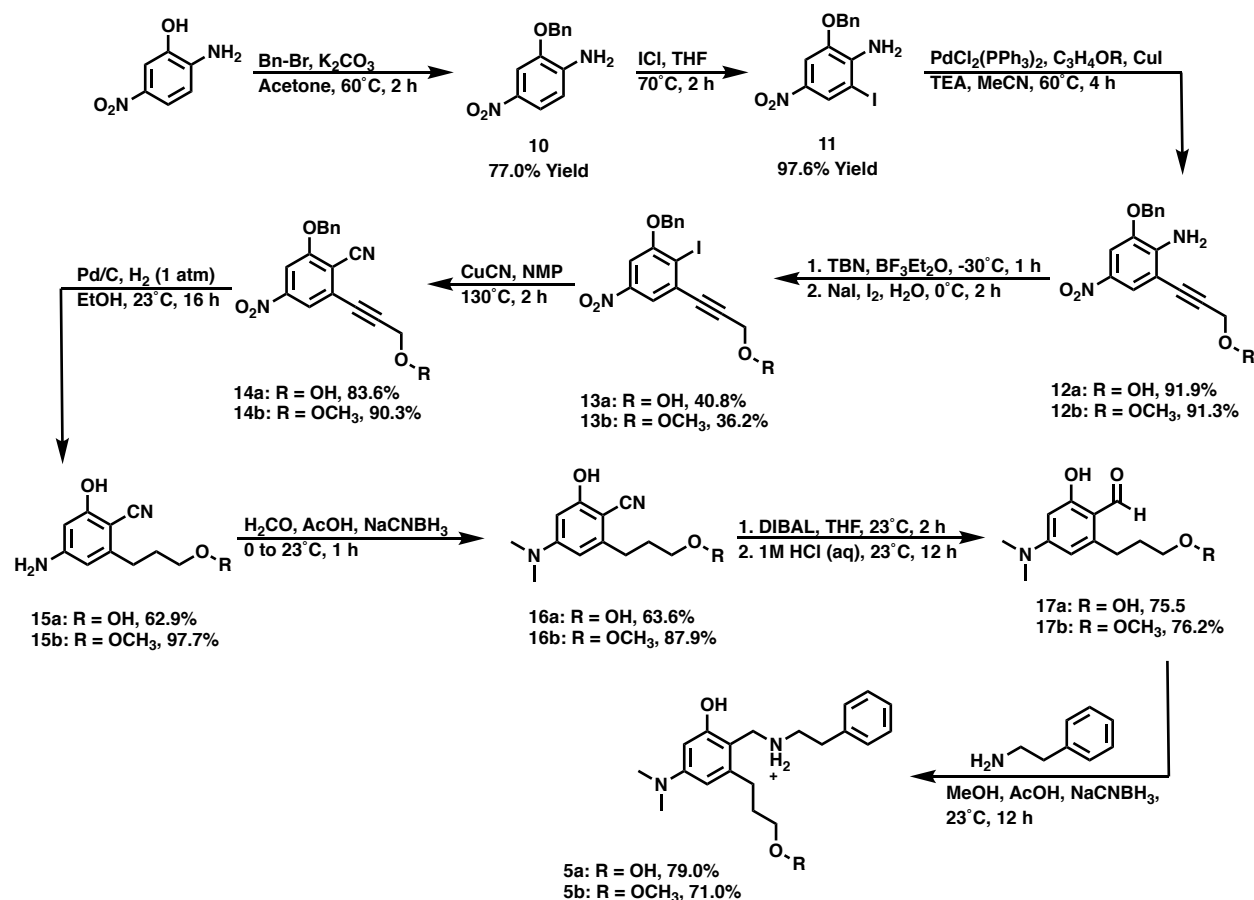
propanethiol arm removed most of the distortion energy due to the increased C-S bond length as compared to the C-O bond. This, in addition to the increased nucleophilicity of the thiol, further lowered the ΔG^\ddagger to 9.6 kcal/mol. This computational work carried out by Joseph Treacy elucidated a path towards mitigating the reversibility problem of the traceless benzylamine linkers.

5.2 Results and Discussion

5.2.1 Preparation of Second Generation Benzylamine Linkers with Release Kinetics

With the DFT calculations showing a significantly lower second transition state, linkers **5a**, **5b**, and **5c** were synthesized (Scheme 5.3). The propanol and propyl methyl ether arms were chosen instead of the propanethiol due to a reduced propensity for disulfide formation, which would lead to competing side reactions in a biological setting. Linkers **5a**, **5b**, and **5c** were prepared using 2-amino-5-nitrophenol as a starting material. Initially, the phenol was selectively benzyl protected, followed by an aniline directed iodination to afford **11**. At this point, the framework for the pendant arm was installed through a Sonogashira coupling with either propargyl alcohol or propargyl methyl ether delivering **12a** and **12b** respectively. Initial attempts to directly install the nitrile group through a Sandmeyer reaction proved unsuccessful, primarily forming the Ullmann-type homodimer. Rather, the nitrile was installed stepwise, initially converting the aniline to an aryl iodide through a Sandmeyer reaction, followed by a Rosenmund-von Braun reaction to furnish **14a** and **14b**. Removal of the benzyl protecting group and simultaneous reduction of the alkyne and nitro groups was accomplished via a palladium mediated reduction. The resulting aniline was selectively dimethylated over the phenol via reductive amination, which was thereupon subjected to a diisobutylaluminum hydride (DIBAL) reduction of the aryl nitrile to afford benzaldehydes **17a** and **17b**. To prepare a linker acting as a negative control for the release studies, **17b** was

methylated using iodomethane to give **33**. Benzaldehydes **17a**, **17b**, and **33** then underwent a final reductive amination with phenethylamine to complete the synthesis of linkers **5a**, **5b**, and **5c** for release studies.



Scheme 5.3. Synthesis of benzylamine traceless linker with the incorporated intramolecular trapping arm.

The release kinetics of the resulting linkers were carried out using a 5 mM solution of the linker in a 1:1 mixture of methanol and Tris buffer (pH 7.4, 100 mM), where the appearance of phenethylamine was monitored via HPLC. Linkers **5a** and **5b** showed roughly a 4- and 5-fold rate enhancement compared to **4a** (Figure 5.2). The additional electronic donation from the alkyl substituent does not fully account for this large of a rate enhancement indicating the intramolecular trap had an additive effect. This rate enhancement between **5a** and **5b** can be attributed to the increased nucleophilicity of the methoxy group compared to the alcohol, which aligned well with

Joseph Treacy's DFT calculations. In order to confirm that the intramolecular trapping arm was in fact quenching INT2a rather than undergoing a nucleophilic substitution reaction, the release from linker **5c** was run as a negative control. If the propyl methyl ether was preferentially undergoing an intramolecular substitution, we would expect little to no change in the rate of release. The release kinetics of **5c** showed a 13-fold reduction in the rate of phenethylamine release compared to **5b**, confirming that these linkers are proceeding through a quinone methide intermediate. Additionally, the successful rate enhancement of **5a** and **5b** compared to **4a** supports our calculations and confirms that TS2 is the primary activation barrier in the release mechanism.

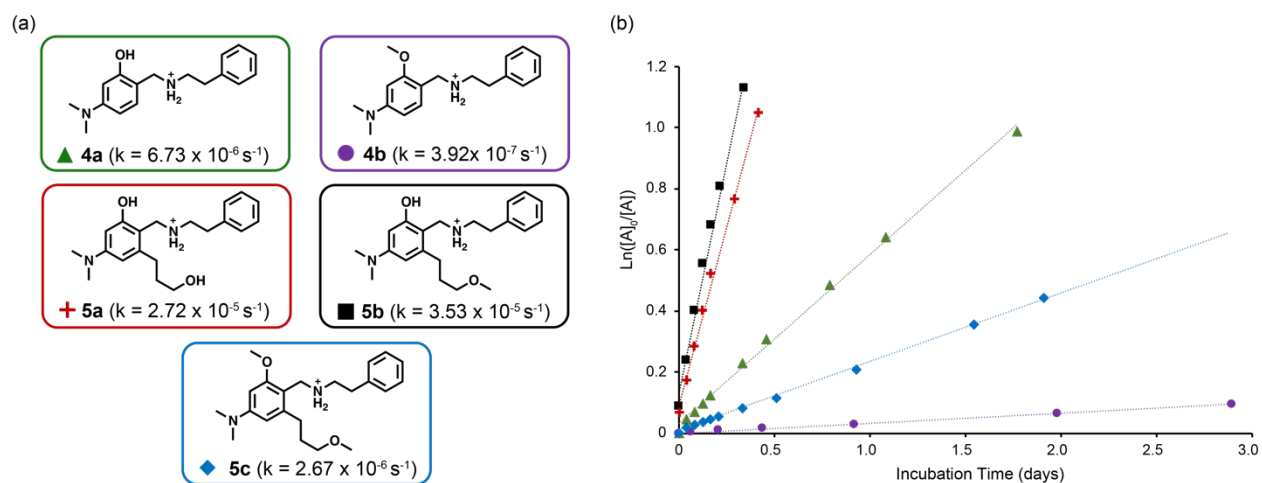


Figure 5.2. Pseudo-first order plot of phenethylamine release kinetics from the benzylamine linker model compounds ($n = 3$, error bars are smaller than markers) carried out at 5 mM of linker in a 1:1 mixture of methanol and buffer. Release kinetics of 4a and 4b were taken from Figure 4.2. as a comparison.

5.2.2 Synthesis of Benzaldehyde Precursors for Traceless Conjugation.

To demonstrate this technology's usefulness as a traceless linker for protein conjugation, **6**, **7**, and **8** were synthesized (Figure 5.3). These three linkers were designed with varying electronics to modulate the rate of release along with the incorporation of the propyl methyl ether intramolecular trapping arm to minimize any reversibility. For the stimuli-responsive trigger, we

chose an acetal protecting group that can be quickly removed in acidic conditions. Masking of the phenol was necessary to limit any unintended release during the conjugation and purification steps.

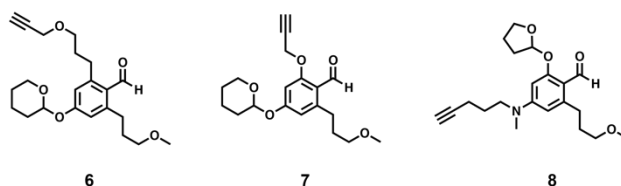
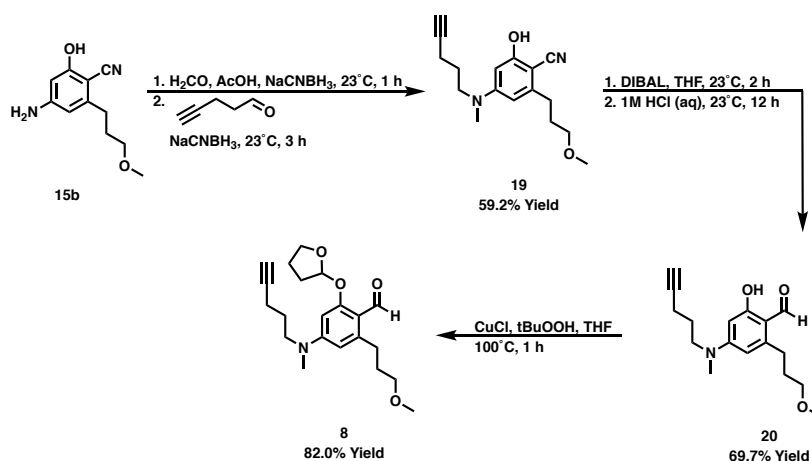


Figure 5.3. Traceless linkers prepared for protein conjugation.

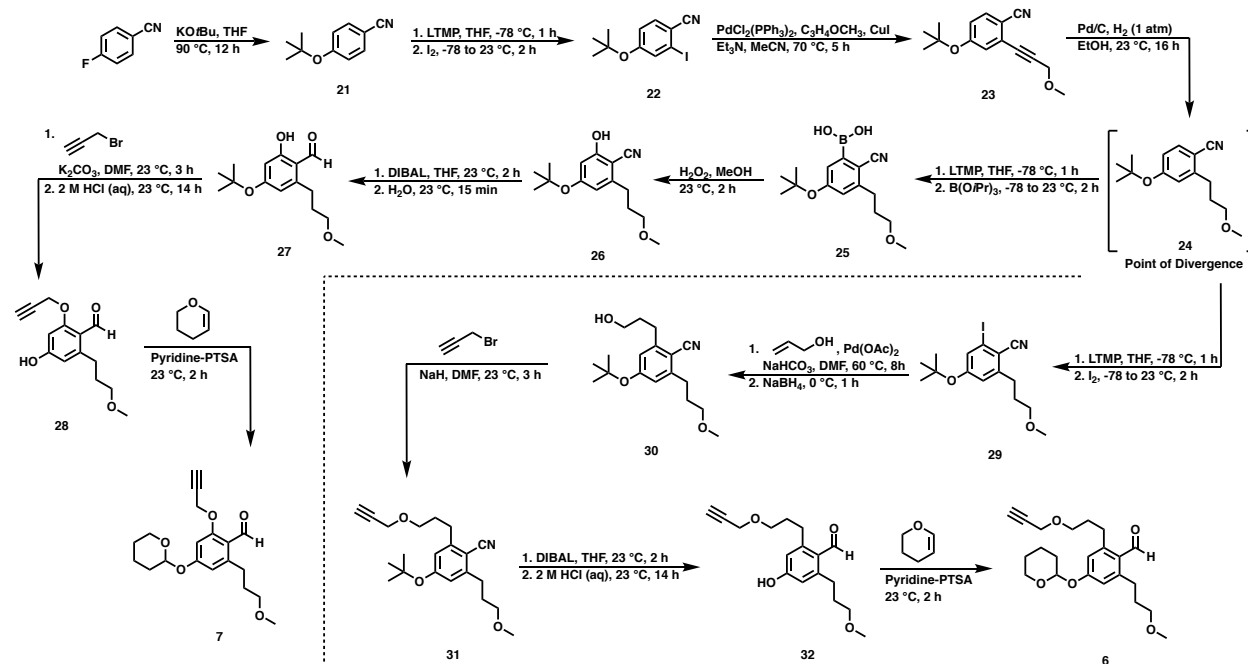
Linker **8** was prepared by monomethylating the aniline of **15b** by reductive amination using formaldehyde followed by a second reductive amination using pent-4-ynal (one-pot) to deliver **19**. Thereupon the aryl nitrile was selectively reduced with DIBAL followed by the conversion of the phenol to a cyclic acetal using a CuCl and peroxide mediated THF addition to afford linker **8**.¹



Scheme 5.4. Synthesis of traceless benzaldehyde precursor **8**.

Linkers **6** and **7** were both prepared using 4-fluorobenzonitrile as a starting material. The aryl fluoride was initially displaced with potassium tert-butyrate to install the protected phenol. Initial pursuits towards **6** and **7** were undertaken using a TIPS protected phenol, however, the TIPS groups proved unstable to the *ortho*-directed lithiation and Sonogashira conditions and was therefore abandoned. The more stable *t*-butyl ether **21** was then iodinated through a nitrile directed

ortho-lithiation intermediate that was subsequently quenched with iodine. The aryl iodide was then coupled to propargyl methyl ether via a Sonogashira reaction followed by a palladium mediated hydrogenation to afford **24**. This is where the synthesis between linkers **6** and **7** diverges in order to vary the electronic nature of the substituent at the position *ortho* to the eventual benzaldehyde. **24** was subjected to another *ortho*-directed lithiation and was quenched with either triisopropyl borate or iodine delivering **25** or **29** respectively, both of which were minimally purified before moving forward. Thereafter, **25** was oxidized to the phenol followed by a DIBAL reduction to furnish **27**. This phenol was then coupled to propargyl bromide followed by the removal of the t-butyl protecting group in one-pot. The resulting phenol was then converted to a cyclic acetal using tetrahydropyran and catalytic pyridine-*p*-toluene sulfonic acid to afford the final benzaldehyde **7** for protein conjugation.²



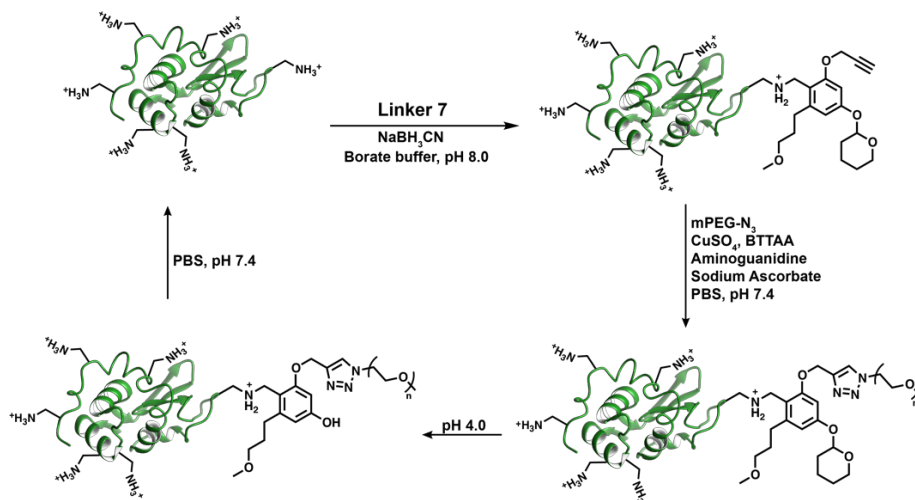
Scheme 5.5. Synthesis of traceless benzaldehyde precursors **6** and **7** from 4-fluorobenzonitrile.

Returning to the point of divergence, the aryl iodide **29** next underwent a Heck coupling with allyl alcohol followed by a sodium borohydride reduction (one-pot) to afford **30**. The propyl

alcohol was then coupled to propargyl bromide, after which the resulting aryl nitrile was reduced with DIBAL. The acidic workup removed the t-butyl ether protecting group from the phenol, which was then converted to a cyclic acetal using tetrahydropyran and catalytic pyridine-p-toluene sulfonic acid to afford the final benzaldehyde **6** for protein conjugation.²

5.2.3 Preparation of Traceless mPEG-Lysozyme Conjugates

The linkers were designed to initially undergo reductive amination with lysozyme followed by a copper-mediated azide alkyne cycloaddition with an azide-containing PEG species (mPEG-N₃) to afford the PEGylated lysozyme conjugates (Figure 5.4). Lysozyme (Lyz) was chosen as the model protein because it has 6 accessible lysine residues along with the N-terminal amine, and the activity assay is well-established.³ This system was synthetically designed in a stepwise manner to aid in the characterization of the intermediates, where the modified protein could be easily characterized via LCMS to ensure the benzylamines were attached as intended. This would aid in identifying potential issues with the traceless release or any potential conjugation inefficiencies.



Scheme 5.6. Representative stepwise protein conjugation scheme for the preparation of traceless mPEG-7-Lyz conjugate.

Reductive amination conditions were initially screened varying the choice of buffer, pH, concentration, and benzaldehyde equivalence. It was found that 0.1 M borate buffer at pH 8.0 using 3.5 equiv. of linker per amine (25 equiv. to Lyz) produced a high percent modification as measured by LCMS. Additionally, conditions consistent with previous reports, selective for the N-terminus over the lysine residues, were found to preferentially produce a single modification.⁴ Unsurprisingly, under more acidic conditions the cyclic acetal groups began to hydrolyze, which in turn allowed for the self-immolative release, decreasing the overall conjugation efficiency. The choice of an alternative masking agent on the phenol that is stable to the acidic conditions would certainly increase the efficiency of the reaction at lower pH's. Targeting a high percent modification with **7** and **8** afforded perfunctionalized lysozyme species within 72 hours, however, **6** proved to be quite sluggish. Attempts to increase the percent modification with **6**, including the addition of catalytic aniline and elevated temperatures, were employed, yet full conversion to the monofunctionalized lysozyme was never observed.⁵ This decreased reactivity is likely due to the increased steric bulk around the benzaldehyde and the increased hydrophobicity compared to **7**

and **8**, which in turn decreased the rate of imine formation and thus favored the competing benzaldehyde reduction.

The copper mediated azide-alkyne cycloaddition was then carried out using previously reported conditions to form the mPEG-linker-Lyz conjugates.⁶ The following copper-click conjugation to mPEG-N₃ was complete within 12 hours. Interestingly, Lyz-**7** formed multipegylated species, while Lyz-**8** preferentially formed the monopegylated conjugate under the same conditions. We believe the competing azaquinone release mechanism reduces the stability of Lyz-**8**, which in turn limits the conjugation efficiency. The monopegylated lysozyme conjugates were purified via size exclusion chromatography and subsequently deprotected under acidic conditions (pH 4.0) to remove the cyclic acetal protecting group.

5.2.4 Traceless Release of Lysozyme and Activity Recovery Studies.

The traceless release of Lyz was monitored from the two purified monopegylated lysozyme conjugates (Figure 7) in phosphate buffer at pH 7.4. The kinetics were obtained by determining the amount of free Lyz in solution using HR-LCMS, thus ensuring that native Lyz was released. The mPEG-**8**-Lyz conjugate reached 98% release within 12 days, while mPEG-**7**-Lyz showed 50% release within the same time period. The trend between the electron donation into the aromatic core and the rate of release aligns with our model system, however, a dramatic decrease in the rate was observed between the small molecule and macromolecular systems.

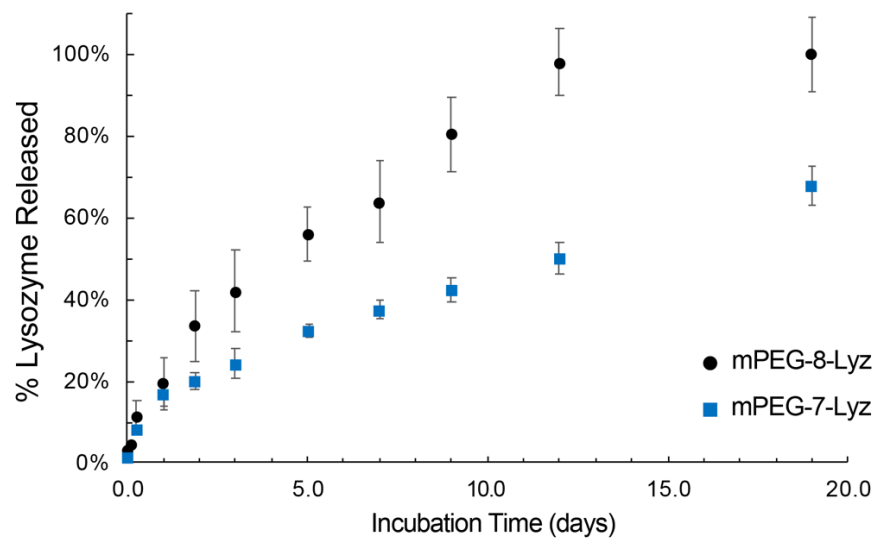


Figure 5.4. Traceless release of lysozyme from Lyz-mPEG conjugates in phosphate buffer (pH 7.4) monitored via HR-LCMS.

Following the release of native lysozyme, the activity of the resulting lysozyme was monitored through the cell lysis of FITC labeled Gram-positive *Micrococcus lueus* in the EnzChek lysozyme activity assay (Figure 8). The lysozyme activity for each of the mPEG-Lyz conjugates was compared before and after traceless release. mPEG-7-Lyz showed a 28% reduction in activity that was restored to 97% upon traceless release. Similarly, the mPEG-8-Lyz showed a 34% reduction in activity that was restored to 94% upon release. An increase in the PEG molecular weight or degree of PEGylation would further exacerbate the activity discrepancy before and after traceless release.

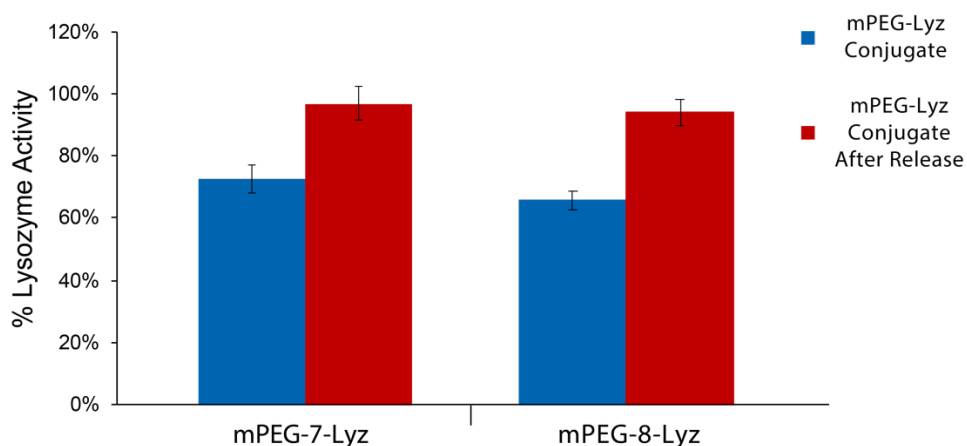


Figure 5.5. Lysozyme activity assay comparison between each mPEG-Lyz conjugate before (blue) and after (red) traceless release.

This work focused on the proof of concept for the design and implementation of this new class of traceless linker. Further adoption into the field of stimuli-responsive, self-immolative linkers is possible. The acetal protecting group on the phenol was chosen as a model stimuli-responsive functional group in this study, which could easily be replaced with other stimuli-responsive groups to impart a site-specific release in the system, adding an additional layer of control. Stimuli-triggered switching of protein activity has long been of interest in biotechnology,⁷ and the strategy has potential for applications such as oral protein delivery,⁸ and targeted drug delivery, reducing off-target effects. This triggering of protein activity further demonstrates the utility of the benzaldehyde linkers in the context of traceless release.

5.3 Conclusions

The observation of reversibility in the initial step acquired through the use of DFT calculations led to the development of traceless benzylamine linkers that contain an intramolecular trapping arm to quench the quinone methide intermediate. Traceless protein-PEG conjugates were prepared using insights gained from the model phenethylamine compounds, and lysozyme

conjugates prepared in Chapter 4. These conjugates were prepared through an initial reductive amination reaction, followed by a copper-click cycloaddition, and subsequent deprotection to afford the mono-PEGylated lysozyme conjugates. These conjugates had reduced enzymatic activity that was subsequently restored upon traceless release of PEG. The rate of traceless release varied between the two conjugates with half-lives of 5 and 12 days depending on the electronics of the linker. This modularity in the rate of release and linker design makes this new class of traceless linkers a useful addition to the bioconjugation toolbox.

5.4 Experimental

5.4.1 Materials

Unless specifically mentioned all solvents were purchased as ACS solvents and used without any further purification. Anhydrous solvents used were either freshly distilled or passed through activated alumina columns. Reagents were purchased at the highest commercial quality and used without further purification, unless otherwise stated. Yields refer to isolated material, unless otherwise stated.

5.4.2 Analytical Techniques

Reactions were monitored by GC/MS, LC/MS, and thin layer chromatography (TLC). TLC was performed using Millipore Sigma silica plates (60F-254), using short-wave UV light as the visualizing agent, acidic ethanolic anisaldehyde, or KMnO₄ and heat as developing agents. NMR spectra were recorded on Bruker AV-400, AV-500, and AV-600 instruments and are calibrated using residual undeuterated solvent (CHCl₃ at 7.26 ppm ¹H NMR, 77.16 ppm ¹³C NMR). The following abbreviations were used to explain multiplicities: s = singlet, d = doublet, t = triplet, q = quartet, m = multiplet. Column chromatography was performed using Silicycle silica (P60,

particle size 40–63 μm) on a Biotage Isolera One 3.0 autocolumn instrument. All silica chromatography unless specifically was carried out on the Biotage using KP-Sil high-performance columns repacked using the Silicycle silica described above (column sizes described in experimental). ESI mass spectra were obtained using an Agilent 6530 QTOF-ESI in tandem with a 1260 Infinity LC. Analytical reverse phase high performance liquid chromatography (HPLC) was carried out on a Agilent 1260 Infinity II HPLC system equipped with an autosampler and a UV detector using a Poroshell 120 2.7- μm C18 120 \AA column (analytical: 2.7 μm , 4.6 \times 100 mm) with monitoring at $\lambda = 220$ and 280 nm and with a flow rate of 0.8 mL/min. Preparatory reverse phase HPLC was carried out on an Agilent 1290 Infinity II high performance liquid chromatography system equipped with a UV detector using a Luna 5 μm C18 100 \AA column (preparatory: 5 μm , 250 \times 21.2 mm) with monitoring at $\lambda = 220$ and 254 nm and with a flow rate of 25 mL/min. Melting points were recorded using a Mettler Toledo 3+ DSC wherein the melting points are listed as the onset temperature T_{on} and the peak temperature T_{peak} running under a nitrogen atmosphere at 5 $^{\circ}\text{C}/\text{min}$.

5.4.3 Methods

Phenethylamine Release Study Procedure

The linker was prepared as a 10mM solution in MeOH in triplicate. Each aliquot was diluted to a final concentration of 5mM with 0.1M Tris buffer (pH: 7.4). This was immediately analyzed on the analytical HPLC to determine the amount of phenethylamine release using a phenethylamine standard curve. Each sample was prepared immediately prior to the first injection to ensure a consistent starting point across the three separate repeats. Time points were taken over a time frame of at least 10 days and longer if necessary.

Lysozyme Reductive Amination Screen

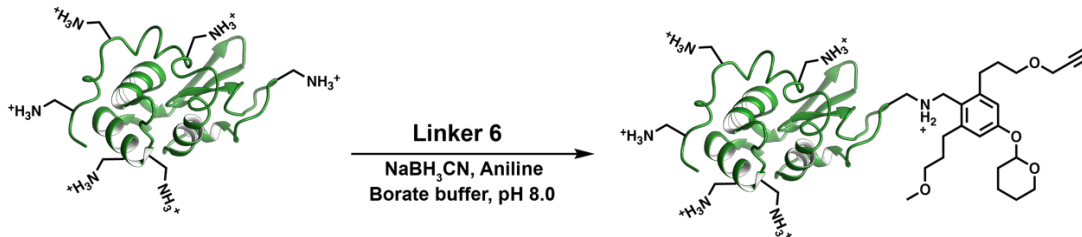
To ensure effective reductive amination of the linkers to lysozyme it was decided to screen conjugation conditions, including choice of buffer, pH, equivalents of benzaldehyde, and final concentration of lysozyme. These experiments were all carried out with using linker 7. It was decided to start screening at pH 5.5 since previous studies with reductive amination to Lysozyme proved effective at this pH. The conversion was monitored at 18 hours for all the conjugation conditions by analysis on the Agilent LC/Q-TOF. Protein peaks were deconvoluted and the mass peaks corresponding to each linker addition was integrated and taken as a percentage of the whole. The benzaldehyde stock solution was prepared in DMSO and the final concentration of DMSO in each condition was adjusted to 10% for consistency across all conditions.

Table 5.1. Reductive amination screen using the benzaldehyde linker 7 and lysozyme in either buffer A (25 mM citric acid), B (100 mM HEPES), or C (100 mM borate). The % modification was monitored using LCMS to determine the number of linkers conjugated to each lysozyme.

Linker Equiv	Buffer	pH	[Lysozyme] μ M	Rxn time (hr)	% Native Lysozyme	Lysozyme + 1 Linker	Lysozyme + 2 Linkers	Lysozyme + 3 Linkers	Lysozyme + 4 Linkers	Lysozyme + 5 Linkers
5	A	5.5	61	18	81%	19%	0%	0%	0%	0%
10	A	5.5	61	18	71%	29%	0%	0%	0%	0%
20	A	5.5	61	18	73%	27%	0%	0%	0%	0%
10	A	6.1	61	18	75%	25%	0%	0%	0%	0%
20	A	6.1	61	18	71%	29%	0%	0%	0%	0%
10	A	6.1	158	18	47%	42%	11%	0%	0%	0%
20	A	6.1	158	18	45%	43%	12%	0%	0%	0%
10	A	6.1	214	18	42%	44%	14%	0%	0%	0%
20	A	6.1	214	18	41%	45%	14%	0%	0%	0%
20	B	7.4	206	18	23%	46%	27%	4%	0%	0%
20	B	7.6	206	18	24%	44%	26%	5%	0%	0%
20	C	8.0	206	18	15%	42%	33%	11%	0%	0%
20	C	8.0	206	48	0%	7%	29%	40%	22%	2%

Not shown above is the occurrence of a side reaction with lysozyme corresponding to a mass adduct of lysozyme + 170.15 Da. This unknown byproduct was minimized when the reductive amination was carried out at higher pH's.

Lysozyme-Linker 6 Conjugation (Reductive Amination)



To a solution of lysozyme (1.5 mg, 1 Eq, 0.105 μmol) in borate buffer (pH 8, 262 μL) was added a solution of benzaldehyde **6** (40.1 μL , 55 mM, 21 Eq, 2.20 μmol) in DMSO, followed by a solution of $NaCNBH_3$ (120.6 μL , 87 mM, 100 Eq, 10.5 μmol) and a solution of aniline (31.5 μL , 1 mM, 0.3 Eq, 0.031 μmol) both in borate buffer (pH 8). This was mixed on an orbital shaker at 22 $^\circ\text{C}$ for 72 hours, while conversion was monitored via LCMS (note 1).

At 72h the conversion had stalled and the resulting lysozyme conjugate was concentrated and buffer exchanged into 100mM PBS using an Amicon Ultra centrifugal filter units with a 10 kDa molecular weight cutoff.

Note 1. The linker does fragment off during the electrospray ionization to a certain extent. This limits the % modification that was determined by the LCMS analysis. Each linker modification appears as an additional 358.16 Da onto the lysozyme (14305 Da).

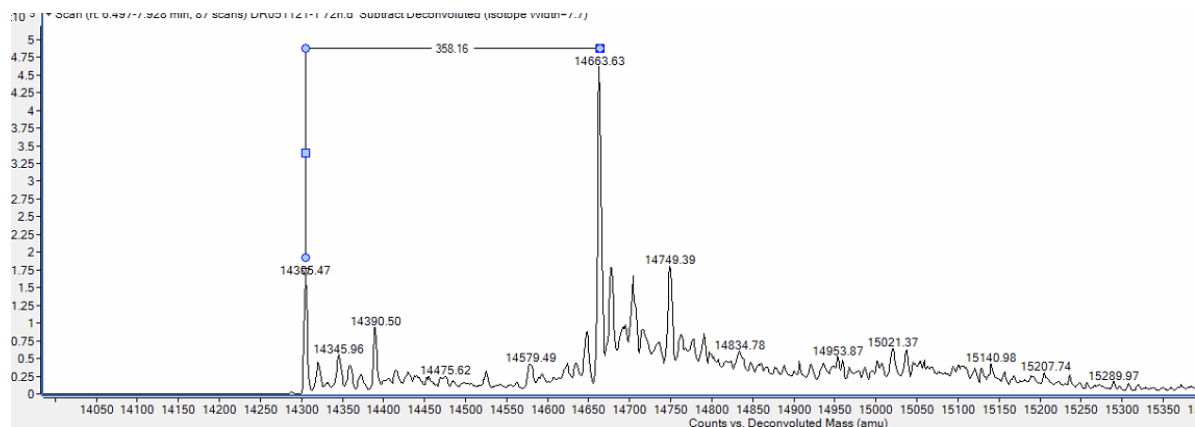
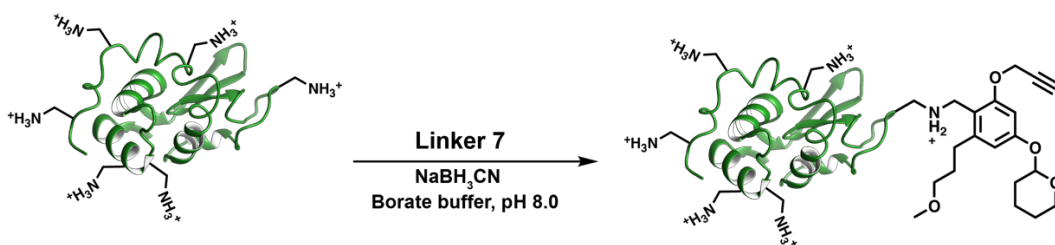


Figure 5.6. LCMS-QTOF of deconvoluted lysozyme-linker-6 mass 72 hours into the reaction

Lysozyme-Linker 7 Conjugation (Reductive Amination)



To a solution of lysozyme (2.0 mg, 1 Eq, 0.140 μmol) in borate buffer (pH 8, 466 μL) was added a solution of benzaldehyde **7** (50.9 μL , 55 mM, 20 Eq, 2.80 μmol) in DMSO, followed by a solution of NaCNBH_3 (160.8 μL , 87 mM, 100 Eq, 14.0 μmol) in borate buffer (pH 8). This was mixed on an orbital shaker at 22 $^\circ\text{C}$ for 72 hours, while conversion was monitored via LCMS (note 1).

At 72h the conversion had stalled and the resulting lysozyme conjugate was concentrated and buffer exchanged into 100mM PBS using an Amicon Ultra centrifugal filter units with a 10 kDa molecular weight cutoff.

Note 1. The linker does fragment off during the electrospray ionization to a certain extent. This limits the % modification that was determined by the LCMS analysis. Each linker modification appears as an additional 316.22 Da onto the lysozyme (14305 Da).

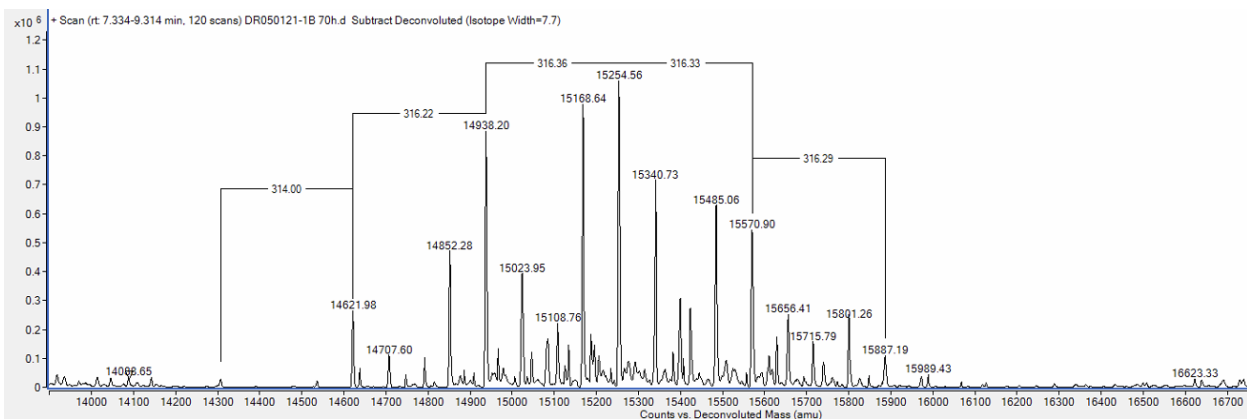
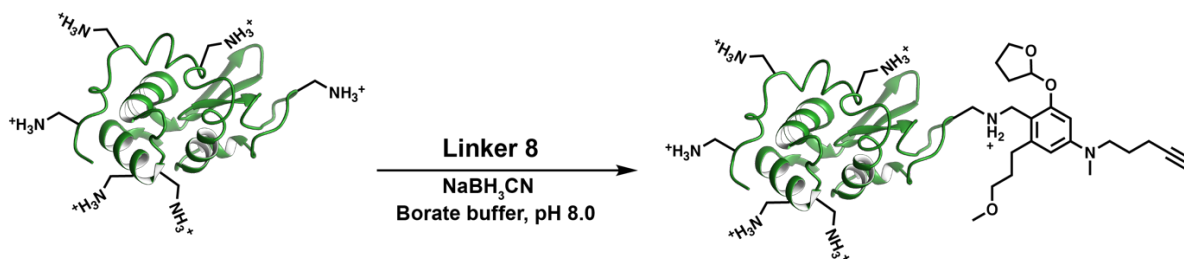


Figure 5.7. LCMS-QTOF of deconvoluted lysozyme-linker-7 mass 72 hours into the reaction

Lysozyme-Linker 8 Conjugation (Reductive Amination)



To a solution of lysozyme (2.0 mg, 1 Eq, 0.140 μmol) in borate buffer (pH 8, 466 μL) was added a solution of benzaldehyde **8** (50.9 μL , 55 mM, 20 Eq, 2.80 μmol) in DMSO, followed by a solution of NaCNBH_3 (160.8 μL , 87 mM, 100 Eq, 14.0 μmol) in borate buffer (pH 8). This was mixed on an orbital shaker at 22 $^\circ\text{C}$ for 72 hours, while conversion was monitored via LCMS (note 1).

At 72h the conversion had stalled and the resulting lysozyme conjugate was concentrated and buffer exchanged into 100mM PBS using an Amicon Ultra centrifugal filter units with a 10 kDa molecular weight cutoff.

Note 1. The linker does fragment off during the electrospray ionization to a certain extent. This limits the % modification that was determined by the LCMS analysis. Each linker modification appears as an additional 342.00 Da onto the lysozyme (14305 Da).

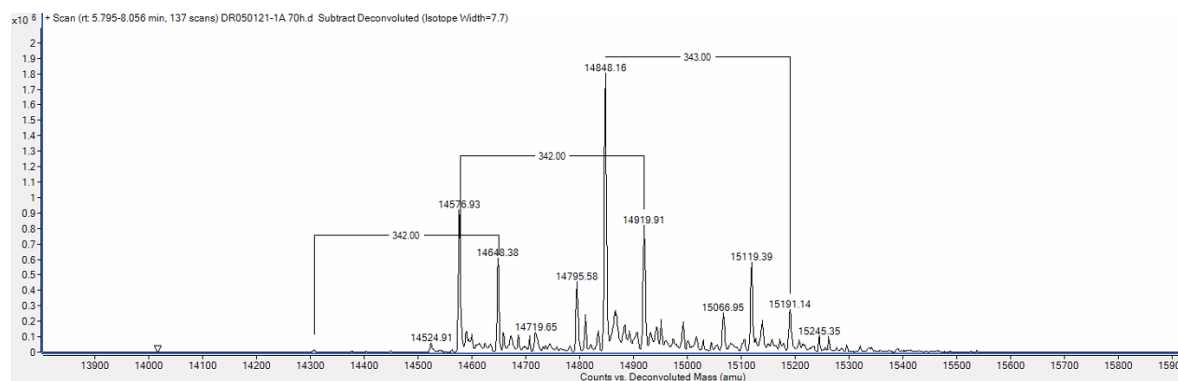
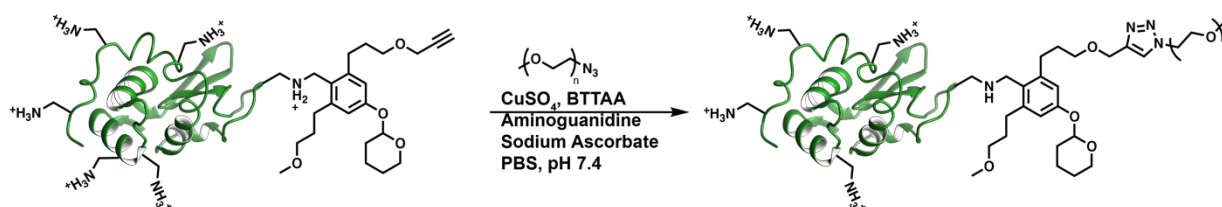


Figure 5.8. LCMS-QTOF of deconvoluted lysozyme-linker-8 mass 72 hours into the reaction

Preparation of mPEG-Lysozyme Conjugates

mPEG-6-Lysozyme



All stock solutions were prepared using 0.1 M PBS (pH 7.4). To a solution of Lysozyme-Linker (570 μL , 0.12 mM, 1 Eq, 68.4 nmol) was added mPEG- N_3 (512.9 μL , 10 mM, 75 Eq, 5.13 μmol). Separately, a solution of BTAA (34.2 μL , 1.0 mM, 0.5 Eq, 34.2 nmol) was combined with a solution of CuSO_4 (34.2 μL , 0.2 mM, 0.1 Eq, 6.84 nmol) and mixed for 5 minutes prior to adding to the lysozyme solution. Lastly, the aminoguanidine (99.1 μL , 3.45 mM, 5 Eq, 0.342 μmol) and sodium ascorbate (99.1 μL , 3.45 mM, 5 Eq, 0.342 μmol) were added to the lysozyme solution and this was placed on an orbital shaker for 12 hours.

The conversion was monitored by SDS-PAGE looking for the appearance of higher MW species. The monopegylated lysozyme appeared on SDS-PAGE and therefore the crude conjugate was purified via size-exclusion chromatography (100 mM PBS, pH 7.1, GE Superdex 75 10/300). The monopegylated lysozyme eluted between 7-8 mL and all corresponding fractions were

concentrated using an Amicon Ultra centrifugal filter units with a 10 kDa molecular weight cutoff. It was recognized that there was very little conjugate present in these fractions due to a relatively low conversion (apparent in FPLC Trace comparison). This bioconjugate was not used for release studies due to the difficulty in preparation and low conversion.

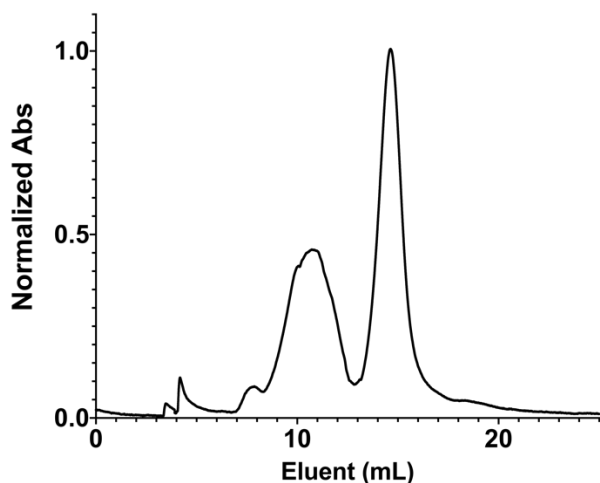
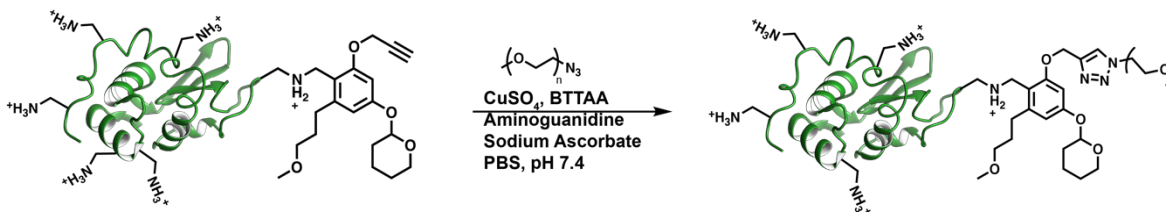


Figure 5.9. FPLC Trace of crude mPEG-6-Lysozyme (GE-Superdex 75 10/300 column, 0.5 mL/min, 100 mM PBS)

mPEG-7-Lysozyme



All stock solutions were prepared using 0.1 M PBS (pH 7.4). To a solution of Lysozyme-Linker (570 μ L, 0.12 mM, 1 Eq, 68.4 nmol) was added mPEG-N₃ (512.9 μ L, 10 mM, 75 Eq, 5.13 μ mol). Separately, a solution of BTTAA (34.2 μ L, 1.0 mM, 0.5 Eq, 34.2 nmol) was combined with a solution of CuSO₄ (34.2 μ L, 0.2 mM, 0.1 Eq, 6.84 nmol) and mixed for 5 minutes prior to adding to the lysozyme solution. Lastly, the aminoguanidine (99.1 μ L, 3.45 mM, 5 Eq, 0.342

μmol) and sodium ascorbate ($99.1 \mu\text{L}$, 3.45 mM , 5 Eq , $0.342 \mu\text{mol}$) were added to the lysozyme solution and this was placed on an orbital shaker for 12 hours.

The conversion was monitored by SDS-PAGE looking for the appearance of higher MW species. A mixture of mono, bi, tri, and tetrapegylated lysozyme appeared on SDS-PAGE. The higher MW species were separated from the mPEG-N₃ and unmodified Lysozyme using an Amicon Ultra centrifugal filter units with a 30 kDa molecular weight cutoff. The filtrate was then purified via size-exclusion chromatography (100 mM PBS , $\text{pH } 7.1$, GE Superdex 75 10/300). The monopegylated lysozyme eluted between 7-9 mL and all corresponding fractions were concentrated using an Amicon Ultra centrifugal filter units with a 10 kDa molecular weight cutoff.

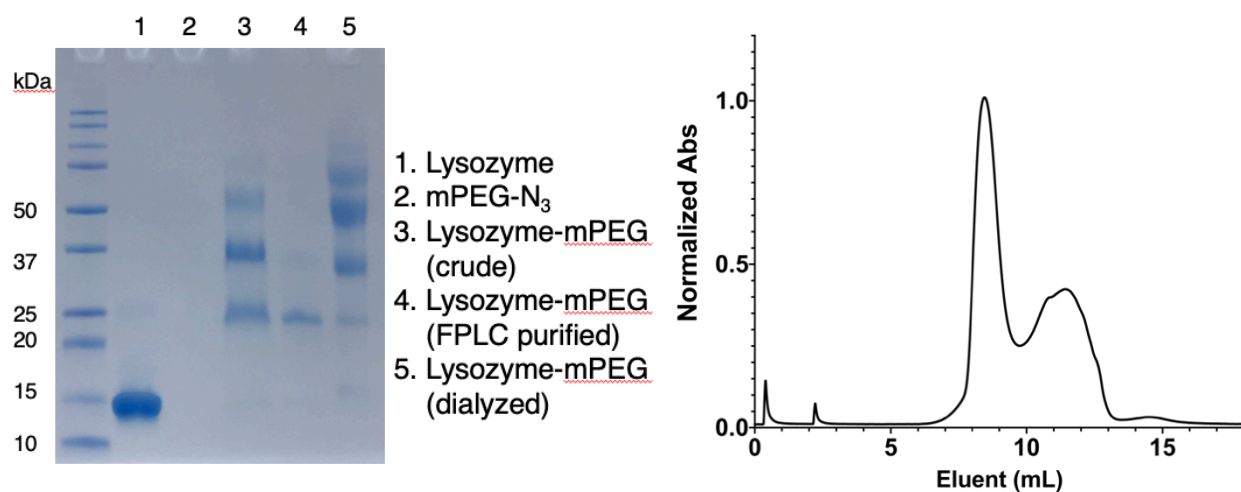
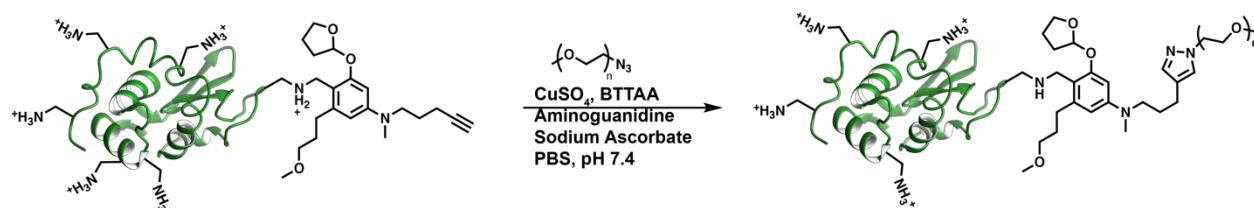


Figure 5.10. (a) SDS-PAGE analysis of conjugation (b) FPLC Trace of crude mPEG-7-Lysozyme (GE-Superdex 75 10/300 column, 0.5 mL/min , 100 mM PBS)

mPEG-8-Lysozyme



All stock solutions were prepared using 0.1 M PBS (pH 7.4). To a solution of Lysozyme-Linker (570 μ L, 0.12 mM, 1 Eq, 68.4 nmol) was added mPEG-N₃ (512.9 μ L, 10 mM, 75 Eq, 5.13 μ mol). Separately, a solution of BTTAA (34.2 μ L, 1.0 mM, 0.5 Eq, 34.2 nmol) was combined with a solution of CuSO₄ (34.2 μ L, 0.2 mM, 0.1 Eq, 6.84 nmol) and mixed for 5 minutes prior to adding to the lysozyme solution. Lastly, the aminoguanidine (99.1 μ L, 3.45 mM, 5 Eq, 0.342 μ mol) and sodium ascorbate (99.1 μ L, 3.45 mM, 5 Eq, 0.342 μ mol) were added to the lysozyme solution and this was placed on an orbital shaker for 12 hours.

The conversion was monitored by SDS-PAGE looking for the appearance of higher MW species. The monopegylated lysozyme appeared on SDS-PAGE and therefore the crude conjugate was purified via size-exclusion chromatography (100 mM PBS, pH 7.1, GE Superdex 75 10/300). The monopegylated lysozyme eluted between 7-9 mL and all corresponding pure fractions were concentrated using an Amicon Ultra centrifugal filter units with a 10 kDa molecular weight cutoff.

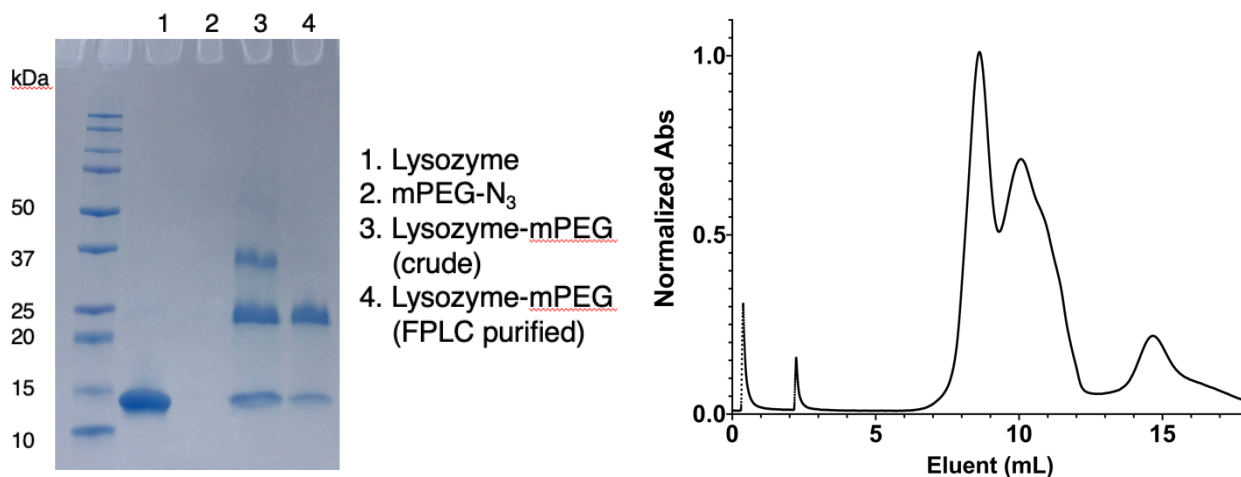


Figure 5.11. (a) SDS-PAGE analysis of conjugation (b) FPLC Trace of crude mPEG-8-Lysozyme (GE-Superdex 75 10/300 column, 0.5 mL/min, 100 mM PBS)

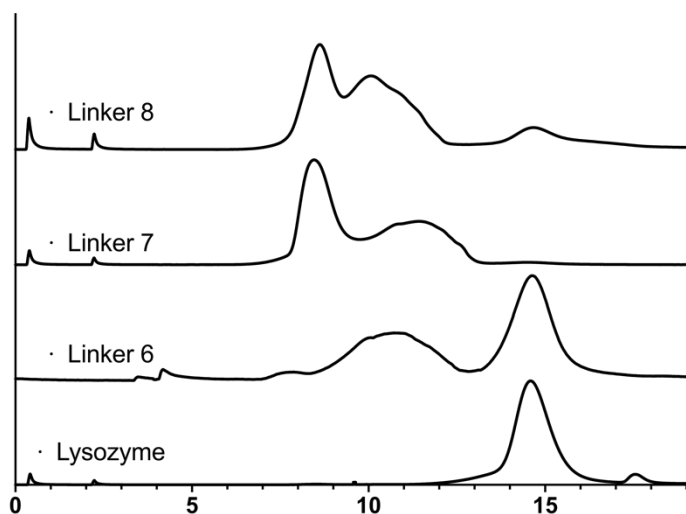
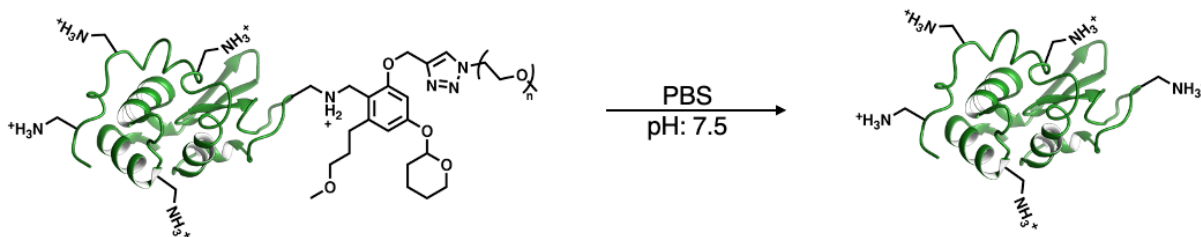


Figure 5.12. FPLC Trace Comparison of the three mPEG-Lysozyme conjugations (GE-Superdex 75 10/300 column, 0.5 mL/min, 100 mM PBS)

mPEG-7-Lysozyme Release



Prior to beginning the release assay the cyclic acetal group was removed by buffer exchanging into 100 mM citric acid buffer (pH 4.0). This solution was mixed on an orbital shaker for 6 hours and then buffer exchanged back into 100 mM PBS (pH 7.4). The protein concentration was determined using BCA and diluted down to 0.2 mg/mL lysozyme-conjugate. This solution was then filtered into a vial and aliquots were taken over 30 days to monitor the amount of lysozyme released using LCMS.

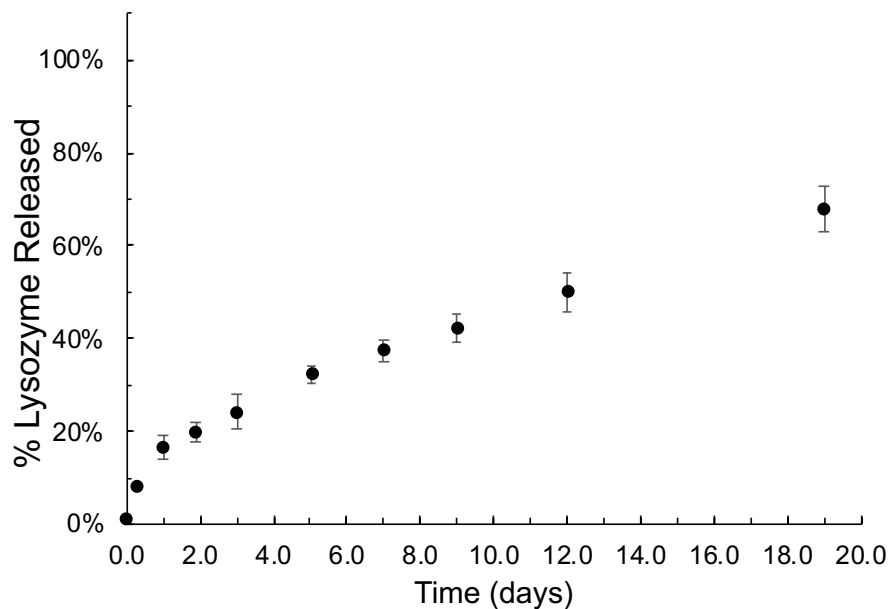
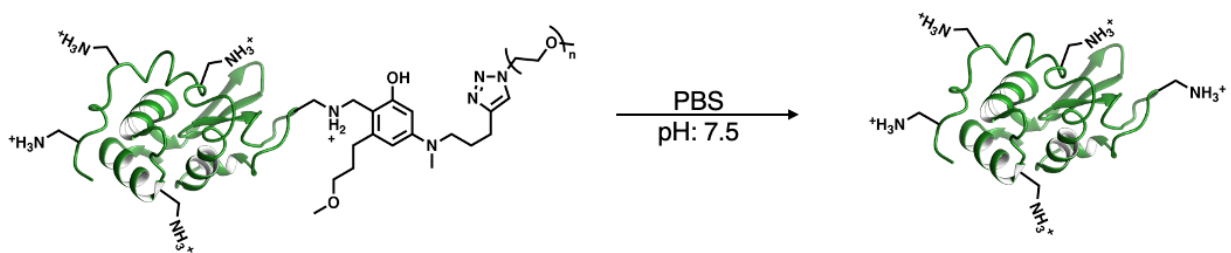


Figure 5.13. Traceless release of lysozyme from mPEG-7-lysozyme conjugate in phosphate buffer (pH 7.4) monitored via HR-LCMS.

mPEG-8-Lysozyme Release



Prior to beginning the release assay the cyclic acetyl group was removed by buffer exchanging into 100 mM citric acid buffer (pH 4.0). This solution was mixed on an orbital shaker for 6 hours and then buffer exchanged back into 100 mM PBS (pH 7.4). The protein concentration was determined using BCA and diluted down to 0.2 mg/mL lysozyme-conjugate. This solution was then filtered into a vial and aliquots were taken over 20 days to monitor the amount of lysozyme released using LCMS.

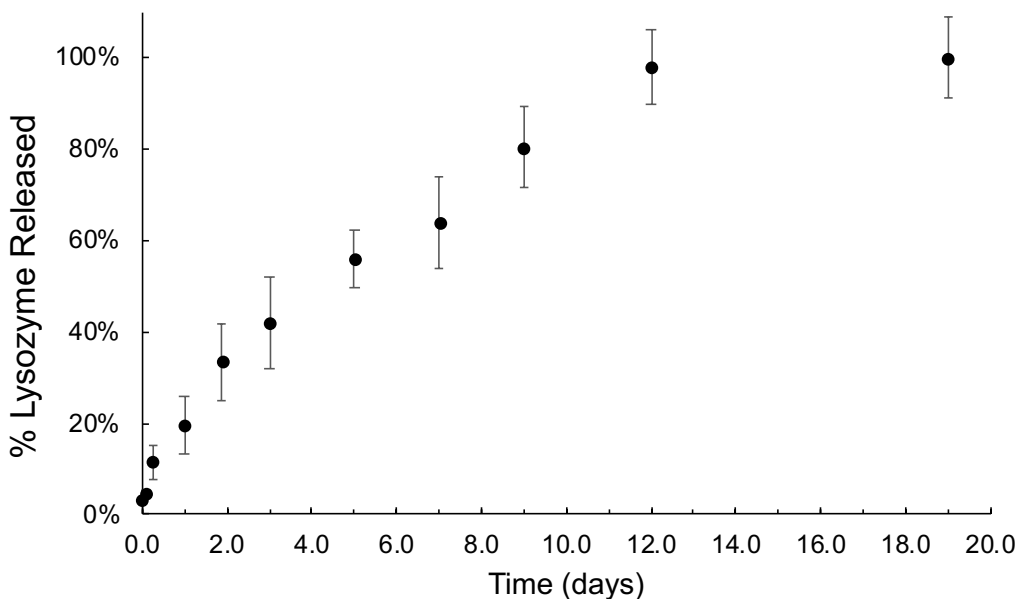


Figure 5.14. Traceless release of lysozyme from mPEG-8-lysozyme conjugate in phosphate buffer (pH 7.4) monitored via HR-LCMS.

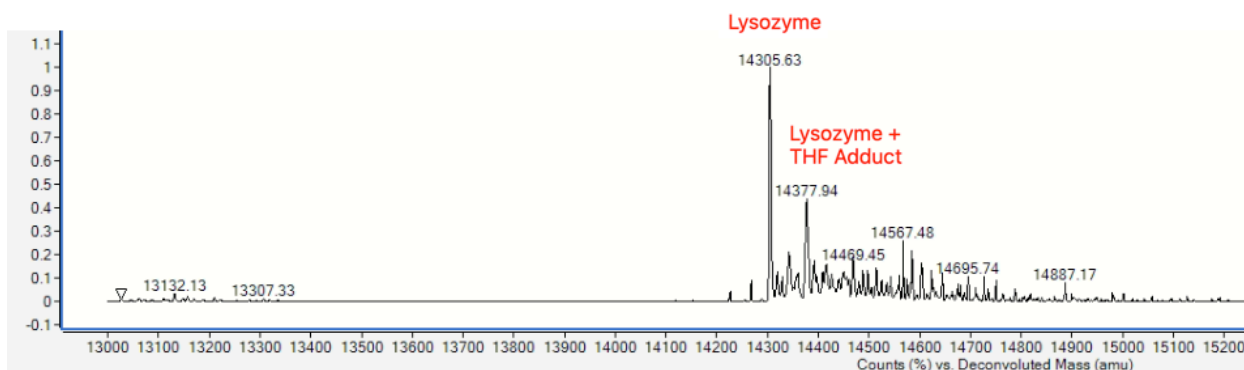


Figure 5.15. Representative deconvoluted LCMS-QTOF mass spectrum of lysozyme after traceless release

Lysozyme Activity Assays

The lysozyme activity assay was conducted using the Invitrogen™ ENZChek™ assay kit, according to the manufacturer instructions. Briefly, 50 μ L of sample (protein concentration was quantified by the bicinchoninic acid (BCA) assay) was mixed with 50 μ L of fluorescein-labeled

Micrococcus luteus in a 96-well plate and incubated at 37 °C. Recovered fluorescein fluorescence from cell lysis was measured (excitation 485 nm, emission 530 nm) and quantified using a standard curve.

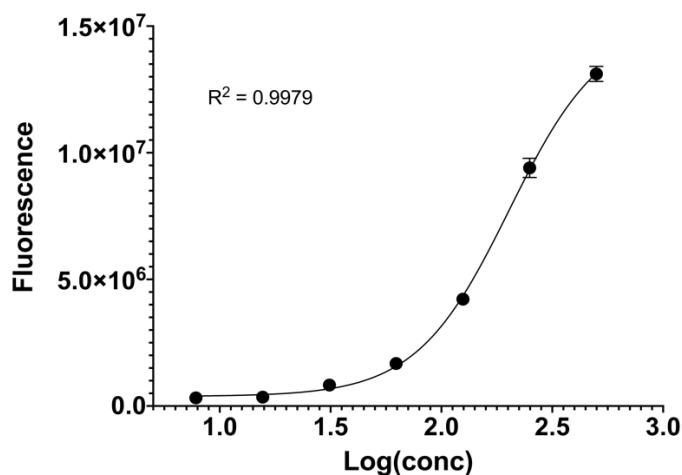
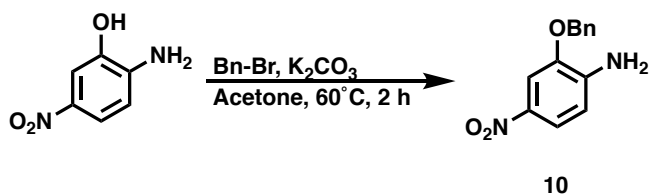


Figure 5.16. Standard curve of lysozyme activity via the ENZChek fluorescence assay (excitation 485 nm, emission 530 nm)

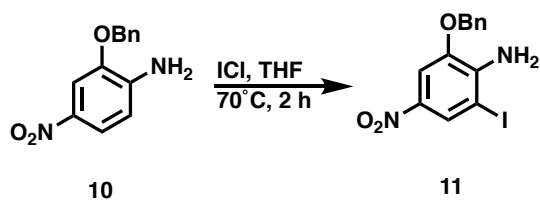
Synthesis of Compound 10



To a solution of 2-amino-5-nitrophenol (7.50 g, 1 Eq, 48.7 mmol) in acetone (350 mL) was added potassium carbonate (13.4 g, 2 Eq, 97.3 mmol) followed by the slow addition of benzyl bromide (8.74 g, 6.08 mL, 1.05 Eq, 51.1 mmol) over 10 minutes. The reaction contents were then brought to reflux and stirred for 3 hours. The reaction was then cooled to 23 °C where the K_2CO_3 salt was filtered away. The solution was then concentrated under reduced pressure and recrystallized using a 1:4 solution of hexanes and ethyl acetate to afford **10** (9.1 g, 77% yield) as

a yellow solid. TLC: R_f 0.53 (2:3 EtOAc:hexanes). ^1H NMR (500 MHz, CD_3CN): δ 7.76 (dd, $J = 2.5, 8.8$ Hz, 1H), 7.73 (d, $J = 2.4$ Hz, 1H), 7.49 (d, $J = 7.5$ Hz, 2H), 7.41 (t, $J = 7.3$ Hz, 2H), 7.36 (m, 1H), 6.72 (d, $J = 8.8$ Hz, 1H), 5.20 (s, 4H). ^{13}C NMR (126 MHz, CD_3CN): δ 145.20, 144.04, 137.45, 136.57, 128.59, 128.19, 127.77, 119.39, 111.50, 107.31, 70.41. IR (film) 3492, 3374, 3030, 2925, 2839, 1615, 1518, 1490, 1382, 1225, 1095 cm^{-1} . HRMS (ESI/Q-TOF): $[\text{M}+\text{H}]^+$ calcd for $\text{C}_{13}\text{H}_{13}\text{N}_2\text{O}_3^+$, 245.0921; found 245.0962. m.p.: T_{on} 148.4 $^\circ\text{C}$: T_{peak} 150.8 $^\circ\text{C}$.

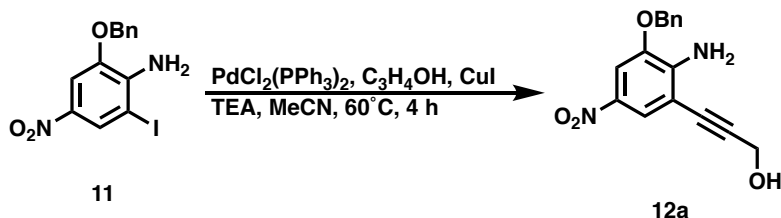
Synthesis of Compound 11



To a solution of 2-(benzyloxy)-4-nitroaniline (3.00 g, 1 Eq, 16.4 mmol) in THF (250mL) was added iodine monochloride (9.97 g, 4.10 mL, 5 Eq, 81.9 mmol), after which the reaction was stirred at reflux for 2 hours. The reaction solution was concentrated down to 50mL under reduced pressure and combined with a biphasic mixture of sat. aq. $\text{Na}_2\text{S}_2\text{O}_3$ (100 mL) and EtOAc (150 mL). The layers were separated and the aq. layer was extracted once again with EtOAc (150mL). The organic layers were combined, washed with sat. aq. NaCl (75 mL), and concentrated under reduced pressure directly onto silica gel (10 g). The crude product was then purified by flash column chromatography (100 g silica gel, 5-50% EtOAc gradient against hexanes over 10 column volumes) to afford **11** (5.30 g, 97.6% yield) as an orange solid. TLC: R_f 0.68 (2:3 EtOAc:hexanes). ^1H NMR (500 MHz, CD_3CN): δ 8.24 (d, $J = 2.3$ Hz, 1H), 7.70 (d, $J = 2.3$ Hz, 1H), 7.39 (m, 5H), 3.66 (t, $J = 6.4$ Hz, 2H), 3.57 (t, $J = 6.6$ Hz, 2H), 1.86 (m, 2H), 1.69 (m, 2H). ^{13}C NMR (126 MHz, CD_3CN): δ 144.10, 143.18, 138.60, 135.26, 128.88, 128.76, 128.18, 128.00, 106.56, 78.40, 71.32,

62.03, 45.09, 29.93, 29.06. IR (film) 3483, 3370, 3090, 3030, 2970, 2925, 1738, 1602, 1496, 1309, 1289, 1217, 1098, 1013 cm^{-1} . HRMS (ESI/Q-TOF): $[\text{M}+\text{H}]^+$ calcd for $\text{C}_{13}\text{H}_{12}\text{IN}_2\text{O}_3^+$, 370.9887; found 370.9942. m.p.: T_{on} 99.5 $^{\circ}\text{C}$: T_{peak} 109.1 $^{\circ}\text{C}$.

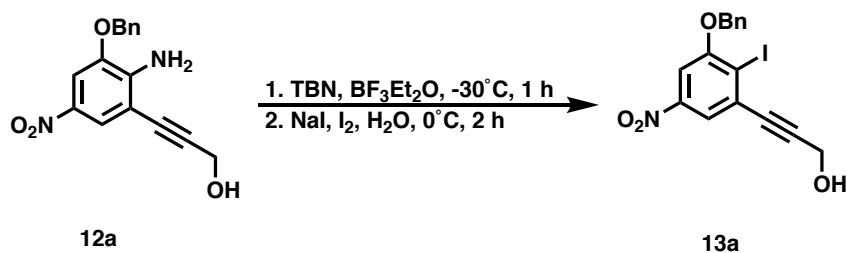
Synthesis of Compound 12a



To a solution of 2-(benzyloxy)-6-iodo-4-nitroaniline, tetrahydrofuran (4.00 g, 1 Eq, 9.04 mmol), copper(I) iodide (172 mg, 0.1 Eq, 904 μmol), and bis(triphenylphosphine)palladium(II) chloride (254 mg, 0.04 Eq, 362 μmol) in a 3:1 solution of acetonitrile:TEA, was added propargyl alcohol (811 mg, 835 μL , 1.6 Eq, 14.5 mmol). The reaction vessel was then quickly evacuated under vacuum and backfilled with argon (this was repeated 2 additional times), after which the contents were heated to 60 $^{\circ}\text{C}$ for 4 hours. The reaction contents were then cooled to 23 $^{\circ}\text{C}$ and filtered over celite. The solvent was removed under reduced pressure directly onto silica gel (10 g). The crude product was then purified by flash column chromatography (100 g silica gel, 10-100% EtOAc gradient against hexanes with a 2% MeOH isocratic primer over 10 column volumes) to afford **12a** (2.48 g, 91.9% yield) as an orange solid. TLC: R_f 0.71 (4:1 EtOAc:hexanes). ^1H NMR (400 MHz, CD_3CN): δ 7.81 (d, $J = 2.4$ Hz, 1H), 7.67 (d, $J = 2.4$ Hz, 1H), 7.48 (d, $J = 7.3$ Hz, 1H), 7.38 (m, 3H), 5.60 (s, 2H), 5.20 (s, 2H), 4.41 (d, $J = 5.3$ Hz, 2H), 3.36 (s, 1H). ^{13}C NMR (126 MHz, CD_3CN): δ 144.92, 144.16, 137.45, 135.41, 128.85, 128.71, 127.99, 122.01, 106.84, 104.74, 94.23, 80.03, 71.14, 51.58. IR (film) 3482, 3367, 3092, 3032, 2970, 2935, 1736, 1499,

1317, 1287, 1167, 1093, 1029 cm^{-1} . HRMS (ESI/Q-TOF): $[\text{M}+\text{H}]^+$ calcd for $\text{C}_{16}\text{H}_{15}\text{N}_2\text{O}_4^+$, 299.1026; found 299.1047. m.p.: T_{on} 130.2 $^{\circ}\text{C}$: T_{peak} 135.2 $^{\circ}\text{C}$

Synthesis of Compound 13a

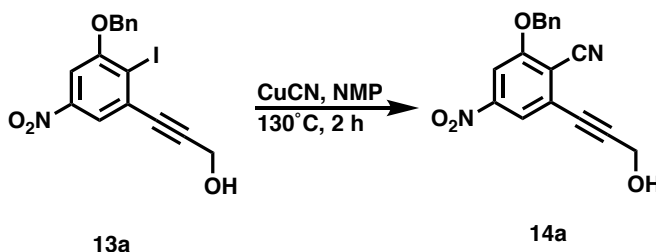


To a solution boron trifluoride etherate (3.81 g, 3.40 mL, 4 Eq, 26.8 mmol) in anhydrous THF (40mL), was added a solution of 3-(2-amino-3-(benzyloxy)-5-nitrophenyl)prop-2-yn-1-ol (2.00 g, 1 Eq, 6.70 mmol) in anhydrous THF (10mL) over 5 minutes and sealed under argon. After cooling the solution to -30°C a solution of tert-butyl nitrite (2.77 g, 3.19 mL, 4 Eq, 26.8 mmol) in anhydrous THF (10mL) was added dropwise over the course of 30 minutes. The reaction was stirred for an additional 15 minutes following full addition of the tert-butyl nitrite solution and then brought up to 5°C for 10 minutes. The diazonium intermediate was then precipitated out of solution by combining the reaction contents with 0.5 L of hexanes. The diazonium salt was filtered off and dissolved in anhydrous THF (10mL). Separately, a solution of potassium iodide (6.68 g, 6 Eq, 40.2 mmol) and iodine (851 mg, 0.5 Eq, 3.35 mmol) was prepared in water (175mL). The diazonium intermediate was added to the aqueous solution dropwise over the course of 30 minutes.

Upon full addition, the reaction was analyzed via analytical HPLC which showed approximately 50% product formation. The reaction contents were then extracted ethyl acetate (3 x 125 mL). The organic layers were combined, washed with sat. aq. $\text{Na}_2\text{S}_2\text{O}_3$ (2 x 100 mL), sat. aq. NaCl (100 mL), dried over MgSO_4 , and concentrated under reduced pressure directly onto

silica gel (5g). The crude product was then purified by flash column chromatography (100 g silica gel, 8-40% EtOAc gradient against hexanes over 10 column volumes) to afford **13a** (1.12 g, 40.8% yield) as a beige solid. TLC: R_f 0.50 (2:3 EtOAc:hexanes). ^1H NMR (400 MHz, CD_3CN): δ 7.86 (d, $J = 2.4$ Hz, 1H), 7.68 (d, $J = 2.4$ Hz, 1H), 7.52 (d, $J = 6.9$ Hz, 2H), 7.40 (m, 3H), 5.27 (s, 2H), 4.42 (d, $J = 6.1$ Hz, 2H), 3.44 (t, $J = 6.2$ Hz, 1H). ^{13}C NMR (126 MHz, CD_3CN): δ 158.39, 148.62, 134.94, 131.86, 128.81, 128.49, 127.20, 119.52, 105.76, 102.53, 93.68, 86.29, 71.78, 51.63. IR (film) 3086, 3029, 2970, 2935, 1740, 1523, 1365, 1344, 1217, 1111 cm^{-1} . HRMS (ESI/Q-TOF): $[\text{M}-\text{H}]^-$ calcd for $\text{C}_{16}\text{H}_{13}\text{N}_2\text{O}_4^-$, 407.9738; found 407.9778. m.p.: T_{on} 170.2 $^\circ\text{C}$: T_{peak} 178.7 $^\circ\text{C}$

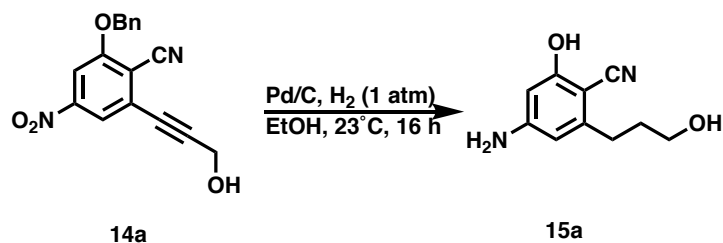
Synthesis of Compound 14a



A solution of 3-(3-(benzyloxy)-2-iodo-5-nitrophenyl)prop-2-yn-1-ol (200 mg, 1 Eq, 489 μmol) and cyanocopper (109 mg, 2.5 Eq, 1.22 mmol) in NMP (1 mL) was stirred at 130 $^\circ\text{C}$ for 2 hours. The reaction contents were cooled to 23 $^\circ\text{C}$ and poured into diethyl ether (175 mL), washed with water (3 x 50 mL), and sat. aq. NaCl (50 mL). The organic layer was dried over MgSO_4 and concentrated under reduced pressure directly onto silica gel (1 g). The crude product was then purified by flash column chromatography (25 g silica gel, 4-50% EtOAc gradient against hexanes over 10 column volumes) to afford **14a** (126 mg, 83.6% yield) as a yellow solid. TLC: R_f 0.39 (2:3 EtOAc:hexanes). ^1H NMR (500 MHz, CD_3CN): δ 7.94 (d, $J = 2.0$ Hz, 1H), 7.80 (d, $J = 2.0$ Hz, 1H), 7.42 (m, 6H), 5.32 (s, 2H), 4.59 (s, 2H). ^{13}C NMR (126 MHz, CD_3CN): δ 160.95, 150.65,

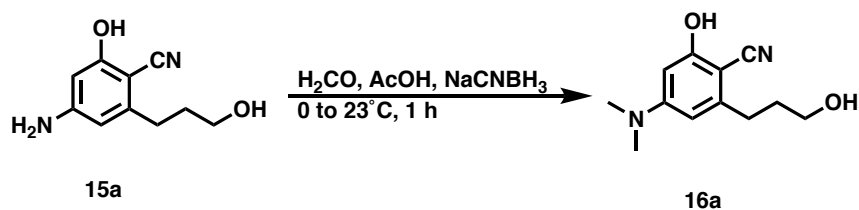
133.97, 129.44, 129.05, 128.94, 127.33, 119.05, 113.41, 110.68, 107.34, 97.01, 80.25, 71.87, 51.40. IR (film) 3096, 2924, 2854, 2341, 1698, 1580, 1532, 1434, 1348, 1318, 1222, 1111 cm^{-1} . HRMS (ESI/Q-TOF): $[\text{M}-\text{H}]^-$ calcd for $\text{C}_{17}\text{H}_{11}\text{N}_2\text{O}_4^-$, 307.0724; found 306.9934.

Synthesis of Compound 15a



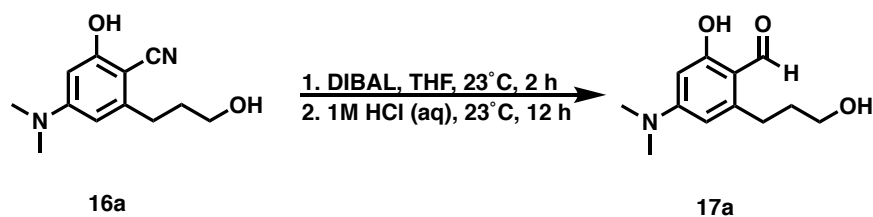
To a slurry of palladium on carbon (95.07 mg, 1 Eq, 893.3 μmol) in ethanol (10 mL) was added 2-(benzyloxy)-6-(3-hydroxyprop-1-yn-1-yl)-4-nitrobenzonitrile (275.4 mg, 1 Eq, 893.3 μmol) and the reaction vessel was sealed under argon. The reaction was sparged with argon for 5 minutes followed by hydrogen for 5 minutes, after which the reaction was stirred under a hydrogen atmosphere for 16 hours. The reaction was filtered through celite and concentrated under reduced pressure directly onto silica gel (1 g). The crude product was then purified by flash column chromatography (25 g silica gel, 10-90% EtOAc gradient against DCM with a 5% MeOH isocratic primer over 10 column volumes) to afford **15a** (108 mg, 62.9% yield) as an orange oil. TLC: R_f 0.34 (40:10:1 EtOAc:DCM:MeOH). ^1H NMR (500 MHz, CD_3CN): δ 6.11 (d, $J = 2.0$ Hz, 1H), 6.03 (d, $J = 2.0$ Hz, 1H), 4.73 (s, 1H), 3.53 (t, $J = 6.4$ Hz, 2H), 2.62 (t, $J = 7.9$ Hz, 2H), 1.76 (m, 3H). ^{13}C NMR (126 MHz, CD_3CN): δ 161.18, 153.17, 148.34, 107.15, 97.49, 87.48, 60.93, 33.13, 30.68. IR (film) 3349, 2921, 2851, 2329, 1611, 1426, 1330, 1258, 1099, 1022 cm^{-1} . HRMS (ESI/Q-TOF): $[\text{M}+\text{H}]^+$ calcd for $\text{C}_{10}\text{H}_{13}\text{N}_2\text{O}_2^+$, 193.0972; found 193.0988.

Synthesis of Compound 16a



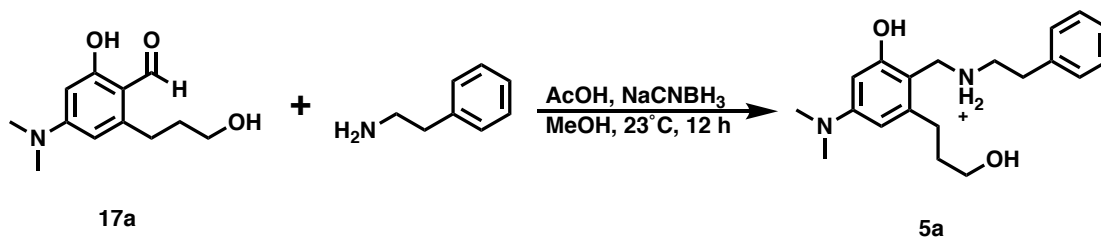
To a solution of 4-amino-2-hydroxy-6-(3-hydroxypropyl)benzonitrile (52.0 mg, 1 Eq, 271 μmol) in MeOH (2mL) at 0 °C was added formaldehyde (220 mg, 201 μL , 37% Wt, 10 Eq, 2.71 mmol), acetic acid (81.2 mg, 77.4 μL , 5 Eq, 1.35 mmol), and sodium cyanoborohydride (68.0 mg, 4 Eq, 1.08 mmol) sequentially. The reaction was brought up to 23 °C and stirred for 1 hour. The reaction was then concentrated under reduced pressure directly onto silica gel (1 g). The crude product was then purified by flash column chromatography (25 g silica gel, 10-100% EtOAc gradient against DCM with a 2% MeOH isocratic primer over 10 column volumes) to afford **16a** (37.9 mg, 63.6 % yield) as a yellow solid. TLC: R_f 0.38 (25:25:1 EtOAc:DCM:MeOH). ^1H NMR (500 MHz, CD_3CN): δ 7.84 (s, 1H), 6.19 (d, $J = 2.3$ Hz, 1H), 6.02 (d, $J = 2.3$ Hz, 1H), 3.54 (t, $J = 7.2$ Hz, 2H), 2.94 (s, 6H), 2.68 (t, $J = 7.9$ Hz, 2H), 2.37 (s, 1H), 1.80 (m, 2H). ^{13}C NMR (126 MHz, CD_3CN): δ 160.87, 153.96, 147.75, 117.59, 105.03, 95.33, 86.26, 61.02, 39.22, 33.44, 31.22. IR (film) 3343, 2928, 2855, 2204, 1607, 1571, 1522, 1400, 1273, 1136, 1062, 1022 cm^{-1} . HRMS (ESI/Q-TOF): $[\text{M}+\text{H}]^+$ calcd for $\text{C}_{12}\text{H}_{17}\text{N}_2\text{O}_2^+$, 221.1285; found 221.1312. m.p.: T_{on} 140.5 °C: T_{peak} 148.6 °C.

Synthesis of Compound 17a



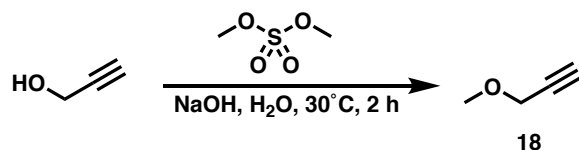
To a solution of 4-(dimethylamino)-2-hydroxy-6-(3-hydroxypropyl)benzonitrile (57.8 mg, 1 Eq, 262 μmol) in anhydrous THF was brought down to 0 °C and a solution of diisobutylaluminum hydride (299 mg, 1.91 mL, 1.1 molar, 8 Eq, 2.10 mmol) in cyclohexanes was added to the reaction dropwise over the course of 10 minutes. Upon complete addition the solution was brought up to room temperature and stirred for an additional 2 hours. The reaction was quenched by the slow addition of MeOH (10 mL) followed by an aq. 1M HCl solution (50 mL) and this solution was stirred for 12 hours. The aqueous solution was then extracted with EtOAc (3 x 75 mL), the organic layers were combined, washed with sat. aq. NaCl (50 mL), dried over MgSO_4 , and concentrated under reduced pressure directly onto silica gel (1 g). The crude product was then purified by flash column chromatography (25 g silica gel, 10-90% EtOAc gradient against DCM with a 1% MeOH isocratic primer over 10 column volumes) to afford **17a** (44.2 mg, 75.5 % yield) as an orange oil. TLC: R_f 0.44 (25:25:1 EtOAc:DCM:MeOH). ^1H NMR (500 MHz, CD_3CN): δ 12.72 (s, 1H), 9.88 (s, 1H), 6.18 (d, $J = 2.5$ Hz, 1H), 5.91 (d, $J = 2.5$ Hz, 1H), 3.54 (q, $J = 5.4$ Hz, 2H), 3.02 (s, 6H), 2.86 (q, $J = 5.7$ Hz, 2H), 2.68 (s, 1H), 1.79 (m, 2H). ^{13}C NMR (126 MHz, CD_3CN): δ 191.13, 165.98, 156.51, 148.50, 108.78, 105.98, 95.11, 60.83, 39.26, 35.42, 28.16. IR (film) 3364, 2926, 2853, 1626, 1562, 1512, 1396, 1309, 1147, 1066 cm^{-1} . HRMS (ESI/Q-TOF): $[\text{M}+\text{H}]^+$ calcd for $\text{C}_{12}\text{H}_{18}\text{NO}_3^+$, 224.1281; found 224.1300.

Synthesis of Compound 5a



Following General Procedure A using 4-(dimethylamino)-2-hydroxy-6-(3-hydroxypropyl)benzaldehyde (17a, 10.0 mg, 44.8 μmol) afforded **5a** (13.1 mg, 79.0% yield) as a purple oil. ^1H NMR (500 MHz, CD_3CN): δ 7.83 (s, 2H), 7.34 (t, $J = 7.3$ Hz, 2H), 7.26 (q, $J = 7.2$ Hz, 3H), 6.54 (d, $J = 2.2$ Hz, 1H), 6.47 (d, $J = 2.3$ Hz, 1H), 4.20 (s, 2H), 3.43 (t, $J = 5.8$ Hz, 2H), 3.25 (s, 2H), 2.99 (t, $J = 8.0$ Hz, 2H), 2.95 (s, 6H), 2.71 (t, $J = 7.2$ Hz, 2H), 1.79 (t, $J = 6.2$ Hz, 2H). ^{13}C NMR (126 MHz, CD_3CN): δ 157.36, 149.89, 144.01, 136.69, 128.86, 128.77, 127.12, 109.03, 107.86, 100.06, 59.61, 48.30, 43.34, 41.47, 33.22, 31.67, 27.66. IR (film) 3065, 2894, 1674, 1612, 1305, 1186, 1134 cm^{-1} . HRMS (ESI/Q-TOF): $[\text{M}+\text{H}]^+$ calcd for $\text{C}_{20}\text{H}_{29}\text{N}_2\text{O}_2^+$, 329.2224; found 329.2228.

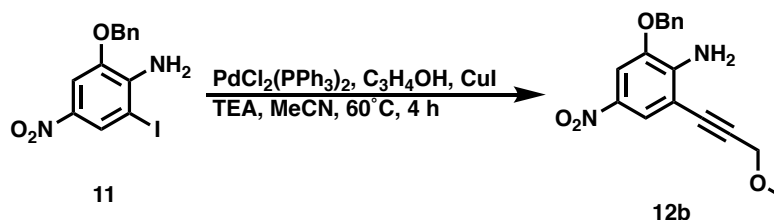
Synthesis of Compound 18



To a solution of propargyl alcohol (3.78 g, 3.89 mL, 1.7 Eq, 67.4 mmol) in water (5 mL) was slowly added an aq. 40% NaOH solution over 5 minutes, followed by the dropwise addition of dimethyl sulfate (5.00 g, 3.79 mL, 1 Eq, 39.6 mmol) over 2 hours (using a syringe pump). The solution was cooled to ensure the reaction contents were kept below 60 $^\circ\text{C}$. Upon complete addition, the solution was quickly distilled over a short distillation setup (1 atm) at 85 $^\circ\text{C}$. A milky white solution was collected and subsequently dried over calcium chloride for 16 hours. This suspension was once again distilled (1 atm) at 85 $^\circ\text{C}$ where the 3-methoxyprop-1-yne (1.71 g, 61.5% yield) was collected as a colorless oil. ^1H NMR (400 MHz, CD_3CN): δ 4.06 (d, $J = 2.4$ Hz,

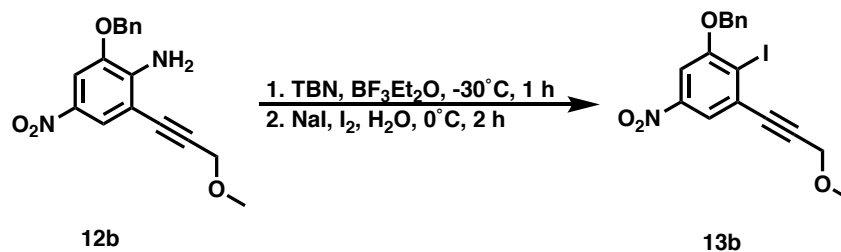
2H), 3.35 (s, 3H), 2.42 (t, $J = 2.4$ Hz, 1H). ^{13}C NMR (101 MHz, CD_3CN): δ 79.48, 74.49, 59.56, 57.49. IR (film) 3292, 2932, 2825, 1451, 1360, 1189, 1092, 1006 cm^{-1} . b.p. (760 Torr): 60 °C.

Synthesis of Compound 12b



To a solution of 2-(benzyloxy)-6-iodo-4-nitroaniline, tetrahydrofuran (4.00 g, 1 Eq, 9.04 mmol), copper(I) iodide (138 mg, 0.1 Eq, 724 μmol), and bis(triphenylphosphine)palladium(II) chloride (254 mg, 0.05 Eq, 362 μmol) in a 3:1 solution of $\text{MeCN}:\text{TEA}$, was added 3-methoxyprop-1-yne (710 mg, 855 μL , 1.4 Eq, 10.1 mmol). The reaction vessel was then quickly evacuated under vacuum and backfilled with argon (this was repeated 2 additional times), after which the contents were heated to 60°C for 4 hours. The reaction contents were then cooled to 23°C and filtered over celite. The solvent was removed under reduced pressure directly onto silica gel (10 g). The crude product was then purified by flash column chromatography (100 g silica gel, 10-80% EtOAc gradient against hexanes over 10 column volumes) to yield **12b** (2.58 g, 91.3% yield) as a brown solid. TLC: R_f 0.48 (2:3 $\text{EtOAc}:\text{hexanes}$). ^1H NMR (500 MHz, CD_3CN): δ 7.86 (d, $J = 2.4$ Hz, 1H), 7.69 (d, $J = 2.4$ Hz, 1H), 7.50 (q, $J = 3.0$ Hz, 2H), 7.40 (m, 3H), 5.60 (s, 2H), 5.22 (s, 2H), 4.36 (s, 2H), 3.39 (s, 3H). ^{13}C NMR (126 MHz, CD_3CN): δ 146.10, 144.07, 136.86, 136.24, 128.61, 128.29, 127.84, 121.61, 107.04, 104.17, 92.42, 80.04, 70.74, 59.86, 56.98. IR (film) 3492, 3376, 3097, 2933, 2884, 2823, 1613, 1504, 1312, 1277, 1167, 1093 cm^{-1} . HRMS (ESI/Q-TOF): $[\text{M}+\text{H}]^+$ calcd for $\text{C}_{17}\text{H}_{17}\text{N}_2\text{O}_4^+$, 313.1183; found 313.1217. m.p.: T_{on} 105.6 °C: T_{peak} 108.3 °C.

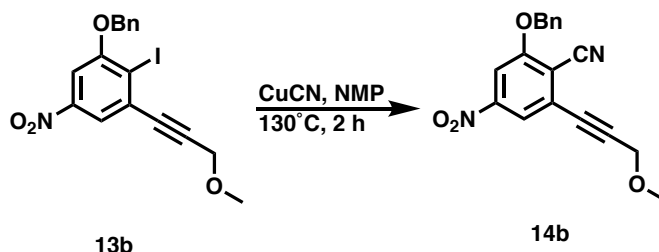
Synthesis of Compound 13b



To a solution boron trifluoride etherate (3.64 g, 3.25 mL, 4 Eq, 25.6 mmol) in anhydrous THF (40mL), was added a solution of 2-(benzyloxy)-6-(3-methoxyprop-1-yn-1-yl)-4-nitroaniline (2.00 g, 1 Eq, 6.40 mmol) in anhydrous THF (10mL) over 5 minutes and sealed under argon. After cooling the solution to -30 °C a solution of tert-butyl nitrite (2.64 g, 3.05 mL, 4 Eq, 25.6 mmol) in anhydrous THF (10mL) was added dropwise over the course of 30 minutes. The reaction was stirred for an additional 15 minutes following full addition of the tert-butyl nitrite solution and then brought up to 5 °C for 10 minutes. The diazonium intermediate was then precipitated out of solution by combining the reaction contents with 0.5 L of hexanes. The diazonium salt was filtered off and dissolved in anhydrous THF (10mL). Separately, a solution of potassium iodide (6.38 g, 6 Eq, 38.4 mmol) and iodine (813 mg, 0.5 Eq, 3.20 mmol) was prepared in water (175mL). The diazonium intermediate was added to the aqueous solution dropwise over the course of 30 minutes. Upon full addition, the reaction was analyzed via analytical HPLC which showed approximately 50% product formation. The reaction contents were then extracted ethyl acetate (3 x 125 mL). The organic layers were combined, washed with sat. aq. Na₂S₂O₃ (2 x 100 mL), sat. aq. NaCl (100 mL), dried over MgSO₄, and concentrated under reduced pressure directly onto silica gel (5g). The crude product was then purified by flash column chromatography (100 g silica gel, 4-30% EtOAc gradient against hexanes over 10 column volumes) to afford **13b** (982 mg, 36.2% yield) as a beige solid. TLC: R_f 0.35 (1:9 EtOAc:hexanes). ¹H NMR (500 MHz, CD₃CN): δ 7.83 (d, J = 2.4 Hz, 1H), 7.65 (d, J = 2.4 Hz, 1H), 7.52 (d, J = 7.4 Hz, 2H), 7.43 (t, J = 7.4 Hz, 2H), 7.37 (t, J = 7.3 Hz, 1H), 5.24 (s, 2H), 4.36 (s, 2H), 3.45 (s, 3H). ¹³C NMR (126 MHz, CD₃CN): δ 158.63, 148.90,

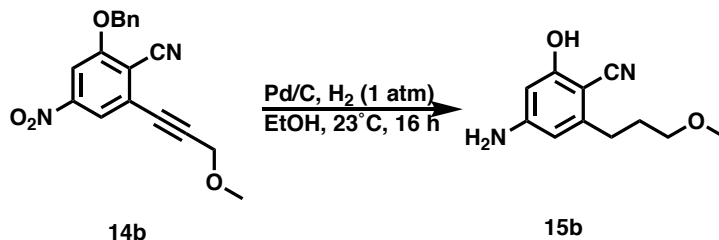
135.72, 131.52, 128.67, 128.35, 127.61, 119.19, 106.19, 101.78, 92.05, 86.27, 71.78, 59.64, 57.31.
IR (film) 3086, 3069, 2928, 2884, 2819, 1698, 1520, 1383, 1317, 1095 cm^{-1} . HRMS (ESI/Q-TOF):
[M+H]⁺ calcd for $\text{C}_{17}\text{H}_{15}\text{IN}_2\text{O}_4^+$, 424.0040; found 423.9999. m.p.: T_{on} 103.8 °C: T_{peak} 105.7 °C.

Synthesis of Compound 14b



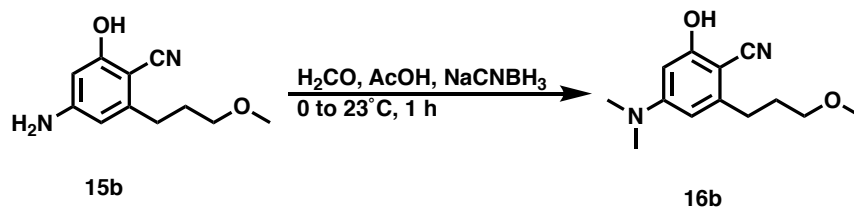
A solution of 1-(benzyloxy)-2-iodo-3-(3-methoxyprop-1-yn-1-yl)-5-nitrobenzene (250 mg, 1 Eq, 591 μmol) and cyanocopper (132 mg, 2.5 Eq, 1.48 mmol) in NMP (1 mL) was stirred at 130 °C for 2 hours. The reaction contents were cooled to 23 °C and poured into diethyl ether (175 mL), washed with water (3 x 50 mL), and sat. aq. NaCl (50 mL). The organic layer was dried over MgSO_4 and concentrated under reduced pressure directly onto silica gel (1 g). The crude product was then purified by flash column chromatography (25 g silica gel, 4-40% EtOAc gradient against hexanes over 10 column volumes) to afford **14b** (172 mg, 90.3% yield) as a yellow solid. TLC: R_f 0.39 (1:4 EtOAc:hexanes). ^1H NMR (500 MHz, CD_3CN): δ 7.96 (d, J = 2.0 Hz, 1H), 7.84 (d, J = 2.0 Hz, 1H), 7.51 (d, J = 7.4 Hz, 2H), 7.46 (m, 2H), 7.40 (m, 1H), 5.33 (s, 3H), 4.42 (s, 2H), 3.49 (s, 4H). ^{13}C NMR (126 MHz, CD_3CN): δ 160.99, 150.68, 134.35, 129.28, 128.91, 128.82, 127.49, 119.10, 113.39, 110.56, 107.38, 94.93, 80.80, 71.95, 59.99, 57.88. IR (film) 3090, 2993, 2931, 2880, 2824, 2228, 1531, 1436, 1346, 1314, 1226, 1211, 1097 cm^{-1} . HRMS (ESI/Q-TOF): [M+H]⁺ calcd for $\text{C}_{18}\text{H}_{15}\text{N}_2\text{O}_4^+$, 323.1026; found 323.1039. m.p.: T_{on} 101.7 °C: T_{peak} 104.5 °C.

Synthesis of Compound 15b



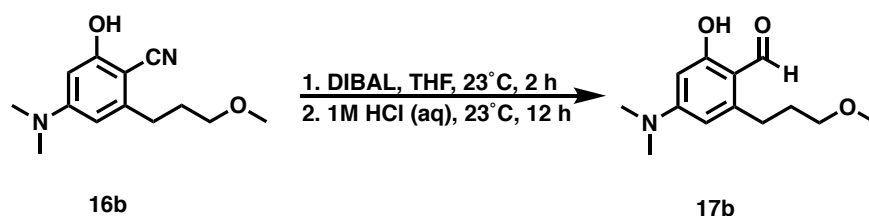
To a slurry of palladium on carbon (46.22 mg, 1 Eq, 434.4 μmol) in ethanol (10 mL) was added 2-(benzyloxy)-6-(3-methoxyprop-1-yn-1-yl)-4-nitrobenzonitrile (140.0 mg, 1 Eq, 434.4 μmol) and the reaction vessel was sealed under argon. The reaction was sparged with argon for 5 minutes followed by hydrogen for 5 minutes, after which the reaction was stirred under a hydrogen atmosphere for 16 hours. The reaction was filtered through celite and concentrated under reduced pressure directly onto silica gel (1 g). The crude product was then purified by flash column chromatography (25 g silica gel, 10-100% EtOAc gradient against hexanes with a 2% MeOH isocratic primer over 10 column volumes) to afford **15b** (87.5 mg, 97.7% yield) as an orange oil. TLC: R_f 0.46 (4:1 EtOAc:hexanes). ^1H NMR (500 MHz, CD_3CN): δ 6.08 (d, $J = 18.5$ Hz, 2H), 4.75 (s, 2H), 3.36 (t, $J = 6.3$ Hz, 2H), 3.27 (s, 3H), 2.61 (t, $J = 7.8$ Hz, 2H), 1.80 (qd, $J = 6.2, 9.6$ Hz, 2H). ^{13}C NMR (126 MHz, CD_3CN): δ 161.22, 153.19, 148.15, 117.18, 107.23, 97.57, 87.43, 71.37, 57.65, 30.86, 30.03. IR (film) 3366, 3227, 2932, 2885, 2205, 1609, 1583, 1467, 1286, 1171, 1106 cm^{-1} . HRMS (ESI/Q-TOF): $[\text{M}+\text{H}]^+$ calcd for $\text{C}_{11}\text{H}_{15}\text{N}_2\text{O}_2^+$, 207.1128; found 207.1174.

Synthesis of Compound 16b



To a solution of 4-amino-2-hydroxy-6-(3-methoxypropyl)benzonitrile (70.0 mg, 1 Eq, 339 μmol) in MeOH (2mL) at 0 °C was added formaldehyde (275 mg, 253 μL , 37% Wt, 10 Eq, 3.39 mmol), acetic acid (102 mg, 97.1 μL , 5 Eq, 1.70 mmol), and sodium cyanoborohydride (85.3 mg, 4 Eq, 1.36 mmol) sequentially. The reaction was brought up to 23 °C and stirred for 1 hour. The reaction was then concentrated under reduced pressure directly onto silica gel (1 g). The crude product was then purified by flash column chromatography (25 g silica gel, 10-80% EtOAc gradient against hexanes over 10 column volumes) to afford **16b** (69.88 mg, 87.9 % yield) as a yellow solid. TLC: R_f 0.28 (1:1 EtOAc:hexanes). ^1H NMR (500 MHz, CD_3CN): δ 7.63 (s, 1H), 6.18 (d, $J = 2.3$ Hz, 1H), 6.02 (d, $J = 2.3$ Hz, 1H), 3.37 (t, $J = 6.3$ Hz, 1H), 3.28 (s, 3H), 2.94 (s, 6H), 2.67 (t, $J = 7.9$ Hz, 2H), 1.84 (qd, $J = 6.2, 9.7$ Hz, 2H). ^{13}C NMR (126 MHz, CD_3CN): δ 160.74, 153.93, 147.57, 117.22, 105.13, 95.37, 86.29, 71.43, 57.66, 39.22, 31.40, 30.37. IR (film) 3203, 2983, 2919, 2868, 2815, 2205, 1607, 1568, 1519, 1399, 1385, 1284, 1115 cm^{-1} . HRMS (ESI/Q-TOF): $[\text{M}+\text{H}]^+$ calcd for $\text{C}_{13}\text{H}_{19}\text{N}_2\text{O}_2^+$, 235.1441; found 235.1483. m.p.: T_{on} 149.9 °C: T_{peak} 153.7 °C.

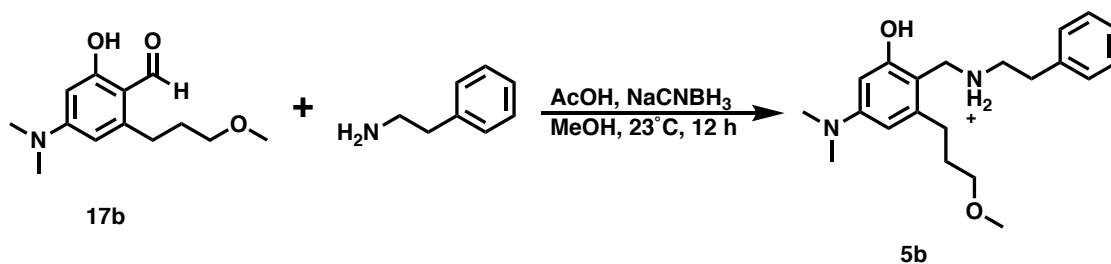
Synthesis of Compound 17b



To a solution of 4-(dimethylamino)-2-hydroxy-6-(3-methoxypropyl)benzonitrile (55.0 mg, 1 Eq, 235 μmol) in anhydrous THF was brought down to 0 °C and a solution of diisobutylaluminum hydride (267 mg, 1.71 mL, 1.1 molar, 8 Eq, 1.88 mmol) in cyclohexanes was added to the reaction dropwise over the course of 10 minutes. Upon complete addition the solution was brought up to

room temperature and stirred for an additional 2 hours. The reaction was quenched by the slow addition of MeOH (10 mL) followed by an aq. 1 M HCl solution (50 mL) and this solution was stirred for 12 hours. The aqueous solution was then extracted with EtOAc (3 x 75 mL), the organic layers were combined, washed with sat. aq. NaCl (50 mL), dried over MgSO₄, and concentrated under reduced pressure directly onto silica gel (1 g). The crude product was then purified by flash column chromatography (25 g silica gel, 10-80% EtOAc gradient against DCM with a 1% MeOH isocratic primer over 10 column volumes) to afford **17b** (42.4 mg, 76.2 % yield) as an orange oil. TLC: R_f 0.57 (1:1 EtOAc:hexanes). ¹H NMR (500 MHz, CD₃CN): δ 12.72 (s, 1H), 9.86 (s, 1H), 6.16 (d, J = 2.5 Hz, 1H), 5.91 (d, J = 2.5 Hz, 1H), 3.36 (t, J = 6.2 Hz, 2H), 3.27 (s, 3H), 3.02 (s, 6H), 2.84 (t, J = 7.8 Hz, 2H), 1.83 (qd, J = 6.2, 9.5 Hz, 2H). ¹³C NMR (126 MHz, CD₃CN): δ 191.06, 165.96, 156.47, 148.16, 108.83, 106.03, 95.16, 71.22, 57.71, 39.25, 32.19, 28.20. IR (film) 2922, 2871, 2826, 1621, 1554, 1510, 1321, 1267, 1144, 1113 cm⁻¹. HRMS (ESI/Q-TOF): [M+H]⁺ calcd for C₁₃H₂₀NO₃⁺, 238.1438; found 238.1458.

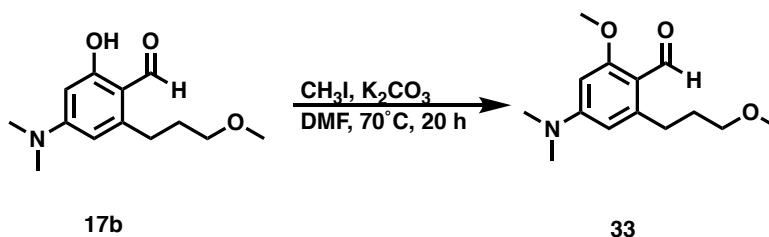
Synthesis of Compound 5b



Following General Procedure A using 4-(dimethylamino)-2-hydroxy-6-(3-methoxypropyl)benzaldehyde (**17b**, 7.5 mg, 32 μmol) afforded **5b** (8.6 mg, 71.0% yield) as a purple oil. ¹H NMR (500 MHz, CD₃CN): δ 7.57 (s, 2H), 7.35 (m, 6H), 6.40 (d, J = 2.3 Hz, 1H), 6.33 (d, J = 2.4 Hz, 1H), 4.17 (s, 2H), 3.32 (t, J = 6.1 Hz, 2H), 3.26 (s, 6H), 3.01 (t, J = 7.8 Hz,

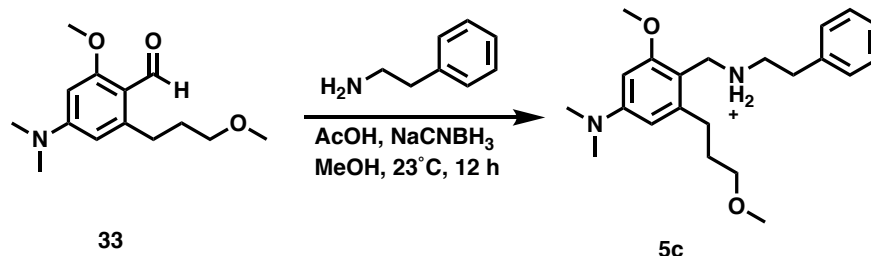
2H), 2.92 (s, 6H), 2.64 (t, $J = 7.6$ Hz, 2H), 1.76 (m, 2H). ^{13}C NMR (126 MHz, CD_3CN): δ 157.14, 150.89, 143.72, 136.64, 128.88, 128.79, 127.15, 107.05, 106.60, 98.91, 70.80, 57.49, 48.28, 43.75, 40.57, 31.63, 30.71, 28.84. IR (film) 3082, 2935, 1675, 1609, 1432, 1304, 1202, 1135 cm^{-1} . HRMS (ESI/Q-TOF): $[\text{M}+\text{H}]^+$ calcd for $\text{C}_{21}\text{H}_{31}\text{N}_2\text{O}_2^+$, 343.2380; found 343.2401.

Synthesis of Compound 33



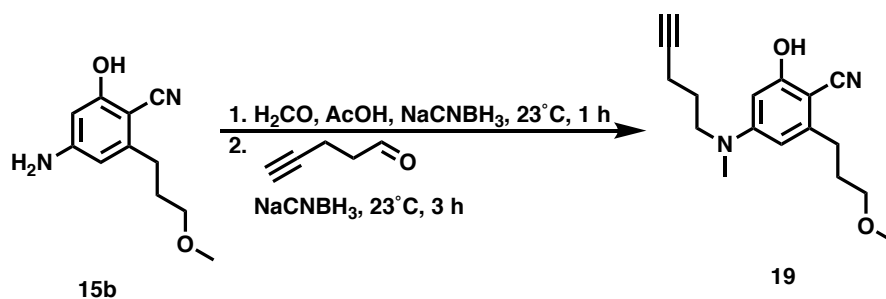
To a solution of 4-(dimethylamino)-2-hydroxy-6-(3-methoxypropyl)benzaldehyde (17.0 mg, 1 Eq, 71.6 μmol) and potassium carbonate (74.3 mg, 7.5 Eq, 537 μmol) in DMF (1 mL) was added the iodomethane (102 mg, 44.8 μL , 10 Eq, 716 μmol). The solution was sealed under argon and the contents were heated to 70 $^\circ\text{C}$ for 20 hours. The reaction was concentrated under reduced pressure directly onto silica (0.5 g). The crude product was then purified by flash column chromatography (10 g silica gel, 10-90% EtOAc gradient against hexanes over 10 column volumes) to afford **33** (7.62 mg, 42.3 %) as a white solid. TLC: 0.47 (1:1 EtOAc:hexanes). ^1H NMR (500 MHz, CD_3CN): δ 10.35 (s, 1H), 6.10 (d, $J = 2.3$ Hz, 1H), 5.97 (d, $J = 2.3$ Hz, 1H), 3.87 (s, 3H), 3.44 (t, $J = 6.4$ Hz, 2H), 3.35 (s, 3H), 3.06 (s, 6H), 3.00 (t, $J = 7.7$ Hz, 2H), 1.83 (m, 2H). ^{13}C NMR (126 MHz, CD_3CN): δ 188.96, 165.74, 154.51, 147.97, 112.58, 106.85, 91.71, 72.56, 58.53, 55.52, 40.10, 31.68, 30.99. IR (film) 2942, 2856, 1652, 1598, 1535, 1368, 1282, 1284, 1243, 1115 cm^{-1} . HRMS (ESI/Q-TOF): $[\text{M}+\text{H}]^+$ calcd for $\text{C}_{14}\text{H}_{22}\text{NO}_3^+$, 252.1594; found 252.1634. m.p.: T_{on} 48.2 $^\circ\text{C}$: T_{peak} 52.7 $^\circ\text{C}$

Synthesis of Compound 5c



Following General Procedure A using the benzaldehyde 33 afforded **5c** (13.2 mg, 22.6 μ mol, 81 %) viscous yellow oil. ¹H NMR (500 MHz, CD₃CN): δ 7.55 (s, 1H), 7.36 (t, J = 7.3 Hz, 5H), 7.28 (m, 8H), 6.30 (d, J = 2.3 Hz, 2H), 6.27 (d, J = 2.3 Hz, 2H), 4.14 (t, J = 5.7 Hz, 2H), 3.75 (s, 3H), 3.32 (t, J = 6.1 Hz, 2H), 3.26 (m, 5H), 3.01 (t, J = 7.7 Hz, 2H), 2.97 (s, 6H), 2.65 (t, J = 7.6 Hz, 2H), 1.76 (m, 2H). ¹³C NMR (126 MHz, CD₃CN): δ 159.28, 151.71, 143.65, 136.64, 128.92, 128.82, 127.19, 106.53, 106.00, 94.11, 70.87, 57.53, 55.12, 48.11, 43.54, 40.19, 31.57, 30.86, 28.94. IR (film) 2997, 1686, 1610, 1465, 1412, 1159, 1114 cm⁻¹. HRMS (ESI/Q-TOF): [M+H]⁺ calcd for C₂₂H₃₃N₂O₂⁺, 357.2537; found 357.2585.

Synthesis of Compound 19



To a solution of 4-amino-2-hydroxy-6-(3-methoxypropyl)benzonitrile (125.0 mg, 1 Eq, 606.1 μ mol) in MeOH (5 mL) at 0 °C was added formaldehyde (49.19 mg, 45.13 μ L, 37% Wt, 1 Eq, 606.1 μ mol), acetic acid (182.0 mg, 173.5 μ L, 5 Eq, 3.030 mmol), and sodium cyanoborohydride (95.21 mg, 2.5 Eq, 1.515 mmol) sequentially. This solution was then brought up to 23 °C and

stirred for 1 hour until full conversion of the starting material was noted via TLC. At this point pent-4-ynal (74.64 mg, 1.5 Eq, 909.1 μmol) was added and the solution was stirred at 23 °C for an additional 3 hours. The reaction was then concentrated under reduced pressure directly onto silica gel (1g). The crude product was purified by flash column chromatography (25 g silica gel, 5-50% EtOAc gradient against hexanes 10 column volumes) to afford **19** (102.8 mg, 59.2 % yield) as a yellow solid. TLC: R_f 0.25 (2:3 EtOAc:hexanes). ^1H NMR (500 MHz, CD_3CN): δ 6.18 (d, $J = 2.3$ Hz, 1H), 6.05 (d, $J = 2.3$ Hz, 1H), 5.94 (s, 1H), 3.44 (m, 4H), 3.36 (s, 3H), 2.98 (s, 3H), 2.75 (t, $J = 7.8$ Hz, 2H), 2.23 (dt, $J = 2.6, 6.7$ Hz, 2H), 2.04 (t, $J = 2.6$ Hz, 1H), 1.93 (qd, $J = 6.2, 9.5$ Hz, 2H), 1.79 (m, 2H). ^{13}C NMR (126 MHz, CD_3CN): δ 160.12, 152.98, 147.32, 117.34, 105.60, 95.82, 86.37, 83.22, 71.74, 69.46, 58.61, 50.91, 38.64, 31.80, 30.46, 25.61, 15.90. IR (film) 3268, 3163, 2926, 2871, 2832, 2210, 1614, 1571, 1517, 1455, 1403, 1368, 1272, 1157, 1110 cm^{-1} . HRMS (ESI/Q-TOF): $[\text{M}+\text{H}]^+$ calcd for $\text{C}_{17}\text{H}_{23}\text{N}_2\text{O}_2^+$, 287.1754; found 287.1758. m.p.: T_{on} 101.4 °C; T_{peak} 112.4 °C

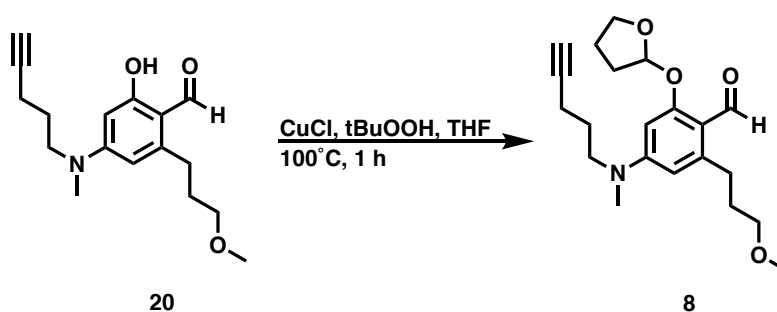
Synthesis of Compound 20



To a solution of 2-hydroxy-6-(3-methoxypropyl)-4-(methyl(pent-4-yn-1-yl)amino)benzonitrile (42.0 mg, 1 Eq, 147 μmol) in anhydrous THF was brought down to 0 °C and a solution of diisobutylaluminum hydride (125 mg, 800 μL , 1.1 molar, 6 Eq, 880 μmol) in cyclohexanes was added to the reaction dropwise over the course of 10 minutes. Upon complete

addition the solution was brought up to room temperature and stirred for an additional 2 hours. The reaction was quenched by the slow addition of MeOH (10 mL) followed by an aq. 1M HCl solution (50 mL) and this solution was stirred for 12 hours. The aqueous solution was then extracted with EtOAc (3 x 75 mL), the organic layers were combined, washed with sat. aq. NaCl (50 mL), dried over MgSO₄, and concentrated under reduced pressure directly onto silica gel (1 g). The crude product was then purified by flash column chromatography (25 g silica gel, 10-60% EtOAc gradient against hexanes over 10 column volumes) to afford **20** (29.6 mg, 69.7 % yield) as an orange oil. TLC: R_f 0.59 (1:1 EtOAc:hexanes). ¹H NMR (500 MHz, CD₃CN): δ 12.66 (s, 1H), 9.88 (s, 1H), 6.10 (d, J = 2.4 Hz, 1H), 5.96 (d, J = 2.4 Hz, 1H), 3.50 (t, J = 7.3 Hz, 2H), 3.38 (t, J = 6.0 Hz, 2H), 3.33 (s, 3H), 3.03 (s, 3H), 2.86 (t, J = 7.7 Hz, 2H), 2.24 (dt, J = 2.6, 6.7 Hz, 2H), 2.04 (t, J = 2.6 Hz, 1H), 1.88 (m, 2H), 1.81 (m, 2H). ¹³C NMR (126 MHz, CD₃CN): δ 190.58, 166.17, 155.35, 147.81, 109.35, 105.84, 95.81, 83.09, 71.43, 69.52, 58.66, 50.88, 38.69, 32.32, 28.73, 25.84, 15.90. IR (film) 3284, 2928, 2879, 2832, 1628, 1556, 1508, 1399, 1317, 1263, 1170, 1114 cm⁻¹. HRMS (ESI/Q-TOF): [M+H]⁺ calcd for C₁₇H₂₄NO₃⁺, 290.1751; found 290.1699.

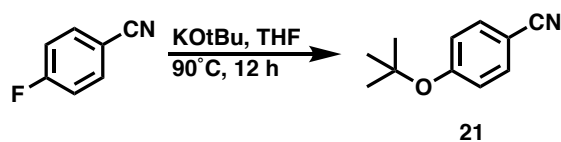
Synthesis of Compound 8



To a suspension of 2-hydroxy-6-(3-methoxypropyl)-4-(methyl(pent-4-yn-1-yl)amino)benzaldehyde (**20**, 6.0 mg, 1 Eq, 21 μmol) and copper(I) chloride (0.10 mg, 0.05 Eq, 1.0 μmol) in tetrahydrofuran (0.45 g, 0.50 mL, 300 Eq, 6.2 mmol) was added tert-butyl hydroperoxide

(8.0 mg, 8.6 μ L, 70% Wt, 3 Eq, 62 μ mol). The reaction contents were then heated to 100 $^{\circ}$ C and stirred for 45 minutes in a sealed dram vial. The reaction was then cooled down to 23 $^{\circ}$ C where full conversion of 20 was noted via TLC. The reaction was then concentrated under reduced pressure directly onto silica (0.5g). The crude product was then purified by flash column chromatography (10 g alumina, 6-50% EtOAc gradient against hexanes over 10 column volumes) to afford **8** (6.1 mg, 82 %) as a red oil. TLC: R_f 0.64 (2:3 EtOAc:hexanes). ^1H NMR (500 MHz, CD_3CN): δ 10.26 (d, J = 0.6 Hz, 1H), 6.35 (d, J = 2.5 Hz, 1H), 6.19 (d, J = 2.4 Hz, 1H), 5.86 (q, J = 1.8 Hz, 1H), 4.04 (m, 1H), 3.94 (m, 1H), 3.52 (m, 2H), 3.40 (t, J = 6.5 Hz, 2H), 3.32 (s, 3H), 3.04 (s, 3H), 2.95 (dt, J = 4.4, 7.7 Hz, 2H), 2.20 (m, 5H), 2.09 (t, J = 2.7 Hz, 1H), 1.97 (m, 1H), 1.83 (m, 2H), 1.77 (m, 2H). ^{13}C NMR (126 MHz, CD_3CN): δ 188.71, 163.72, 153.46, 147.34, 113.24, 107.68, 103.28, 95.92, 83.40, 72.41, 68.99, 68.37, 58.18, 50.81, 38.38, 32.73, 31.54, 30.89, 25.84, 23.38, 15.80. IR (film) 2925, 2875, 2832, 1659, 1598, 1546, 1386, 1284, 1160, 1114, 1035 cm^{-1} . HRMS (ESI/Q-TOF): $[\text{M}+\text{H}]^+$ calcd for $\text{C}_{21}\text{H}_{30}\text{NO}_4^+$, 360.2173; found 360.2150.

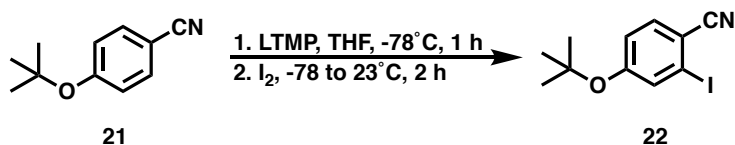
Synthesis of Compound 21



To a solution of 4-fluorobenzonitrile (5.00 g, 1 Eq, 41.3 mmol) in anhydrous THF (100 mL), potassium *tert*-butoxide (5.79 g, 1.25 Eq, 51.6 mmol) was added and the reaction contents were heated to reflux for 22 hours. The reaction contents were combined with 300mL of diethyl ether, which was washed with 1M aq. NaOH (2x 100 mL), sat. aq. NaCl (75 mL), the organic layer was dried over MgSO_4 and concentrated under reduced pressure directly onto silica gel (5 g). The crude product was then purified by flash column chromatography (25 g silica gel, 10-100% DCM

gradient against hexanes over 10 column volumes) to afford **21** (6.56 g, 90.7 % yield) as a tan oil. TLC: R_f 0.45 (1:9 EtOAc:hexanes). ^1H NMR (400 MHz, CD_3CN): δ 7.53 (d, $J = 8.9$ Hz, 2H), 7.02 (d, $J = 8.9$ Hz, 2H), 1.39 (s, 9H). ^{13}C NMR (101 MHz, CD_3CN): δ 159.92, 133.38, 122.96, 119.13, 105.65, 80.19, 28.83. IR (film) 2980, 2935, 2225, 1602, 1499, 1368, 1250, 1152 cm^{-1} . HRMS (ESI/Q-TOF): $[\text{M}+\text{H}]^+$ calcd for $\text{C}_{11}\text{H}_{14}\text{NO}^+$, 176.1070; found 176.1099.

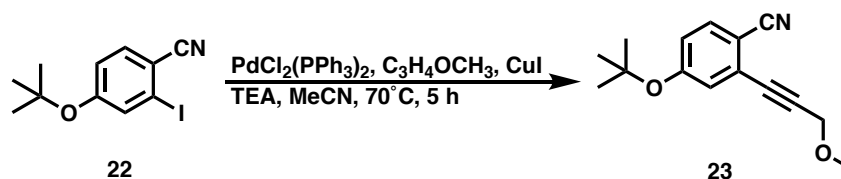
Synthesis of Compound 22



A solution of 2,2,6,6-tetramethyl piperidine (11.9 g, 14.3 mL, 1.2 Eq, 84.2 mmol) in anhydrous THF (50 mL) was cooled to -30 °C and a solution of nBuLi (5.40 g, 35.1 mL, 2.4 molar, 1.2 Eq, 84.2 mmol) in hexanes was added dropwise over 5 minutes. This solution was stirred for 30 min at -30 °C and then cooled to -78 °C. This LiTMP solution was then slowly cannulated (~15 minutes) into a solution of 4-(tert-butoxy)benzonitrile (12.3 g, 1 Eq, 70.2 mmol) in anhydrous THF (120 mL). Upon full addition, the reaction was stirred for 1 hour at -78 °C. At this point, a solution of iodine (31.2 g, 1.75 Eq, 123 mmol) in anhydrous THF (10 mL) was added to the reaction dropwise over 5 minutes forming a red solution upon full addition. Following one hour of stirring at -78 °C the solution was brought up to 23 °C and combined with diethyl ether (400mL). This solution was washed with sat. aq. $\text{Na}_2\text{S}_2\text{O}_3$ (2 x 100 mL), 0.1M aq. HCl (2 x 50 mL), sat. aq. NaCl (50 mL), dried over MgSO_4 , and concentrated under reduced pressure. The crude product was then purified by a manual flash column chromatography (200 g, 3:2 petroleum ether to benzene isocratic solvent system) affording **22** (11.1 g, 52.5% yield) as a yellow solid. TLC: R_f 0.44 (benzene). ^1H NMR (600 MHz, CD_3CN): δ 7.56 (d, $J = 8.6$ Hz, 1H), 7.53 (d, $J = 2.2$ Hz, 1H), 7.11

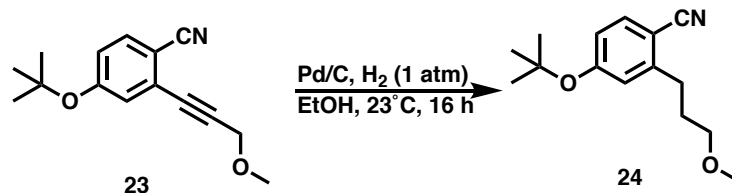
(dd, $J = 2.3, 8.6$ Hz, 1H), 1.37 (s, 9H). ^{13}C NMR (126 MHz, CD_3CN): δ 160.04, 135.08, 132.91, 122.10, 119.61, 113.37, 98.29, 81.09, 27.91. IR (film) 2980, 2934, 2217, 1578, 1546, 1478, 1458, 1366, 1301, 1233, 1156, 1021 cm^{-1} . HRMS (ESI/Q-TOF): $[\text{M}+\text{H}]^+$ calcd for $\text{C}_{11}\text{H}_{13}\text{INO}^+$, 302.0036; found 302.0057. m.p.: T_{on} 84.3 $^{\circ}\text{C}$: T_{peak} 89.7 $^{\circ}\text{C}$

Synthesis of Compound 23



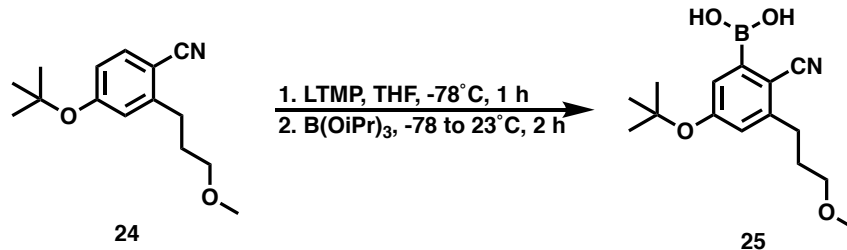
To a solution of 4-(tert-butoxy)-2-iodobenzonitrile (2.00 g, 1 Eq, 6.64 mmol), copper(I) iodide (126 mg, 0.1 Eq, 664 μmol), and bis(triphenylphosphine)palladium(II) chloride (233 mg, 0.05 Eq, 332 μmol) in a 3:1 solution of $\text{MeCN}:\text{TEA}$, was added 3-methoxyprop-1-yne (745 mg, 1.6 Eq, 10.6 mmol). The reaction vessel was then quickly evacuated under vacuum and backfilled with argon (this was repeated 2 additional times), after which the contents were heated to $70\text{ }^{\circ}\text{C}$ for 4 hours. The reaction contents were then cooled to $23\text{ }^{\circ}\text{C}$ and filtered over celite. The solvent was removed under reduced pressure directly onto silica gel (10 g). The crude product was then purified by flash column chromatography (100 g silica gel, 4-40% EtOAc gradient against hexanes over 10 column volumes) to afford **23** (1.44 g, 89.1% yield) as a brown oil. TLC: R_f 0.46 (1:4 $\text{EtOAc}:\text{hexanes}$). ^1H NMR (400 MHz, CD_3CN): δ 7.61 (d, $J = 8.6$ Hz, 1H), 7.14 (d, $J = 2.4$ Hz, 1H), 7.08 (dd, $J = 2.4, 8.6$ Hz, 1H), 4.33 (s, 2H), 3.40 (s, 3H), 1.36 (s, 9H). ^{13}C NMR (101 MHz, CD_3CN): δ 159.73, 134.12, 127.27, 125.89, 123.16, 117.57, 108.23, 91.48, 82.00, 80.67, 59.57, 57.06, 27.95. IR (film) 2980, 2934, 2824, 2226, 1592, 1553, 1485, 1369, 1301, 1159, 1097 cm^{-1} . HRMS (ESI/Q-TOF): $[\text{M}+\text{H}]^+$ calcd for $\text{C}_{15}\text{H}_{18}\text{NO}_2^+$, 244.1332; found 244.1345.

Synthesis of Compound 24



To a slurry of palladium on carbon (3.5 g, 1 Eq, 32 mmol) in ethanol (80 mL) was added 4-(tert-butoxy)-2-(3-methoxyprop-1-yn-1-yl)benzonitrile (7.9 g, 1 Eq, 32 mmol) and the reaction vessel was sealed under argon. The reaction was sparged with argon for 5 minutes followed by hydrogen for 5 minutes, after which the reaction was stirred under a hydrogen atmosphere for 16 hours. The reaction was filtered through celite and concentrated under reduced pressure directly onto silica gel (2 g). The crude product was then purified by flash column chromatography (50 g silica gel, 3-30% EtOAc gradient against hexanes over 10 column volumes) to afford **24** (7.71 g, 96.1% yield) as a beige oil. TLC: R_f 0.49 (1:4 EtOAc:hexanes). ¹H NMR (500 MHz, CD₃CN): δ 7.56 (d, $J = 8.5$ Hz, 1H), 6.98 (d, $J = 2.3$ Hz, 1H), 6.94 (dd, $J = 8.5, 2.4$ Hz, 1H), 3.37 (t, $J = 6.2$ Hz, 2H), 3.28 (s, 3H), 2.82 (t, $J = 7.8$ Hz, 2H), 1.87 (m, 2H), 1.38 (s, 9H). ¹³C NMR (126 MHz, CD₃CN): δ 160.87, 148.65, 134.86, 124.32, 121.45, 119.06, 106.36, 80.79, 72.05, 58.60, 28.98. IR (film) 2978, 2931, 2871, 2827, 2219, 1600, 1561, 1489, 1368, 1247, 1156, 1116 cm⁻¹. HRMS (ESI/Q-TOF): $[M+H]^+$ calcd for C₁₅H₂₂NO₂⁺, 248.1645; found 248.1664.

Synthesis of Compound 25

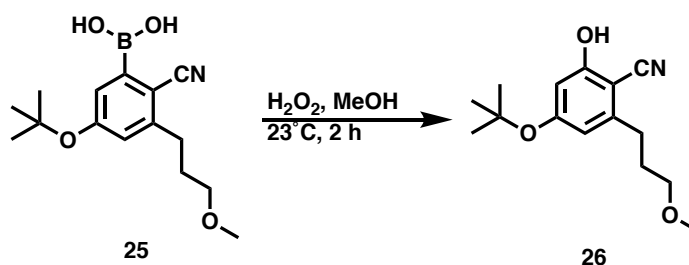


A solution of 2,2,6,6-tetramethyl piperidine (500 mg, 599 μ L, 1.75 Eq, 3.54 mmol) in anhydrous THF (50 mL) was cooled to -30 $^{\circ}$ C and a solution of nBuLi (227 mg, 1.42 mL, 2.5 molar, 1.75 Eq, 3.54 mmol) in hexanes was added dropwise over 5 minutes. This solution was stirred for 30 min at -30 $^{\circ}$ C and then cooled to -78 $^{\circ}$ C. This LiTMP solution was then slowly cannulated (~15 minutes) into a solution of 4-(tert-butoxy)-2-(3-methoxypropyl)benzonitrile (500 mg, 1 Eq, 2.02 mmol) in anhydrous THF (120 mL). Upon full addition, the reaction was stirred for 1 hour at -78 $^{\circ}$ C. At this point, a solution of triisopropyl borate (760 mg, 933 μ L, 2 Eq, 4.04 mmol) in anhydrous THF (10 mL) was added to the reaction dropwise over 5 minutes. Following one hour of stirring at -78 $^{\circ}$ C the reaction was quenched by the slow addition of MeOH (5 mL) followed by aq. 0.1M HCl (5 mL). The reaction contents were brought up to 23 $^{\circ}$ C and combined with a biphasic mixture of ethyl acetate (300mL) and aq. 0.1M HCl (100 mL). The organic layer was collected and washed with sat. aq. NaCl (50 mL), dried over MgSO₄, and concentrated under reduced pressure. The crude product was then purified by recrystallization (1:20 benzene to hexanes) affording **25** (279 mg, 47.4% yield at 90% purity*) as a beige solid. ¹H NMR (400 MHz, CD₃CN): δ 7.01 (d, J = 2.1 Hz, 1H), 6.96 (d, J = 2.3 Hz, 1H), 3.38 (t, J = 6.2 Hz, 2H), 3.30 (s, 3H), 2.83 (t, J = 7.7 Hz, 2H), 1.87 (m, 2H), 1.37 (s, 9H). ¹³C NMR (101 MHz, CD₃CN): δ 158.99, 147.66, 133.67, 123.68, 123.15, 120.24, 118.30, 79.53, 71.11, 57.42, 30.81, 30.22, 27.85. IR (film) 3210, 2977, 2927, 2871, 2218, 1720, 1601, 1586, 1449, 1427, 1367, 1273, 1248, 1156, 1114 cm⁻¹

¹. HRMS (ESI/Q-TOF): [M+H]⁺ calcd for C₁₅H₂₃NBO₄⁺, 292.1715; found 292.1733. m.p.: T_{on} 141.2 °C: T_{peak} 170.1 °C

*Note 1. The aryl boronic acid was only purified to ~90% purity where the impurity was the unmodified aryl starting material which is nonreactive in the subsequent oxidation and can be easily purified away from the phenol.

Synthesis of Compound 26

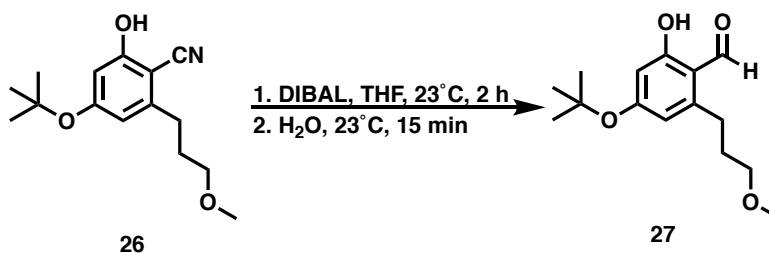


A solution of (5-(tert-butoxy)-2-cyano-3-(3-methoxypropyl)phenyl)boronic acid (175.0 mg, 1 Eq, 601.1 μmol) (~90% pure from the previous step) in ethanol (4 mL) was added hydrogen peroxide (204.4 mg, 184.2 μL, 30% Wt, 3 Eq, 1.803 mmol) and this was stirred at 22 °C for 2 hours. The reaction was then concentrated under reduced pressure directly onto silica gel (1g). The crude product was then purified by flash column chromatography (25 g silica gel, 8-80% EtOAc gradient against hexanes over 10 column volumes) to afford **26** (130 mg, 82.1% yield) as a yellow oil. TLC: R_f 0.40 (2:3 EtOAc:hexanes). ¹H NMR (500 MHz, CD₃CN): δ 6.47 (d, J = 1.8 Hz, 1H), 6.45 (d, J = 1.9 Hz, 1H), 3.36 (t, J = 6.3 Hz, 2H), 3.27 (d, J = 0.4 Hz, 3H), 2.73 (t, J = 7.8 Hz, 2H), 1.84 (m, 2H), 1.38 (d, J = 0.5 Hz, 9H). ¹³C NMR (126 MHz, CD₃CN): δ 161.70, 160.89, 147.57, 115.85, 114.40, 106.21, 93.42, 79.41, 71.12, 57.37, 30.63, 30.00, 27.81. IR (film) 3257,

2979, 2934, 2872, 2219, 1738, 1702, 1604, 1580, 1432, 1368, 1315, 1278, 1251, 1152, 1117 cm^{-1}

¹. HRMS (ESI/Q-TOF): $[\text{M}+\text{H}]^+$ calcd for $\text{C}_{15}\text{H}_{22}\text{NO}_3^+$, 264.1594; found 264.1609.

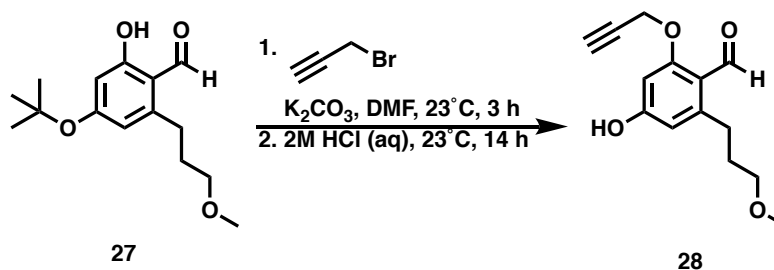
Synthesis of Compound 27



To a solution of 4-(tert-butoxy)-2-hydroxy-6-(3-methoxypropyl)benzonitrile (200.0 mg, 1 Eq, 759.5 μmol) in anhydrous THF was brought down to 0 °C and a solution of diisobutylaluminum hydride (864.1 mg, 5.523 mL, 1.1 molar, 8 Eq, 6.076 mmol) in cyclohexane was added to the reaction dropwise over the course of 10 minutes. Upon complete addition the solution was brought up to room temperature and stirred for an additional 2 hours. The reaction was quenched by the slow addition of MeOH (10 mL) followed by an aq. 0.1M HCl solution (20 mL) and this solution was stirred for 15 minutes. The reaction contents were then added to aq. 0.1M HCl (100mL), extracted with EtOAc (3 x 100 mL), the organic layers were combined, washed with sat. aq. NaCl (50 mL), dried over MgSO_4 , and concentrated under reduced pressure directly onto silica gel (1 g). The crude product was then purified by flash column chromatography (25 g silica gel, 8-70% EtOAc gradient against hexanes over 10 column volumes) to afford **27** (111.2 mg, 55.0 % yield) as a tan solid. TLC: R_f 0.73 (2:3 EtOAc:hexanes). ¹H NMR (500 MHz, CD_3CN): δ 12.34 (s, 1H), 10.11 (s, 1H), 6.38 (d, $J = 2.3$ Hz, 1H), 6.36 (d, $J = 2.3$ Hz, 1H), 3.34 (t, $J = 6.2$ Hz, 2H), 3.27 (s, 3H), 2.91 (t, $J = 7.7$ Hz, 2H), 1.84 (m, 2H), 1.44 (s, 9H). ¹³C NMR (126 MHz, CD_3CN): δ 194.22, 165.35, 164.08, 148.61, 114.87, 113.08, 105.67, 80.16, 70.92, 57.66, 32.00, 28.09, 27.61. IR (film)

3275, 2979, 2931, 2873, 2828, 1623, 1563, 1482, 1369, 1296, 1228, 1204, 1158, 1118 cm^{-1} . HRMS (ESI/Q-TOF): $[\text{M}+\text{H}]^+$ calcd for $\text{C}_{15}\text{H}_{23}\text{O}_4^+$, 267.1591; found 267.1585.

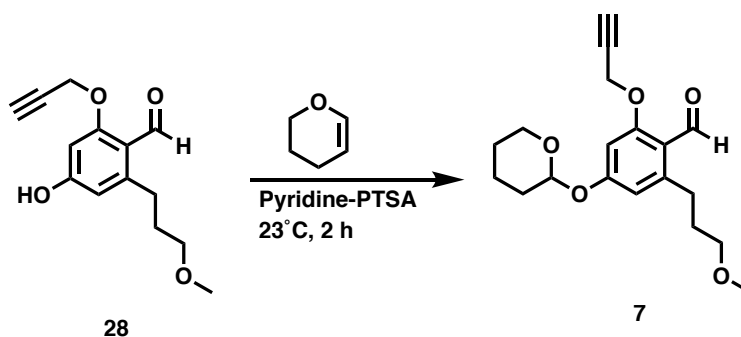
Synthesis of Compound 28



A solution of 4-(tert-butoxy)-2-hydroxy-6-(3-methoxypropyl)benzaldehyde (100.0 mg, 1 Eq, 375.5 μmol) and potassium carbonate (77.83 mg, 1.5 Eq, 563.2 μmol) in anhydrous DMF (4 mL) was stirred at 23°C for 5 minutes. The propargyl bromide, (72.58 mg, 52.63 μL , 80% Wt, 1.3 Eq, 488.1 μmol) was then slowly added over 5 minutes and the reaction was stirred for 3 hours. At this point, 12 mL of aq. 1M HCl was added and the reaction contents were vigorously stirred at 23°C for 14 hours. The reaction contents were poured into EtOAc (200 mL), washed with aq. 0.1M HCl (50 mL), with sat. aq. NaCl (50 mL), dried over MgSO_4 , and concentrated under reduced pressure directly onto silica gel (0.5 g). The crude product was then purified by flash column chromatography (25 g silica gel, 7-80% EtOAc gradient against hexanes over 10 column volumes) to afford **28** (85.6 mg, 91.8 % yield) as a brown solid. TLC: R_f 0.39 (1:1 EtOAc:hexanes). ^1H NMR (500 MHz, CD_3CN): δ 10.37 (s, 1H), 6.49 (d, $J = 2.2$ Hz, 1H), 6.36 (d, $J = 2.3$ Hz, 1H), 4.80 (d, $J = 2.5$ Hz, 2H), 3.36 (t, $J = 6.5$ Hz, 2H), 3.28 (s, 3H), 2.90 (q, $J = 5.2$ Hz, 2H), 2.87 (t, $J = 2.4$ Hz, 1H), 1.73 (m, 2H). ^{13}C NMR (126 MHz, CD_3CN): δ 189.24, 163.69, 162.65, 148.43, 116.40, 111.23, 98.53, 78.08, 76.44, 71.81, 57.54, 56.48, 30.55, 30.44. IR (film) 3286, 2927, 2872, 2828,

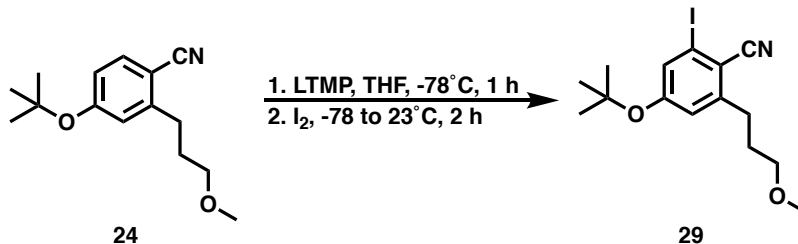
1656, 1598, 1573, 1450, 1319, 1273, 1152, 1102 cm^{-1} . HRMS (ESI/Q-TOF): $[\text{M}+\text{H}]^+$ calcd for $\text{C}_{14}\text{H}_{17}\text{O}_4^+$, 249.1121; found 249.1129. m.p.: T_{on} 84.0 $^{\circ}\text{C}$: T_{peak} 94.4 $^{\circ}\text{C}$

Synthesis of Compound 7



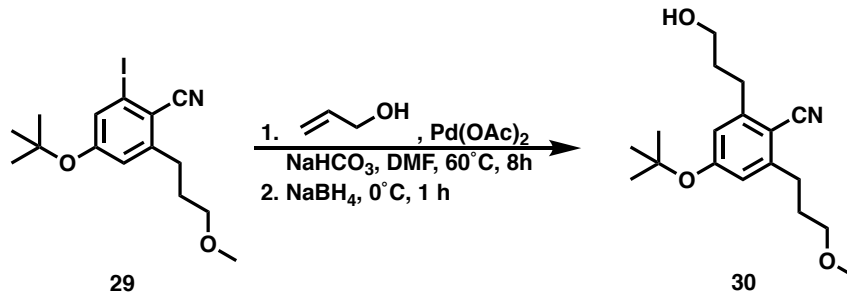
To a solution of 4-hydroxy-2-(3-methoxypropyl)-6-(prop-2-yn-1-yloxy)benzaldehyde (15.0 mg, 1 Eq, 60.4 μmol) and pyridinium p-toluenesulfonate (759 μg , 0.05 Eq, 3.02 μmol) in DCM (2 mL) was added 3,4-dihydro-2H-pyran (15.2 mg, 16.5 μL , 3 Eq, 181 μmol). This solution was stirred at 23 $^{\circ}\text{C}$ for 2 hours, after which the reaction contents were concentrated under reduced pressure directly onto silica gel (0.1 g). The crude product was purified by flash column chromatography (10 g silica gel, 4-50% EtOAc gradient against hexanes over 10 column volumes) affording **7** (13.2 mg, 39.7 μmol , 65.7 %) as a colorless oil. TLC: R_f 0.76 (2:3 EtOAc:hexanes). ^1H NMR (500 MHz, CD_3CN): δ 10.46 (s, 1H), 6.67 (d, $J = 2.3$ Hz, 1H), 6.58 (d, $J = 2.2$ Hz, 1H), 5.51 (t, $J = 3.2$ Hz, 1H), 4.80 (d, $J = 2.4$ Hz, 2H), 3.85 (m, 1H), 3.63 (m, 1H), 3.40 (t, $J = 6.4$ Hz, 2H), 3.32 (s, 3H), 2.97 (m, 2H), 2.64 (t, $J = 2.4$ Hz, 1H), 1.99 (m, 1H), 1.87 (m, 2H), 1.79 (m, 2H), 1.69 (m, 2H), 1.61 (q, $J = 5.6$ Hz, 1H). ^{13}C NMR (126 MHz, CD_3CN): δ 189.74, 163.16, 161.89, 148.18, 117.81, 111.82, 99.27, 96.35, 77.85, 75.95, 72.11, 62.17, 58.16, 56.67, 30.90, 30.76, 30.06, 25.04, 18.56. IR (film) 2932, 2871, 1677, 1598, 1571, 1440, 1285, 1153, 1114 cm^{-1} . HRMS (ESI/Q-TOF): $[\text{M}+\text{Na}]^+$ calcd for $\text{C}_{19}\text{H}_{24}\text{O}_5\text{Na}^+$, 355.1516; found 355.1525.

Synthesis of Compound 29



A solution of 2,2,6,6 tetramethyl piperidine (2.5 g, 3.0 mL, 1.75 Eq, 18 mmol) in anhydrous THF (10 mL) was cooled to -30 °C and a solution of nBuLi (1.1 g, 7.1 mL, 2.5 molar, 1.75 Eq, 18 mmol) in hexanes was added dropwise over 5 minutes. This solution was stirred for 30 min at -30°C and then cooled to -78 °C. This LiTMP solution was then slowly cannulated (~15 minutes) into a solution of 4-(tert-butoxy)-2-(3-methoxypropyl)benzonitrile (2.5 g, 1 Eq, 10 mmol) in anhydrous THF (40 mL). Upon full addition, the reaction was stirred for 1 hour at -78 °C. At this point, a solution of iodine (5.1 g, 2 Eq, 20 mmol) in anhydrous THF (5 mL) was added to the reaction dropwise over 5 minutes forming a red solution upon full addition. Following one hour of stirring at -78 °C the solution was brought up to 23 °C and combined with diethyl ether (400mL). This solution was washed with sat. aq. Na₂S₂O₃ (2 x100 mL), 0.1M aq. HCl (2 x 50 mL), sat. aq. NaCl (50 mL), dried over MgSO₄, and concentrated under reduced pressure directly onto silica gel (2 g). The crude product was then purified by a flash column chromatography (100 g, 5-50% diethyl ether gradient against hexanes over 10 column volumes) affording **29** (1.82 g, 48.0% yield) as an orange oil. TLC: R_f 0.45 (1:4 EtOAc:hexanes). ¹H NMR (500 MHz, CD₃CN): δ 7.41 (d, J = 2.2 Hz, 1H), 6.99 (d, J = 2.2 Hz, 1H), 3.36 (t, J = 6.2 Hz, 2H), 3.27 (s, 3H), 2.84 (t, J = 7.8 Hz, 2H), 1.85 (m, 2H), 1.38 (s, 9H). ¹³C NMR (126 MHz, CD₃CN): δ 159.76, 149.89, 130.80, 122.87, 118.78, 113.53, 98.86, 80.88, 70.99, 57.68, 31.96, 30.07, 27.97. IR (film) 2978, 2931, 2870, 2827, 2220, 1687, 1583, 1538, 1445, 1368, 1252, 1156, 1112 cm⁻¹. HRMS (ESI/Q-TOF): [M+H]⁺ calcd for C₁₅H₂₁INO₂⁺, 374.0611; found 374.0665.

Synthesis of Compound 30

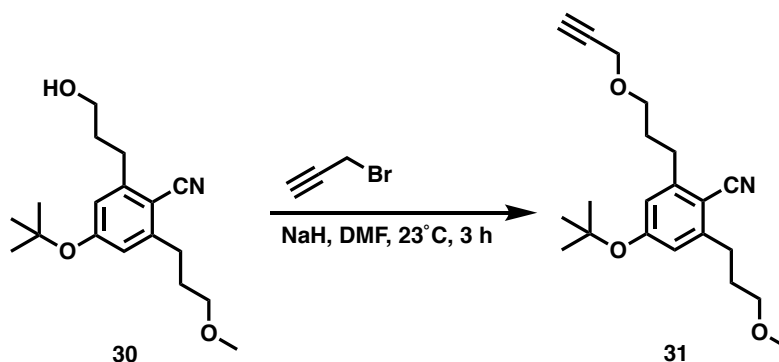


To a suspension of 4-(tert-butoxy)-2-iodo-6-(3-methoxypropyl)benzonitrile (500.0 mg, 1 Eq, 1.340 mmol), palladium(II) acetate (30.08 mg, 0.1 Eq, 134.0 μ mol), and sodium bicarbonate (562.7 mg, 5 Eq, 6.698 mmol) in DMF (4 mL) was added the allyl alcohol (116.7 mg, 137 μ L, 1.5 Eq, 2.009 mmol). The reaction vessel was then quickly evacuated under vacuum and backfilled with argon (this was repeated 2 additional times), after which the contents were heated to 60 °C for 8 hours. The reaction contents were then cooled to 23 °C where it was noted via TLC that the reaction had reached 100% conversion. The reaction contents were then cooled to 0 °C and the sodium borohydride (50.68 mg, 1 Eq, 1.340 mmol) was slowly added over 10 minutes. Upon full addition the reaction was slowly brought back up to 23 °C over the course of 1 hour after which TLC showed fully consumption of the intermediate.

The reaction contents were then filtered over celite (washing with EtOAc). The organic solution was then diluted further with EtOAc (for a total volume of 350 mL). The organic layer was washed with 0.1M HCl (2 x 75 mL), H₂O (2 x 75 mL), and sat. aq. NaCl (75 mL). The organic layer was then dried over MgSO₄, and concentrated under reduced pressure directly onto silica gel (10 g). The crude product was then purified by flash column chromatography (50 g silica gel, 10-100% EtOAc gradient against hexanes over 10 column volumes) to afford **30** (320.1 mg, 1.048 mmol, 78.23 %) as a tan oil. TLC: R_f 0.37 (1:1 EtOAc:hexanes). ¹H NMR (500 MHz, CD₃CN): δ 6.83 (d, J = 2.3 Hz, 1H), 6.82 (d, J = 2.3 Hz, 1H), 3.53 (t, J = 5.6 Hz, 2H), 3.37 (t, J = 6.2 Hz, 2H),

3.27 (s, 3H), 2.81 (m, 4H), 2.66 (s, 1H), 1.83 (m, 4H), 1.38 (s, 9H). ¹³C NMR (126 MHz, CD₃CN): δ 159.47, 148.14, 147.92, 120.93, 120.89, 117.14, 105.70, 79.65, 71.19, 60.69, 57.65, 33.43, 31.11, 30.91, 30.31, 28.09. IR (film) 3443, 2978, 2933, 2870, 2214, 1595, 1459, 1367, 1169, 1132, 1117 cm⁻¹. HRMS (ESI/Q-TOF): [M+H]⁺ calcd for C₁₈H₂₈NO₃⁺, 306.2064; found 306.2017.

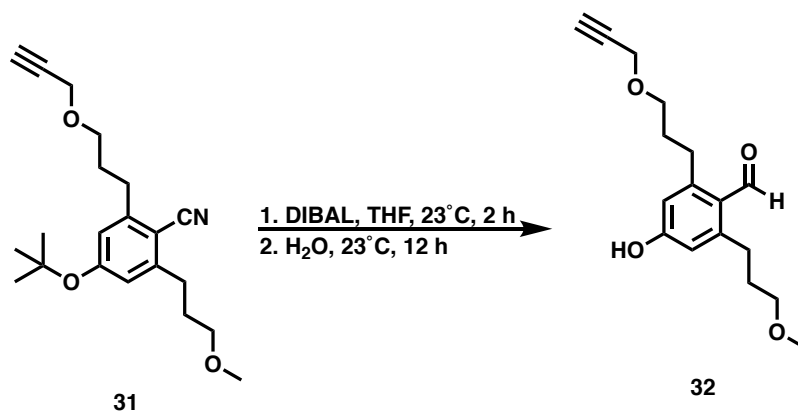
Synthesis of Compound 31



A solution of 4-(tert-butoxy)-2-(3-hydroxypropyl)-6-(3-methoxypropyl)benzonitrile (200.0 mg, 1 Eq, 654.8 μmol) and sodium hydride (52.39 mg, 60% Wt, 2 Eq, 1.310 mmol) in anhydrous DMF (4 mL) was stirred at 23 °C for 5 minutes. Then propargyl bromide, (72.58 mg, 52.63 μL, 80% Wt, 1.3 Eq, 488.1 μmol) was then slowly added over 5 minutes and the reaction was stirred for 3 hours. The reaction contents were then poured into EtOAc (200 mL), washed with H₂O (2 x 50 mL), aq. 0.1M HCl (2 x 50 mL), with sat. aq. NaCl (50 mL), dried over MgSO₄, and concentrated under reduced pressure directly onto silica gel (0.5 g). The crude product was then purified by flash column chromatography (25 g silica gel, 7-50% EtOAc gradient against hexanes over 10 column volumes) to afford **31** (163.2 mg, 72.6 % yield) as a tan oil. TLC: R_f 0.37 (1:4 EtOAc:hexanes). ¹H NMR (600 MHz, CD₃CN): δ 6.77 (d, J = 2.2 Hz, 1H), 6.76 (d, J = 2.1 Hz, 1H), 4.15 (d, J = 2.4 Hz, 2H), 3.55 (t, J = 6.2 Hz, 2H), 3.41 (t, J = 6.3 Hz, 2H), 3.34 (s, 3H), 2.86 (m, 4H), 2.42 (t, J = 2.45 Hz, 1H) 1.94 (m, 4H), 1.39 (s, 9H). ¹³C NMR (126 MHz, CD₃CN): δ

159.32, 147.79, 147.58, 121.19, 121.15, 117.37, 106.14, 79.81, 79.79, 74.36, 71.53, 68.92, 58.60, 58.11, 31.40, 31.36, 30.42, 30.30, 28.93. IR (film) 2975, 2929, 2870, 2214, 1596, 1460, 1368, 1170, 1128, 1105 cm^{-1} . HRMS (ESI/Q-TOF): $[\text{M}+\text{H}]^+$ calcd for $\text{C}_{21}\text{H}_{30}\text{NO}_3^+$, 344.2220; found 344.2218.

Synthesis of Compound 32

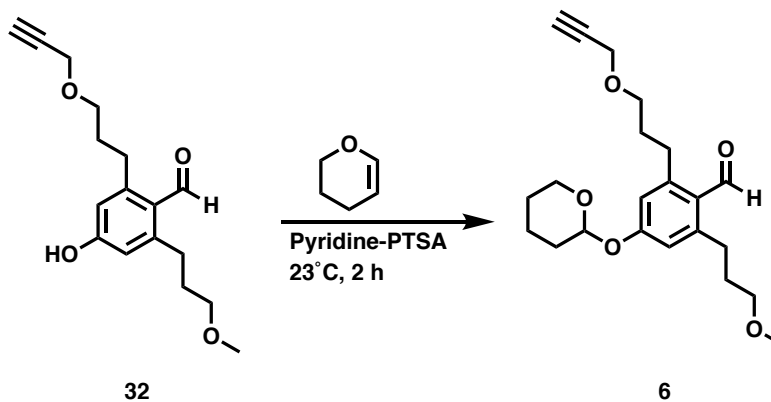


A solution of 4-(tert-butoxy)-2-(3-methoxypropyl)-6-(3-(prop-2-yn-1-yloxy)propyl)benzonitrile (95.0 mg, 1 Eq, 277 μmol) in anhydrous THF was brought up to 60 °C and a solution of diisobutylaluminum hydride (197 mg, 1.26 mL, 1.1 molar, 5 Eq, 1.38 mmol) in cyclohexanes was added to the reaction portion-wise.* Upon complete addition the reaction was quenched by the slow addition of MeOH (10 mL) followed by an aq. 1M HCl solution (50 mL) and this solution was stirred for 12 hours. The aqueous solution was further diluted with 1M aq. HCl (50 mL), extracted with EtOAc (3 x 75 mL), the organic layers were combined, washed with sat. aq. NaCl (50 mL), dried over MgSO_4 , and concentrated under reduced pressure directly onto silica gel (1 g). The crude product was then purified by flash column chromatography (25 g silica gel, 5-50% EtOAc gradient against hexanes with a 1% MeOH isocratic primer over 10 column volumes) to afford **32** (46.2 mg, 159 μmol , 57.5 %) as a colorless oil. TLC: R_f 0.42 (1:1

EtOAc:hexanes). ^1H NMR (500 MHz, CD_3CN): δ 10.39 (s, 1H), 6.60 (d, $J = 2.6$ Hz, 1H), 6.58 (d, $J = 2.6$ Hz, 1H), 4.15 (d, $J = 2.4$ Hz, 2H), 3.56 (t, $J = 6.2$ Hz, 2H), 3.44 (t, $J = 6.3$ Hz, 2H), 3.36 (s, 3H), 3.00 (q, $J = 8.0$ Hz, 4H), 2.43 (t, $J = 2.4$ Hz, 1H), 1.88 (m, 4H). ^{13}C NMR (126 MHz, CD_3CN): δ 191.34, 159.87, 149.23, 149.12, 124.90, 116.26, 116.09, 79.84, 74.45, 71.92, 69.18, 58.51, 58.08, 31.58, 31.49, 30.27, 30.24. IR (film) 3289, 2934, 2871, 1674, 1604, 1582, 1458, 1277, 1148, 1102 cm^{-1} . HRMS (ESI/Q-TOF): $[\text{M}+\text{H}]^+$ calcd for $\text{C}_{17}\text{H}_{23}\text{O}_4^+$, 291.1591; found 291.1582.

*Note 1. The DIBAL was added one equivalence at a time and one hour was allowed to pass between each addition. The conversion was monitored after each hour via analytical HPLC. The product readily reduces down to the benzylamine (appears to be more significant at room temperature) as the major byproduct. DIBAL is added up to the point where all the starting material is consumed while trying to maintain minimal benzylamine formation.

Synthesis of Compound 6



To a solution of 4-hydroxy-2-(3-methoxypropyl)-6-(3-(prop-2-yn-1-yloxy)propyl)benzaldehyde (32, 15.0 mg, 1 Eq, 51.7 μmol) and pyridinium p-toluenesulfonate (649 μg , 0.05 Eq, 2.58 μmol) in DCM (2 mL) was added 3,4-dihydro-2H-pyran (13.0 mg, 14.1 μL , 3 Eq, 155 μmol). This solution was stirred at 23 $^\circ\text{C}$ for 2 hours, after which the reaction

contents were concentrated under reduced pressure directly onto silica gel (0.1 g). The crude product was purified by flash column chromatography (10 g silica gel, 20-100% DCM gradient against hexanes with a 7% EtOAc isocratic primer over 10 column volumes) affording **6** (11.3 mg, 30.2 μ mol, 58.4 %) as a colorless oil. TLC: R_f 0.79 (2:3 EtOAc:hexanes). ^1H NMR (500 MHz, CD_3CN): δ 10.43 (s, 1H), 6.79 (d, J = 1.4 Hz, 2H), 5.50 (t, J = 3.0 Hz, 1H), 4.15 (t, J = 1.9 Hz, 2H), 3.84 (td, J = 10.7, 3.0 Hz, 1H), 3.58 (m, 3H), 3.40 (t, J = 6.2 Hz, 2H), 3.34 (s, 3H), 3.01 (m, 4H), 2.42 (t, J = 2.3 Hz, 1H), 1.99 (m, 1H), 1.87 (m, 6H), 1.70 (m, 2H), 1.60 (m, 1H). ^{13}C NMR (126 MHz, CD_3CN): δ 191.50, 160.33, 148.65, 148.35, 125.70, 116.72, 116.67, 95.79, 79.98, 74.25, 71.83, 69.27, 62.07, 58.55, 58.05, 31.84, 31.64, 30.44, 30.37, 30.11, 25.08, 18.49. IR (film) 2927, 2871, 1721, 1680, 1596, 1455, 1278, 1148, 1109 cm^{-1} . HRMS (ESI/Q-TOF): $[\text{M}+\text{H}]^+$ calcd for $\text{C}_{22}\text{H}_{31}\text{O}_5^+$, 375.2166; found 375.2151.

5.5 References

- (1) Barve, B. D.; Wu, Y.-C.; El-Shazly, M.; Korinek, M.; Cheng, Y.-B.; Wang, J.-J.; Chang, F.-R. Copper-Catalyzed Selective C₁O Bond Formation by Oxidative α -C(Sp³)₂H/O₂H Coupling between Ethers and Salicylaldehydes. *Tetrahedron* **2015**, *71* (15), 2290–2297. <https://doi.org/10.1016/j.tet.2015.02.035>.
- (2) Sterzycki, R. Pyridinium Tosylate, A Mild Catalyst for Formation and Cleavage of Dioxolane-Type Acetals. *Synthesis* **1979**, *1979* (9), 724–725. <https://doi.org/10.1055/s-1979-28814>.
- (3) Masuda, T.; Ide, N.; Kitabatake, N. Structure–Sweetness Relationship in Egg White Lysozyme: Role of Lysine and Arginine Residues on the Elicitation of Lysozyme Sweetness. *Chem. Senses* **2005**, *30* (8), 667–681. <https://doi.org/10.1093/chemse/bji060>.

- (4) Chen, D.; Disotuar, M. M.; Xiong, X.; Wang, Y.; Chou, D. H.-C. Selective N-Terminal Functionalization of Native Peptides and Proteins. *Chem. Sci.* **2017**, *8* (4), 2717–2722. <https://doi.org/10.1039/C6SC04744K>.
- (5) Guerry, A.; Bernard, J.; Samain, E.; Fleury, E.; Cottaz, S.; Halila, S. Aniline-Catalyzed Reductive Amination as a Powerful Method for the Preparation of Reducing End-“Clickable” Chitooligosaccharides. *Bioconjug. Chem.* **2013**, *24* (4), 544–549. <https://doi.org/10.1021/bc3003716>.
- (6) Presolski, S. I.; Hong, V. P.; Finn, M. G. Copper-Catalyzed Azide–Alkyne Click Chemistry for Bioconjugation. *Curr. Protoc. Chem. Biol.* **2011**, *3* (4), 153–162. <https://doi.org/10.1002/9780470559277.ch110148>.
- (7) Stayton, P. S.; Shimoboji, T.; Long, C.; Chilkoti, A.; Ghen, G.; Harris, J. M.; Hoffman, A. S. Control of Protein–Ligand Recognition Using a Stimuli-Responsive Polymer. *Nature* **1995**, *378* (6556), 472–474. <https://doi.org/10.1038/378472a0>.
- (8) Fuhrmann, G.; Grotzky, A.; Lukić, R.; Matorri, S.; Luciani, P.; Yu, H.; Zhang, B.; Walde, P.; Schlüter, A. D.; Gauthier, M. A.; Leroux, J.-C. Sustained Gastrointestinal Activity of Dendronized Polymer–Enzyme Conjugates. *Nat. Chem.* **2013**, *5* (7), 582–589. <https://doi.org/10.1038/nchem.1675>.

5.6 Appendix C

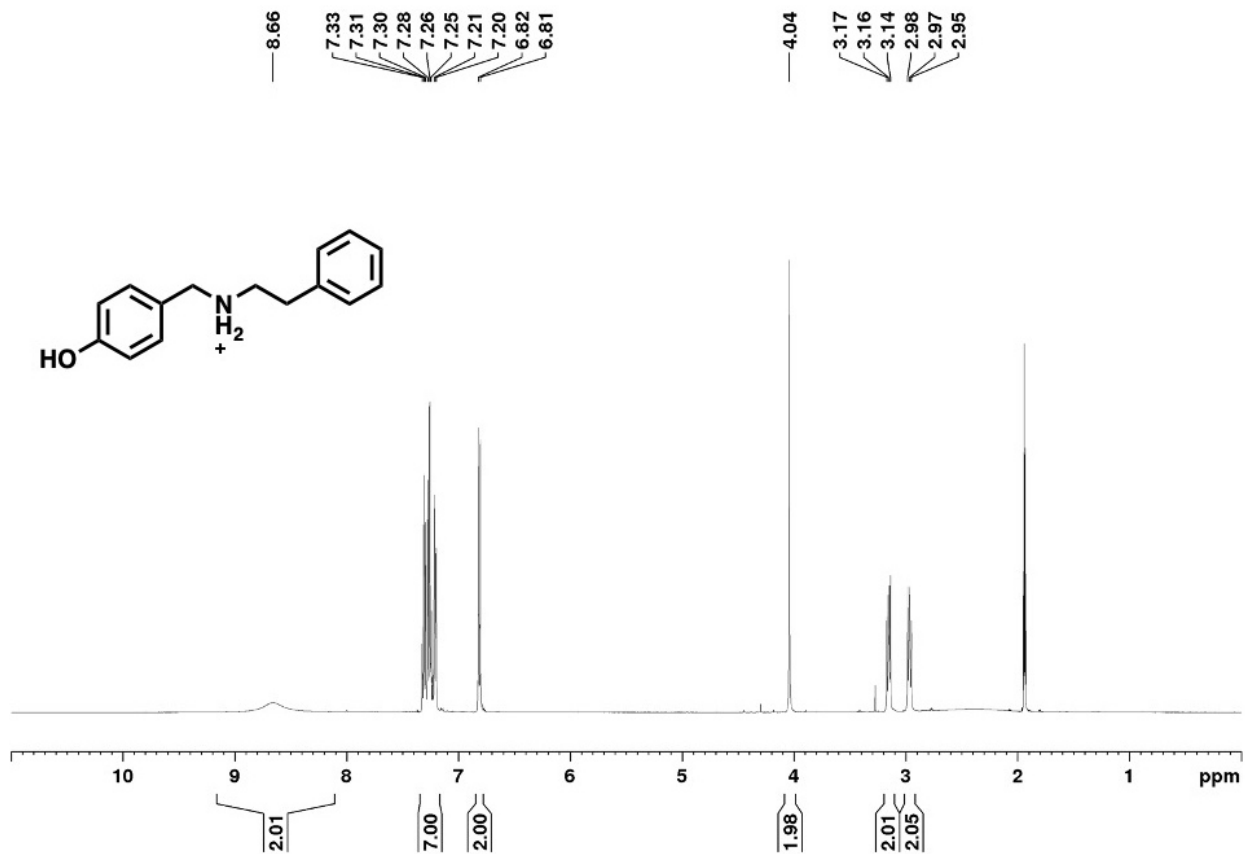


Figure 5.17. ^1H NMR Spectrum of Compound 1 in CD₃CN

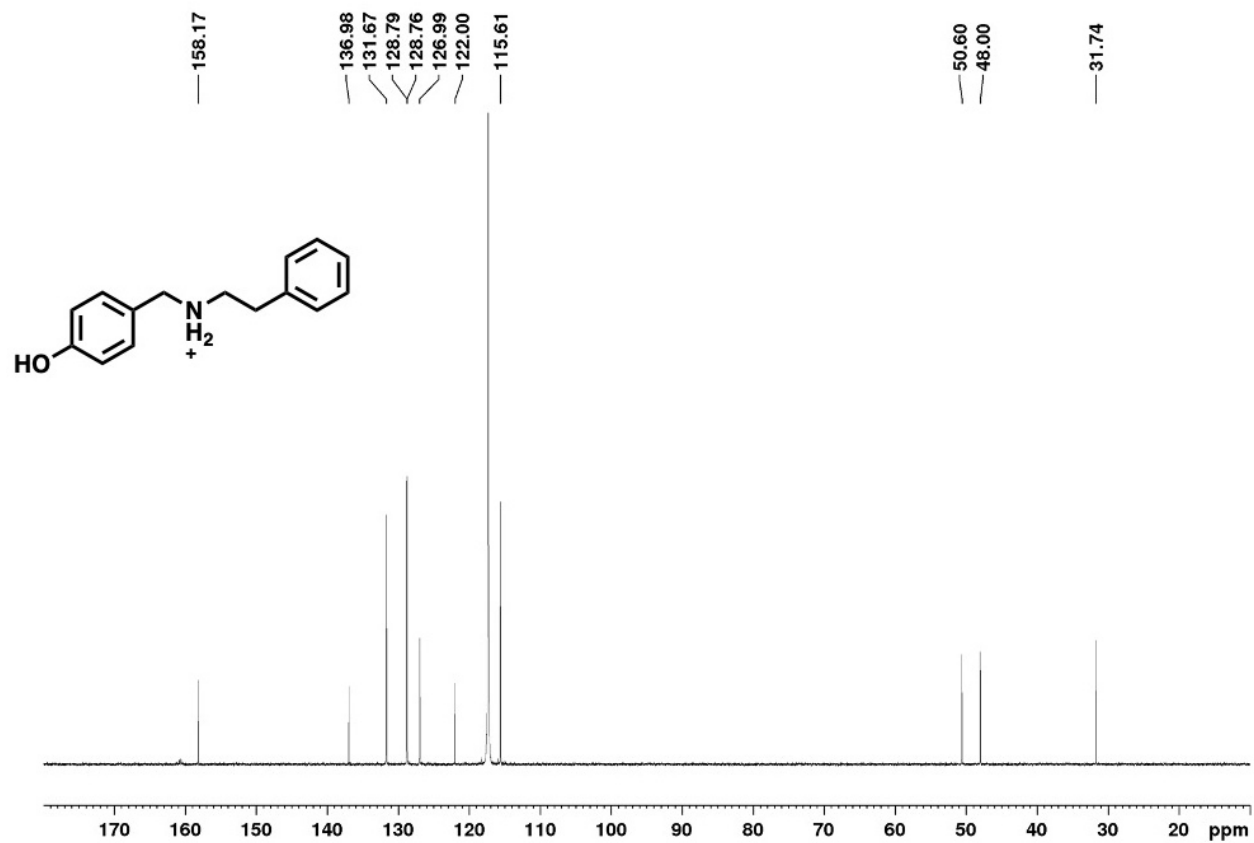


Figure 5.18. ^{13}C NMR Spectrum of Compound 1 in CD_3CN

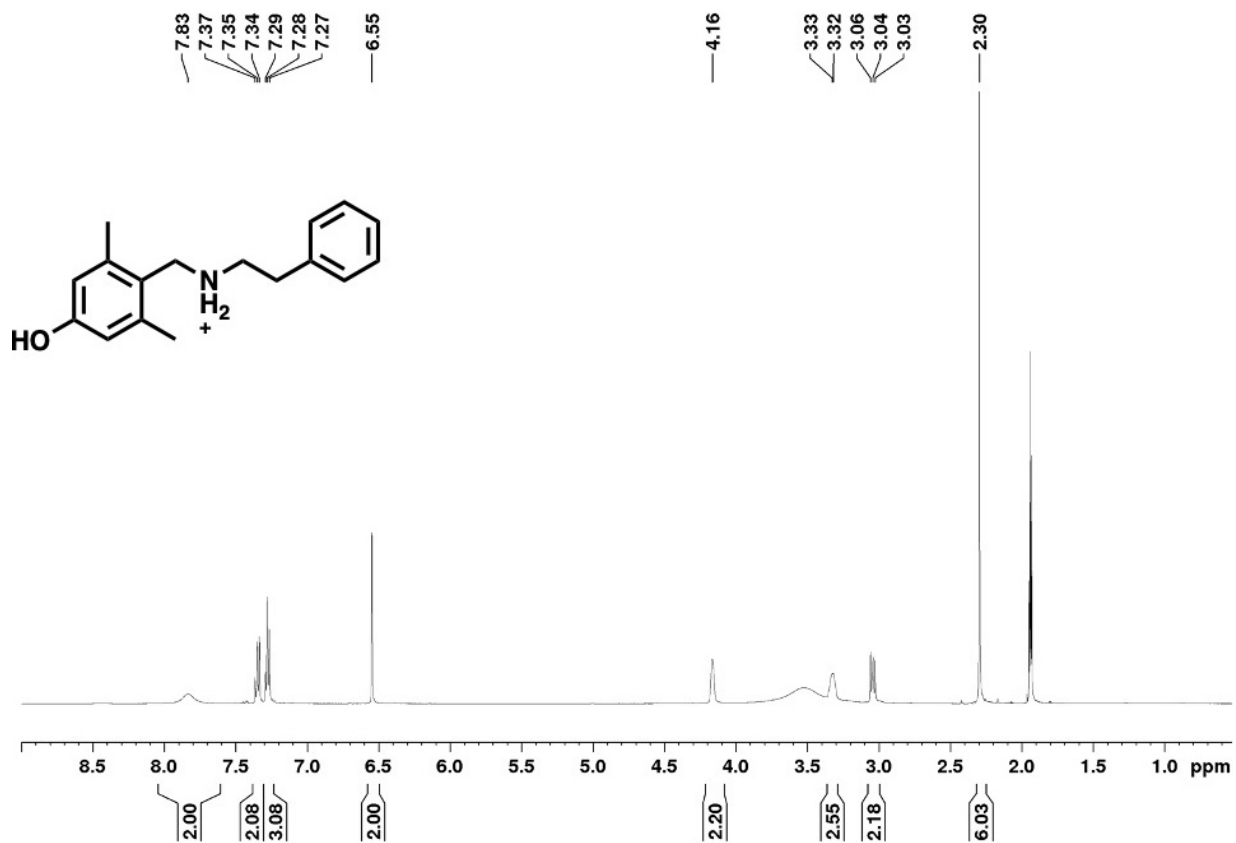


Figure 5.19. ¹H NMR Spectrum of Compound 2 in CD₃CN

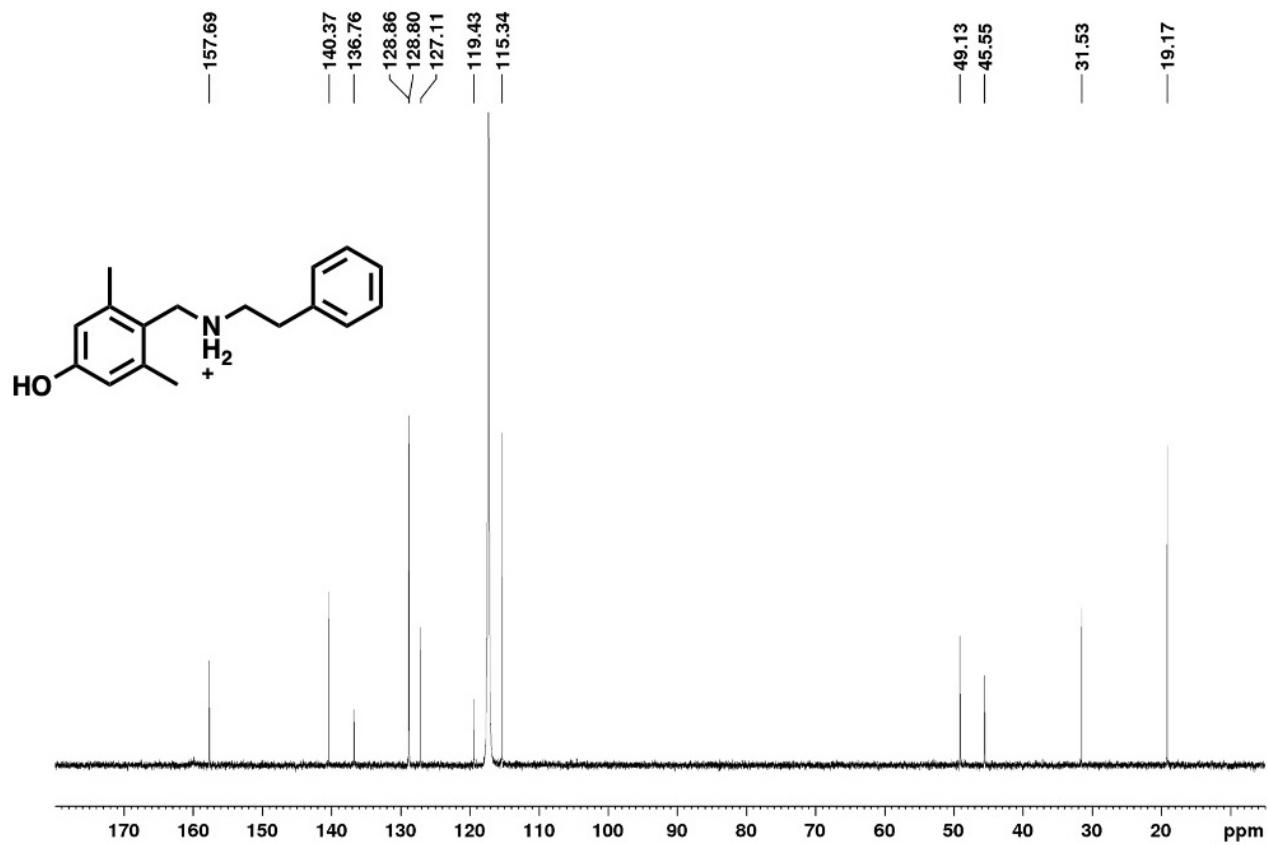


Figure 5.20. ^{13}C NMR Spectrum of Compound 2 in CD_3CN

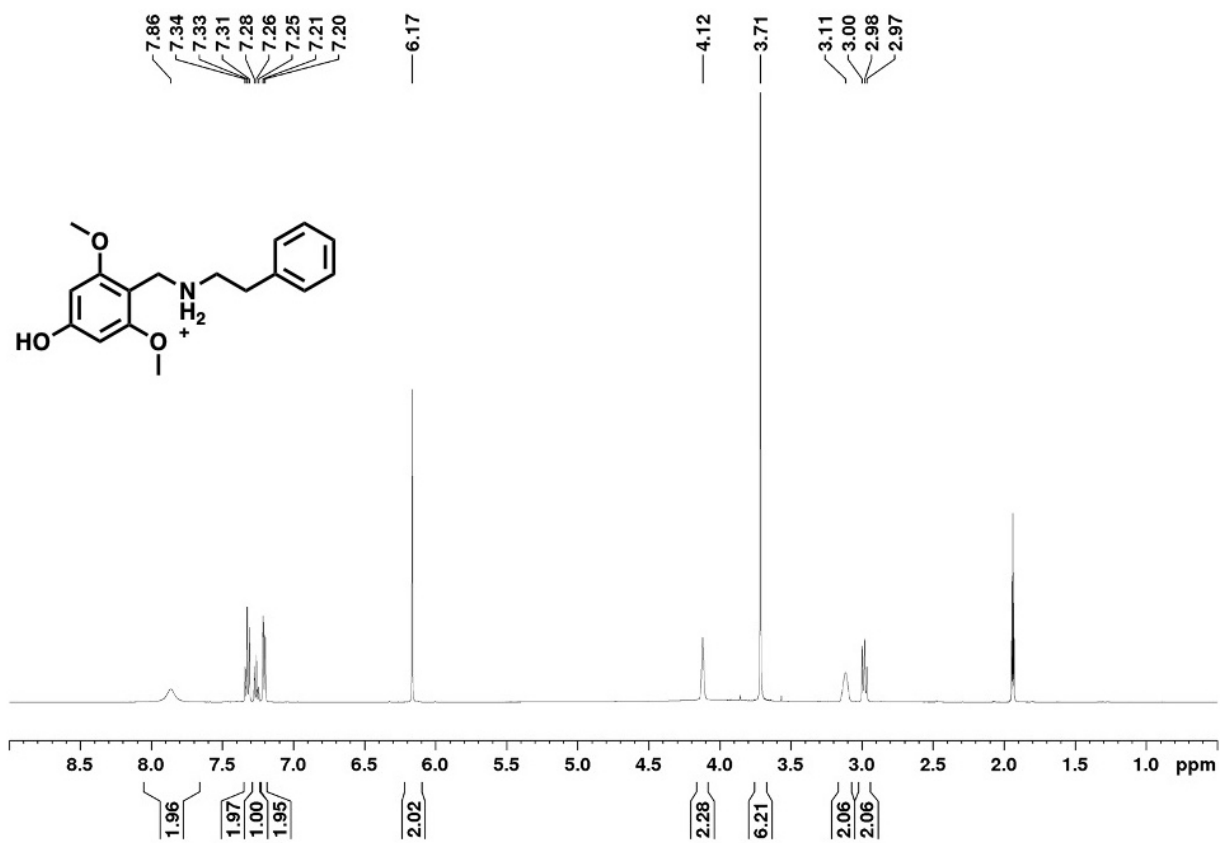


Figure 5.21. ¹H NMR Spectrum of Compound 3a in CD₃CN

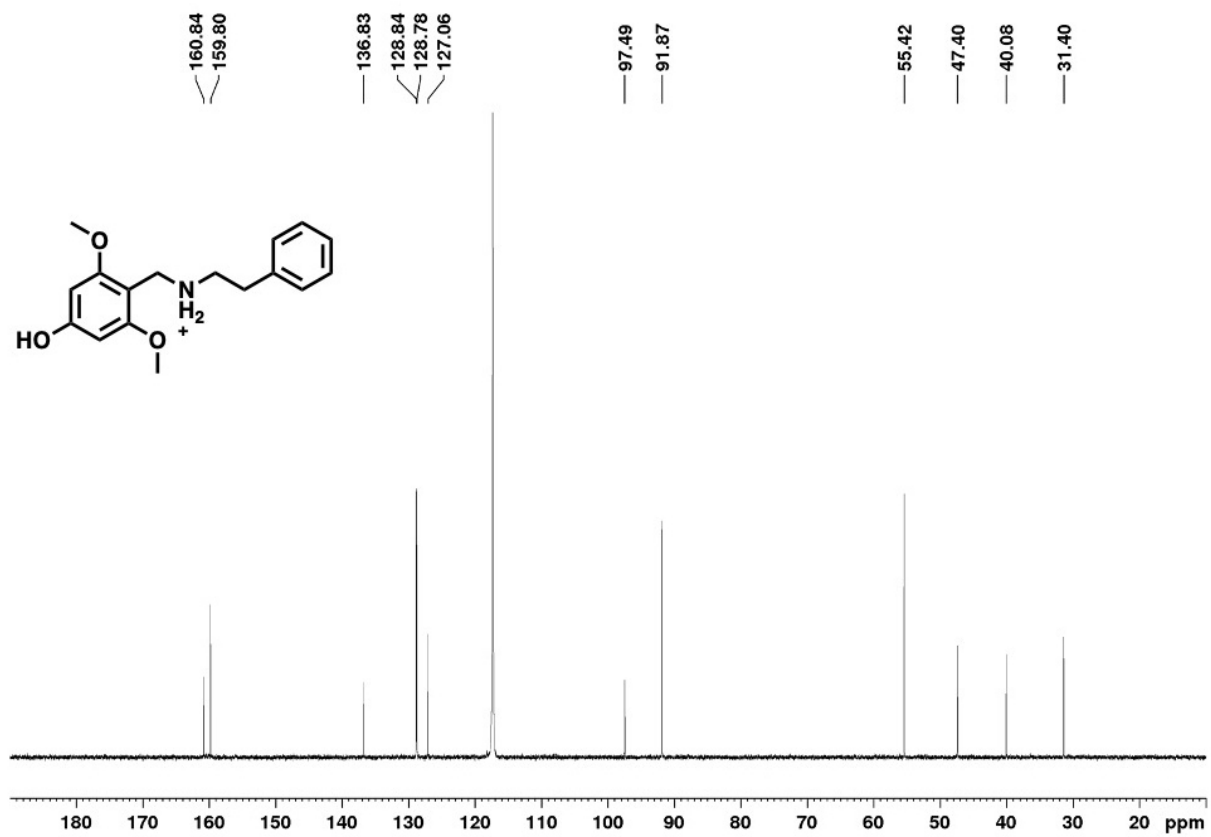


Figure 5.22. ^{13}C NMR Spectrum of Compound 3a in CD_3CN

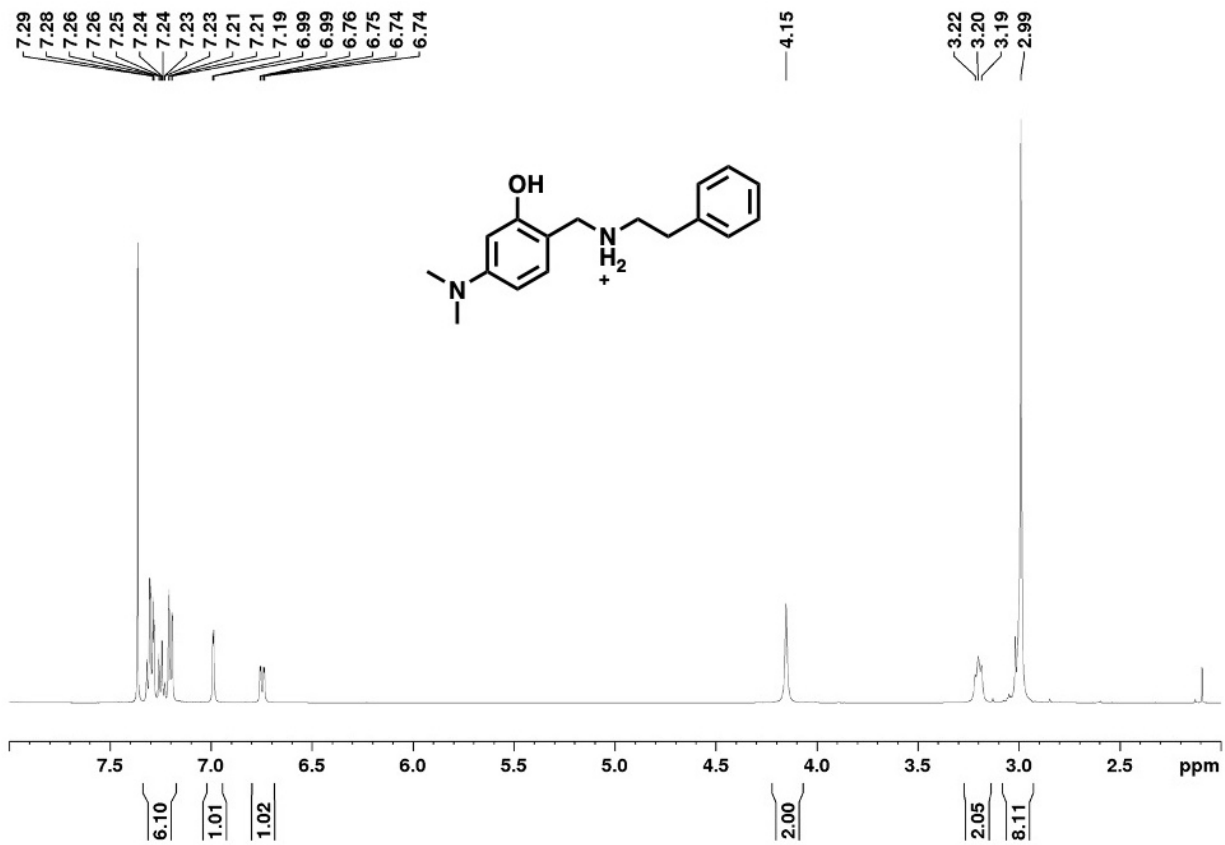


Figure 5.23. ¹H NMR Spectrum of Compound 4a in CD₃CN

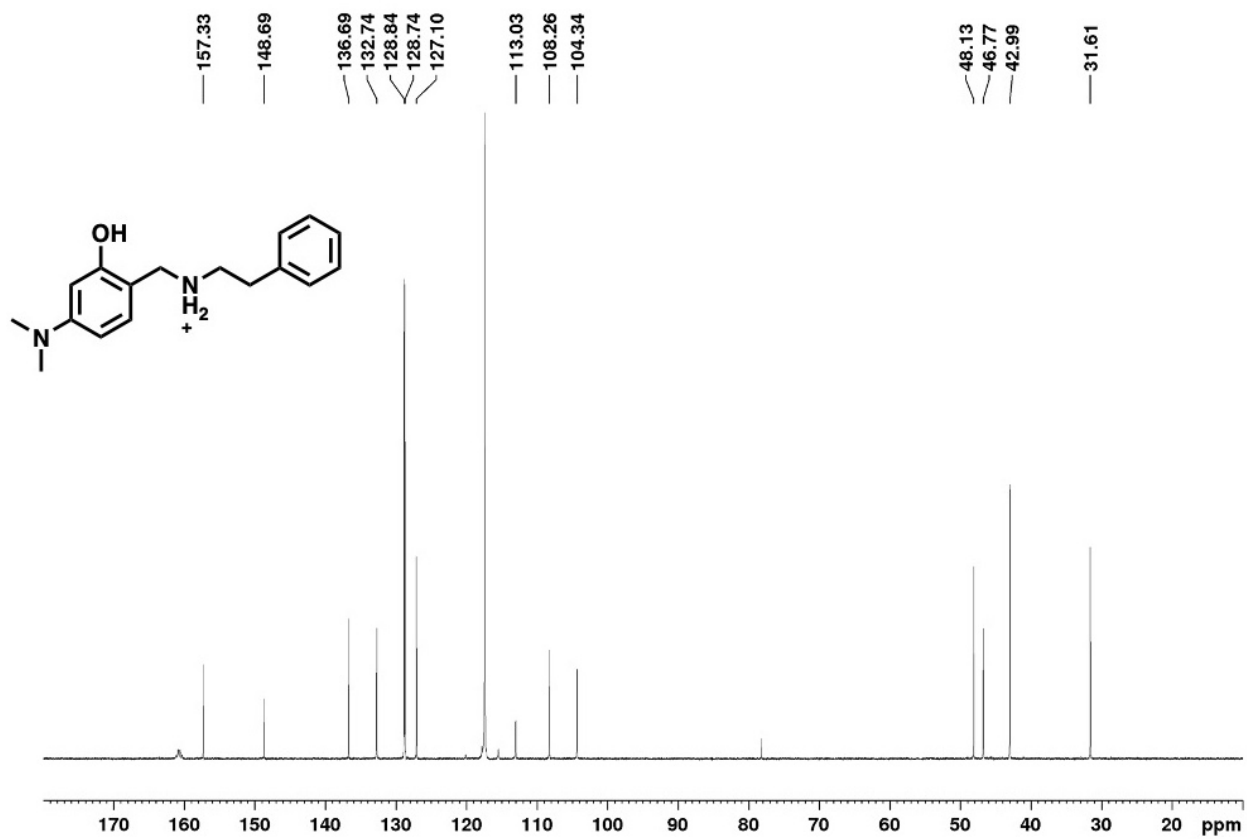


Figure 5.24. ^{13}C NMR Spectrum of Compound 4a in CD_3CN

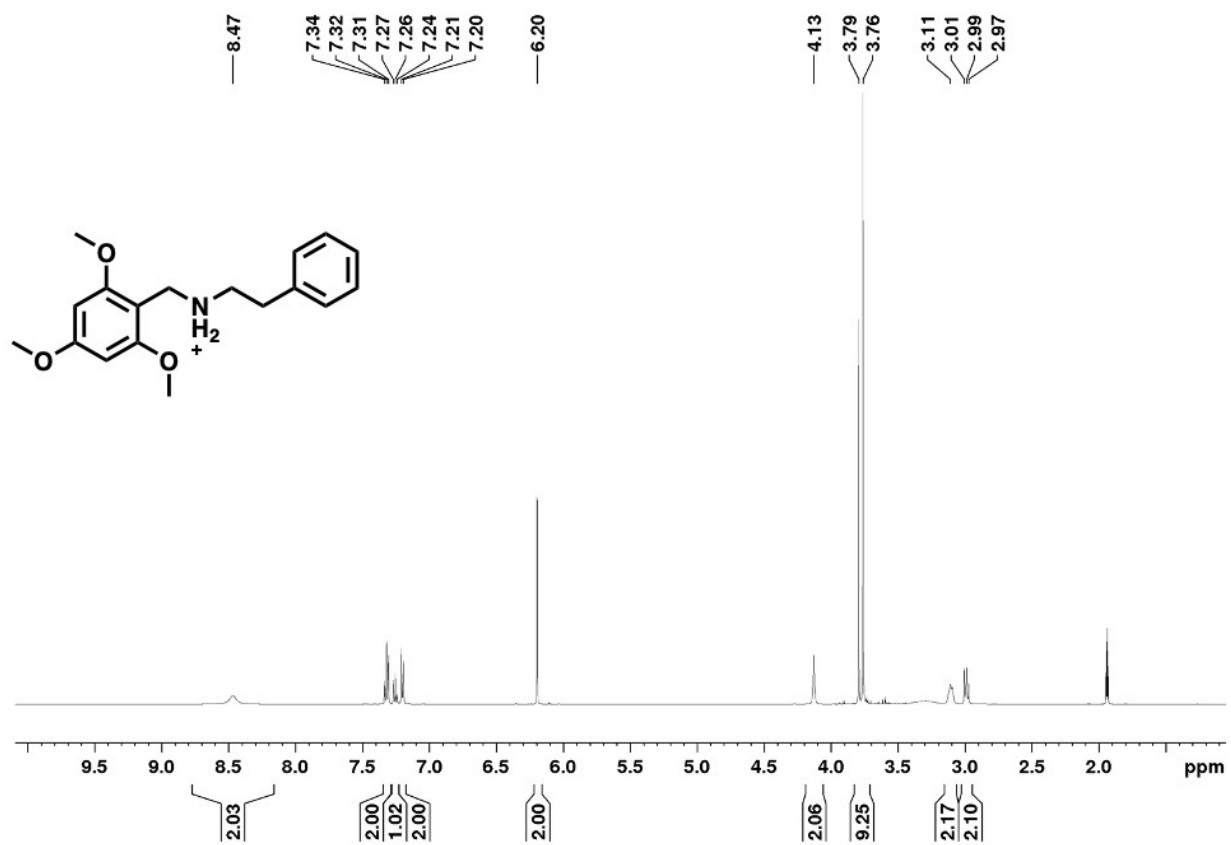


Figure 5.25. ¹H NMR Spectrum of Compound 3b in CD₃CN

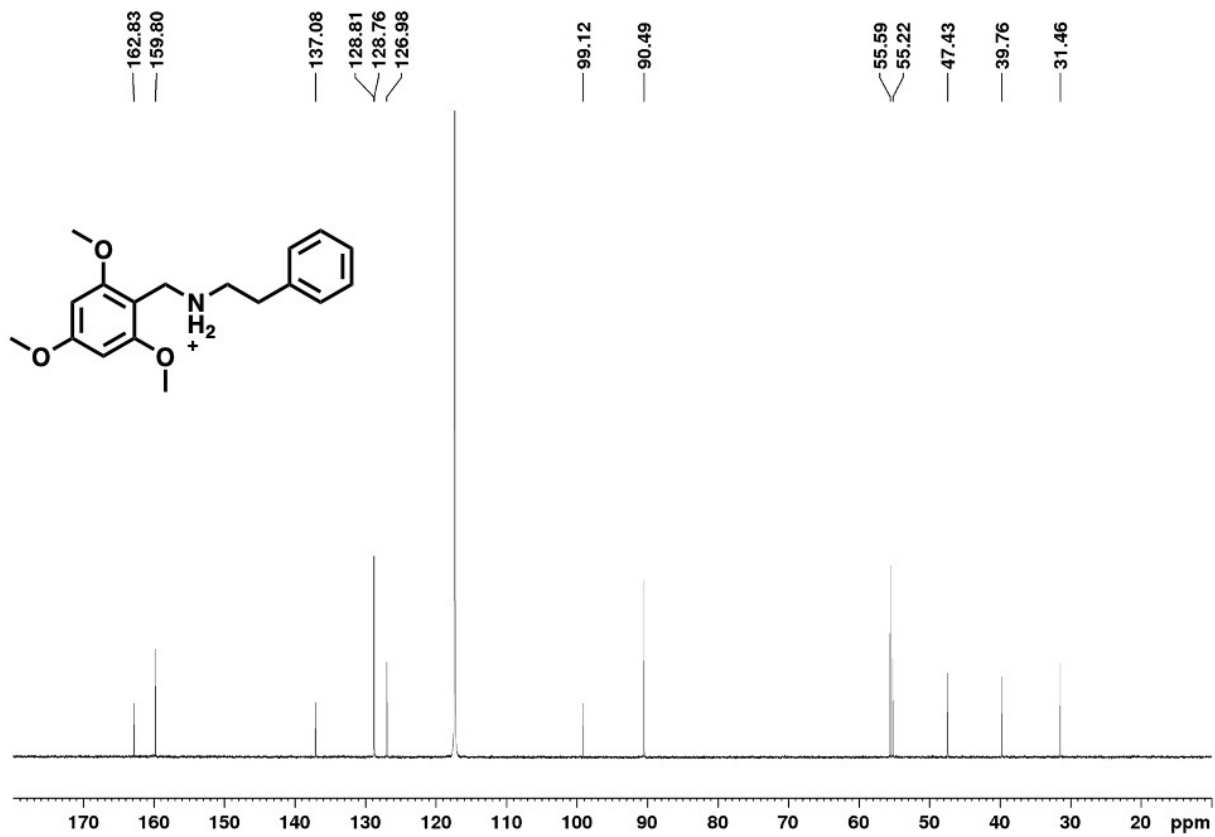


Figure 5.26. ¹³C NMR Spectrum of Compound 3b in CD₃CN

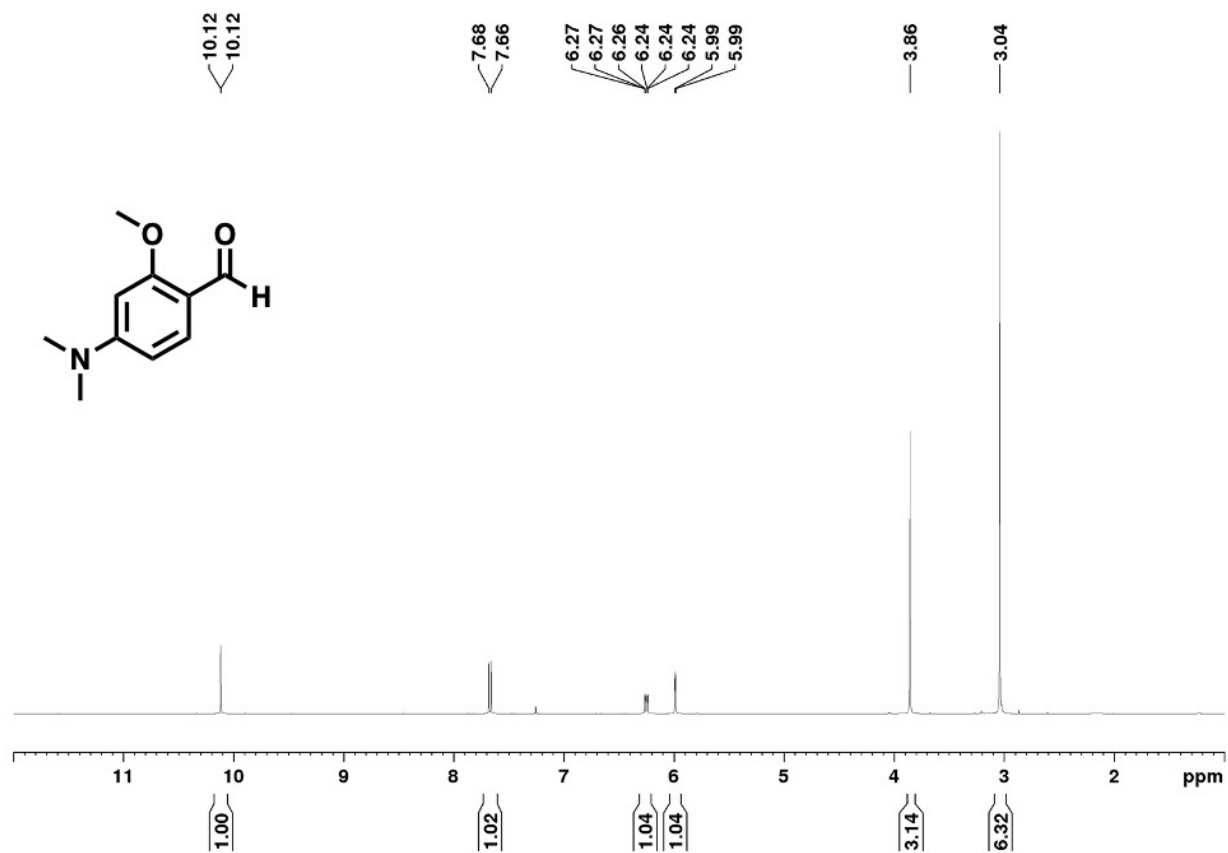


Figure 5.27. ¹H NMR Spectrum of Compound 9 in CDCl₃

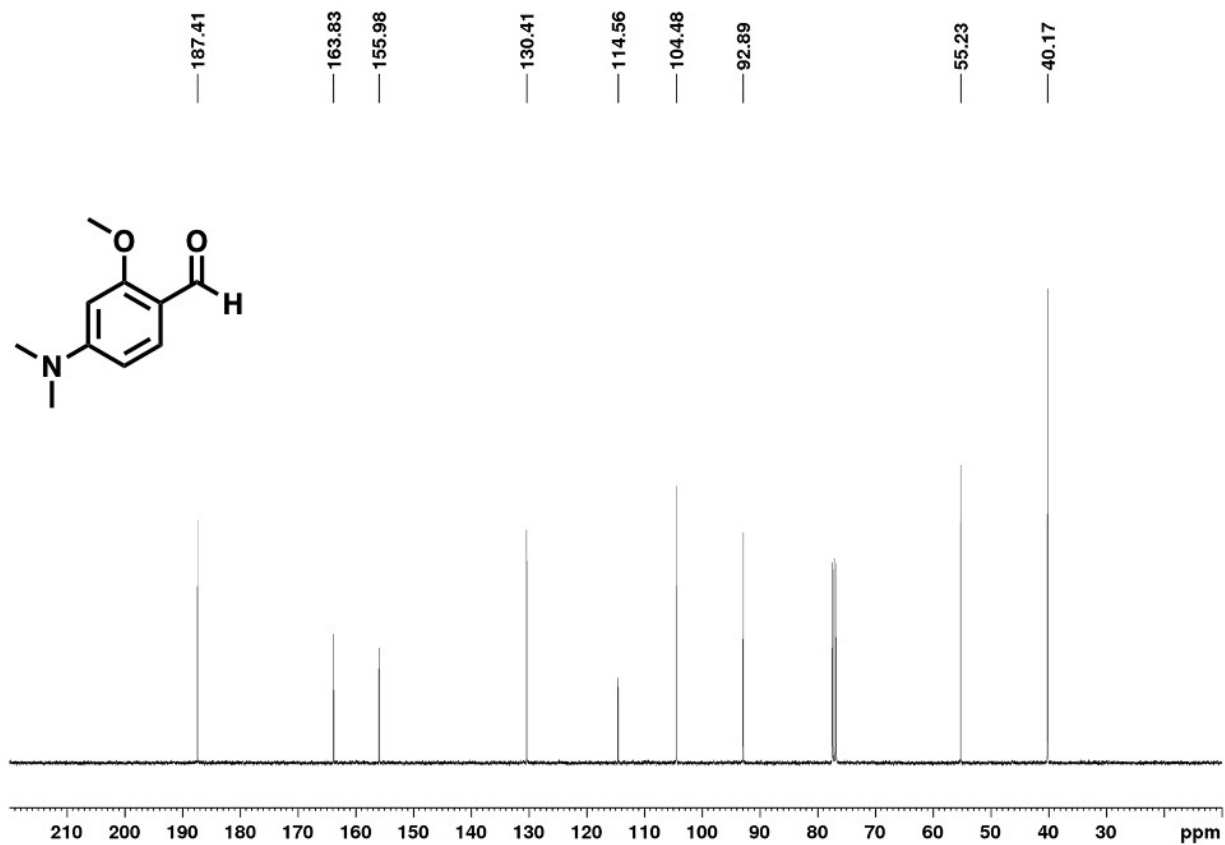


Figure 5.28. ¹³C NMR Spectrum of Compound 9 in CDCl₃

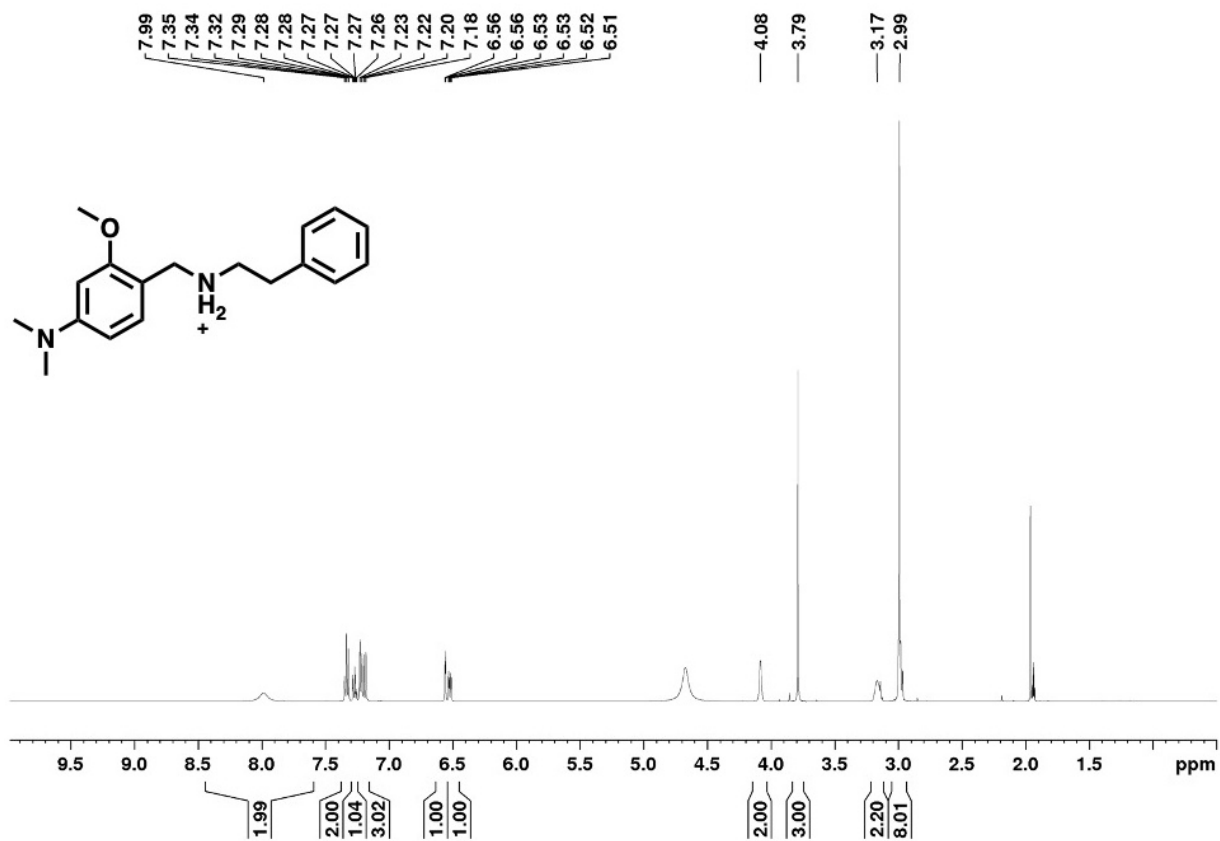


Figure 5.29. ¹H NMR Spectrum of Compound 4b in CD₃CN

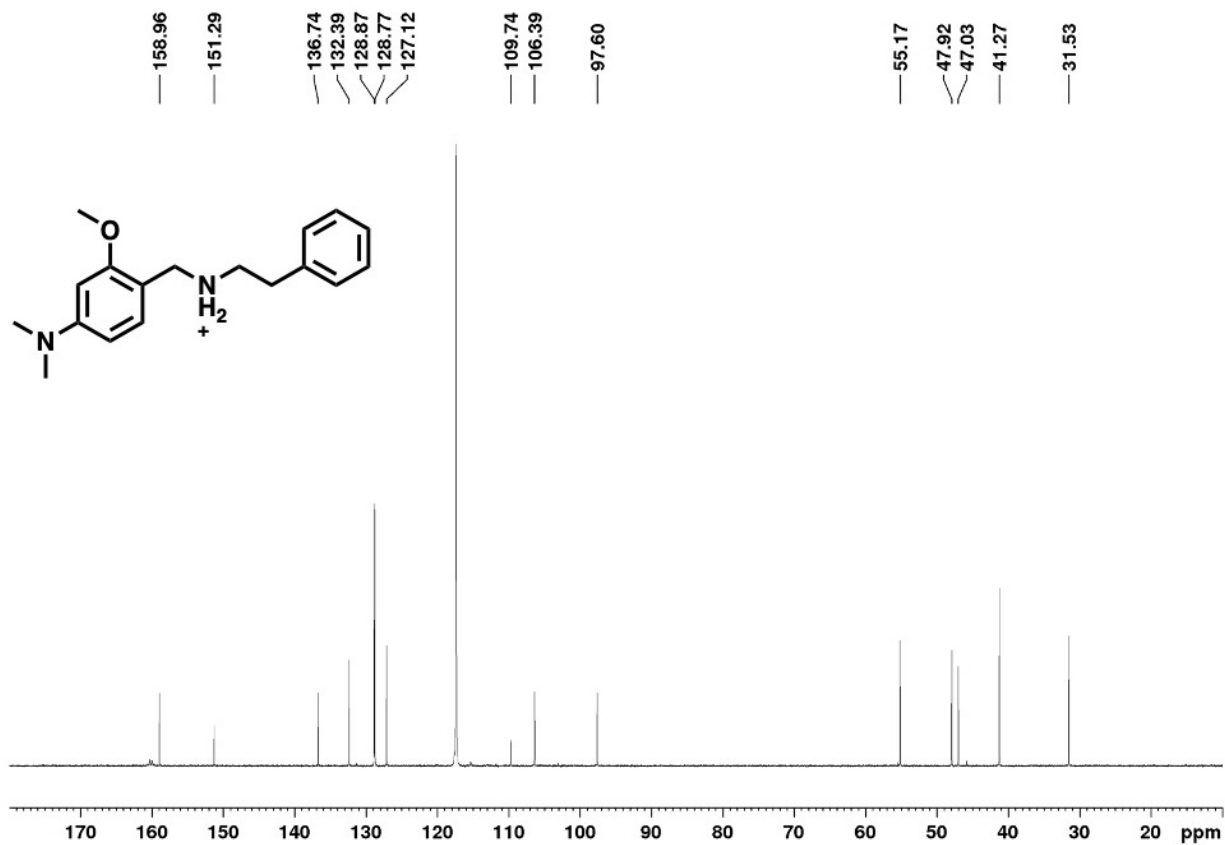


Figure 5.30. ^{13}C NMR Spectrum of Compound 4b in CD_3CN

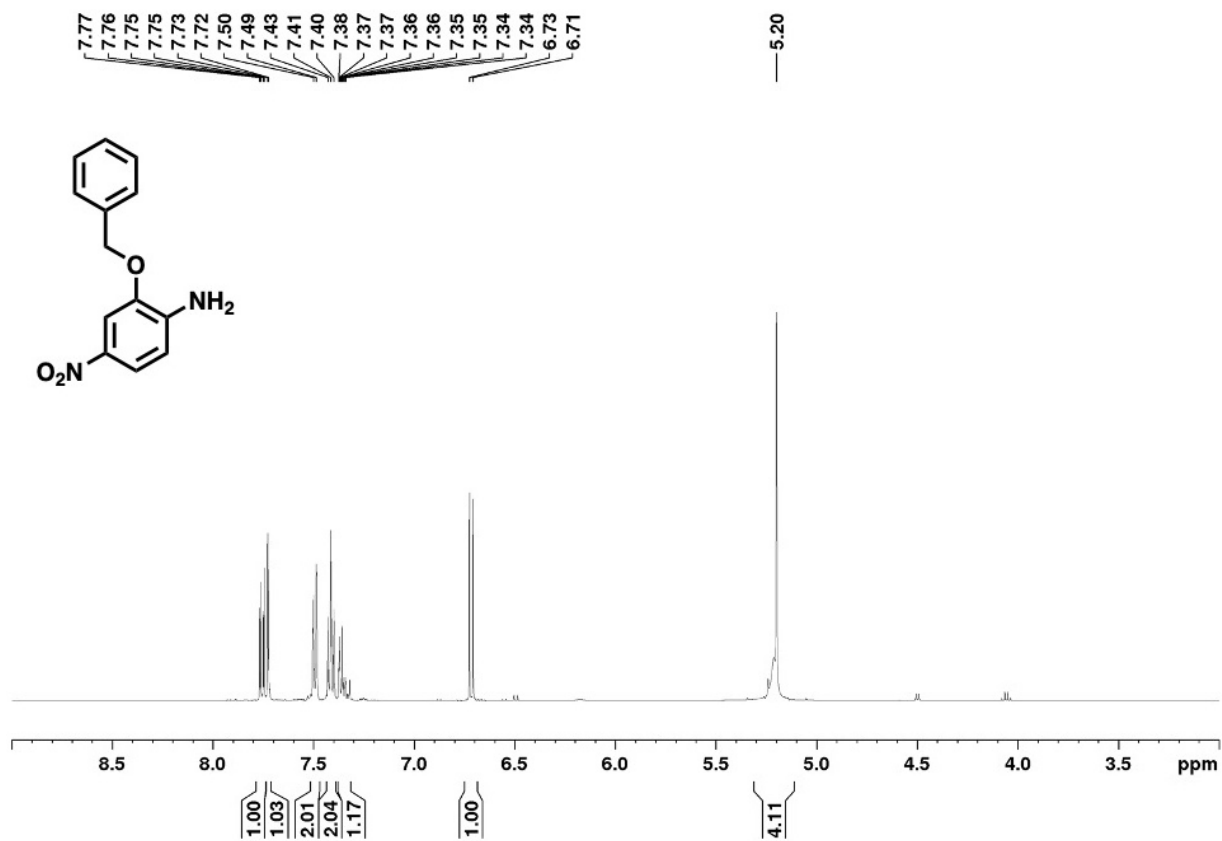


Figure 5.31. ¹H NMR Spectrum of Compound 10 in CD₃CN

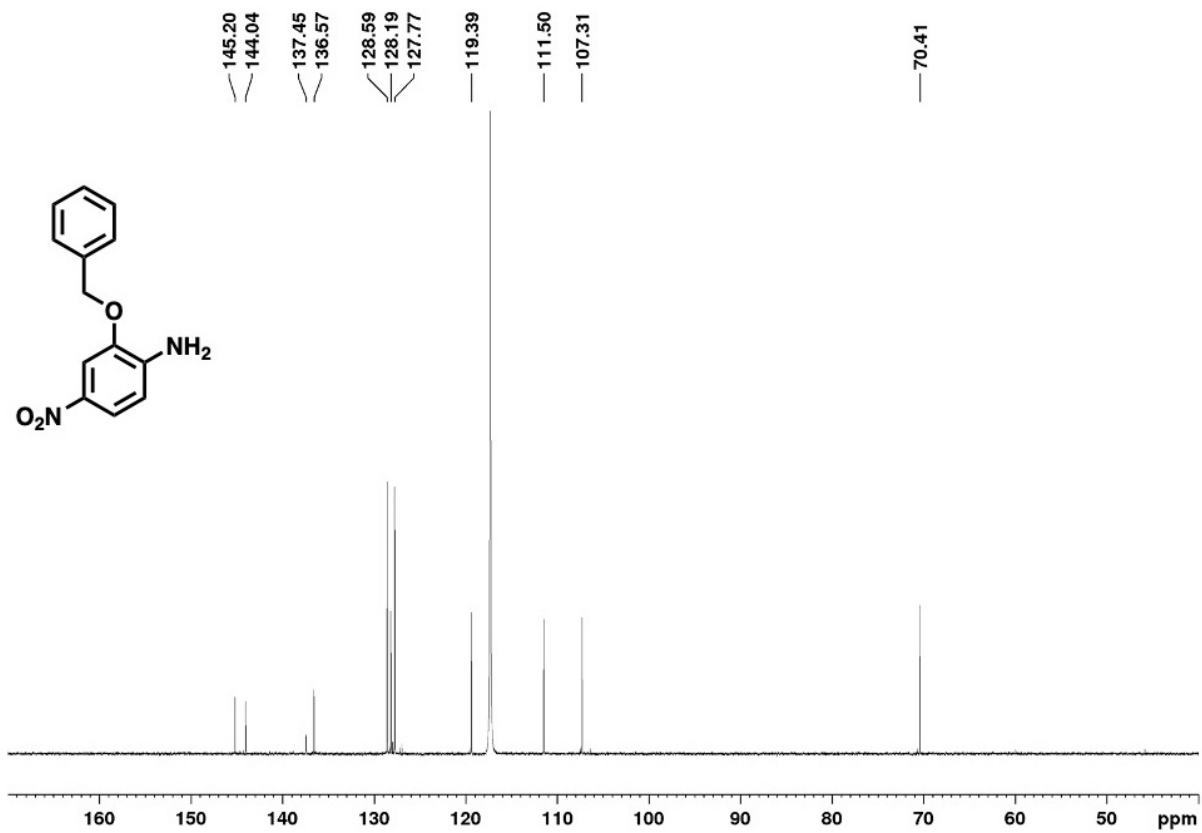


Figure 5.32. ^{13}C NMR Spectrum of Compound 10 in CD_3CN

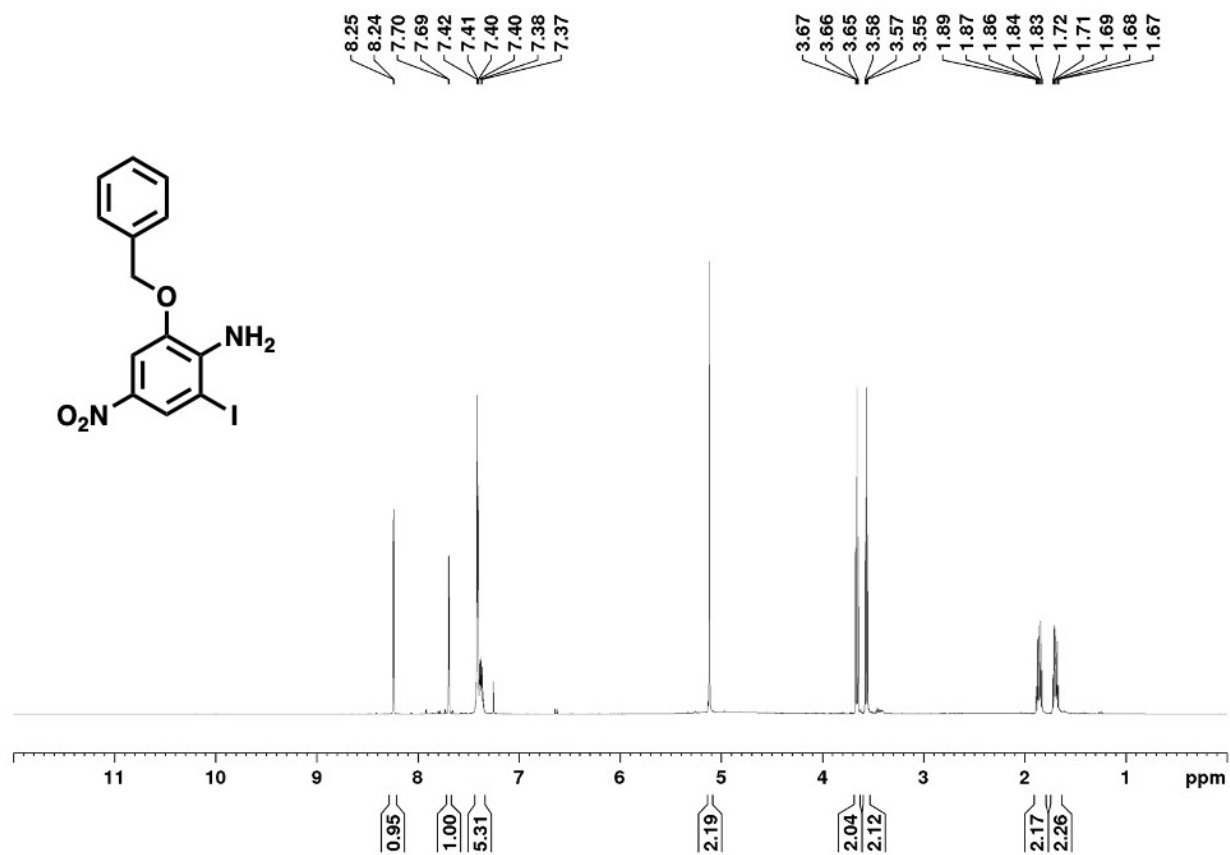


Figure 5.33. ¹H NMR Spectrum of Compound 11 in CDCl₃

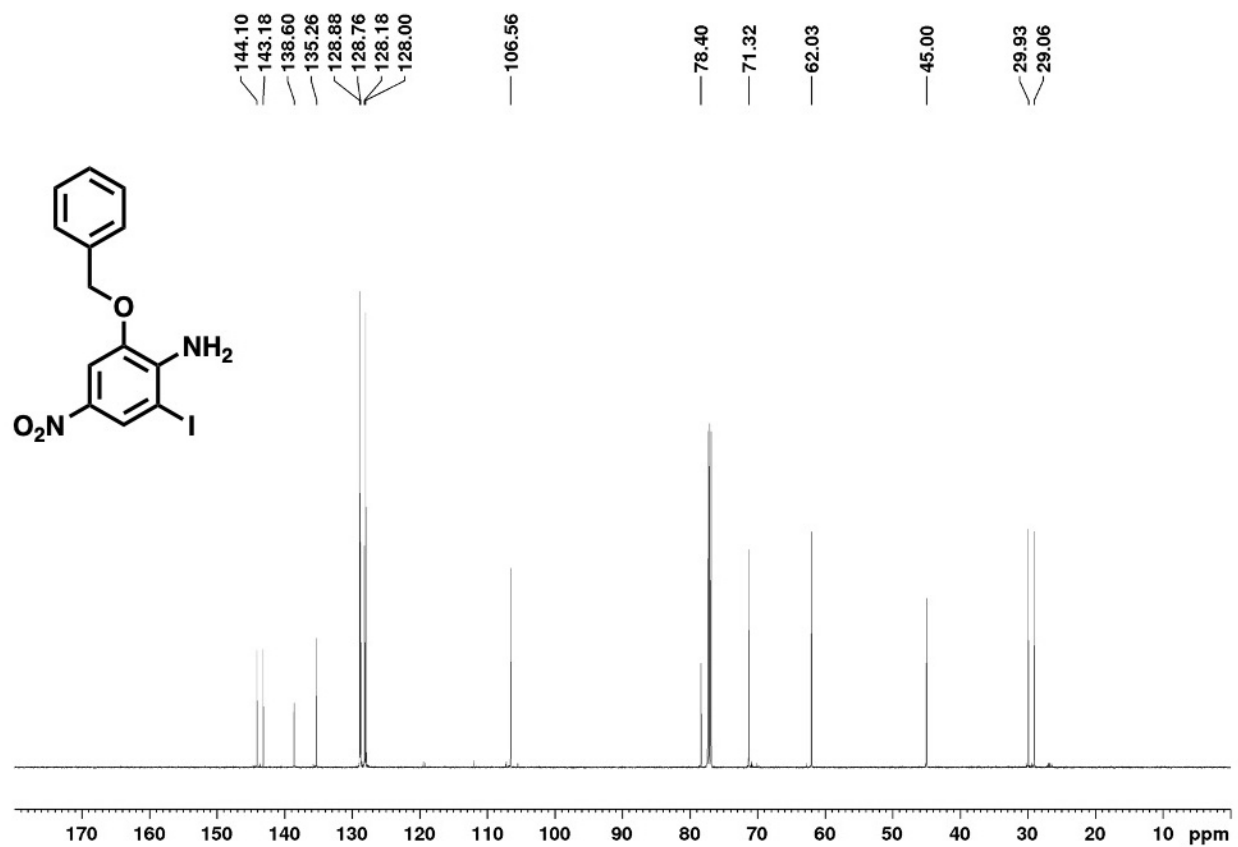


Figure 5.34. ^{13}C NMR Spectrum of Compound 11 in CDCl_3

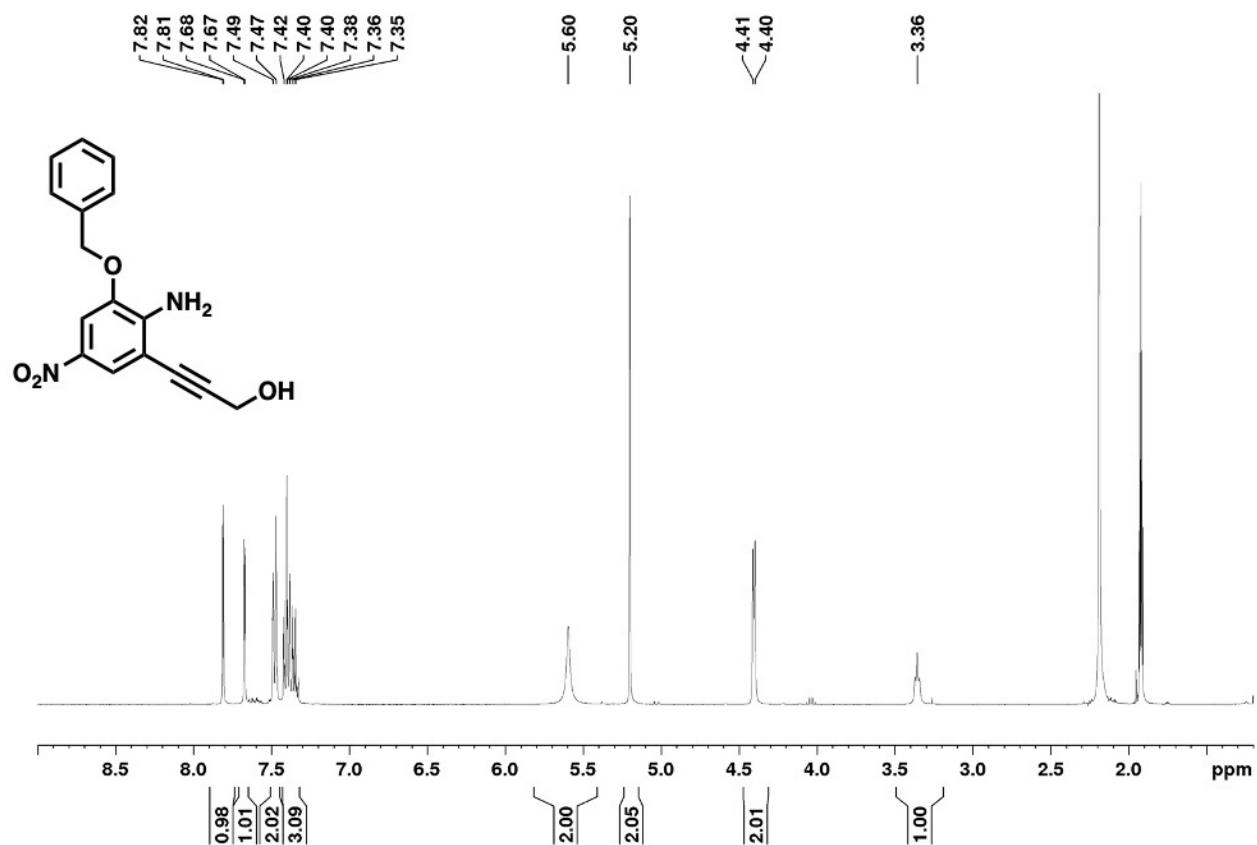


Figure 5.35. ¹H NMR Spectrum of Compound 12a in CD₃CN

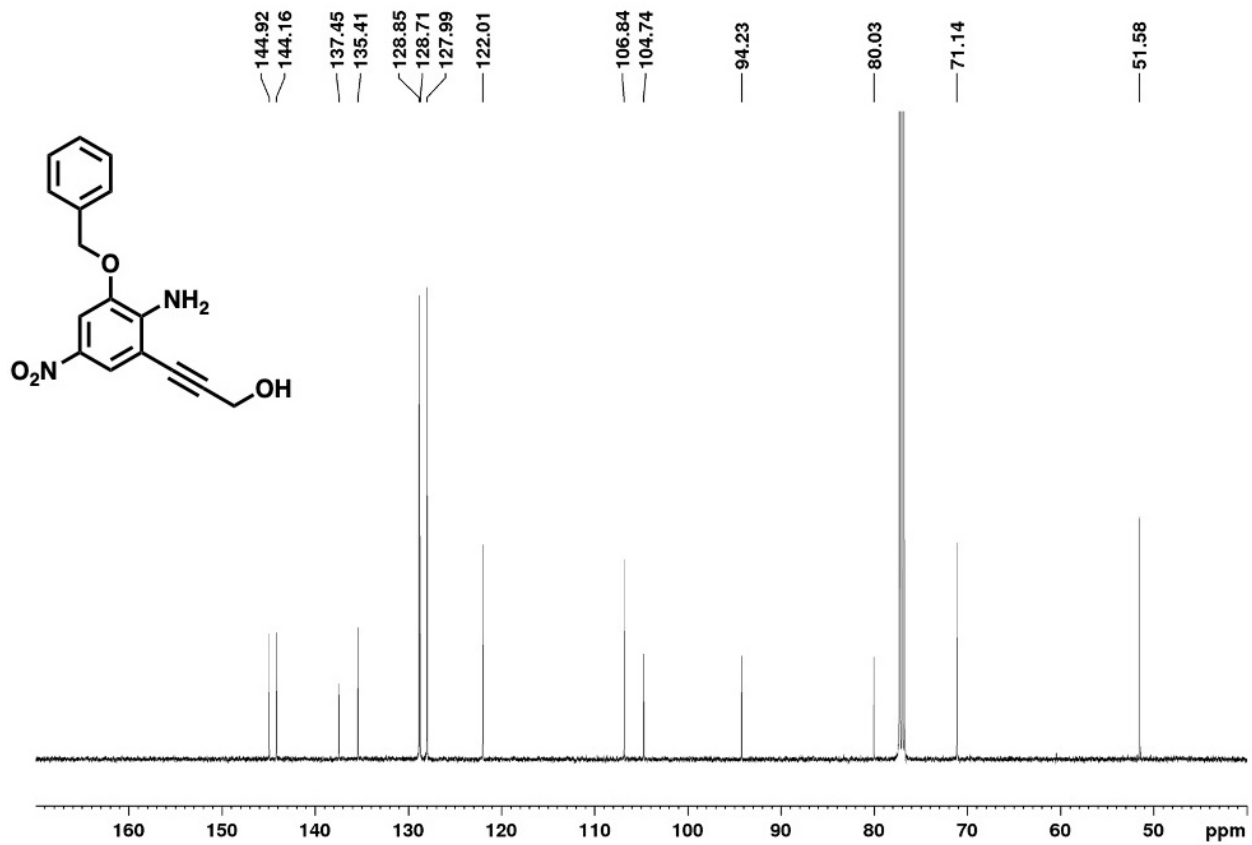


Figure 5.36. ¹³C NMR Spectrum of Compound 12a in CDCl₃

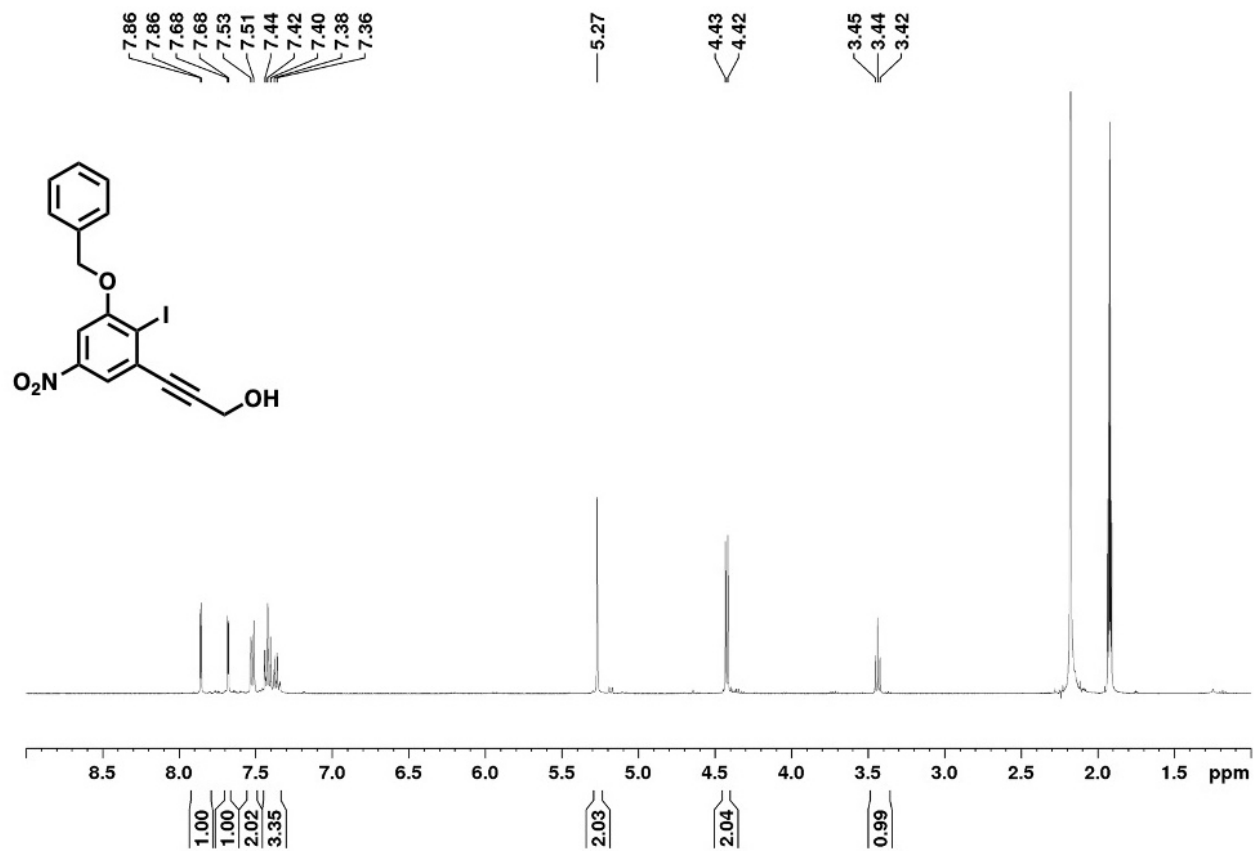


Figure 5.37. ¹H NMR Spectrum of Compound 13a in CD₃CN

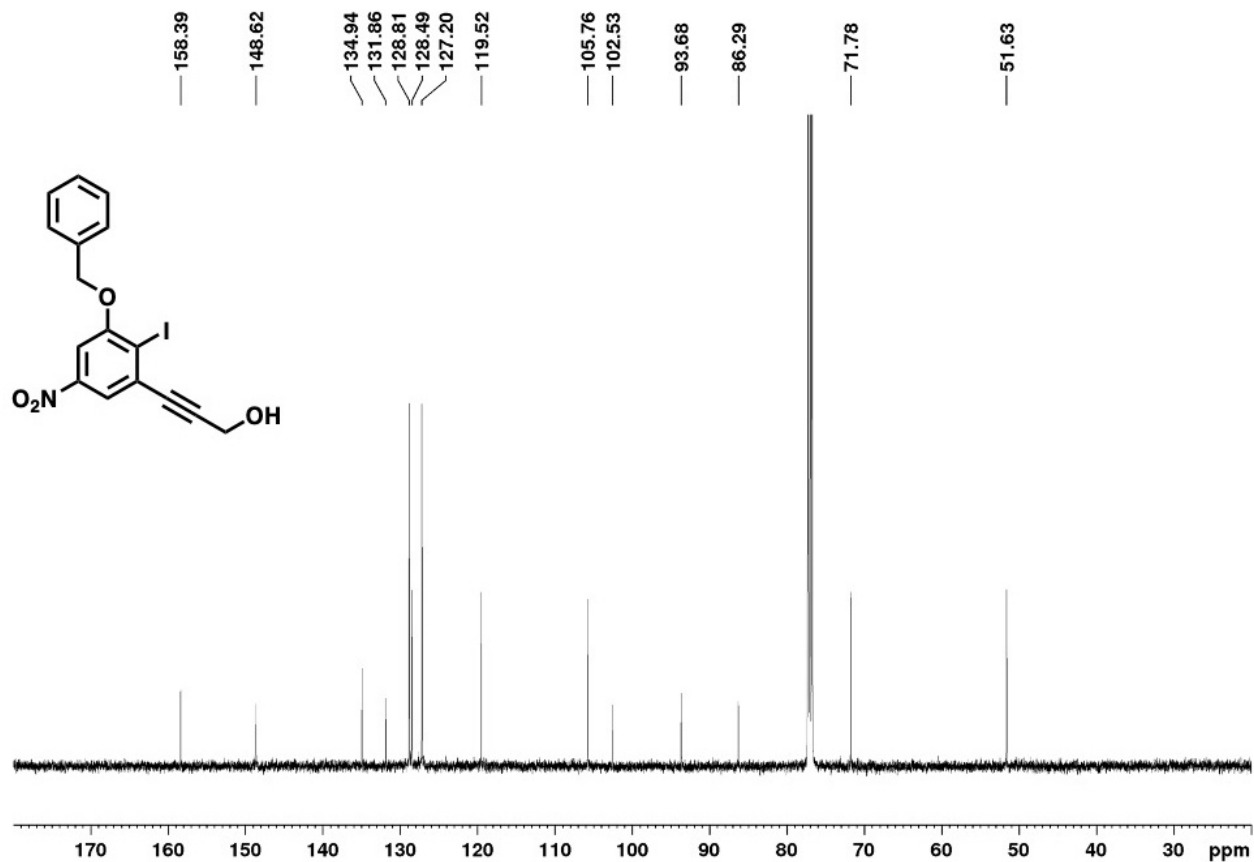


Figure 5.38. ¹³C NMR Spectrum of Compound 13a in CD₃CN

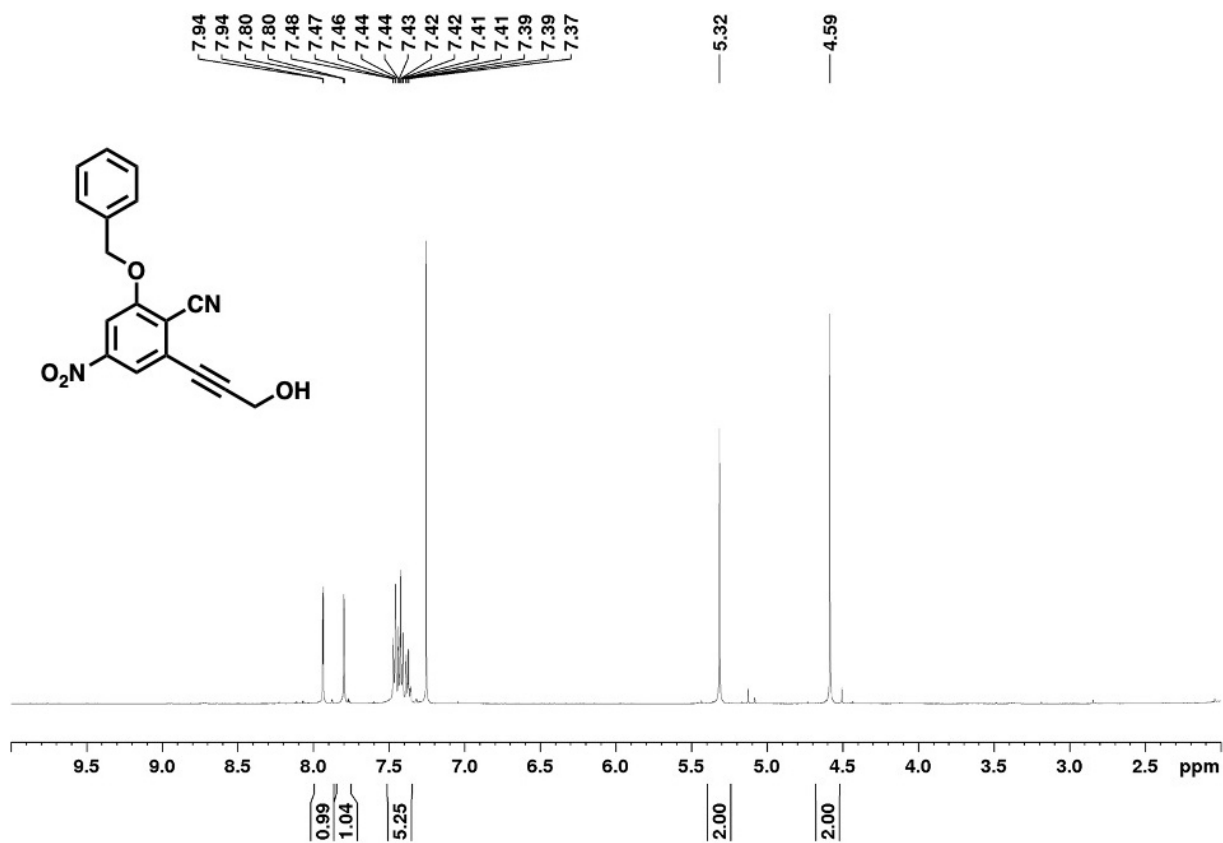


Figure 5.39. ¹H NMR Spectrum of Compound 14a in CDCl₃

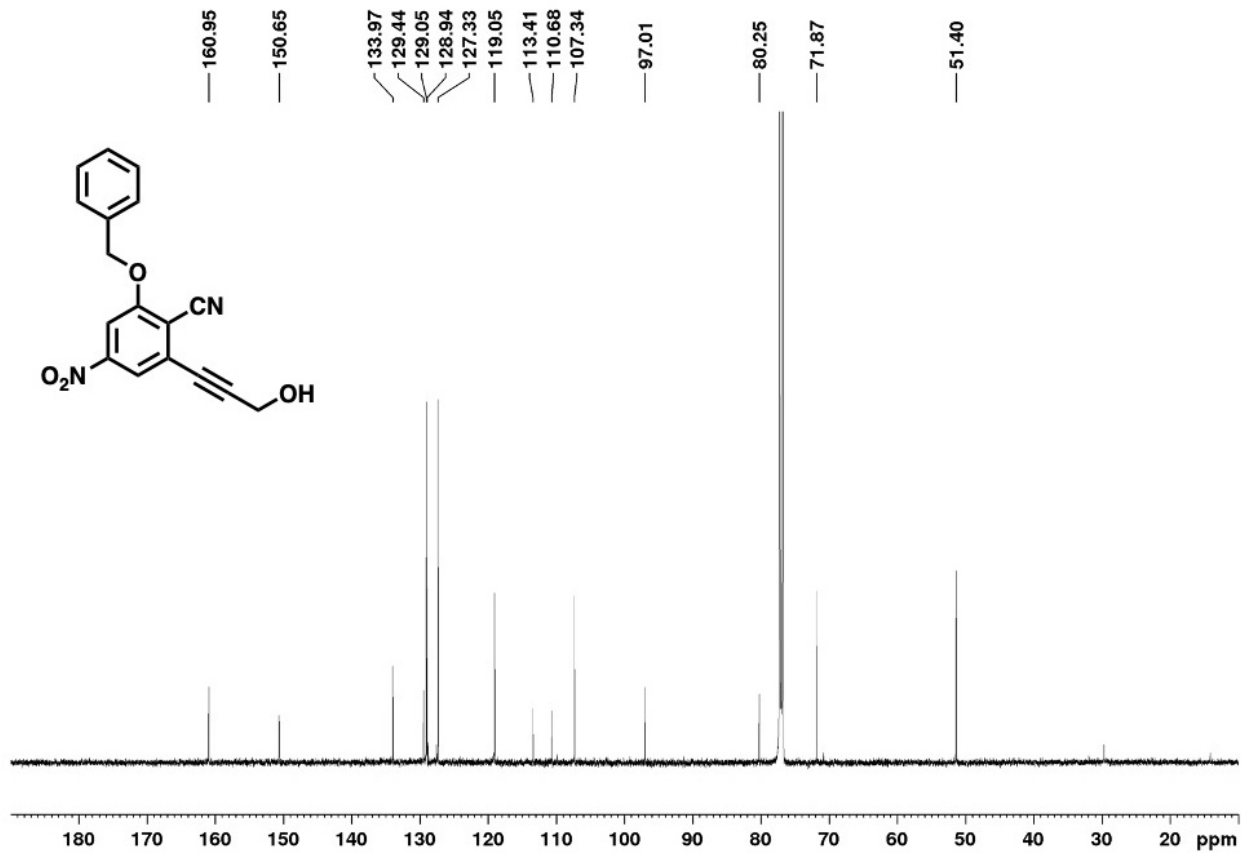


Figure 5.40. ¹³C NMR Spectrum of Compound 14a in CDCl₃

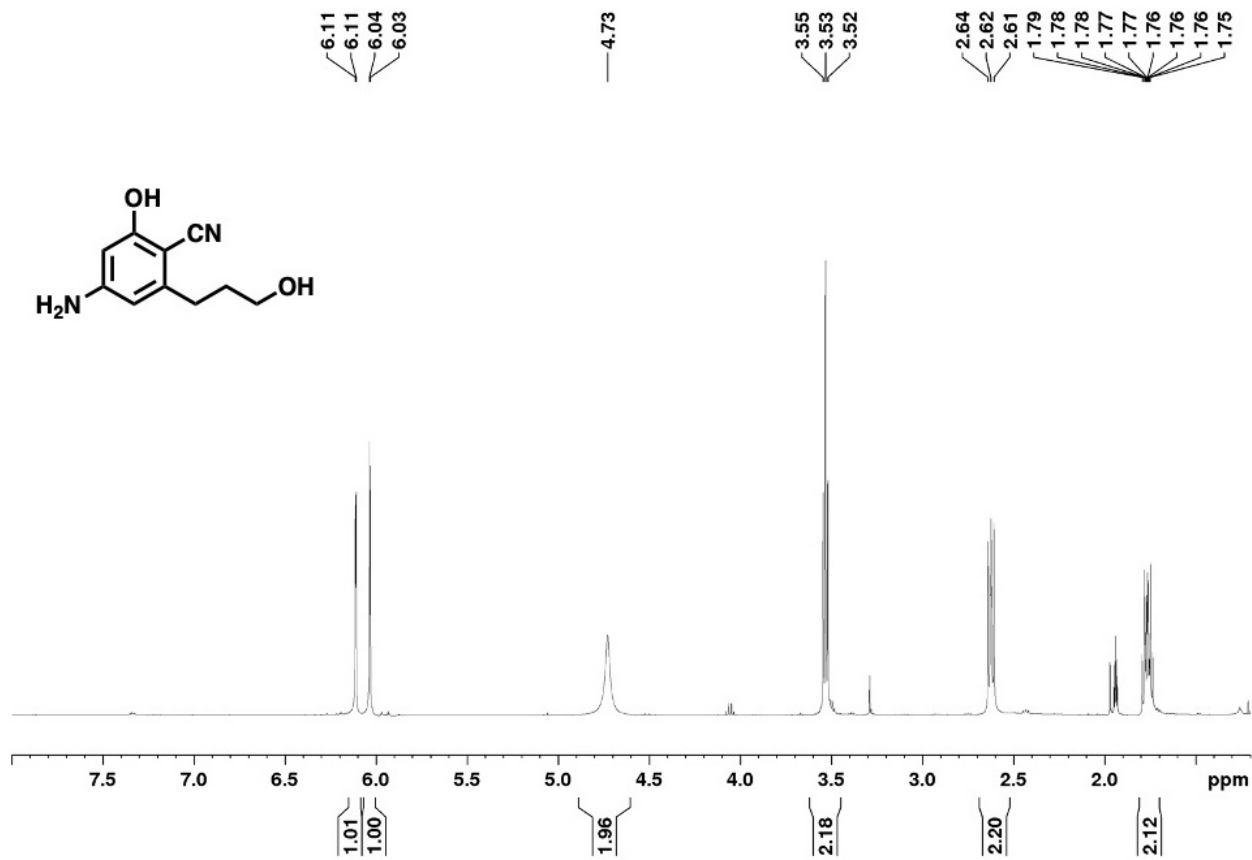


Figure 5.41. ¹H NMR Spectrum of Compound 15a in CD₃CN

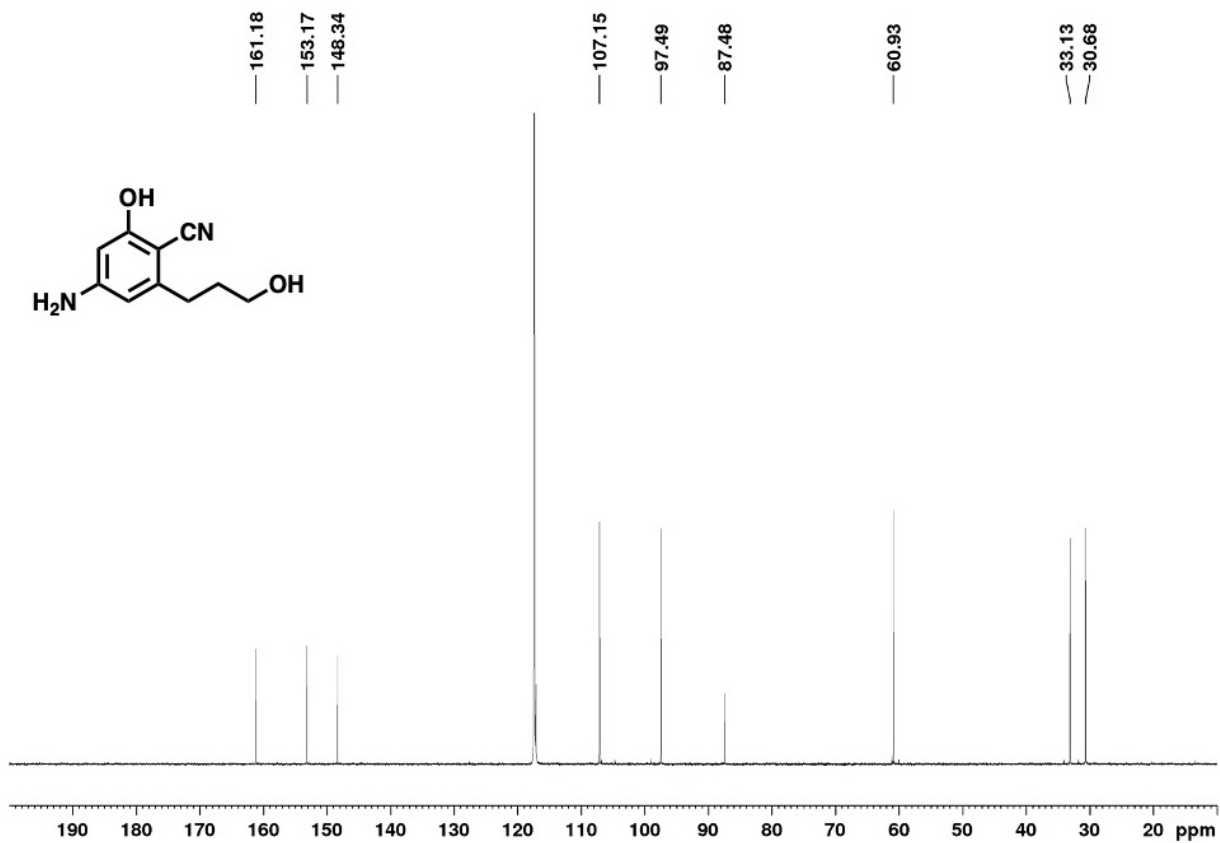


Figure 5.42. ^{13}C NMR Spectrum of Compound 15a in CD_3CN

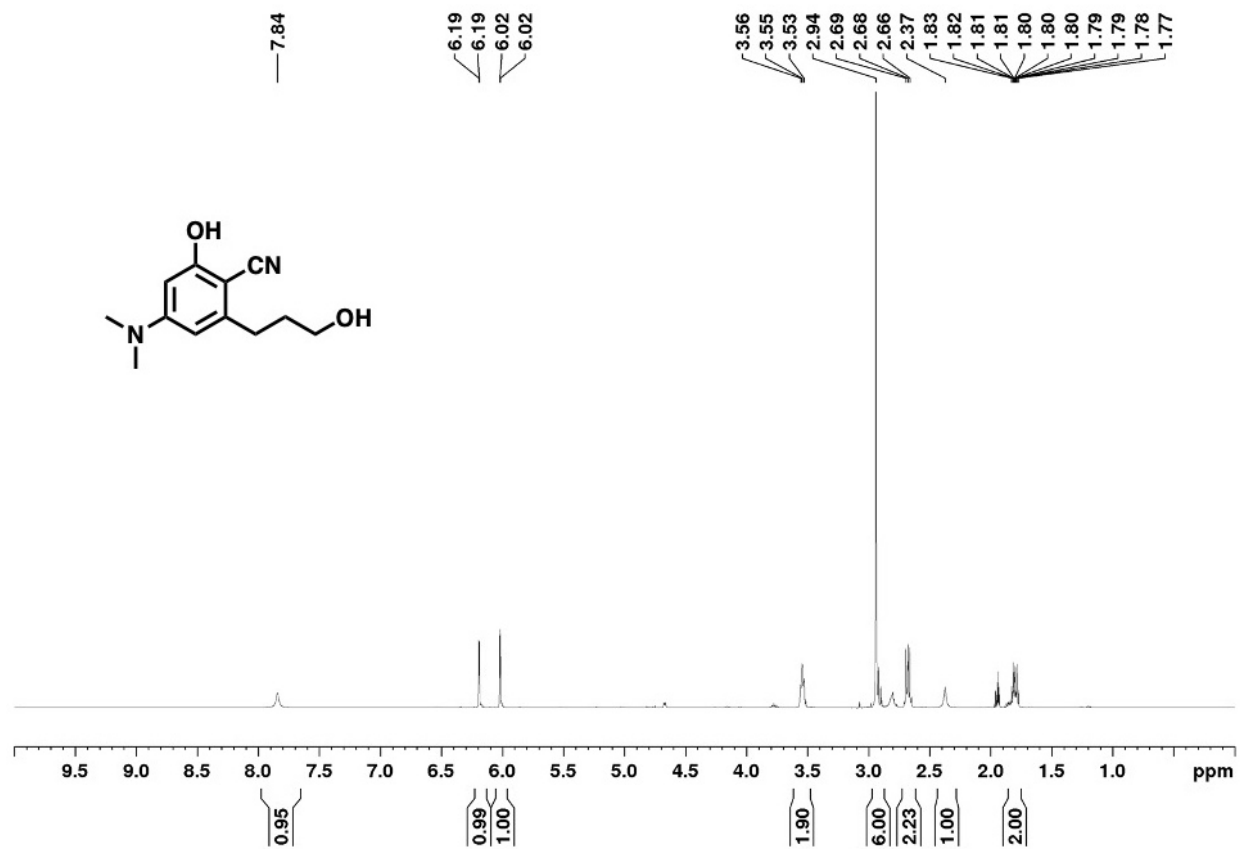


Figure 5.43. ¹H NMR Spectrum of Compound 16a in CD₃CN

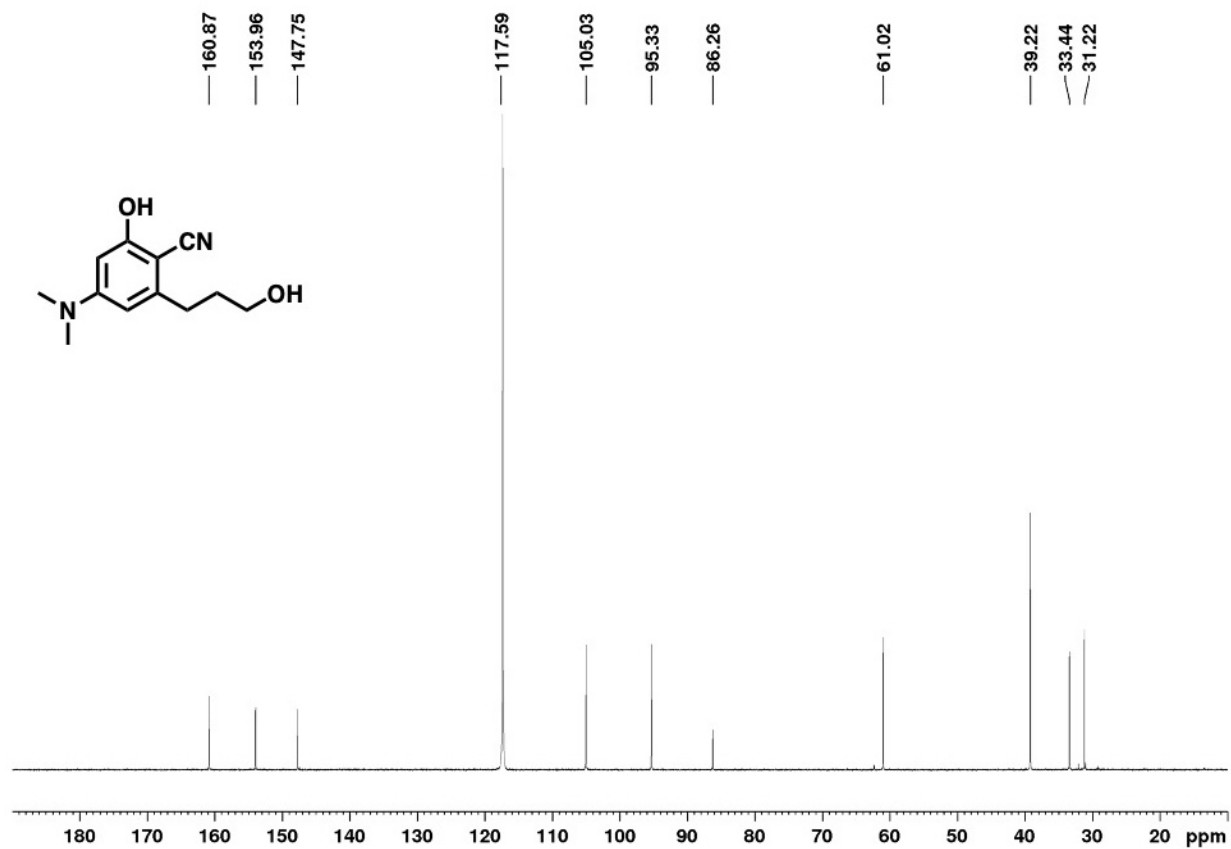


Figure 5.44. ¹³C NMR Spectrum of Compound 16a in CD₃CN

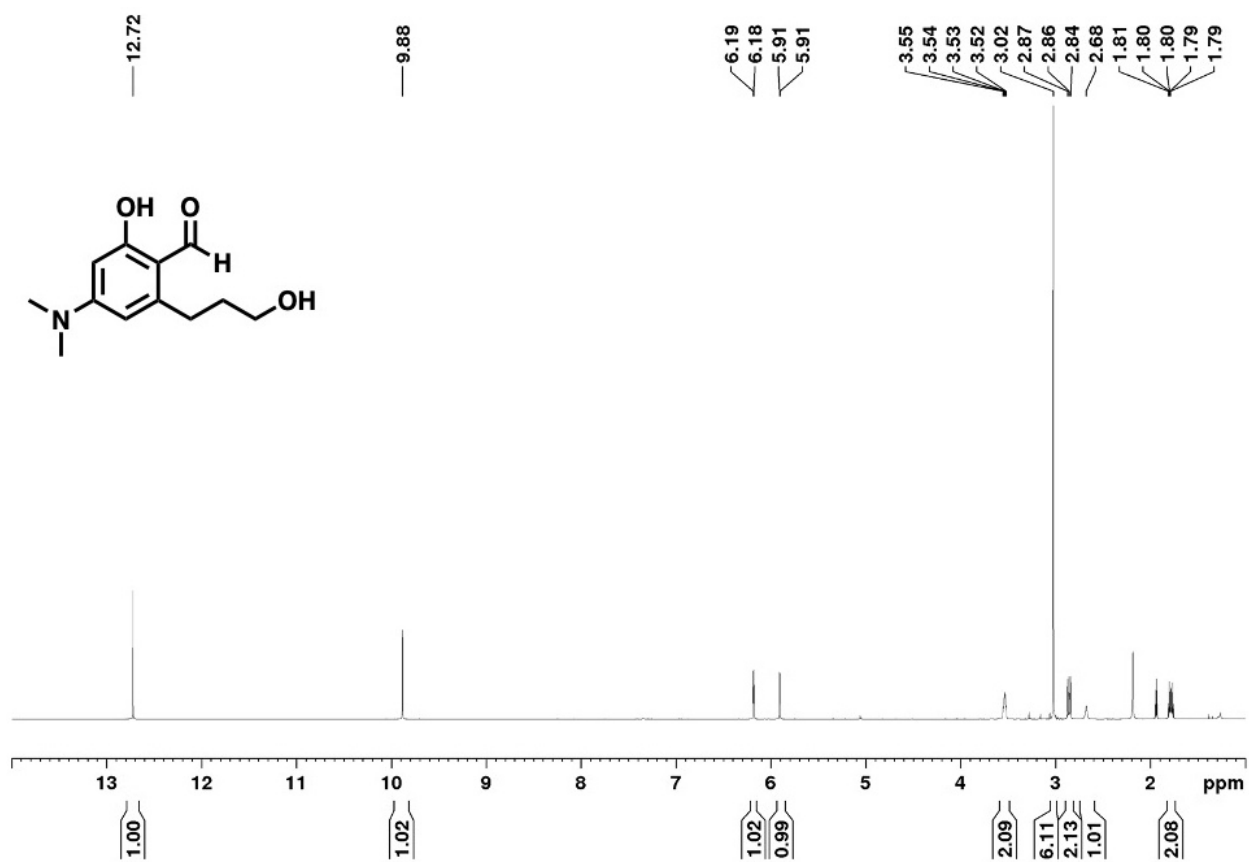


Figure 5.45. ¹H NMR Spectrum of Compound 17a in CD₃CN

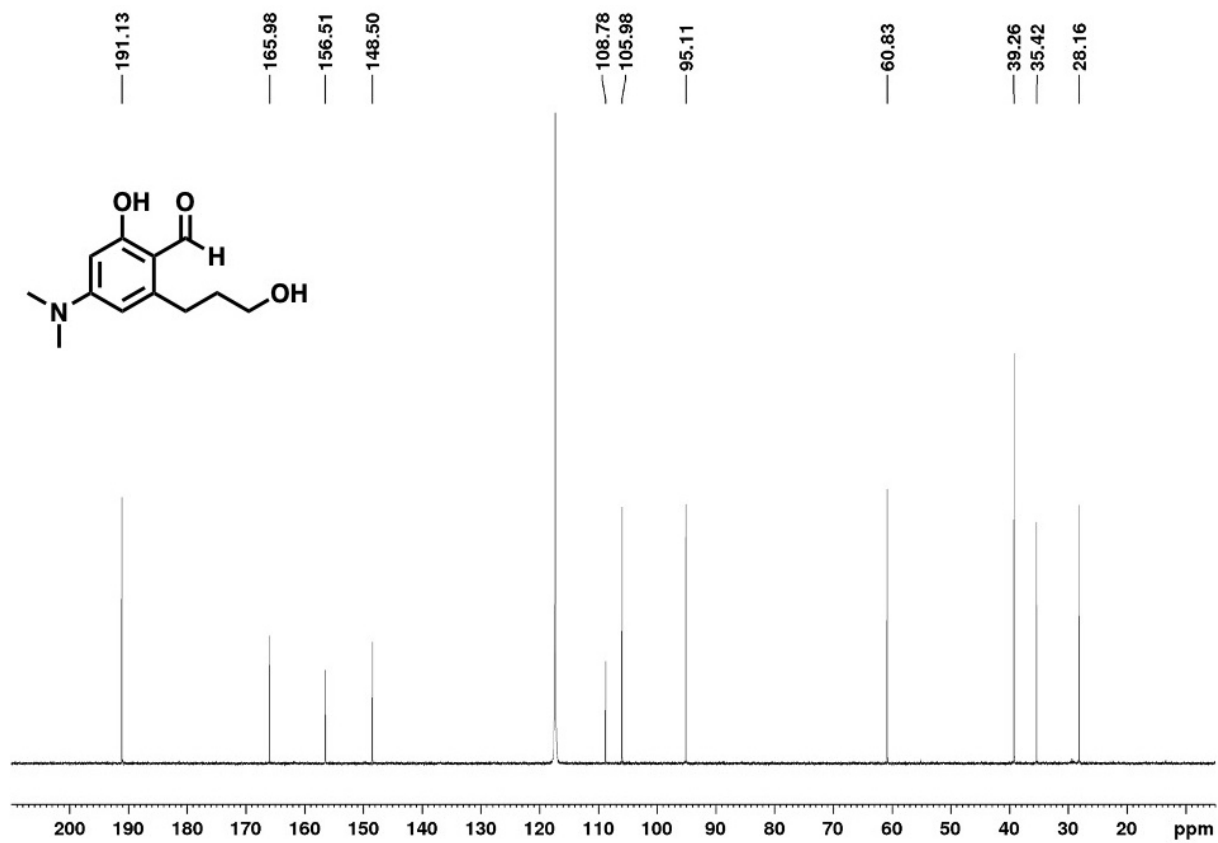


Figure 5.46. ^{13}C NMR Spectrum of Compound 17a in CD_3CN

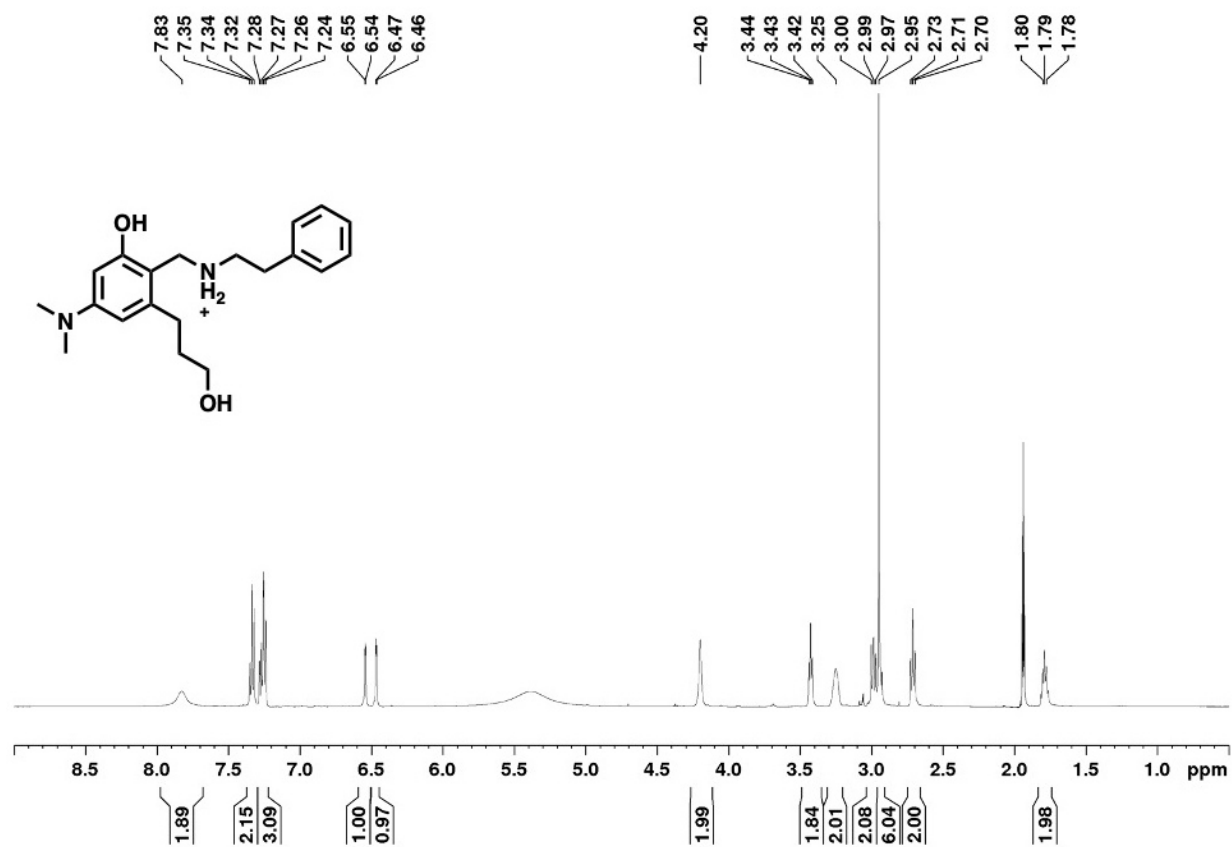


Figure 5.47. ¹H NMR Spectrum of Compound 5a in CD₃CN

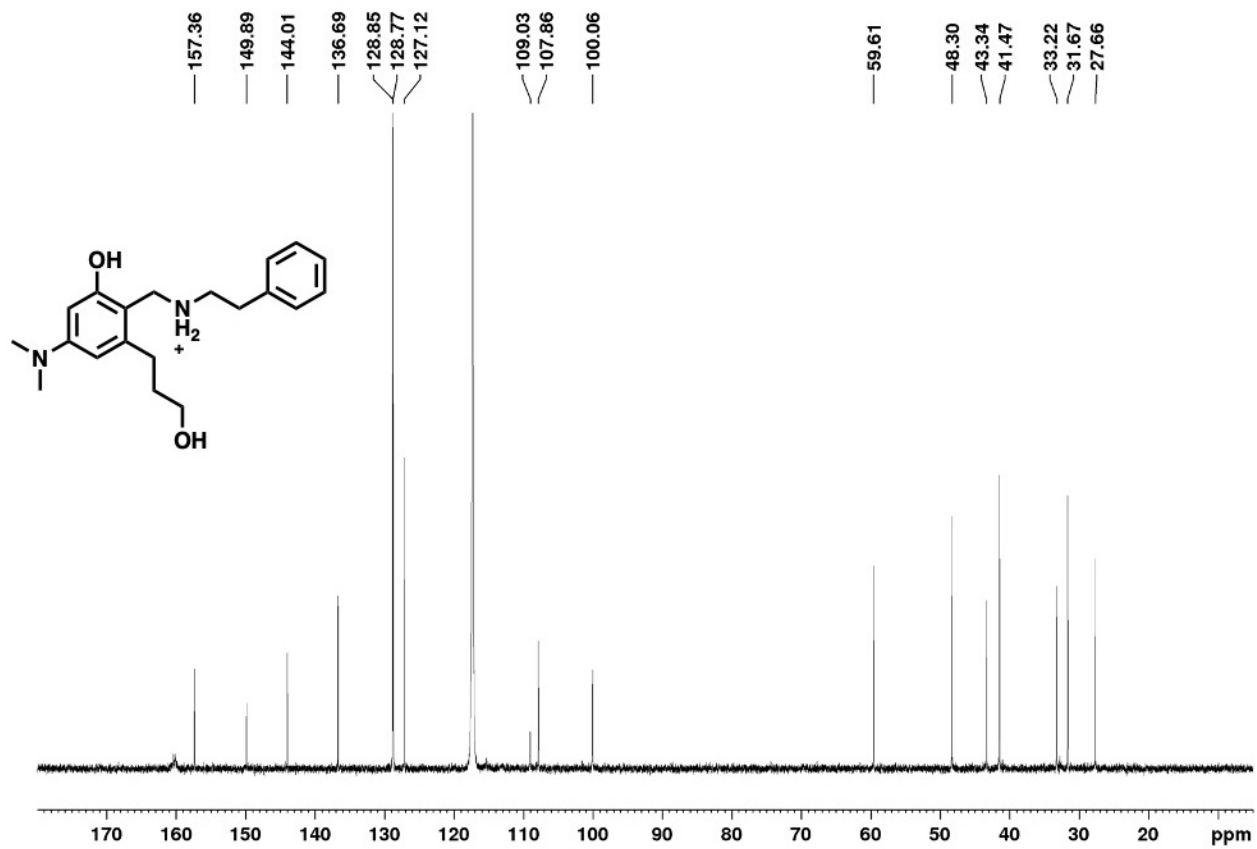


Figure 5.48. ^{13}C NMR Spectrum of Compound 5a in CD_3CN

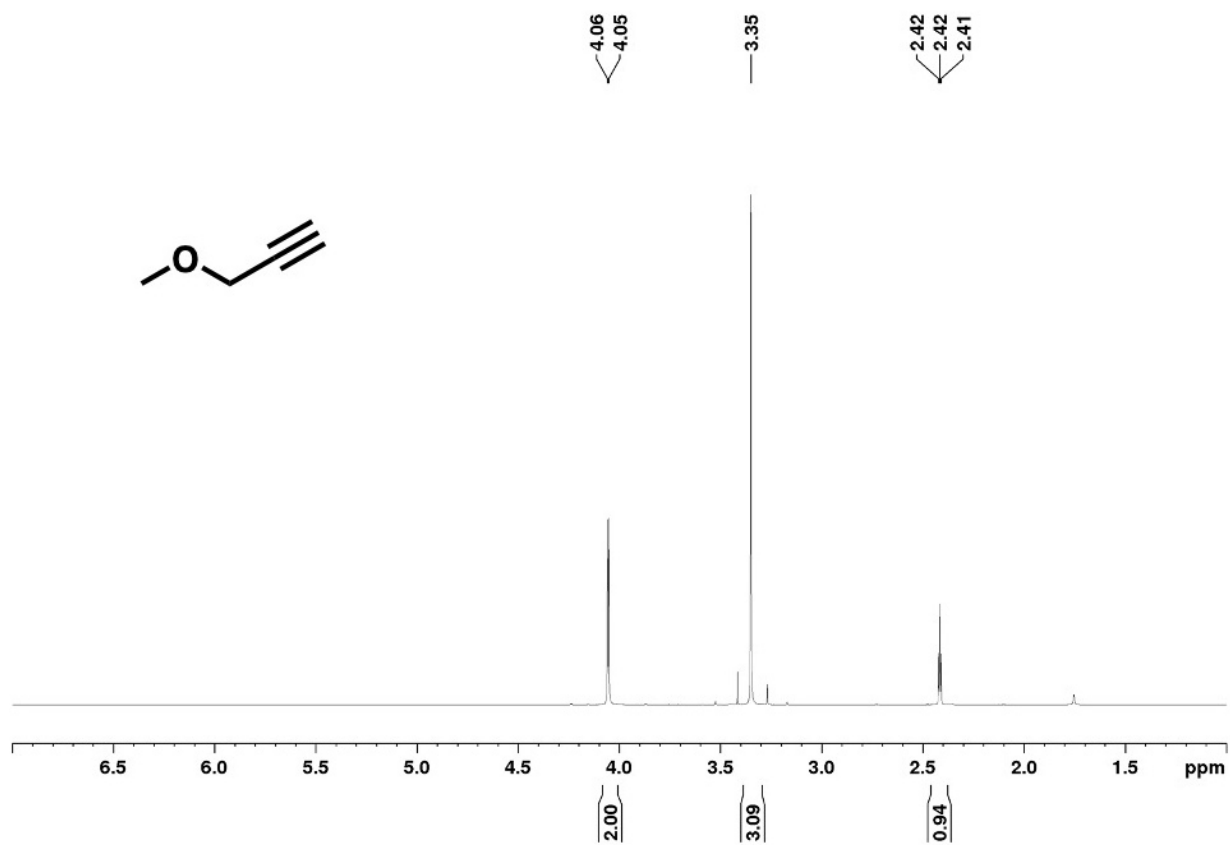


Figure 5.49. ^1H NMR Spectrum of Compound 18 in CDCl_3

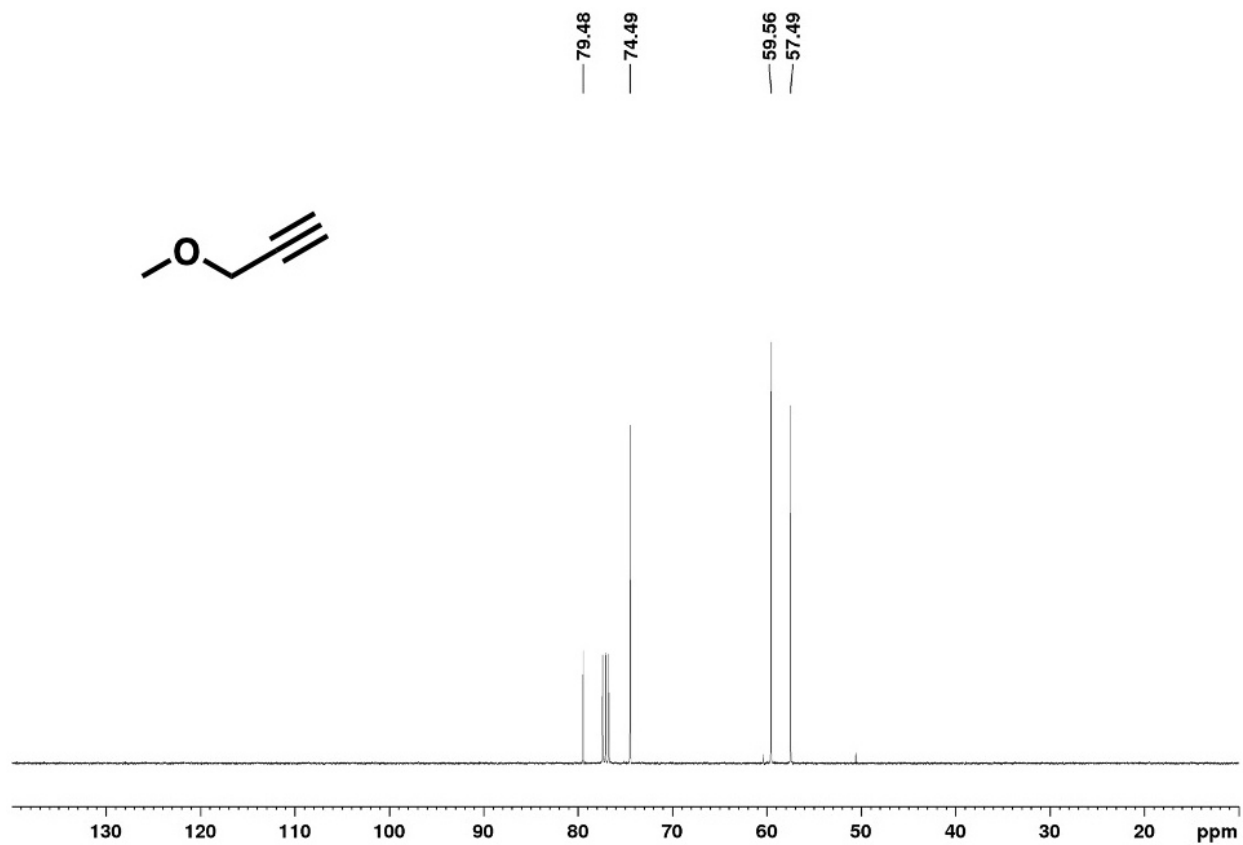


Figure 5.50. ^{13}C NMR Spectrum of Compound 18 in CDCl_3

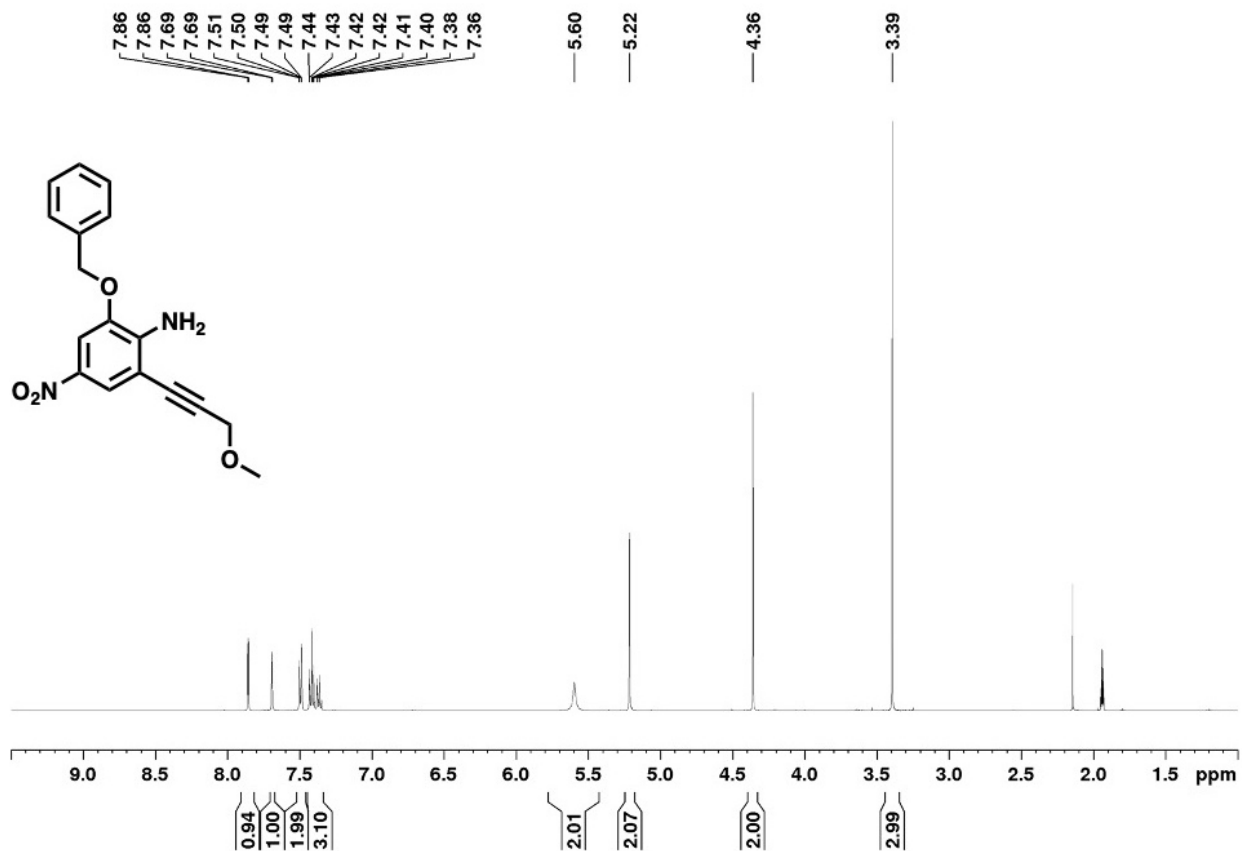


Figure 5.51. ¹H NMR Spectrum of Compound 12b in CD₃CN

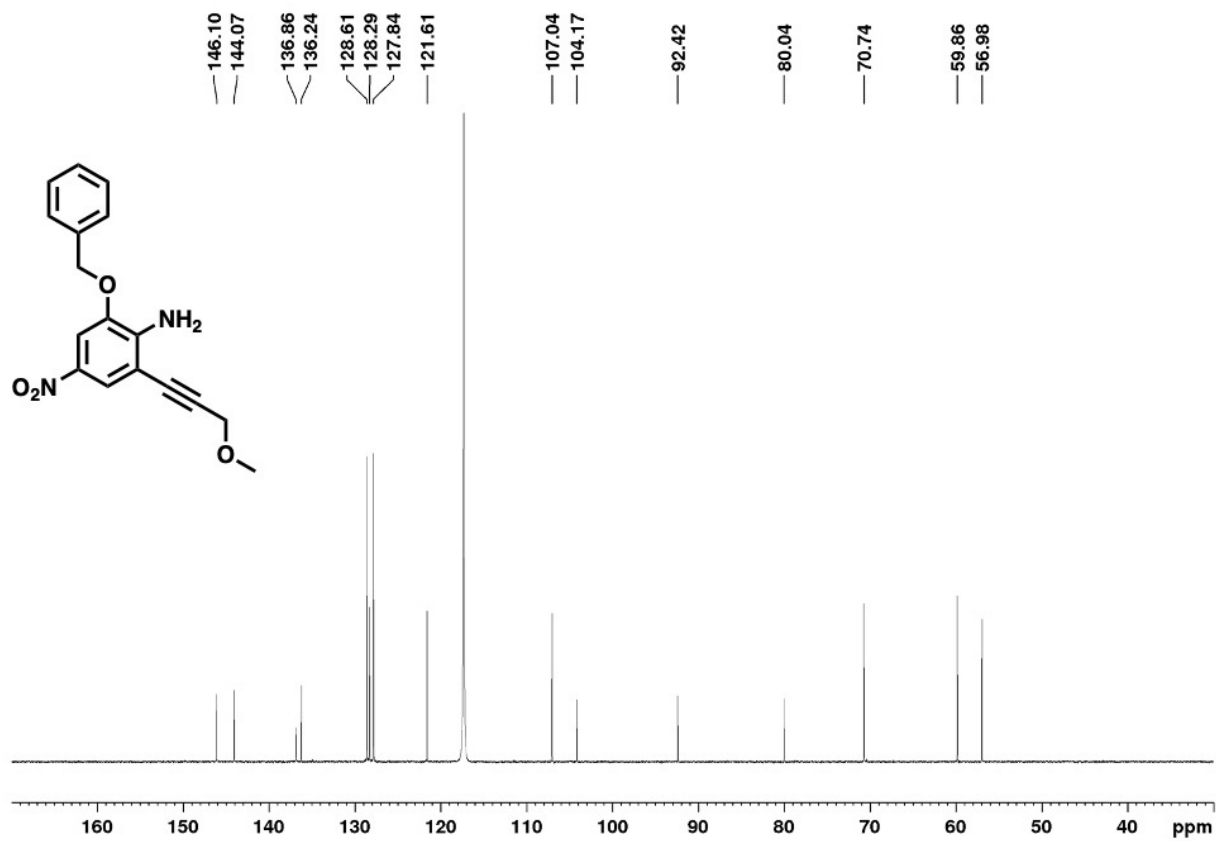


Figure 5.52. ^{13}C NMR Spectrum of Compound 12b in CD_3CN

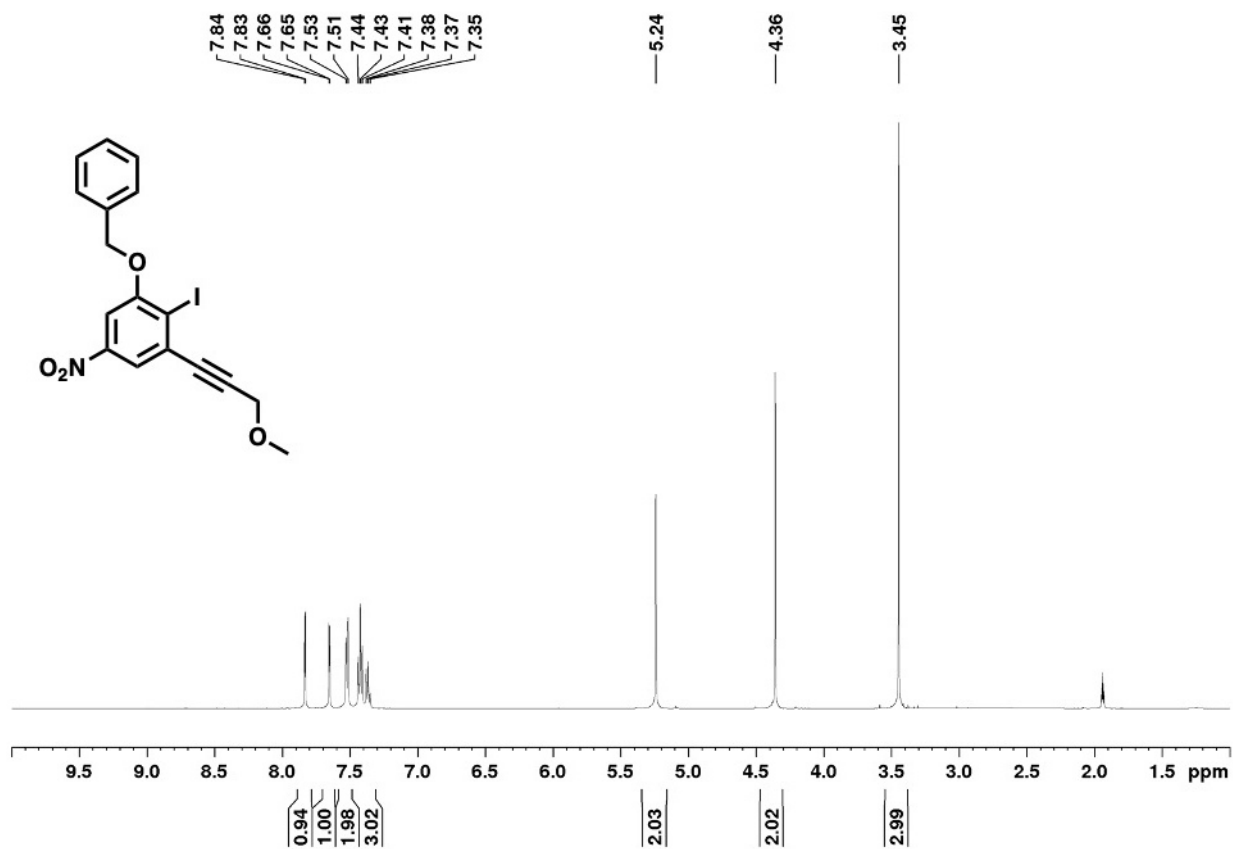


Figure 5.53. ¹H NMR Spectrum of Compound 13b in CD₃CN

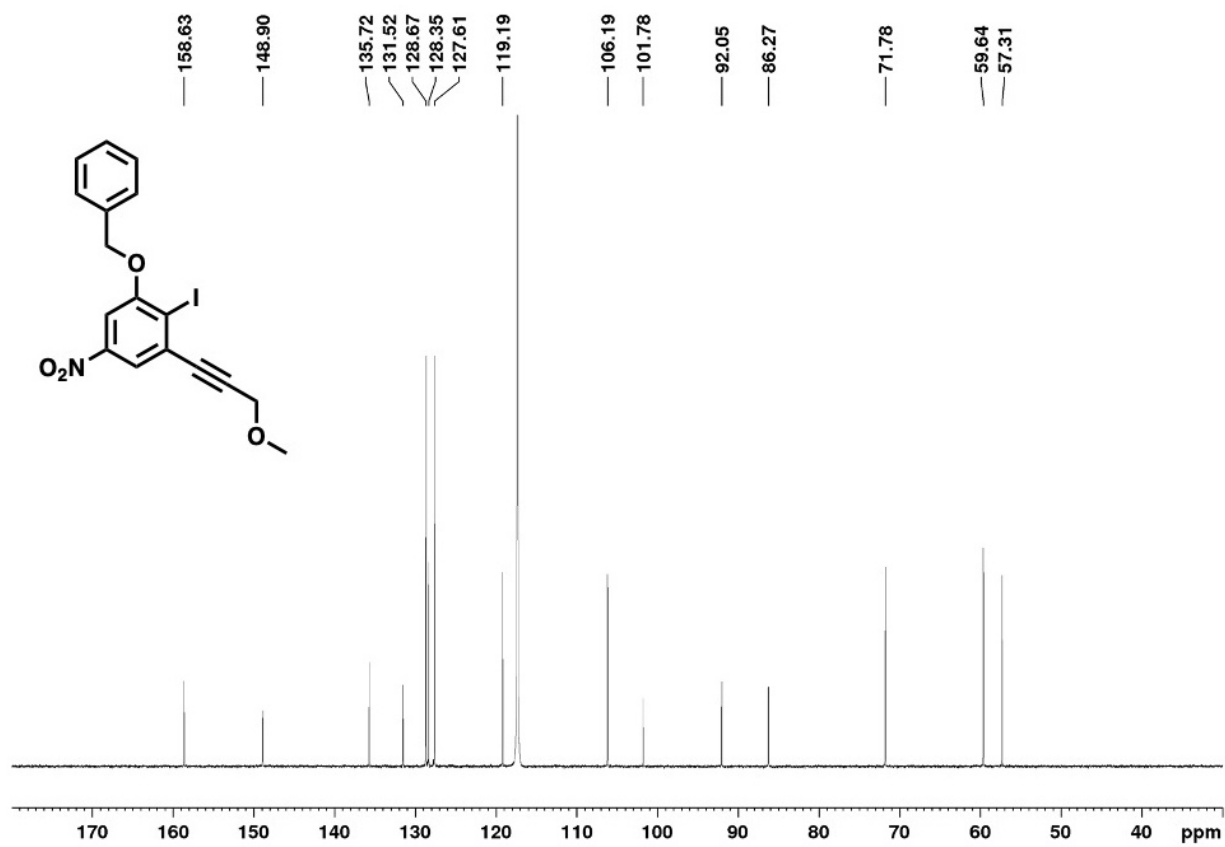


Figure 5.54. ^{13}C NMR Spectrum of Compound 13b in CD_3CN

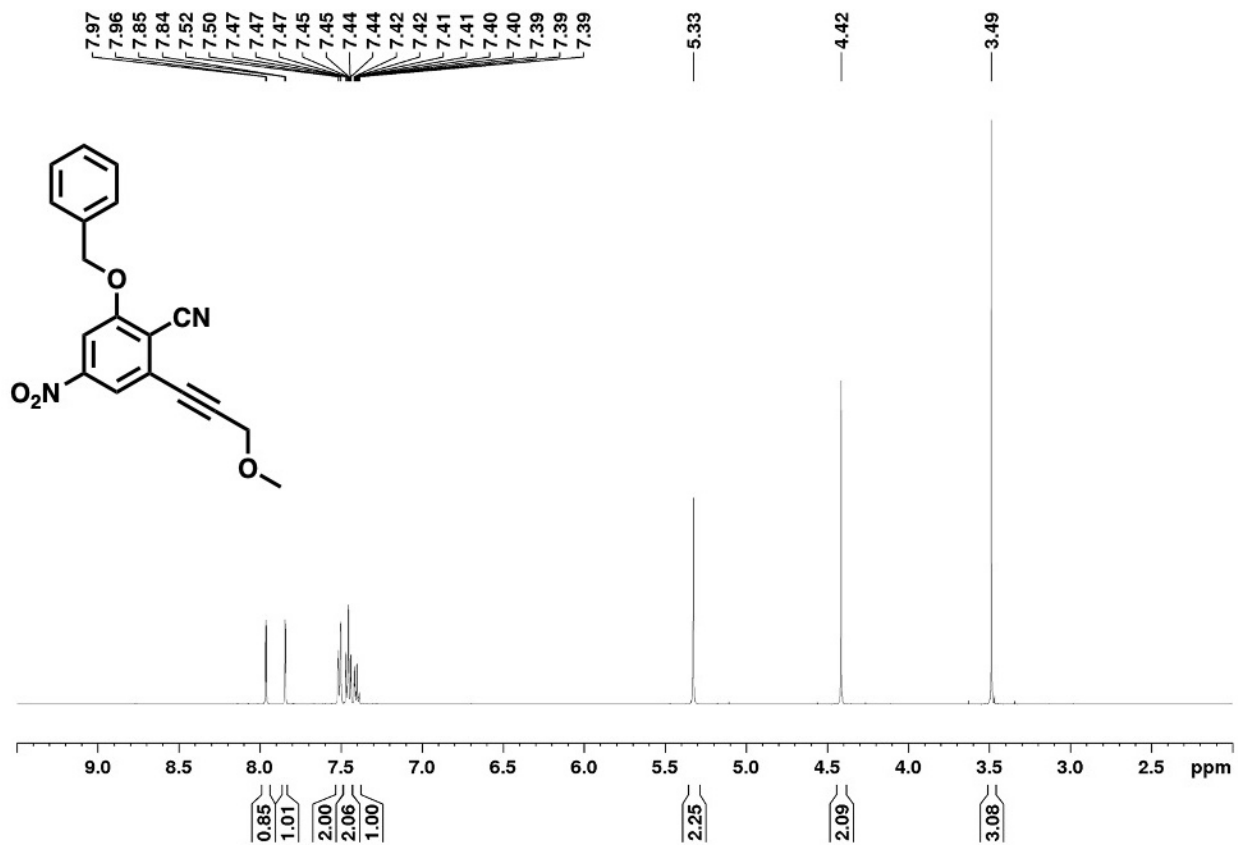


Figure 5.55. ¹H NMR Spectrum of Compound 14b in CD₃CN

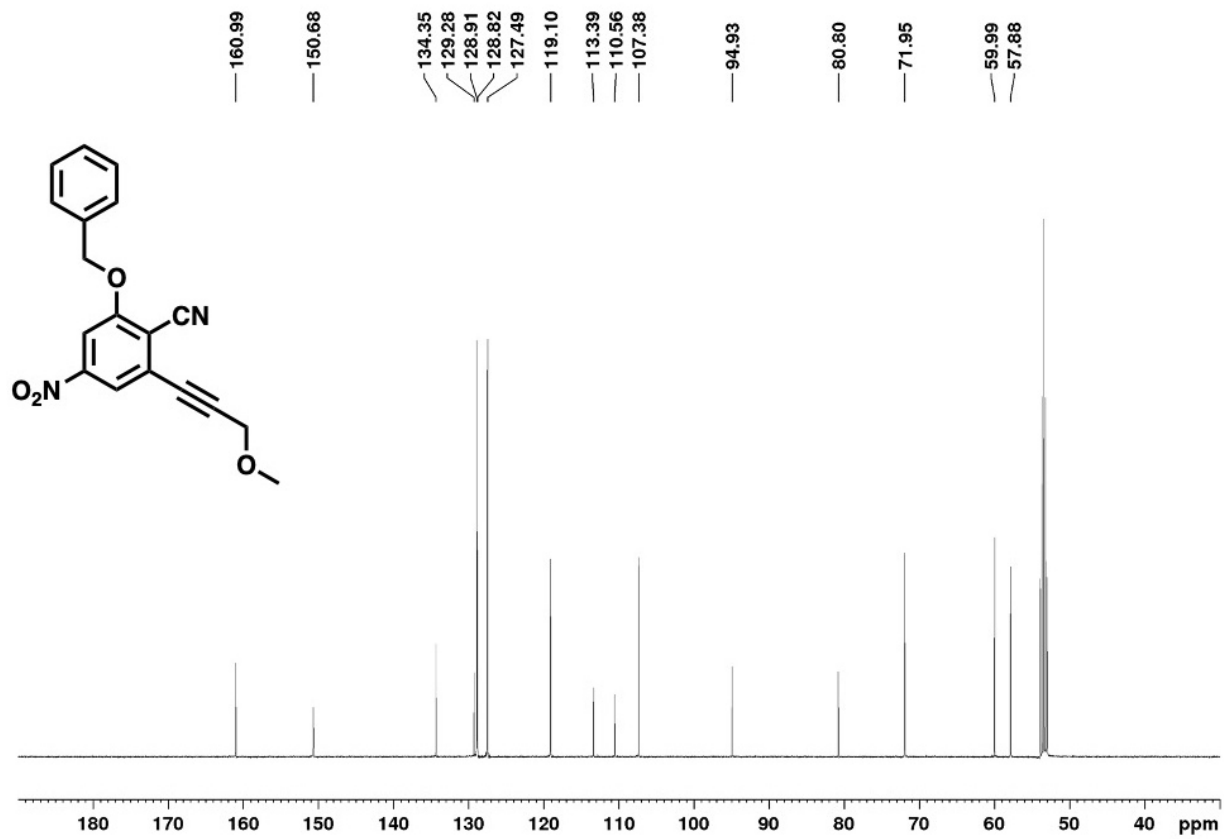


Figure 5.56. ^{13}C NMR Spectrum of Compound 14b in CD_2Cl_2

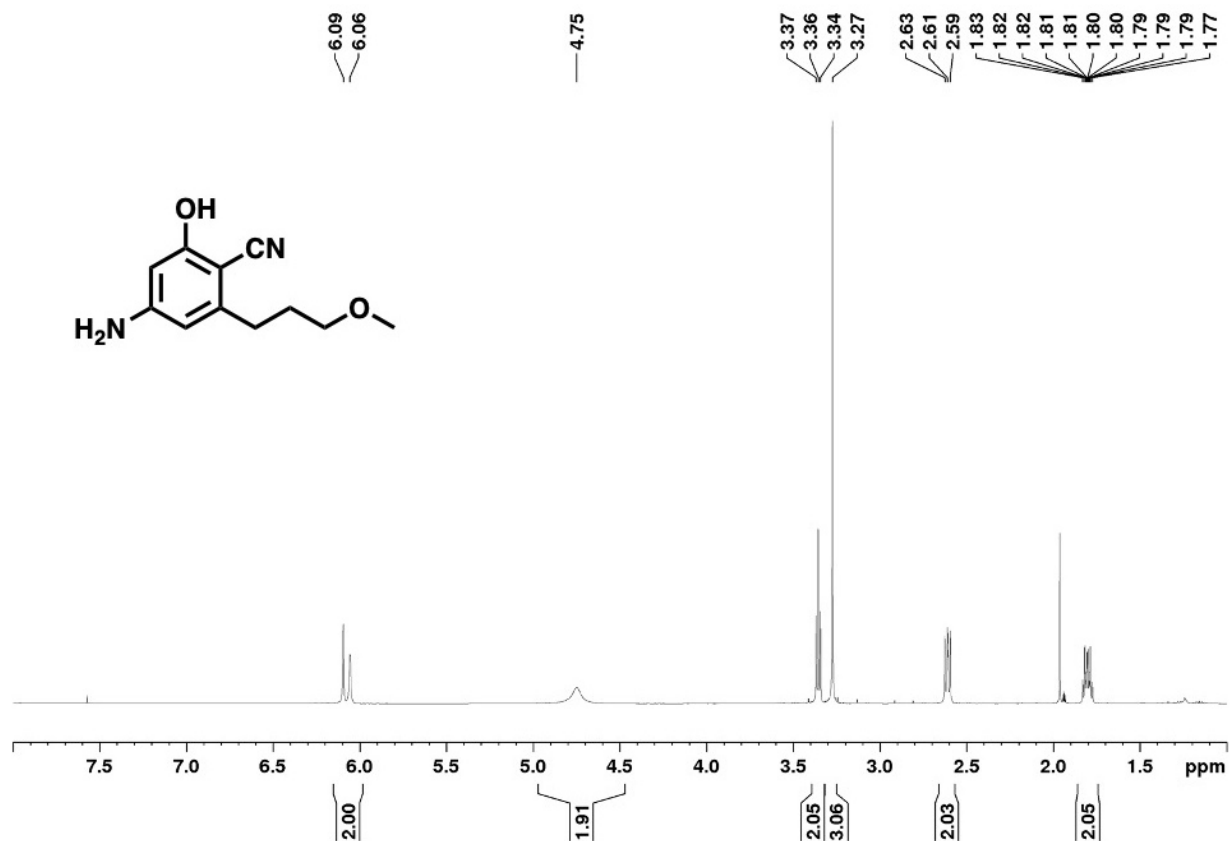


Figure 5.57. ¹H NMR Spectrum of Compound 15b in CD₃CN

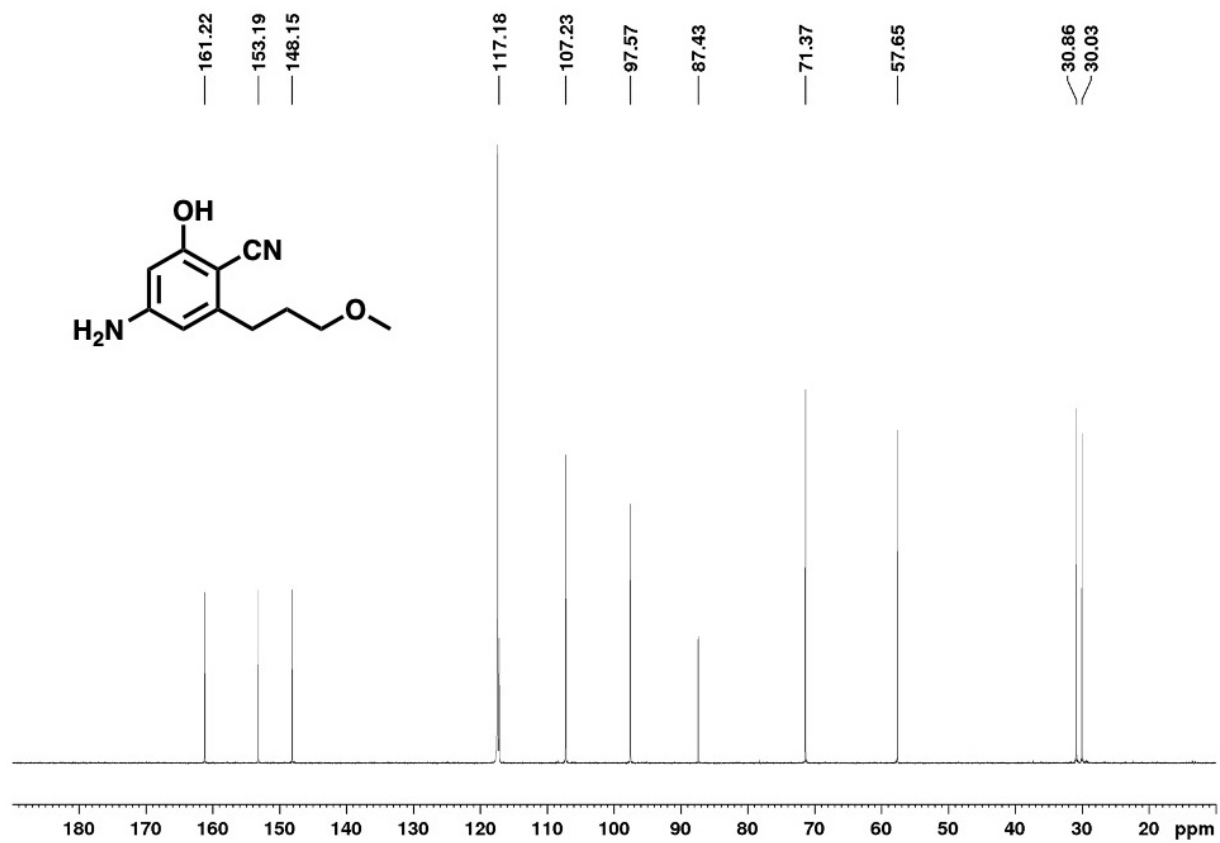


Figure 5.58. ^{13}C NMR Spectrum of Compound 15b in CD_3CN

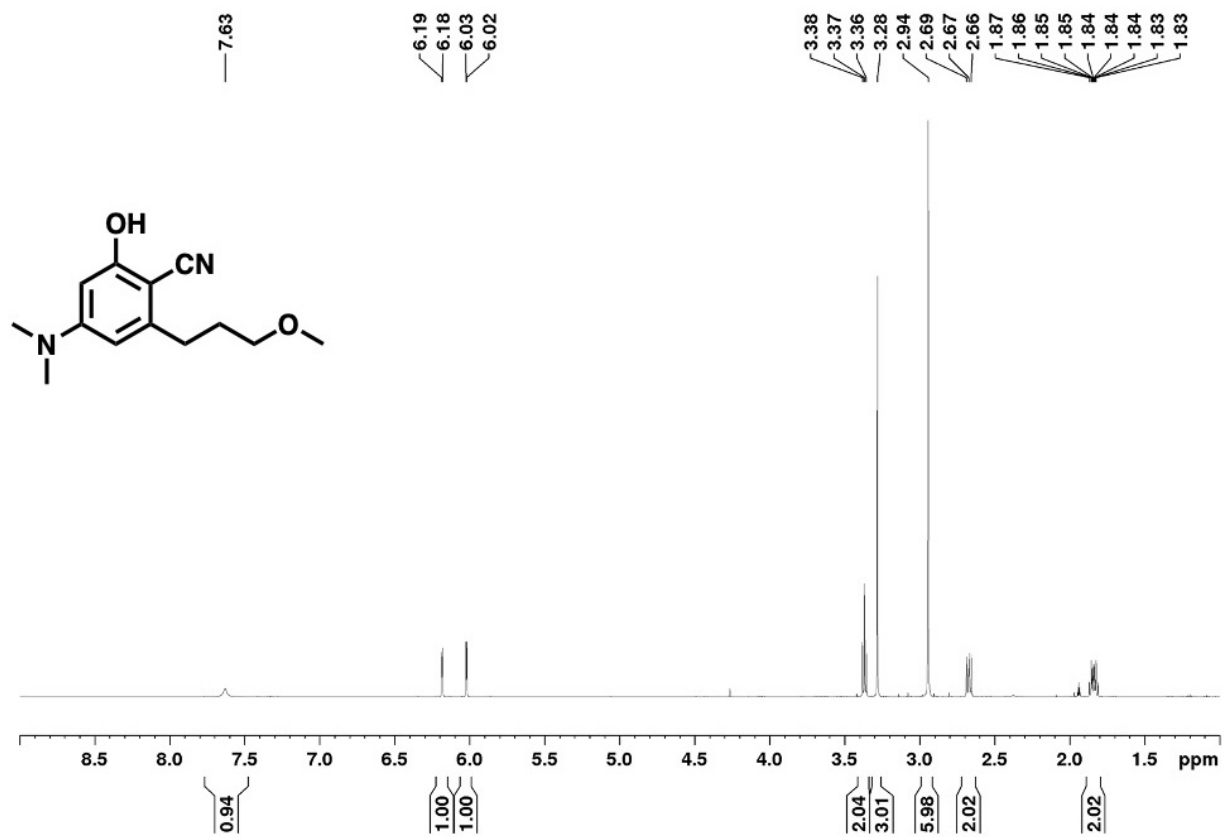


Figure 5.59. ¹H NMR Spectrum of Compound 16b in CD₃CN

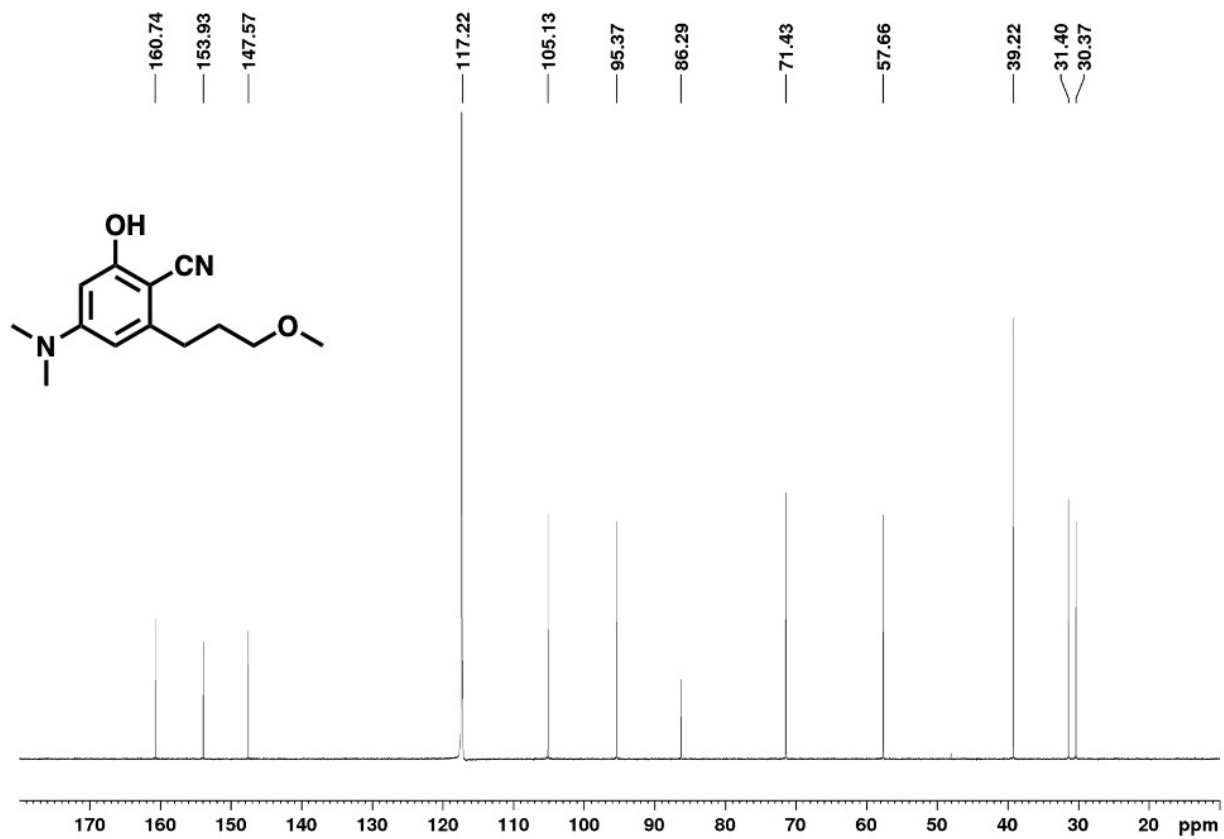


Figure 5.60. ¹³C NMR Spectrum of Compound 16b in CD₃CN

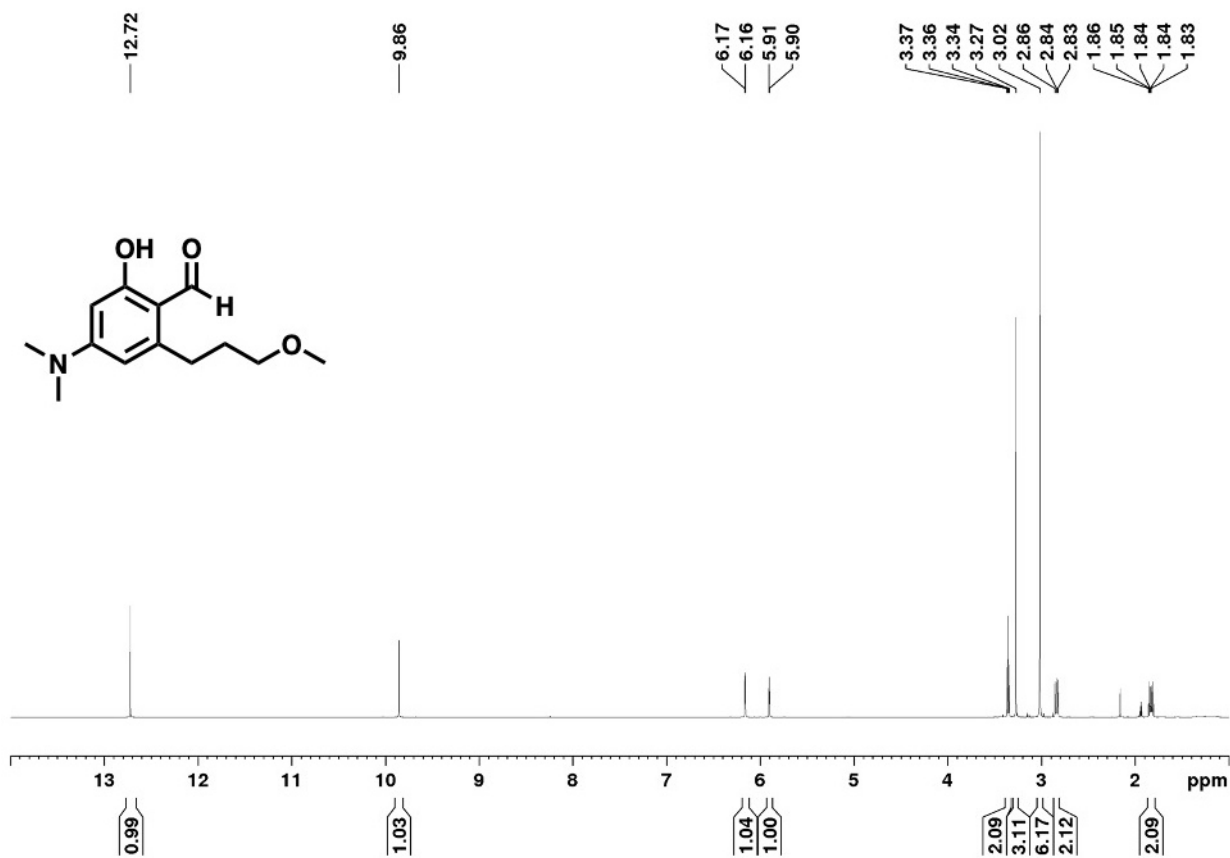


Figure 5.61. ¹H NMR Spectrum of Compound 17b in CD₃CN

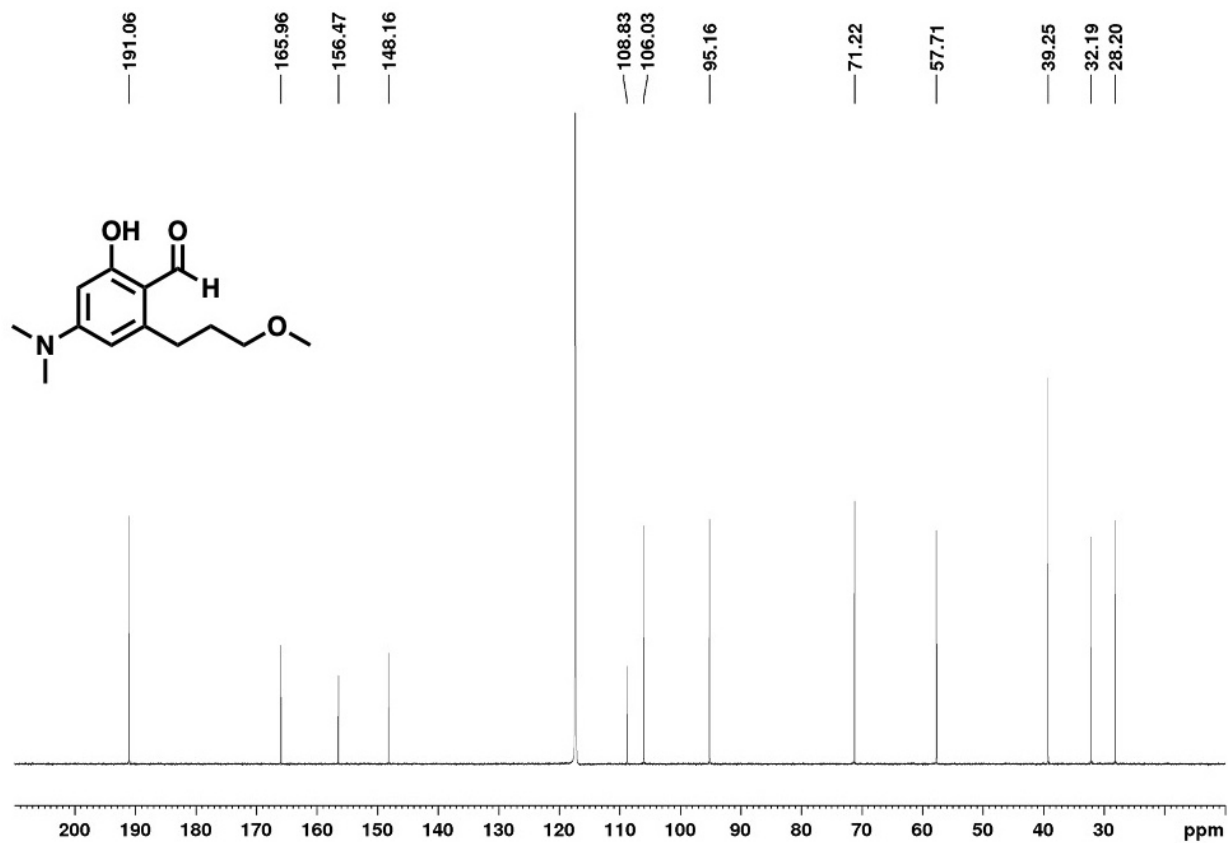


Figure 5.62. ^{13}C NMR Spectrum of Compound 17b in CD_3CN

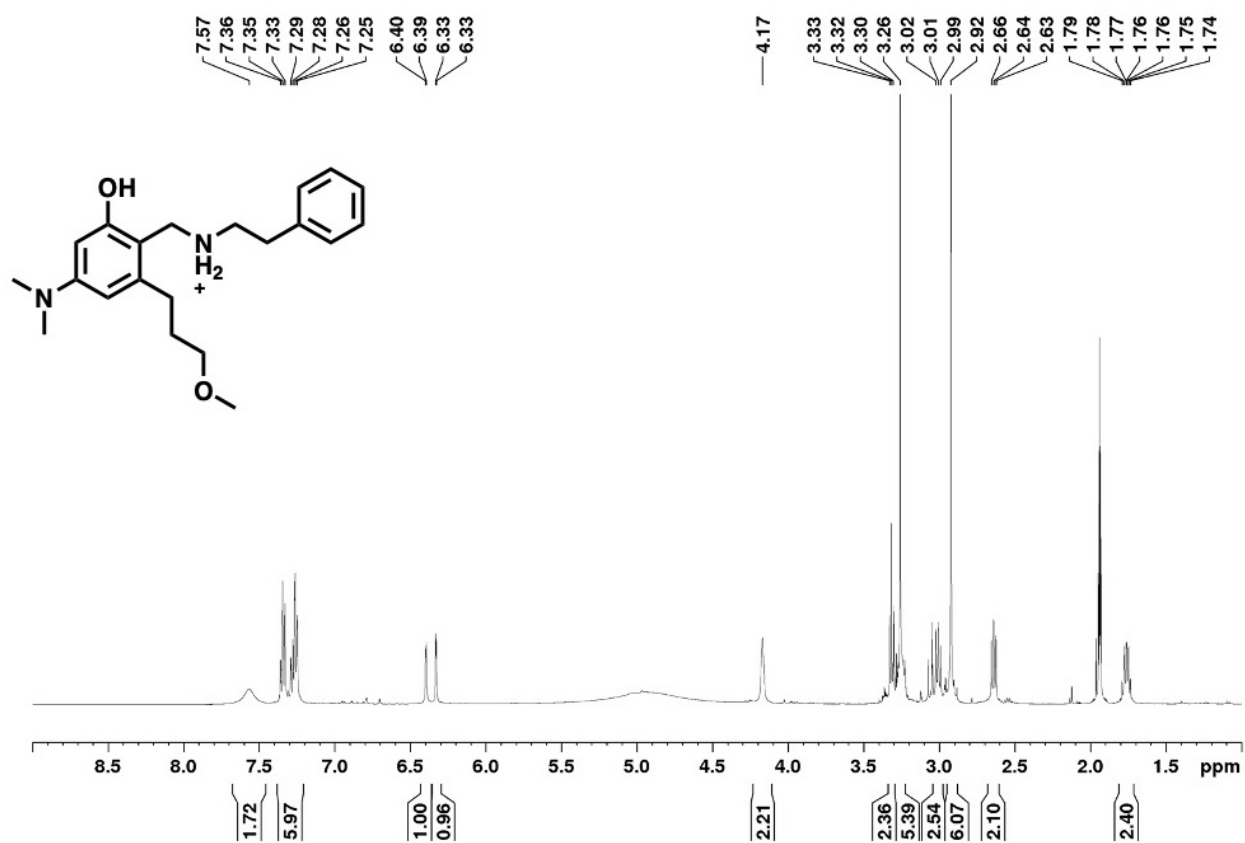


Figure 5.63. ¹H NMR Spectrum of Compound 5b in CD₃CN

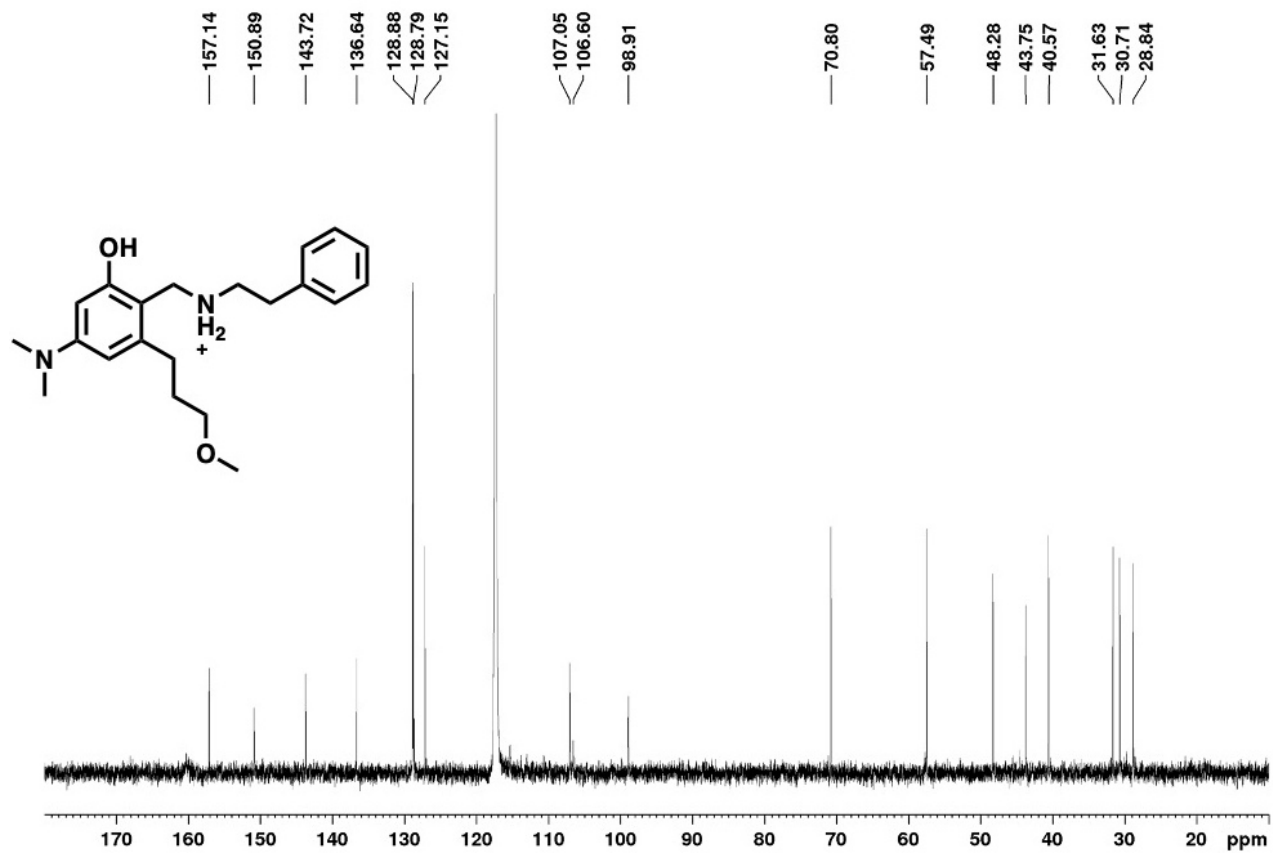


Figure 5.64. ^{13}C NMR Spectrum of Compound 5b in CD_3CN

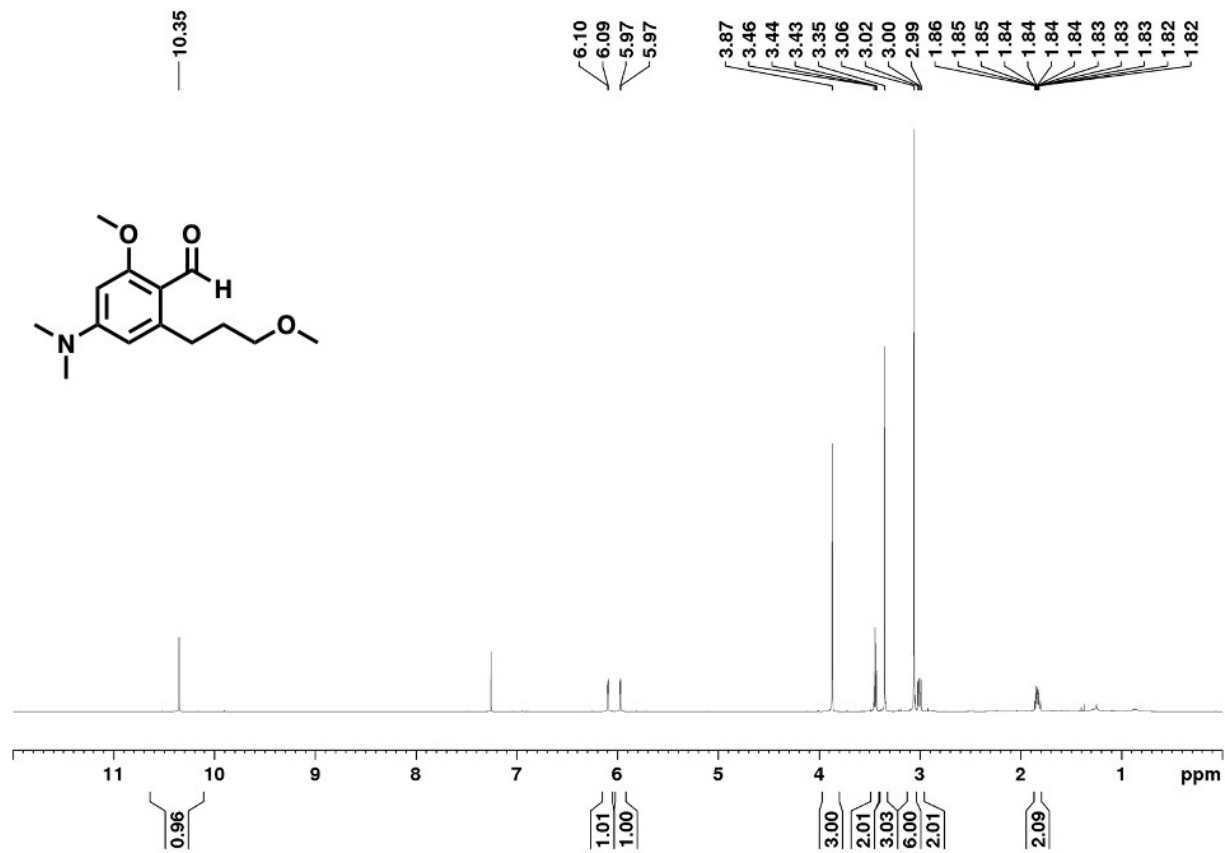


Figure 5.65. ¹H NMR Spectrum of Compound 33 in CDCl₃

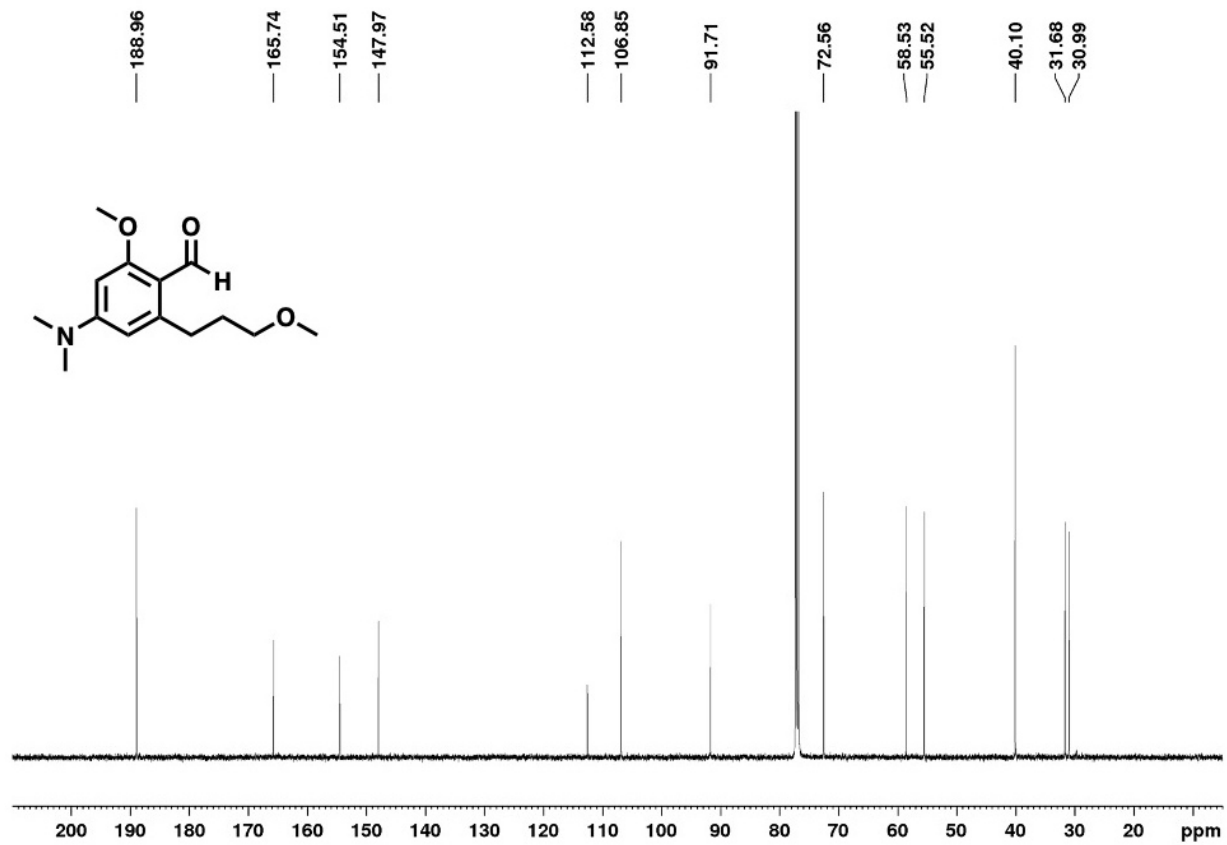


Figure 5.66. ^{13}C NMR Spectrum of Compound 33 in CDCl_3

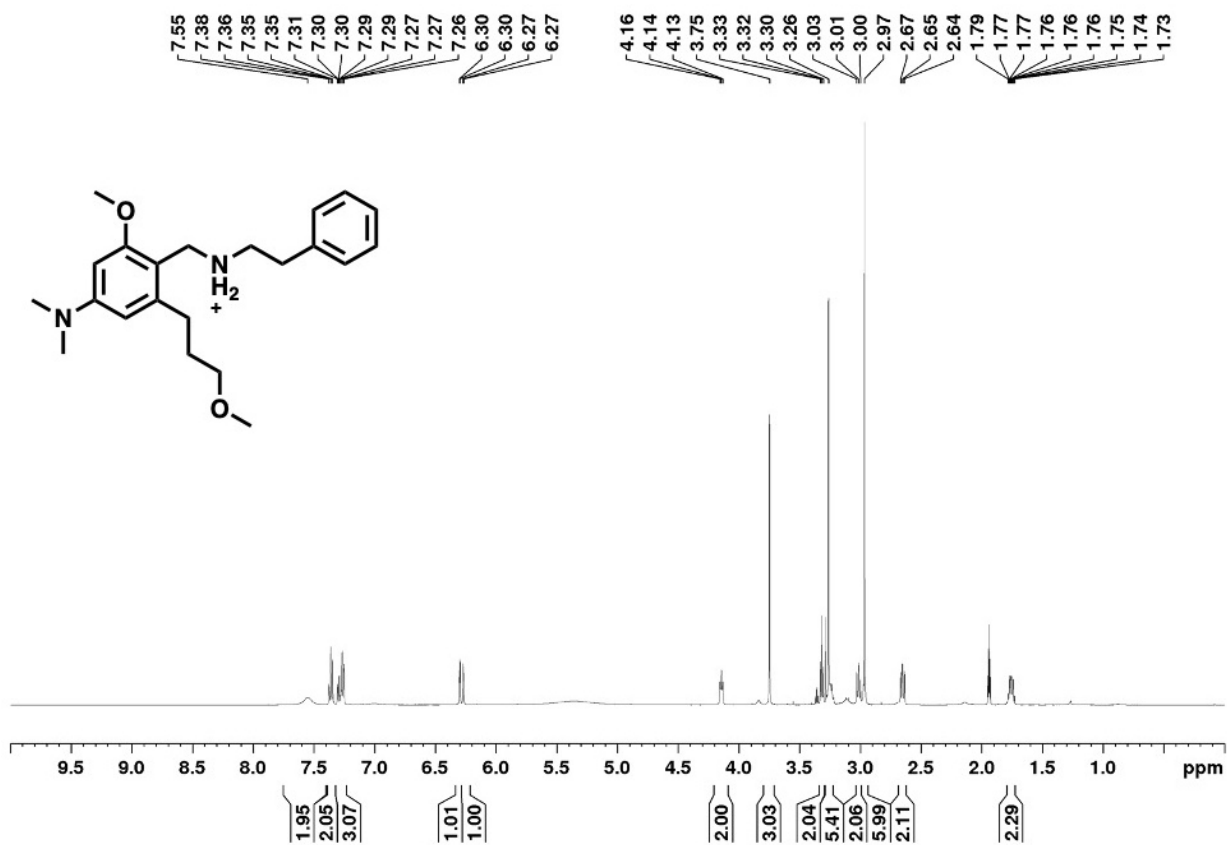


Figure 5.67. ¹H NMR Spectrum of Compound 5c in CD₃CN

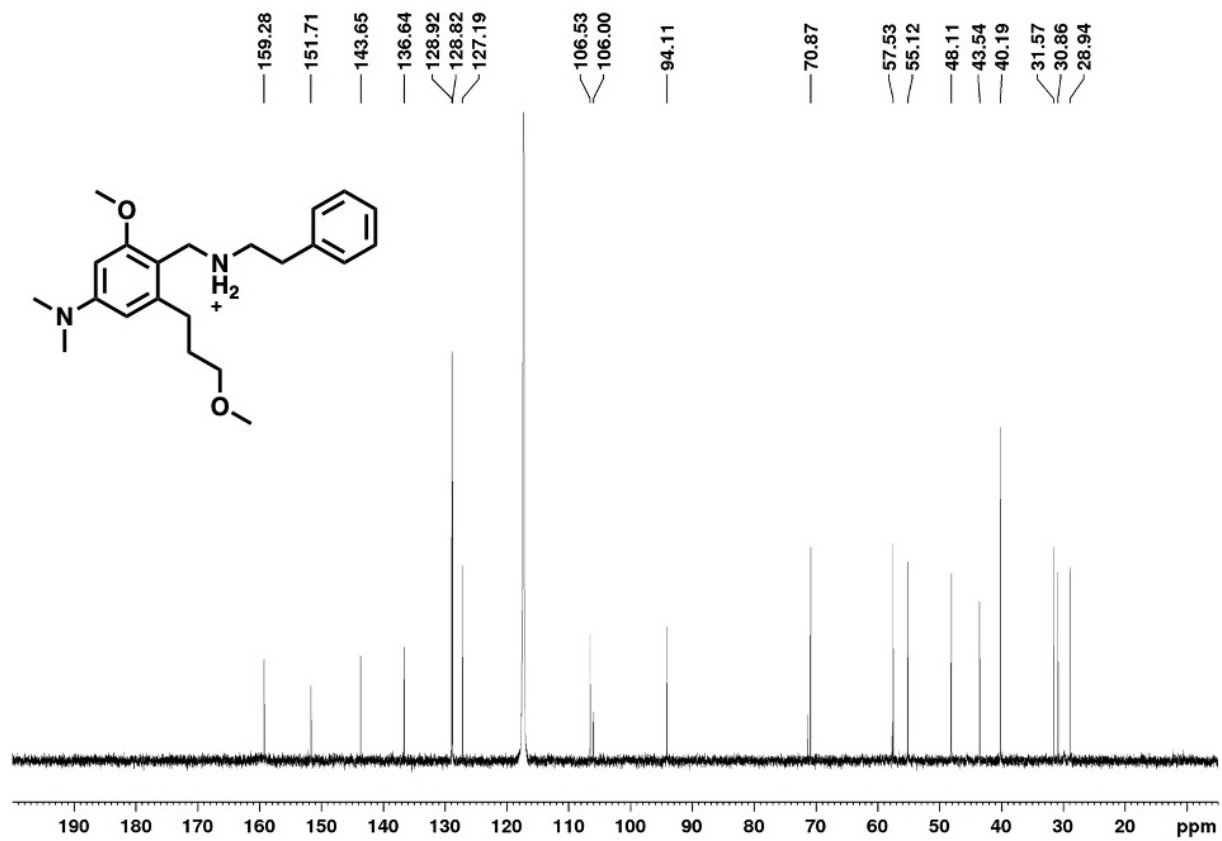


Figure 5.68. ¹³C NMR Spectrum of Compound 5c in CD₃CN

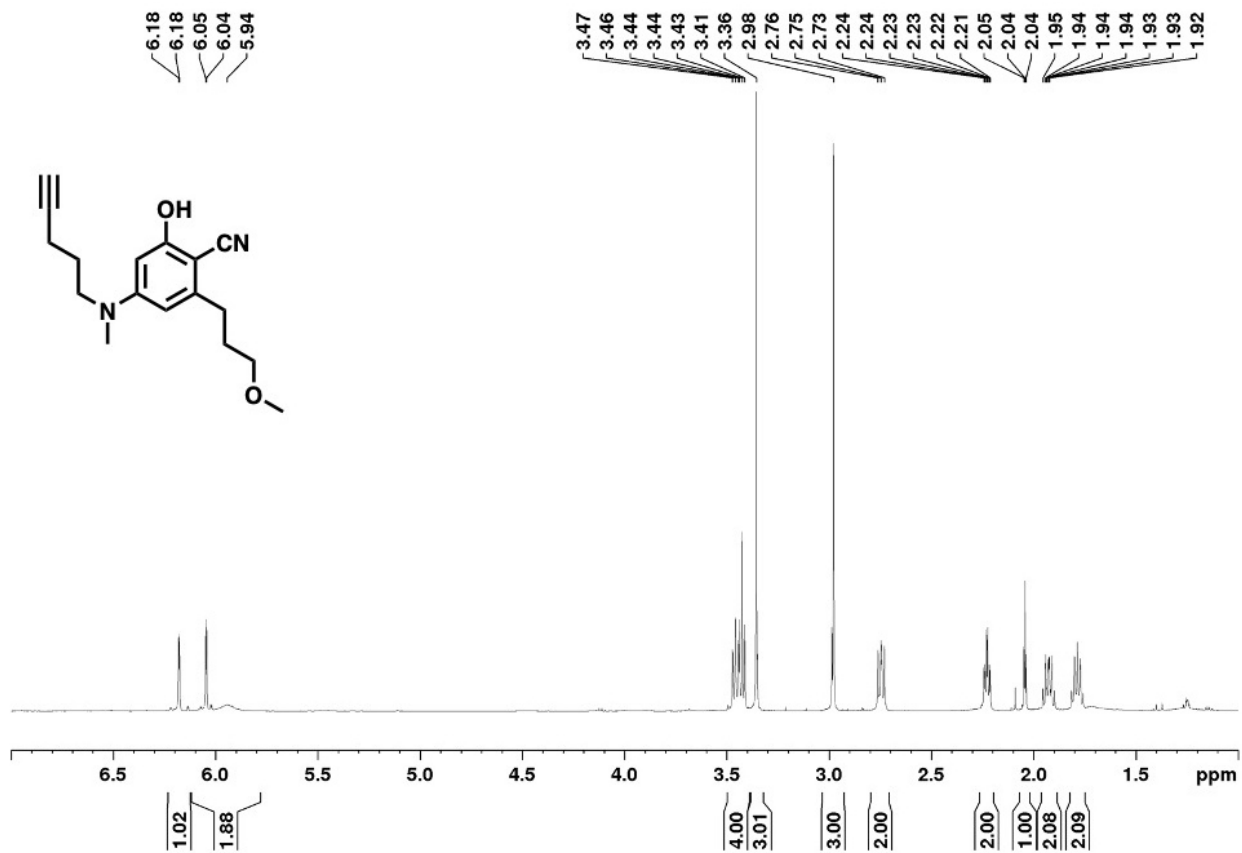


Figure 5.69. ¹H NMR Spectrum of Compound 19 in CDCl₃

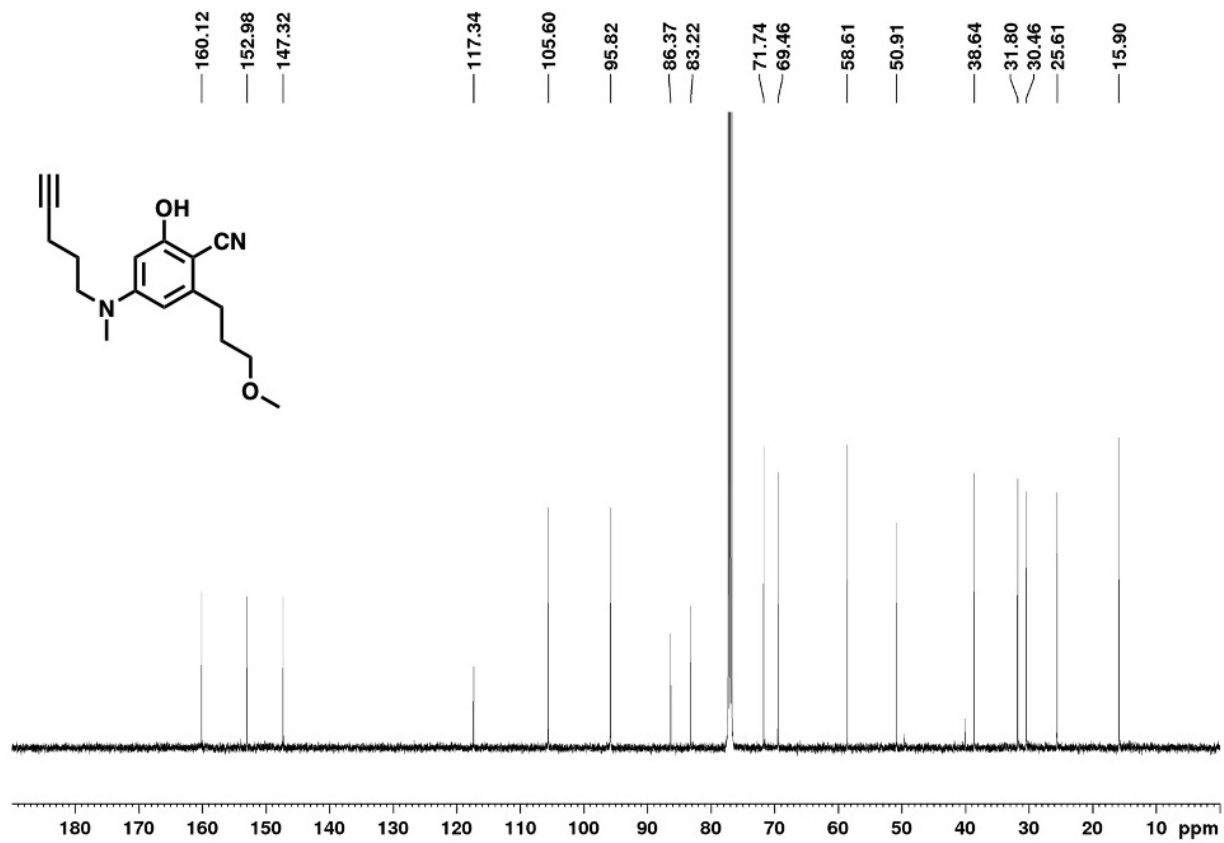


Figure 5.70. ^{13}C NMR Spectrum of Compound 19 in CDCl_3

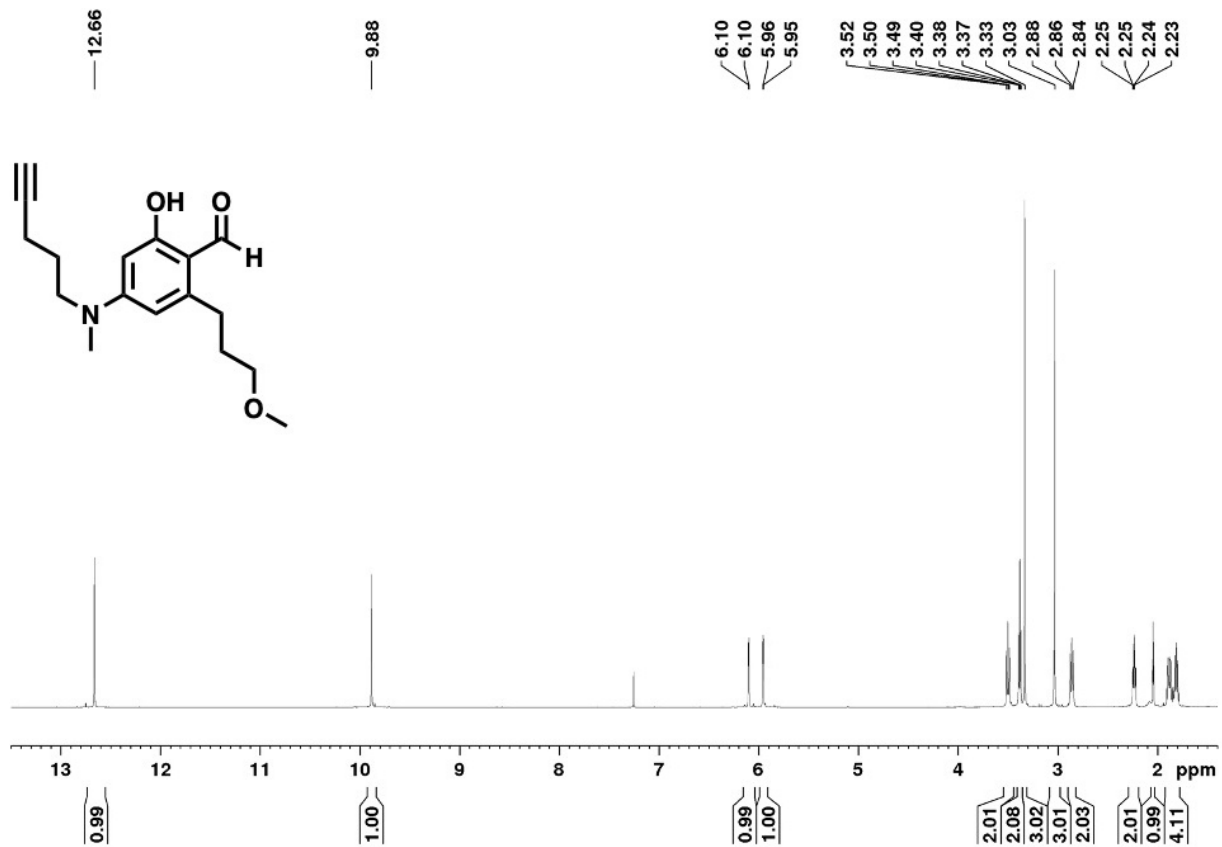


Figure 5.71. ¹H NMR Spectrum of Compound 20 in CDCl₃

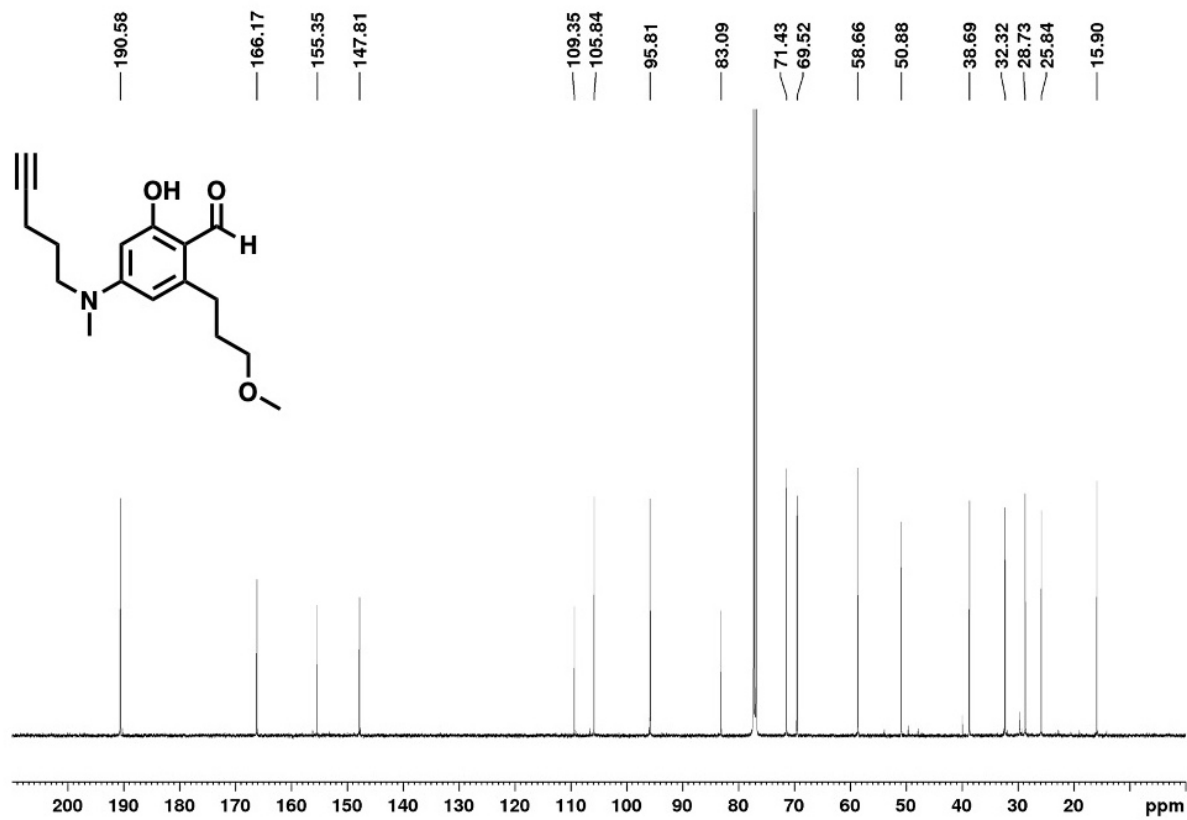


Figure 5.72. ^{13}C NMR Spectrum of Compound 20 in CDCl_3

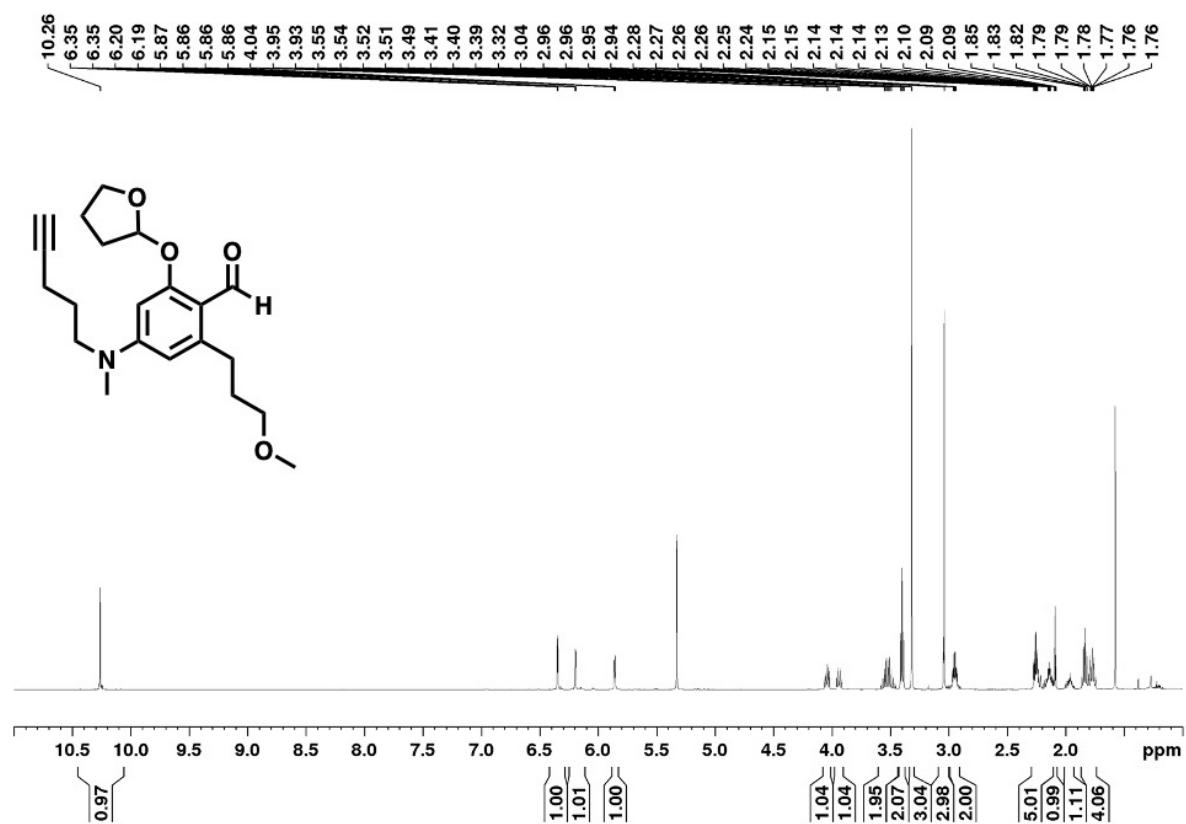


Figure 5.73. ¹H NMR Spectrum of Compound 8 in CD₂Cl₂

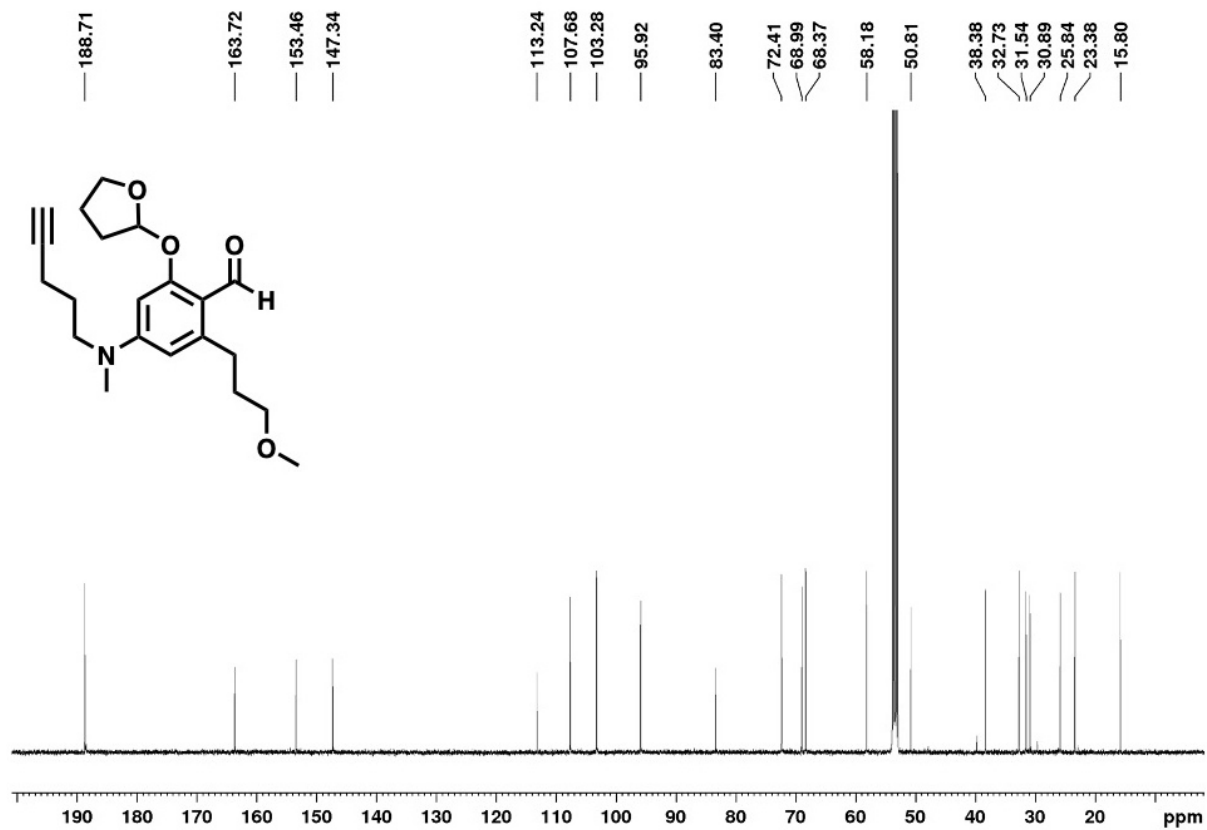


Figure 5.74. ¹³C NMR Spectrum of Compound 8 in CD₂Cl₂

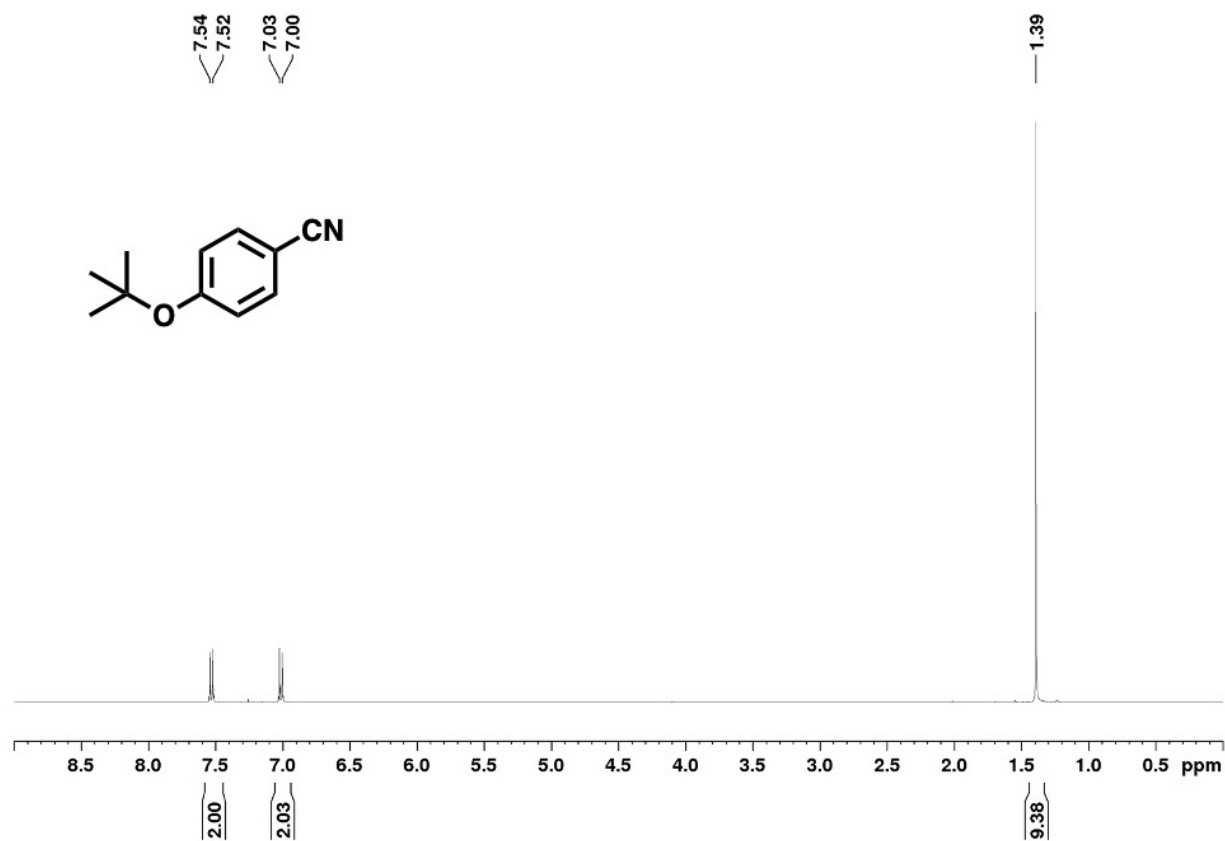


Figure 5.75. ¹H NMR Spectrum of Compound 21 in CDCl₃

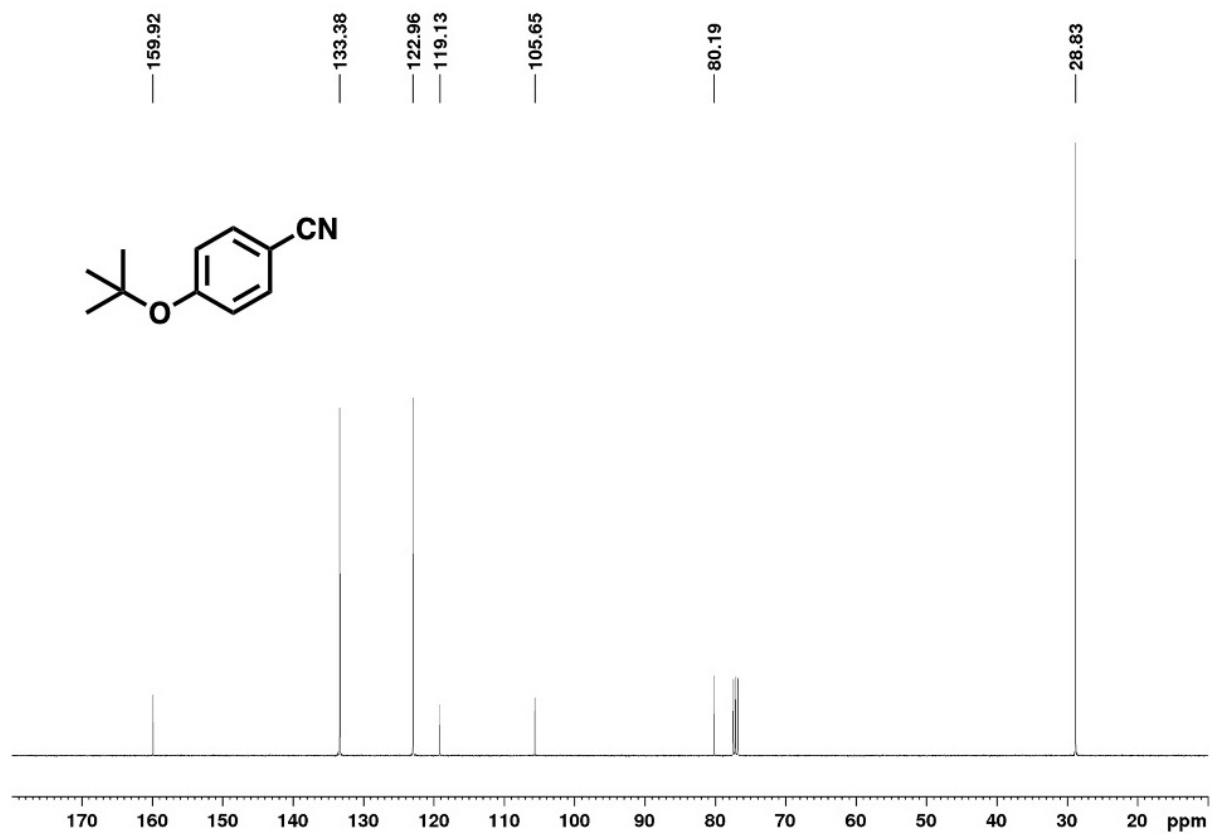


Figure 5.76. ^{13}C NMR Spectrum of Compound 21 in CDCl_3

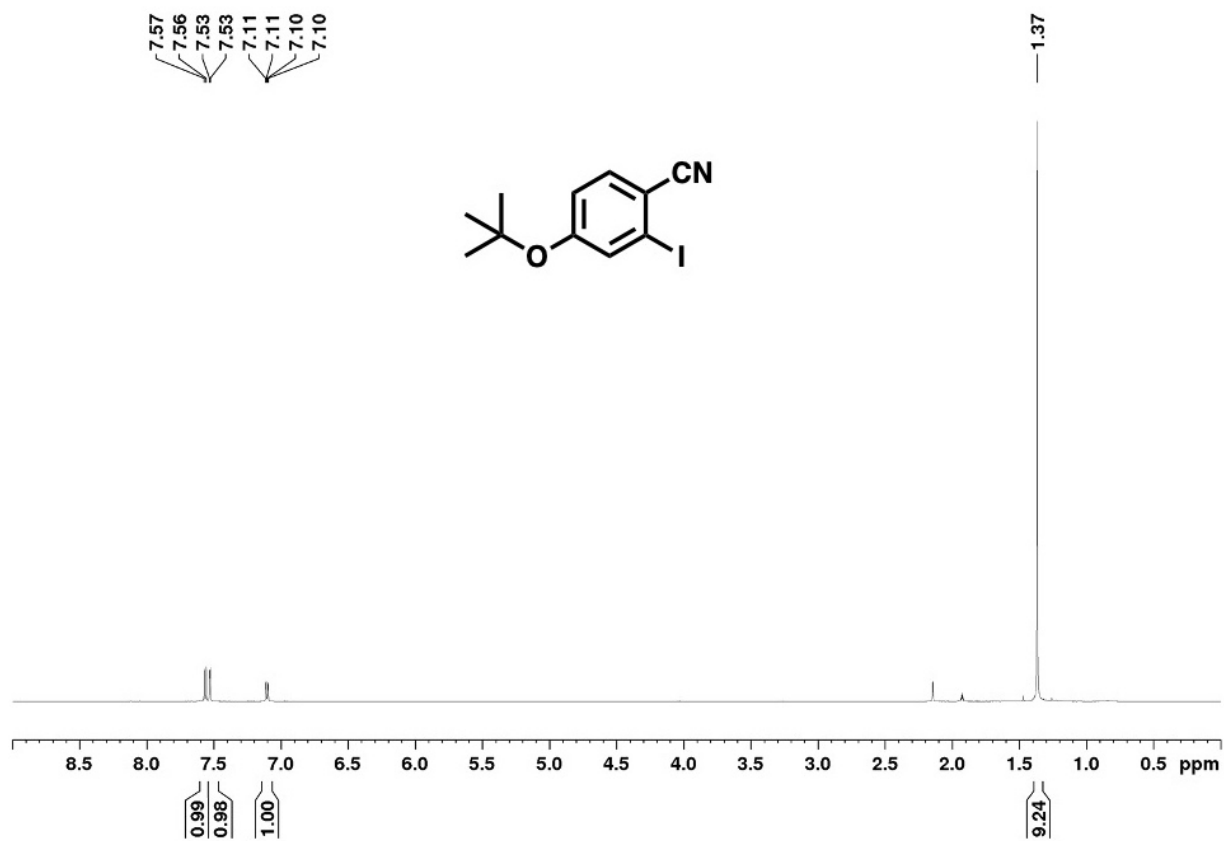


Figure 5.77. ¹H NMR Spectrum of Compound 22 in CD₃CN

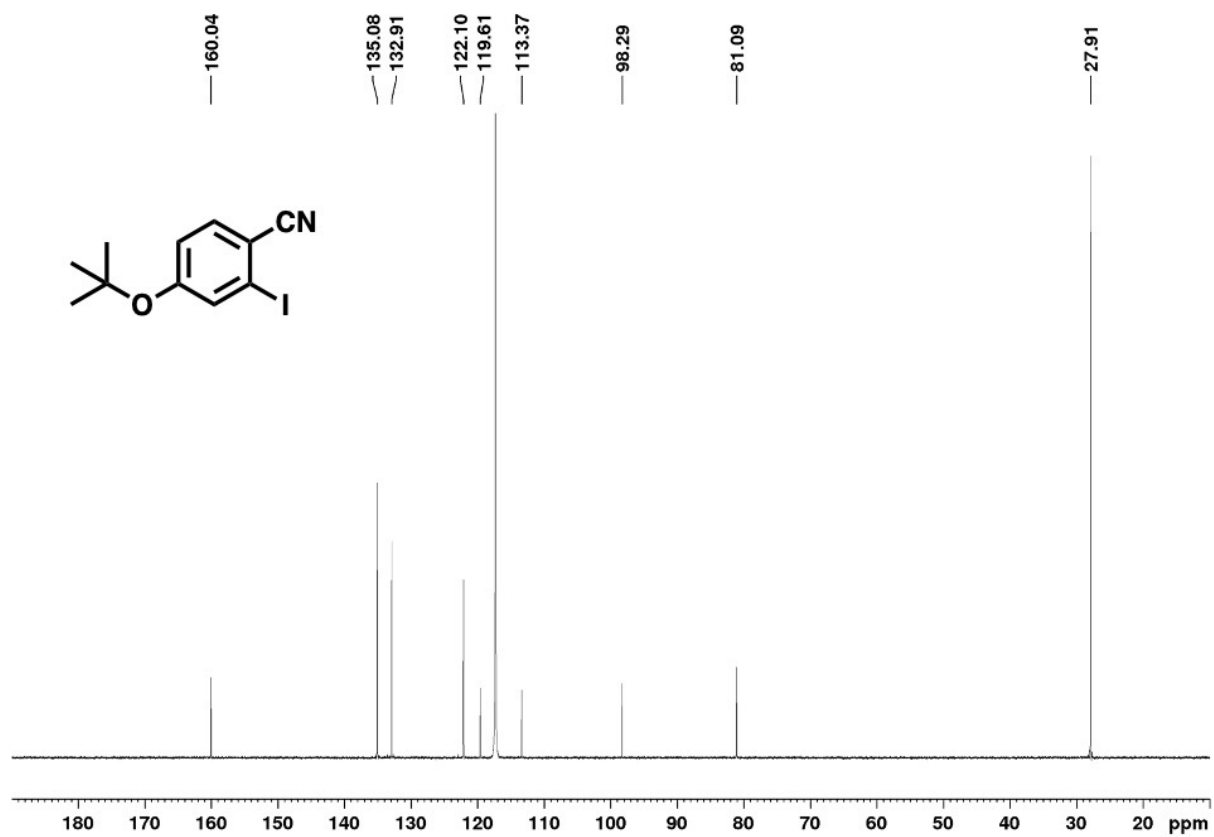


Figure 5.78. ^{13}C NMR Spectrum of Compound 22 in CD_3CN

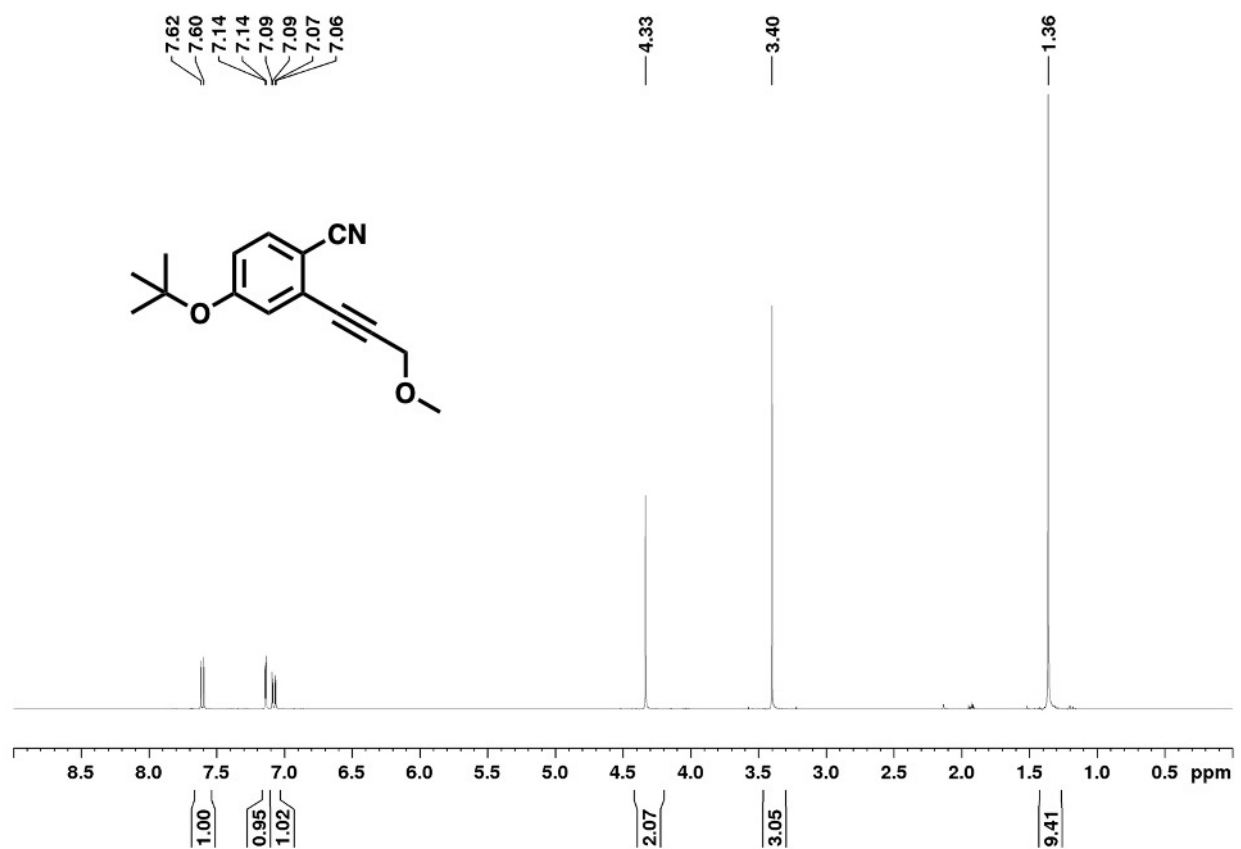


Figure 5.79. ¹H NMR Spectrum of Compound 23 in CD₃CN

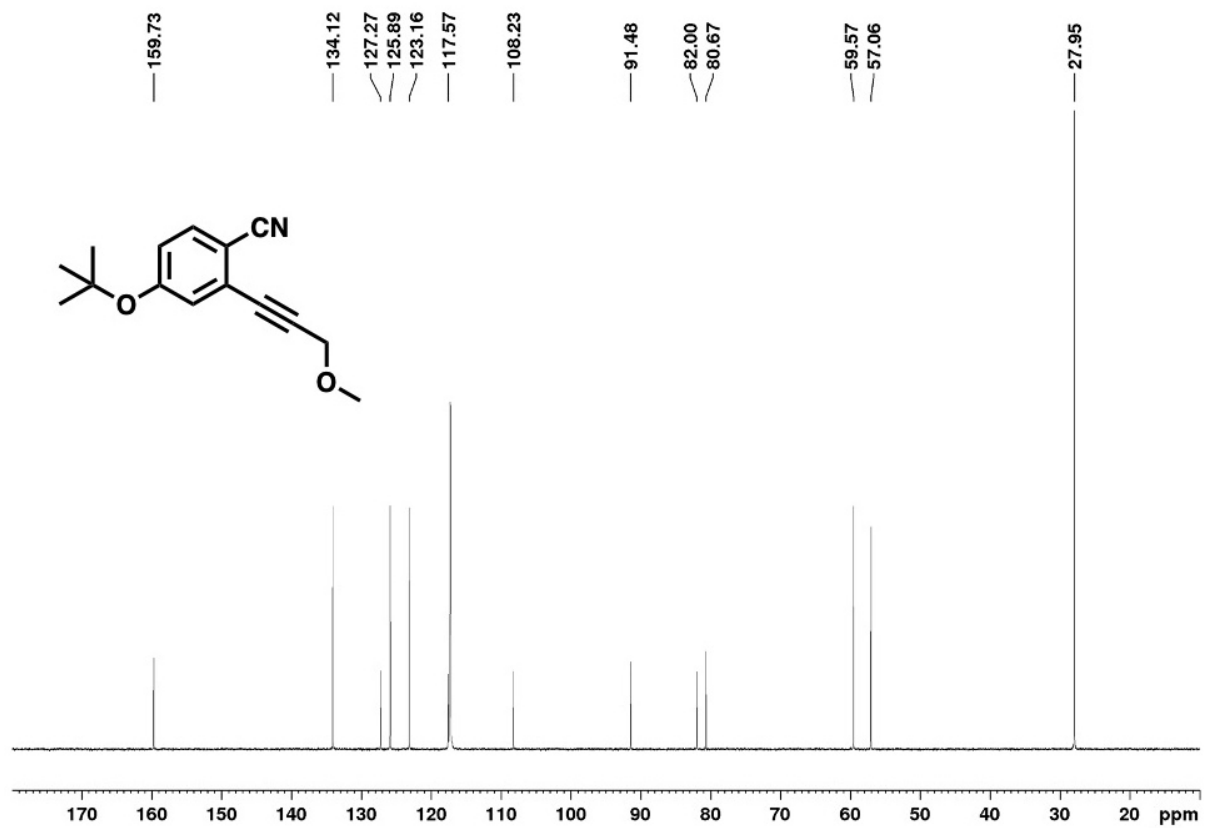


Figure 5.80. ^{13}C NMR Spectrum of Compound 23 in CD_3CN

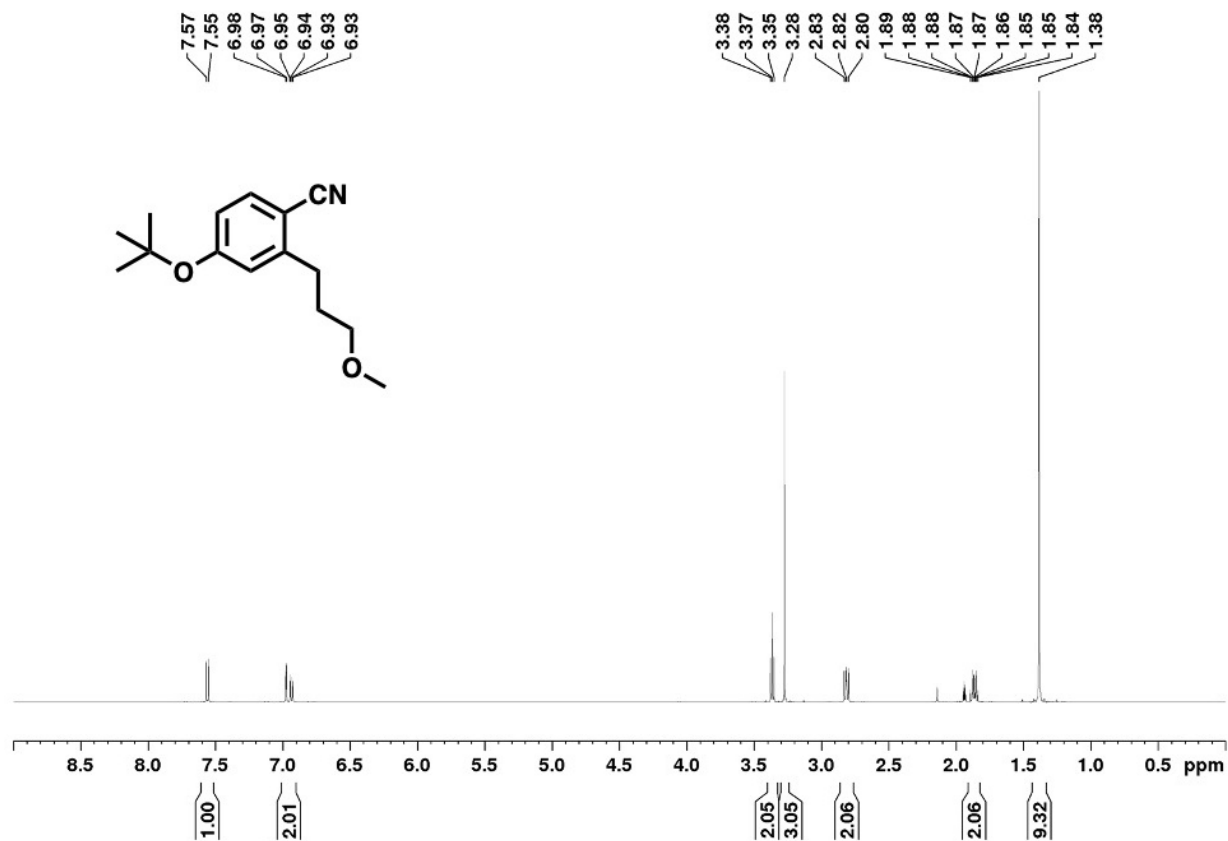


Figure 5.81. ¹H NMR Spectrum of Compound 24 in CD₃CN

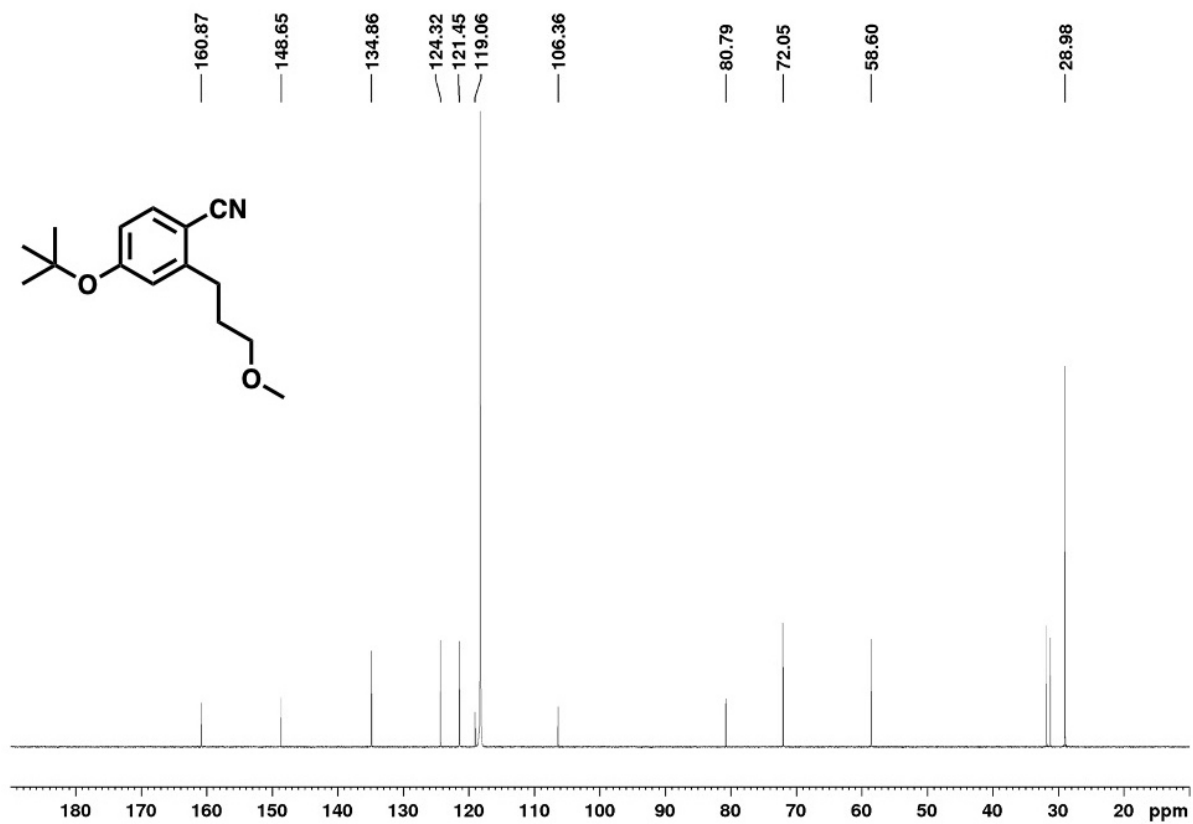


Figure 5.82. ^{13}C NMR Spectrum of Compound 24 in CD_3CN

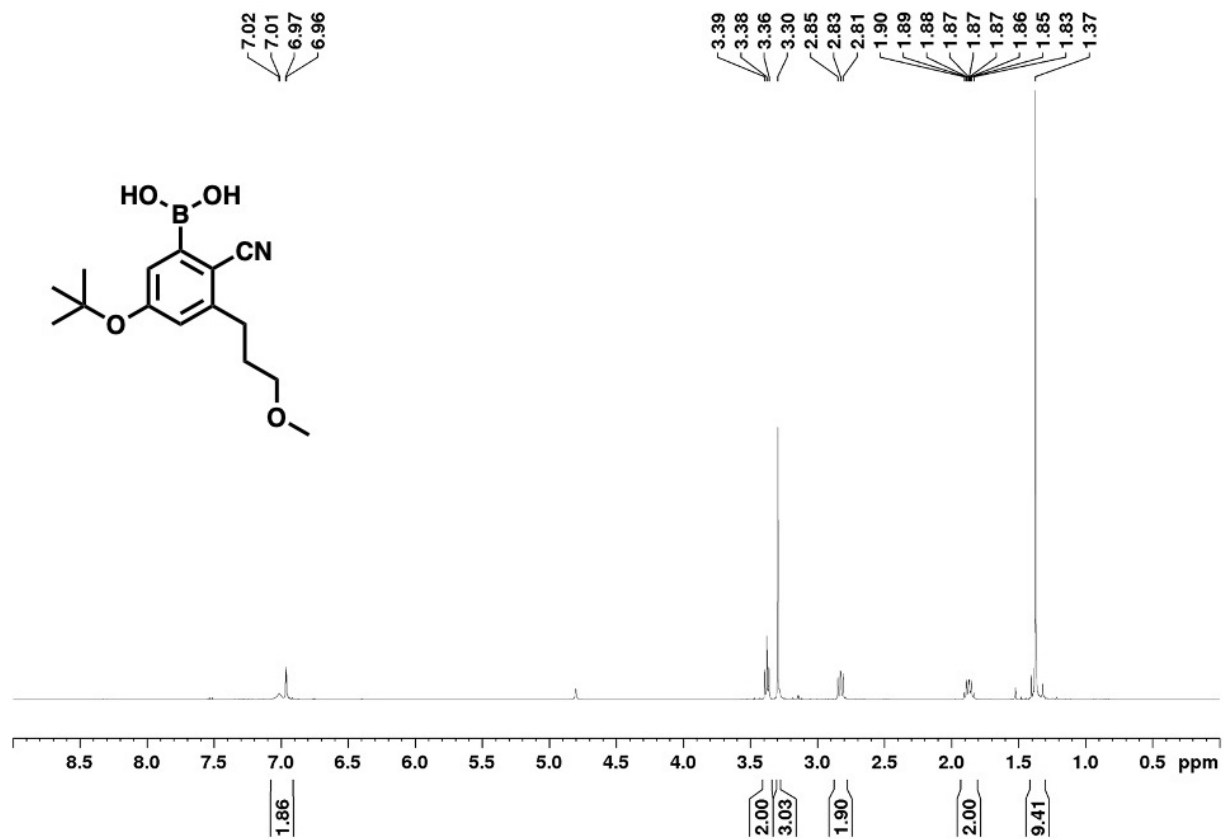


Figure 5.83. ¹H NMR Spectrum of Compound 25 in CD₃OD

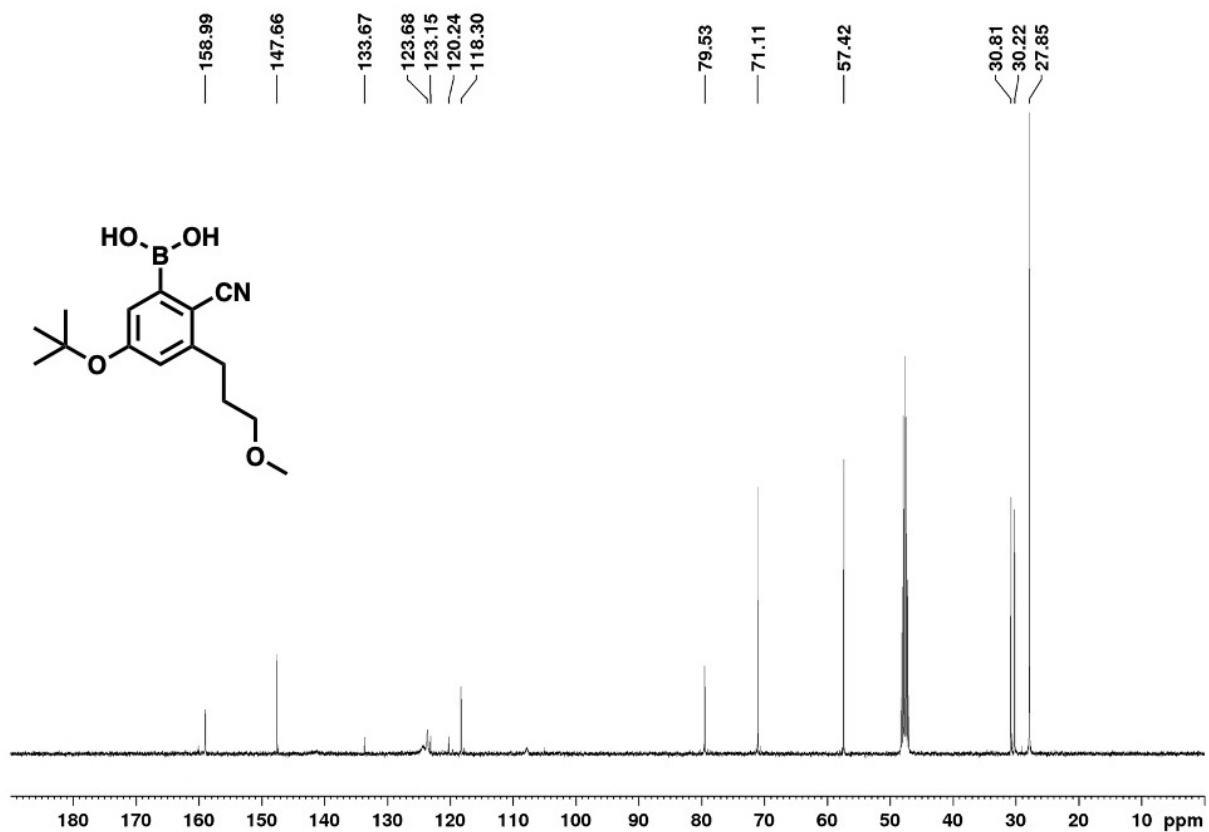


Figure 5.84. ¹³C NMR Spectrum of Compound 25 in CD₃OD

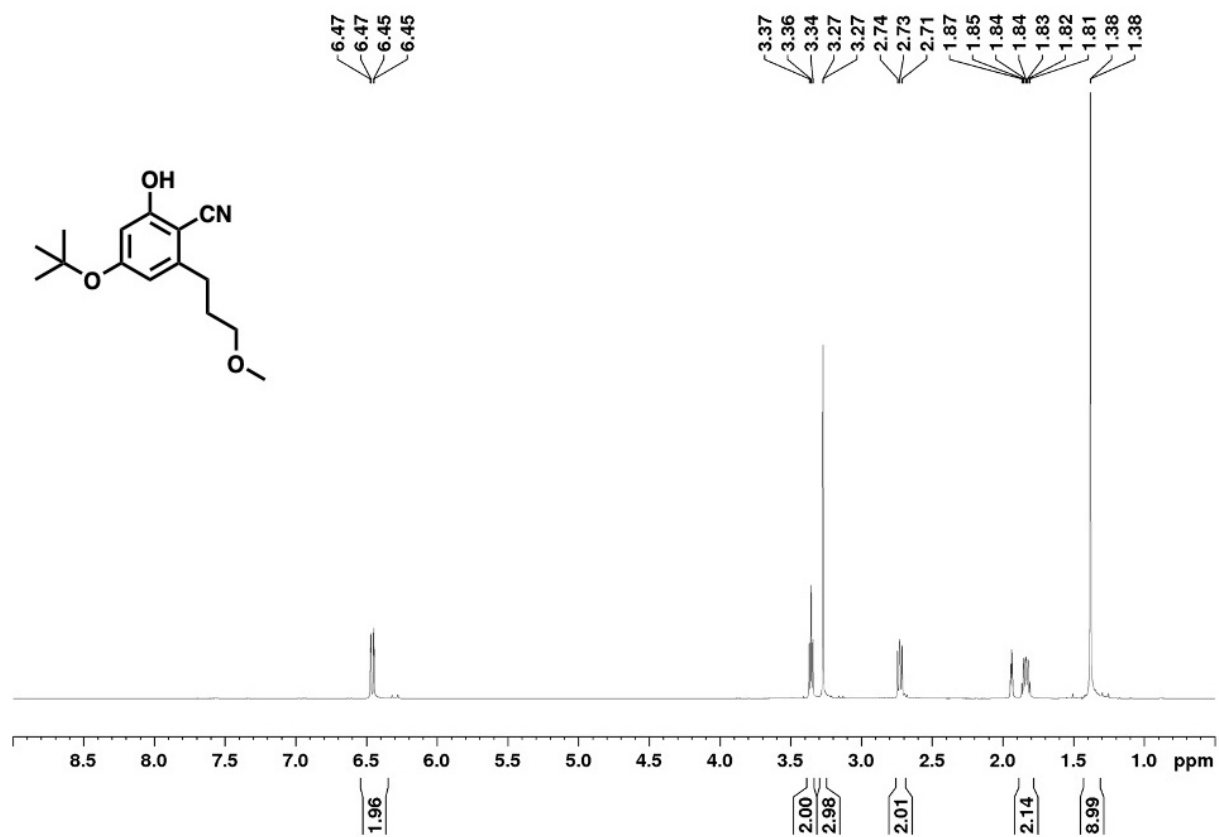


Figure 5.85. ¹H NMR Spectrum of Compound 26 in CD₃CN

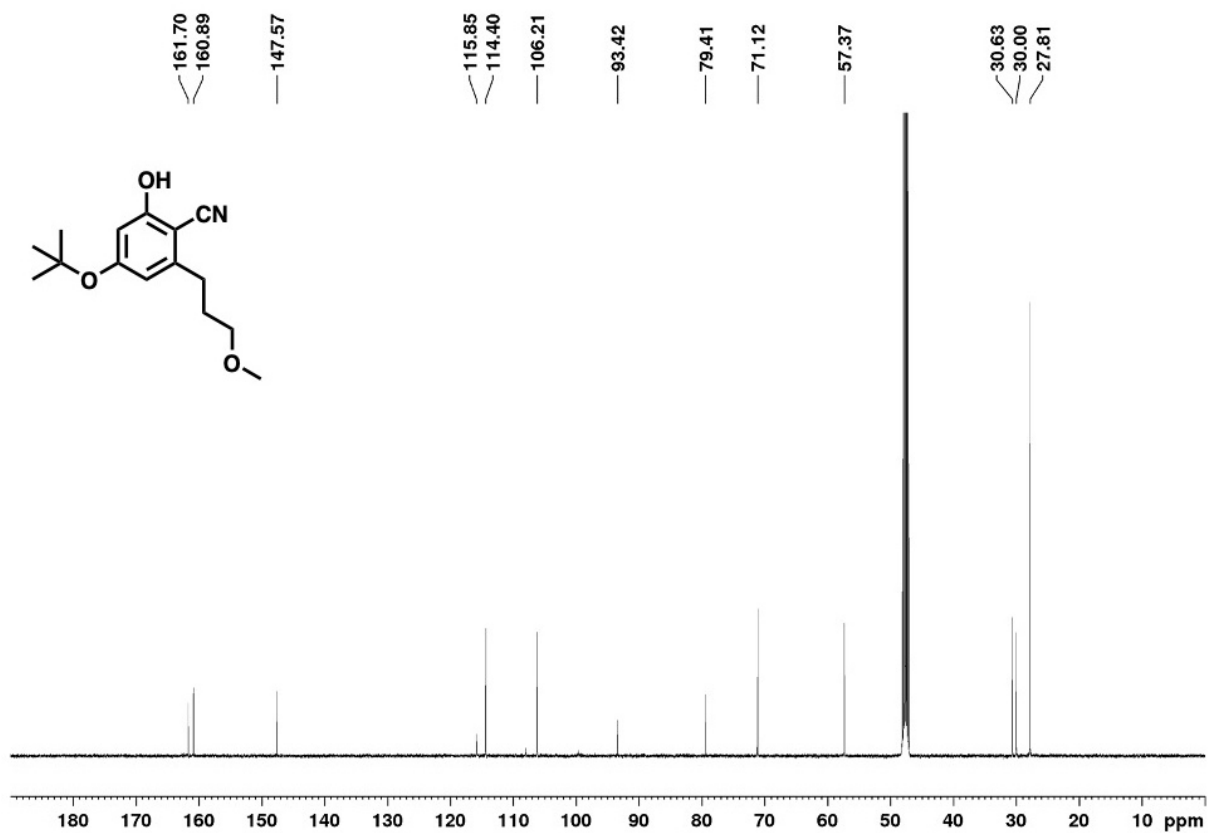


Figure 5.86. ¹³C NMR Spectrum of Compound 26 in CD₃OD

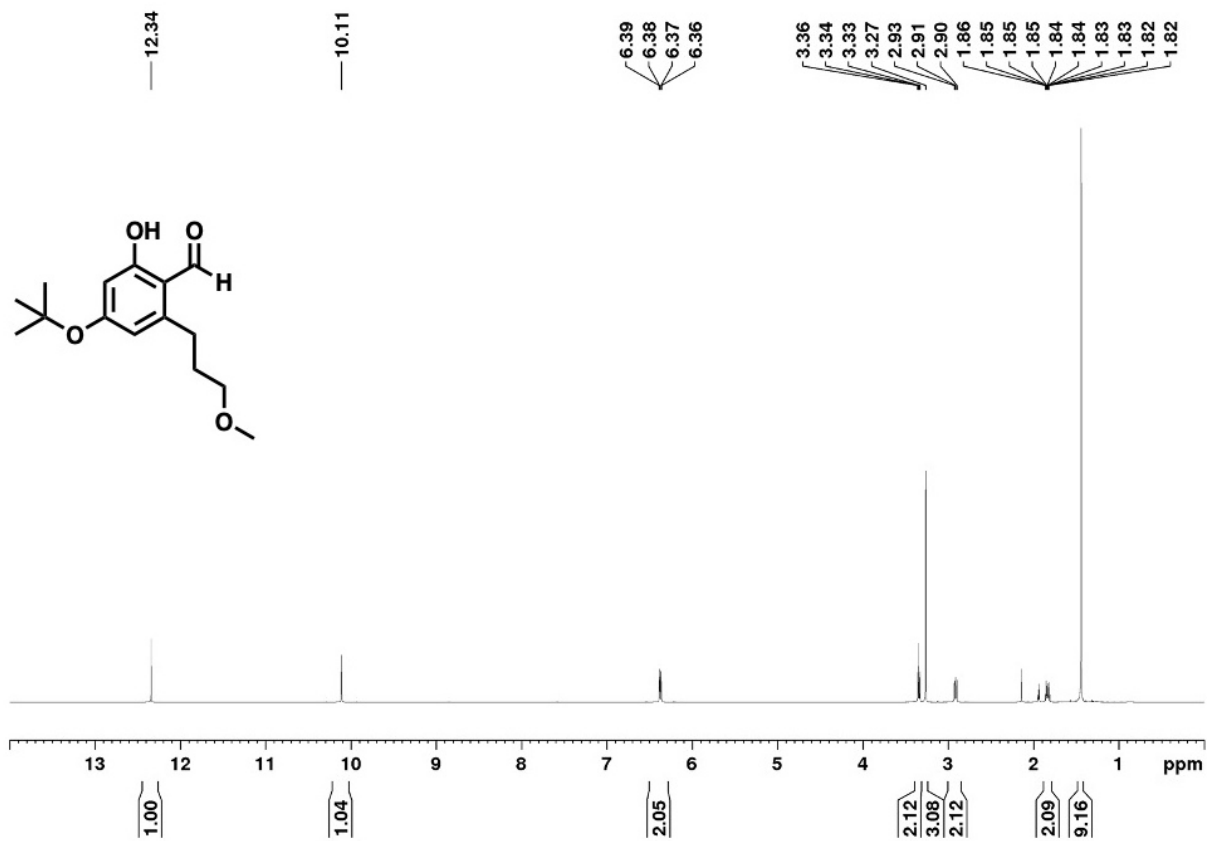


Figure 5.87. ¹H NMR Spectrum of Compound 27 in CD₃CN

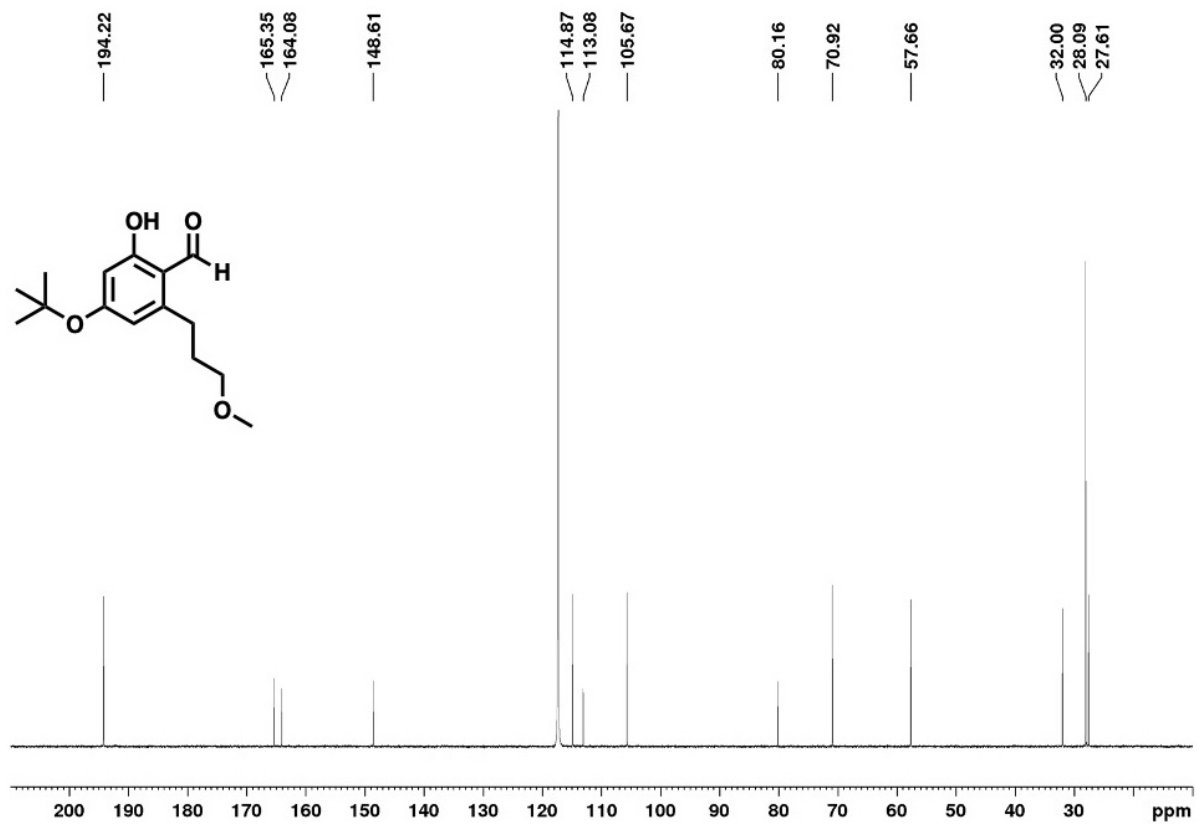


Figure 5.88. ¹³C NMR Spectrum of Compound 27 in CD₃CN

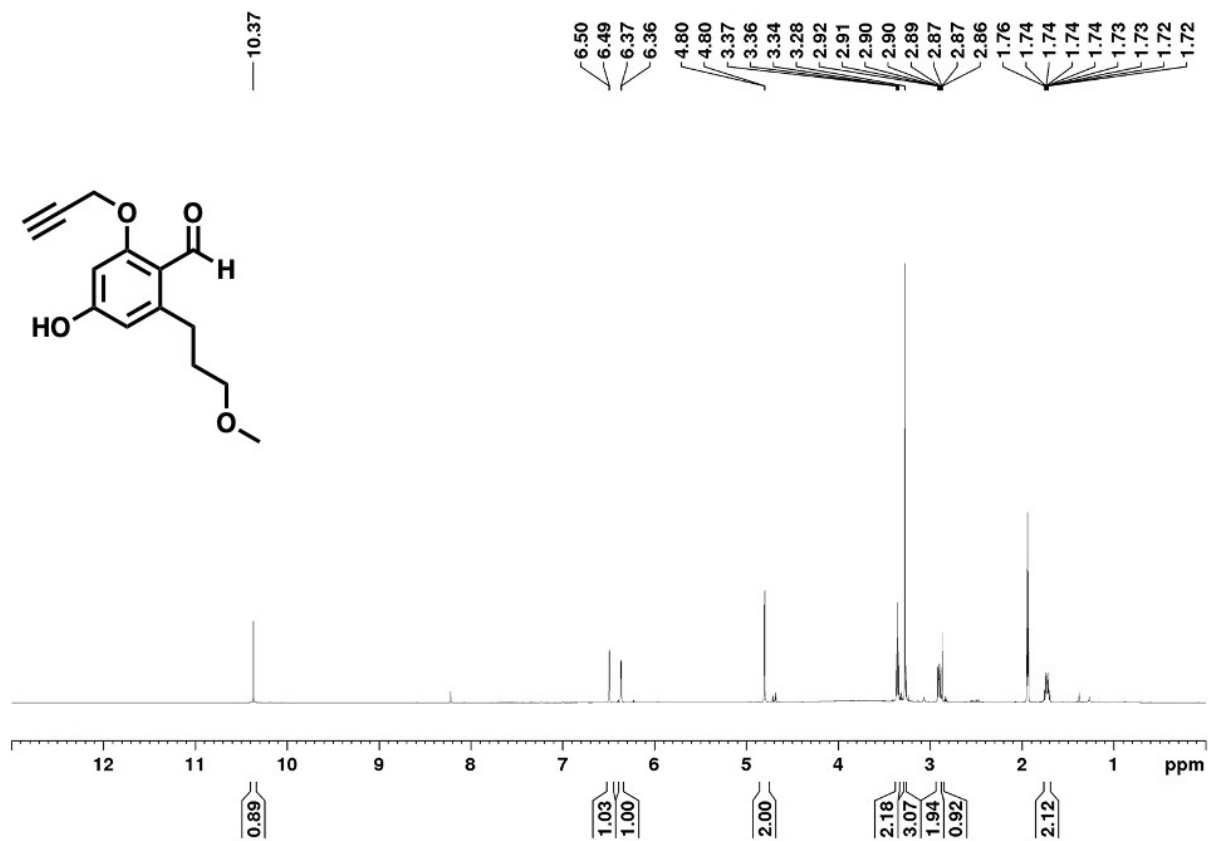


Figure 5.89. ^1H NMR Spectrum of Compound 28 in CD_3CN

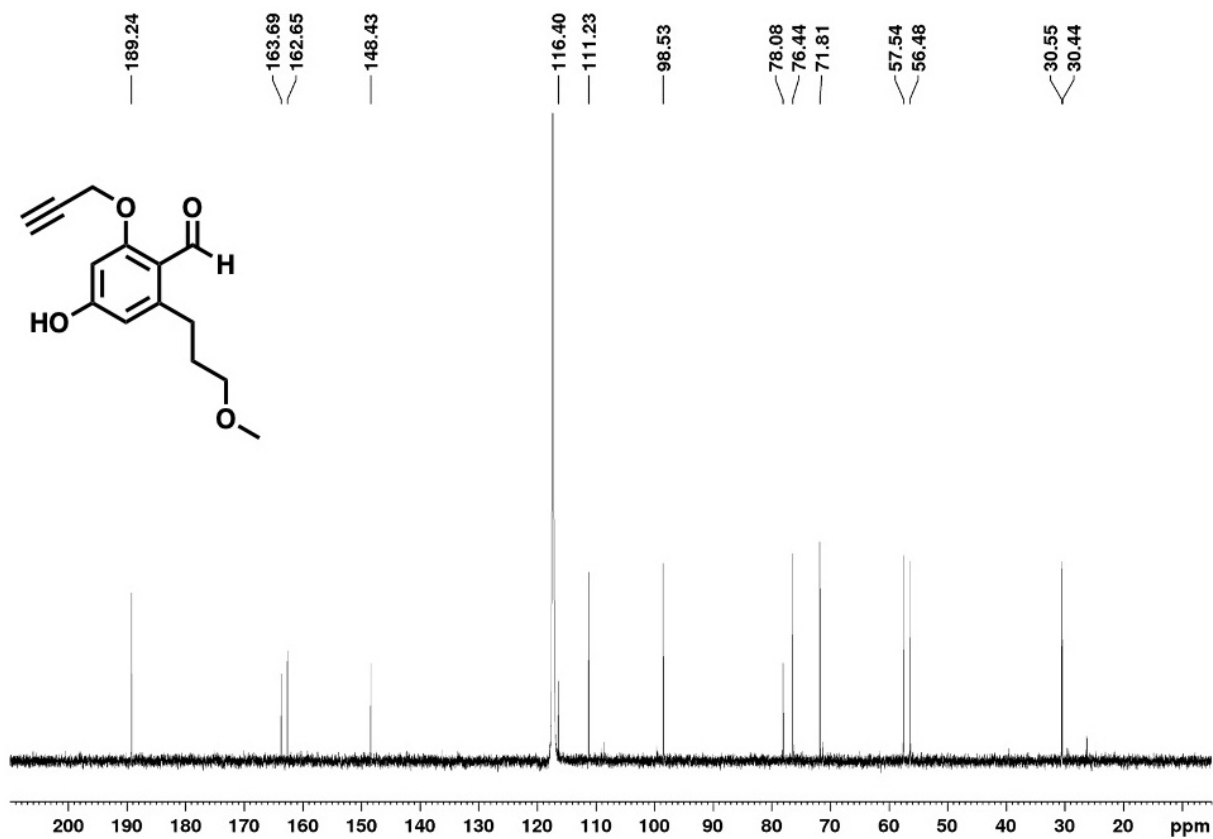


Figure 5.90. ¹³C NMR Spectrum of Compound 28 in CD₃CN

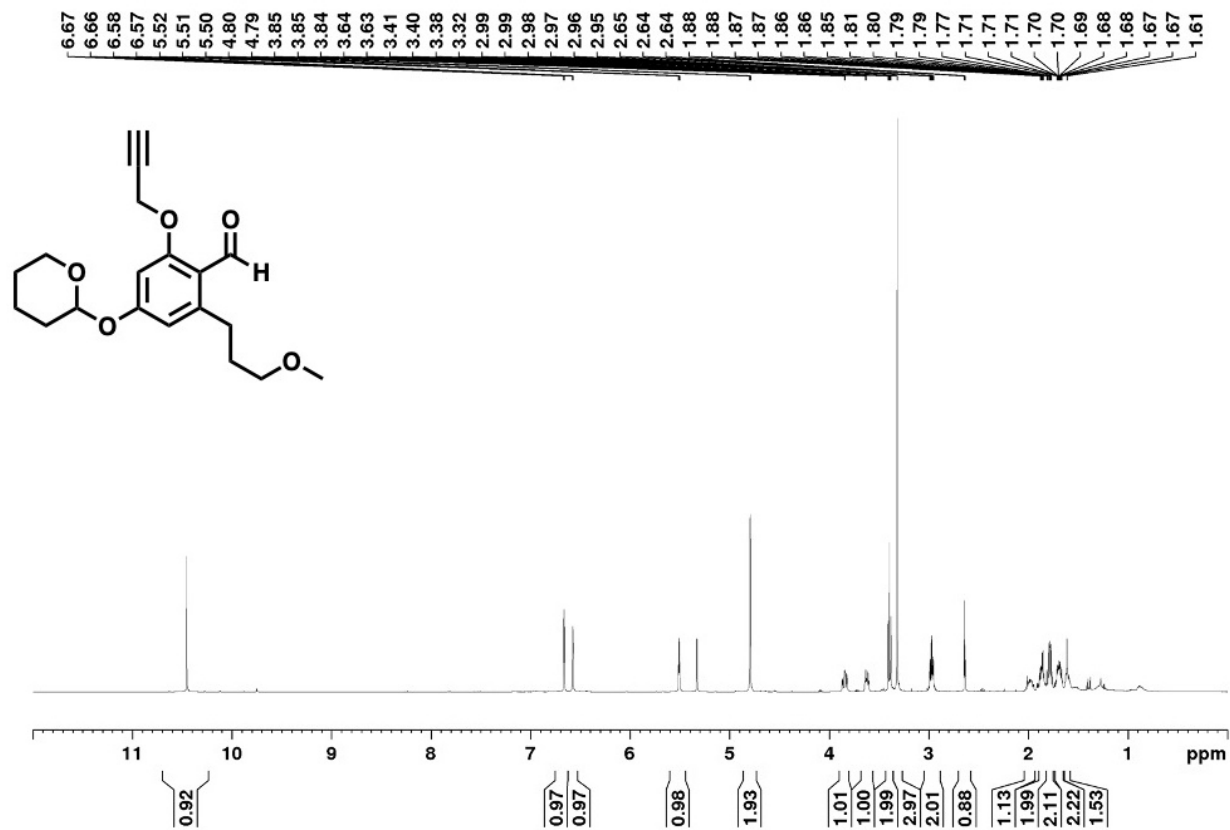


Figure 5.91. ¹H NMR Spectrum of Compound 7 in CD₂Cl₂

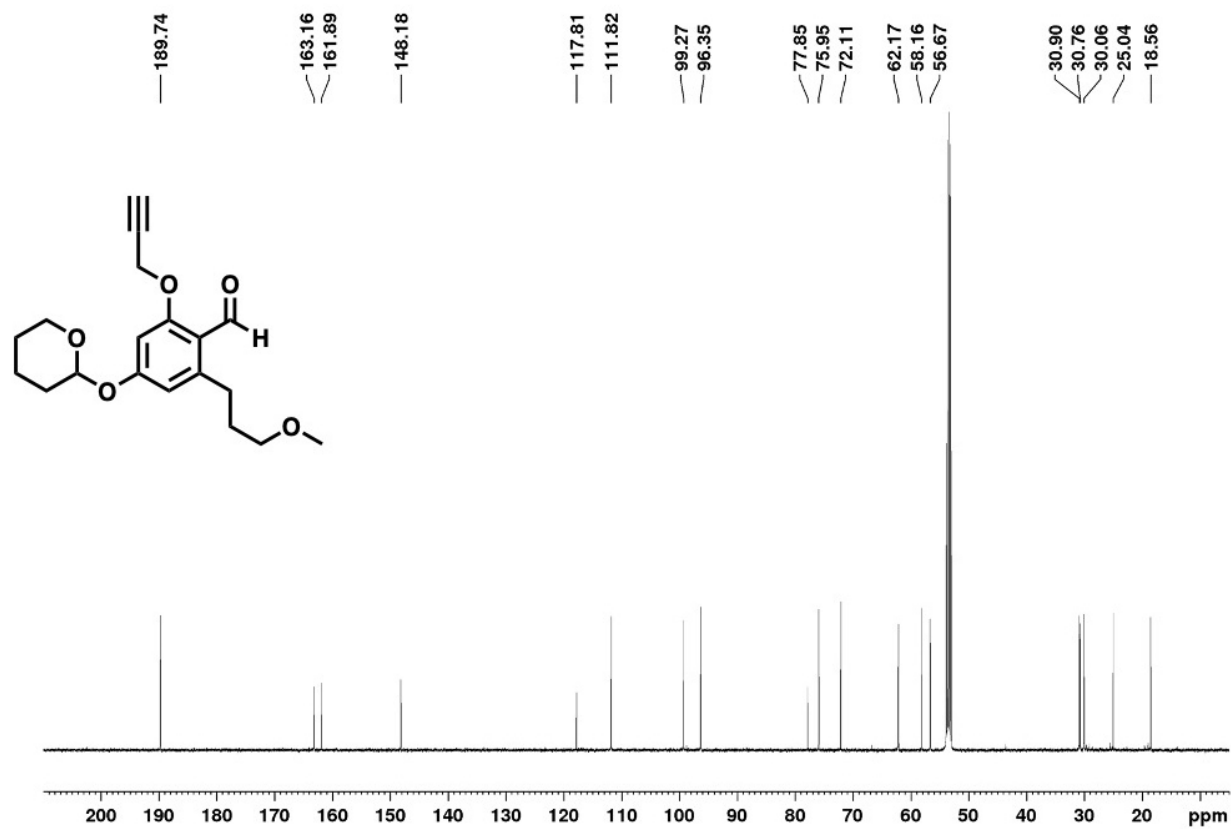


Figure 5.92. ^{13}C NMR Spectrum of Compound 7 in CD_2Cl_2

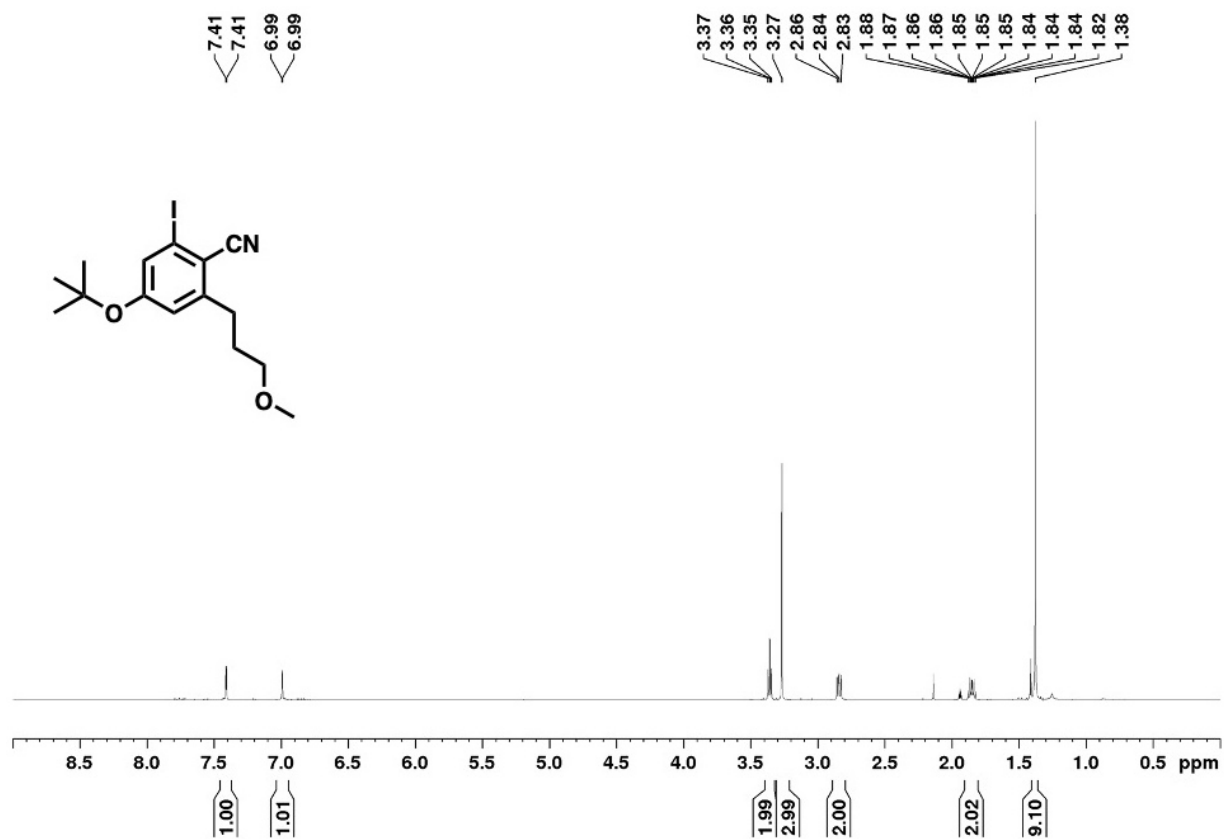


Figure 5.93. ¹H NMR Spectrum of Compound 29 in CD₃CN

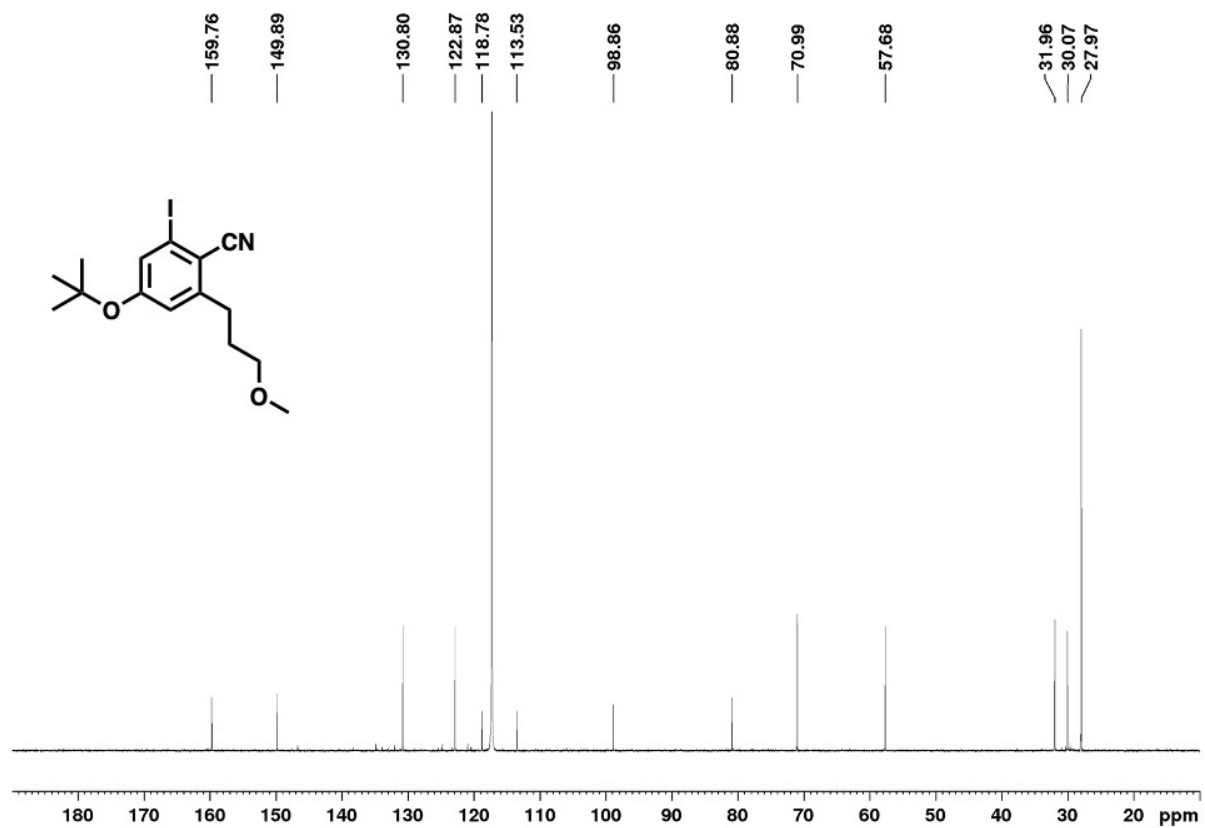


Figure 5.94. ^{13}C NMR Spectrum of Compound 29 in CD_3CN

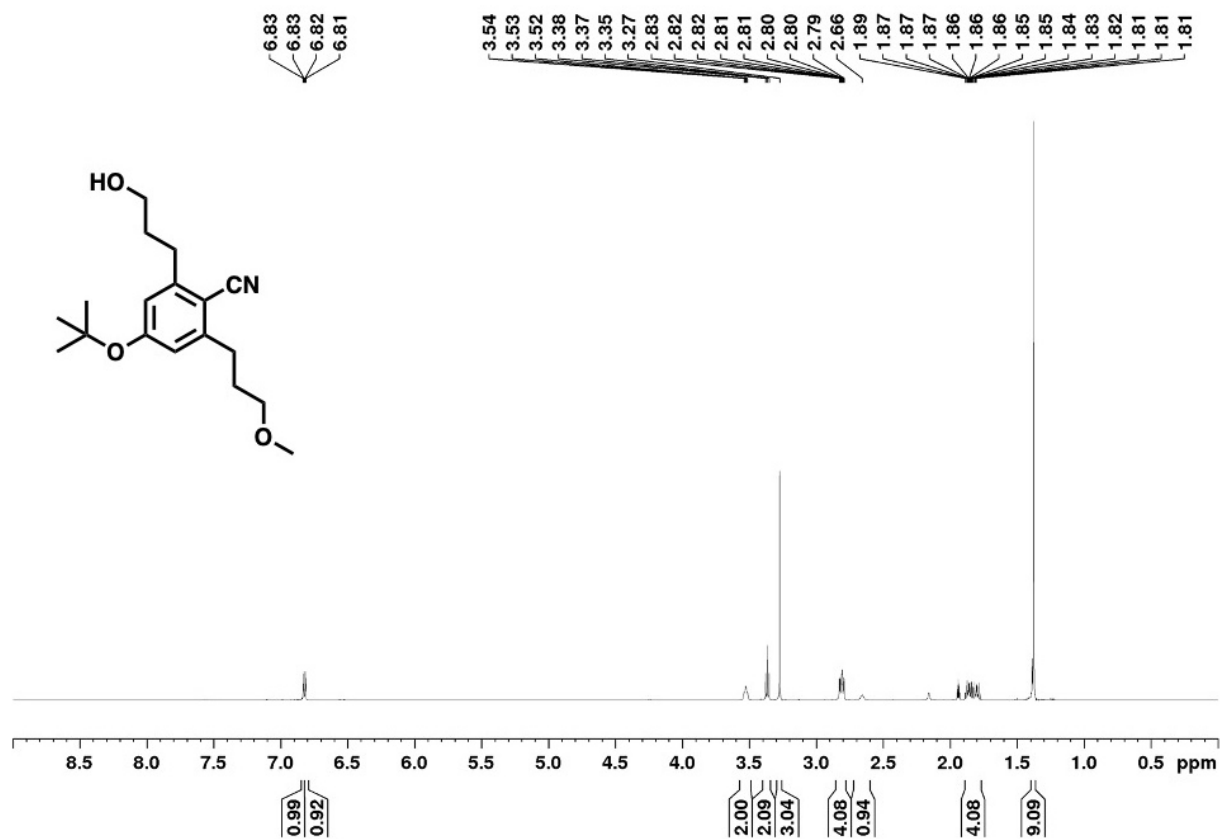


Figure 5.95. ¹H NMR Spectrum of Compound 30 in CD₃CN

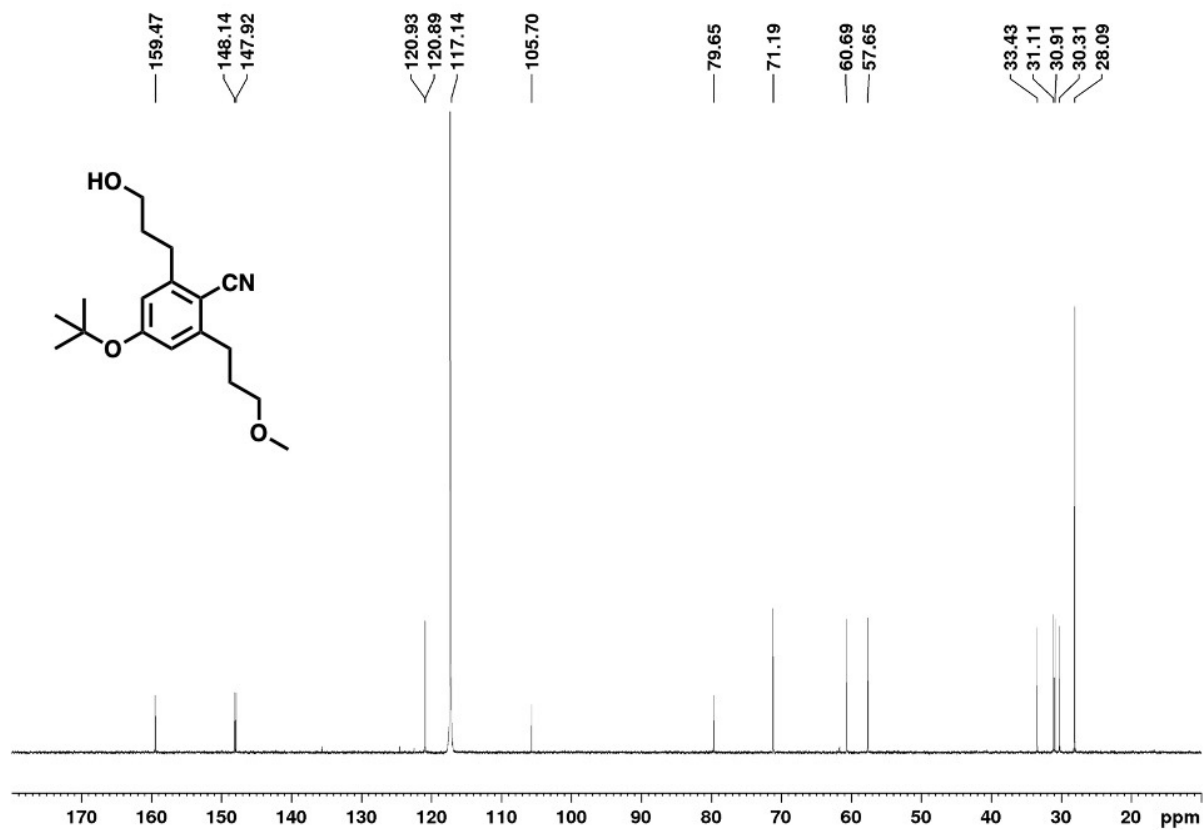


Figure 5.96. ^{13}C NMR Spectrum of Compound 30 in CD_3CN

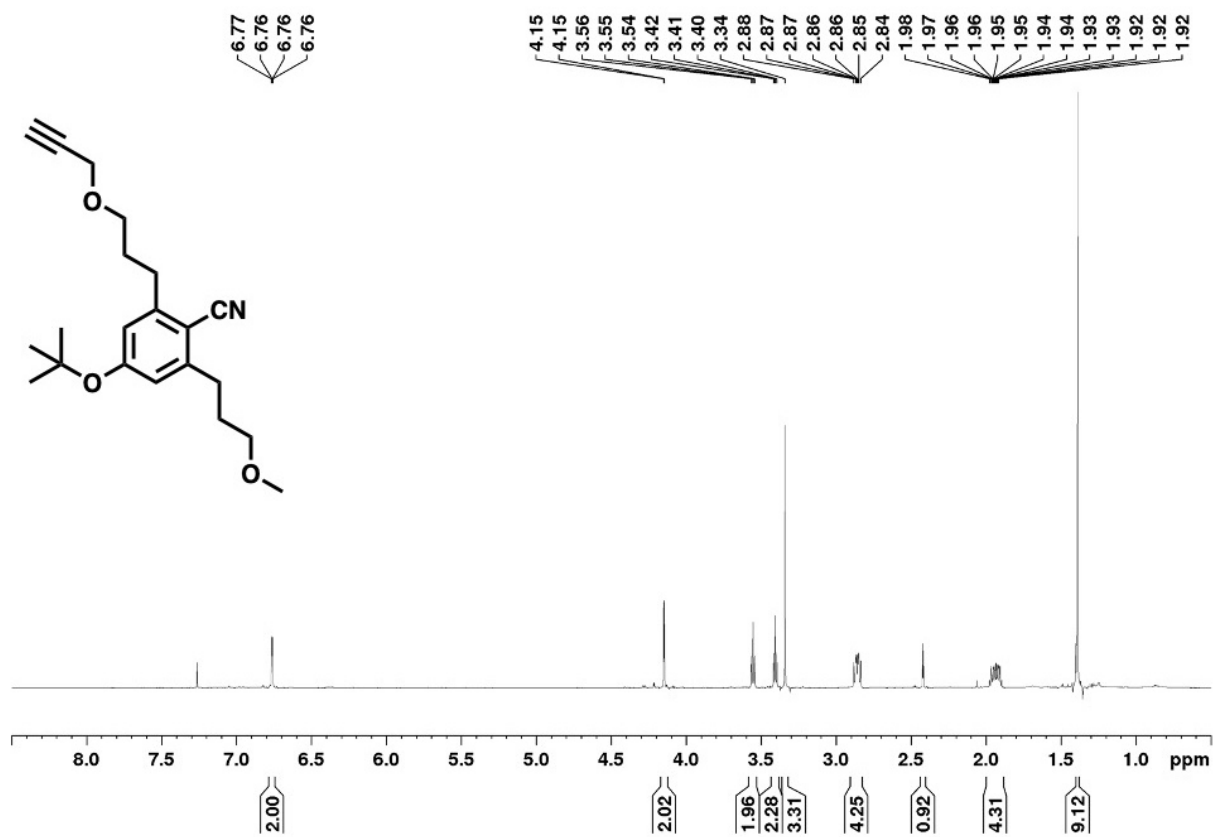


Figure 5.97. ¹H NMR Spectrum of Compound 31 in CDCl₃

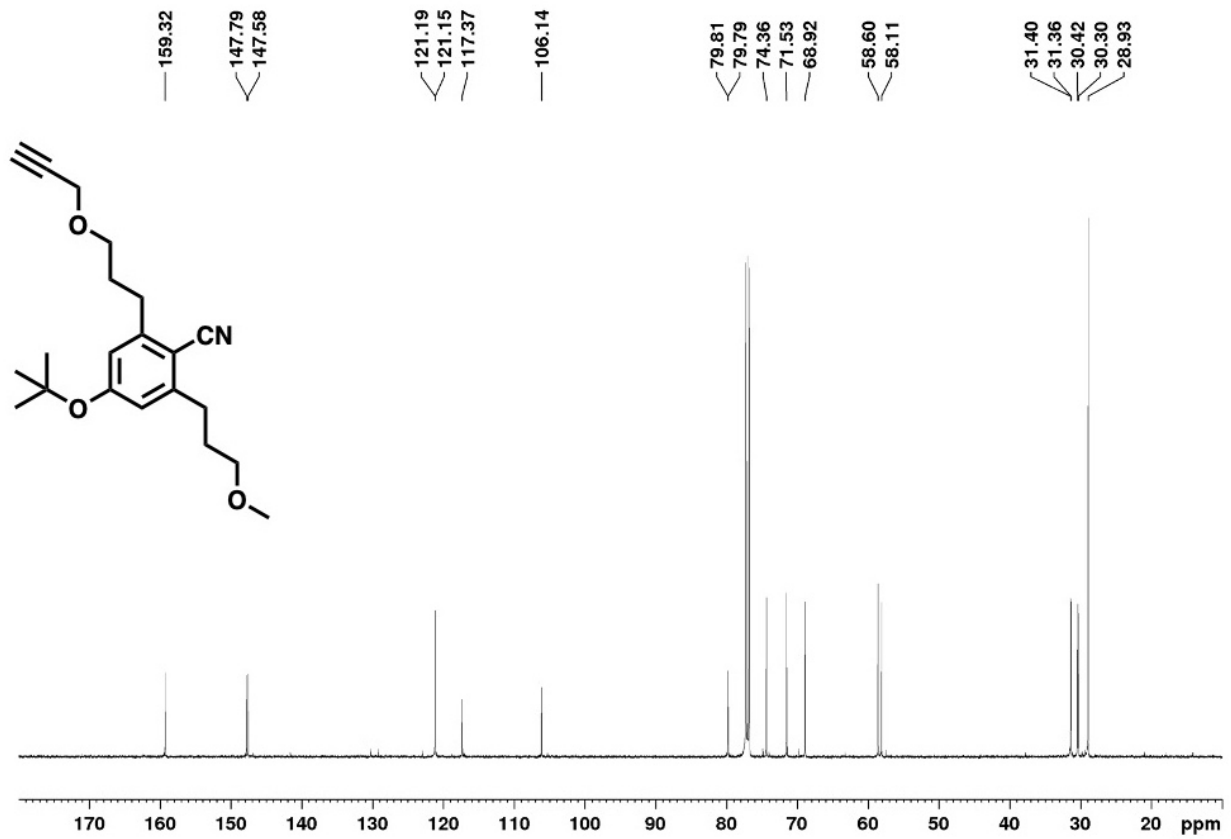


Figure 5.98. ^{13}C NMR Spectrum of Compound 31 in CDCl_3

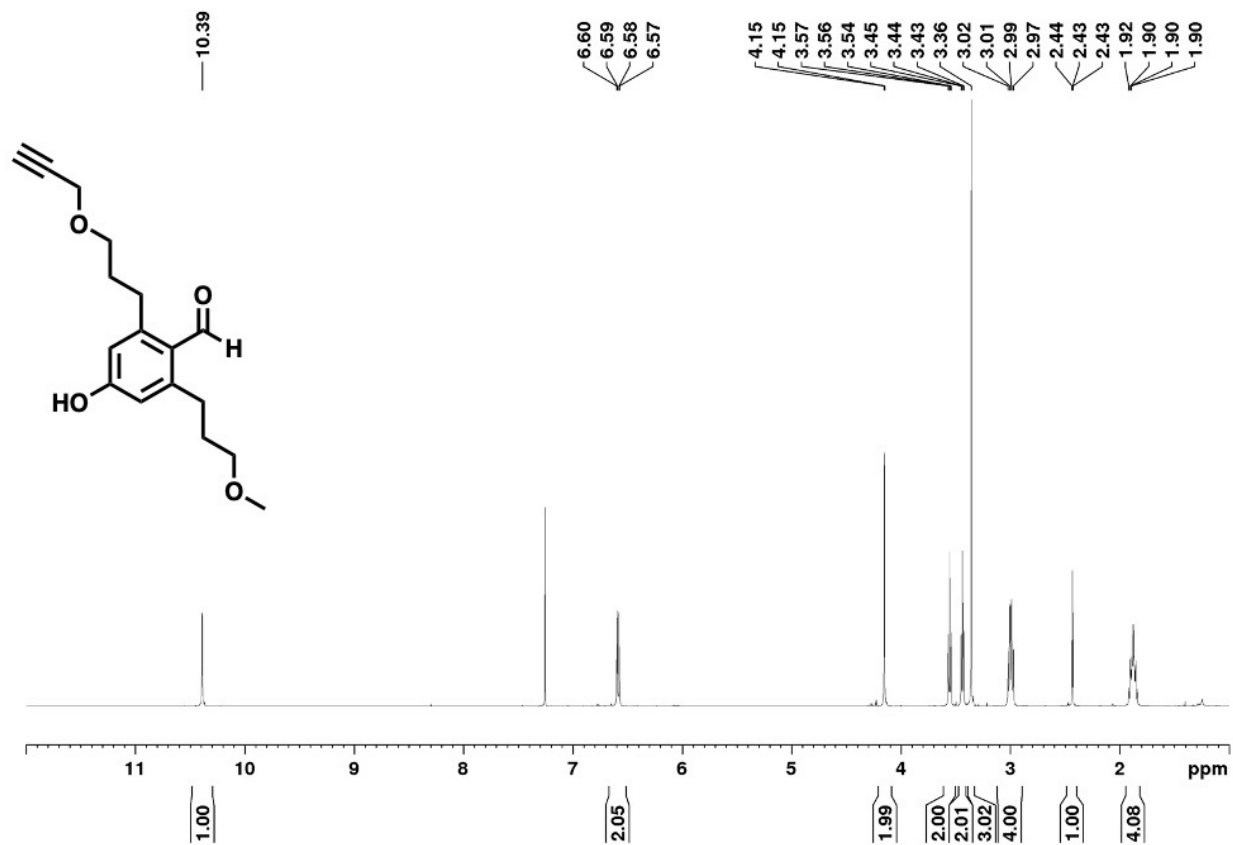


Figure 5.99. ¹H NMR Spectrum of Compound 32 in CDCl₃

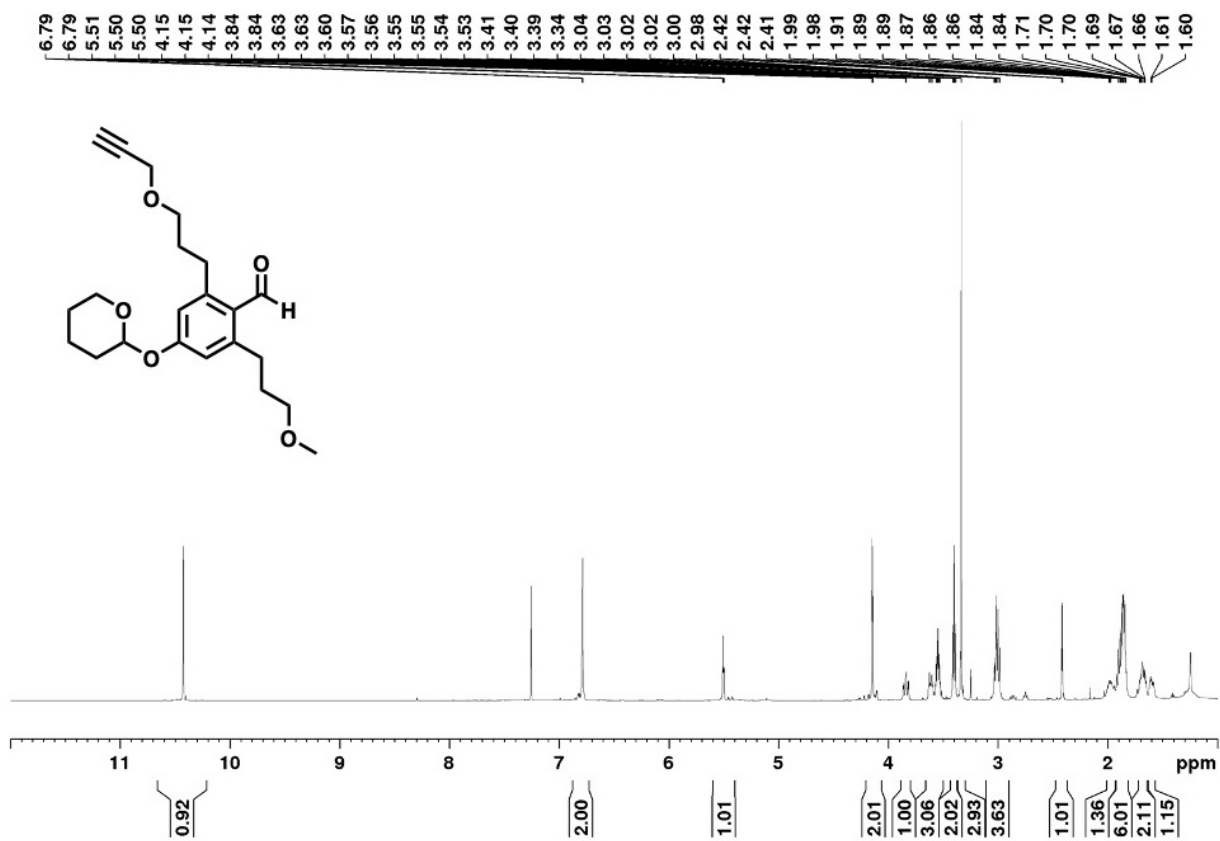


Figure 5.101. ¹H NMR Spectrum of Compound 6 in CDCl₃

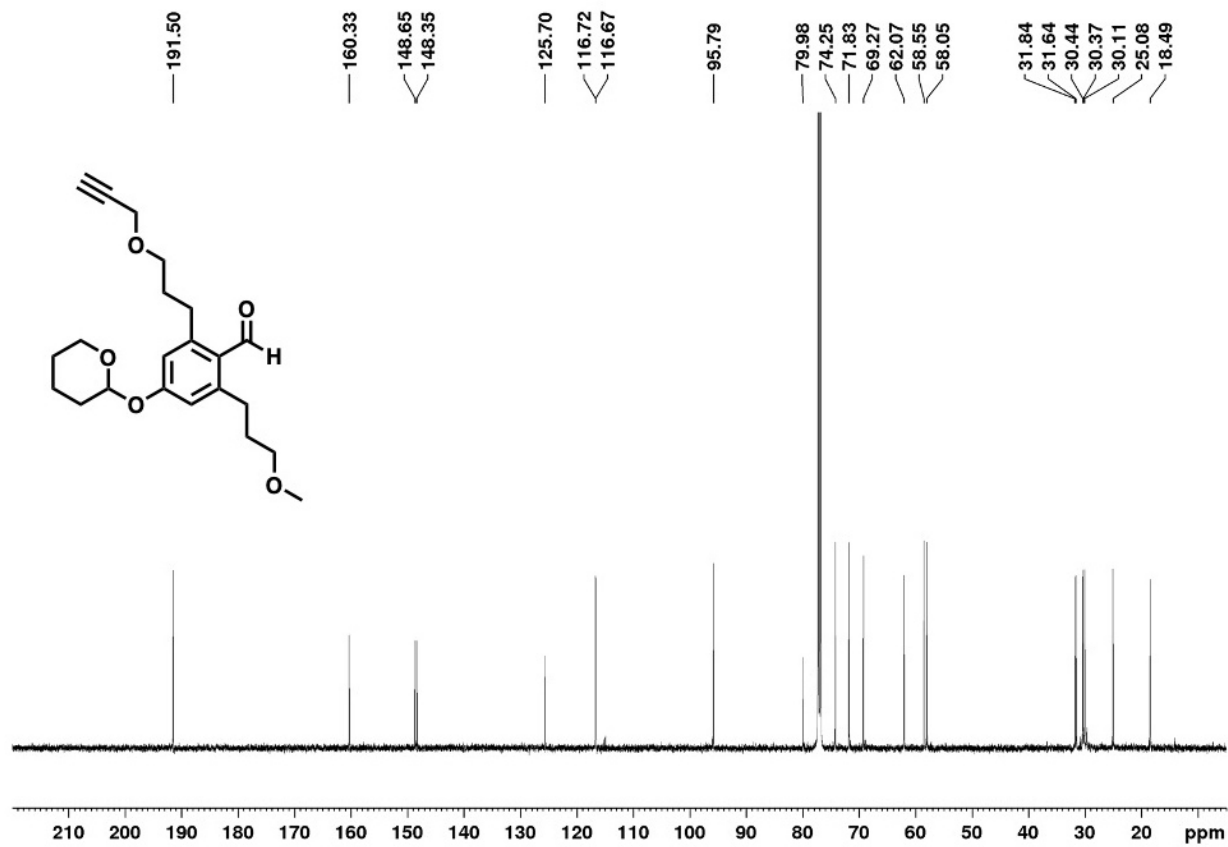


Figure 5.102. ¹³C NMR Spectrum of Compound 6 in CDCl₃

